UNIVERSITY OF
LINCOLN

RECQL4; Linking DNA Replication and Bone Tumourigenesis

Tammy Wiltshire

A thesis submitted in partial fulfilment of the requirements of the University of Lincoln for the degree of Doctor of Philosophy

School of Life Sciences

October 2019

Abstract

As part of cell division, the initiation of DNA replication is an important regulatory mechanism that maintains genomic stability over generations. RECQL4 belongs to the RecQ DNA helicase family holding an important role in the initiation of DNA replication. RECQL4 mutations can lead to disorders including type II Rothmund-Thomson (RTS) syndrome. These patients demonstrate predisposition to osteosarcoma (OS) development. OS is a primary bone tumour showing extensive chromosomal instability. We hypothesise mesenchymal stem cells (MSC) differentiating to osteoblasts are particularly sensitive to RECQL4 mutations, which may lead to impaired differentiation and OS. Our aim is to establish a direct link between the impairment of replication initiation, consequent chromosomal instabilities and deregulation in osteoblast differentiation, and OS development.

A model that phenocopies the effect of *RECQL4* mutations was established in ASC52telo cells to apply acute and chronic pressure on replication initiation using PHA-767491, which inhibits DDK that acts upstream of RECQL4 in replication initiation (PHA cells). We monitored cell viability and chromosomal instability characteristics in these cells, and RTS cell lines. To establish if PHA cells sustained differentiation capability, the cells were cultured using supplemented media for osteoblast and adipocyte differentiation, and were analysed by histochemical staining and immunofluorescence. Presence of DNA damage was quantified using γH2AX, and activation of the DNA damage response was assayed by western blotting. The cells were cultured in ultra-low attachment plates to test for anchorage-independent growth, and further analysed by cell count, MTS and luminescence assays. To identify protein-protein interactions of RECQL4, GFP-tagged RECQL4 HeLa and U2OS cells were treated with SAHA, or hydroxyurea, pulled down with GFP-nanotrap, and analysed by mass spectrometry and western blot.

We confirmed reduced proliferation rate while maintaining viability in PHA cells. Assaying mitochondrial membrane potential revealed no significant effect on mitochondrial function. Successful differentiation of PHA treated MSCs into osteoblasts and adipocytes was confirmed. Expression of osteoblast differentiation markers: calcium, and RUNX2 was influenced by PHA. An increase was also observed in chronic PHA cells under normal medium, indicating malignant transformation. Sustained DNA damage was shown in chronic PHA-767491

treated ASC52telo cells, with a higher degree of CHK1 phosphorylation, anchorage-independent growth and reduced contact inhibition.

We found that the RECQL4 mutated cell line AG05013tert was more sensitive to inhibition of replication initiation. Increase of DNA damage markers was observed in AG05013tert cells, but not in AG18375 and AG03587. Presence of MCM10 and PP2A in RECQL4 complexes was confirmed, and novel interactions with HDX and EN-2 were found.

Overall, we demonstrated that chronic interference with DNA replication initiation leads to sustained DNA damage with characteristics of genomic instability, activated DNA damage response that may become impaired over time, and may induce transformation.

To further these studies, RECQL4 knockdown using lentiviral transduction in osteoblasts would verify the cellular changes we propose, which lead to chromosomal instabilities and OS development. Novel protein interactions with RECQL4 could highlight new pathways with a direct and/or indirect role in tumourgenesis.

Acknowledgements

I would like to acknowledge and thank my supervisor Dr Csanád Z. Bachrati for all the support and encouragement within the project. I would like to acknowledge Timea Palmai-Pallag for producing the data required within the study, thank you so much to you both for your time you gave. I would also like to thank my family for all off their support.

Contents

Figures

Tables

Schematics

Abbreviations

3-isobutyl-1-methylxanthine (IBMX)
Activating Protein-1 (AP-1)
Acute promyelocytic leukemia (APL)
Adenomatosis poliposis coli (APC)
Adenosine triphosphate (ATP)
Adipose derived mesenchymal stem cells (ascs)
Alkaline phosphatase (ALP)
Alkaline phosphatase, and collagenase-3 (matrix metalloproteinase-13, MMP-13)
Alpha splice variant Ca^{2+}/Calmodulin-dependent kinase II (α-CAMKII)
Alternative lengthening of telomerase (ALT)
Aprataxin-and-PNK-like factor (APLF)
Ascorbic acid (ASC)
Ataxia-telangiectasia mutated (ATM)
ATM and Rad3- related (ATR)
A-thalassemia/mental retardation X-linked (ATRX)
Baller–Gerold syndrome (BGS)
Base excision repair (BER)
BCL2-binding component 3 (BBC3)
BMP ligand heterodimer (BMPR)
Bone marrow (BM)
Bone Marrow Derived Cells (BMDCS)
Bone morphogenetic protein 9 (BMP9)
Bone morphogenic protein (BMP)
Bone morphogenic protein 2 (BMP-2)
Bone sialoprotein (BSP)
Bovine Serum Albumin (BSA)
Break induced replication (BIR)
Breast-ovarian cancer gene 1 (BRCA1)
Ca^{2+}/Calmodulin-dependent kinase II (camkii)
Calcium ions (Ca^{2+})
Calcium sensing receptor (casr)
Camp-responsive element binding protein (CREB)
Camptothecin (CPT)
Casein Kynase 1 (CK1)
CCAAT-enhancer-binding proteins (C/EBP)
Cdc10-dependent transcript 1 (Cdt1)
Cdc45/MCM2–7/GINS (CMG)
Cell division cycle (Cdc)
Checkpoint kinase-1 (Chk1)
Checkpoint kinase-2 (Chk2)
Chromosomal instabilities (CIN)
Chronic lymphocytic leukemia (CLL)
C-Jun N-terminal kinase (JNK)
Class switch recombination (CSR)
Colony-forming-unit-fibroblasts (CFU-f)
Colorectal cancer cells (crcs)
Copy number variations (cnvs)
Core-binding factor alpha 1 (Cbfa1)
Cyclic AMP receptor element-binding protein binding protein-associated factor (PCAF)

Cyclin D1 (CCND1)
Cyclin-dependent kinase (CDK)
Cyclin-dependent kinases (CDK)
Cyclooxygenase-2 (COX2)
Dbf4-dependent kinases (DDK)
Delta-like ligand (DLL)
Dentin matrix protein-1 (DMP1)
Dexamethasone (DEX)
Dimethyl sulfoxide (DMSO)
Dishevelled (DSH)
DNA damaged response (DDR)
DNA double-stranded breaks (dsbs)
DNA polymerases (Pol)
DNA single-strand breaks (ssbs)
E2F transcription factor 2 (E2F2)
Electron transport chain (ETC)
Engrailed-1 (EN-1)
Engrailed-2 (EN-2)
Epithelial-mesenchymal transition (EMT)
Extracellular matrix (ECM)
Extracellular related kinase (ERK/12)
Fibroblast growth factor (FGF)
Gamma-H2AX (□H2AX)
Gap phase (G2)
Gap phase 1 (G1)
Global genome NER (GG-NER)
Glycerol-3-phosphate dehydrogenase (GPDH)
Glycogen synthase kinase 3b (GSK3b)
Helicase rnased C-terminal (HRDC)
Heterogeneous Nuclear Ribonucleoprotein-A1 (HNRPA1)
Heterogeneous Nuclear Ribonucleoprotein-A2/B1 (HNRPA2B1)
Highly divergent homeobox (HDX)
Histone acetyltransferases (hats)
Histone deacetylases (hdacs)
Homologous recombination repair (HR)
Human umbilical cord mesenchymal stem cells (HUC-mscs)
Hydrogen peroxide (H_2O_2)
Hydroxyurea (HU
Hypoxia inducible factor-1 alpha (HIF-1α)
Hypoxia inducible factors (HIFS)
IGF-I receptor (IGF-IR)
Immunofluorescence (IF)
Inner membrane (IN)
Inorganic phosphate (Pi)
Insulin-Like Growth Factors (IGF)
Integrin α5 (ITGA5)
Intermediate filaments (IFS)
Ironizing radiation (IR)
Ligase (LIG)
Linker of nucleoskeleton and cytoskeleton (LINC)
Liproprotein lipase (LPL)
Lysophosphatidic acid (LPA)
Matrix metalloprotease 9 (MMP9)

Matrix metalloproteinase (mmps)
MCM (minichromosome maintenance)
Meiotic Recombination-11 (MRE11)
Melanocyte-stimulating hormone 2 (MSH2)
Mesenchymal stem cells (mscs)
Methylenetetrahydrofolate reductase (MTHFR)
Micrornas (mirnas)
Microsatellite instability (MIN)
Minichromosome Maintenance (MCM)
Mitochondrial DNA (mtdna)
Mitochondrial DNA (mtdna)
Mitochondrial DNA copy number (mtdna)
Mitochondrial permeability transition pore (mptp).
Mitochondrial transcription factor A (mttfa)
Mitofusins (Mfn)
Mitogen activated protein kinases (mapks)
Mitogen-activated protein kinase (MAPK)
Monocytic leukemia zinc finger protein (MOZ)
MOZ-related factor (MORF)
MRE11/NBS1/RAD50 complex (MRN)
Multicentric OS (OSMC)
Next-generation sequencing (NGS)
Nijmegen Breakage Syndrome-1 protein (NBS1)
Nitric oxide (NO)
Non-homologous end joining repair (NHEJ)
Non-targeting (NT)
Nuclear envelope (NE)
Nuclear targeting sequences (NTS)
Nuclear-pore complexes (npcs)
Nucleophosmin (NPM)
Nucleotide excision repair (NER)
Nucleotide excision repair (NER)
Nucleotide instability (NIM)
Numerical chromosomal instabilities (N-CIN)
Origin recognition complex (ORC)
Osteoprotegrin (OPG)
Osteosarcoma (OS)
Outer membrane (OM)
Oxidative phosphorylation system (OXPHOS)
Parathyroid hormone (PTH)
Parathyroid hormone-related protein (PTHRP)
Partitioning-defective (par)
Patched 1 (PTCH1)
Peroxisome proliferation-activated receptor (ppar)
Peroxisome proliferator-activated receptor-γ (pparγ)
PHA-767491 (PHA)
Phosphatase and tensin homologue deleted from chromosome 1 (PTEN)
Phosphate Buffered Saline (PBS)
Phosphatidyl inositol-3 kinase (PI3K)
Phosphatidylinositol-3 (PI-3)
Phosphatidylinositol-3 kinase-like kinase family (PIKK).
Phosphoinositide 3-kinase pathway (PI3K/Akt)
Poly(adpribose) polymerase 1 (PARP1)

Polyomavirus enhancer-binding protein 2/core binding factor (PEBP2/CBF)
Pre-initiation complex (pre-IC)
Pressure of oxygen (po_2)
Proliferator activated receptor gamma coactivator-1 α (PGC-1α),
Prostaglandin E2 (PGE2)
Protection Of Telomeres-1 (POT1)
Protein phosphatase 2A (PP2A)
Protonophore p-trifluoromethoxy carbonyl cyanide phenyl hydrazone (FCCP)
PTH-related protein (PTH-rp)
Pyruvate dehydrogenase kinase (PDK)
RAPADILINO (RAPA)
Reactive oxygen substances (ROS)
Receptor activator of nuclear factor kappa B–receptor activator of nuclear factor kappa B ligand (RANK-RANK-L)
Receptor activator of nuclear factor κb ligand (RANKL)
Receptor activator of nuclear factor-kappa B ligand (RANKL)
Recq carboxy-terminal (RQC)
RecQ like helicase 4 (RECQL4)
Replication protein A (RPA)
Repressor Activator Protein-1/Telomeric Repeat Binding Factor 2 Interacting Protein (RAP-1/TERF2IP)
Retinoblastoma protein (RB)
Rhodamine 123 (R123)
Ribosomal protein S3 (RPS3)
Rothmund-Thomson syndrome (RTS)
Runt-related transcription factor 2 (RUNX2)
sealing zone (SZ)
Sex determining region Y box (Sox)
Short-hairpin rnas (shrnas)
Small Integrin Binding N-Linked Glycoproteins (SIBLING)
Small integrin-binding ligand N-linked glycoprotein (SIBLING)
Small interfering RNA (sirna) Flp recombination (FRT)
Smoothened (SMO)
Sonic hedgehog (SHH)
S-phase cycling dependent kinases (S-CDK)
SRY-related high-mobility group box 9 (SOX9)
Stromal cell-derived factor (SDF1)
Structural chromosomal instabilities (S-CIN)
Structural variations (svs)
Suberoylanilide hydroxamic acid (SAHA)
Synthesis-dependent strand annealing (SDSA)
T-cell factor/lymphocyte enhancer factor (LEF/TCF)
Telomerase activation (TA)
Telomerase reverse transcriptase catalytic subunit (htert)
Telomerase RNA (htr)
Telomeric Repeat Binding Factor (TRF)
Tet repressor (tetr)
Tetracycline inducible gene expression (Tet-on)
Tetramethylrhodamine methyl ester (TMRM)
Tetramethylrhodamine, ethyl ester, perchlorate (TMRE)
The citric acid (TCA)
The pre-replicative complex (pre-RC)
Thymine glycol (Tg)

Topoisomerase (TOP)
Topoisomerase 2-binding protein 1 (topbp1)
Transcriptional-coupled repair (TCR)
Transcription-coupled NER (TC-NER)
Transforming growth factor-b1 (TGF-b1)
Transforming growth factor-beta (TGF-β)
Transforming growth factor-β family of ligands (TGF-β)
TRF1-interacting Ankyrin-related ADP-ribose polymerase (TANK)
TRF1-Interacting Nuclear Factor-2 (TIN2)
Type II collagen (Col2)
Type XI collagen (Col11)
Ultrafine DNA bridges (ufbs)
Ultra-violet (UV)
Vascular endothelial growth factor (VEGF)
VEGF receptors 1 (VEGFR-1)
VEGF receptors 2 (VEGFR-2)
Werner syndrome (WS)
Western Blot (WB)
Wingless-type signalling (Wnt)
Xeroderma pigmentosum group A (XPA)
X-ray cross complementing protein 4 (XRCC4)
XRCC4-like factor (XLF)

1 Introduction

1.1 Cell division

Humans begin as a single cell; the fertilised egg, and through cell division adults are built from around 10^{13} cells. During development, a large number of cells are produced, and the process is precisely regulated to ensure this and the generation of a variety of cell types. The cell diversity is achieved through asymmetric cell division. During asymmetric division, the daughter cells inherit different cellular components such as proteins and RNA, resulting in cellular heterogeneity, leading to divergent fates (Gönczy, 2008; Knoblich, 2010). Complex regulatory mechanisms are in place to achieve proliferation of eukaryotic cells. The chromosomes are required to be duplicated precisely and segregated forming daughter cells to maintain genomic stability over generations. The precise regulatory mechanisms ensure DNA replication is only restricted for occurrence once per cell cycle. Failure of the process to occur accurately leads to the development of lethality and severe diseases, including cancer (Tanaka and Araki, 2011). Studies using *Drosophila melanogaster* and *Caenorhabditis elegans* models identified the basic molecular mechanisms behind asymmetric division (Gönczy, 2008). The process requires coordination between spindle orientation and temporal events. As part of the process partitioning-defective (par) proteins localise along a polarity axis asymmetrically which controls the orientation of the spindle and asymmetric localization of determinants of cell fate. This inherited cell fate is only passed on to one of the two daughter cells (Fisher et al., 2012; Hoege and Hyman, 2013; Noatynska et al., 2013; Thompson, 2013).

1.1.1 Cell cycle

The cell cycle defines the process of cell division as a sequence of events leading to the rise of two genetically identical daughter cells. The cell cycle is regulated to ensure normal development of multicellular organisms. The initiation of the process is well maintained and regulated to ensure proper progression, and completion form one phase to the next. Once commenced, the completion of the cycle must follow. The cell cycle consists of four distinct phases, which includes G1 (Gap1), S (DNA synthesis), G2 (Gap2), and M phase

Figure 1.1-a). Each phase controls the process of the cell division progression, and the transition is tightly regulated by various kinases which will be discussed later. Cell cycle progression is monitored by checkpoints; G1/S, G2/M, and the spindle checkpoint located in M phase, to ensure faithful completion of steps prior to engaging in the next cell cycle phase. During S phase, genetic material is replicated. Chromosomes condense and segregate during M phase, equally distributing the genetic material forming daughter cells. The M phase is complex, containing five steps; prophase, prometaphase, metaphase, anaphase and telophase. Gap phases (G1 and G2) allow for cell growth and preparation for DNA synthesis. The G0 phase of the cell cycle allows the cell to go into quiescence. It is an irreversible/reversible state of replicative dormancy, a period of cell cycle arrest to allow continuation, when progression is appropriate. Cell type and external stimuli can lead a cell into this state (Murray, 1993; Coudreuse and Nurse, 2010; Pagliuca et al., 2011; Bertoli et al., 2013; Foley and Kapoor, 2013). The duration of each phase of the cell cycle can be very variable. In mammalian cells, the cell cycle usually takes around 24 hours (Foley and Kapoor, 2013; Araujo et al., 2016).

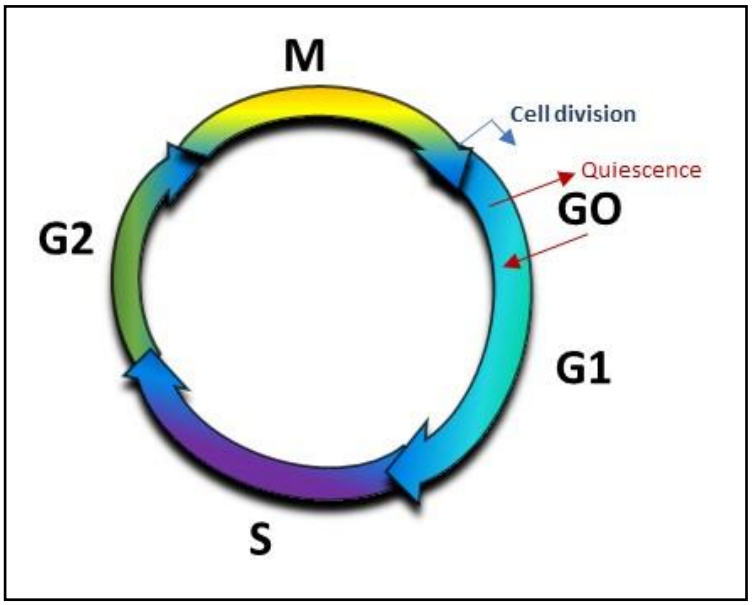

Figure 1.1-a Cell cycle division phases. Cell division involves the tightly regulated, ordered events of the cell cycle. A new cell cycle commits the cell for division and activates G1-S phase transcription. The DNA is replicated during S phase, the chromosomes are condensed, sorted and passed on to the new daughter cells during M phase. The GO phase is a state of irreversible or reversible. replicative dormancy (Quiescence) (Adapted from Foley and Kapoor, 2013).

1.1.1.1 Cyclin-dependent kinases

In higher eukaryotes, the restriction of replication was initially described in 1974 (Pardee, 1974; Blagosklonny and Pardee, 2002). This process occurs via the

sequential assembly of the replication initiation complex in G1, and the regulation of origin firing in S phase by cyclin-dependent kinases (CDK). The activity of CDKs is dependent on the binding with cyclin protein family members (Tanaka and Araki, 2011). The cyclin/Cdk complexes are a family of conserved heterodimeric serine/threonine kinases which are made of a regulatory subunit known as cyclins, and a Cdk which is the catalytic component. In higher eukaryotes five Cdks (1,2,3,4,and 6), have been shown to be associated with cell cycle progression, including Cdk1 which is activated by A- and B-type cyclins, Cdk2 by E- and A-type cyclins, Cdk3 by C-type cyclins, and Cdk4 and Cdk6 by D-type cyclins (Stern and Nurse, 1996; Morgan, 1997; Malumbres and Barbacid, 2009; Uhlmann et al., 2011; Symeonidou et al., 2012). Interestingly, while there is some functional redundancy of some cyclin/Cdk complexes, Cdk1 is essential. Studies have shown in yeast, mice and flies that Cdks are required for proliferation, survival, and have a role in polarity regulation as well (Coudreuse and Nurse, 2010; Noatynska et al., 2013).

1.1.2 Replication initiation

The initiation of DNA replication is an important regulatory step to ensure activation occurs appropriately to prevent over-replication, which would lead to possible heterogeneity and therefore loss of genome integrity, lethality and severe diseases, including cancer. In eukaryotes origins of replication initiate chromosomal DNA replication (Tanaka and Araki, 2011; Chen at al, 2018; Kang et al, 2018)

1.1.2.1 Replication initiation; RECQL4

During cell division, the onset of DNA synthesis requires the interaction of initiator proteins at the site of replication initiation, prior to the loading of the replication machinery. These sites are referred to as replication origins (Leonard and Méchali, 2013). Replication origin activation a conserved chain of events. The first step is called licensing, and generates the specific protein-origin DNA complex, the pre-replicative complex (pre-RC) (see Figure 1.1-b) (Tanaka and Araki, 2011). The protein part of the Pre-RC comprises the hexameric origin recognition complex (ORC). The binding of ORC is followed by the recruitment of additional factors. The complex contains Cdc10-dependent transcript 1 (Cdt1), Cdc6, which further recruits the Mcm2–7 (Minichromosome Maintenance: MCM) replicative helicase (Tatiana and Bakkenist, 2018). The accumulation of Cdt1 promotes the formation of pre-RC (Ballabeni et al., 2013). During late mitosis, and G1 phase of the cell cycle the pre-

RC assembles at origins by the loading of Mcm2-7 as an inactive helicase complex (see Figure 1.1-b).

Initiation is the second step reaction that occurs at the transition from G0 to S cell cycle phase, activating the pre-RC (Tanaka and Araki, 2011). Pre-RCs are activated by conversion into pre-initiation complexes (pre-ICs), via recruitment of initiation factors (Symeonidou et al., 2012), the Cdc7-Dbf4 (DDK), and S-phase cycling dependent kinases (S-CDK); Cdk2-cyclinE (see Figure 1.1-b) (Labib, 2010). The origin firing is triggered by the phosphorylation events of DDK and S-CDK, which promotes the binding of the cdc45 initiator factor, in the presence of Mcm10, TopBP1 and the GINS complex (Labib, 2010). The protein Treslin associates with TopBP1 in a Cdk2-dependent manner, mediating the loading of Cdc45 onto the replication origins (Kumagai et al., 2010). It has been suggested that the participation of RECQL4 in nuclear DNA replication occurs due to its N terminal domain, which resembles Sld2; a protein in yeast with a crucial role in DNA replication. The study by Ohlenschläger *et al*., (2012) demonstrated that the N-terminus of RECQL4 adopts a fold, similar to that of homeodomains. This domain serves as a DNA binding module and is also implicated in the interaction with human replication factor TopBP1. TopBP1 a key mediator crucially involved in DNA replication initiation and is involved in the formation of the active replicative helicase complex on replication origins, (see Figure 1.1-b) (Sanchez et al., 1999; Ohlenschläger et al., 2012; Tanaka et al., 2013). MCM10 interacts with RECQL4, enabling the localization of RECQL4 to the origins (Im et al., 2015), and the association of RECQL4 with the MCM2-7 complex (see Figure 1.1-b) (Xu et al., 2009b). The MCM2-7 complex plays an important central role as the replicative DNA helicase by acting as a DNA unwinding enzyme both during DNA replication initiation and elongation (Labib et al., 2000; Forsburg, 2004). The process of unwinding the double-stranded DNA is catalysed by the replicative helicase Cdc45/MCM2–7/GINS (CMG) complex, the defining step in replication initiation (Muramatsu et al., 2010; Sengupta et al., 2013; Medagli et al., 2016) and leads to polymerase loading (Labib, 2010) (Figure 1.1-b). For processive DNA synthesis; two sister replisomes are formed at each origin, and proceed bidirectionally along the DNA following the recruitment of additional replication factors to the CMG (Aria and Yeeles, 2019). At the end of mitosis, the degradation of geminin is required for initiating a new round of licensing. Geminin is a negative regulator of licensing by

binding to Cdt1 (Figure 1.1-b) (Nishitani and Lygerou, 2002; Symeonidou et al., 2012; Ballabeni et al., 2013).

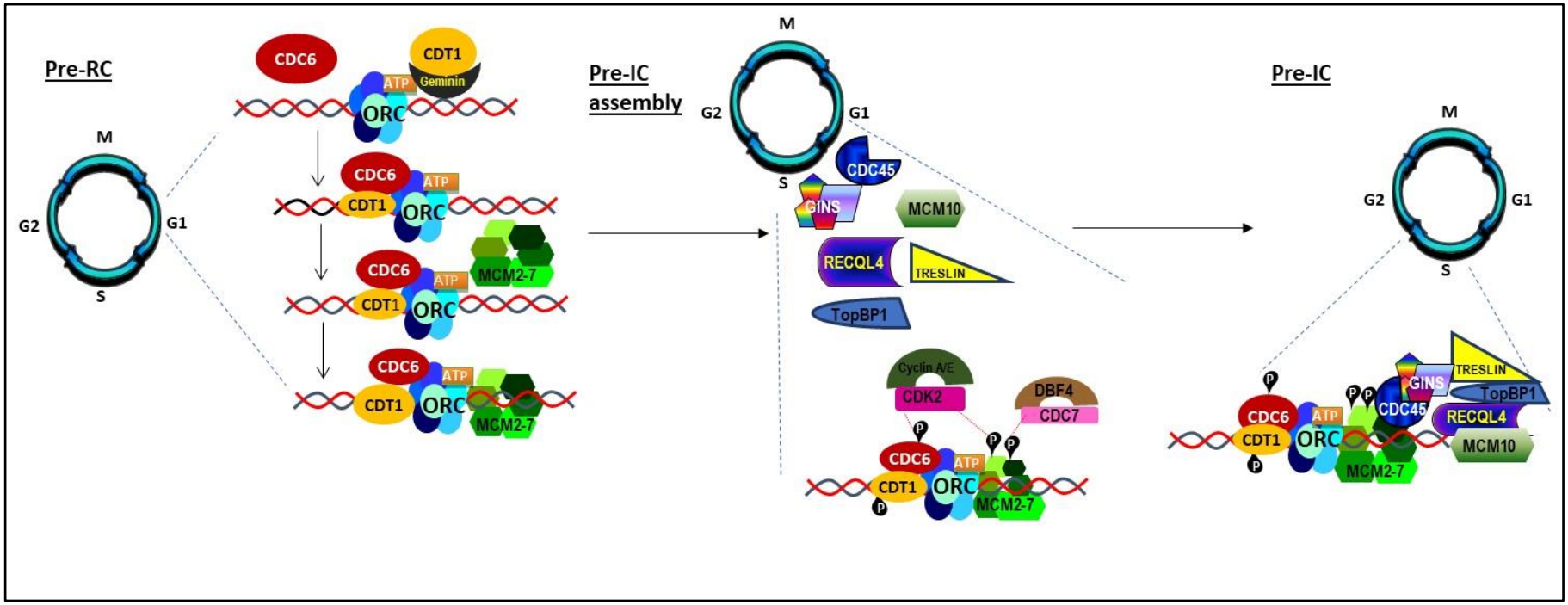

Figure 1.1-b DNA replication licensing and the initiation steps, in budding yeast and human cells, based primarily on studies in budding yeast and analogies drown for human cells. At the late M and G1 phases of the cell cycle the sequential loading of ORC, Cdc6 and Cdt1proteins onto the chromatin recruits the MCM2-7 hexameric helicase to the replication origins, generating the assembly of pre-replicative complex (pre-RC). Other proteins associate with the DNA replication origins (Pre-IC assembly), and the formation of the preinitiation complex (Pre-IC) occurs following phosphorylation by DDK and CDK kinase. This leads DNA unwinding and polymerase loading; Pol, α Pol ε and Pol δ, initiating DNA replication (Moiseeva and Bakkenist, 2018)

1.1.2.2 Impaired DNA replication initiation can lead to oncogenesis

The faithful transfer of the genome and viability from the parental cell onto the daughter cells is a very elaborately controlled mechanism (Lau et al., 2007). Eukaryotes have evolved regulation at several stages, which safeguards the process of DNA replication initiation, DNA repair, and checkpoints that are critical for replication precision. This ensures the prevention of erroneous genomic instabilities and aneuploidy, which has been found a common trait in most cancers (Lengauer et al., 1998; Depamphilis et al., 2006; Duesberg et al., 2006; Lau et al., 2007). Defects in DNA replication have been shown to be a result of direct inhibition or the abrogation of checkpoint and repair mechanisms. Furthermore, studies have shown a link between replication initiation proteins and oncogenesis, as illustrated in (Figure 1.1-c) (Lau et al., 2007). The lack of or impaired function of pre-RC proteins in the relevant cell cycle phases may give rise to different phenotypes, which could lead to possible therapeutic and diagnostic developments (Lau and Jiang, 2006; Lau et al., 2007).

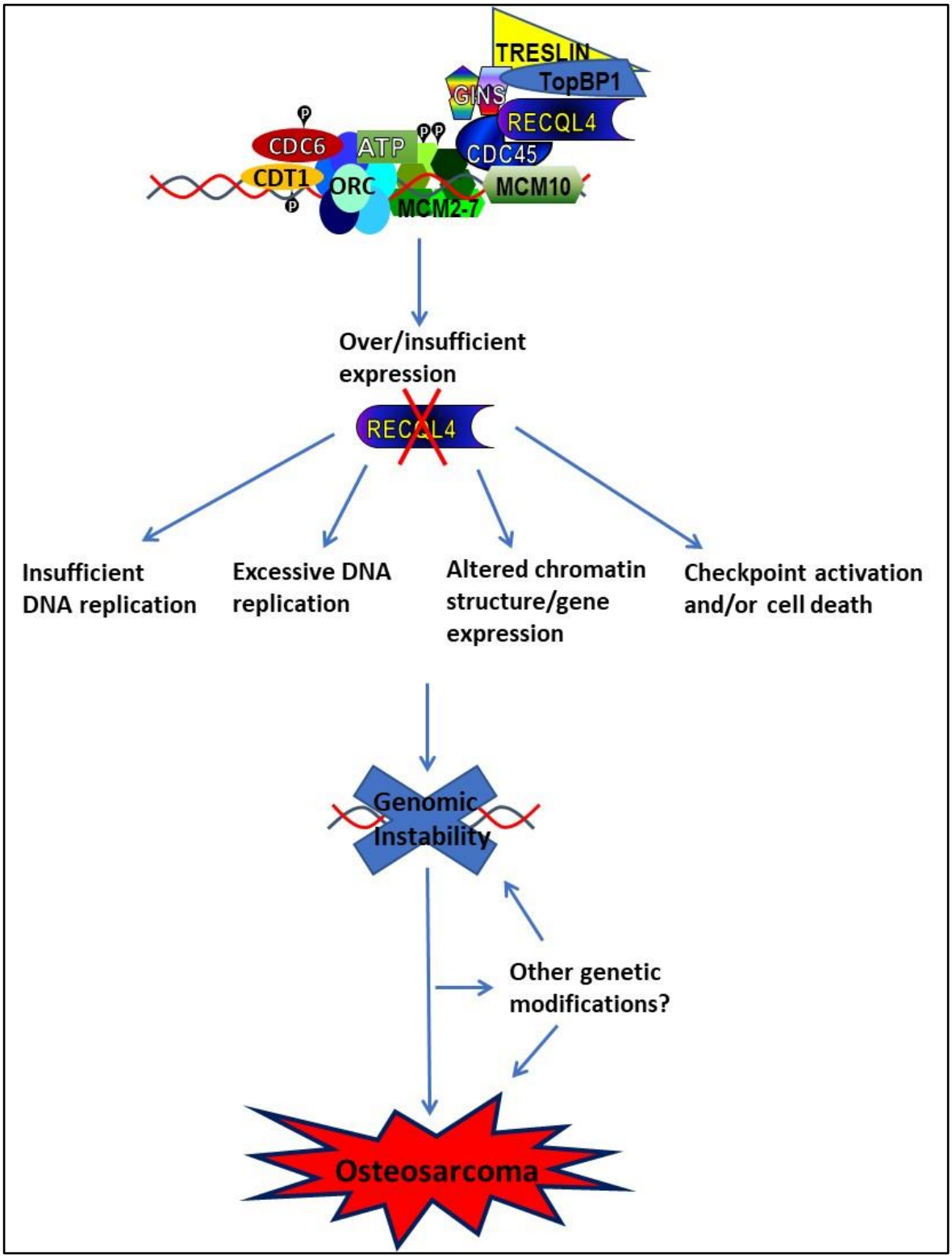

Figure 1.1-c Impairment of Pre-RC/DNA replication proteins and its involvement in oncogenesis. Impaired function of pre-RC proteins can result in incomplete DNA replication leading to cell death or chromosomal instability by reducing licensed origins. De-regulation can lead to re-firing, which if undetected can lead to subsequent amplifications and aneuploidy (Lau et al., 2007).

1.2 RECQL4

RECQL4 belongs to the family of RecQ DNA helicases. There are five members of this family in humans: *WRN*, *BLM*, *RECQL4*, *RECQL1*, and *RECQL5* (Figure 1.2-a)

(Kitao et al., 1999b; Croteau et al., 2012b). The RecQ helicase family is highly conserved, and along with other proteins such as BRCA1 and BRCA2 have been termed *'the guardians of the genome'* due to their involvement in DNA metabolism related processes including repair, homologous recombination or replication fork restart, replication, transcription, and chromatin organization (Croteau et al., 2012b; Larsen and Hickson, 2013; Nahhas et al, 2018). The *RECQL4* gene was first cloned and mapped to chromosome 8q24.3 by Kitao *et al* (1999a). *RECQL4* is a small gene of 6.5 kb, with 21 exons and with most introns less than 100 bp in length (Kitao et al., 1999a; Wang et al., 2002a). The gene encodes a 1208 amino acid protein. Unlike other human RecQ helicases, RECQL4 lacks the RecQ carboxy-terminal (RQC), and helicase RNaseD C-terminal (HRDC) domains (Figure 1.2-a) (Ohlenschläger et al., 2012).

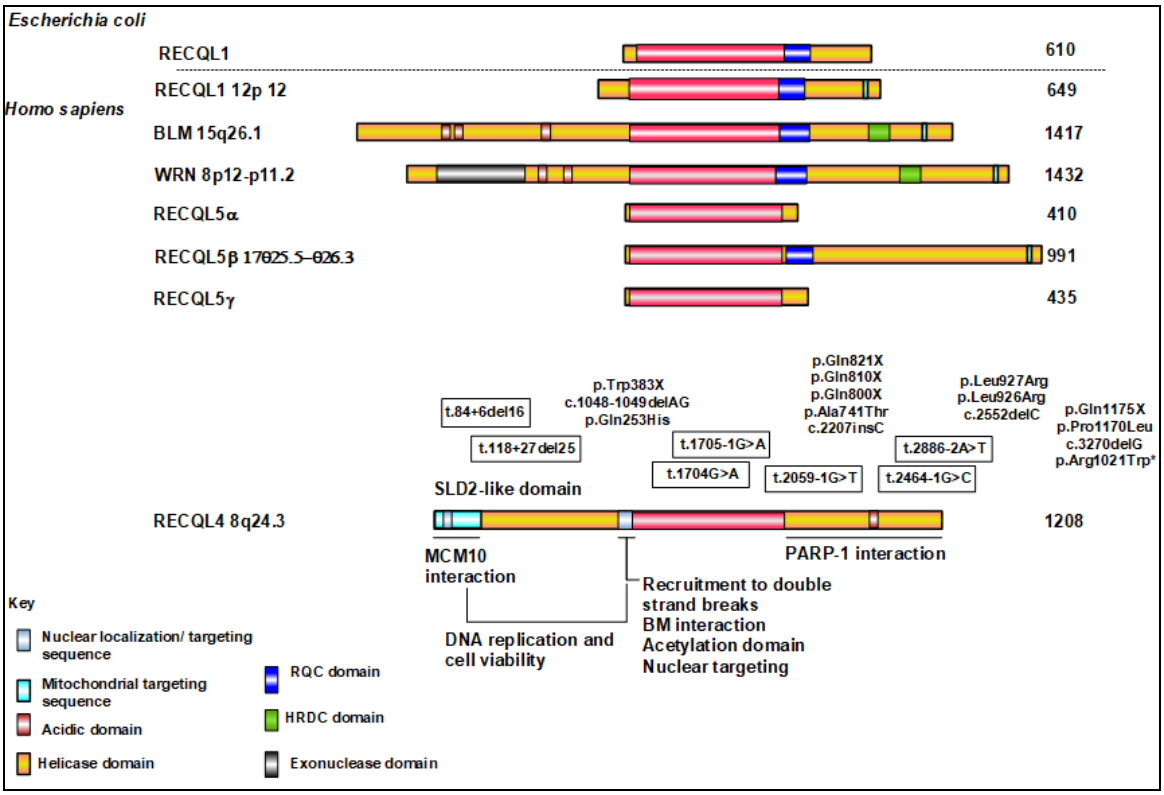

Figure 1.2-a Structural organization of human RecQ helicases. RecQ helicase members possess a highly-conserved helicase domain (pink). The nuclear localization signal (greyish-blue) is present mostly at the C-terminus, RECQL4 is an exemption, which has two nuclear targeting sequences (NTS1 and NTS2) that are present at the N-terminus. The N-terminus of RECQL4 shows sequence similarity with the Sld2 protein in yeast that is important for DNA replication and cell viability. A putative mitochondrial targeting sequence is present at the N-terminus of RECQL4. The location of some of the known RECQL4 mutations are depicted. * Mutations shared by RTS and BGS (Adapted image, from Croteau *et al.,* 2012; Sidorova and Monnat., 2015.

1.2.1 Biochemical activity of RECQL4

Studies have highlighted roles and functions of RECQL4, including DNA strand-annealing activity and ATPase activity activated by ssDNA. RECQL4 has also been shown to be involved in DNA repair (Yin et al., 2004; Macris et al., 2006; Maire et al., 2009) and is capable of unwinding various DNA structures (Xu and Liu, 2009a). RECQL4 was thought not to possess DNA helicase activity, unlike other members of the RecQ helicases (Yin et al., 2004; Macris et al., 2006). However, RECQL4 was shown to possess *in vitro* 3′→5’ helicase activity by other authors, which might have been masked by strand annealing activity (Xu and Liu, 2009a; Capp et al., 2010; Croteau et al., 2012b; Larsen and Hickson, 2013). It has been suggested that there is a second helicase activity harboured at the 400 amino-terminal amino acid by a study by Xu and Liu, (2009), even in the absence of notable nucleotide binding and helicase motifs (Xu and Liu, 2009a).

1.2.2 RECQL4 localisation

Northern blotting analysis showed high expression in human thymus, testis, and placenta, with moderate expression in the heart, brain, colon, and the small intestines. Peak of expression is seen at S-phase of the cell cycle (Yin et al., 2004; Dietschy et al., 2009; Croteau et al., 2012a). Within the RecQ helicase family, RECQL4 is the only known to be found both in the nucleus and cytoplasm (Yin et al., 2004; Petkovic et al., 2005; Burks et al., 2007). It localizes predominantly to the nucleoplasm, with fraction to telomeres and nucleolus, and more recently found inside the mitochondria (Croteau et al., 2012a). A study by Burks *et al.,* (2007), identified two nuclear targeting signals located in the N-terminus; NTS1 amino acids 37–66 and NTS2 amino acids 363-492, of RECQL4 (Burks et al., 2007). The acetylation of RECQL4 by histone acetyltransferase p300 has been shown to lead to localisation of RECQL4 to the cytosol from the nucleus (Dietschy et al., 2009). A study by Chi *et al.,* (2012) reported the identification of nuclear exporting signals pNES2 and pNES3 at the C-terminus. Diminished cytoplasmic localization was observed following pNES2 deletion. They also found that in the presence of functional pNES2 RECQL4 cytoplasmic fraction was enriched following the addition of ubiquitination tail at the C-terminus. Using immunofluorescence Chi *et al.,* (2012) demonstrated cytoplasmic RECQL4 to be located within the mitochondria, suggesting a regulatory role in mitochondrial DNA (mtDNA) copy number maintenance. An increase in mtDNA copy number was demonstrated in HEK293

cells following RECQL4 expression elevation, while RECQL4 knockdown in U2OS cells resulted in a decrease in mtDNA copy number. In *RECQL4* deficient human fibroblasts and RECQL4 suppressed cancer cells mitochondrial superoxide production and a decrease in repair function was reported following oxidative DNA damage, further demonstrating the role of RECQL4 in mitochondrial stability (Chi et al., 2012). The intracellular distribution and dynamic relocalization of RECQL4 to sites of DNA damage has suggested a possible contribution to the phenotypes, and associated heterogeneity, which has been found in RECQL4-associated diseases (Croteau et al., 2012a).

1.2.3 Mutations in the *RECQL4* gene

Almost half of the mutations in *RECQL4,* representing missplicing, nonsense, or frameshift mutations, occur before or in regions coding for the helicase domain suggesting that the helicase domain is critical for accurate function of the protein (Siitonen et al., 2009; Larizza et al., 2010; Kohzaki et al., 2012). Most of the mutations are predicted to cause a truncated protein (Kitao et al., 1998; Larizza et al., 2010; Wang et al., 2017a).

DT40 cells with homozygous deletions of the *RECQL4* gene failed to proliferate, however rescue was achieved by ectopic expression of the N-terminal Sld2-like domain leading to proliferation. This suggests that the C-terminus, including the helicase domain is not essential for cell proliferation (Abe et al., 2011). However, other studies suggest the C-terminus as well as the helicase domain to be a requirement for DNA replication (Sangrithi et al., 2005; Matsuno et al., 2006; Capp et al., 2009). The knockout of the *Recql4* gene entirely, or the part encoding the Sld2-like N-terminus has been found to lead to embryonic lethality in mice and flies (Hoki et al., 2003; Sangrithi et al., 2005; Matsuno et al., 2006; Xu et al., 2009a).

RECQL4 mutations (Figure 1.2-a) give rise to autosomal recessive overlapping diseases in humans: Rothmund–Thomson syndrome (RTS, OMIM #268400) RAPADILINO (RAPA, OMIM #266280), and Baller–Gerold syndrome (BGS, OMIM #218600). The majority of mutations detected have been found to be 3’ to the codon of amino acid 496 (Larizza et al., 2010). The loss of helicase domain causes a severe phenotype reminiscent of RTS (Mann et al., 2005). Studies have suggested that the mutations found within the RECQL4 protein in RTS individuals permit partial

activity (hypomorphic), even though the expression may be detected at very low levels (Ouyang et al., 2008).

1.2.3.1 Baller-Gerold (BGS) syndrome

BGS is inherited in an autosomal recessive manner and was first described in 1950. Its hallmark presentations include radial aplasia/hypoplasia and craniosynostosis. Craniofacial manifestations are not seen in all patients (Petkovic et al., 2005; Van Maldergem et al., 2006). The Hallmark feature of RTS, poikiloderma, is also found in patients with BGS (Petkovic et al., 2005). The most frequent mutations of *RECQL4* are the R1021W missense, and the 2886 delta T frameshift mutations of exon 9 (Van Maldergem et al., 2006).

1.2.3.2 RAPADILINO syndrome

RAPADILINO is an autosomal recessive disease, involving *RECQL4* mutations, and was originally described in Finland in 14 patients. The acronym RAPADILINO stands for the characteristic clinical features often presented: RAdial hypo-/aplasia, Patellae hypo-/aplasia and cleft or highly arched PAlate, DIarrhoea and DIslocated joints, LIttle size and LImb malformation, NOse slender and NOrmal intelligence. Patients most commonly represent in-frame deletions of exon 7, which is thought not to affect the helicase domain (Siitonen et al., 2003). Interestingly, while there are overlaps in RTS and RAPADILINO symptoms, joint dislocations and patellar hypo/aplasia, found to be more common in female RAPADILINO patients, are not characteristic to RTS (Kellermayer et al., 2005; Van Maldergem et al., 2006). Around 7% have been found to develop tumours, mainly lymphomas and osteosarcoma (Kellermayer et al., 2005; Siitonen, 2008).

1.2.3.3 Rothmund Thomson Syndrome (RTS)

RTS was first described by Rothmund in 1868, characterising it as a familial occurrence of skin changes with bilateral juvenile cataracts. In 1936 Thompson reported subsequent cases, and in 1957 it was suggested by Taylor that these were of the same disease (Rothmund, 1868; Thomson, 1936; Taylor, 1957). RTS is a rare autosomal recessive genodermatosis, therefore both parents of proband are obligate heterozygotes, leaving the siblings a 25% chance of being affected, 25% chance of not being carriers, and a 50% chance of being carriers but asymptomatic.

RTS patients appear to be phenotypically and genetically heterogeneous (Wang et al., 2003; Larizza et al., 2006; Larizza et al., 2010).

Recurrent *RECQL4* mutations have been found to include exon 9 c.1573delT (p.Cys525AlafsX33), which accounts for around one-third of RTS mutations. This mutation was found in compound heterozygous patients from multiple ethnic backgrounds (Wang et al., 2003; Larizza et al., 2010; Croteau et al., 2012b). The amino-terminal region has an essential functional role in the cell, although not necessarily for cell viability but can lead to severe phenotype reminiscent of RTS if lost (Kitao et al., 1999b; Ichikawa et al., 2002; Hoki et al., 2003; Mann et al., 2005). RTS patients have been found to have common phenotypes caused by mutations that target the helicase domain or the C-terminal region, suggesting the C-terminus acts as one unit (Kohzaki et al., 2012).

1.2.3.3.1 Symptoms

Pathological changes of the skin are the main hallmark characteristic presentation seen in RTS patients (Larizza et al., 2010). Poikiloderma, a skin rash seen in RTS patients, usually presented around the age of 3-6 month and typically the pattern of spread involves the cheeks, and then to other extremities, sparing the trunk and abdomen. The rash is sun-sensitive with redness and blisters, involving patches of skin. The patient may develop variable pigmentation, atrophy; areas of thinning of the skin, and telangiectases; small clustering of blood vessels under the skin. This presentation is a crucial criterion for diagnosing RTS (Pujol et al., 2000; Wang et al., 2001; Beghini et al., 2003; Larizza et al., 2010). Ectodermal dysplasia is often seen in type I RTS (Larizza et al., 2010). Ectodermal dysplasia was previously defined as a congenital disorder presenting with alterations in at least to ectodermal structures including the hair, teeth, nails, or sweat glands (Freire-Maia, 1971). The classification has been modified to include gene defects and clinical manifestations (Visinoni et al., 2009). Sparse or absent hair, eyelashes and eyebrows is a common feature. In a cohort of 41 RTS sufferers, 50% and 73% of the patients presented with sparse, brittle, thin or absent scalp hair and sparse hair on eyelashes and/or eyebrows, respectively (Wang et al., 2001). Poorly formed and dystrophic nails (Larizza et al., 2010), and dental abnormalities were first described in the early study of 1868, and are also common features (Rothmund, 1868).

Ocular lesions are often present, with rapid onset of bilateral cataracts is the most common ocular sign (Nathanson et al., 1983; Stinco et al., 2008).

Rothmund-Thomson syndrome does not appear to show cognitive impairment (Larizza et al., 2010), however, one patient has been recorded in the literature with sensorineural deafness (Beghini et al., 2003).

Haematological signs have been reported, ranging from myelodysplasia to aplastic anaemia, and leukaemias have also been identified (Rizzari et al., 1996; Knoell et al., 1999; Porter et al., 1999; Narayan et al., 2001; Pianigiani et al., 2001).

The loss of or underdeveloped bone and reduced growth syndromes leading to patterning-like phenotype are often referred to as “dysostoplasias”. They can occur following genetic defects leading to defects in mesenchymal condensation and/or differentiation (Mundlos and Olsen, 2002). Radial ray defects appear to follow all three overlapping *RECQL4* mutation disorders; BGS, RTS, and RAPADILINO (Siitonen et al., 2003; Larizza et al., 2006; Van Maldergem et al., 2006; Burks et al., 2007; Larizza et al., 2010). An early review has reported about 68% of the patients were found to display skeletal anomalies, including frontal bossing, saddle nose and abnormalities of the long bones (Vennos et al., 1992; Wang et al., 2003). A latter study of 28 subjects found around 75% of patients with RTS presented at least one skeletal abnormality (Mehollin-Ray et al., 2008). In at least two-third of patients low birth weight, slow weight gain, and linear growth deficiency are present, and they are proportionally small (Wang et al., 2001)**.** Those patients without *RECQL4* mutations and RTS appear to share some similar symptoms including skeletal abnormalities, however, those patients with *RECQL4* mutations and RTS show a higher percentage of presenting with small stature, sparse brows or lashes, and radial ray defects (Radial hypo/aplasia and/or aplastic/hypoplastic thumbs. The symptoms of RTS patients have been shown to involve highly proliferative cells, including developing teeth, nails, skin, intestines and blood (Larizza et al, 2010; Wang and Plon, 2019). Involvement of RECQL4 in DNA replication initiation could explain this, suggesting RECQL4 may be important for viability of highly proliferative cells. The dysfunction of RECQL4 could lead to reduced cellular proliferative potential, leading to tissue damage and a lower potential for tissue regeneration, and the development of pathological disorders, such as RTS (Lu *et al,* 2014).

1.2.3.3.2 Diagnosis

The symptoms of RTS are relatively non-specific, leading to clinical diagnostics criteria to be variable. Clinical diagnosis is therefore based on the time of onset, spreading, and clinical presentation of the characteristic poikiloderma. The

probability of an RTS diagnosis, according to is determined by an atypical rash and the presence of two of the following signs: short stature, congenital bone defects, sparse hair found on the scalp, eyebrows, and eyelashes, abnormalities of the teeth and nails, cataracts, and hyperkeratosis. RTS diagnosis is usually considered in patients with osteogenic sarcoma, especially if presenting with skin changes (Nahhas et al, 2018; Wang and Plon 2019). RTS molecular genetic tests currently include sequence analysis/mutation scanning to identify point mutations in the RECQL4 gene, and deletion/duplication analysis for the detection of partial or whole genome deletions in cytogenetic testing. Lymphocytes or skin fibroblasts can reveal chromosome 8 abnormalities: trisomy 8, tetrasomy 8q, partial 8q duplication, and isochromosome 8q (Wang and Plon, 2016). It has been suggested that primary defects of the replication and repair functions of RecQ helicase mutant cells, chromosomal instability is a secondary occurrence (Bachrati and Hickson, 2008). Chromosomal instabilities are not a hallmark feature, however, to act as an adjunct to clinical diagnosis, nevertheless, when found it appears as distinctive mosaic aneuploidies and isochromosomes (Larizza et al., 2006).

1.2.3.3.3 Subtypes

There are two subtypes of RTS based on molecular and clinical analysis: type I and type II. Type I is characterised by poikiloderma, ectodermal dysplasia, and juvenile cataracts and shows no *RECQL4* mutations on gene analysis. The aetiology of these cases is unknown, gene mutations have not been associated. Those patients with type II RTS have documented *RECQL4* mutations with an associated risk of malignancy, and characterised further by poikiloderma and congenital bone defects (Wang et al., 2003; Larizza et al., 2010; Croteau et al., 2012b). Mutations may render the RECQL4 protein in RTS individuals partially active, even though the expression may be detected at very low levels (Ouyang et al., 2008). It is unclear if the two types of RTS represent different syndromes demonstrating similar clinical features, or the possibility of involving different genes linking to the same pathway (Larizza et al, 2010), suggesting a link between RECQL4 and cancer predisposition in RTS patients.

1.2.4 RTS and cancer predisposition

Cancer is a developmental process, and cancer cells are formed following complex cell transformation, often due to mutations or DNA-rearrangements which undermine the former cellular phenotype. This generates a cell population with large variability in gene expression, chromatin organisation, and interactome composition formation (Huang et al., 2009b; Greaves and Maley, 2012; Huang, 2013; Wang et al., 2013a; Wang et al., 2013b)

RTS patients can present with multiple malignancies, in particular osteosarcoma (Dick et al., 1982; Varughese et al., 1992; Drouin et al., 1993). Studies have shown susceptibility can also be induced by chemotherapy (Simon et al., 2010; Carlson et al., 2011). Around two thirds of patients with mutations in *RECQL4* have RTS (Wang et al, 2003; Siitonen et al., 2009; Larizza et al, 2010; Croteau et al, 2012). A clinical cohort study looked at 41 RTS patients and found 30% diagnosed with osteosarcoma (Wang et al., 2001). The median age of diagnosis of osteosarcoma is 11 years in RTS patients, which is slightly lower than those in general public without RTS (Lindor et al., 2000; Wang et al., 2001), suggesting RTS as a premature aging syndrome that may lead to cell susceptibility to OS (Croteau et al., 2012b; Larsen and Hickson, 2013). Proliferative defects could lead to tissue damage and reduced regeneration, leading to many of the symptoms associated with RTS (Lu et al, 2014). This could also link the age of OS development occurring in younger patients in those with RTS (Lindor et al., 2000; Wang et al., 2001). RTS type II patients have demonstrated a second peak of incidence of OS in the elderly (Unni, 1996; Dorfman and Czerniak, 1998). OS in older patients have also demonstrated worse prognosis (Longhi et al., 2008). Epithelial tumours including squamous cell and basal cell carcinomas, Bowens disease, and melanoma of the skin have also been demonstrated in some RTS patients (Wang et al., 2001; Wang et al., 2003; Howell and Bray, 2008). Skin malignancy may be related to skin sensitivity, and use of sunscreen protection is recommended (Kiss and Anstey, 2013; Morales-Sánchez et al., 2016). The development of skin cancers can occur at any age, however, often presented earlier in RTS patients (Stinco et al., 2008). Interestingly, many RTS patients develop more than one tumour of the same or of different type. This supports RTS as a cancer predisposition syndrome (Hees et al., 1996; Stinco et al., 2008).

The burden of cancer correlates with the increase of the age of the population (Jones et al., 2012). The biological functions of the association of aging and cancer is not yet fully understood. Aging leads to physiological deterioration which contributes to the development of some human cancers (Kennedy et al., 2014), and could be a driver of the significance risk of cancer development seen on premature aging diseases (Figure 1.2-b).

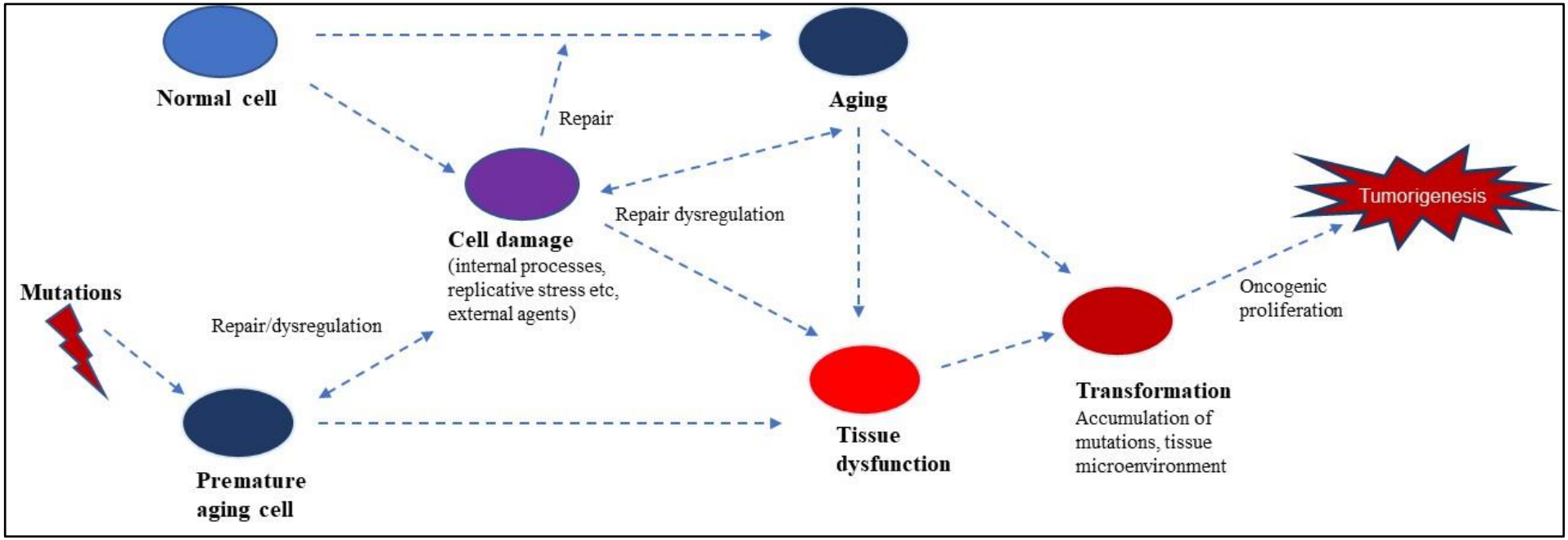

Figure 1.2-b– Schematic linking premature/normal aging and cancer development. Mutations can lead to premature aging syndromes. Key hallmarks of aging include; telomere attrition, mitochondrial dysfunction, genomic instability, loss of proteostasis, epigenetic alterations, stem cell exhaustion, cellular senescence, deregulated nutrient sensing, and altered intercellular communication. This could lead to cell susceptibility driving cancer development (Anisimov, 2009; López-Otín et al., 2013).

1.3 Mesenchymal stem cells

The first report of MSCs was in 1867 by pathologist Julius Friedrich Cohnheim, who described them as fibroblastoid, adherent, and extravasated cells at sites of injury (Cohnheim, 1867). Later, these ossifying cells were isolated in cell culture, and reported as a plastic-adhering colony forming cell population, originally harvested from bone marrow (Friedenstein et al., 1970). In 1990 they were found to exhibit the ability of multipotent differentiation, and from then referred to as mesenchymal stem cells, capable of osteoblastic, adipocytogenic, and chondrogenic potential (Caplan, 1991). Mesenchymal stem cells (MSCs) are now widely available, have few ethical concerns, low immunogenicity, and multi-lineage differentiation potential (Figure 1.3-a) (Jung et al., 2012; Wang et al., 2014).

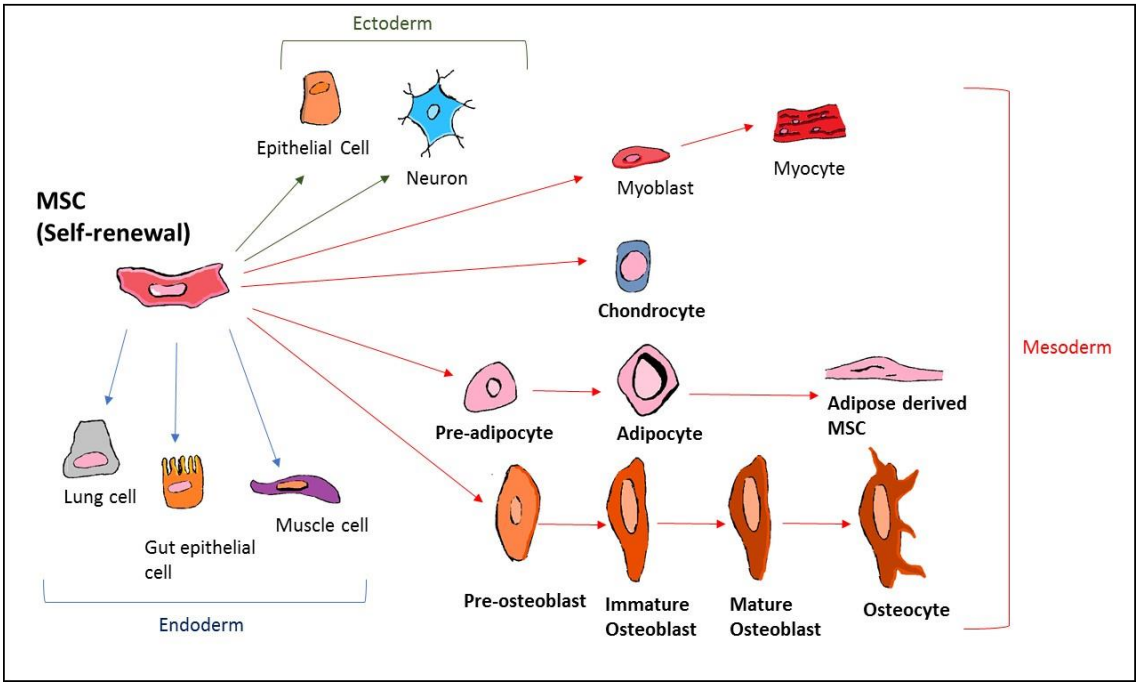

Figure 1.3-a Mesenchymal stem cell multipotentiality. Mesenchymal stem cells (MSCs) are able to differentiate into mesodermal, ectodermal, and endodermal lineages (Ullah et al., 2015). Adapted from (Uccelli et al., 2008).

There are many sources of MSCs (Crisan et al., 2008; Choudhery et al., 2013; Patel et al., 2013). MSCs can be isolated efficiently from bone marrow (Pittenger et al., 1999), amniotic fluid (Scherjon et al., 2003; Tsai et al., 2004), amniotic membrane (Cai et al., 2010), dental tissue (Huang et al., 2009a; Seifrtová et al., 2012), endometrium (Schüring et al., 2011), peripheral (Ab Kadir et al., 2012), and adipose tissue (Wagner et al., 2005; Zhang et al., 2006), to name a few. The bone marrow is often utilised for isolating multipotent MSCs, however, the harvest procedure is

highly invasive, and the quantity, differentiation potential, and lifespan has been reported to decline with age (Nishida et al., 1999; Mueller and Glowacki, 2001; Stenderup et al., 2003). Adipose tissue is easier to obtain as less invasive then many other sources, such as the bone marrow. Adipose tissue has been identified with relatively high abundance of stem cells (Dicker et al., 2005; Fraser et al., 2006). Large quantities of adipose tissue can be isolated following liposuction, therefore attractive for requirements of large scale productions of MSCs (Zuk et al., 2002; Wang et al., 2014). MSCs from different sources have been shown to demonstrate variations on proliferation rates, and suggested that human umbilical cord mesenchymal stem cells (HUC-MSCs) have highest proliferation potential (Choudhery et al., 2013; Wang et al., 2014). However, these are more difficult to obtain, compared to adipose derived cells. The success of isolation has also been reported to be variable (Erices et al., 2000; Goodwin et al., 2001; Mareschi et al., 2001; Wexler et al., 2003; Bieback et al., 2004; Kögler et al., 2004; Lee et al., 2004).

MSCs hold typical characteristics, such as fibroblast like morphology, formation of fibroblastoid colony-forming units, differentiation ability, and expression of certain classical markers. MCSs have been found to be positive for markers CD44, CD105, CD73, and CD90, and negative for CD3, CD14, CD19, CD34, and CD45 (Choudhery et al., 2013; Wang et al., 2014). However, studies have found some controversy, with different marker expression seen (Kern et al., 2006). MSCs are defined by the International Society for Cellular Therapy as holding specific characteristics. The criteria include: exhibiting plastic adherence, specific set of cell surface markers (as listed above), and have the ability to differentiate *in vitro* into adipocytes, chondrocytes and osteoblasts (Dominici et al., 2006; Bourin et al., 2013).

The ability to differentiate is dependent on MSC type (Cohen and Chen, 2008), involving signalling pathways and transcription factors promoting lineage selection. Some of these well regulated pathways include Wnt (Clevers et al., 2014; Park et al., 2015), Hedgehog (Spinella-Jaegle et al., 2001; Deng et al., 2008; Fontaine et al., 2008), Notch (Deng et al., 2008; Lin and Hankenson, 2011; Shimizu et al., 2011; Song et al., 2015), chemical factors, and physical factors; ECM, integrins, cell shape, external mechanical forces, geometric structures such as contractile cytoskeleton (Engler et al., 2006; Chen et al., 2016).

1.3.1 Bone formation

The bone holds many roles in the human body. Functions of the bone include the maintaining of calcium levels in the blood, establishing and maintaining the mechanical support of soft tissue, and skeletal structure; growth and support, acting as levers in muscle action, supporting the process of haematopoiesis, acting as a hold surrounding the brain and spinal cord. Bone tissue is unlike other tissue, in respect to its ability to regenerate rather than heal (Marzona and Pavolini, 2009). Bone is a very dynamic form of tissue that undergoes a constant state of remodelling under normal conditions, in response to changes that include hormone levels, growth factors, and mechanical load. The efficiency of bone structure is dependent on the biochemical properties of different bone components (Ducy et al., 2000). There are three main types of bone cells: osteoblasts, osteocytes and osteoclasts, which work collectively coordinating bone maintenance (Curtis et al., 2016). There is a finely regulated balance in bone structure formation that involves the deposition of bone extracellular matrix (ECM), hydroxylapatite [$Ca_5(PO_4)_3(OH)$] crystals on the collagen fibres, by differentiated osteoblasts and resorption by osteoclast Boonrungsiman et al., 2012; Luukkonen et al, 2019). Osteocytes occupy single lacunae and hold an extensive network of dendritic processes. They act as a mechanosensory system around Haversian canals allowing communication between neighbouring osteocytes directly via Cx43 at gap junctions, or through endocrine, paracrine (receptor activator of nuclear factor-kappa B ligand (RANKL)) and autocrine signalling factors, crucial for bone modelling and remodelling (Yellowley et al., 2000; Curtis et al., 2016). Defects in osteoblasts be it qualitative or quantitative, acquired or inherited, would lead to disruption of bone maintenance causing many pathophysiological presentations, such as short stature, bone fragility, osteoporosis, and metabolic bone disease (Ducy et al., 1999).

Macrophages hold a known role in repair and inflammation. Interestingly, they are also found within the developing marrow cavity in normal bone. Macrophages, like osteoclasts are of monocytic lineage. The function of macrophages in the bone is not fully understood, as they have not been found to co-localise with osteoclasts (Godwin et al., 2013). They may promote osteoblast differentiation leading to repair and maintenance of bone density (Vi et al., 2015).

Throughout life this maintenance is achieved through the process of continuous tissue renewal known as remodelling (Figure 1.3-b), which occurs asynchronously

throughout the skeleton at basic multicellular units. During childhood there is a positive balance, which reaches a peak of bone mass in early adulthood (Ducy et al., 1999; Hernandez et al., 2003). This is followed by a period of stability before a negative balance occurs in older age, leading to a greater activity of osteoclasts and bone loss (Zebaze et al., 2010). In adults the BMU (basic multicellular unit) takes around 3 weeks with 3 to 4 months for the formation response, resulting in about 5-10% of the skeleton is replaced each year, and the replacement of the whole adult human skeleton takes around 10 years (Frost and Straatsma, 1964; Parfitt, 1980; Harada and Rodan, 2003).

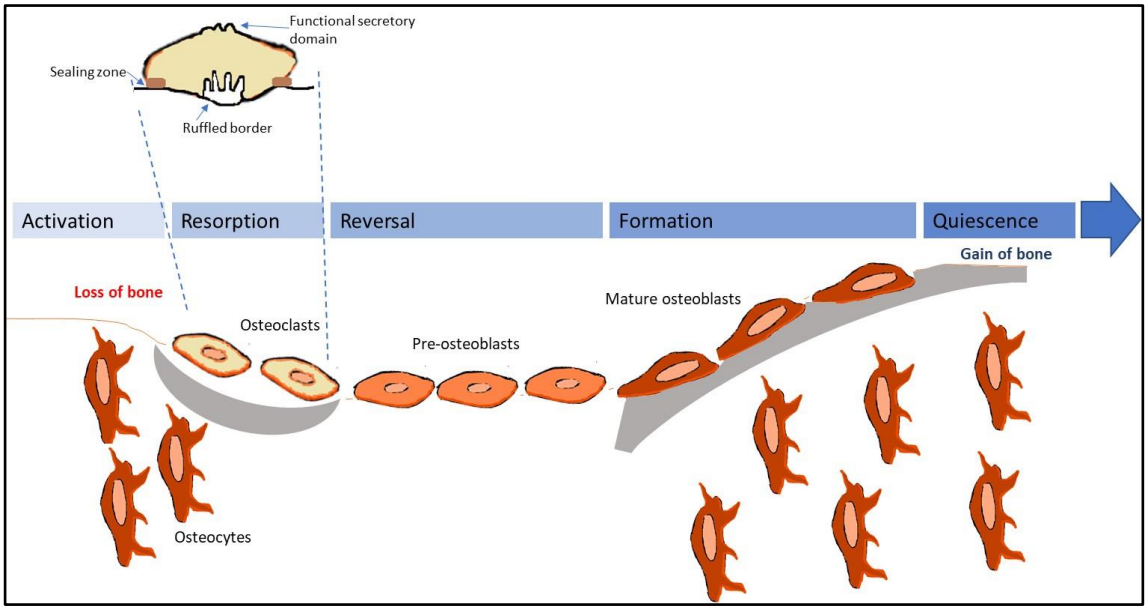

Figure 1.3-b The sequential stages of bone remodelling. Activation; signal via osteocytes or endocrine signals osteoclast precursors the remodelling site. Resorption; the bone matrix is resorbed by fully differentiated and mature osteoclasts which adhere to the mineralized bone matrix, and secrete protons and proteases, such as cathepsin-K, and matrix metalloprotease 9 (MMP9). The membrane-rich ruffled border dissolves the mineral phase of the bone and releases proteases to further degrade the organic phase. A 'sealing zone' is formed where they adhere tightly to the matrix confining to the lacuna, and allows efficient bone degradation. The reversal stage; the removal of most osteoclasts, Mesenchyme derived osteoblasts then rebuild this resorbed bone by producing mineralized matrix. Termination phase (Quiescence) ends the differentiation of osteoblasts and the bone surface is maintained until further remodelling is signalled (Duong et al., 1998; Coxon and Taylor; Bellido et al., 2014; Georgess et al., 2014). Adapted from (Everts et al., 2009; Siddiqui and Partridge, 2016)

Skeletal growth occurs from the beginning of development in foetal life to second decade during longitudinal growth. This requires the process of modelling which differs from remodelling that occurs throughout life. The cells hold the same roles, however, the bone is formed at the sites that have not undergone resorption (Figure 1.3-c). The changes generated in the size and shape of the bone follow the widening of long bones at the periosteal surface, and the development of medullary cavity due to resorption at the endosteal surface (Sims and Martin, 2014). The

development of bone is referred to as osteogenesis. The skeleton is formed from three distinct lineages: the somites generating the axial, the lateral plate mesoderm generating the limb, and the cranial neural crest forming the branchial arch and craniofacial bones and cartilage. Bone formation involves the transformation of existing mesenchyme tissue forming bone tissue, directly referred to as intramembranous ossification; and forming post differentiation into cartilage, which is replaced by bone; termed endochondral ossification. In humans in long bones, endochondral ossification forms outwards in both directions from the centre of the bone. The cartilage ends of the long bones are called epiphyseal growth plates. The bone continues to grow, if these areas produce chondrocytes, which are required to proliferate and push out the cartilaginous ends of the bone (Gilbert, 2000). Intramembranous ossification involves mesenchymal cells condensing and differentiating into osteoblasts directly, which deposit the osteoid matrix leading to calcification, and form an outer fibrous membrane surrounding the bone known as the periosteum. The inner surface of the periosteum is highly cellular, while the peripheral surface is rich in vascular and neural sympathetic network, mesenchymal progenitor cells differentiating into osteoblasts, fibroblasts and osteogenic progenitor cells that also form an osteoid matrix, which therefore leads to layers of bone formation (Squier et al., 1990; Gilbert, 2000; Dwek, 2010). The inner layer has also been referred to as the cambium and found to be essential for bone growth (Ito et al., 2001; Bilkay et al., 2008) that involves bone elongation and modelling (Dwek, 2010). The cambium becomes thinner with age, and in adults the periosteum is only a thin layer of tissue of which envelopes the bone structure (Allen et al., 2004). Following terminal differentiation of osteoblasts, osteocytes become trapped within the bone matrix and are the most abundant cell within the bone. The lifespan of these cells is long, reported at around 25 years (Polig and Jee, 1990; Mulhern and Van Gerven, 1997; Franz-Odendaal et al., 2006). However, other factors influence this, such as bone age and cell location from the surface of remodelling (Parfitt et al., 2000; Qiu et al., 2002).

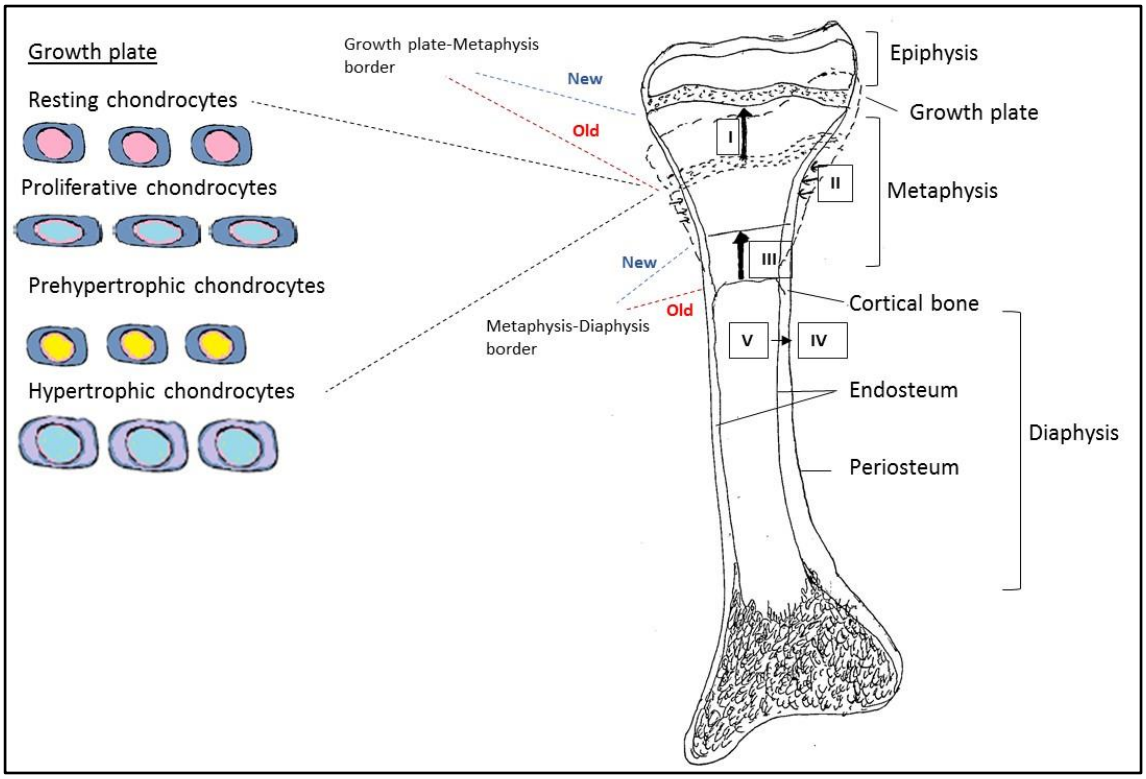

Figure 1.3-c Schematic diagram of the interior of a typical long bone showing the growing proximal end with a growth plate and a distal end with the epiphysis fused to the metaphysis (Jee, 1988; Zoetis et al., 2003). During growth (dashed lines) (I), the external shape of the metaphysis is maintained, (II). A constant length of the metaphysis is achieved by resorbing central trabeculae at the border between the metaphysis and the diaphysis (III). At the diaphysis level, the outer bone size expands through periosteal apposition (IV). The marrow cavity enlarges through endocortical resorption (V) (Rauch, 2012). The growth plate is divided into three well-defined zones, which disappears after puberty (Karimian et al., 2011). The resting zone contains embedded single cells or pairs of small, uniformly round in shape, and generally quiescent cells (Ballock and O'keefe, 2003; Melrose et al., 2008). Immediately beneath this zone lies the proliferative zone, the chondrocytes are flatten, and begin to divide forming parallel to the bone alignment, and synthesize collagen of types II and XI (Ballock and O'keefe, 2003). In the hypertrophic zone, the chondrocytes are larger in shape and more swollen, here they initiate terminal differentiation. The cells demonstrate reduced cell division, an increase in alkaline phosphatase activity and the synthesis of large amounts of various elements of the ECM, including type-X collagen. Elongation occurs until adulthood, when the epiphyses fuse by ossification (O'keefe et al., 1994; Scheuer and Black, 2000; Karimian et al., 2008; Karimian et al., 2011). Image adapted from (Jee, 1988; Karimian et al., 2011; Rauch, 2012; Alman, 2015).

The regulation of MSC differentiation into osteoblasts and adipocytes have been implicated in conditions which relate to defective bone remodelling (Horwitz et al., 1999; Kawai et al., 2012; Pino et al., 2012). An increase of bone marrow adiposity has been seen in conditions relating to bone loss, such as aging and pathological conditions (Justesen et al., 2001; Moerman et al., 2004; Dudley-Javoroski and Shields, 2008; Bredella et al., 2011; Cao, 2011; Motyl et al., 2011; Cohen et al., 2012; Mcgee-Lawrence et al., 2016). In support of our hypothesis, studies have suggested impaired differentiation in the osteogenic, or chondrocyte pathway may play a role in OS development (Taitz et al., 2004; Walkley et al., 2008; Wagner et al., 2011; Mutsaers et al., 2013; Sun et al., 2014).

1.4 Primary bone malignancies

1.4.1 Ewing sarcoma

Ewing sarcoma is an example of a pediatric solid tumour of the bone, derived from mesenchymal cells (Riggi et al., 2005; Chen et al., 2015). Specific initiation by chromosomal translocations have been reported in Ewing sarcomas, including the t(11;22)(q24:q12) that generates the EWS-FLI1 fusion protein (Tirode et al., 2014) the most frequent oncogenic driver (Chen et al., 2015). Ewing sarcoma presents with a peak incidence in adolescence, but unlike OS, a second peak is not seen in the elderly (Damron et al., 2007). The development of Ewing is thought to be prenatal, whereas OS appears to show a link between bone growth during puberty in its aetiology (Parkin et al., 1988; Stiller, 2007). Both commonly demonstrate fibro-osseous lesions (Lee et al., 2012).

1.4.2 Osteosarcoma

Osteosarcoma (OS) is the most common primary bone cancer. The incidence of OS appears to show a bimodal distribution, the first peak is associated with rapid growth of the skeletal system, occurring during adolescence (Mirabello et al., 2009; Yamaguchi et al., 2015). This is highlighted also as females present earlier than males, which is linked to the earlier development age seen in females (Mirabello et al., 2009). The second peak occurs in the elderly (Yamaguchi et al., 2015).

OS mostly occurs in the metaphyseal areas (91%) of long bones of the extremities, including lower end of femur, upper end of the tibia, upper end of humerus, and the upper end of the femur (descending order). Only around 9% are seen in the diaphysis. A common site is the knee joint. The involvement with other sites of non-long bone are less common, but the occurrence appears associated with an increase with age (Kaya et al., 2000; Bielack et al., 2002; Cleton-Jansen et al., 2009; Fletcher, 2014; Kundu, 2014). The characteristic radiological feature of OS is the sun-burst appearance with periosteal lifting with a Codmans' triangle formation, identified by x-ray. There is usually further evidence of new bone formation in soft tissue with a permeative pattern of destruction of bone (Resnick, 1995; Dorfman and Czerniak, 1998; Fletcher, 2014; Kundu, 2014).

The classification of osteosarcoma is based on the predominant cell lineage, and the extracellular matrix produced by the malignant cells (Fletcher, 2014). The most common primary osteosarcoma is osteoblastic (osteoid matrix) accounting for about

50%, chrondroblastic (cartilaginous tissue) about 25%, and fibroblastic (fibrous tissue) about 25%. Other primary classifications include small cell, telangiectatic, low grade central, and surface osteosarcomas; parosteal, periosteal, and high-grade surface. There are further unusual types which demonstrate similar biological behaviour to conventional osteosarcoma such as osteoblastic osteosarcoma-sclerosing type, chondroblastoma-like osteosarcoma, and clear-cell osteosarcoma, to name a few (Huvos, 1993; Broadhead et al., 2011a; Hameed et al., 2011; Tesser-Gamba et al., 2012; World Health, 2013; Fletcher, 2014; Kundu, 2014). Cases of multicentric OS (OSMC) have been reported (Sim et al., 1992; Varughese et al., 1992; El-Khoury et al., 1997; Miozzo et al., 1998; Spurney et al., 1998; Pujol et al., 2000; Wang et al., 2001; Leonard and Méchali, 2013), which refers to the tumour occurring at multiple sites with the absence of pulmonary metastases. This is further classified as synchronous if more than one lesion is found, and metachronous if a new tumour is found at new site (Currall and Dixon, 2006). There appears to be an increased risk of OSMC in RTS patients reported in the literature (Hicks et al., 2007; Cabral et al., 2008; Stinco et al., 2008; Larizza et al., 2010). Asymptomatic osteosarcoma has been reported; however, most patients present with symptoms related to location of lesion (Yamaguchi et al., 2015). The most likely cell type of OS origin is the osteogenic cell lineage, as they are prevalent in the bone microenvironment. Interestingly, OS occurs more commonly at the sites of bone growth, suggesting proliferation of osteoblastic cells may acquire mutations required for transformation (Rosenberg, 2010). Studies have suggested MSC under osteoblast commitment were the cells of origin, however, although only present at low incidence, early mesenchymal progenitors targeted with specific mutations could also generate OS. This suggested the micro-environment signals may be a contributing factor. The level of tumour differentiation did not relate to the level of cell of origin differentiation. Supporting epigenetic differentiation mechanisms could be involved, particularly in mature osteoblasts during tumour initiation (Calo et al., 2010; Rodriguez et al., 2013; Chan et al., 2014; Quist et al., 2015). Undifferentiated MSCs may lead to OS following oncogenic events (Mohseny et al., 2009; Lemos et al., 2015).

Current treatment for OS involves a combination of adjuvant and neoadjuvant chemotherapy, and surgery (Hong at al, 2013; Harrison et al 2018). Survival rate of osteosarcoma has remained fairly unchanged over the past 20 years (Bishop et al., 2016). Around 70% of patients with osteosarcoma and no metastasis at diagnosis

will have a 5-year survival rate, which falls to <30% in patients with metastasis, or <20% reoccurrence following remission, following current treatments. Around 80% of patients will develop or present with radio-graphically undetectable micro-metastases (Marina et al., 2004; Chou et al., 2005; Daw et al., 2006; Tang et al., 2008; Li et al., 2014). The survival rates appear similar between RTS patients and non-RTS patients (Hicks et al., 2007). A study demonstrated some patients with RTS and osteosarcoma led to remission following appropriate multimodal therapy, although survival rates still low overall. Treatment was advised as the same as sporadic OS, with the exception of chemotherapy, as increased toxicity has been seen in RTS patients; this would need additional monitoring and altering on the patients response (Hicks et al., 2007; Zils et al., 2015). Better understanding could improve treatment developments (Gorlick, 2002; Kundu, 2014; Cui et al., 2016). Early metastasis is often seen, and often the main reason for the poor prognosis with OS (Ta et al., 2009; Tesser-Gamba et al., 2012; Botter et al., 2014).

1.4.2.1 Cell cycle dysregulation and OS

Dysregulation of cell cycle checkpoints has been demonstrated in many tumours (Hartwell and Kastan, 1994; Taylor and Mckeon, 1997; Bower et al., 2010).The deregulation of mitotic checkpoint control is thought to be an underlying cause of chromosomal instabilities (Savage and Mirabello, 2011; Martin et al., 2012). The tumour suppressor Phosphatase and tensin homolog (PTEN) supresses unscheduled mitotic checkpoint complex to maintain chromosomal stability (Choi et al., 2017), as a regulator of cyclin D and PI3K-Akt signalling (Weng et al., 2001). The loss of PTEN may aid tumour growth and expansion in the bone (Xi and Chen, 2017). Nuclear α-thalassemia/mental retardation X-linked (ATRX) has multiple roles, including histone modifications and transcription (Ratnakumar and Bernstein, 2013). In childhood cancers mutation in the epigenetic regulator *ATRX* is common, with around 29% of osteosarcomas (Chen et al., 2014a). The loss of ATRX can lead to an upregulation of transcription, aberrant epigenetic alterations, and DNA damage at telomeres (Wong et al., 2010; Heaphy et al., 2011a; Lovejoy et al., 2012). The phosphoinositide 3-kinase (PI3K/Akt) pathway is known to be an important cell survival pathway in OS (Cenni et al., 2004; Inoue et al., 2005; Díaz-Montero et al., 2006). Akt regulates several downstream targets, enabling OS cell growth and survival (Chirgwin and Guise, 2000).

1.4.2.2 OS and known gene involvements

To date, 14 main drivers have been described that may account for around 87% of cases of osteosarcoma; some novel in the context of osteosarcoma (*ATRX, FANCA, NUMA1* and *MDC1)*, some known including *RECQL4*, *TP53*, and *RUNX2* (Kovac et al., 2015). Altered expression of genes associated with cell adhesion, DNA repair, and cell cycle progression may also be involved in the development of OS (Yang and Wang, 2016), a few of which will be discussed in more detail below.

1.4.2.2.1 P53

P53 belongs to a family of transcription factors, encoded by *TP53* gene in humans. P53 holds an important role in the regulation in MSC differentiation, including osteogenic (Kim et al., 2014; Li et al., 2015), maintaining genomic stability (Lane and Crawford, 1979; Levine et al., 1991), regulation of cell cycle (El-Deiry et al., 1992), apoptosis (Shaw et al., 1992), senescence (Yonish-Rouach and Resnitzky, 1991), and metabolism (Berkers et al., 2013). Around 50% of human cancers were reported to hold P53 mutations (Olivier et al., 2010; Robles and Harris, 2010). P53 mutations appear to be a significant oncogenic driver in OS (Diller et al., 1990; Helman and Meltzer, 2003; Mirabello et al., 2015; Velletri et al., 2016). Next generation sequencing approaches have identified a specific translocation event in the first intron of the TP53 tumour suppressor gene in the majority of OS cases, leading to the inactivation of TP53 in almost all osteosarcomas (Chen et al., 2014a). A high level of genomic instability is seen in OS cells with P53 mutations (Overholtzer et al., 2003; Liu et al., 2009). The lack of P53 in MSCs may lead to disruption of differentiation into mature osteoblasts as a consequence of the upregulation of Runx2 and Osterix, establishing impaired bone remodelling, and an osteosclerotic phenotype, demonstrated in mice (Lin et al., 2009; Solomon et al., 2014; Zambetti, 2014). The bone tumour microenvironment could signal MSCs lacking or having mutant P53 to promote OS development (Cheng et al., 2014; Alfranca et al., 2015). RECQL4 has been found to interact with P53 (De et al., 2012; Xavier et al., 2014; Lu et al., 2015). Interestingly, an increase of P53 protein levels have been reported in RTS cells (Davis et al., 2013).

1.4.2.2.2 RECQL4 and tumour development

The mechanisms behind tumorigenesis and association with mutations in *RECQL4* remain unknown (Lin et al, 2017). The most common cause of death in patients presenting with *RECQL4* mutations is cancer (Croteau et al., 2014; Lu et al., 2017). Overexpression and amplification of *RECQL4* has been reported in colorectal cancer (Buffart et al., 2005), furthermore, a study by Lao *et al*, (2013) found RECQL4 and BLM expression are significantly increased in colorectal cancer cells (CRCs), when compared to matched normal colonic mucosa and in contrast to RECQL and RECQL5. The study indicates the possibility of increased expression of BLM and RECQL4 to support the ability of CRC cells to tolerate genotoxic stress (Lao et al., 2013). RECQL4 expression is also increased in metastatic prostate cancer cell lines (Su et al., 2010). The loss of RECQL4 expression has been shown to lead to the accumulation of double-strand breaks, while following knockdown tumourigenicity (*in vivo*) and invasiveness (*in vitro*) was shown to decrease in metastatic prostate cancer cells (Su et al., 2010), These data suggest that RECQL4 might be an important factor in the pathogenesis and tumorigenesis of CRC and prostate cancer (Su et al., 2010; Lao et al., 2013). Overexpression and amplification of RECQL4 has also been reported in breast cancer (Thomassen et al., 2009), late stage laryngeal squamous cell carcinomas (Saglam et al., 2007) as well as in sporadic osteoblastomas (Maire et al., 2009). Thomassen *et al*, (2009) even suggests RECQL4 to be a potential metastasis promoting gene in breast cancers. Yong *et al,* (2014), found frequent amplifications of RECQL4, however, did not find associations between these amplifications and late stage oral squamous cell carcinomas (OSCCs). Despite significant amplifications were shown, the expression of RECQL4 was not shown to be affected in the samples (Yong et al, 2014).

1.4.2.2.2.1RECQL4 and OS

RECQL4 expression is found abundantly in actively forming bone; in osteoblasts lining the trabecular surface, bone lining cells, and in chondrocytes of the growth plate. RECQL4, therefore, may have an important role in bone growth (Delagoutte and Von Hippel, 2003; Siitonen, 2008; Ng et al., 2015). A correlation has been shown between the presence of pathogenic variants of *RECQL4*, low bone mineral density, and a history of increased fracture risk in RTS patients (Cao et al., 2017), and risk of OS development (Mehollin-Ray et al., 2008). RECQL4 has been found to be a requirement for skeletal development through interaction with p53 (Lu et al.,

2015). In conditional mouse models, disruption of Recql4 function in skeletal cells leads to bone abnormalities, such as osteoporosis, however, it would appear not to always lead to OS development but may lead to OS susceptibility (Lu et al., 2015; Ng et al., 2015), and the type of mutation may be an influencing factor. In Recql4-deficient mice ($Recql4^{HD}$), Lu *et al,* (2014) found evidence of bone marrow and/or haematological defects indicating possible senescence of bone marrow cells. Interestingly, some RTS patients have shown to have progressive leukopenia, chronic microcytic hypochromic anaemia, myelodysplasia, aplastic anaemia and leukaemia (Larizza et al, 2010); disorders that are associated with the dysfunction of bone marrow (Kohzaki et al., 2012), suggesting that RECQL4 deficiency may lead to bone marrow dysfunction. RECQL4 expression may be up-regulated by RANKL during osteoclast differentiation (Mccardle, 2013). RANKL has been shown to facilitate the migration of cancer cells into the bones (Jones et al., 2006), while high levels of RANKL in osteosarcoma leads to poor response to preoperative chemotherapy (Lee et al., 2011b). The increase in the generation of osteoclasts resulting in the resorption of normal bone is also a part of OS pathogenesis and aggressiveness (Bathurst et al., 1986; Avnet et al., 2008; Broadhead et al., 2011b), which could be linked to high levels of RANKL observed (Mori et al., 2007). RANKL pathway has been found to be crucial for tumourigenic osteolysis, and allows tumour expansion (Chirgwin and Guise, 2000). An association has also been made with over-expression of RECQL4 in osteosarcoma tumours and an increase in genome instability (Maire et al., 2009; Thomassen et al., 2009). Interestingly, in sporadic osteosarcoma somatic mutations of RECQL4 have not been detected (Martin et al., 2014).

1.4.2.2.3 RUNX2 and cancer

The mammalian Runx family of transcription factors, which includes RUNX1, RUNX2, and RUNX3, have an important role in cell fate determination into specific lineages (Komori, 2010; Ito et al., 2015). The RUNX genes encode the α subunits of PEBP2/CBF (polyomavirus enhancer-binding protein 2/core binding factor) transcription factors required for skeletal development (Wang et al., 1993; Yoshida et al., 2002). The key role of RUNX2 is in the regulation of osteoblast differentiation, therefore maintaining bone, bone development, and maturation (Komori, 2007). RUNX2 is regulated by Vitamin D (Lim et al., 2010; Martin et al., 2010; Hoshino et al., 2015; Garimella et al., 2017). Patients with OS present aberrations in vitamin D regulatory system and sub optimal vitamin D levels (Lee at al., 2013; Kurucu et al

2019). Vitamin D targets the RUNX2 pathway, specifically inhibiting genes required for cell cycle, proliferation, survival, interactions, cytoskeletal dynamics, migration, and invasion, reported in an OS cell line (Garimella et al., 2017).

RUNX2 may increase the expression of prometastatic RUNX2 target genes, including integrins, focal adhesion kinase, *PTHrP*, *VEGF*, bone sialoprotein (*BSP*), osteopontin and survivin (Van Der Deen et al, 2012; Rustamov et al, 2019). RUNX2 has been shown to be overexpressed in metastatic breast cancer cells, leading to the promotion of transcription of genes such as MMP and VEGF, which are involved in migration and invasiveness (Javed et al., 2005). RUNX2 has been shown to act in rapidly proliferating tumour cells in the bone microenvironment through the promotion of PTH or PTHrP mediated antiapoptototic effects. RUNX2 expression here appears to be pro-survival for the tumour cells, promoting tumour growth. To aid this RUNX2 also induces survivin expression (Bellido et al., 2003). In OS, many growth factors have been reported to activate RUNX2, promoting RUNX2 phosphorylation directly, or indirectly. Survivin is an important biomarker in OS, and recently Runx2 has been shown to activate survivin and Bcl2 which inhibits apoptosis, aiding in tumour cell survival (Lim et al., 2010). The overexpression of RUNX2 can generate osteopenia and fractures as receptor activator of NF-κB ligand (RANKL) expression is increased, leading to stimulation of osteoclast activity (Liu et al., 2001; Gupta et al., 2012) In OS cell lines, RUNX2 may also regulate the focal adhesion pathway by mediating genes, such as TLN1 and FAK (Van Der Deen et al., 2012).

Interestingly, RUNX2 has also been implicated in osteomimicry which promotes breast and prostate cancer metastasis to the bone (Akech et al., 2010; Brubaker et al., 2003; Leong et al., 2010). Osteomimicry is the ability of cancer cells to behave like bone cells, assuming osteoblast like phenotype. This has been demonstrated by breast and prostate cancer cells expressing bone matrix proteins, alkaline phosphatase, and molecules involved in the cross talk between osteoclasts and osteoblasts (Gonzalez-Suarez et al., 2010; Rucci and Teti, 2010).

1.4.2.3 OS and bone dysregulation

OS commonly occurs in the metaphysis region, and the most common primary site of OS is the distal femur (Girish et al., 2012; Haynes et al., 2017; Kumar and Singh, 2017). During bone growth, the metaphyseal cortex of the distal radius appears thin and porous. The observed cortical porosity may be an influential factor to the

increased rates of distal fractures seen in puberty (Parfitt, 1994). Cortical porosity refers to the average fraction of the void volumes within the volume of the cortical bone (Kalkwarf et al., 2011; Zebaze et al., 2013). An early study suggests the incomplete trabecular coalescence as the main process leading to fragility, rather than bone remodelling (Rauch et al., 2007), as rapid modelling drift of the metaphyseal cortex occurs (Rauch, 2012). This could suggest, however, the lack of osteoblast involvement to recover the situation (Rauch, 2012). Another study has suggested mechanical loading cycles leading to the coalescence of metaphyseal trabeculae, which may link to the metaphyseal cortical thickness and porosity (Tanck et al., 2006; Rauch, 2012). Further factors which may be involved include the short life cycle of metaphyseal trabeculae. Pathological fractures can present at diagnosis or form during treatment in patients with OS, with an incidence of around 5-12% (Chandrasekar et al., 2012).

1.5 The DNA damage response and genome instability

A fundamental pre-requisite for life involves completeness and integrity of genomic information (Utani et al., 2010). DNA damage is a generic term which is used to describe DNA modifications with the ability to generate cell death response, in particular apoptosis. If DNA damage is not repaired or does not lead to apoptosis, loss of genomic stability can follow the genomic alterations (Roos and Kaina, 2013).

1.5.1 DNA damage

DNA damage can originate from exogenous and endogenous (internal) sources. Endogenous sources can be related to physiological processes, such as during replication following DNA mismatches, and DNA strand breaks can follow abortive topoisomerase I and II activity. DNA lesions can also occur due to damage arising from hydrolytic reactions, and methylation (Valko et al., 2006). Double-stranded DNA breaks (DSBs) can also arise following V(D)J recombination and immunoglobulin gene class switch recombination (CSR) during development of the adaptive immune system leading to induced chromosome breakage (Dudley et al., 2005; Daniel and Nussenzweig, 2013). Inflammation and infection recruits macrophages and neutrophils to the site, and reactive oxygen and nitrogen compounds are produced (Kawanishi et al., 2006). This can lead to DNA single-strand breaks (SSBs), DSBs or base damage (Khanna and Jackson, 2001). Further examples include oxidative DNA damage (Li et al., 2002), lipid peroxidation (Esterbauer et al., 1990), propano adducts (Hecht et al., 2001), etheno adducts

(Chung et al., 1996), endogenous alkylating agents (Holliday and Ho, 1998), and endogenous oestrogens (Yager and Leihr, 1996), to name a few.

A major environmental risk of exogenous sources comes from ultra-violet light. A common cancer-causing reagent prevalent today includes tobacco (Doll and Peto, 1981; Pfeifer et al., 2002; Wogan et al.; Gao et al., 2014; Wei et al., 2014). Exogenous and endogenous sources can be influenced by an interaction between them, leading to DNA damage and diseases, such as cancer (Jackson and Loeb, 2001).

1.5.2 Hallmark features of genomic instability

Genomic instability refers to a range of alterations of DNA from single nucleotide to whole chromosomal changes. Based on the level of genetic disruption genomic instabilities are typically divided into three categories.

Nucleotide instability (NIM) is characterised by high occurrence of nucleotide deletions, base substitutions, and insertions. NIM occurs due to replication errors and impairment of nucleotide excision repair and base excision repair pathways. This form may be less common, however can lead to dramatic phenotypes. An example is germline mutations in XPC that lead to *Xeroderma pigmentosum*, an autosomal recessive disease. It is characterised by impaired nucleotide excision repair and sensitivity to UV light and often skin cancer (Al-Tassan et al., 2002; Dworaczek and Xiao, 2007).

A microsatellite is a tract of repetitive DNA which leads to the repeats of specific DNA motifs ranging between 2 to 5 base pairs, at typically 5 to 50 times (Turnpenny and Ellard, 2016). They can occur at various locations within the genome, and demonstrate a high mutation rate and diversity, establishing microsatellite instability (MIN). MIN usually originates from defects in mismatch repair genes (Weissenbach et al., 1992; Ionov et al., 1993; Geiersbach and Samowitz, 2011).

Chromosomal instabilities (CIN) involve the increased rate of loss or gain of entire or part of chromosomes and can be categorised as numerical (N-CIN), and structural (S-CIN), although with some overlapping features (Cisyk et al., 2014). N-CIN can occur as a result of defects in chromosomal segregation, and S-CIN can follow aberrant genomic rearrangements and chromosomal breakages, which can include duplications, translocations, and deletions (Rajagopalan et al., 2003), and usually but not always alterations to gene copy numbers. S-CIN can form as a result

of ineffective DNA damage response mechanism often in response to exogenous insults that cause errors in replication (Bayani et al., 2003).

In cancer cells some of the mechanisms involved in maintaining genomic stability can be disrupted, which leads to genomic instability and can contribute to the malignant transformation of these cells through, for example, the amplification of oncogenes or drug-resistance genes (Utani et al., 2010). CIN frequently leads to karyotypic complexity in tumours which is associated with high expression levels of survival and tissue invasion genes, and decreased expression of cell cycle and DNA repair regulators (Roschke et al., 2008). It is thought that around 90% of human cancers exhibit chromosomal abnormalities and aneuploidy (Lengauer et al., 1997; Gagos and Irminger-Finger, 2005). CIN is related to poor prognosis and drug resistance (Gagos and Irminger-Finger, 2005; Carter et al., 2006; Walther et al., 2008; Lee et al., 2011a). The underlying mechanism of CIN in sporadic cancers is not yet fully understood, partly due to the wide range of genes that can give rise to CIN following disruption of normal processes, demonstrating the heterogeneous nature found in sporadic cancers.

Importantly for the work presented in this thesis, a study found an association of CIN, and in particular errors in chromosomal segregation leading to centrosome aberrations, to be a feature of OS development (Al-Romaih et al., 2003; Ottaviani and Jaffe, 2009). Osteosarcoma has a high level of genetic and cytogenetic heterogeneity, not just between patients but also within the same patient (Selvarajah et al., 2008). *RECQL4* mutations can lead to replicative stress and genomic instability (Burrell et al., 2013; Flach et al., 2014; Zeman and Cimprich, 2014). Interestingly, a relationship of RECQL4 overexpression and S-CIN development in osteosarcomas has been reported (Bayani et al., 2007; Maire et al., 2009). MIN has been demonstrated in several cancers (Wang et al., 2005; Sheng et al., 2006; Weisenberger et al., 2006; Geigl et al., 2008), and reported in a few OS tumours as well (Heinsohn et al., 2007; Ahmed et al., 2012).

1.5.3 Single stranded DNA

Single-stranded DNA is an ubiquitous and a very important intermediate structure formed throughout the cells' life cycle. It is therefore crucial that single-stranded DNA is protected from DNA damage. Replication protein A (RPA) is the main ssDNA binding protein in eukaryotes, and has many roles required for ssDNA formation, including DNA replication, recombination, DNA damage checkpoints, and

DNA repair mechanisms (Zou et al., 2006). During DNA damage response RPA is required for the formation of γH2AX foci (Anantha et al., 2007) and RAD51 foci (Anantha et al., 2008).

1.5.4 Double stranded DNA break

DNA double strand breaks (DSB) are the most dangerous type of DNA lesions, as they can lead to the loss of large chromosomal regions (Chang et al., 2017). DSBs can also occur following two single-strand breaks in close proximity, or following DNA damage response during DNA replication (Khanna and Jackson, 2001), but many other mechanisms are also involved, both physiological and pathological (Lieber, 2016). If not repaired these lesions can block transcription and genome replication, and can lead to serious consequences such as mutations and genome aberration resulting in reduced cell viability (Valko et al., 2006).

1.5.5 DNA repair pathways

In eukaryotes, the DNA damaged response (DDR) aids in maintaining genomic stability following DNA damage. The site of the lesion on the DNA can alter subsequent response mechanism. The DNA damage response pathway is a complex, well-organised pathway comprising biochemical signalling and effector pathways that functions to repair and restore the original configuration of DNA, following damage (Kavanagh et al., 2013), involving many proteins with variable roles, including detectors, mediators and effectors (Sancar et al., 2004).

Defects in DNA repair have been shown to strongly link to predisposition to cancer, neurodegeneration, immune deficiency and aging (Coon and Benarroch, 2018; Gorgoulis et al, 2018). RECQL4 has been shown to participate in a range of DNA repair pathways (Petkovic et al., 2005; Fan and Luo, 2008; Schurman et al., 2009; Shamanna et al., 2014), and mutations may cause impairment of these pathways following DNA damage.

1.5.5.1 DNA damage response pathways

The DNA damage response pathways include the PI 3-kinase-related kinase (PIKK) family of proteins *Ataxia telangiectasia* mutated (ATM) and *Ataxia telangiectasia* and RAD 3-related (ATR). These act as detectors and initiate the DNA damage response. DSBs activate ATM, and ssDNA, which may arise during replication fork

stalling or collapse following endogenous and exogenous induced lesions in S phase, bound by RPA and ATRIP activates ATR (Friedel et al., 2009).

Mediator proteins include breast cancer 1, early onset (BRCA1), Mediator of DNA damage checkpoint 1 (MDC1) and p53 binding-protein 1 (53BP1), following phosphorylation by ATM or ATR. These processes are aimed to stop cell cycle progression, and to activate proteins required for DNA repair, (Podhorecka et al., 2010). This can further a response to effector proteins such as RAD51, checkpoint kinase-1 (CHK1), checkpoint kinase-2 (CHK2) and p53 (Kobayashi, 2004). There have been two characterised pathways of the DNA damage response involving CHK1. The ATM/ATR-CHK1/CHK2-Cdc5s pathway is reversible and demonstrates a fast response to DNA damage. CHK1, a key distal signal transducer, is activated by 'proximal transducers' ATR, and to some extent ATM, and other PI3 kinase like proteins, activating DNA damage "sensor" proteins linked with "mediator" proteins (Dai and Grant, 2010). The second pathway is the p53-dependent pathway, which is a much slower response and is irreversible. It involves Chk1/Chk2 with ATM/ATR phosphorylating p53 or MDM2, which subsequently promotes the stabilization of p53 (Zhou and Bartek, 2004; Dai and Grant, 2010).

1.5.5.2 Homologous recombination

Relatively benign DNA lesions found during G1 or G2 phase in a repair-competent cell can generate DSB during DNA replication (Nagaraju and Scully, 2007; Petermann and Helleday, 2010). If a break occurs during the S phase of the cell cycle, DSBs are formed at blocked replication forks, which are usually repaired by homologous recombination between sister chromatids that is an error-free but complex repair pathway (Figure 1.5-a). Following damage recognition, the intact homologous strand of DNA is detected, and is transported near the lesion. The broken ends undergo 5'→3' end resection, and the liberated 3' single-stranded tail invades the intact neighbouring sister chromatid. Using the complementary strand of the intact sister chromatid the broken end is extended by DNA polymerase, copying the missing information from the template into the broken chromatid. The DNA strand is separated following ligation and the DNA is restored via the dissolution pathway resulting in non-crossover outcome, or holiday junction resolution resulting in non-crossover or cross over outcome in equal probability (Pâques and Haber, 1999; San Filippo et al., 2008; Krejci et al., 2012). Other pathways include synthesis-dependent strand annealing (SDSA) favoured during

mitosis, and break induced replication (BIR) involving the formation of replication fork in a D-loop structure (Krejci et al., 2012).

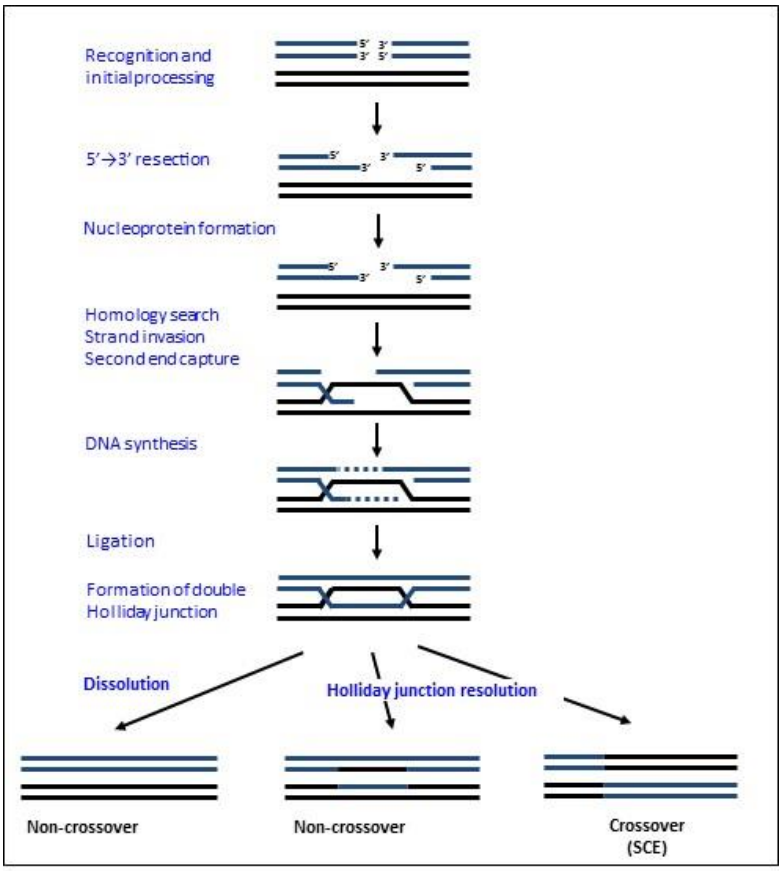

Figure 1.5-a A schematic of the execution step of homologous recombination repair (HR) of double-stranded DNA breaks (DSB). The DNA at the break site is resected, the degradation of one strand at both sides of the break at 5'→3' direction exposes the DNA as a single stranded DNA with 3' tail, and coated with RPA. It recruits RAD52 interacting with RAD51. The resected ssDNA nucleoprotein filament tail engages in active strand invasion. Strand exchange and DNA synthesis follows the dissociation of RAD51 exposing the 3'-OH, and newly synthesised DNA is ligated forming a double Holiday junction. Separation of the double Holiday junction can be via dissolution, or resolution that can follow different paths, producing either a crossover or a non-crossover end product (Cromie et al., 2001; West, 2003; Krejci et al., 2012).

ATM/ATR signalling is important for the phosphorylation of proteins involved in homologous recombination, including BRCA1, BRCA2, WRN, BLM, and FANCD2 (Roos and Kaina, 2013). Following DNA damage leading to DSB, ATM phosphorylates CHK2 (checkpoint kinase-2) at Thr68 (Matsuoka et al., 2000). ATM is a homodimeric serine/threonine protein kinase and normally is in an inactive state. Recruitment to the break by the MRE11/NBS1/RAD50 (MRN) complex results in its activation by auto-phosphorylation at Ser1981 (Bakkenist and Kastan, 2003). ATR phosphorylates CHK1 (checkpoint kinase-1) at Ser345 in response to stalled DNA replication forks (Guo et al., 2000), which occur following lesions due to replication blockage or interstrand crosslinks preventing DNA synthesis due to modifications on DNA template. Detection of stalled forks and transduction of the signal requires

the ATR-ATRIP complex, TopBP1 (DNA topoisomerase 2-binding protein 1) and the 9-1-1 complex (Ward and Chen, 2001). CHK1 and CHK2 phosphorylate the transcription factor p53 at Ser20 (Shieh et al., 2000), which is a key decision-making step between DNA repair and apoptosis (Oda et al., 2000; Roos et al., 2007).

1.5.5.3 Non-homologous end-joining

In a cell that is not replicating, an alternative route is taken outside of late S and G2 phases, when homologous recombination is the dominant pathway to repair double-stranded breaks: non-homologous end joining repair (NHEJ) repairs DSBs, not restricted by cell cycle phase (Figure 1.5-b). HR is essentially error free, while NHEJ is mostly error-prone potentially leading to mutations (Lieber, 2010). The cause of DSB and cell cycle phase influences the repair process chosen. NHEJ does not require the homologous template for the repair of the DNA. NHEJ is capable of repairing a wide range of DNA-end configurations, which can however lead to the repaired DNA junctions containing mutations (Chang et al., 2017). An important step is the recognition and binding of the Ku heterodimer to the DSB (Mari et al., 2006; Uematsu et al., 2007), which acts as a scaffold and recruits other factors such as DNA-PKcs (Uematsu et al., 2007), X-ray cross complementing protein 4 (XRCC4) (Mcelhinny et al., 2000; Mari et al., 2006; Costantini et al., 2007), DNA Ligase IV (Costantini et al., 2007), XRCC4-like factor (XLF) (Yano et al., 2008), and Aprataxin-and-PNK-like factor (APLF) (Grundy et al., 2013). DNA-PKcs is a member of phosphatidylinositol-3 (PI-3) kinase-like kinase family (PIKK), similar to ATM and ATR (Abraham, 2004; Bakkenist and Kastan, 2004).

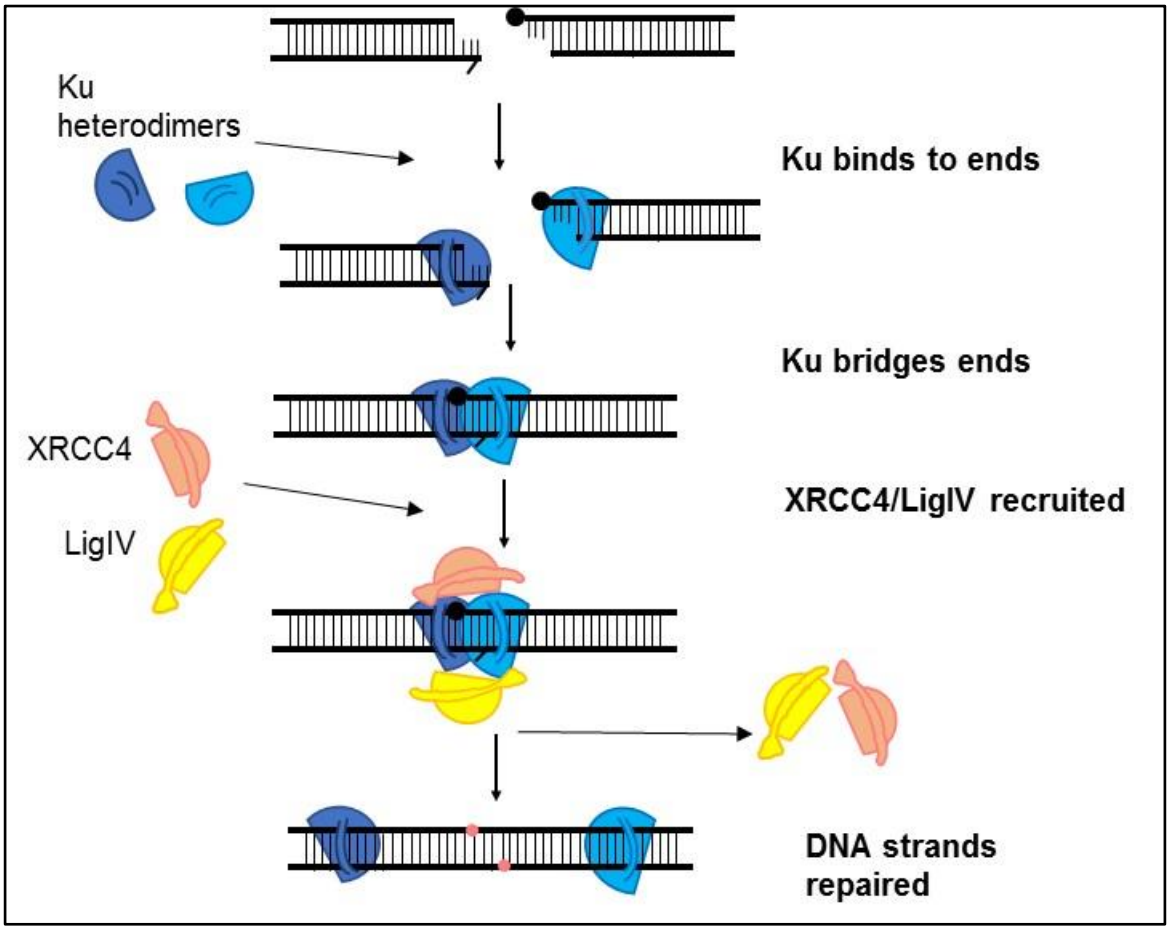

Figure 1.5-b DSB repair by NHEJ pathway. The DSB initiates the recognition of the DNA end, the NHEJ complex is assembled at the DSB. The DNA ends form a bridge by Ku heterodimers (Ku70/Ku80), leading to end stability, and processing. The gap generated is filled in by processing enzymes, and the ends are ligated by XRCC4/LigIV. The dissolution of the NHEJ complex follows as DNA strands are repaired (Davis and Chen, 2013). Adapted from (Pardo et al., 2009).

Chromatin structure appears to be an important context of the choice and completion of DSB repair pathway selection, which was first suggested following a study which investigated UV induced DNA damage and repair following nucleotide excision repair (Cleaver, 1977). Histone H2AX, a variant form of histone H2A, is phosphorylated on serine 139 of the C terminal tail following DNA damage, such as ironizing radiation (IR), forming gamma-H2AX (γH2AX). The γH2AX site seems to be a target of the nuclear DNA damage PI3 kinase-like signalling kinases, ATM, ATR, and DNA-PKcs, dependent on source and timing of DNA damage (Rogakou et al., 1998; Rogakou et al., 1999; Bonner et al., 2008; Kinner et al., 2008). The presence of γH2AX foci is a widely used marker for the detection of DNA damage and repair or to determine the effectiveness of radiation treatment and cancer therapies (Celeste et al., 2003b; Bonner et al., 2008; Mariotti et al., 2013). It has also been suggested that γH2AX may also be important in allowing repair proteins to access damaged DNA regions and remodelling chromatin process, and may have a role in processes of apoptotic cell death (Baritaud et al., 2012). Chromatin

complexity affects the selection and rate of DNA repair processes. Slowly repaired DNA may be in regions of heterochromatin, where prolonged chromatin relaxation takes much longer for intermediates to reach the break sites. ATM is crucial for this by activating KAP1, a KRAB- associated protein that forms foci and colocalizes with γH2AX. Repair in heterochromatic regions occurs primarily in G2 phase by HR, and DSBs in euchromatic regions is repaired by NHEJ (Ziv et al., 2006; Goodarzi et al., 2010; Jakob et al., 2011; Goodarzi and Jeggo, 2012).

1.5.5.4 Telomeres are disguised double-stranded breaks

Normal somatic cells hold a finite proliferative capacity termed the molecular clock (Harley et al., 1992; Wright and Shay, 1992; Cong et al., 2002), also referred to as the Hayflick limit (Hayflick and Moorhead, 1961; Hayflick, 1965). Warson and Olovnikov hypothesized that DNA would be progressively lost at the ends of chromosomes as the cell divides. Telomeres, initially reported in the late 1930s (Blackburn, 2001), act as essential regulators of both cell life span and chromosomal integrity (Hahn, 2003). Telomeres are repetitive DNA sequences (TTAGGG/ AATCCC) located at the ends of linear chromosomes. In normal cells, these shorten during each cell division cycle, *in vitro*, and with age *in vivo,* leading to replicative mortality via senescence, as the cell reaches the Hayflick limit known as stage 1 (M1) (Shay and Wright, 2004; Shay and Wright, 2019). If the cell is able to avoid this trigger by inactivating p53, it leads to further proliferation and telomere loss until stage 2 (M2) is reached. M2 has been shown to lead to cell death following the critically short and dysfunctional telomeres. Further cell survival can be achieved following the escape of this crisis by the activation of telomerase (Cong et al., 2002). Telomeres are also important structures in the protection of DNA ends from degradation, stem cell self-renewal, and DNA replication attrition (Burrow et al., 2017), as they play a role in the cell cycle, DNA replication, MMR processes involved in maintaining chromosomal stability, relating to cell pluripotency and self-renewal (Kapinas et al., 2013). Telomeres end in a 3' overhang, known as the G-strand overhang, which bends back on itself and anneals with the complementary sequences in the 5' end of the opposite strand, displacing part of the 5' end in a D-loop and creates a telomere or T-loop (Figure 1.5-c). T-loops facilitate the formation of a higher order structure mediating the end capping by masking telomeric DNA ends from recognition by the DNA repair system as a double-stranded break (Espejel et al., 2002). Regulating factors of telomerase-mediated telomere

elongation include the telomere-binding protein TRF1 (Telomeric Repeat Binding Factor-1), a negative regulator of telomere length, interacting with POT1 (Protection Of Telomeres-1; a single-stranded telomeric DNA-binding protein) (Sfeir et al., 2009). TRF2 assists in the formation of the T-loop, and maintains the secondary structure of the telomere to stabilize the T-loop and protects from unscheduled nucleolytic processing. TRF2 also interacts with the human Repressor Activator Protein-1/Telomeric Repeat Binding Factor 2 Interacting Protein (RAP-1/TERF2IP), and the MRN complex, which is implicated in response to DNA damaging agents (Wang et al., 2004; Doksani et al., 2013). The Ku complex has a role in the repair of DSB and localizes to the telomere (Chai et al., 2002; Tsai et al., 2002; Hahn, 2003). Further proteins involved in the T-loop stabilization and maintaining telomere includes TRF1-interacting Ankyrin-related ADP-ribose polymerase (TANK) (Sbodio and Chi, 2002), TRF1-Interacting Nuclear Factor-2 (TIN2) (Ye et al., 2004), and heterogeneous nuclear ribonucleoproteins such as Heterogeneous Nuclear Ribonucleoprotein-A1 (HNRPA1) (Ishikawa et al., 1993), and Heterogeneous Nuclear Ribonucleoprotein-A2/B1 (HNRPA2B1) (Kamma et al., 2001; Chai et al., 2002; He and Smith, 2009). Exogenous activation of telomerase is an *in vitro* method for immortalization of cell lines, and it can lead to unlimited proliferation capacity (Cong et al., 2002).

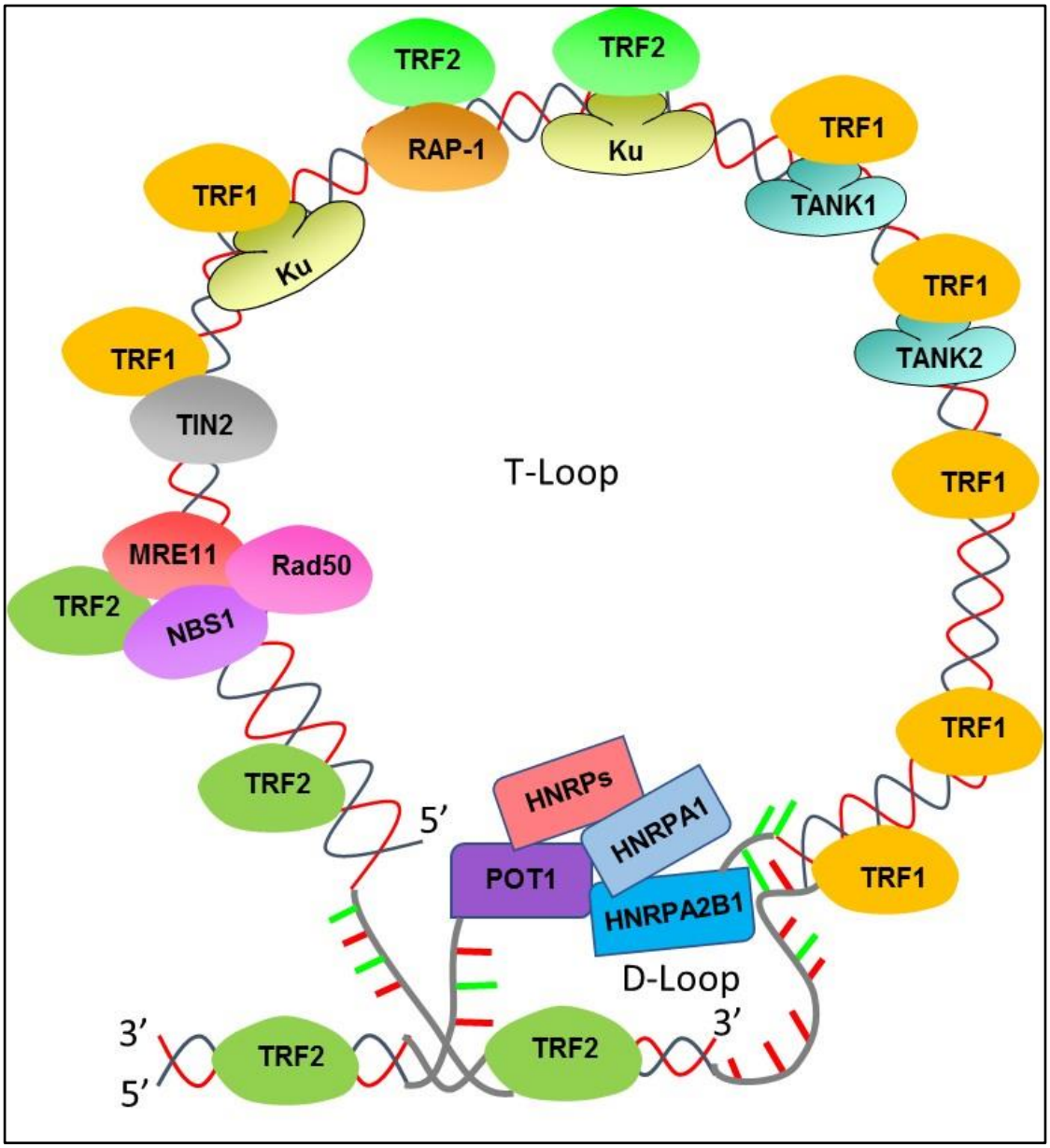

Figure 1.5-c Formation of T-loop. The T-loop is formed as both strands of chromosome join by an early point in a double-stranded DNA by 3' strand end invading the strand pair and forming a D-loop (Greider, 1999; Griffith et al., 1999). The T-loop is stabilised with additional proteins; TANK:TRF1-interacting, Ankyrin-related ADP-ribose polymerase, TIN2;TRF1-Interacting Nuclear Factor-2, HNRPA1; Heterogeneous Nuclear Ribonucleoprotein-A1, and HNRPA2B1; Heterogeneous Nuclear Ribonucleoprotein-A2/B1. This image is a modification of QIAGEN's original (Qiagen, 2018).

In cancer cells, a common feature involves the activation of telomere maintenance mechanisms, enabling the cells to avoid telomere shortening checkpoint, allowing the cell to continue to divide, and overcome replicative senescence. Telomere maintenance in tumours involves two mechanisms in humans, either telomerase activation (TA), or alternative lengthening of telomeres (ALT) (Granger et al., 2002; Maser and Depinho, 2002; Artandi and Depinho, 2009; Cesare and Reddel, 2010; Shay and Wright, 2011). It is thought around 85% of carcinomas maintain telomeres using TA, with the synthesis of new telomeric DNA via telomerase; a holoenzyme, comprising functional telomerase RNA (hTR), and telomerase reverse transcriptase

catalytic subunit (hTERT) (Feng et al., 1995; Nakamura et al., 1997; Granger et al., 2002; Shay and Wright, 2006). In around 5-15% of human cancers, in the absence of TA, the cancer cell can utilise ALT via homologous recombination (Henson et al., 2002). This process involves the elongation of telomeres via recombination (Bechter et al., 2003). In early studies, OS cells interestingly have been reported to demonstrate both TA and ALT with even expressions, unlike other cancer cells (Bryan et al., 1997; Scheel et al., 2001). However, ALT appears to be more prevalent in OS (Scheel et al., 2001; Heaphy et al., 2011b).

Telomeres have been found to hold additional functions to suppress the DNA damage response via telosome. This prevents potentially lethal telomere fusion, translocation, and genomic instability which can form following DSB repair at telomeres (Burgess, 2013). Interestingly, many proteins involved in DNA repair also have a functional role in telomeres (Marcomini and Gasser, 2015). The interaction of nucleoprotein complexes on telomeric DNA aids the maintenance of telomere integrity. Following disruption of shelterin components, which can lead to exposure of the DNA structures at the ends of disrupted telomere, a DNA damage response may follow. The shelterin complex consists of six major proteins, TRF2, TRF1, POT1, TPP1, Rap1, and TIN2 (Palm and de Lange, 2008). The shelterin complex protects chromosomal ends from erosions. POT1–TPP1 complex has been found to compete with the CST (CTC1, STN1, and TEN1) complex which terminates telomerase activity (Chen et al., 2012). In particular, TRF2, is thought to perform an important role in the protection of telomeres from erosion by binding to telomeric repeats to form the T-loop (Palm and De Lange, 2008) (Figure 1.5-c). The Loss of TRF2 protein and the consequent disruption of the shelterin complex, both expression and activity has been shown to induce telomere shortening, DNA damage response, chromosomal instability, and replicative senescence (Oh et al., 2003; Denchi and De Lange, 2007; Okamoto et al., 2013). Telomere shortening leads to reduced TRF2 (Saha et al., 2013). On the other hand, artificially increased TRF2 have been found to develop a delay in the onset of senescence (Karlseder et al., 1999). It has been suggested TRF1 and TRF2 activity via telomere length may play a role in initial transformation phases, and tumourigenesis (Matsutani et al., 2001; Nakanishi et al., 2003; Nijjar et al., 2005; Oh et al., 2005; Muñoz et al., 2006).

1.5.5.5 Base excision repair

A common form of endogenous DNA damage includes base modifications (Lindahl, 1993), that can lead to alterations of base pairing, and if not repaired, can lead to mutagenesis (Gelfand et al., 1998). A primary repair mechanism of oxidative lesions is base excision repair (BER) (Croteau et al., 2012b), and often follows ROS induced damage. There are two main pathways (Figure 1.5-d) short patch and long patch BER (Kim and M Wilson Iii, 2012). The pathway mainly repairs non-bulky small nucleotide lesions, the excision and replacement of incorrect bases such as uracil, or damaged bases such as 3-methyladenine or 8-oxoG generated by alkylation or oxidation, respectively (Kim and M Wilson Iii, 2012). The initiation occurs following at least one of distinct glycosylases (NTHL1, NEIL1, NEIL2, NEIL3 MPG, TDG, UNG, MUTYH, OGG1, MPG, MPD4 and SMUG1), depending on the type of the lesion, and further influences the choice of pathway (Fortini et al., 1999). Other influential factors include the cell type, and the availability of BER factors (Narciso et al., 2007; Bauer et al., 2011; Tichy et al., 2011). Short-patch BER requires specific repair proteins which are not necessary for replication, and therefore, the process shows efficiency in proliferating and non-proliferating cells. Following initiation by DNA glycosylase, further steps require AP-endonuclease APE1, DNA polymerase β (Pol β), and DNA ligase I or III (LIG1/3) (Krokan and Bjørås, 2013). poly(ADPribose) polymerase 1 (PARP1) and XRCC1 may also participate, but has been suggested these may not always be involved (Hanssen-Bauer et al., 2011). The long-patch repair pathway has been found to primarily take place in proliferating cells, and to a large extent utilises replicative proteins during the process by APE1, including, PCNA, FEN1, DNA polymerase δ/ε and LIG1. However, this is dependent on proliferative state of the cell. Pol β is found to be used in non-proliferating cells with primarily Pol δ/ε in proliferating cells (Akbari et al., 2009; Svilar et al., 2011). The core steps of BER (Figure 1.5-d) are excision of the base, incision, end processing, repair synthesis, and gap filling and ligation. A variation of proteins utilised downstream of the base excision is dependent on the short-patch repair with a single nucleotide gap is generated, filled and ligated, or long-patch repair with a gap of 2-10 nucleotides is generated and filled (Lindahl, 2001; Almeida and Sobol, 2007; Fortini and Dogliotti, 2007; Robertson et al., 2009; Svilar et al., 2011; Wallace et al., 2012).

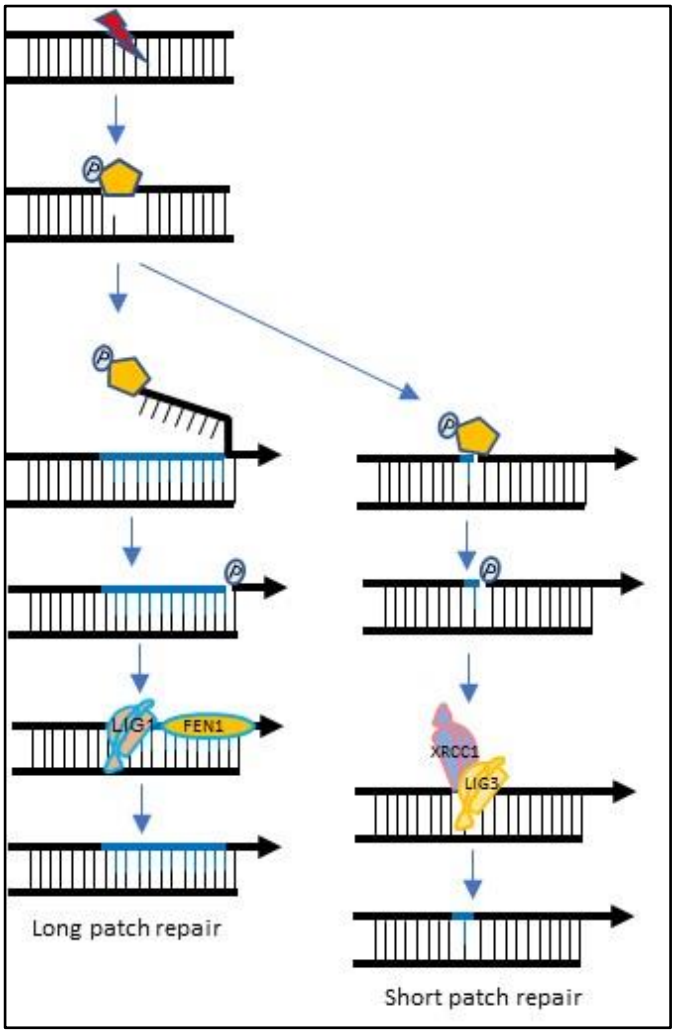

Figure 1.5-d The core steps of BER. The DNA glycosylase excises the damaged base producing an abasic or AP site. The DNA backbone is cleaved by AP enonuclease at 5', generating a 5' deoxyribose phosphate end and a free 3'OH end. During short-patch repair DNA polymerase β (Pol β) adds a nucleotide to the 3'-OH end and removes the 5'-deoxyribose phosphate group. Then DNA ligase (LIG3+ XRCC1) joins the ends to form an intact strand. Long-patch repair: DNA polymerase δ or ε (Pol δ or ε) acting with RFC and PCNA adds 2-8 nucleotides to the 3'-OH group, while displacing the 5'-deoxyribose phosphate group and further nucleotides to generate a flap. The flap endonuclease FEN1 removes the flap, then ligase (LIG1) joins the ends. Image adapted from (Schärer, 2003).

1.5.5.6 Nucleotide excision repair

A lesion on the transcribed template strand can lead to stalling of RNA polymerase inducing nucleotide excision repair (NER) (Hu et al, 2017). In mammals, Nucleotide excision repair (NER) (Figure 1.5-e) usually occurs following UV induced DNA damage (Lu et al., 2017). It is the main pathway for removing bulky DNA lesions caused by UV, and environmental mutagens, and some chemotherapeutic agents (Friedberg et al., 2005; Schärer, 2013).

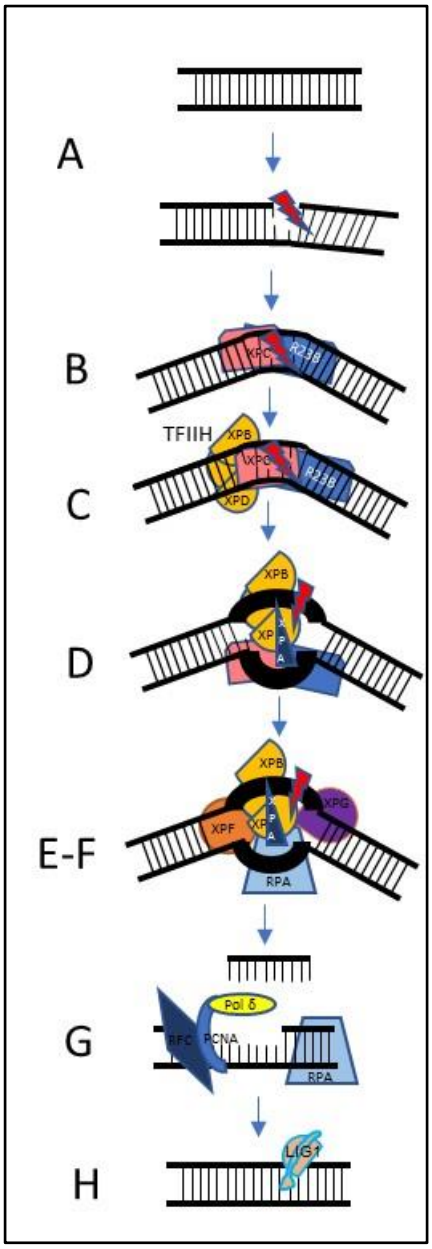

Figure 1.5-e Schematic of the core NER reaction. (A) Damaging agents induce bulky DNA lesions that destabilize duplex DNA, leading to DNA helix distortion. (B) In GG-NER, XPC-HR23B recognize the lesions and binds the undamaged strand opposite, stabilizing the DNA bend. (C) TFIIH is recruited and interacts with XPC-RAD23B. (D) TFIIH in an ATP dependent manner, unwinds the DNA helix. One subunit (here XPD) encounters the chemically modified base, while XPB (second helicase subunit) continues unwinding the DNA. (E) Stalling at the lesion allows the formation of "preincision" complex with the recruitment of XPA, RPA, and XPG. (F) ERCC1-XPF interacts with XPA and is recruited to the complex, creating a dual incision; 5' by ERCC1-XPF and followed by the incision at 3' by XPG. (G) RPA remains bound to ssDNA facilitating the transition to repair synthesis by Pol δ and Pol κ or Pol ε and associated factors; PCNA and RFC. (H) The sealing of the nick of DNA completes the repair synthesis, by DNA ligase IIIα/XRCC1 or DNA ligase I (LIG1, shown here) completes the process (Gillet and Schärer, 2006; Schärer, 2013). Image adapted from (Gillet and Schärer, 2006).

The NER pathway recognises UV induced DNA damage by dual incision with XPG and XPF-ERCC1 endonucleases, leading to a region of ssDNA about 22-35 nucleotides long. This region is then coated with RPA. Further, this can trigger the GG-NER-dependent ATR activation for repair (Marteijn et al., 2014). The initiation of NER can occur by two subpathways; global genome NER (GG-NER), and transcription-coupled NER (TC-NER) (Gillet and Schärer, 2006; Hanawalt and

Spivak, 2008). TC-NER is more specific and acts on lesions in the transcribed strand of active genes, whereas GG-NER can act at any location of the genome. The GG-NER specific factor XPC-RAD23B, and sometimes the UV-damaged DNA-binding protein initiate the GG-NER pathway. RNA polymerase stalled at lesions initiate the TC-NER pathway, with the aid of TC-NER specific factors, such a CSA and XAB2. The core NER factors are crucial for each pathway for the completion of the excision process (Tubbs et al., 2009; Latypov et al., 2012; Schärer, 2013). During the synthesis step of NER damage signalling can be triggered under certain circumstances. These occasions can include too high damage load, the inhibition of repair synthesis following nucleotide depletion or inhibition of polymerases (Hanasoge and Ljungman, 2007; Matsumoto et al., 2007; Marteijn et al., 2009; Overmeer et al., 2011), and if the incision at 3' does not occur. The signalling follows the replacement of EXO1 with XPG (Schärer, 2013). The NER intermediate forms a ssDNA which is coated with RPA which binds ATRIP/ATR, activating the ATR kinase (Zou and Elledge, 2003; Novarina et al., 2011). A signal cascade with MDC1, RNF8, 53BP1, and BRCA1 forms chromatin marks including the phosphorylation of γH2AX (Marteijn et al., 2009; Schärer, 2013). The NER pathway demonstrates heterogeneity, which occurs due to the molecular mechanisms involved, and the crosstalk between other processes. The NER pathway is able to repair a wide range of structurally unrelated DNA lesions, such as cyclobutene-pyrimidine dimers, and lesions generated by UV, chemical adducts, intrastrand crosslinks and ROS (Marteijn et al., 2014).

1.5.6 Involvement of RECQL4 in processes of DNA repair

Patients with RTS cells were found to show sensitivity to DNA damaging agents, suggesting an implication of RECQL4 within the DNA damage response (Cabral et al., 2008; Fan and Luo, 2008; Jin et al., 2008). Studies have investigated *RECQL4* mutant cells in response to genotoxic agents, however, results have been varied, possibly due to different primary cells and assays utilised (Lu et al., 2014a). Some of the agents include ionizing radiation, UV, topoisomerases inhibitors, and chemotherapy agents (Werner et al., 2006; Cabral et al., 2008; Fan and Luo, 2008; Jin et al., 2008; Singh et al., 2010; Crevel et al., 2012; Kohzaki et al., 2012). Viable RTS patient fibroblasts were shown to undergo irreversible growth arrest following the recovery from damage caused by oxidative stress, with significantly reduced DNA synthesis (Werner et al., 2006).

RTS patient cells show chromosomal instabilities, mainly mosaicism and isochromosomes (most often 8, 7 and 2 trisomies) (Ying et al., 1990; Orstavik et al., 1994; Wang et al., 2001; Beghini et al., 2003; Larizza et al., 2006). In mouse embryonic fibroblasts aneuploidy and an increase in premature centromere separation was observed, leading to chromosomal instability (Mann et al., 2005). Sister chromatid segregation errors were also seen by others (Dietschy et al., 2007), and it was suggested to reflect the activity of RECQL4 in the N-end rule pathway (Yin et al., 2004). In lymphocytes of RTS patients, chromosome breaks also occur frequently (Der Kaloustian et al., 1990; Lindor et al., 1996; Miozzo et al., 1998; Grant et al., 2000), although a few exceptions have been seen (Kerr et al., 1996; Beghini et al., 2003). Spontaneous breaks have been found to occur in skin fibroblasts as well (Vennos et al., 1992; Miozzo et al., 1998).

Following induction of DNA double-stranded breaks (DSBs) in human cells, endogenous RECQL4 was found to interact with RAD51; they co-localize and form a complex at sites representing homologous recombination repair. It is proposed RECQL4 could resolve aberrant DNA structures formed during DNA replication, and recombinational repair processes, or signal interactions with other proteins during these processes, suggesting a potential reason for genomic instability found in RTS cells and the predisposition to cancer (Petkovic et al., 2005). Silencing of *RECQL4* also led to reduced RAD51 foci numbers in cells treated with ionizing radiation, and an increase of PARP inhibitor sensitivity was shown. Further to this, *RECQL4*-slienced cells were sensitive to cisplatin induced DNA damage repair via HR, suggesting reduced HR repair ability following DSB (Santarpia et al., 2013).

PARP-1 is a single-strand break repair protein and is activated by a wide variety of DNA damaging agents. PARP-1 also modulates cellular sensitivity to γ-irradiation and holds an important role in BER (Bohr, 2002). Woo et al (2006) found an interaction of RECQL4 and poly(ADP-ribose) polymerase-1 (PARP-1). The study by Schurman et al, (2009) found RECQL4 regulates BER capacity directly and indirectly. They showed the colocalization of RECQL4 with key factors in BER; APE1 and FEN1 following H_2O_2 induced oxidative DNA damage. Interestingly, RTS cells were shown to express an upregulation of BER pathway genes, but fail to respond as normal cells under the same oxidative stress conditions (Schurman et al., 2009).

RECQL4 is also thought to coordinate with BLM in DNA replication and DNA repair, and the interaction has been shown to be stronger in S-phase and following ionizing radiation. BLM has many cellular roles including involvement in homologous recombination (Singh et al., 2012). The intracellular distribution and dynamic relocalization of RECQL4 to sites of DNA damage has suggested a possible role to the phenotypes, and associated heterogeneity, which has been found in RECQL4-associated diseases (Croteau et al., 2012b). Studies have highlighted functional roles of RECQL4 associated with aging and cellular senescence, oxidative DNA damage repair, telomere maintenance and mitochondrial dysfunction. Genomic instability and cellular senescence can be caused by the disruption of normal replication and transcription (Croteau et al., 2012b).

RECQL4 may interact with *Xeroderma pigmentosum* group A (XPA) demonstrated by GST-pulldown assay, as part of the NER pathway. A further increase of interaction was observed in cells under UV irradiation (Fan and Luo, 2008). A study demonstrated co-immunoprecipitation of RECQL4 with the Ku70/Ku80 heterodimer and the depletion of RECQL4 in human cells has been suggested to decrease NHEJ activity (Shamanna et al., 2014).

Interestingly, increased fragility of telomeric ends have been found in RTS patient cells and human cells following RECQL4 knockdown. Human RECQL4 has been shown to localise to telomeres and interact with the shelterin protein telomeric repeat-binding factor 2 (TRF2), and TRF1. On telomeric D-loops, RECQL4 has been shown to interact and stimulate WRN activity. RECQL4 has been demonstrated to be able to resolve telomeric D-loops also, which is a requirement for replication at the telomeres (Ghosh et al., 2012). WRN, BLM, and RECQL4 appear to be more active at telomeric D-Loops containing 8-oxoguanine base lesions, results of oxidative damage. The unwinding of D-Loops containing thymine glycol (Tg) lesions have been shown to be a preference of RECQL4 (Ferrarelli et al., 2013). Therefore, RECQL4 appears to have an important role in maintaining telomeric stability. Mutations in *RECQL4* could therefore lead to the dysfunction of telomeres, which is involved in tumour suppression and progression (Xu et al., 2013). RTS patient cells were shown to have an elevated level of fragile telomeric ends (Ghosh et al., 2012). A study by Yin et al (2004), reported an interaction between RECQL4 and cytosolic ubiquitin ligases UBR1 and UBR2, which have a function in the N-end rule pathway involving protein ubiquitination and degradation (Yin et al., 2004).

1.6 Aims of project

RECQL4 mutations in RTS patients lead to genomic instabilities, in particular chromosomal instabilities. We hypothesise that differentiating osteoblast become increasingly sensitive to DNA lesions, leading to malignant transformation. Using a cellular system that interferes with the initiation of DNA replication, and therefore recapitulates defects in *RECQL4* mutated cells we aim to determine the cellular changes this may generate during osteocyte differentiation of mesenchymal stem cells. To achieve interference with replication initiation during osteogenic differentiation we follow two related approaches:

1) We utilize PHA-767491, a specific inhibitor of DDK at sub-lethal concentrations to put a continuous pressure on the initiation machinery in proliferating and differentiating mesenchymal stem cells. DDK acts upstream of RECQL4 recruitment, and we hypothesise that its inhibition can copy the phenotypes of RECQL4 impairment in a system that is simple to establish and maintain.

2) While RTS fibroblasts cell lines are readily available from cell repositories, *RECQL4* mutated mesenchymal stem cells are not. We aim to establish an immortalized MSC cell line in which RECQL4 is depleted by lentiviral transduction of shRNA.

RECQL4 holds a critical role in predisposing RTS patients to OS development, perhaps directly or indirectly. We aim to identify RECQL4 interacting partners that may lead to understanding important interactions or pathways, which may enable the development or sensitizing of cells to tumorigenesis in RECQL4 mutated cells.

2 Materials and Methods

2.1 Stock solutions

Chemical reagents made up following manufacturer's protocols. Cell culture reagents were prepared in a Thermo Scientific Safe 2020 class II biological safety cabinet. Unless otherwise stated procedures were performed at room temperature. All solutions were made with Milli-Q® ultra-pure water with a resistivity of about 18 MΩ/cm.

2.1.1 Stock solutions and chemical reagents

Table 2.1-a Stock solutions and buffers

Stock solutions	Composition
Fixing solution with 4% paraformaldehyde	Prepared with the 9 x dilution of Formaldehyde (Sigma 36.5-38% F8775; 4% final concentration) in 250nM HEPES (4-(2-hydroxyethethyl)-1-piperazineethanesulfonic acid; Life Technologies, 2013a). Made up with distilled water.
Permeabilising solution	0.3% Triton X-100 (Sigma-Aldrich 93422) (v/v) in 1X PBS
IF Blocking buffer	10% FBS 0.1% Triton-X100 (Sigma-Aldrich 93422), (v/v) in 1X PBS
1X PBS	1X phosphate buffered saline tablet (Gibco® PBS Tablet, Thermo Fisher Scientific BR014G), per 100ml H2O, 0.01M.
1X PBS-Tween 20	1X PBS, 0.1% (v/v) Tween-20 (Sigma-Aldrich).
Oil red O stock solution	300mg Oil Red O (Thermo Fisher Scientific, 15244664) in 99% isopropranol
Oil red O working Solution	Oil red O stock solution was diluted in distilled H2O in 3:2, stirred for 10 minutes. Filtered before use.
Alizarin Red S staining solution	2g Alizarin Red S (Santa Cruz Biotechnology, sc-205998), dissolved in distilled H2O, pH adjusted to 4.3. Stored in dark.
Alcian blue staining solution	10mg Alcian blue (Santa Cruz Biotechnology, sc-214517) dissolved in a mixture of 60ml of absolute ethanol and 40ml Acetic acid (98%).
Destaining solution	Mixture of 120ml of absolute ethanol and 80ml Acetic acid.
Membrane blocking buffer	5% non-fat milk (w/v) in 1x PBS Tween 20, or 5% (w/v) BSA in 1x PBS Tween-20; stirred for 30 minutes
WB blocking buffer	2% (w/v) non-fat milk in 1x PBS Tween-20
WB blocking buffer BSA	2% (w/v) BSA in 1x PBS Tween 20
Anti-fading mounting medium	For 1 ml: 1 µl Para-phenylenediamine (10mM), 49 µl pure water, 50 µl 1M TRIS pH 7.4, and 900 µl Glycerol
Acid stripping	4M HCl in distilled H2O
Pulldown lysis buffer	1ml phosphosafe (Sigma-Aldrich), 30µl 5M NaCl (Melford D23735 7647-14-15), 10µl phosphatase inhibitor #3 (Sigma-Aldrich, P0044 lot-033M4020V), 10µl phosphatase inhibitor #2 (Sigma-Aldrich, P5726), 10µl phosphatase inhibitor cocktail (Sigma-Aldrich, P8340 lot-033M4023V), 40µl 25x complete mini (1 tablet in 420 µl H2O), (Roche 11836153001), 1µl 1M DTT, 10µl PMSF phenylmethanesulfonyl fluoride solution (Sigma-Aldrich, 93482).
2x lysis solution	25mM Tris-HCl (pH7.6), 150mM NaCl, 1% NP-40, 1% sodium-deoxycholate, 0.1% SDS.

Protease inhibitor cocktail	1 mini complete tablet in 1ml deionised water.
Protein lysis buffer stock	5ml 2x lysis solution, 100 µl 10mM Sodium fluoride (NaF), 500 µl 5mM Sodium pyrophosphate (NaPPi), and 3ml MiLLiQ water.
Western blotting lysis buffer	420 µl Protein lysis buffer stock and 71.4 µl protease inhibitor cocktail.
TBE buffer 10x	Tris (1M)-borate (1M)-EDTA (0.02M) (ThermoFisher Scientific)
Agarose gel 0.8%	0.32g agarose gel in 40ml TBE 1x
25 x Tris-Glycine buffer	18.2g Tris base (12mM) (Melford B2005) 90g Glycine (96mM) (Fisher Scientific, BP381-1 130837 To 500ml with deionised water
Criterion gel running buffer (10x)	30g Tris Base (Melford B2005), 144g Glycine (Fisher Scientific, BP381-1 130837), 10g SDS (pH 8.3) in 1000ml deionised H2O diluted 1x.
Invitrogen gel running buffer	NuPAGE MOPS SDS (20x) NP001 25ml in 500ml H2O.
Invitrogen Nupage Novex LDS sample buffer (4x)	Glycerin, Sulfuric acid, monododecyl ester, lithium salt (NP0008, ThermoFisher Scientific)
Membrane transfer buffer	40ml 25x Tris-Glycine buffer, 760ml deionised H2O, 200ml methanol.
2x RealTime-Glo™	NanoLuc ® Enzyme was equilibrated to 37℃. 1000x MT cell viability substrate and 1000x NanoLuc ® Enzyme was added to media and mixed well.
PHA-767491 (PHA)	PHA-767491 (Sigma-Aldrich, PZ0178), dissolved in DMSO (Dimethyl Sulfoxide; Santa Cruz Biotechnology, sc-358801).
NEBuffer 2	10 mM Tris-HCl, 50 mM NaCl, 10 mM $MgCl_2$, 1 mM DTT (pH 7.9@25°C)

Table 2.1-b Nucleic acid stains

Cell stain	Colour	Dilution	Cell permeability	Mounting media	Detection	Excitation /Emission (nm)	Molecular formula
Hoechst 1mg/ml (Sigma-Aldrich, 33258)	Blue	1: 20000 in H_2O	Cell-permeable	Anti-fading mounting medium	Fluorescent	352/461	$C_{25}H_{37}Cl_3N_6O_6$
DAPI (4', 6-diamidino-2-phenylindole; Life Technologies).	Blue	1: 20000 in H_2O	Cell-Impermeable	Anti-fading mounting medium	Fluorescent	358/461	$C_{16}H_{17}Cl_2N_5$
Vectashield mounting medium with DAPI (Vector, H-1200)	Blue	-	Cell-Impermeable		Fluorescent	360/460	$C_{16}H_{17}Cl_2N_5$

Table 2.1-c Primary antibodies. WB – Western blot, IF – Immunofluorescence

Antigen	Dilution	Clonality	Raised in / isotype	Immunogen	kDa
Tubulin WB	1:5000 in WB blocking buffer	Monoclonal	Mouse		50
RECQL4 (Cell Signalling Technology, 2814) WB	1:1000 in WB blocking buffer BSA	Polyclonal	Rabbit	Synthetic peptide corresponding to amino acids near the amino terminus of human *RECQL4*	150
Ki-67 (Dako, M7240) IF, WB	1:300 in IF blocking buffer	Monoclonal Clone-MIB-1	Mouse, IgG1κ	Human recombinant peptide corresponding to a 1002 bp Ki-67 cDNA fragment	55
RUNX2 (Santa Crux, M-70 sc-10758) 200µg/ml IF	1:300 in blocking buffer -IF	Polyclonal	Rabbit IgG	Epitope corresponding to amino acids 294-363 RUNX2 mouse origin PQVATYHRAIKVTVD GPREPRRHRQKLDD SKPSLFSDRLSDLGR IPHPSMRVGVPPQNP RPSLNSAPSPF	
Phospho CHK-1 (Bethyl A300-163A), (1mg/ml) WB	1:250 in WB blocking buffer BSA	Polyclonal	Rabbit IgG	phosphorylated synthetic peptide, which represented a portion of human Checkpoint Kinase 1 (GeneID 1111) around serine 317 according to the numbering given in entry NP_001265.1	55
HDX (Aviva Systems, QC11406, ARP39), (1µg/ml), WB	1:500 in WB blocking buffer BSA	Polyclonal	Rabbit	Synthetic peptide sequence derived from: MNLRSVFTVEQQRIL QRYYENGMTNQSKN CFQLILQCAQETKLD FSVVRT	77
HDX (Abcam, 94475), (1µg/ml), WB	1:1000 WF blocking buffer BSA	Polyclonal	Rabbit		77
γH2AX, (Abcam, phospho-2139, ab2893n, 1mg/ml), IF	1:500 IF blocking buffer	Polyclonal	Rabbit		
TRF2 (Novus Biologicals NB100-56506, 1mg/ml), IF	1:500 IF blocking buffer	Monoclonal	Mouse		
53BP1, (Novus Biologicals, NB100-305, 1mg/ml), WB	1:5000 in WB blocking buffer BSA	Polyclonal	Rabbit		220
PP2A A subunit (PP2a), (Cell Signalling 2039s), WB	1:1000 in WB blocking buffer BSA	Polyclonal	Rabbit		62
MCM10 (Proteintech, 12251-AP), WB	1:800 in WB blocking buffer BSA	Polyclonal	Rabbit	MCM10 fusion protein ag2899	97-105
Chk-1 (Santa Cruz, sc-7898), WB	in WB blocking buffer BSA	Polyclonal	Rabbit		56
Engrailed homolog 2 (EN2), (Thermo Fisher Scientific, PA5-28953, 1mg/ml), WB	1:10,000 in WB blocking buffer BSA	Polyclonal	Rabbit		30

Table 2.1-d Secondary antibodies.

Secondary antibody	Dilution	Clonality	Raised in
Alexa-fluor 488 anti-rabbit, (invitrogen, A11008)	1:500 in IF blocking buffer		Goat
Alexa fluor 555 anti-mouse, (Invitrogen, A21422)	1:500 in IF blocking buffer		Goat
Anti-Rabbit Horseradish Peroxidase, (Millipore, 12-348)	1:5000 in WB blocking buffer/ WB blocking buffer BSA	Polyclonal	Goat
Anti-Mouse Horseradish Peroxidase (Millipore AP501P)	1:5000 in WB blocking buffer/ WB blocking buffer BSA	Polyclonal	Goat
Anti-Goat Horseradish Peroxidase (Millipore AP180P)	1:10,000 in WB blocking buffer/ WB blocking buffer BSA	Polyclonal	Donkey

Table 2.1-e Cell lines and culture details. DMEM - Dulbeccos modified minimal essential medium (Gibco™, Thermo Fisher Scientific). EMEM - Eagle's Minimum Essential Medium (Gibco™, Thermo Fisher Scientific). MEM α - Minimum Essential Medium alpha (Gibco™, Thermo Fisher Scientific). FBS – fetal bovine serum (Gibco™, Thermo Fisher Scientific).

Cell line	Species/details	Tissue/cell type	Disease/mutation	Growth medium	Freezing medium	Obtained
HeLa LacZeoTO (HeLa)	Human	Cervical	Carcinoma	DMEM with 10% FBS Antibiotic (complete media) + 1% penicillin/streptomycin	DMEM + 20% Foetal calf serum + 10% DMSO	Stephen Taylor, University of Manchester
U2OS Flp-In™ T-REx™ (U2OS)	Human		Osteosarcoma	DMEM with 10% FBS Antibiotic (complete media) + 1% penicillin/streptomycin	DMEM + 20% Foetal calf serum + 10% DMSO	Catherine Miller, University of Manchester
AG05013htert immortalized	Human, male, 10 years of age	Skin,fibroblast	RTS/RECQL4	DMEM with 10% FBS	DMEM + 20% Foetal calf serum + 10% DMSO	Coriell Cell Repositories
HS68htert immortalized	Human, male, new born	Skin,fibroblast	aspartoacylase deficiency; possible Canavan disease	DMEM with 15% FBS	DMEM + 20% Foetal calf serum + 10% DMSO	Immortalisation performed by CRUK Cell Cervices at Clare Hall
MRC5	Human	Lung, fibroblast		DMEM with 10% FBS	DMEM + 20% Foetal calf serum + 10% DMSO	(ATCC® CCL-171™)
ASC52telo htert immortalized	Human	adipose derived mesenchymal stem cells		MesenPRO RS™ Medium kit (Thermo Fisher Scientific)	MesenPRO RS™ Medium (Thermo Fisher Scientific) + 10% DMSO	ATCC® SCRC 4000™) P13
AG03587	Human, Caucasian, male, 7 years of age.	Fibroblast,	RTS	EMEM with 15% FBS,	EMEM with 15% FBS + 10% DMSO	Coriell Cell Repositories
AG18375	Human, Caucasian, male, 22 years of age.	Fibroblast	RTS/RECQL4 Osteosarcoma at 21 years of age.	MEM α +10% FBS	MEM α 10% FBS + 10% DMSO	Coriell Cell Repositories

Table 2.1-f siRNA details

siRNA		Target sequence
AllStars Non-Targeting (NT), (Qiagen, 1027280),	No homology to any known mammalian gene.	Non-targeting
RECQL4 siRNA (pool), (Qiagen)	#1SI03091732 #2 SI00061866 #3 SI00061859 #4 SI00061852	Entrez gene 9401
RECQL4 siRNA #9		5'-caggguguggaacgaggauu-3'
RECQL4 siRNA#10		5' aggcuagggcagugacug auu-3'
HDX (Qiagen) pool	HS cxorf43 8 (5104269097) HS cxorf43 5 (5103160745) HS cxorf43 7 (5104257617) HS HDX 1 (5105393444)	Entrez gene 139324

Table 2.1-g Delivery agent to DNA ratio

Delivery system	**Ratio reagent:DNA** (PEYFP-C1 at 200ng)			
Fugene 6	2:1	3:1	3:2	4:1
Lipofectamine 2000	2:1	3:1	3:2	4:1

Table 2.1-h Control plasmid

Plasmid	Type	Promoter	Size	5'sequencing primer	1	Tag 1	Constitutive	Viral
pEYFP-C1	Mammalian expression	CMV	4700	5'd[CATGGTCCTGCT GGAGTTCGTG]		EYFP (Nterm)	Constitutive	Nonviral

Table 2.1-i concentrations of plasmid for inoculation

Plasmid and vector	Soc medium	Ratio
10 µl	40 µl	1:4
20 µl	30 µl	2:3
50 µl	-	-

Table 2.1-j Digest mix

Digest		
NcoI	**XhoI**	**HinfI**
3µl plasmid DNA or empty vector	5µl plasmid DNA or empty vector	5µl plasmid DNA or empty vector
1µl 10x BSA	1µl 10x BSA	1µl 10x BSA
1µl 10x NEB3 (Biolabs B72035)	1µl 10x NEB4 (Biolabs B70045)	1µl 10x NEB3 (Biolabs B72035)
0.5µl NCOI (10 n/ µl)	0.5µl digest (Biolabs R01465)	0.5µl digest (Boehringer monheim 13607322-43)
4.5µl H_2O	2.5µl H_2O	2.5µl H_2O
Incubated at 37℃ for 2 hours	Incubated at 37℃ overnight	Incubated at 37℃ overnight

Table 2.1-k RECQL4 oligonucleotides

Oligonucleotides	Concentration	Sequence
9 Top - Sh RECQL4_9 (Sigma-Aldrich 8017856206 0010 403)	200µm	5'CCGGCACAGGGTGTGGGAACGAGGACTCGAGTCCTCGTTCCCACACCCTGTGTTTTTG-3'
9 Bottom - Sh RECQL4_9 (Sigma-Aldrich 8017856206 0020 403)	200µm	5'AATTCAAAAACACAGGGTGTGGGAACGAGGACTCGAGTCCTCGTTCCCACACCCTGTG-3'
10 Top - Sh RECQL4_10 (Sigma-Aldrich 8017856206 0030 403)	200µm	5'CCGGAGAGGCTAGGGCAGTGACTGACTCGAGTCAGTCACTGCCCTAGCCTCTTTTTTG-3'
10 Bottom - Sh RECQL4_10 (Sigma-Aldrich 8017856206 0040 403)	200µm	5'AATTCAAAAAAGAGGCTAGGGCAGTGACTGACTCGAGTCAGTCACTGCCCTAGCCTCT-3'

Table 2.1-l Annealing mix

ML Protocol (A)		Addgene Protocol (B) (modified)	
TE pH 8.0	43µl	H_2O	43 µl
100 mM $MgCl_2$	5µl	NEBuffer 2 10x	5 µl
200 pmol of Top oligo (200 µM)	1µl	200 pmol of Top oligo (200 µM)	1µl
200 pmol of Bottom oligo (200 µM)	1µl	200 pmol of Bottom oligo (200 µM)	1µl

Table 2.1-m Ligation Reagent mix

	Empty vector	RECQL4 9 (A)	RECQL4 9 (B)	RECQL4 10 (A)	RECQL4 10 (B)
PLK0.1 (93.5ng/µl	1µl	1µl	1µl	1µl	1µl
10x annealed insert	-	0.5µl	0.5µl	0.5µl	0.5µl
T4 ligase	0.2µl	0.2µl	0.2µl	0.2µl	0.2µl
10x ligase buffer	1µl	1µl	1µl	1µl	1µl
10x BSA	1µl	1µl	1µl	1µl	1µl
H_20	6.8µl	6.3µl	6.3µl	6.3µl	6.3µl
Adenosine triphosphate (ATP)	0.1µl	0.1µl	0.1µl	0.1µl	0.1µl

Table 2.1-n PCR amplification mix

PCR amplification mix component	Volume per reaction
Amplification grade water	To final volume (25µl)
GenePrint® 10 5X Master Mix	5µl
GenePrint® 10 5X Primer Pair Mix	5µl
template DNA (10ng)	Up to 15µl
Total reaction volume	25µl

2.2 Cell Culture

All cell culture procedures were performed in a clss II Thermo Scientific Safe 2020 Biological safety cabinet. Separate solutions were used between cell lines to reduce the risk of cross contamination. Cells were incubated in a Panasonic MCO-19A1C-PE humidified cell culture incubator, CO_2 controlled at 5%, at 37℃. All solutions were equilibrated to 37℃ before usage in a Grant waterbath.

2.2.1 Cell maintenance

Cells were maintained in 25cm^2 T-flasks in 5ml of suitable medium (Table 2.1-e) at around 80-90% confluency (2-4 days).

For passaging and seeding, the media was removed using aspiration, and the cells were washed with 1x PBS. 500µl 1x trypsin-EDTA (0.25% trypsin, 0.53mM EDTA, Gibco) in 1x PBS was added to detach the cells, for 5-10 minutes at 37 ℃. Detached cells were re-suspended in suitable media (Table 2.1-e) and the cells were counted before each assay, seeding, and passaging by haemocytometer or a BioRad TC20

cell counter. Desired cell density was seeded onto plate wells, or in 25cm^2 T-flask for continual culture. If required during culture, cell growth was recorded using phase contrast images taken with a Nikon eclipse T5100 and DN100 camera.

2.2.2 Freezing

The cells were detached from the culture vessel using trypsin-EDTA, as previously described, and were placed in separate conical tubes and centrifuged down at 1000rpm for 5 minutes. The medium was carefully removed leaving the cells at the base of the 15ml conical centrifuge tube. Light tapping was applied to mix the remaining cells and suitable 1ml freezing medium was added (Table 2.1-e). The suspension was transferred into cryo-vials and stored via slowly cooling to -80℃, then transferred to vapour phase of a liquid nitrogen container.

2.2.3 Recovery

The cells were rapidly thawed by placing in a 37℃ water bath for 2 minutes, to prevent the formation of water crystals. The cells were suspended in 10 ml media then centrifuged down at 1000rpm for 5 minutes and the freezing media (Table 2.1-e) was removed by aspiration. The cells were re-suspended in the appropriate growth media (Table 2.1-e) and transferred to a 25cm^2 T-flask.

2.2.4 Proliferation titration

Cells were harvested as previously described, were seeded at suitable densities and incubated at 37°C. At various time points the cells were harvested as previously described and counted. The cells were viewed using Nikon Eclipse TE2000 inverted stage microscope.

2.2.5 ASC52telo differentiation ability

ASC52telo cells were seeded at 5000 cells per cm^2 on 24 well plate. The cells were allowed to reach around 80% confluency (control cells). The cells were treated with selected differentiation media: chondrocyte differentiation (StemPro chondrocyte kit, Thermo Fisher Scientific), osteocyte differentiation (StemPro osteogenesis kit, Thermo Fisher Scientific), and adipocyte differentiation (StemPro adipocyte kit, Thermo Fisher Scientific). Medium was changed every 3 days. Full differentiation

was expected following at least 21 days of culture. Differentiation was confirmed with histochemical staining.

2.2.5.1 Adipocyte differentiation detection - Oil red o

Following cell incubation for adipocyte differentiation (21 days, unless stated otherwise), the medium was aspirated gently; the cells were not allowed to remain dry for no longer than 30 seconds. All rinsing was carried out gently, in order not to disturb the monolayer. The cells were washed with 1x PBS, and fixed in 4% fixing solution (Table 2.1-a) for 10 minutes at 4℃. The fixing solution was then removed and 1x PBS washes performed 2 times. The cells were washed with distilled H2O. 60% Isopropanol was added to cover the cells for 5 minutes. This was removed and 2ml of Oil red O working solution (Table 2.1-a), was added to cover the cells for 5 minutes. The solution was removed and the cells washed with tap water until running clear. 2ml of Harris haematoxylin (Thermo Fisher Scientific) counterstain was added for 1 minute and rinsed with warm tap water. The cells were observed using transmitted light microscopy, the nuclei staining blue, and the lipid droplets staining red.

2.2.5.2 Osteoblast differentiation detection - Alizarin red S

Following cell incubation for osteoblast differentiation (21 days, unless stated otherwise), the medium was aspirated gently. All rinsing was carried out gently, in order not to disturb the monolayer. The cells were washed with 1x PBS, and fixed in 4% fixing solution (Table 2.1-a) for 10 minutes at 4℃. The fixing solution was then removed and 1x PBS washes performed 2 times. The cells were washed with distilled H_2O, and Alizarin Red S staining solution (Table 2.1-a), was added to cover the cells for 5 hours. The plate was wrapped in foil to protect from light. The solution was carefully removed and cells washed 4x with H_2O and maintained in 1x PBS. The cells were observed using transmitted light microscopy, extracellular calcium deposits staining orange-red.

2.2.5.3 Chondrocyte differentiation detection – Alcian blue

Following cell incubation for chondrocyte differentiation (21 days, unless stated otherwise), the medium was aspirated gently. The cells were washed with 1x PBS, and fixed in 4% fixing solution (Table 2.1-a) for 10 minutes at 4℃. The fixing solution

was then removed and 1x PBS washes performed 2 times. The cells were washed with distilled H_2O and Alcian blue staining solution was added to cover the cells overnight. The staining solution was carefully removed and the cells were washed 2x with destaining solution (Table 2.1-a) for 20 minutes each time. The cells were maintained in 1x PBS and observed using transmitted light microscopy. Cartilage stains dark blue.

2.2.6 Anchorage-independent growth

ASC52telo cells were seeded at 2000 cells per well in Costar flat bottom ultra-low attachment surface non pyrogenic (3474) 96 well plate. The cells were incubated as indicated in the legend of the respective figures. Every 3 days the plate was centrifuged at 1000rpm, the media was carefully removed leaving 20ul on the cells. The cells were re-suspended in media under the same conditions with/without treatment (PHA-767491). MTS assay (Section 2.2.7.2) was performed at indicated days.

2.2.7 Cell quantification and viability analysis

2.2.7.1 Cell quantification

Cell quantification was performed before each assay to seed cells at desired density, and for analysis of cell proliferative rate. Obtained cell suspension was mixed with Trypan blue at a 1:1 ratio to measure cell viability, was added to a clean haemocytometer, and viewed using Nikon Eclipse TE2000 inverted microscope with 10x objective. In total 8 quadrants were used to provide a mean. The mean was calculated, and the cell concentration was expressed as $n \times 10^5$. Alternatively, a Bio-Rad TC20 automated cell counter was used with a cell suspension prepared (see Table 2.1e).

2.2.7.2 MTS viability assay

The procedure was carried out in dark conditions. MTS solution was prepared using MTS (CellTiter 96® -A Queous MTS Reagent Powder, Promega), dissolved in 1x PBS and mixed with the electron coupling reagent phenazine methosulfate (PMS), (Sigma-Aldrich, P9625). Cells were seeded at appropriate densities in 96-well plate

and following incubation the media was replaced with 100ul fresh media and 20ul of MTS/PMS solution was added to the culture medium at a final concentration of 1.9 mg/ml MTS and 44 µg/ml PMS in 1x PBS, and cells were incubated for 3 hours at 37°C. Post incubation, the coloured product generated by viable cells was measured at 490 nm and quantified using a Spectra Max Plus (Molecular Devices) plate reader with Softmax pro 5.2 software.

For drug treatments, the drug was added 24 hours following cell seeding and maintained throughout the assay until MTS/PMS was added.

2.2.7.3 RealTime-Glo™ MT assay

ASC52telo cells were seeded at 5000 cells per cm^2 on a 96 well plate in triplicates, and treated as required. A well was left blank either side. The cells were incubated, and the media was changed every 3 days. On day 21 fresh media was added, 2x RealTime-Glo™ was added to the wells in media to form 1x concentration, and incubated for 1 hour. The plate was covered with PCR film to reduce contamination to cells, covered with tin foil to protect from light during incubation. Luminescence was read using Hidex Chameleon plate reader. The plate was returned for incubation and on day 24 the RealTime-Glo™ MT assay was repeated, and cells returned for incubation. To analyse the cells further an MTS assay (Section 2.2.7.2) was performed on day 28.

2.2.8 PHA-767491 titration

A suitable concentration of PHA-767491 (pyridin-4-yl)-6,7-dihydro-1H-pyrrolo[3,2-c]pyridin-4(5H)-one; Sigma-Aldrich, PZ0178), was determined in a range of cell lines to establish mild proliferation inhibition. Cells were harvested as previously described, and seeded at 2000 cells per well in a 96-well plate and incubated for 24 hours. Wells with media alone were used as background control. Media was replaced with 100ul fresh media containing a range of PHA-767491 concentrations after the cells had safely attached to the substrate. The cells were incubated for 7-10 days and an MTS assay performed as described previously.

A PHA-767491 model (PHA model) (Figure 2.2-a) was generated to establish ASC52telo cell lines which would represent: 1) short term treatment (referred to as ‘acute’); 2) continuous, prolonged treatment (‘chronic’); 3) cells released from

chronic treatment for the duration of experiment (‘chronic recovery); 4) and untreated cells (no treatment) in low and high passage cells. Low passage chronic PHA treatment started at P+6, high passage chronic PHA treatment started at P+13. Cells treated with PHA for a period of time and through a number of passages prior to further plating were deemed ‘chronic’.

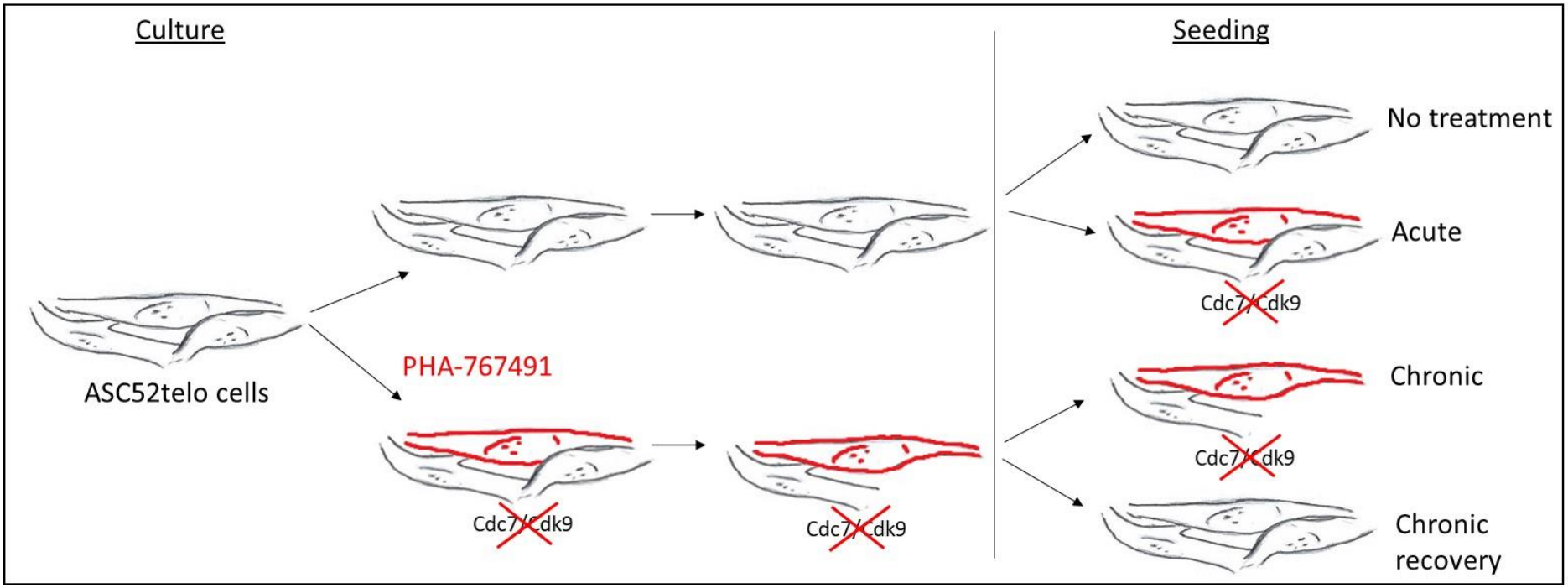

Figure 2.2-a A schematic showing ASC52telo cells and various culture conditions that established a model of PHA-767491 treatment. ASC52telo cells were passaged and maintained under PHA-767491 at 1.5μm as per model. 'Chronic' represents cells under treatment during culture that continued throughout any further analysis. 'Acute' represents cells without treatment under culture but the addition of PHA-767491 during assays. 'Recovery' cells were treated during culture but no treatment during further analysis.

2.2.9 Titration of selection reagents

Optimum selection concentration of Blasticidin-S® (Thermo Fisher Scientific) in HeLa and U2OS cells had been previously determined to be 4µg/ml and 15µg/ml, respectively.

HeLa and U2OS cells were seeded into petri dishes containing 10ml DMEM medium (Table 2.1-e) with Blasticidin-S® (Thermo Fisher Scientific) as above and concentrations of Hygromycin B (Calbiochem, 400053) varying between 0 µg/ml with 50µg/ml increments and incubated for 2 and 3 weeks. The cells were observed microscopically using Nikon Eclipse TE2000 inverted stage microscope for the rate of cell growth / cell death to determine an appropriate concentration of Hygromycin B with the Blasticidin-S® co-treatment. The optimal concentration of Hygromycin B for co-selection was found to be 225 µg/ml (45 µl in 10ml medium) in HeLa cells, and and100 µg/ml (20 µl in 10ml medium) in U2OS cells.

2.2.10 Transfection

2.2.10.1 siRNA transfection

All siRNA transfections were performed as reverse transfections, under RNAse-free conditions, and conducted in 96 well plates. For one well of the 96-well plate 0.1 µl DharmaFECT 1 (Dharmacon) delivery reagent was diluted in 9.9µl OptiMEM medium (Gibco, Thermo Fisher Scientific), and 0.5µl 2µM siRNA (Table 2.1-f) was diluted in 9.5µl OptiMEM. The diluted reagents were mixed via vortexing and incubated at room temperature for 5 minutes. Following incubation the transfection reagents (diluted siRNA and diluted transfection reagent) were combined, mixed, and incubated at room temperature for 20 mins, then placed into the wells. Cell suspension of 12,000 cells per well was set up and 80µl was added to each well. The reagent mixes and cell suspension were scaled up as required for the number of wells. The media was topped up 18 hours post transfection and incubated for further 2 days. Whole cell protein was extracted (Section 2.3.1) and further analysis was performed.

2.2.10.2 Optimisation of plasmid transfection

HeLa LacZeo cells were seeded at $1x10^5$per well onto glass coverslips in 24 well plate and incubated overnight. The cells were transfected with variety of ratios

(Table 2.1-g) of delivery agent : plasmid DNA, using either Fugene 6 (Promega), or Lipofectamine 2000 (Invitrogen, Thermo Fisher Scientific), and pEYFP-C1 control plasmid (Table 2.1-h). For Lipofectamine 2000, 6 hours post transfection the media was removed and replaced with media alone, while additional media was added to Fugene 6 wells. Analysis was performed 72 hours post transfection.

2.2.10.3 Plasmid transient transfection

$1x10^5$ HeLa or U2OS cells were seeded into wells of a 24 well plate and incubated overnight. The medium was then replaced with 500 µl fresh medium. 300 ng of plasmid DNA diluted in OptiMEM (Gibco, Thermo Fisher Scientific) was mixed with Lipofectamine 2000 at a ratio of 3:1 Lipofectamine 2000 to DNA, and incubated at room temperature for 25 minutes. A 100 µl aliquot of the transfection mix was added into the appropriate wells and incubated for 6 hours. 6 hours post transfection additional 500 µl medium (Table 2.1-e) was added to each well, and incubated for 72 hours, until analysis.

2.2.10.4 Co-transfection for inducible expression

For the generation of stable cell lines the FlipIn / FRT site-specific recombination system was used. The host cell lines, HeLa-LacZeo and U2OS-FLIPINTREX, contain a single-copy integrated FRT recombination site, which is utilized by the FLP recombinase. The FLP recombinase is introduced into the system via the co-transfection of the pOG44 plasmid (Invitrogen, Thermo Fisher Scientific).

HeLa-LacZeo and U2OS-FLIPINTREX cells were seeded onto 10cm plates and cultured to reach around 50% confluency. 800ng of pXPfrtto-RECQL4-Emerald maxiprep plasmid DNA (2.6.5) (4294.5ng/µl) was mixed with 7.2µg pOG44 (1940.1 ng/ µl) to reach a ratio of 9:1 in OptiMEM and allowed to stand for 5 minutes. Lipofectamine 2000 transfection reagent was diluted in OptiMEM to allow a ratio 3:1 with DNA reagent, mixed well, and allowed to stand for 5 minutes at room temperature. The diluted plasmids and the Lipofectamine reagent were mixed well and allowed to stand at room temperature for 25 minutes then added to the cells drop-wise and incubated for 5 hours. Post transfection the medium was removed and was replaced with 10ml of fresh medium. The transfected cell population was selected for correct integration and Tet repressor expression with Blasticidin-S®

(Thermo Fisher Scientific) and Hygromycin B (Calbiochem, 400053), at concentrations determined previously.

2.2.11 Verification of inducible Emerald-GFP tagged RECQL4

Emerald-GFP tagged RECQL4 clones (in HeLa-LacZeo and U2OS-FLIPINTREX hosts) under selection were maintained in 6 well plates to reach around 90% confluency. The cells were harvested using trypsin as previously described and seeded at suitable density onto ethanol sterilised glass coverslips in 1ml medium (Table 2.1-e). Doxycycline at 2 µg/ml was added to the wells and incubated for 3 days. Fixing, mounting and analysis was performed as described in section 2.4.

2.3 Protein isolation and analysis

2.3.1 Whole cell protein extraction

Adherent cells (ASC52telo) were allowed to reach around 80% confluence, for approximately three days. The cell medium was removed from the dishes using an aspirator, and cells were washed x3 with 1X Phosphate Buffered Saline (PBS). Remaining PBS was aspirated. An appropriate amount of cold lysis buffer supplemented with protease and phosphatase inhibitors was added for 5 minutes at 4 ℃. The lysate was then collected and was transferred into a new 1.5ml micro-centrifuge tube and sonicated with 4x 5 second bursts at 18 microns of amplitude (Soniprep 150, MSE). The cells were then centrifuged at 13,000 rpm for 20 minutes at 4℃ to sediment the cell debris, and the lysate was transferred to a new 1.5ml micro-centrifuge tube and stored at -80℃.

2.3.2 Protein quantification

Protein concentration of whole cell lysate was determined by Bradford assay. For each sample 1 µl was assayed in 4 µl of H_2O in 96-well plate. Bovine Serum Albumin (BSA, Sigma-Aldrich, A9647) 0-2mg/ml was used as standards at 5 µl per well. 250 µl of Quick Start Bradford 1x dye (Bio-Rad, 500-0205) was added to each well, and was incubated for 5 minutes in tin foil to protect from light. Absorbance was read at 595nm using Infinite® M200 Tecan or spectra Max Plus Molecular Devices plate reader with Softmax pro 5.2 software.

2.3.3 Sodium dodecyl sulphate polyacrylamide gel (SDS page)

Proteins were separated by electrophoresis using polyacrylamide gel. Depending on the number of parallel samples either a small or a large gel was run. A small Novex NuPage 4-12% Bis-Tris pre-cast gel was run in an XCell *sure*Lock Mini-Cell tank with 1x Invitrogen NuPage MOPS SDS running buffer. A large Criterion TGX pre-cast 4-15% gel was run in a Criterion cell (Bio-Rad) in 1x Criterion gel running buffer (Table 2.1-a). Protein concentrations in each lysate were determined (Section 2.3.2) and normalised to the most dilute sample to maintain equal loading. To denature the proteins each lysate was heated at 100℃ for 5 minutes with 1x Nupage Novex LDS sample buffer (Table 2.1-a) and allowed to cool on ice. The gel was run at 100v for 2.5 hours (Nupage) or 120v for 1.5 hours (Criterion). Following the separation of the proteins the gel was either cut (Section 2.3.4) and sent for mass spectrometry, or western blot was performed (Section 2.3.5)**.**

2.3.4 Gel section cutting

Sections of the gel previously ran by SDS page (Section 2.3.3), were then cut according to ladder markings. To help maintain sterility and to avoid keratin contamination, equipment was cleaned with ethanol and Teknon 100. The sections were stored in micro-centrifuge tubes, at -80℃, and sent for mass spectrometry analysis.

2.3.5 Western blotting

To identify specific proteins extracted from cells a western blot was performed. The proteins were separated by size using SDS-page (2.3.3), transferred onto Amersham Hybond ECL nitrocellulose membrane (RPN303D GE-Healthcare) and were blocked in membrane blocking buffer (Table 2.1-a) for 1 hour. Targeted proteins were marked using appropriate primary and secondary antibodies: the membrane was incubated overnight at 4 °C with primary antibodies in blocking buffer (Table 2.1-c), sealed in a polyethylene bag on a rotary wheel. Unbound antibody was removed in 5x washes for 10 minutes each in PBS Tween-20. A targeted horseradish peroxidase-conjugated secondary antibody (Table 2.1-c) was then applied for 1 hour at room temperature sealed in a polyethylene bag on a rocking platform. Unbound antibody was removed in 5x washes for 10 minutes each in PBS Tween-20. The signal from targeted protein was detected using an enhanced

chemiluminescence detection kit: ECL substrate BioRad (Bio-Rad**,**170-5060s) for 5 mins, or Pierce™ ECL Western Blotting Substrate (Thermo Scientific Fisher ™) for 1 minute. The signal was captured on film and developed using an Xograph Compact x4, or imaged using Bio-Rad ChemiDoc™ MP imaging system (Bio-Rad) with Image lab 4.1 software. Band densities were measured using ImageJ software, and normalized to Tubulin to express relative density where appropriate.

2.3.6 Stripping and re-probing

The membrane previously probed was stripped to allow re-probing with different antibody. The membrane was placed into stripping solution (Table 2.1-a) for 30 minutes on a rocking platform, followed by 2x washes in 1xPBS-Tween. The membrane was then blocked and appropriate antibody applied as described above (Section 2.3.5).

2.3.7 Immunoprecipitation of GFP-RECQL4 fusion proteins

Cells expressing Emerald-GFP tagged RECQL4 in a doxycycline inducible manner were established in HeLa and U2OS background. HeLa GFP-RECQL #2 and U2OS GFP-RECQL4 #15 cells were recovered. Confluency was established in selection medium (Table 2.1-e). The cells were then detached as previously described and re-seeded into separate 3x 10cm petri dishes for each cell line with medium (Table 2.1-e). GFP-RECQL4 expression was induced with the addition of 2ug/ml doxycycline and the cells were allowed to establish confluency. The cells were then trypsinised and transferred into 8 x 10 cm petri dishes separately for each cell line and incubated overnight. Late evening the following day the cells were treated as follows: 2 of the petri dishes of each cell line were treated with 2µm Suberoylanilide hydroxamic acid (SAHA); 2 were treated with 4mM hydroxyurea; two were left untreated, and the final two with Dimethyl Sulfoxide (DMSO) and incubated for 18 hours. The medium was then removed and on ice using 3ml of cold PBS the cells were detached by scraping and transferred into 15ml falcon tubes. The falcon tubes were then centrifuged at 1,000rpm for 5 minutes at 4℃. The supernatant from each tube was carefully removed and the pellet was re-suspended in 5ml cold PBS, and centrifuged at 1,000rpm for 5 minutes at 4℃. The supernatant was carefully removed and the pellet was re-suspended in 1ml cold PBS and transferred into

separate 1.5ml micro-centrifuge tubes. These were then centrifuged again at 1,000rpm for 5 minutes at 4℃, and the supernatant discarded.

GFP-tagged proteins were isolated via immunoprecipitation using Chromotek GFP-trap®_A. The pellet was flicked to mix well before the addition of lysis buffer to each and allowed to rotate on a rotary wheel at 4℃ 20rpm for 1 hour. Following incubation, the crude lysate was centrifuged at 13,000rpm for 30 minutes at 4℃. The supernatant was transferred to new 1.5ml micro-centrifuge tubes on ice. 50µl of the cell lysate was diluted with 50µl 4x LDS-sample buffer with 13mM DTT and heated at 100℃ for 5 minutes, allowed to cool on ice before storage at -80℃ for western blotting (input). 25µl of GFP-trap®_A beads were equilibrated with 500µl of ice cold dilution buffer for each sample in 1.5ml micro-centrifuge tubes. The tubes were centrifuged at 2700xg for 2 minutes at 4℃, and the supernatant was discarded; this process was repeated a further 2 times. The cell lysate was then added to the appropriate 1.5ml micro-centrifuge tube containing the beads. They were then rotated on a rotary wheel for 2 hours at 12rpm at 4℃. Following incubation, the tubes were centrifuged at 2000xg for 2 minutes at 4℃. The supernatant was then transferred to new 1.5ml micro-centrifuge tubes. From this a 50 µl of aliquot was diluted with 50µl 4x LDS-sample buffer with 13mM DTT and heated at 100℃ for 5 minutes, allowed to cool on ice and stored at -80℃ for western blotting (cleared lysate). The remaining supernatant was discarded. The beads were then washed with 500µl ice cold dilution buffer and centrifuged at 2000xg for 2 minutes at 4℃, the supernatant discarded, and the wash step repeated. The beads were then re-suspended in 4x LDS-sample buffer with 13mM DTT and heated at 95℃ for 10 minutes, allowed to cool on ice before storage at -80℃. SDS page, gel section cutting, and western blotting was performed as described above (Sections 2.3.3, 2.3.4, 2.3.5, respectively).

2.4 Epifluorescent microscopy

Glass coverslips (Thermo Fisher Scientific 12392128, MNJ-500, 13mm), were sterilised in 70% ethanol and allowed to dry in wells of a 24-well plate. Cells were seeded at appropriate concentrations with suitable media and cell treatments, on the glass coverslips. The cells were incubated and allowed to reach around 70-90% confluency. Then the medium was removed using aspiration and the cells were washed with 1x PBS. The cells were fixed in 4% paraformaldehyde for 12 minutes on ice. The fix was removed, and the cells were washed in PBS 5 times. The cells

were then permeabilised for 20 minutes on ice and then blocked (IF blocking buffer) for 1hr at 37°C (Table 2.1-a). Primary antibody (Table 2.1-c) was diluted in blocking buffer and applied to glass slide, 15 µl per coverslip. The glass coverslip was applied onto this with cells facing down and cemented down using Fixogum. This was stored in a humidified chamber overnight at 4°C. The coverslips were then placed back into a 24 well plate with cells facing upwards, and washed 5x with 1x PBS for 5 minutes. The appropriate targeting secondary Alexa Fluor antibody (Table 2.1-d) was applied for 1 hr at 37 °C; the plate was covered in tin foil to protect the secondary antibody from light. The cells were washed 5x with 1x PBS for 5 minutes. The coverslips were allowed to dry on Whatman paper. To visualize the nuclei a counterstaine was applied, either DAPI, or Vectashield, or Hoechst (Table 2.1-b). The coverslips were sealed using clear nail polish and stored at 4°C. The cells were viewed microscopically using Nikon E800 microscope with DN100 imaging camera and imaging software, 100x objective, using FITC and DAPI filters, or using Leica SP8 Laser Scanning Confocal Microscope equipped with a 63x objective. Analysis was performed using CellProfiler software, minimum 100 cells viewed per control/ treatment.

For the analysis of signal from fluorescent proteins from either transient transfection or inducible expression, cells were seeded and transfected as described in section 2.2.10.3, or seeded and induced as described in section 2.2.11. Following the required incubation, the medium was removed and the cells were washed x2 with PBS and fixed using 4% fixing (Table 2.1-a**Error! Reference source not found.**) s olution for 10 minutes at 4℃. The fixing solution was then removed and 1x PBS washes performed 2 times. The cells were stained with 20000x Dapi and viewed microscopically using Nikon E800 microscope with DN100 imaging camera and imaging software, 100x objective, using FITC and DAPI filters.

2.5 Analysis of mitochondrial membrane potential

ASC52telo cells were seeded at 5000 cells per cm^2 in two 96 well plates, with blank wells either side; both plates were kept under the same conditions. PHA-767491 treatment was applied following the PHA model. The cells were incubated for 72 hours. One plate was analysed with the MTS viability assay (Section 2.2.7.2). The other plate was analysed using TMRE (tetramethylrhodamine, ethyl ester) assay (abcam 113852), for this, FCCP (20µm) (carbonyl cyaninde 4-(trifluoromethoxy)

phenylhydrazone) was added in FCCP control wells at 1000x dilution in culture media, cells incubated for 3 hours. TMRE at 400µm in culture media was added to each well and incubated for 30 minutes, plate wrapped in foil to protect from light. All wells were washed x2 with 0.2% BSA. TMRE was read at Ex/Em 549/575nm**,** Infinite® M200 from Tecan.

2.6 Molecular cloning

2.6.1 RECQL4-Emerald tagged construct

The Emerald-GFP tagged expression construct, pXPfrtto-RECQL4-Emerald, was generated with the Gateway® site-specific recombination cloning system by recombining the pENTR-RECQL4(F0) entry clone with the pDESTfrtto-Emerald-N0 expression vector, and was performed by Dr Csanad Bachrati. The recombinant constructs were verified with restriction fragment mapping.

2.6.2 Preparation of LB-Agar plates and LB-broth

1l of LB was prepared by the addition of 25g LB broth (Miller) powder (Sigma-Aldrich) to 1l distilled water and sterilised by autoclaving. 1l LB-agar was prepared by dissolving 25g of LB broth (Miller) powder (Sigma-Aldrich) and 8g of agar powder (Sigma-Aldrich) in 1l of deionised water, and sterilised by autoclaving. When the LB-agar was cooled to ~50°C Ampicillin was added to the final concentration of 100 µg/ml. 20ml of LB-agar/Amp was poured into 10cm diameter bacterial petri dishes and allowed to cool to room temperature.

2.6.3 Transformation

Transformation procedure was performed using aseptic technique, over Bunsen flame.

A 25 µl aliquot of bacterial host cells (*Escherichia coli* NEB5α; fhuA2 Δ[argF-lacZ]U169 phoA glnV44 Φ80Δ [lacZ]M15 gyrA96 recA1 relA1 endA1 thi-1 hsdR17; New England Biolabs) was thawed on ice slowly. 1 µl RECQL4 construct was added and mixed and was incubated on ice for 30 minutes. The bacterial cells were heat shocked at 42℃ for 35 seconds, and were transferred onto ice for 2 minutes. 75 µl SOC medium was added to top up to 100 µl and the cell suspension was

incubated for 1 hour at 37℃ with vigorous shaking. Aliquots of the recovered culture were spread onto previously cooled agar plates, at variable concentrations (Table 2.1-i). The plates were then incubated at 37℃ overnight upside down for the prevention of condensation formation.

2.6.4 Small scale purification of plasmid DNA (miniprep)

Eight single colonies were selected from the 10 µl transformation plate, and inoculated into 5 ml LB and ampicillin at 100 µg/ml in separate vented-lid tubes, and incubated overnight at 37℃, with shaking at 190 rpm.

The isolation of high purity plasmid DNA was performed as per Miniprep Qiagen protocol (Qiagen, 2012). Bacterial cells following overnight growth in LB were harvested by centrifugation at 13,000rpm at room temperature for 3 minutes. The cell pellet formed was re-suspended in 250µl P1 buffer followed by lysing with mixing 250 µl P2 buffer. 350 µl of P3 buffer was added and mixed to precipitate genomic DNA. Precipitated genomic DNA and cell debris was sedimented by centrifuging at 13.000 rpm for 10 minutes at room temperature. The supernatant was collected into a QIAprep spin column. The column was centrifuged for 1 minute at 13,000 rpm and the flow through discarded. 500 µl PB buffer was used to wash the columns, centrifuged at 13,000 rpm for 1 minute. 750 µl PE buffer was added and again centrifuged. The flow-through was discarded and the column was again spun down to remove residual wash buffer. Bound plasmid was eluted by the addition of 50 µl EB buffer, followed by centrifugation. DNA concentration was determined using Nanodrop as per manufacturer's instructions.

2.6.5 Medium scale plasmid purification (maxiprep)

High yield isolation of high purity plasmid DNA was performed as per Maxiprep Qiagen protocol (Qiagen, 2012). 200ml of selective LB was inoculated with 1ml of starter culture and was incubated overnight in a 500ml conical flask at 37°C with shaking at 250rpm. Bacterial cells were harvested by centrifugation at 6000g for 15 minutes at 4°C, and the pellet was re-suspended in 10ml P1 buffer. 10ml P2 buffer was added to this suspension to lyse the cells, mixed and incubated at room temperature for 5 minutes. 10ml of 4°C P3 buffer was added with mixing and incubated on ice for 20 minutes. This was centrifuged at 20000g at 4°C for 30 minutes to remove precipitated material. The Qiagen-tip 500 column was

equilibrated with QBT buffer. The supernatant of centrifuged sample was then applied to the Qiagen-tip 500 column and washed 2x with 30 ml QC buffer and eluted with 15ml QF buffer. Precipitation followed using isopropanol, the sample was centrifuged at 15000g for 20minutes at 4°C and washed with 70% ethanol. Once dried the pellet was re-suspended in 1ml nuclease-free water and stored at -20 °C. DNA concentration was determined using Nanodrop as per manufacturer's instructions.

2.6.6 Analysis of plasmids via restriction digestion and gel electrophoresis

Plasmid DNA was purified using the Miniprep protocol (Section 2.6.4). The recombinant constructs were verified with restriction fragment mapping. A digest mix (Table 2.1-j) was incubated at 37℃. An agarose gel was prepared (Table 2.1-a), with the addition of 4 µl Safeview and was poured into Biolab mini-sub cell GT tray with combe and allowed to cool and set. Samples were centrifuged briefly at 13000rpm, followed by the addition of 1/5th volume of 6x loading dye (New England Biolabs, B7024S). Undigested controls were made using plasmid, water and loading dye. Samples were run alongside a 2 log DNA ladder (New England Biolabs) at 80 V for 60 minutes. Gel images were captured using Bio-Rad ChemiDoc™ MP imaging system (Bio-Rad), with Image lab 4.1 software.

2.6.7 Generation of shRNA constructs

Two pairs of oligonucleotides coding for the stem-loop structure of an shRNA that target the 3' untranslated region of RECQL4 were custom synthesised (Table 2.1-k). The annealing reaction mix was set up as shown in (Table 2.1-l) and a PCR machine was programmed to anneal the top and bottom oligonucleotides (Table 2.6-a). The pLKO.1 vector was digested with EcoRI, heat inactivated, purified (Qiagen PCR purification kit), further AgeI digested and the digested pLKO.1 plasmid was purified following agarose gel electrophoresis (Qiagen gel extraction kit) (Addgene). A ligation reaction (Table 2.1-m) was set up and the ligated constructs were transformed into STABL-1 (Invitrogen, Thermo Fisher Scientific) competent cells using the protocol described in section 2.6.3.

Table 2.6-a PCR set up in (PCR-C100 Touch thermal cycler, BioRad).

Temperature (℃)	Time (minutes)
95	10
94	2.5
93	2.5
92	2.5
91	2.5
90	2.5
89	2.5
88	2.5
87	2.5
86	2.5
85	2.5
84	2.5
83	2.5
82	2.5
81	2.5
80	2.5
79	2.5
78	2.5
77	2.5
76	2.5
75	2.5
74	∞

2.6.8 Generation of lentiviral vector and transduction of ASC52telo cells

Generation of 4th generation lentiviral particles was performed by Dr Timea Palmai-Pallag following the well established protocol of Addgene (Adggene). The shRNA constructs were co-transfected with pRSV/REV, pMDLg/pRRE, pMD2G plasmids into 293T cells. The resulting supernatant, containing the infectious lentiviral particles was used to transduce ASC52telo cells.

2.7 DNA fingerprinting

2.7.1 Preparation of genomic DNA with phenol-chloroform extraction

Cells were cultured in T25 flask until around 90% confluency. Cells were harvested following trypsin-EDTA treatment (Section 2.2.1), centrifuged at 1000rpm for 5 minutes, and the supernatant was removed to establish a cell pellet. The cell pellet was washed by re-suspending in PBS and centrifuging at 1000rpm for 5 mins. The wash step was repeated 3x and cell pellet was stored at -20℃. The pellet was re-

suspended in 300µl DNA lysis buffer (100mM Tris Hcl and 5mM EDTA in H2O) and mixed well by vortex for 1 minute. 15µl of 20% SDS and 6 µl of 10mg/ml Proteinase K (Thermo Fisher Scientific) was added, mixed and incubated at 55°C overnight. 1 volume of Phenol:Chloroform:Isoamyl alcohol 25:24:1 (Thermo Fisher Scientific) was added and mixed well by inverting for 3 minutes,+ and centrifuged at 13200rpm for 5 minutes. The supernatant was carefully removed into a new 1.5ml microcentrifuge tube and the precipitate discarded. The extraction step was repeated with an equal volume of chlorophorm. 0.1 volumes of 3M sodium-acetate pH 5.2 and 2.5 volumes of 100% ethanol was added to the DNA solution mixed and incubated at -20°C overnight. The precipitated DNA was centrifuged at 4℃ for 30 minutes at 13000rpm. The supernatant was discarded and to wash the DNA 500µl of 70% ethanol was added, the pellet was mixed with vortexing for 20 seconds, and centrifuged again at 4℃ for 30 minutes at 13000rpm. The supernatant was carefully removed and DNA pellet was air dried, and resuspended in nuclease free H_2O.

2.7.2 DNA fingerprinting with the GenePrint 10 kit

For amplification, the extracted DNA concentration was determined using NanoDrop. The GenePrint® 10 5X Master Mix and GenePrint® 10 5X Primer Pair Mix were completely thawed and centrifuged briefly to bring the contents to the bottom, and vortexed to mix well. Samples were prepared in the order as listed in Table 2.1-n. For the positive control 2800M DNA (part of the kit) was added (1µl), and amplification grade water was used as negative control, in place of DNA template. The reaction mixture was then run in Thermal cycle (PCR-C100 touch thermal cycler BioRad) as shown in Table 2.7-a .

Table 2.7-a Thermal cycling settings

Temperature (℃)	Time (seconds)
96	60
94	10
59	60
72	30
For 30 cycles then;	
60	600
4	soak

2.7.3 The detection of amplified fragments

A loading cocktail was prepared by combining the internal lane standard 600 (0.5µl) and Hi-Di™ formamide (9.5µl) per sample. This was mixed and added to tubes before the addition of 1µl of amplified sample, or 1µl of GenePrint® 10 Allelic Ladder Mix; used to provide sizing and genotyping of the amplified fragments. The samples were centrifuged briefly, and denatured at 95°C for 3 minutes, before chilling on ice for a further 3 minutes. The samples were loaded into Applied Biosystems ABI Prism 310 genetic analyser and ran with parameters set out in Table 2.7-b.

Table 2.7-b Applied ABI prism 310 genetic analyser parameters

Parameter	
Amplification type	HID
Capillary length	36cm
Polymer	POP-4® (ThermoFisher Scientific P/N 402838)
Running Buffer	10x with EDTA (ThermoFisher Scientific P/N 402824)
Dye set	Promega 4Dye
Internal colour	60
Temperature	Red
Pre-Injection EP time	120 seconds
Syringe pump time	150 seconds
Injection time	24 seconds
EP voltage	15kV
Laser	9.8mW
Run time	1440 seconds

2.7.4 Statistical analysis

Statistical significance was calculated by the Tukey post hoc test following one-way ANOVA analysis. Significant P-value determined as >0.05.

3 Chapter 1 Interfering with DNA replication initiation

Results

Literature data supports that replication initiation is impaired in cells that contain either mutated or no RECQL4 protein (Matsuno et al., 2006). Establishing our model system in mesenchymal stem cells was hindered by the lack of availability of mutated MSCs. To determine a potential link between interference of DNA replication initiation and tumourigenesis, we employed the dual Cdc7/Cdk9 inhibitor, (PHA-767491) to establish a model of mild replication initiation inhibition in ASC52telo cells, which was expected to reduce proliferation.

ASC52telo cells can differentiate into three lineages, adipocytes, chondrocytes, and osteocytes. It was important to determine if this capability was maintained in cells under PHA-767491 treated model.

Several studies have suggested that RECQL4 may have a role in mitochondrial DNA maintenance (Croteau et al., 2012; Chi et al., 2012; Gupta et al., 2014), which in turn can lead to mitochondrial dysfunction. To determine if the PHA-model generates changes in mitochondrial function, mitochondrial membrane potential was measured, which closely relates to mitochondrial membrane permeability (Dai et al., 2015).

3.1 Establishing the model system for inhibition of DNA replication initiation

The first step for mild proliferation inhibition through the interference of DNA replication initiation was the identification of a suitable PHA-767491 concentration. A suitable seeding density in 96 well plate was determined in a preliminary experiment first using the MRC5 normal fibroblast cell line. The seeding density of 2000 cells per well over 8 days showed steady cell proliferation while maintaining cell viability (Figure 3.1-a), PHA-767491 was found to inhibit cellular growth following the treatment in MRC5 using a range of concentrations. A reduced but steady proliferation rate was shown with around 1.5µM PHA-767491 (Figure 3.1-b). A range of other cell lines: MRC5, AG05013tert, and HS68tert, showed a similar sensitivity profile (Figure 3.1-c), however with very wide variability. We concluded that the large observed variability seen in (Figure 3.1-c) could be due to the instability of PHA-767491 and repeated the experiment with media changes every

3 days. Under these conditions, PHA-767491 treated HS68tert cells showed a more stable inhibition of proliferation, confirming the degradation of the PHA-767491 over time (Figure 3.1-d).

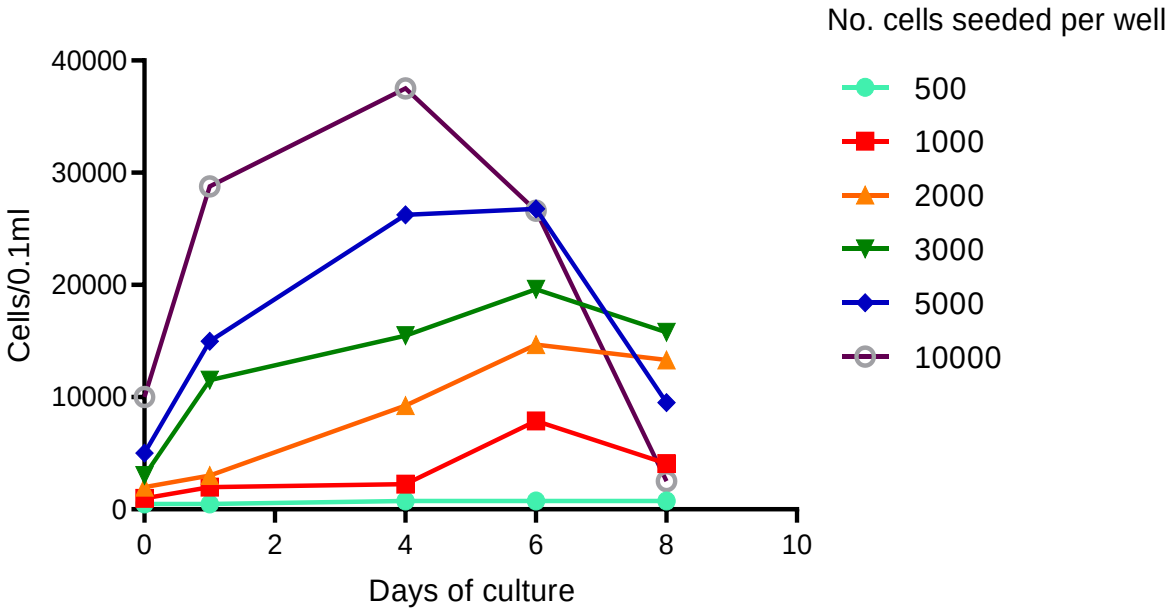

Figure 3.1-a Establishment of a suitable seeding density. MRC5 cells were seeded at the indicated densities in a 96 well plate, and cell number was established using a BioRad TC20 cell counter daily for 8 days. The seeding density of 2000 cells per well was found to be appropriate, showing steady proliferation rate while maintaining cell viability. Graph shows results of one experiment (n=1).

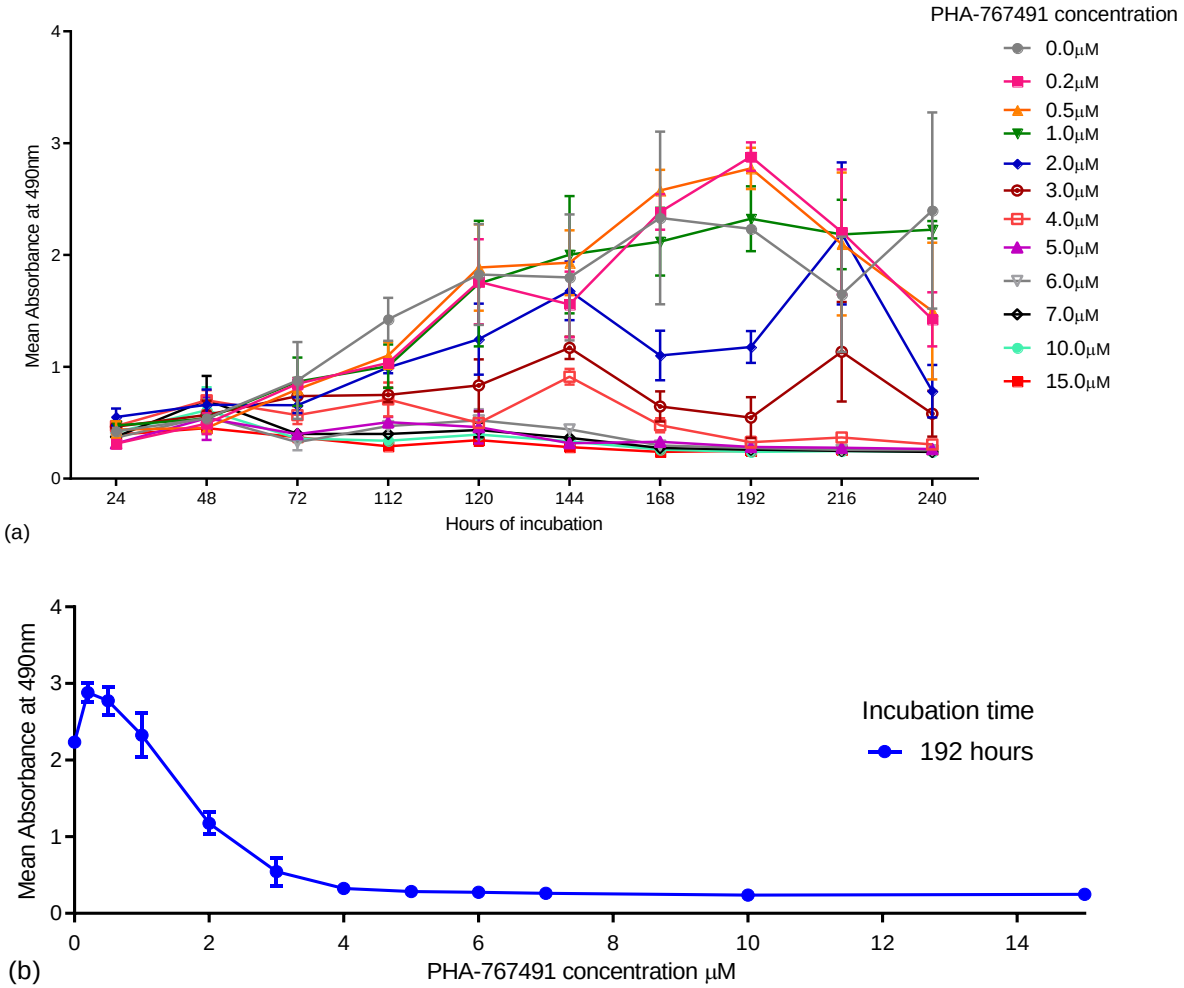

Figure 3.1-b Sensitivity of MRC5 cells to PHA-767491. MRC5 cells were seeded at 2000 cells per well in 96 well plate, and incubated overnight. The cells were then treated with the indicated concentrations of PHA-767491. (a) Cell proliferation was established using the MTS assay daily for 10 days, read at 490nm, (b)192 hours IC50 1.58µM. Data represents SD of triplicates, from one experiment (n=1).

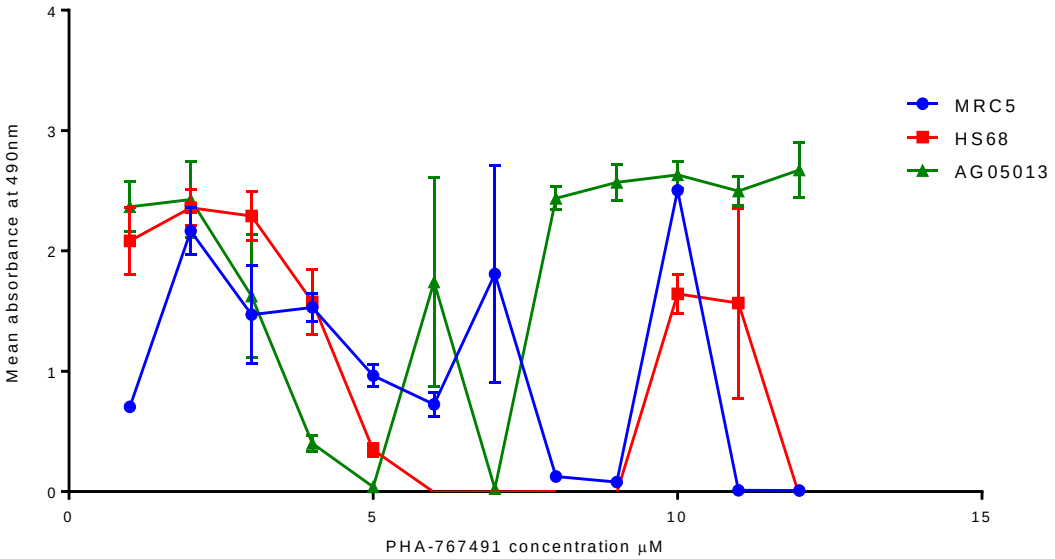

Figure 3.1-c Sensitivity of MRC5, AG05013tert, and HS68tert cells to PHA-767491. Each cell line was seeded at 2000 cells per well as triplicates and incubated overnight. The cells were then treated with the indicated concentration of PHA-767491. Cell proliferation was established using the MTS assay 7 days post PHA treatment. Data represents SEM of triplicates, from one experiment (n=1). Proliferation of cells showed a decrease in response to increased PHA-767491 concentration; however, was highly variable most likely due to instability of the drug.

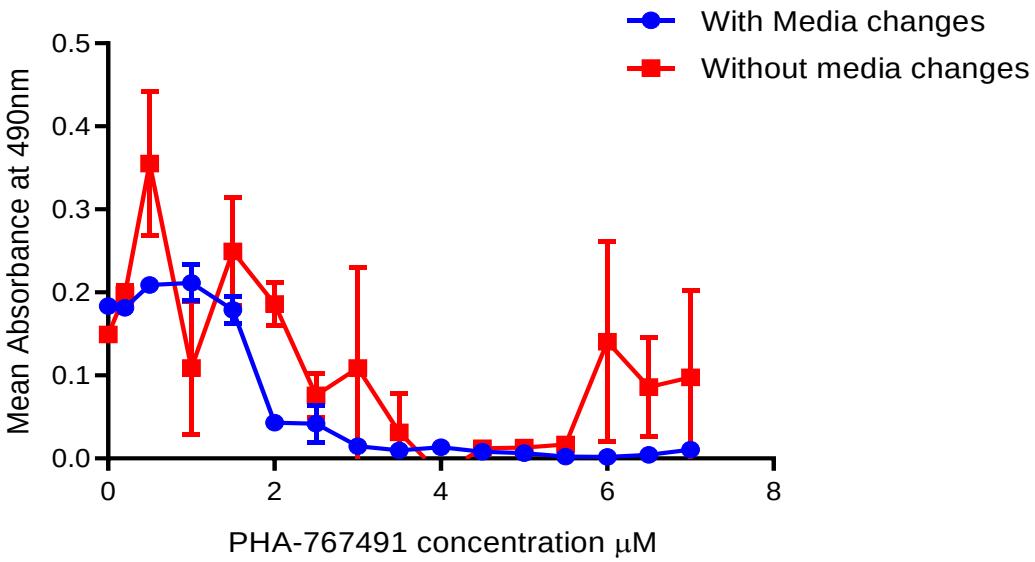

Figure 3.1-d Sensitivity of HS68tert cells to PHA-767491 with or without media changes. Cells were seeded at 2000 cells per well in 96 well plate in triplicates, and were treated with the indicated concentrations of PHA-767491, alongside controls. On one plate the medium was changed every three days. Cell viability was established after 7 days of incubation following PHA-767491 treatment using the MTS assay. Averages were taken of the absorbance readings. The graphs indicated that medium changes are required to produce steady and reproducible response. Data represents means ± SEM of triplicates from one experiment (n=1). With media changes the IC50 of PHA-767491 was calculated to be 1.7µM.

To determine sensitivity of mesenchymal stem cells to inhibition of replication initiation, ASC52telo cells (hTERT immortalized adipose derived mesenchymal stem cells) were treated with PHA-767491. A reduction in cell viability was demonstrated with the increase of PHA-767491 concentration, suitable viability

seen with 2500 cells seeded per well and so 5000 cells per well seeding was not repeated (Figure 3.1-e). Low passage ASC52telo cells appeared to be more sensitive to low concentrations of PHA (Figure 3.1-f), with increase in cell viability at higher PHA concentrations. This is not expected or explicable, and although was seen twice, would need repeating to verify. PHA-767491 at around 1.5 µM demonstrated a reduction in cell proliferation while maintaining cell viability.

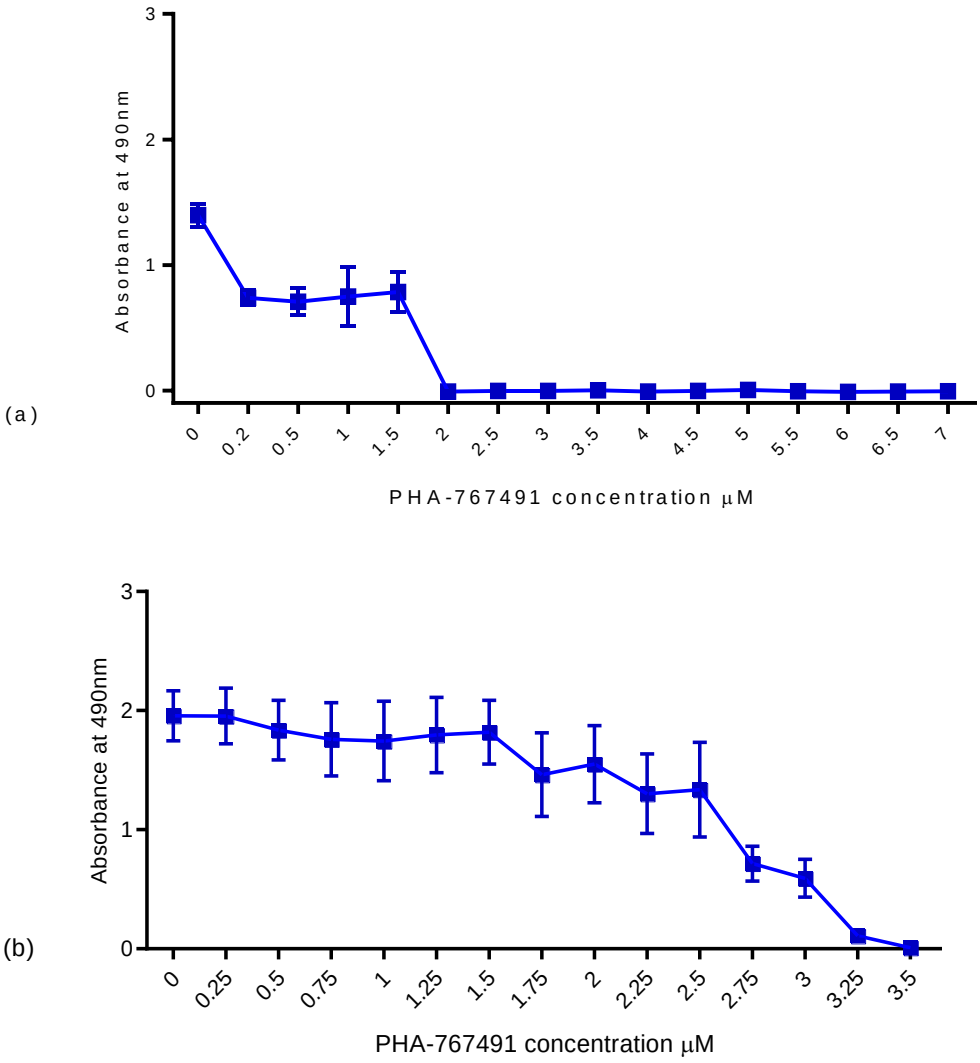

Figure 3.1-e PHA-767491 sensitivity in ASC52telo cells. 5000 (a) and 2500 (b) ASC52telo cells (p+6) were seeded per well in a 96 well plate, in triplicates. 18 hours post seeding medium was changed with the addition of PHA-767491 at the indicated concentrations, with media changes with PHA-767491 at appropriate concentrations every 3 days. MTS absorbance was read at 490nm 10 days post initial PHA767491 treatment. Error bars represent the standard error of means (SEM) of triplicates combined from one (a) or two (b) independent experiments. Sensitivity to PHA-767491 was observed with increasing concentrations, with more steady reduction of cell viability observed with 2500 cells per well. (a) IC50 = 0.48 µM, (b) IC50 = 2.5 µM.

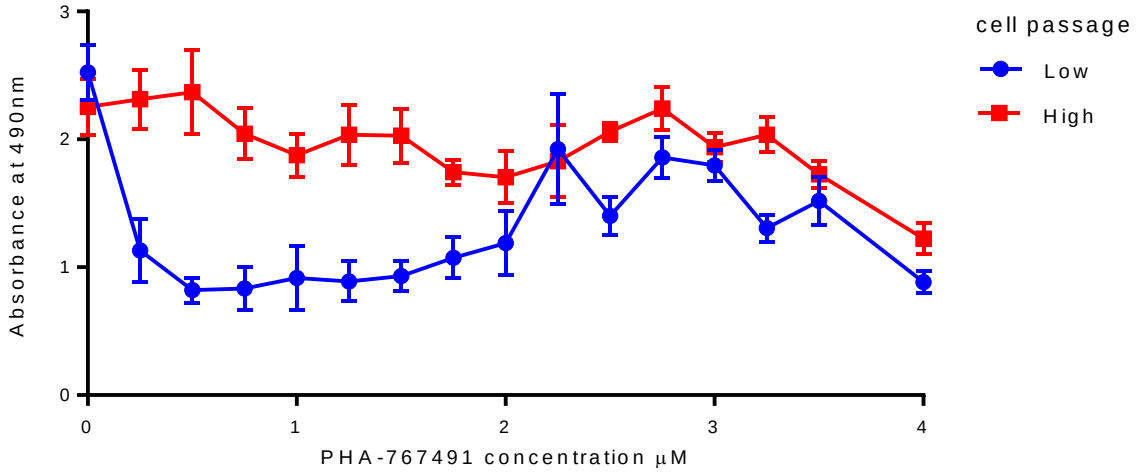

Figure 3.1-f PHA-767491 sensitivity of high and low passage ASC52telo cells. 2500 ASC52telo hTERT immortalized adipose derived mesenchymal stem cells were seeded per well in a 96 well plate, in triplicates. 18 hours post seeding medium was changed with the addition of PHA-767491 treatment at variable concentrations, and then again every 3 days. MTS absorbance was read at 490nm 10 days post PHA-767491 initial treatment. Low; P+13, P+14, High: P+66, P+67, Error bars represent the standard error of means (SEM) of combined data from two independent experiments (n=2), Mann-Whitney test was applied to test statistical significance *** P≤0.001. Low passage ASC62telo appeared more sensitive to PHA-767491.

These preliminary experiments determined a PHA-767491 concentration appropriate for mild interference with DNA replication initiation at 1.5 µM. Using this concentration, a PHA-767491 model (PHA model) was set up to establish ASC52telo cell lines under acute treatment (low passages +6 to +38, high passages +43 to +96), chronic PHA-767491 treatment (low passages +18 to +41, high passages +53 to +90) and recovery in low and high passage cells.

Using this model, we first determined how chronic PHA-767491 treatment affects the viability and proliferative capacity of cells, and further verified the suitability of the selected PHA-767491 concentration. As cells were routinely cultured, at each passage, cell numbers (haemocytometer) and viability (trypan blue) was determined before the same number of cells were re-seeded. Cells under continuous PHA treatment showed a significant reduction in proliferation rate compared to untreated cells under the same conditions, verifying the effect of interference in DNA replication. A decrease of viability was also seen; however, this was not significant (Figure 3.1-g). Changes in cell morphology were also observed, cells appeared larger with chronic PHA treatment (Figure 3.1-h).

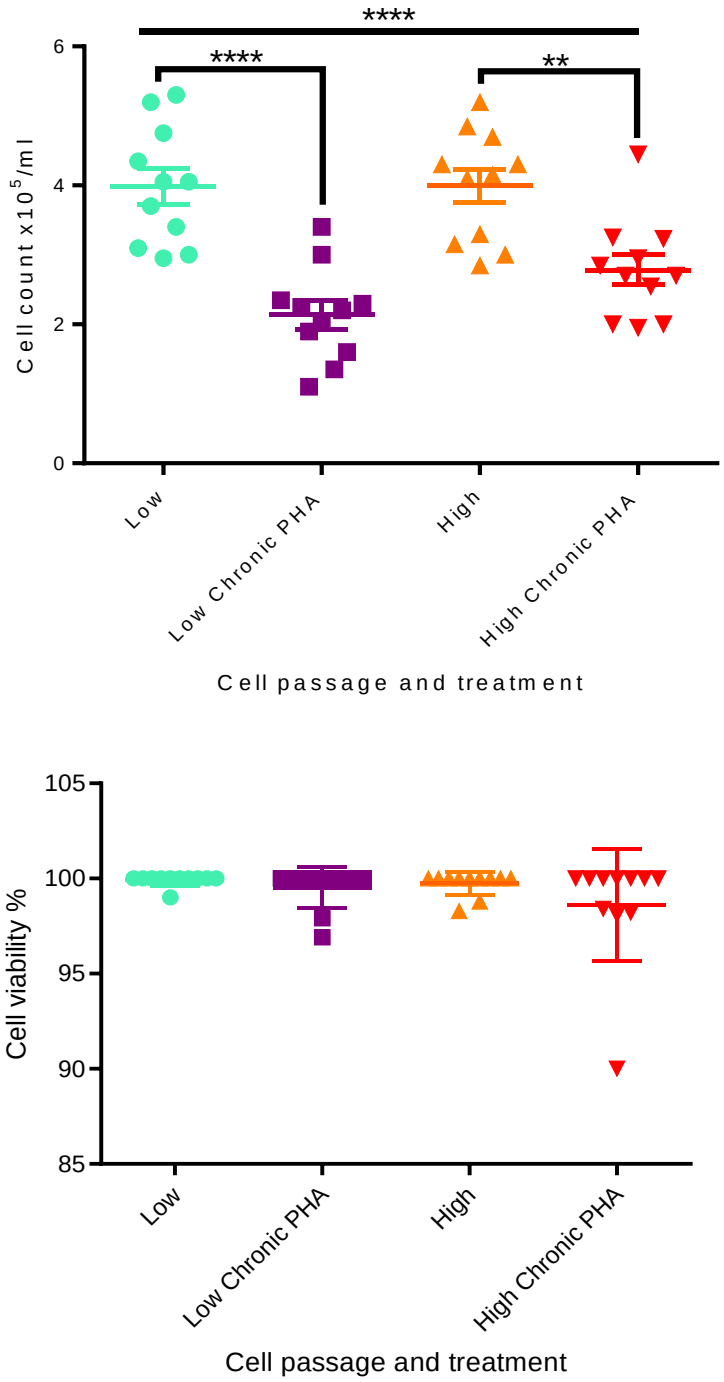

Figure 3.1-g Cell count and viability following chronic PHA-767491 treatment of ASC52telo cells. High and low passage ASC52telo cells were seeded at 5000 cells per cm^2 in T25 flasks, with or without chronic PHA-767491 treatment. At each passaging (every 3 days) cell count and viability was measured before cells were reseeded. Measurements were taken over several passages. Low – P+12 to 18, P+26-29, Low Chronic PHA – P+12 to 18, P+29 to 32, High – P+63 to 65, P+68 to 71, P+79 to 82. High Chronic PHA- P+53 to 57, P+67 to 73. Error bar represents SEM, statistical significance was calculated by the Tukey post hoc test following one-way ANOVA analysis. ** $P \leq 0.01$, ****$P < 0.0001$, graph shows data from two independent experiments combined (n=2). Chronic PHA treatment leads to decrease in proliferative rate while maintaining cell viability.

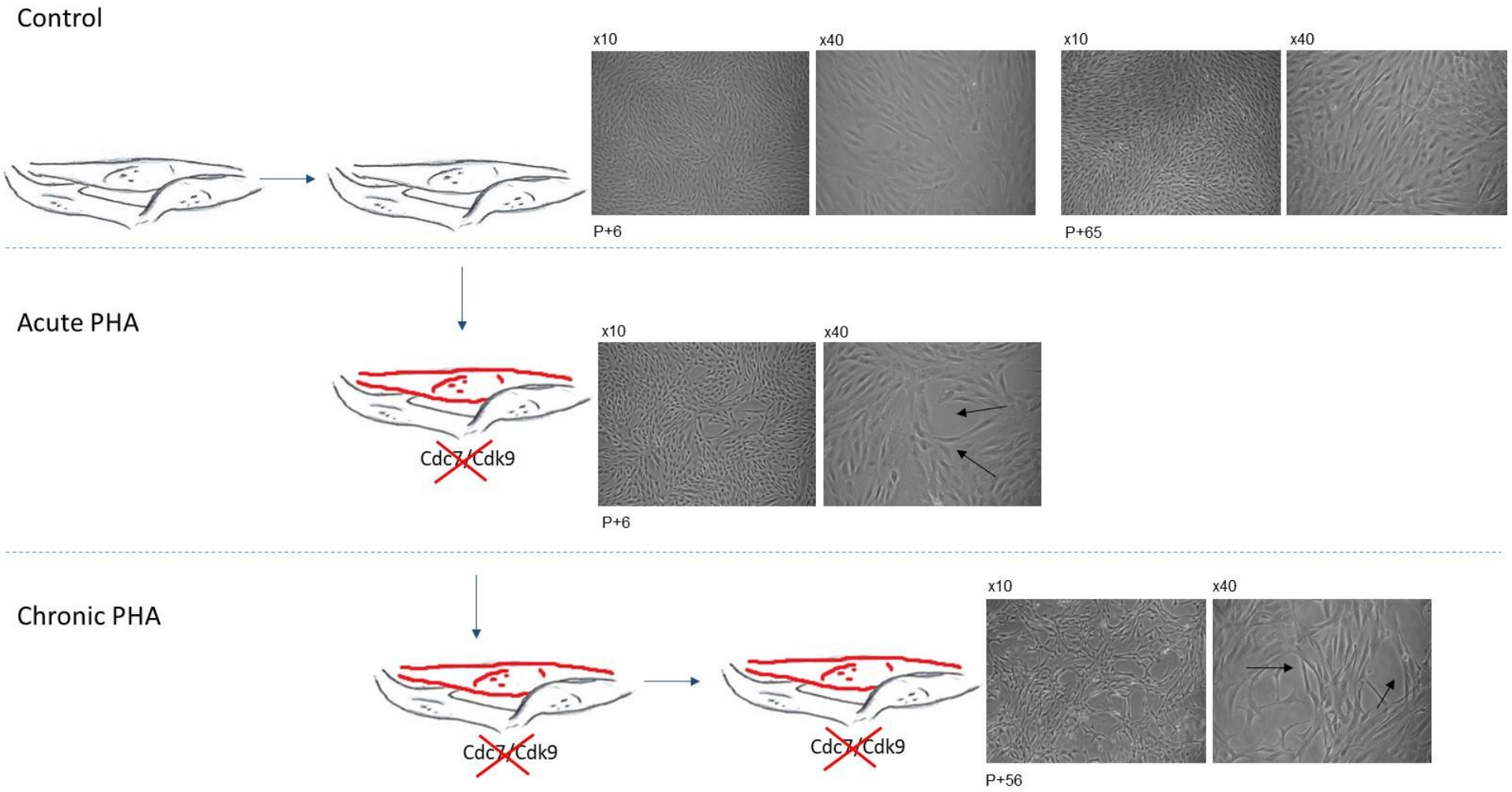

Figure 3.1-h Cell morphology of ASC52telo cells following acute and chronic PHA-767491 treatment. High and low passage ASC52telo cells were seeded at 5000 cells per cm^2 in T25 flasks, with or without PHA-767491 treatment. Low passage cells; PHA started at p+6. High passage chronic PHA; PHA started p+13 meaning that these cells have been cultured with PHA over 43 passages. Phase contrast images were taken during cell culture using a Nikon Eclipse TE2000 inverted microscope with x10 and x40 objective. Black arrows: reduced cell numbers are observed in cells treated with PHA-767491, and cells appeared larger.

Ki67 is a marker of proliferation; actively cycling cells stain strongly with Ki67, while resting G0 cells show low expression. In order to test how acute and chronic PHA treatment influences the proliferation capacity of ASC52telo cells low and high passage cells were fixed and stained with Ki67 and the signal intensity of the population was quantified. Interestingly, acute PHA treatment in ASC52telo cells appeared to have a level of Ki67 expression generally similar to non-treated cells, with a general increase seen compared to DMSO control cells. A decrease of Ki67 signal intensity was seen in cells treated with PHA for an extended period (chronic treatment). Cells were also treated with Camptothecin (CPT) as a control to demonstrate that while cells undergo DNA damage response a reduction of Ki67 expression is seen (Figure 3.1-i).

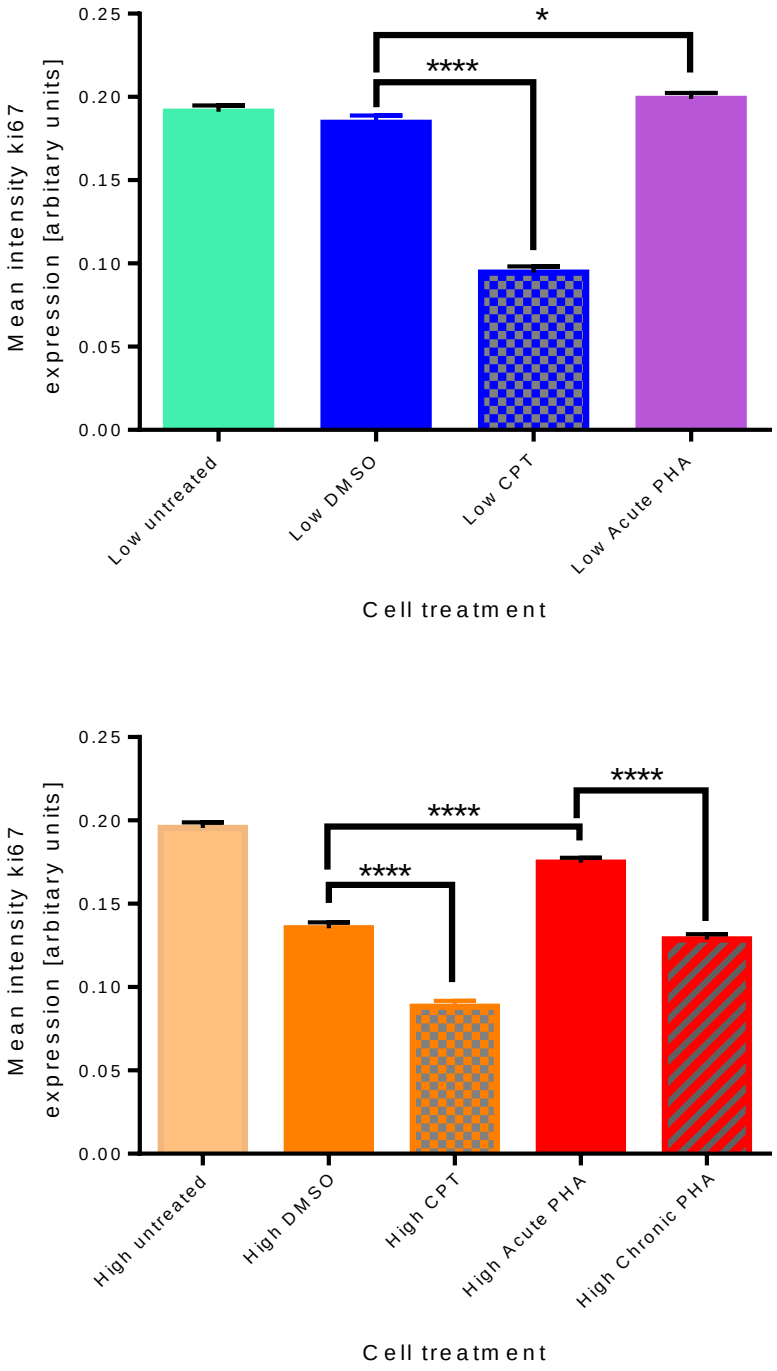

Figure 3.1-i proliferative state of ACS2telo cells following mild inhibition of replication initiation. High and low passage ASC52telo cells were seeded at 5000 cells per cm^2 in 24 well plate on glass coverslips, with or without acute or chronic PHA-767491 treatment. Camptothecin (CPT) was added for 24 hours. The cells were incubated for 72 hours before fixing in 4% paraformaldehyde and stained for Ki67 and DAPI. Images were collected using a Leica SP8 confocal microscope and analysed and quantified using CellProfiler. Statistical significance of difference was calculated by the Tukey post hoc test following one-way ANOVA analysis, *P≤ 0.05, ****P≤0.0001. Low passage cells: P+11, P+20, P+22, High Passage cells: P+62, P+90, P+88, High DMSO: P+62, P+90, P+88, Chronic PHA: P+62, P+90, P+88. Error bars represent the standard error of means (SEM) of combined data from three independent experiments (n=3). Reduced Ki67 expression observed in cells with CPT, and return to basal levels seen in chronic PHA-767491 cells.

3.1.1 PHA-767491 effect on osteocyte differentiation

ASC52telo cells undergoing acute and chronic PHA treatment, and without PHA treatment were successfully differentiated into osteoblasts. Cell morphology changes were seen (Figure 3.1-j), and osteoblast differentiation was verified by staining mineralised calcium deposits using Alizarin Red S stain (Figure 3.1-k, Figure 3.1-l, and Figure 3.1-n), and following chronic PHA-767491 (Figure 3.1-m). Differentiation capability was also followed and verified over time at 7, 14 and 21 days in low and high passage cells (Figure 3.1-n, and Figure 3.1-o). Generally, higher levels of calcified extracellular matrix was observed following PHA-767491 treatment (Figure 3.1-l, and Figure 3.1-o).

ASC52telo cells were successfully differentiated into adipocytes, as demonstrated with the appearance of lipid droplets stained red with Oil Red O (Figure 3.1-l), with and without acute PHA treatment over 7, 14, and 21 days (Figure 3.1-n and Figure 3.1-o). High passage acute PHA treated cells seem to have a reduced amount of lipid droplets.

Osteoblast, adipocyte, and chondrocyte differentiation was also verified in high passage ASC52telo cells, following Alizarin Red S, Oil Red O, and Alcian Blue staining, respectively (Figure 3.1-p).

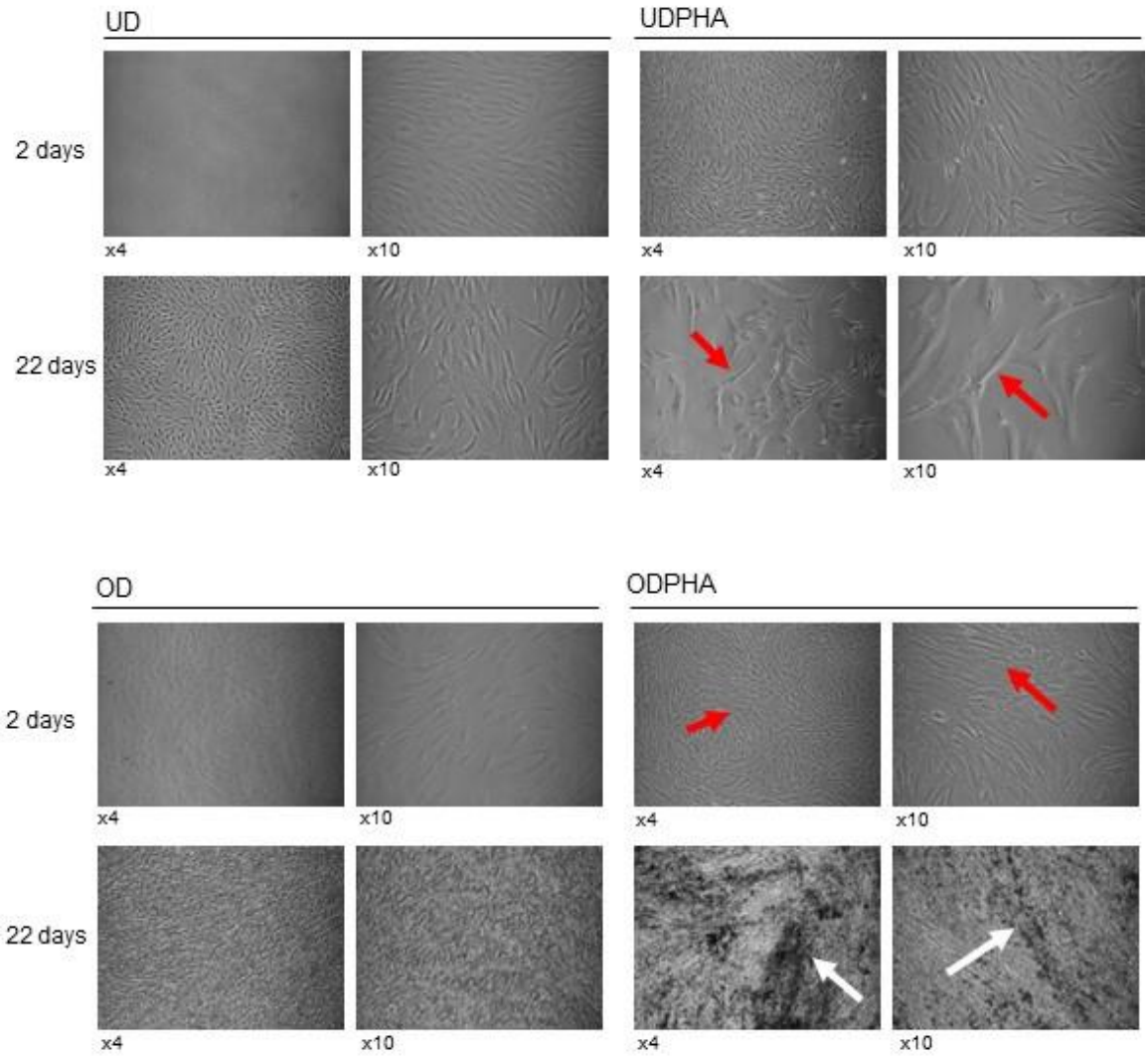

Figure 3.1-j Morphology changes of ASC52telo cells under osteoblast differentiation and acute PHA treatment. Low passage ASC52telo cells (p+13*)* were seeded at 5000 cells per cm^2 on 24 well plate and allowed to differentiate for 22 days. UD- undifferentiated cells, UD PHA- un-differentiated cells, acute PHA treatment. OD- Osteoid differentiation, OD PHA- acute PHA treatment and osteoid differentiation. Phase contrast images were taken on a Nikon Eclipse TE2000-s inverted microscope and Nikon DN100 camera with x4 and x10 objective. Changes in cell morphology were observed following differentiation, as expected, and confirm the differentiation capabilities of ASC52telo cells. PHA-767491 treated cells appeared larger (red arrows) and show signs of increased mineralisation (white arrows).

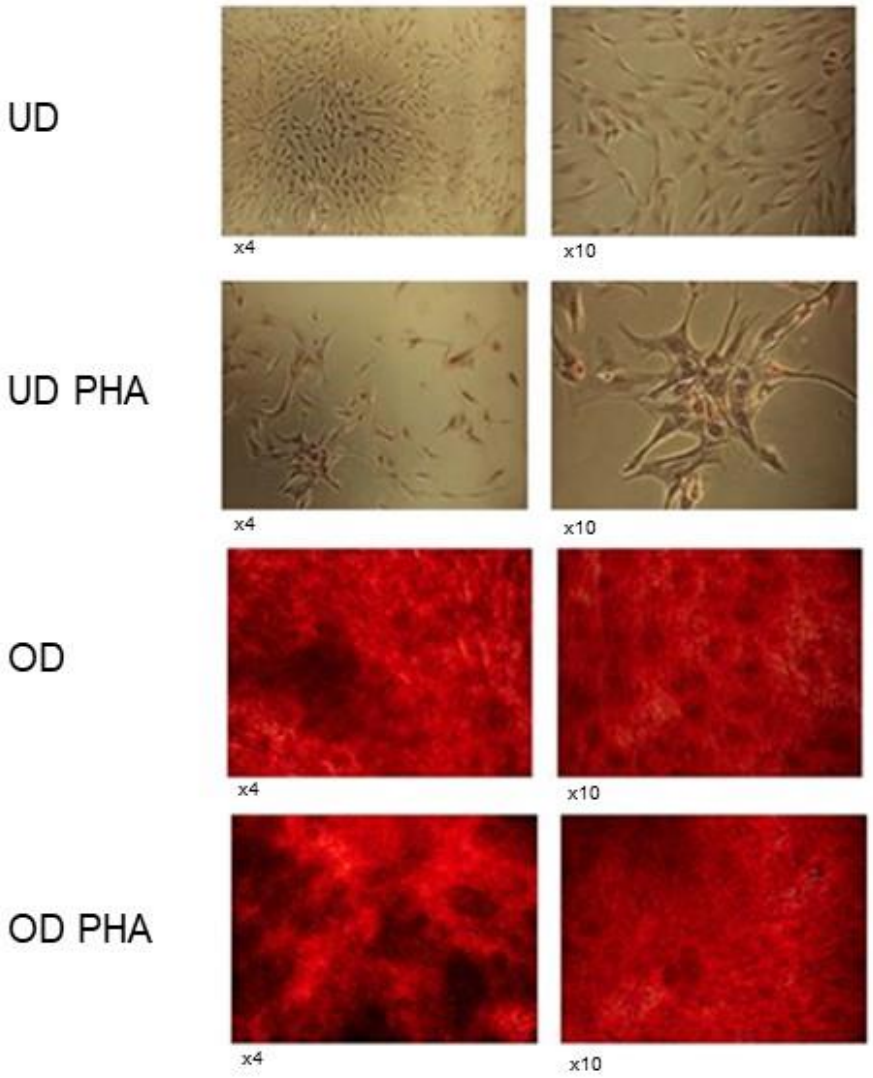

Figure 3.1-k Differentiation of ASC52telo cells to osteoblasts under acute treatment with PHA-767491. ASC52telo cells p+13 were seeded at 5000 cells per cm^2 on 24 well plate, and allowed to differentiate for 22 days with or without acute PHA treatment. Medium was changed every 3 days. Cells were fixed in 4 % formaldehyde in PBS and stained with Alizarin Red S (as per protocol). UD- undifferentiated cells, UD PHA- acute PHA treatment, un-differentiated cells. OD- Osteoid differentiation, OD PHA- acute PHA treatment, osteoid differentiation. Images were taken on a Nikon eclipse TE2000-s inverted microscope with a Nikon DN100 camera and x4, x10 objectives. Bright orange-red staining shows calcified deposits synthesised by MSC-derived osteoblasts.

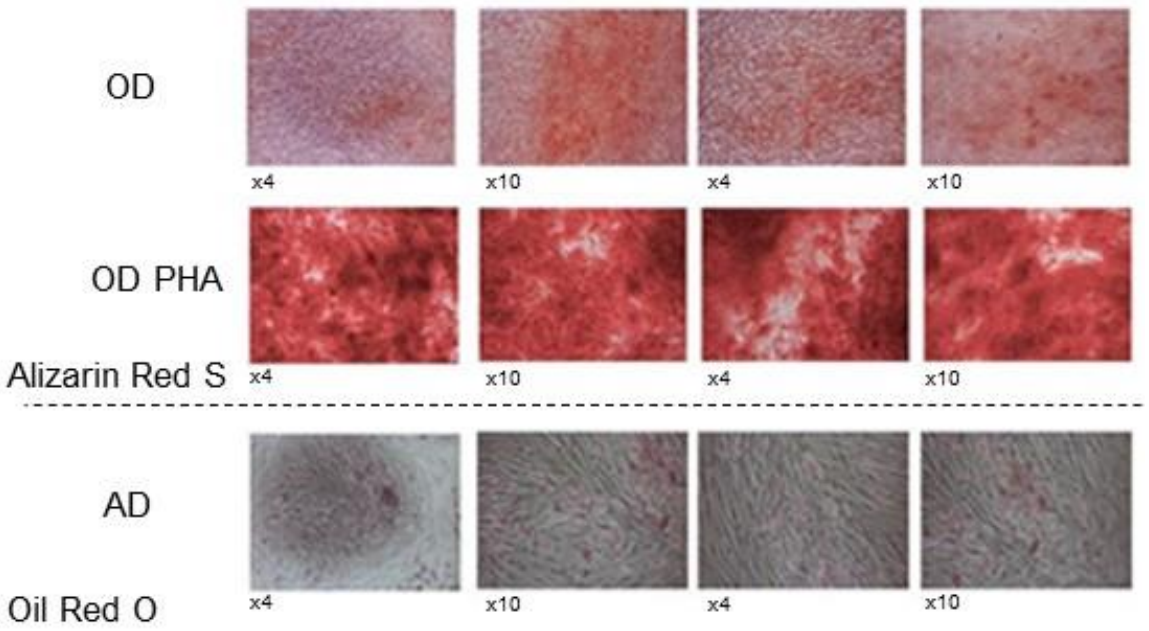

Figure 3.1-l Differentiation of low passage ASC52telo cells under acute PHA treatment. Low passage (P+17) ASC52telo cells were seeded at 5000 cells per cm^2 in 24 well plate and allowed to differentiate for 21 days in the presence or absence of PHA. Cells were fixed in 4 % paraformaldehyde in PBS and stained with Alizarin Red S. Bright orange-red staining demonstrates calcified deposits synthesised by differentiated osteoblasts. Oil Red O highlights lipid droplets in adipocyte differentiated cells. OD- Osteoid differentiation, OD PHA- acute PHA treatment, osteoid differentiation AD: Adipocyte differentiation. Images were taken on a Nikon Eclipse TE2000-s inverted microscope and a Nikon DN100 camera and x4, x10 objectives. Increased alizarin Red S staining seen between OD and OD acute PHA-767491 treated cells.

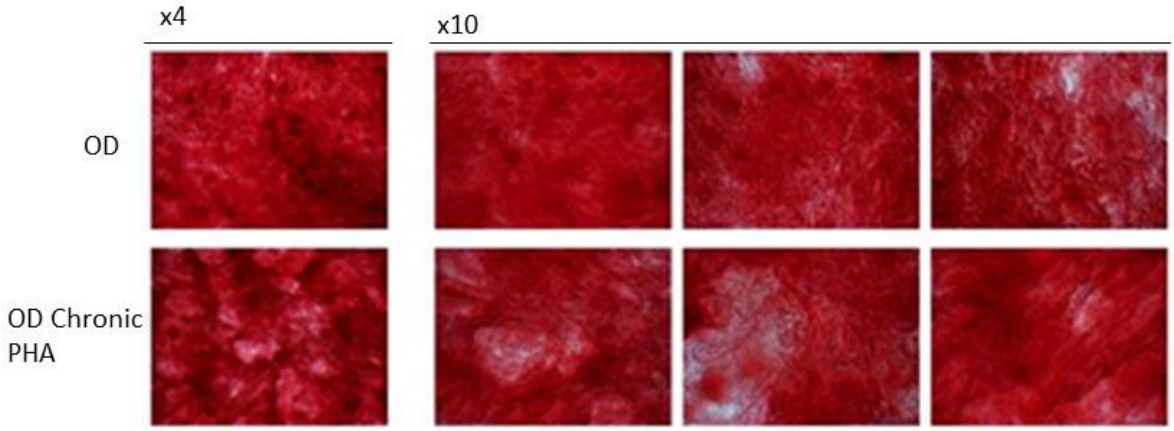

Figure 3.1-m Osteoblast differentiation in ASC52telo under Chronic PHA-767491 treatment. ASC52telo cells P+22 were seeded at 5000 cells per cm^2 and chronic PHA cells continued with PHA treatment (commenced P+13). Cells were allowed to differentiate for 21 days, with media changes every 3 days, were fixed with 4% formaldehyde in PBS and stained with Alizarin Red S. Images were taken on a Nikon Eclipse TE2000-s inverted microscope and a Nikon DN100 camera and x4, x10 objectives. Bright orange-red staining demonstrates calcified deposits synthesised by differentiated osteoblasts. OD: osteoid differentiation, OD Chronic PHA: osteoid differentiation with continual PHA-767491 treatment.

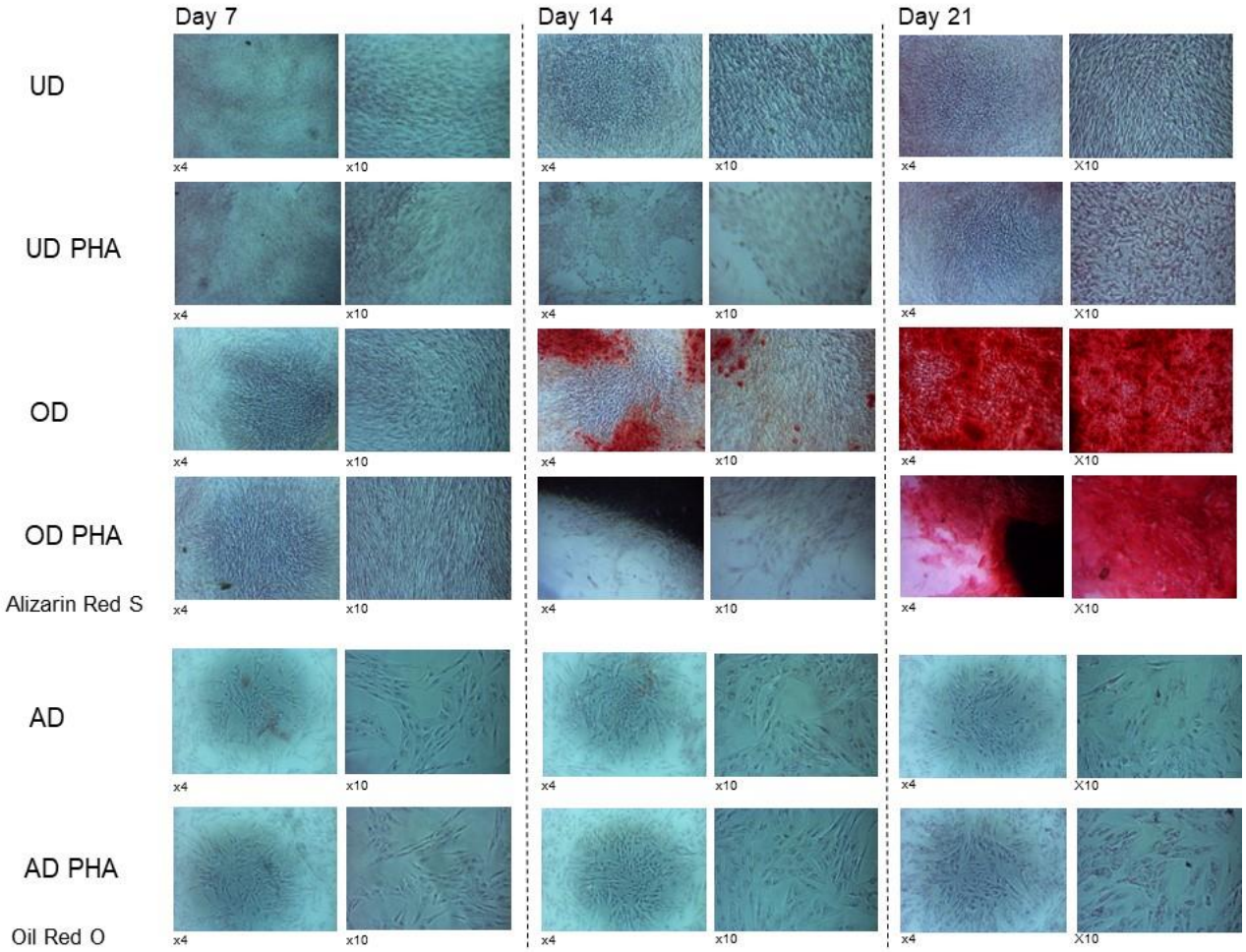

Figure 3.1-n Monitoring of osteocyte and adipocyte differentiation capability over 7, 14, and 21 days in acute PHA-767491 treated low passage ASC52telo cells. Low passage (P+28) ASC52telo cells were seeded at 5000 cells per cm^2 in 24 well plate and allowed to differentiate for 7, 14, and 21 days before being fixed in 4 % formaldehyde in PBS and stained with Alizarin Red S. Bright orange-red cells demonstrate calcified deposits, synthesised by osteoblasts. Oil Red O highlights lipid droplets in adipocyte differentiated cells. UD: un-differentiated, UD PHA: acute PHA treated, un-differentiated cells, OD: osteoid differentiation, OD PHA- acute PHA treated cells, osteoid differentiation, AD: Adipocyte differentiation, AD PHA: acute PHA treated cells, adipocyte differentiation. Images were taken on a Nikon Eclipse TE2000-s inverted microscope and Nikon DN100 camera, with x4, x10 objective.

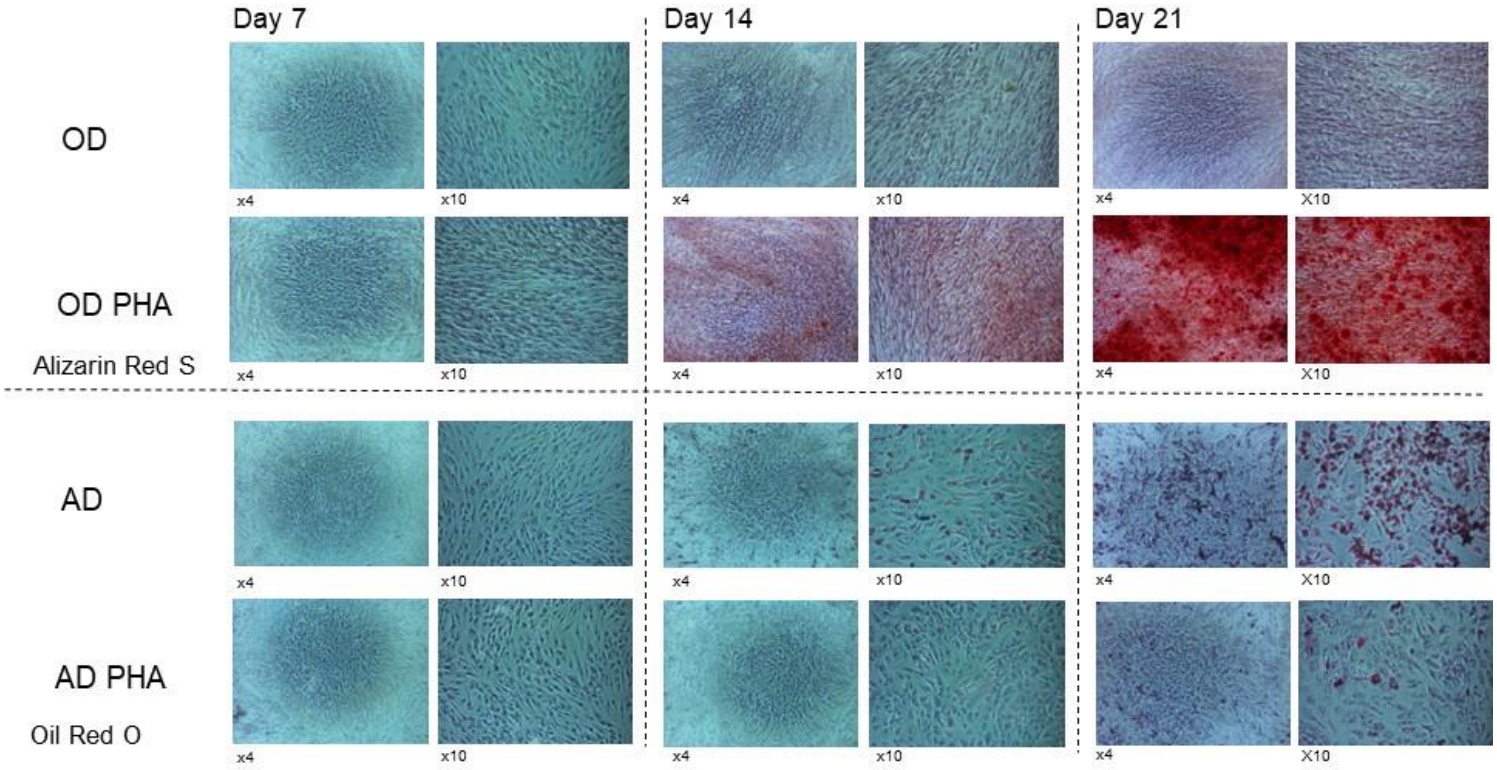

Figure 3.1-o Monitoring of osteocyte and adipocyte differentiation ability over 7, 14, and 21 days with acute PHA-767491 in high passage ASC52telo cells. High passage (P+81) ASC52telo cells were seeded at 5000 cells per cm^2 in 24 well plate, and allowed to differentiate for 7, 14, and 21 days before fixing in 4 % formaldehyde in PBS and stained with Alizarin Red S. Bright orange-red cells demonstrate calcified deposits synthesised by osteoblasts. Oil Red O highlights lipid droplets in adipocyte differentiated cells. OD: osteoid differentiation, OD PHA: osteoid differentiation with acute PHA-767491 treatment, AD: Adipocyte differentiation, AD PHA: adipocyte differentiation with acute PHA treatment. Images were taken on a Nikon Eclipse TE2000-s inverted microscope with Nikon DN100 camera and x4, x10 objectives

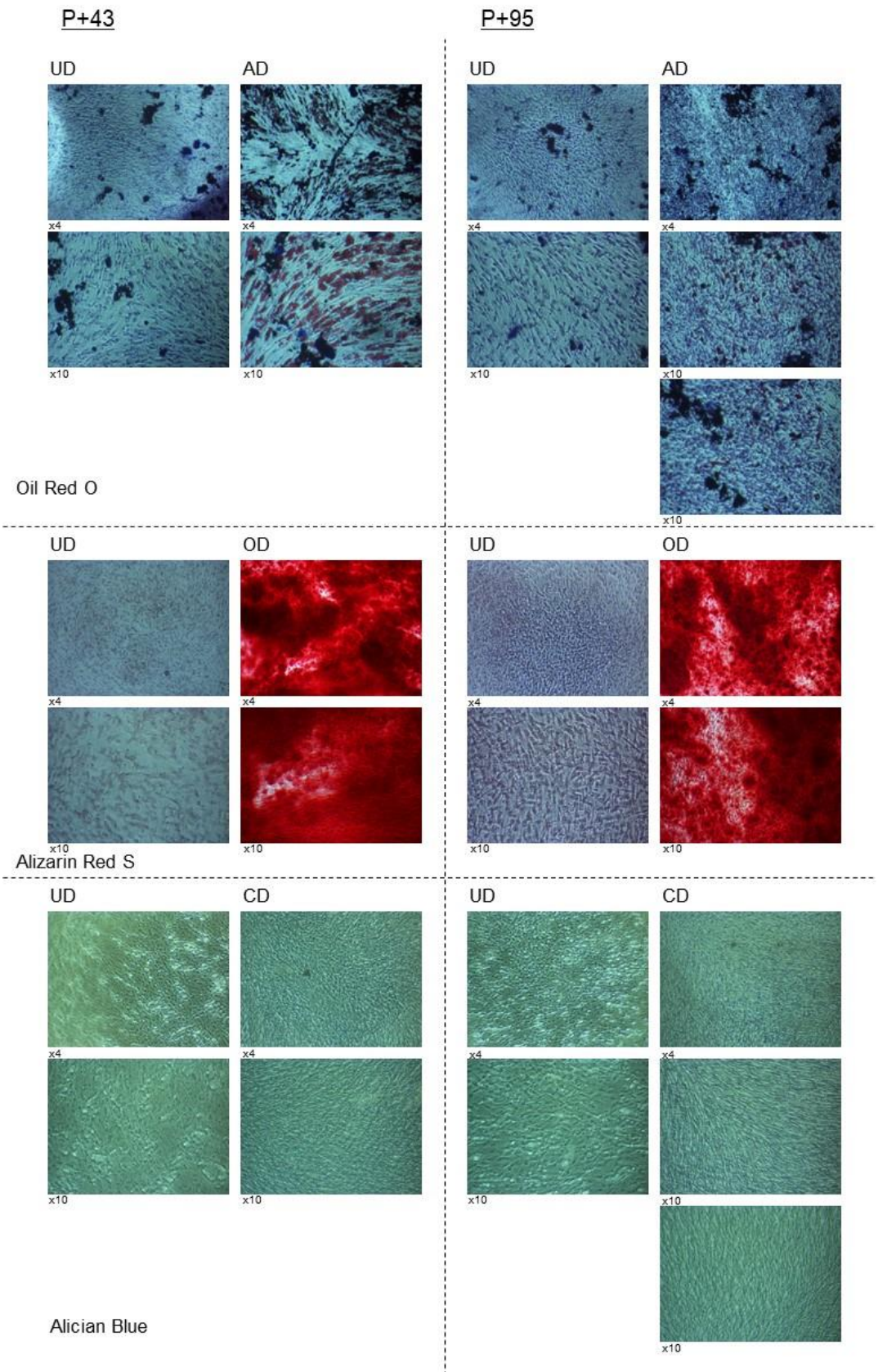

Figure 3.1-p Osteocyte, adipocyte, and chondrocyte differentiation in high passage ASC52telo cells. High passage (P+43 and P+95) ASC52telo cells were seeded at 5000 cells per cm^2 on 24 well plate, and allowed to differentiate for 21 days before fixing in 4 % formaldehyde in PBS and staining. Alizarin Red S staining highlights calcified deposits synthesised by osteoblasts, Oil Red O highlights lipid droplets in adipocyte differentiated cells, and Alcian Blue demonstrates the presence of proteoglycans synthesised by chondrocytes. UD: un-differentiated, OD: osteoid differentiation, AD: Adipocyte differentiation, CD: Chondrocyte differentiation. Images were taken on a Nikon Eclipse TE2000-s inverted microscope with Nikon DN100 camera and x4, x10. objectives.

In addition to using histological stains as described above, differentiating cells were stained for the expression of differentiation and proliferation markers. RUNX2 is a marker of osteoblast differentiation, with the most abundant expression seen in early differentiation, which reduces upon maturation. RUNX2 showed reduced expression upon osteoblast differentiation (Figure 3.1-q and Figure 3.1-r). Interestingly, RUNX2 expression appeared to increase in low passage ASC52telo cells with acute PHA-767491 treatment during osteoblast differentiation (Figure 3.1-q). A trend of this increase was also seen in subsequent experiments under chronic PHA-767491 (Figure 3.1-r and Figure 3.1-s) however, it was not always consistent, or proved statistically significant.

Ki67, as discussed above, is a marker of proliferation. Interestingly, cells kept in culture for long term (21 days) undisturbed, demonstrated an increase in Ki67 positive cells under acute PHA treatment. Although we have not formally verified this finding, it is likely that due to their slower proliferation rate under interference with replication initiation they reach confluency and exit the cell cycle later then the untreated culture, therefore contain more cycling cells at the day 21 timepoint (Figure 3.1-t).

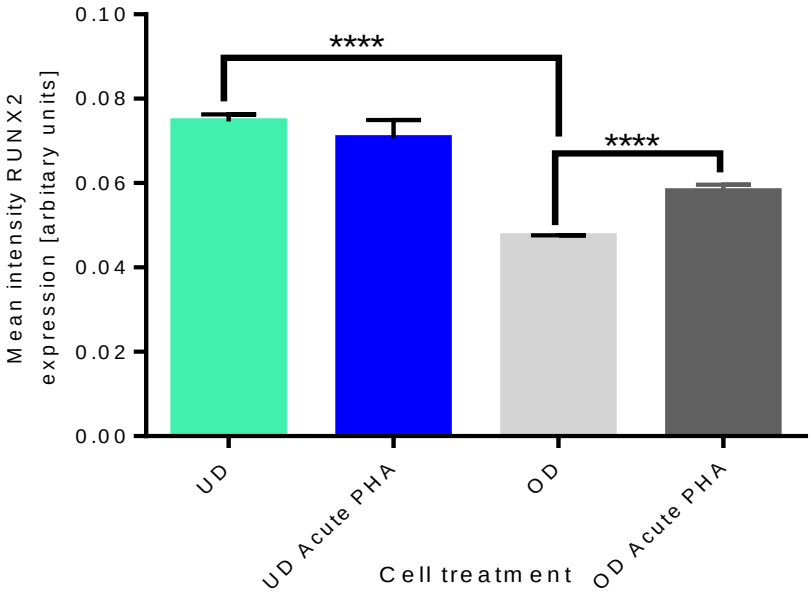

Figure 3.1-q RUNX2 expression in ASC52telo cells with acute PHA-767491 treatment and osteoid differentiation. Low passage (P+13) ASC52telo cells were seeded at 5000 cells per cm^2 onto glass coverslips in 24 well plate, with or without PHA-767491. Cells were differentiated for 22 days with media changes every 3 days; control cultures were kept in normal MSC medium but otherwise were treated similarly. Cells were fixed with 4% formaldehyde and stained for RUNX2 and DAPI. Images were collected using a Leica SP8 confocal microscope and quantified using CellProfiler. Error bars represent SEM from one experiment. Statistical significance was calculated by the Tukey post hoc test following one-way ANOVA analysis, ****P<0.0001. UD: un-differentiated, UD acute PHA: un-differentiated with PHA treatment, OD: osteoid differentiation, OD acute PHA: osteoid differentiation with PHA-767491 treatment. Reduced levels of RUNX2 expression following mature osteoblast differentiation, with an increase seen in PHA-767491 acute treated cells.

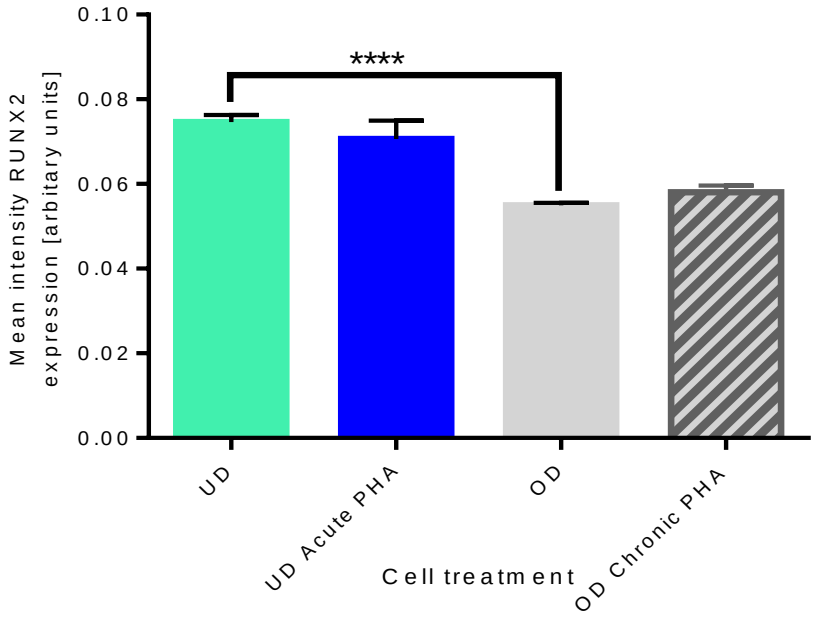

Figure 3.1-r RUNX2 expression in ASC52telo cells under chronic PHA-767491 treatment and osteocyte differentiation. ASC52telo cells p+22 were seeded at 5000 cells per cm^2 and kept treated with PHA (Chronic PHA started at p+13). Cells were allowed to differentiate for 21 days, with media changes every 3 days; parallel control cultures were kept in normal MSC media but otherwise were treated similarly. Cells were fixed with 4% formaldehyde and stained for RUNX2 and DAPI. Images were collected with a Leica SP8 confocal microscope and quantified using CellProfiler. Error bars represent SEM from one experiment. Statistical significance was calculated by the Tukey post hoc test following one-way ANOVA analysis. UD: un-differentiated, UD acute PHA: un-differentiated with PHA treatment, OD: osteoid differentiation, OD chronic PHA: osteoid differentiation with continual PHA-767491 treatment. Reduced levels of RUNX2 expression following mature osteoblast differentiation, ****P≤0.0001.

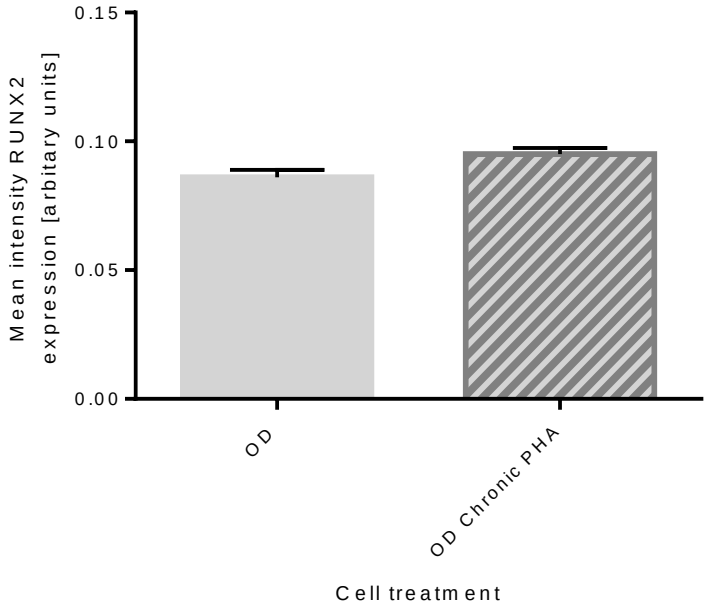

Figure 3.1-s RUNX2 expression in ASC52telo under Chronic PHA-767491 treatment and Osteoid differentiation. Low passage (P+17) ASC52telo cells were seeded at 5000 cells per cm^2 and continued with PHA treatment (commenced at P+13). Cells were allowed to differentiate for 21 days, with media changes every 3 days, were fixed with 4% formaldehyde and stained for RUNX2 and DAPI. Images were collected on a Leica SP8 confocal microscope and quantified using CellProfiler. Error bars represent SEM from one independent experiment. Statistical significance was calculated by the Tukey post hoc test following one-way ANOVA analysis. OD: osteoid differentiation, OD PHA: osteoid differentiation with PHA-767491 treatment. Although RUNX2 expression intensity appears higher in PHA-767491 treated differentiated cells, this increase is not statistically significant.

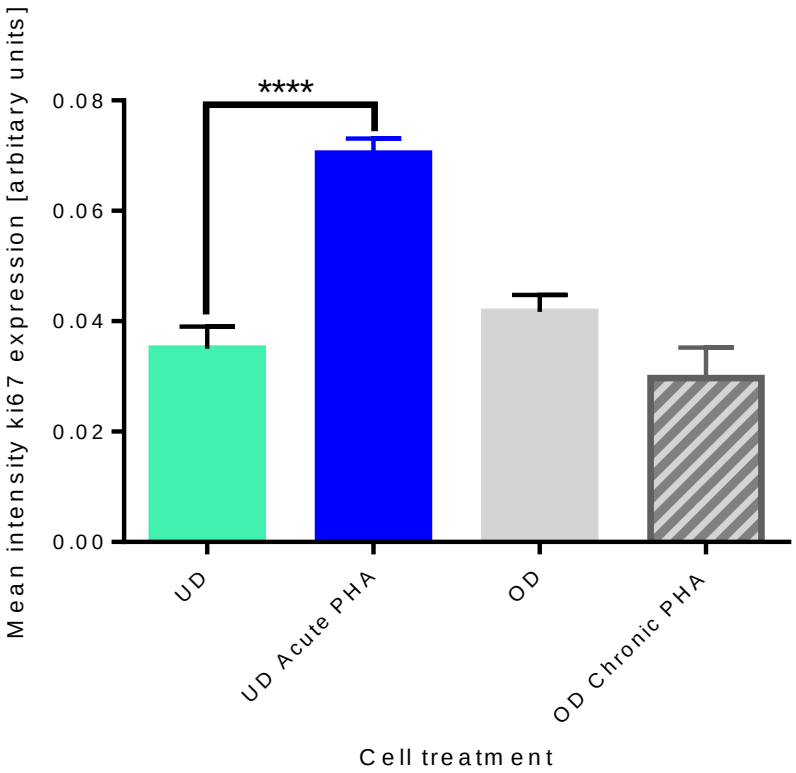

Figure 3.1-t Ki67 expression in chronic PHA -767491 treated ASC52telo cells. ASC52telo cells p+22 were seeded at 5000 cells per cm^2. Media was changed to Osteoid differentiating media or maintained in Mesenpro media with or without PHA (Chronic PHA started p+13). The cells were incubated for 21 days. Media was changed every 3 days. The cells were fixed with 4% formaldehyde and stained for Ki67 and DAPI. Images were collected on a Leica SP8 confocal microscope and quantified using CellProfiler. Error bars represent SEM from one independent experiment. Statistical significance was calculated by the Tukey post hoc test following one-way ANOVA analysis. ****P≤0.0001. An increase of Ki67 observed in UD PHA cells. UD: un-differentiated, UD PHA: un-differentiated with PHA treatment, OD: osteoid differentiation, OD PHA: osteoid differentiation with PHA-767491 treatment.

3.1.2 Relationship of DNA replication initiation and cellular transformation

Mesenchymal stem cell differentiation into osteoblasts, chondrocytes, and adipocytes (Pittenger et al., 1999) was previously verified in ASC52telo cells using differentiation inducing media. RUNX2 staining in previous experiments raised the possibility of spontaneous differentiation, which was investigated in more detail. Spontaneous differentiation is the occurrence of differentiated cells during culturing in non-inducing media. Appearance of such cells was investigated following chronic PHA treatment kept in normal MSC media and analysed by histochemical and immunohistochemical staining for differentiation markers.

Differentiation of ASC52telo cells into osteoblasts is shown in high passage cultures under continuous (chronic) mild proliferation inhibition, shown by red staining of calcium deposits, which persists after withdrawal of chronic PHA treatment (recovery) (Figure 3.1-u). Low and high passage cells show an increase of RUNX2

expression in response to acute PHA treatment. High passage cells under chronic treatment have high RUNX2 expression, which falls to normal levels following cessation of PHA treatment (Figure 3.1-v).

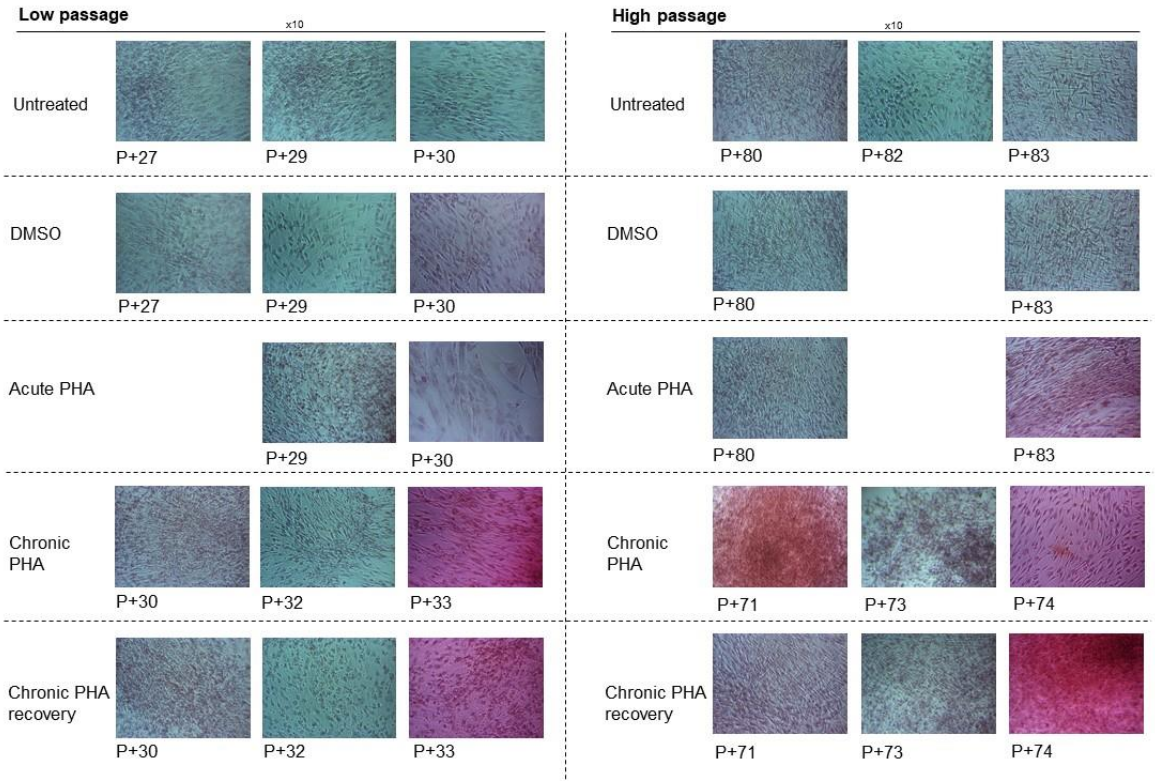

Figure 3.1-u Production of calcified matrix by ASC52telo cells following chronic PHA-767491 treatment in normal Mesenpro media. ASC52telo cells were cultured as per PHA model and seeded at 5000 cells per cm^2 on 24 well plate, and incubated for 3 days**,** Cells were fixed in 4 % paraformaldehyde in PBS and stained with Alizarin Red S. Bright orange-red staining demonstrated calcium deposits. Images were taken on a Nikon Eclipse TE2000-s inverted microscope with Nikon DN100 camera and x10 objectives. P+: cell passage.

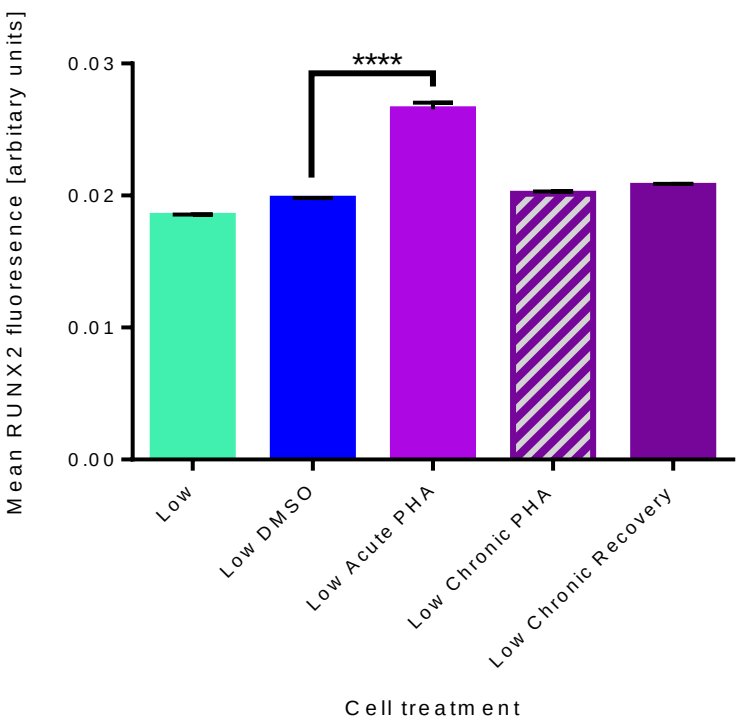

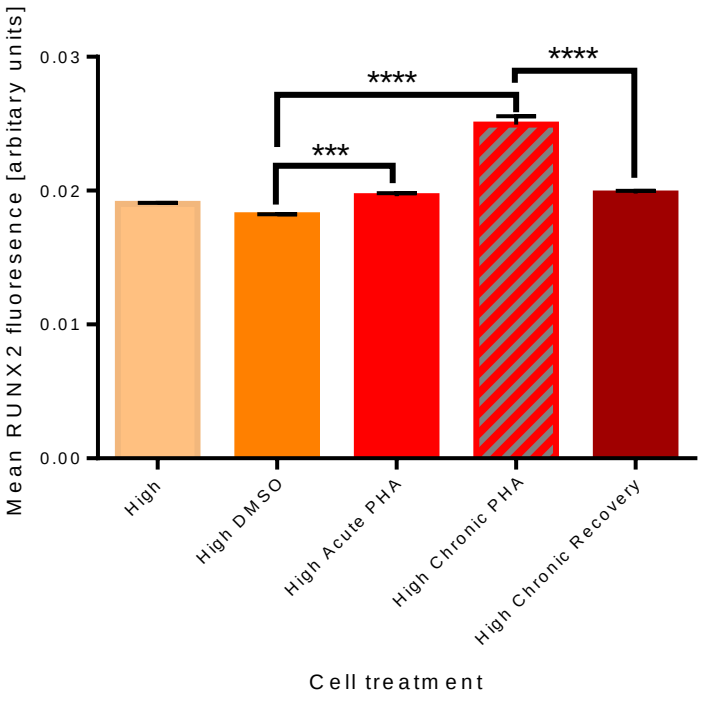

Figure 3.1-v RUNX2 levels in undifferentiated ASC52telo cells cultured under replication stress. ASC52telo cells precultured according to the PHA model were seeded at 5000 cells per cm^2 and kept treated as before or released (recovery). Cells were incubated for 3 days, were fixed with 4% formaldehyde and stained for RUNX2 and DAPI. Images were collected using a Leica SP8 and quantified using CellProfiler. Error represents SEM. Statistical significance was calculated by the Tukey post hoc test following one-way ANOVA analysis. Low – P+35, P+37, P+38, High – P+88, P+90, P+91, High chronic-P+83, P+85, P+86, Low chronic – P+37, P+40 P+41. *** P≤0.001, ****P≤0.0001. Graph represents combined data from three independent experiments.

3.1.3 Relationship of DNA replication initiation and Membrane potential

Membrane potential appeared to remain unchanged following mild proliferation inhibition in ASC52telo cells (Figure 3.1-w). In parallel wells MTS reading was also taken to reflect cell viability, and the readings taken from TMRE were divided by MTS reading to give a representative effect to cell viability. The protonophore p-trifluoromethoxy carbonyl cyanide phenyl hydrazone (FCCP), a mitochondrial uncoupler, induces mitochondrial depolarization leading to a rapid release from quenched matrix into the cytoplasm, abolishes ATP synthesis, and can deplete the cytoplasmic pool of ATP. FCCP was used as a control to induce mitochondrial membrane depolarization generating the loss of fluorescent intensity (Perry et al., 2011; Wang et al., 2017b; Nicholls, 2018) a significant reduction was seen.

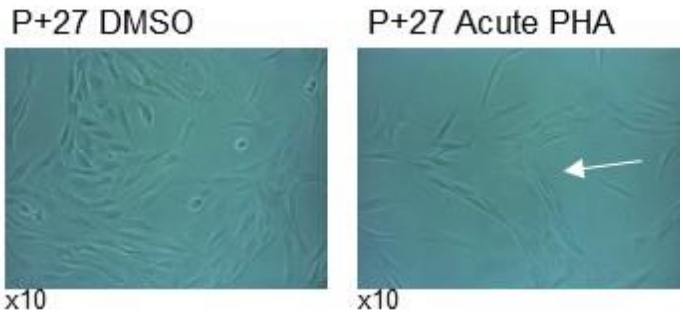

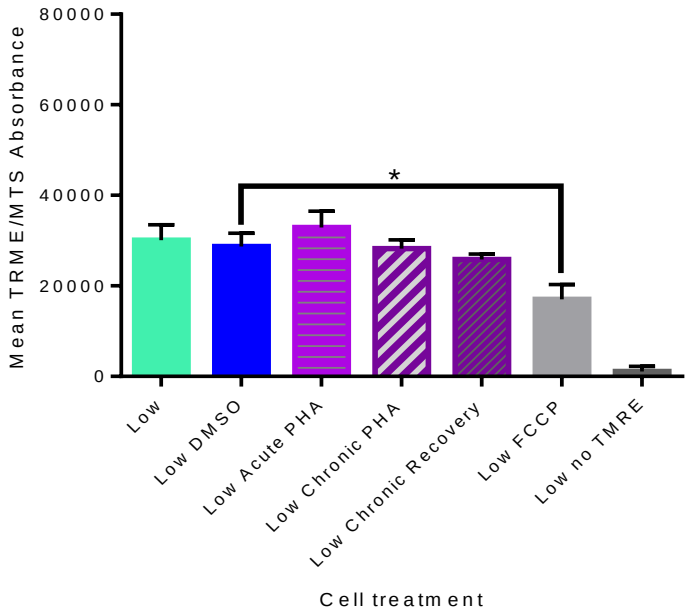

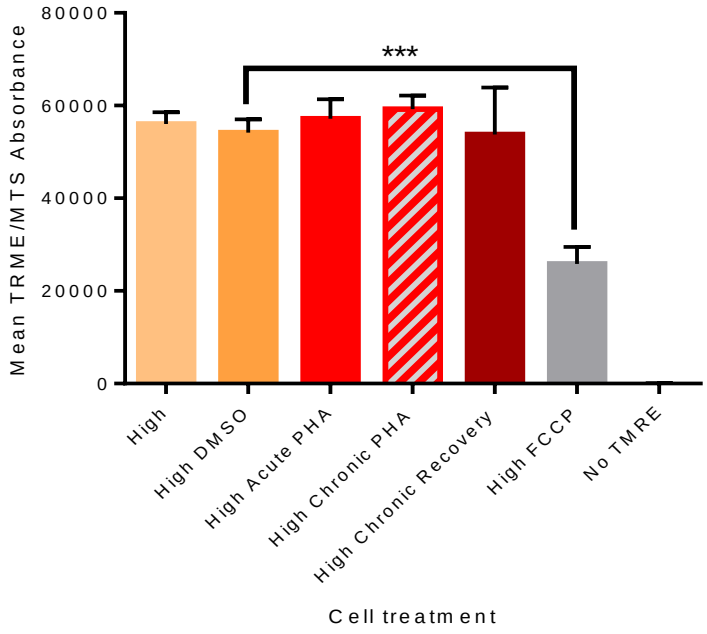

Figure 3.1-w Mitochondrial activity in acute and chronic PHA-767491 ASC52telo cells. ASC52telo cells were seeded at 5000 cells per cm^2 in two 96 well plates in triplicates, and kept under the same conditions except PHA treatment was applied as per the representative PHA model. The cells were incubated for 72 hours. One plate was analysed using MTS and the other using the TMRE assay, TMRE readings were averaged against MTS reading. Error bars represent SEM; graphs represent combined data from three independent experiments (n=3), Low: p+23, P+26, P+27, Low Chronic PHA/recovery: P+26, P+29, P+30, High: P+78. P+79, P+80 High Chronic PHA/recovery: P+68, P+69 P+70 Statistical significance was calculated by the Tukey post hoc test following one-way ANOVA analysis, * $P \leq 0.05$, *** $P \leq 0.001$. No significant differences in mitochondrial activity have been demonstrated in ASC52telo cells under PHA-model. White arrow; slow proliferation.

3.1.4 Summary

To establish a model of mild replication initiation inhibition in mesenchymal stem cells, ASC52telo cells were treated with PHA. This was to enable further investigations on the effects of this treatment on cell morphology, physiology, and differentiation into osteoblasts. ASC52telo cells have been employed in many studies (Wolbank et al., 2009; Hasebe-Takada et al., 2016; Nardone et al., 2017; Pitrone et al., 2017). We surprisingly demonstrated more pronounced PHA sensitivity at low concentrations in low passage cells, with an unexpected increase in cell viability at higher PHA concentrations. This is not expected or explicable, and although was seen twice, would need repeating to verify.

We wanted to put a continuous pressure on replication initiation without affecting viability in ASC52telo cells, therefore we selected 1.5 µM, the highest concentration that showed the minimal effect on cell survival (Figure 3.1-b and Figure 3.1-e). A model of PHA-767491 was established in low and high passage ASC52telo cells with acute and chronic PHA treatment, and withdrawal of treatment in either case ('recovery'). This enabled us to further understand the effects of reduced replication over time and the potential cellular stress this generates, similar to the effect of *RECQL4* mutations, and if and how the cells may recover following the cessation of treatment with PHA-767491. Reduced proliferative rate was verified using cell count (haemocytometer), and maintained viability was measured using trypan blue. Interestingly, PHA-767491 treated cells appeared to lead to cell morphology changes, as the cells appeared larger, which is an indication of cellular morphological modifications that have been further explored in this study.

Successful adipocyte, chondrocyte, and osteoblast differentiation was achieved in the ASC52telo cells, under PHA-767491 treatment, and cells under long term culture. PHA-767491 treated ASC52telo cells were further analysed for induced and spontaneous differentiation. RUNX2 expression suggests the commitment of the MSCs towards osteoblast differentiation (Ducy et al., 1997; Komori et al., 1997), which was evaluated to determine if the cells showed signs of this commitment under normal media. An increase in RUNX2 expression was demonstrated following acute PHA-767491 treatment in low passage cells and following chronic PHA-767491 treatment in high passage cells, while reduced levels were seen following recovery. The difference between passages suggests that low passage

cells may be more sensitive to the initial treatment, and chronic treatment also leads to sensitivity over long term culture. Further studies are needed to identify if the association of the cell cycle is the link to the data obtained. However, these results taken together with the mineralised calcium levels also observed within these treated cells, suggest differentiation into osteoblasts, or disruption of the regulation of these markers. The ASC52telo cells were not investigated for spontaneous differentiation into the other forms of cell lineages. This would be useful to further our understanding of the transformation mechanisms that appeared to establish following chronic replicative stress in these cells.

The mitochondrial membrane appeared stable following PHA treatment, no significant changes of membrane potential was seen.

4 Chapter 2 The interference with DNA replication initiation generates genomic instability

Results

We established that ASC52telo cells under acute and chronic mild replication interference using PHA-767491 held the ability for osteoblast differentiation. In addition, dysregulation of differentiation markers, suggestive of transformation may follow chronic treatment. We hypothesis these cells established genomic instability, promoting transformation. A characteristic of OS is chromosomal instabilities; markers of this were investigated as the next step using the established model.

4.1 PHA-767491 induces chromosomal instabilities in ASC52telo cells

To establish if continuous interference with replication initiation influences the DNA damage response, ASC52telo cells under the PHA-767491 model were treated with Camptothecin and cell viability was analysed. The sensitivity of acute and chronic PHA-767491 cells to Camptothecin induced DNA damage did not appear to be significantly different (Figure 4.1-a).

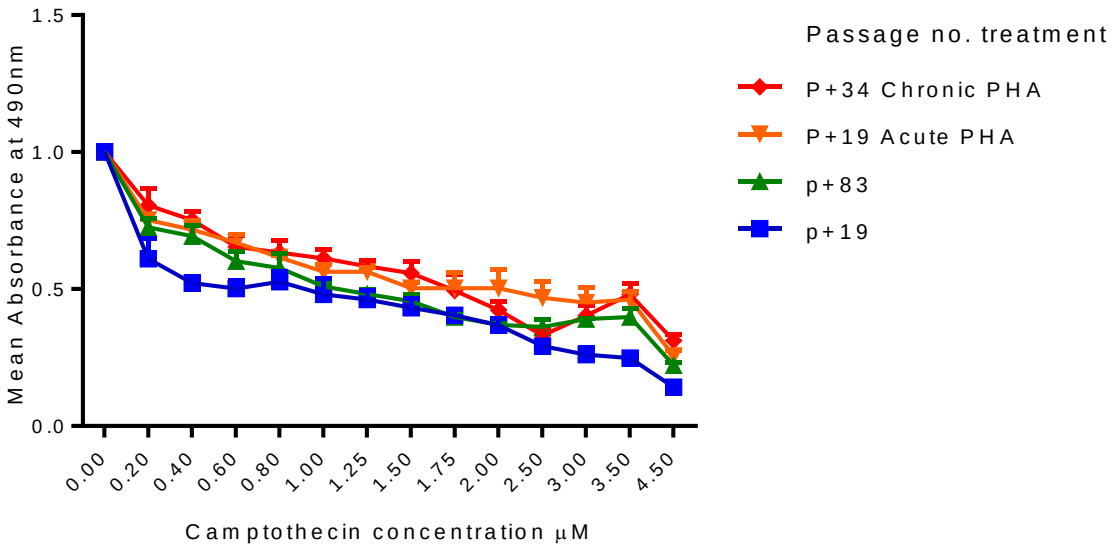

Figure 4.1-a Camptothecin sensitivity of ASC52telo cells under acute and chronic PHA-767491 treatment. 2500 high and low passage ASC52telo cells treated according to the PHA model were seeded per well in a 96 well plate. Treatment was administered in triplicates. 18 hours post seeding medium was changed with the addition of Camptothecin at variable concentrations with or without PHA-767491. MTS assay was performed 24 hours post Camptothecin treatment. Data represent means ± SD of triplicates; representative graph from two independent experiments. A decline of cell viability was observed on increasing CPT concentrations. Data was normalised to media and CPT alone. P+19 IC50 = 0.3890, p+83 IC50 = 0.5485, p+19 Acute PHA IC50 = 0.6926, p+34 Chronic PHA IC50 = 0.6535; calculated from one repeat shown above.

Chromosomal instabilities can be demonstrated in cells following DNA damage through observing cell morphology changes and known markers including micronuclei, budding, chromatin bridges etc. (Wilkens et al., 2004; Verma and Dey, 2014; Tyagi et al., 2015). These markers were found in ASC52telo cells under the PHA model (Figure 4.1-b). To establish a baseline of potential DNA damage in low and high passage untreated ASC52telo cells, these changes in nuclear morphology were observed and quantified in control untreated cells and cells treated according to the PHA model. High passage cells appeared to demonstrate a higher percentage of chromosomal instability markers in comparison to lower passage cells (Figure 4.1-c and Figure 4.1-d). Although not always significant, a further increase was observed in acute and chronic PHA-767491 treated cells (Figure 4.1-c). Ki67 and γH2AX staining was also observed in the micronuclei (Figure 4.1-e).

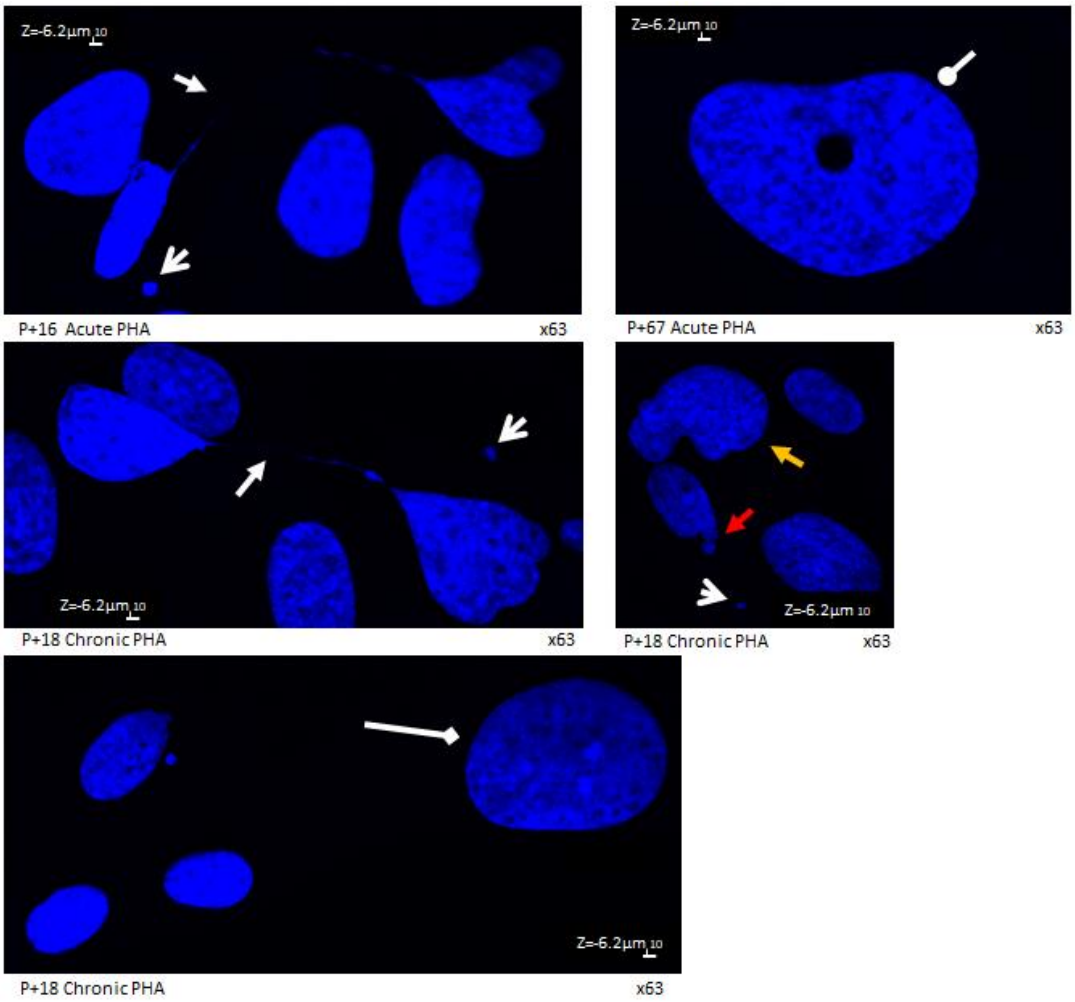

Figure 4.1-b Chromosomal instability markers observed in acute and chronic PHA-767491 treated ASC52telo cells. ASC52telo cells were seeded onto coverslips at 5000 cells per cm2. The cells were treated with PHA-767491 as per the PHA model. The cells were fixed in 4% paraformaldehyde and stained with DAPI. Images were collected with a Leica SP8 confocal microscope x63 objective. Morphology changes observed: White arrow head: Bridge, white open arrow head: micronuclei, red arrow head: bleb, yellow arrow head: multi-lobed, white oval arrow: doughnut -shaped, white diamond arrow head: enlarged nuclei.

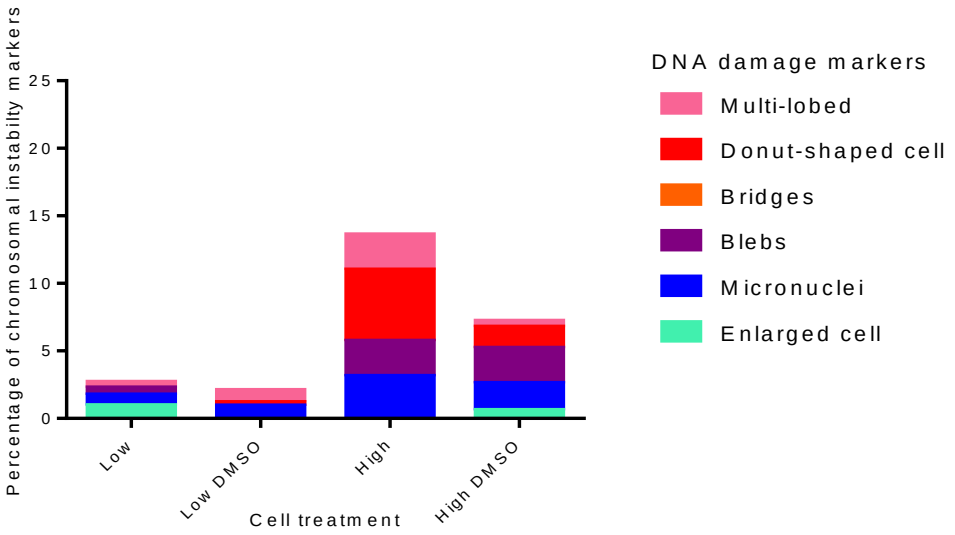

Figure 4.1-c Chromosomal instability markers in untreated ASC52telo cells. ASC52telo cells were seeded onto coverslips at 5000 cells per cm^2 and allowed to reach around 80% confluence. The cells were fixed in 4% paraformaldehyde and stained with DAPI. Images were collected with a Leica SP8 confocal microscope, graph represents combined data from three independent experiments (n=3). Changes in nuclear morphology were observed and quantified. Low: P+ 20, 14, 22, High: P+ 67, 88, 90,

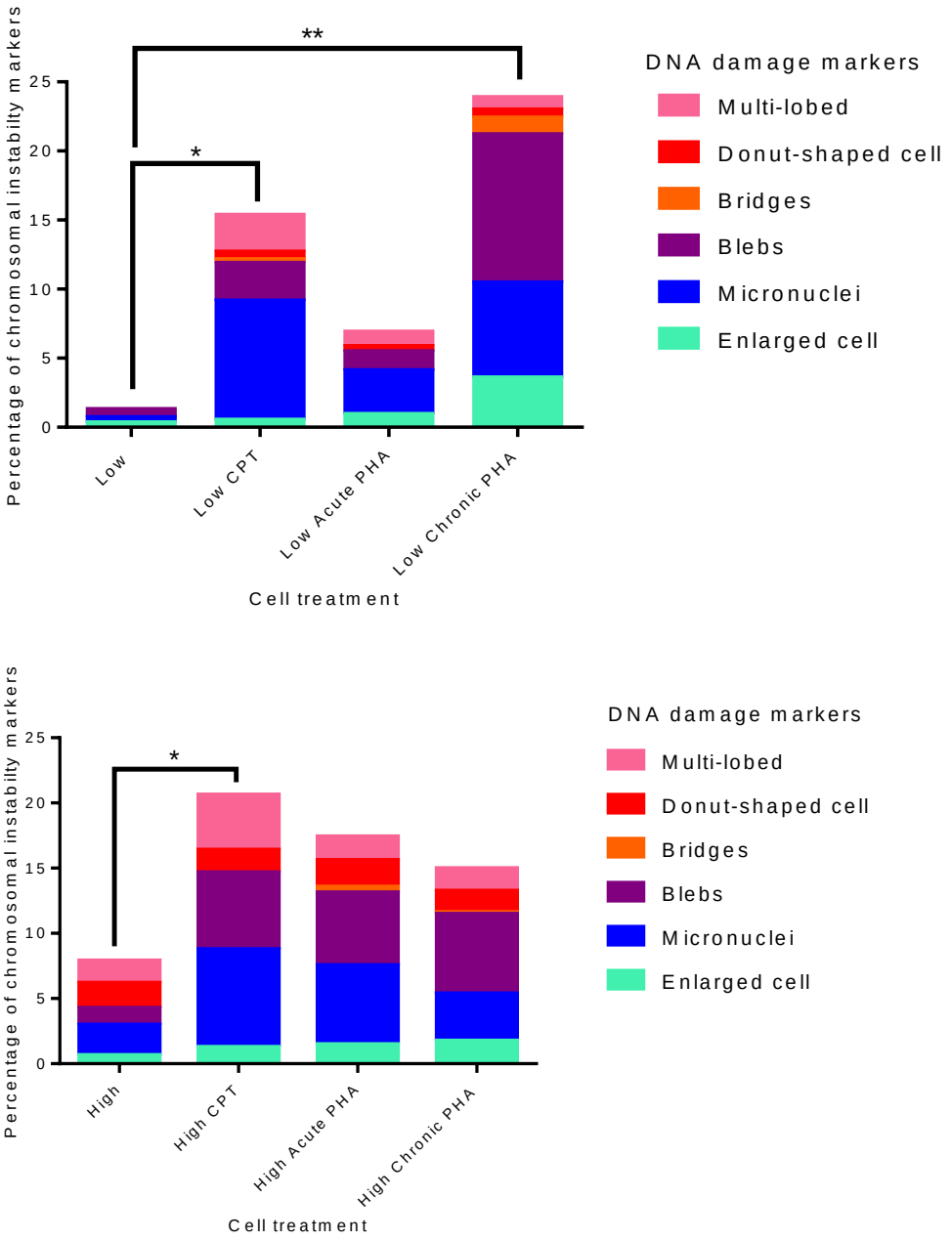

Figure 4.1-d Chromosomal instability markers in ASC52telo under acute and chronic PHA-767491 treatment. ASC52telo cells were seeded onto glass coverslips at 5000 cells per cm^2. The cells were treated with PHA in acute or chronic way as indicated. Camptothecin (CPT) was used to generate DNA damage as control; cells were treated at 0.8µM for 24 hours. The cells were fixed in 4% paraformaldehyde and stained with DAPI. Images were collected with a Leica SP8 confocal microscope. Low and Low acute PHA: p+20, 22, 11, and 13, Low chronic PHA: p+11,13, 20, 22. High and High acute PHA: p+62, 65, 88, and 90, High chronic PHA: p+47, 49, 53, and 55. Graphs represent data combined from four independent experiments (n=4). Statistical significance was calculated by the Tukey post hoc test following one-way ANOVA analysis, * $P \leq 0.05$, ** $P \leq 0.01$. Chromosomal instability markers were detected at high rate following CPT treatment in high and low passage cells, and also present in PHA-747691 treated cells.

γH2AX

P+9 acute PHA

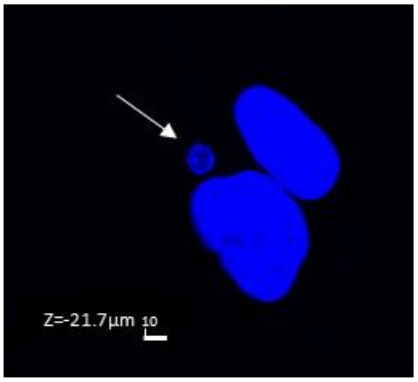

Dapi

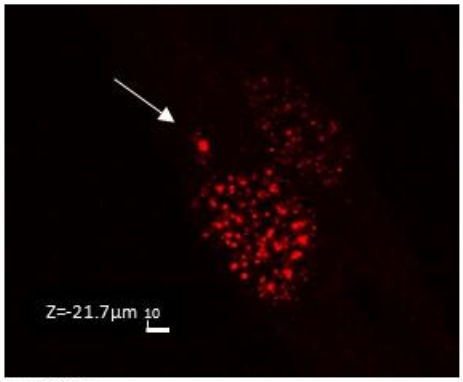

γH2AX

P+62 Chronic PHA

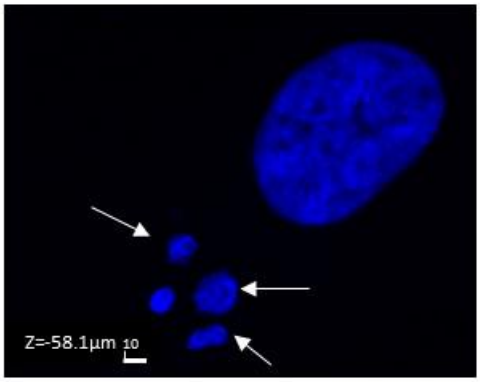

Dapi

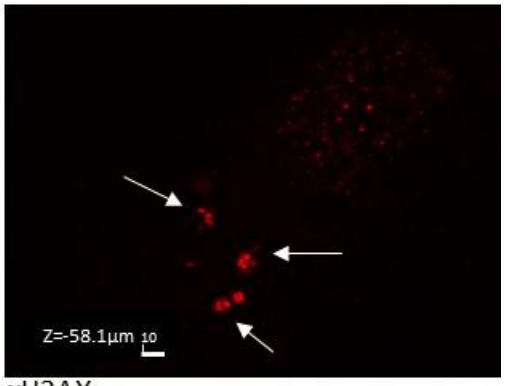

γH2AX

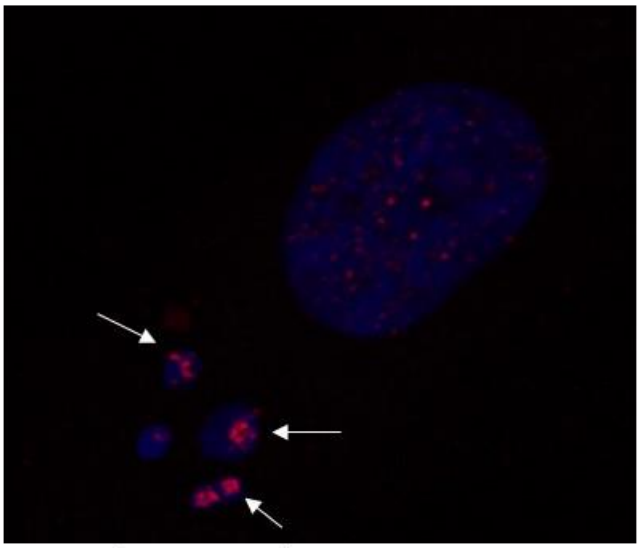

Dapi and γH2AX overlay x63

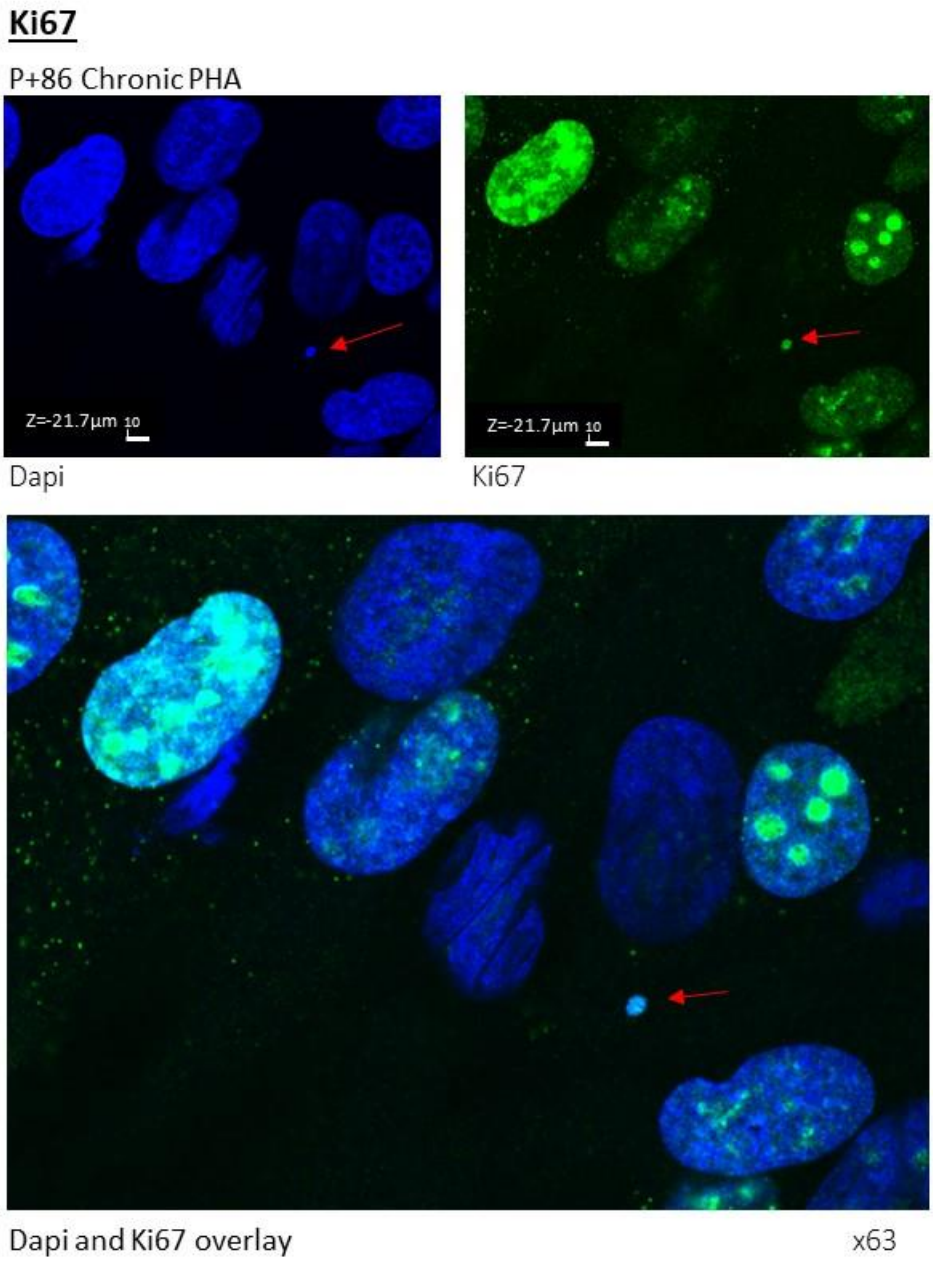

Figure 4.1-e ASC52telo cells form micronuclei staining positive for Ki67 and γH2AX, following mild inhibition of replication initiation. High and low passage ASC52telo cells were seeded at 5000 cells per cm^2 in 24 well plate on glass coverslips, with acute or chronic PHA-767491 treatment. The cells were incubated for 72 hours before fixing in 4% paraformaldehyde and stained for Ki67 and DAPI and γH2AX. Images were collected using a Leica SP8 confocal microscope, x63 objective. Intense staining observed in some micronuclei; representative images are shown.

4.1.1 DNA damage marker and mild proliferation inhibition

To further characterize the origin of observed signs of chromosomal instabilities, the existence of spontaneous DNA damage was examined in our model of cells exposed to mild proliferation inhibition by assessing γH2AX expression, which is a marker of DNA double strand breaks. We demonstrated that Camptothecin (CPT) treatment induces γH2AX foci formation with strong intensity of expression (Figure 4.1-f) as expected.

A significant increase in the number of spontaneous γH2AX foci was shown in high and low passage ASC52telo cells under acute and chronic PHA-767491 treatment (Figure 4.1-f). Importantly, the number of γH2AX foci was decreased to basal level in low passage cells under recovery, however, the same was not observed in high passage cells indicating persistent DNA damage. Quantifying the intensity of γH2AX signal in the nuclei is another method of assessing DNA damage, albeit not as sensitive as foci count. Acute and chronic PHA-767491 in low passage cells led to an increase in γH2AX intensity, with recovery again seen. In high passage cells chronic PHA treatment did not significantly cause an increase in expression compared to acute treatment, but a reduction was also seen in recovering cells (Figure 4.1-f). The discrepancy between the two measurements is interesting and probably reflects the overall size of the individual foci: high number of small foci are still detectable with counting but cause a lower signal intensity.

Unrepaired double-stranded breaks can be a source of chromosomal instabilities resulting in chromosome fusions and breaks, changing the number of telomeres directly, or can influence telomere maintenance via other mechanisms indirectly. To assess telomere numbers in our PHA model, the expression of TRF2, a member of the telomeric shelterin complex was quantified. TRF2 foci count and intensity (Figure 4.1-g) increased following PHA treatment in low passage cells, with recovery as the PHA treatment was withdrawn in the released population, as observed with γH2AX expression previously. High passage cells showed an increase in TRF2 foci count following acute treatment, however this was not seen in chronic PHA-767491, interestingly, the cells under recovery demonstrated an increase in TRF2 foci count. TRF2 intensity was only increased in acute PHA-767491 cells (Figure 4.1-g).

We also tested if the increased occurrence of γH2AX foci observed previously is concentrated specifically to the telomeres, which would indicate telomere erosion or specific telomeric damage. We co-stained ASC52telo cells with γH2AX and TRF2, and quantified their co-localization (Saha et al., 2013). Significant telomeric damage was only demonstrated in low passage cells with acute and chronic PHA-767491, with recovery seen (Figure 4.1-h), following analysis of γH2AX foci co-localized with TRF2.

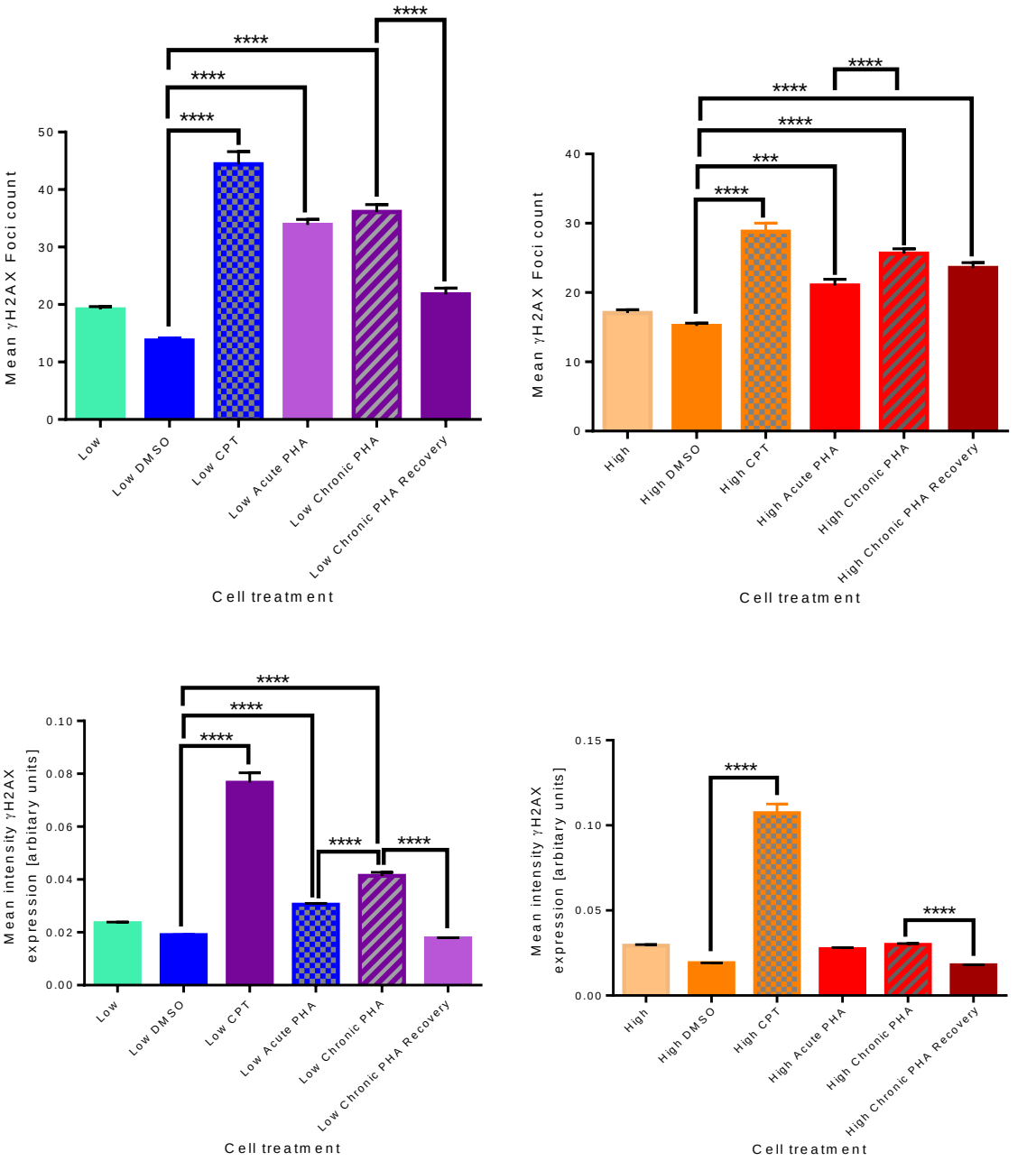

Figure 4.1-f γH2AX foci and intensity following mild inhibition of replication initiation, in high and low passage ASC52telo cells. ASC52telo cells were seeded at 5000 cells per cm^2 onto glass coverslips. The cells were incubated until the untreated cells reached around 80% confluency. PHA was added to short term treated cells throughout this incubation (acute treatment; 3 days), while long term (chronic) treatment was maintained continuously. The cells were fixed in 4% paraformaldehyde and and probed for γH2AX. Low: P+16, 11, 17, 13, 9, 14, Low DMSO: P+ 16, 17, 14, Low CPT: P+11, 18, 13 , Low acute PHA-767491: P+16, 17, 11, 9, 14, Low chronic PHA-767491: P+17, 18, 13, 11, 12, Low chronic PHA-767491 recovery: P=16,P+17, 18, High: P+69, 70 62, 65, 67, High DMSO: P+69, 70, 67, DMSO, High CPT: P+62, 65, 67, High acute PHA-767491: P+69, 62, 65, 67, High chronic PHA-767491: P+68, 69, 55, 67, High chronic PHA-767491 recovery: P+68, 69, 67. Images were collected with a Leica SP8 confocal microscope and quantified using CellProfiler. Error bars represent SEM of combined data from three independent experiments (n=3), statistical significance was calculated by the Tukey post hoc test following one-way ANOVA analysis. ***P≤0.001, ****P≤0.0001. An increase of γH2AX foci was shown in high and low passage ASC52telo cells under acute and chronic PHA-767491 treatment,

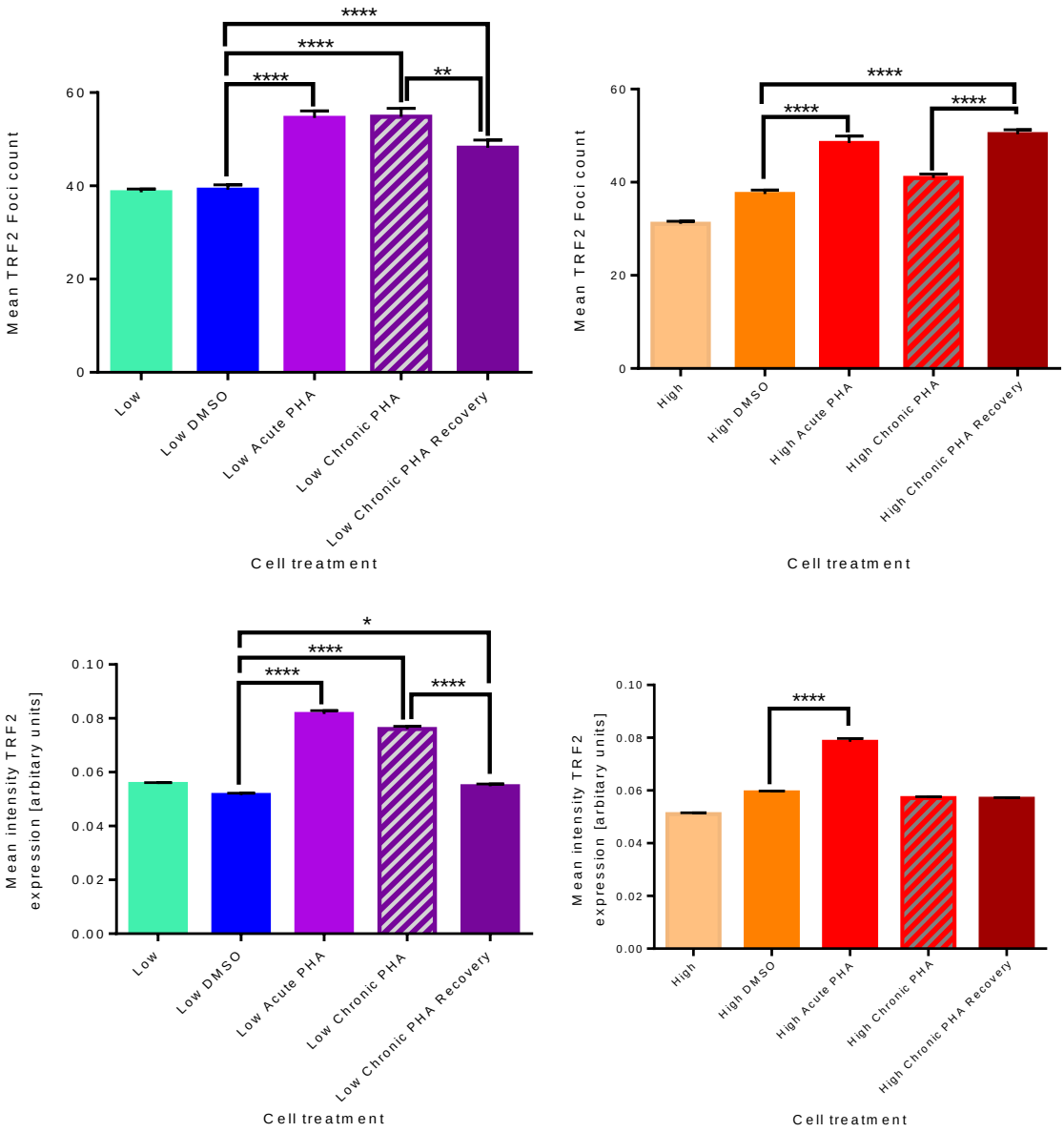

Figure 4.1-g Quantification of TRF2 foci and intensity following mild inhibition of replication initiation, in high and low passage ASC52telo cells. ASC52telo cells were seeded at 5000 cells per cm^2 onto glass coverslips. The cells were incubated until the untreated cells reached around 80% confluency. PHA was added to short term treated cells throughout this incubation (acute treatment; 3 days), while long term, chronic, treatment was maintained continuously. The cells were fixed in 4% paraformaldehyde and stained for TRF2. Images were collected with a Leica SP8 confocal microscope and quantified using CellProfiler. Passage numbers; Low: p+16, 11, 17, 13, 9, 14, Low DMSO: p+16, 17, 14, Low acute PHA: p+16, 17, 11, 9, 14, Low Chronic PHA: p+17, 18, 13, 11, 12 (n=5), Low chronic PHA Recovery: P+16, p+17, 18, High: p+ 69, 70 62, 65, 67, High DMSO: p+69, 70, 67, High acute PHA: p+69, 62, 65, 67, High chronic PHA: p+68, 69, 55, 67, High chronic PHA recovery: p+68, 69, 67. Error bars represent SEM of combined data from three independent experiments (n=3), statistical significance was calculated by the Tukey post hoc test following one-way ANOVA analysis. * P≤0.05, ** P≤0.01, ****P≤0.0001. TRF2 foci count and intensity increased in Low acute and chronic PHA treated cells.

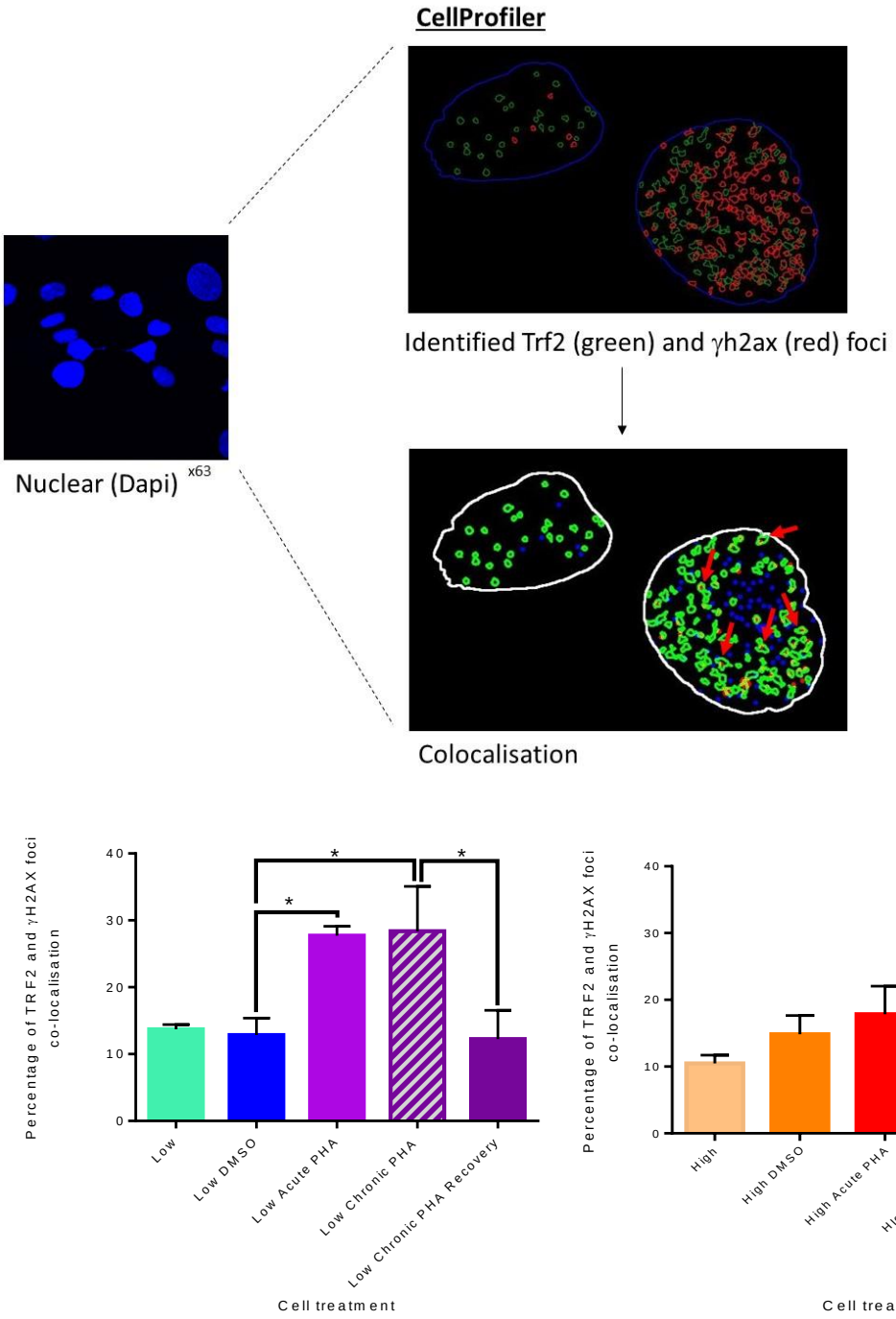

Figure 4.1-h Co-localisation of TRF2 with γH2AX following mild inhibition of replication initiation in high and low passage ASC52telo cells. ASC52telo cells were seeded at 5000 cells per cm^2 onto glass coverslips. The cells were incubated until the untreated cells reached around 80% confluency. PHA was added to short term treated cells throughout this incubation (acute treatment, 3 days), while long term (chronic) treatment was maintained continuously. The cells were fixed in 4% paraformaldehyde and co-stained for TRF2 and γH2AX. Images were collected with a Leica SP8 confocal microscope and quantified using CellProfiler. Passage numbers; Low: P+16, 11, 17, 13, 9, 14, Low DMSO- p+16, 17, 14, Low acute PHA: p+16, 17, 11, 9, 14 , Low chronic PHA: p+17, 18, 13, 11, 12, Low chronic PHA recovery: P=16, p+17, 18, High: P+ 69, 70 62, 65, 67, High DMSO: p+69, 70, 67, High acute PHA: p+69, 62, 65, 67, High Chronic PHA: p+ 68, 69, 55, 67, High chronic PHA recovery: p+68,69, 67. Error bars represent SEM of combined data from three independent experiments (n=3). Statistical values were calculated by the Tukey post hoc test following one-way ANOVA analysis. * $P \leq 0.05$. Percentage of co-localisation represents TRF2 foci also positive for γH2AX foci (white arrows). Significant co-localisation seen in low passage PHA treated cells.

Resolving and regulating a response following DNA damage is maintained by a number of pathways; ATM and ATR initiating a DNA response via phosphorylation of mediator proteins, including 53BP1, and effector protein CHK1 (Friedel et al., 2009; Dai and Grant, 2010). Low passage ASC52telo under acute PHA-767491 showed a significant decrease in 53BP1 (DSB interacting protein); although not significant a similar finding appeared in the high passage cells under the same conditions. 53BP1 expression significantly increased in the low passage acute PHA-767491 cells with suggested rise in phosphorylated-CHK1 (Phospho-CHK1, the activated form) (Figure 4.1-i). However, further repeats are necessary to verify these findings.

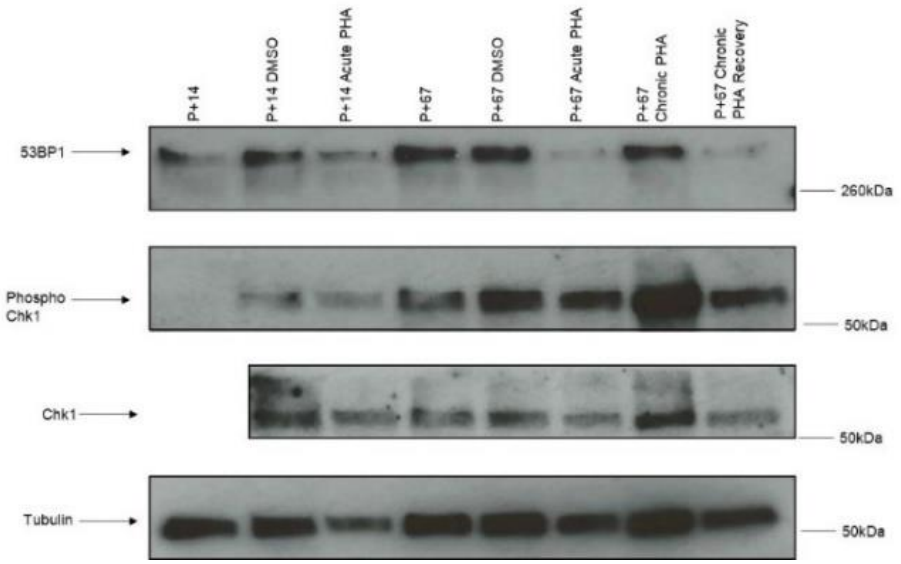
P+14
P+14 DMSO
P+14 Acute PHA
P+67
P+67 DMSO
P+67 Acute PHA
P+67 Chronic PHA
P+67 Chronic PHA Recovery
53BP1
260kDa
Phospho Chk1
50kDa
Chk1
50kDa
Tubulin
50kDa

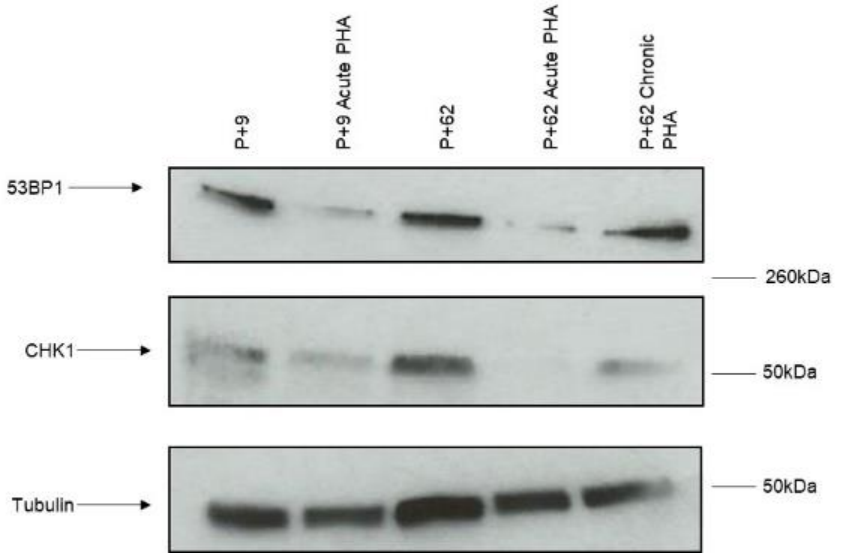
P+9
P+9 Acute PHA
P+62
P+62 Acute PHA
P+62 Chronic PHA
53BP1
260kDa
CHK1
50kDa
Tubulin
50kDa

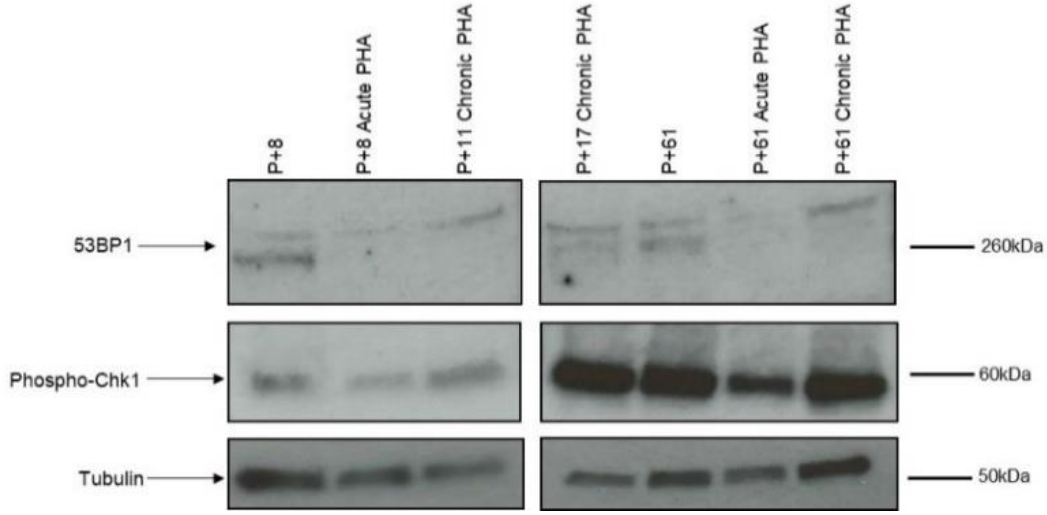
P+8
P+8 Acute PHA
P+11 Chronic PHA
P+17 Chronic PHA
P+61
P+61 Acute PHA
P+61 Chronic PHA
53BP1
260kDa
Phospho-Chk1
60kDa
Tubulin
50kDa

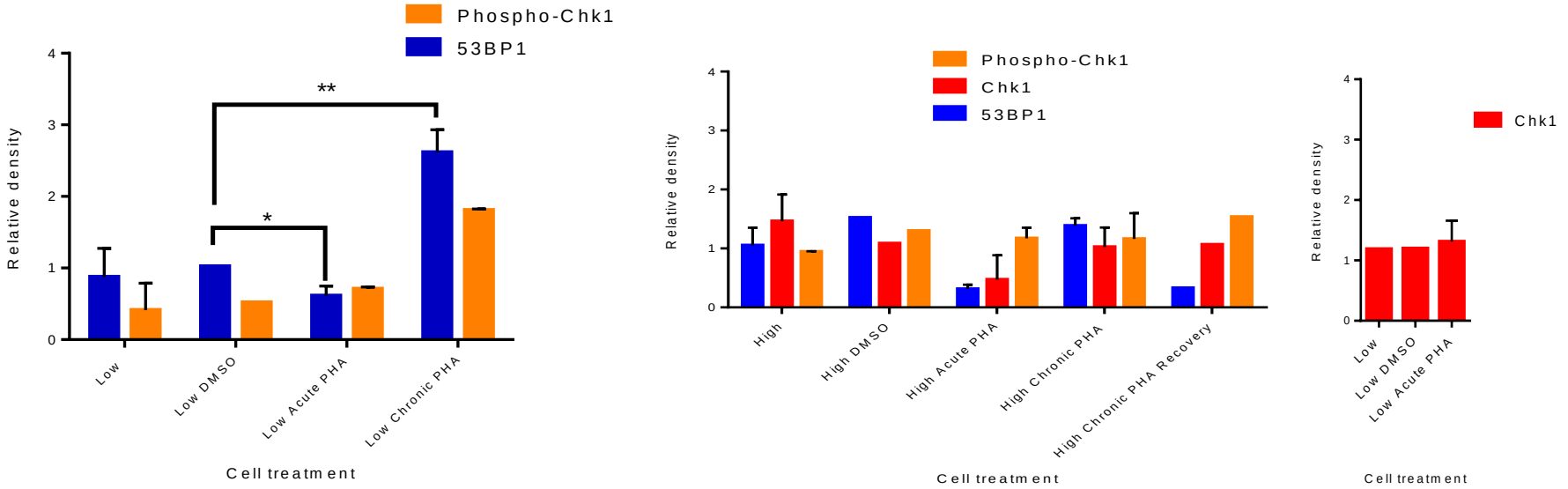

Figure 4.1-i Expression of markers of the DBS damage response pathway in ASC52telo cells following acute and chronic PHA-767491 treatment. ASC52telo cells were seeded at 5000 cells per cm^2 in 24 well plate, and incubated until the untreated cells reached around 80% confluency (4 days). Cells were treated as per PHA model with media changes at day 3. Cell lysate was collected and SDS PAGE and western blot was performed. The membrane was probed with antibodies detecting 53BP1, Phospho-Chk1, Chk1, and tubulin, and quantified using ImageJ. Intensity values are presented as relative intensity. Statistical significance of difference was calculated by the Tukey post hoc test following two-way ANOVA analysis * $P \leq 0.05$, ** $P \leq 0.01$, graphs and error bars SEM represent data combined of number of independent experiments as indicated in brackets. 53BP1: Low/High, Low/High Acute PHA, High Chronic PHA (n=3), Low Chronic PHA (n=2). Low/High DMSO, High Chronic PHA recovery (n=1). Chk1: Low/High, Low/High Acute PHA, Low/High Chronic PHA (n=2), Low/High DMSO, High Chronic PHA recovery (n=1), Phospho-Chk1: Low, Low/High DMSO, High Chronic PHA recovery (n=1), High, Low/High Acute PHA, High Chronic PHA (n=2). DNA damage response markers were present, with some correlation in PHA-767491 treated cells.

4.2 Markers of cellular transformation in ASC52telo cells following chronic inhibition of replication initiation

The model of cancer proposed by Vogelstein and Kinzler suggests that cancer is a disease of damaged DNA, accumulating a range of genetic mutations capable of transforming normal cells into cancer cells (Kinzler and Vogelstein et al., 1996; Hanahan and Weinberg, 2000). Cancer is generated in response to exposure to external sources of damage, and genetic predisposition (Sonnenschein and Soto, 2008). Malignant cellular transformation refers to the process of cells acquiring properties and hallmarks of cancer (Parsa, 2012). We showed previously that the ASC52telo cells under chronic PHA-767491 treatment have established persistent DNA damage. To establish if mild proliferation inhibition leads to cellular transformation *in vitro*, some further hallmarks or properties of cancer cells were investigated. A fundamental feature of cancer biology is the ability of the cell to exhibit anchorage-independent cell growth, which is the capability of colony forming in semisolid media. This feature is associated with tumour cell aggressiveness *in vivo*, including tumour cell metastasis, and a marker of transformation *in vitro* (Mori et al., 2009).

The ASC52telo cells were to be cultured for an extended period of time and a suitable density, while maintaining viability was to be established. ASC52telo cells were seeded at a range of densities and viability was measured by morphology appearance, cell count, and percentage of viability during cell culture over 5 days. These parameters were maintained over the culture time in ASC52telo cells seeded at 2000 cells per 96 well, which was deemed a suitable seeding density for both high and low passages (Figure 4.2-a). To establish if ASC52telo cells under the PHA-model acquired anchorage independent growth, the cells were seeded onto ultra-low attachment 96 well plates, alongside adherent plates. Cell morphology changes were shown with viable cells forming clumps while cultured under anchorage-independent conditions, with large clumps were seen (Figure 4.2-b). Cell viability of these cells was measured using MTS assay with a significant difference seen in High passage chronic PHA-767491 ASC52telo cells. This measurement was normalised against ASC52telo cells treated under the same conditions except seeded onto the adherent (standard) plate, representing an appropriate baseline of cell viability (Figure 4.2-c). When the cells were collected following anchorage-independent growth and reseeded onto adherent plates, continued cell growth was observed (Figure 4.2-d)

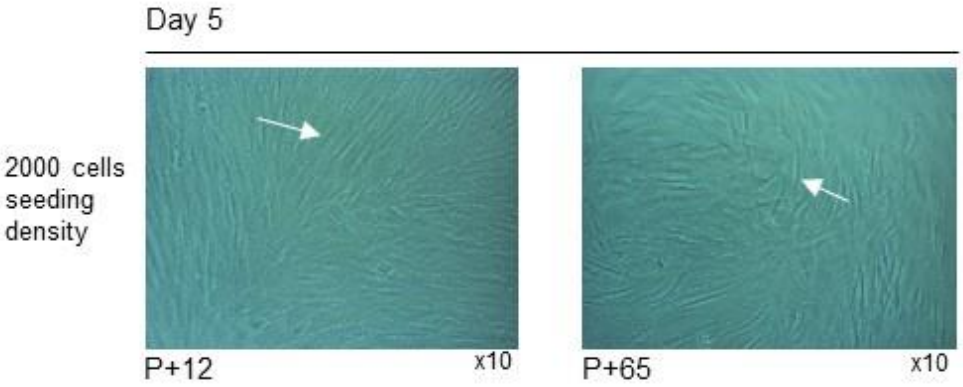
Day 5
2000 cells seeding density
P+12
x10
P+65
x10

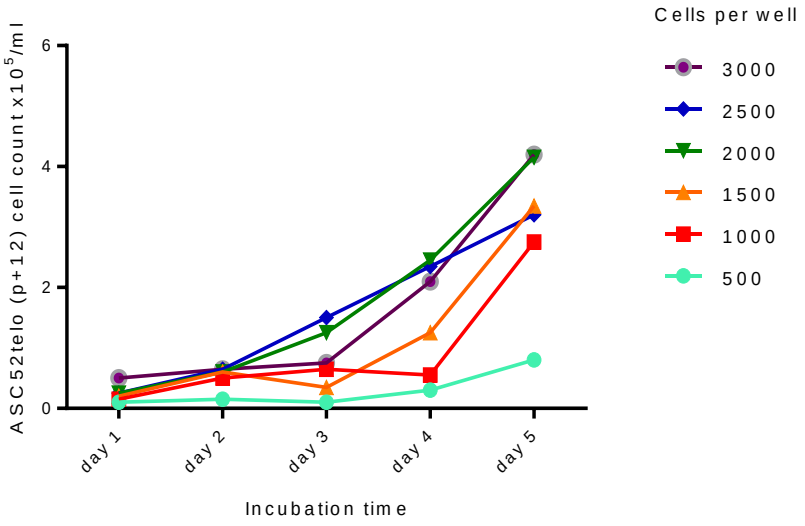
ASC52telo (p+12) cell count x10^5/ml
0
2
4
6
day 1
day 2
day 3
day 4
day 5
Incubation time
Cells per well
3000
2500
2000
1500
1000
500

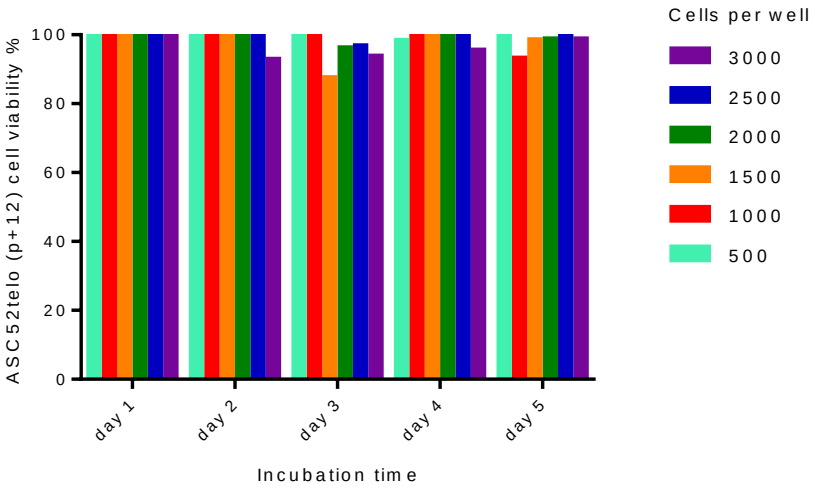
ASC52telo (p+12) cell viability %
0
20
40
60
80
100
day 1
day 2
day 3
day 4
day 5
Incubation time
Cells per well
3000
2500
2000
1500
1000
500

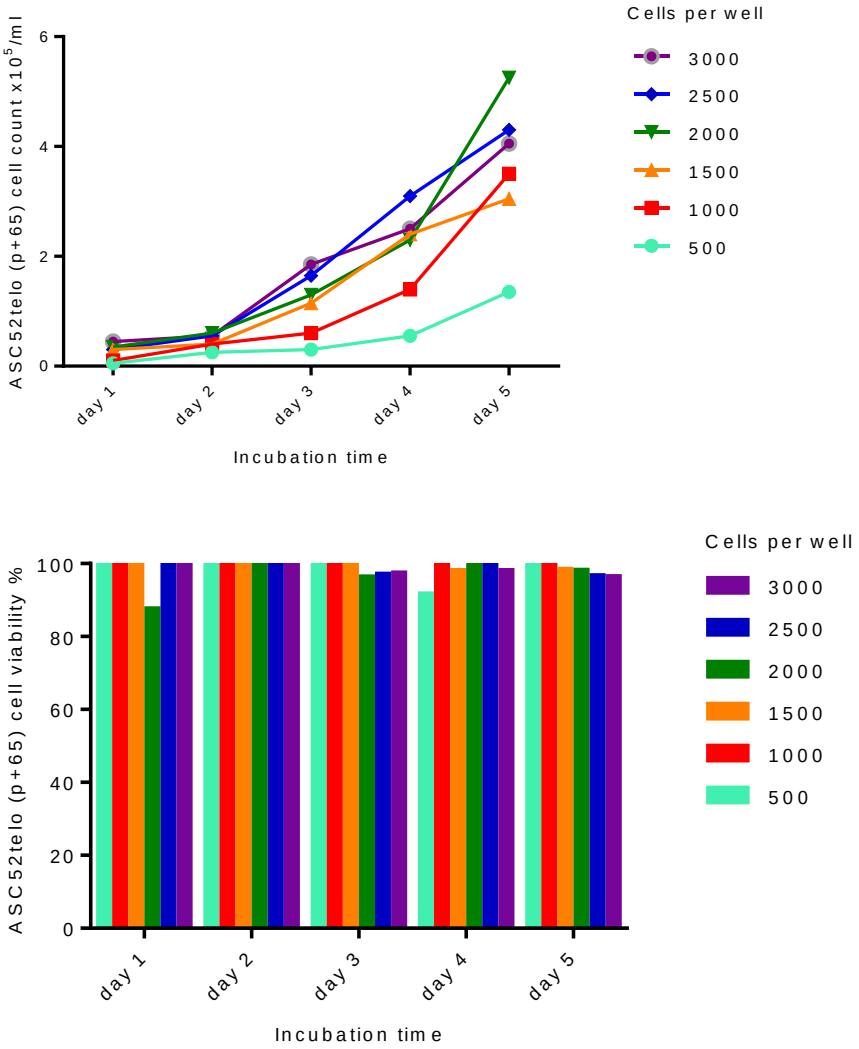

Figure 4.2-a Cell viability with varied seeding density in ASC52telo cells. ASC52telo low (p+12) and high (p+65) passage cells were seeded at a range of seeding densities (as indicated in the legend) in a 96 well plate and incubated for 5 days. Each day the cells were detached using trypsin and counted using haemocytometer in trypan blue to measure cell viability. Seeding at 2000 cells per well showed steady increase in cell count while maintaining cell viability in both high and low passages, graphs represent one independent preliminary experiment (n=1). Phase contrast images were collected using a Nikon Eclipse T5100 inverted microscope and DN100 camera with x10 objective. Cell growth and confluence were observed while maintaining normal morphological appearance, over the culture period, white arrows-normal elongated cells.

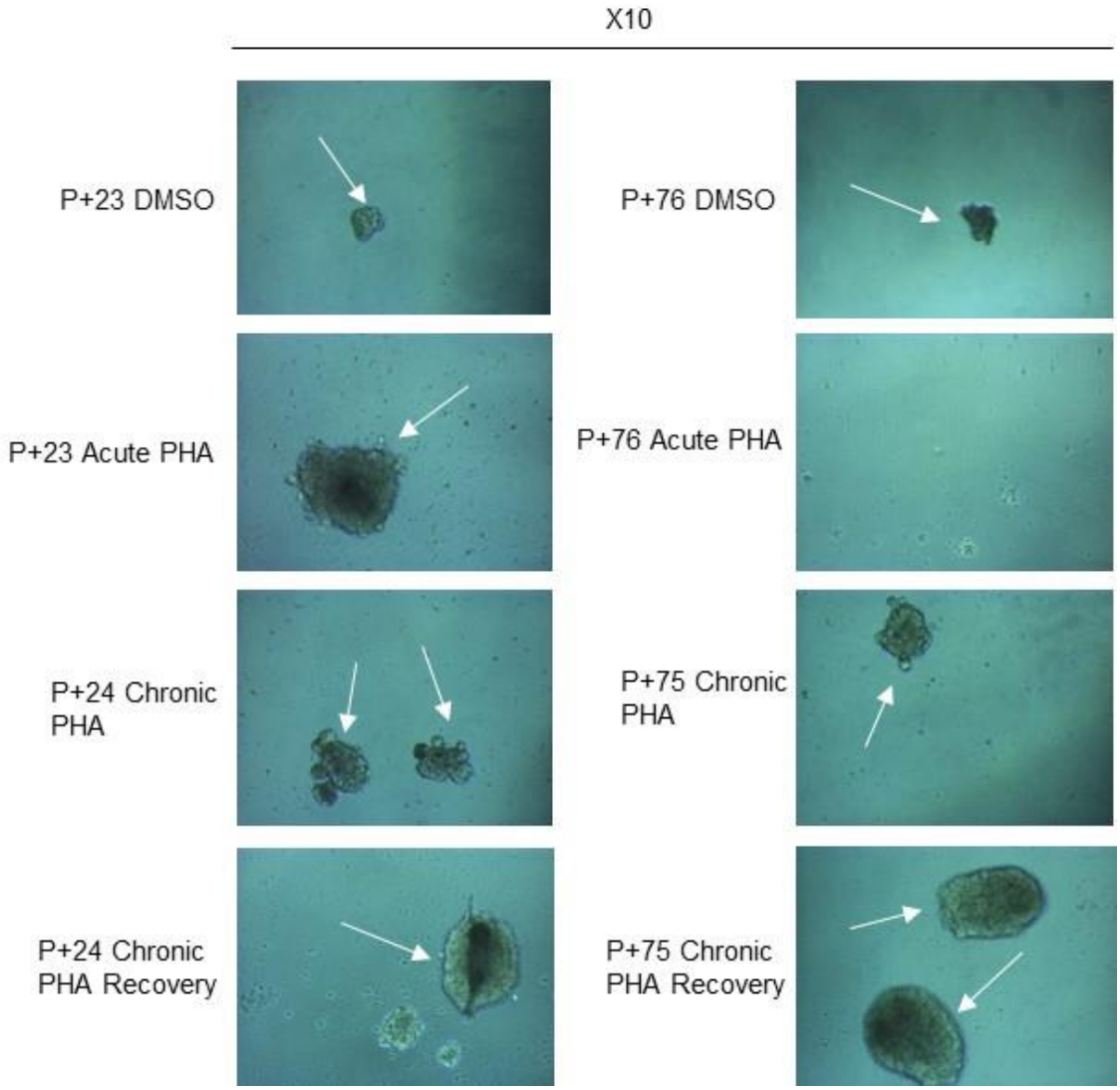

Figure 4.2-b Cell morphology and anchorage-independent growth in ASC52telo cells treated according to the PHA model. ASC52telo cells were seeded at 2000 cells per well in Costar flat bottom ultra-low attachment surface non-pyrogenic (3474) 96 well plate. PHA-767491 was added to short term treated cells throughout this incubation (15 days), while long term treatment was maintained continuously. Phase contrast images were taken using a Nikon Eclipse T5100 inverted microscope and DN100 camera, with x10 objectives. Cell clump formation was observed (white arrows) to a different degree in correlation with treatment.

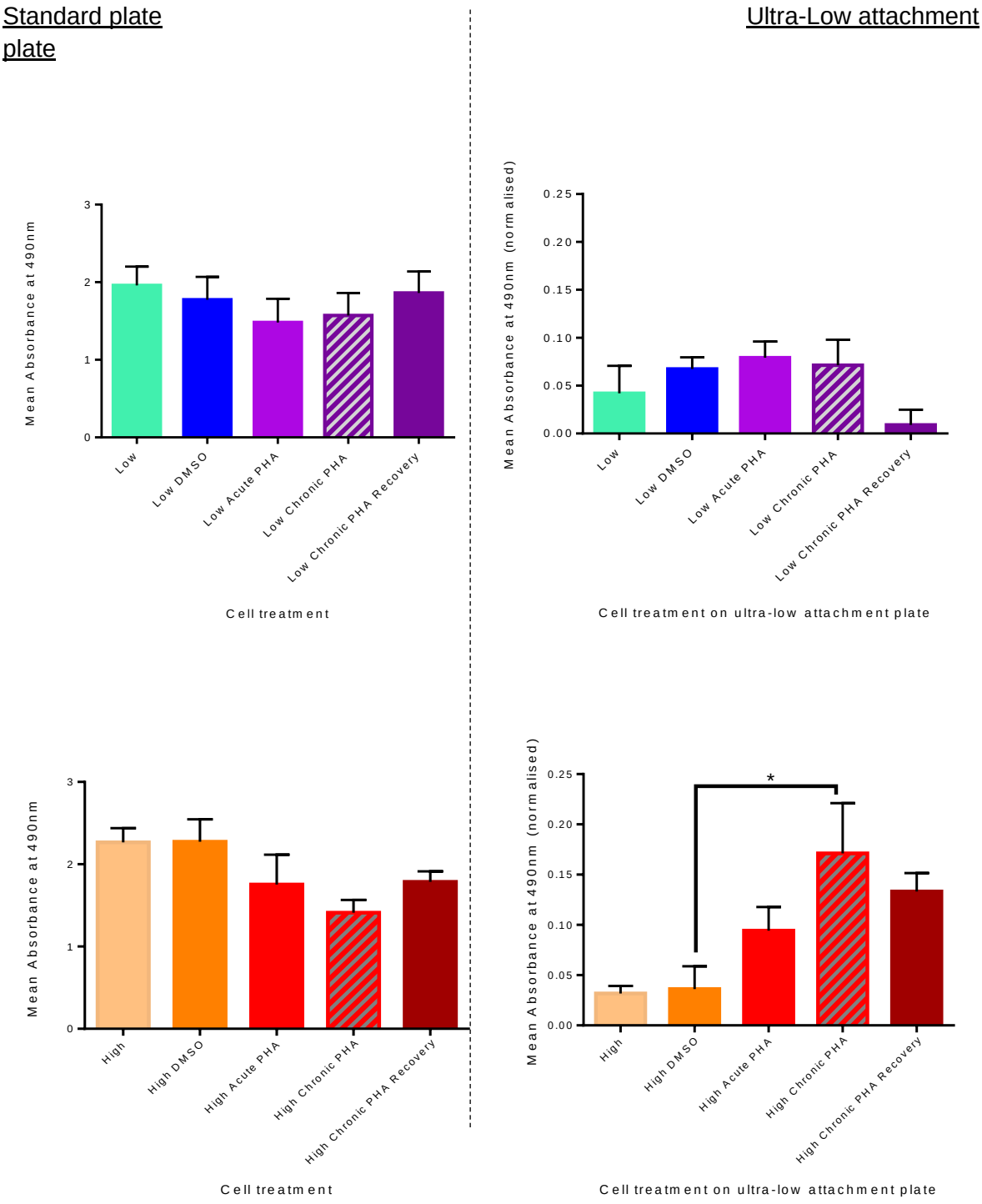

Figure 4.2-c Anchorage-independent growth in ASC52telo cells under PHA-model. ASC52telo cells were seeded at 2000 cells per well in triplicates in Costar flat bottom ultra-low attachment surface non pyrogenic (3474) 96 well plate, and control standard 96 well plate. The cells were incubated and the media was changed carefully every 3 days. MTS assay was performed at day 15. Low/Low DMSO/Low Acute PHA: P+15, 17, and 23, Low Chronic/Recovery: P+18, 19, 24. High/High DMSO/ High Acute PHA: P+68,70, 76, High Chronic/Recover: P+68, 69, 75. Error bars represents SEM, statistical values were calculated by the Tukey post hoc test following one-way ANOVA analysis * P≤0.05, Graphs represent combined data of three independent experiments (n=3). Cell viability was maintained over the culture time on standard plate, significant reduced proliferative rate was not seen in PHA-767491 treated cells over long-term culture (standard plate). Following growth on ultra-low attachment plate high passage chronic PHA-767491 cells demonstrated an increase in MTS signal, suggesting growth under anchorage independent conditions.

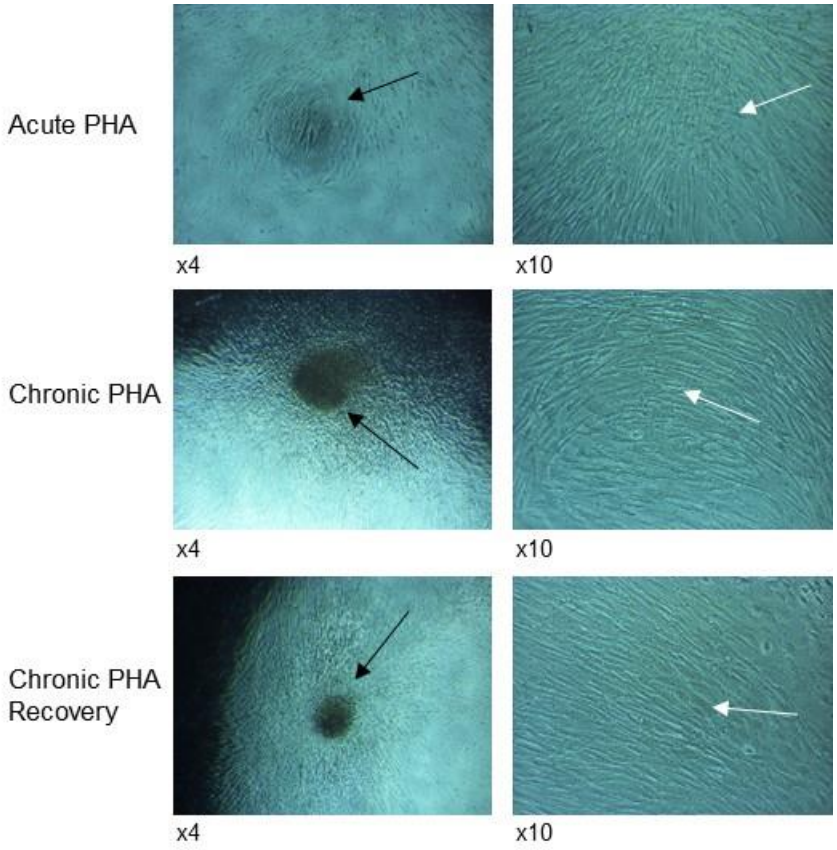

Figure 4.2-d Recovery of ASC52telo cells cultured according to the PHA model, following anchorage-independent growth. ASC52telo cells P+68 were seeded at 2000 cells per well in Costar flat bottom ultra-low attachment surface non-pyrogenic (3474) 96 well plate for 15 days, with careful media changes, under PHA-model. After culturing under anchorage independent conditions, the cells were trypsinised and re-seeded onto standard adherent plate for 10 days. Phase contrast images were taken using a Nikon Eclipse T5100 inverted microscope and DN100 camera, with x4, x10 objectives. Cell recovery was seen with adherent growth observed (white arrow), cell clump adhering to plate surface (black arrow),

4.2.1 Contact inhibition

A hallmark of cell transformation is impaired contact inhibition (Abercrombie, 1979). To determine if ASC52telo treated with PHA-767491 for an extended period have acquired this characteristic, analysis of contact inhibition was performed using a range of methods.

ASC52telo cells were cultured as per the PHA-767491 model for 18 days with cell count and cell viability analysed. As expected, untreated ASC52telo cells under normal growth conditions (high and low passage) demonstrated a steady increase of cell numbers, which reached a plateau during long term culture to 18 days. Acute PHA-767491 treated cells demonstrated a steady reduced proliferative rate up to day 4 as found previously, however an increase similar to untreated cells was seen following extended culture time. Chronic PHA-767491 cells appeared to increase in cell number further, suggesting reduced contact inhibition as a possibility. Cell viability was also analysed and verified to be >95% in all cell treatments. Although

increased cell growth may have been seen, the PHA treated cells appeared to form clumps which would result in discrepancies in cells count, resulting in inaccurate representation (Figure 4.2-e).

Therefore, the cells were lysed and protein concentration was analysed as a measure of growth. Low passage acute culture showed an increase which then fell again. Continual cell growth was further demonstrated in high passage chronic PHA-767491 treated cells following recovery (Figure 4.2-f), while MTS assay suggested continued cell proliferation (Figure 4.2-g), however, this finding needs to be verified. The cells were also assayed with the Promega Real-time Glo MT assay using luminescence, which allows non-endpoint measurements, unlike the MTS assay. It showed steady cell growth at day 21. We hoped to analyse these cells using the same method at day 24, but luminescence was lost, therefore an MTS assay was performed on these cells at day 28. It suggested continual growth in high passage chronic PHA-767491 cells compared to same passage cells with no treatment (Figure 4.2-h).

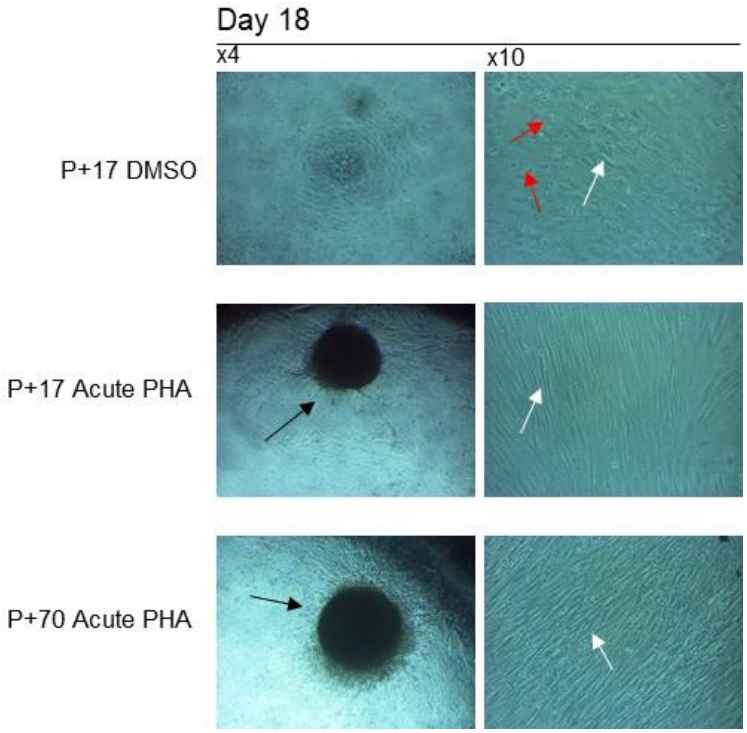
Day 18
x4
x10
P+17 DMSO
P+17 Acute PHA
P+70 Acute PHA

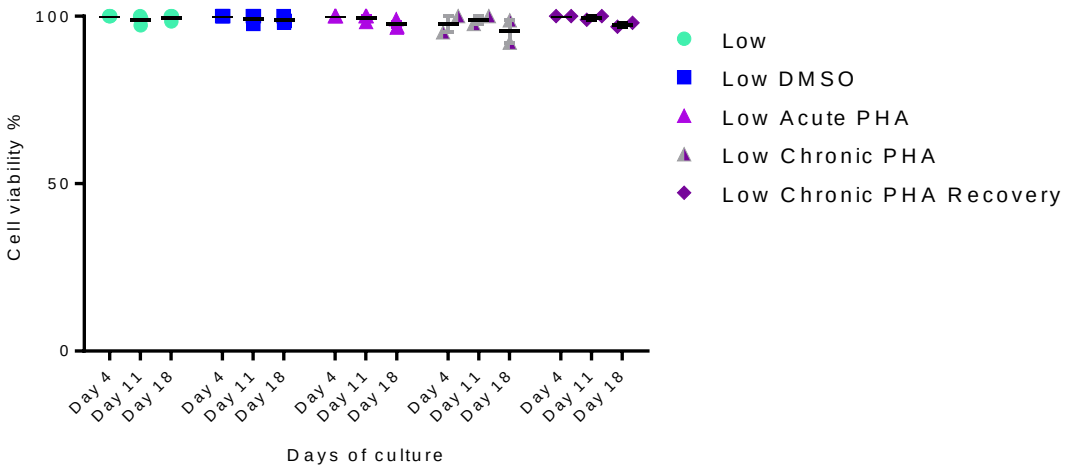
100
50
0
Cell viability %
Day 4
Day 11
Day 18
Days of culture
Low
Low DMSO
Low Acute PHA
Low Chronic PHA
Low Chronic PHA Recovery

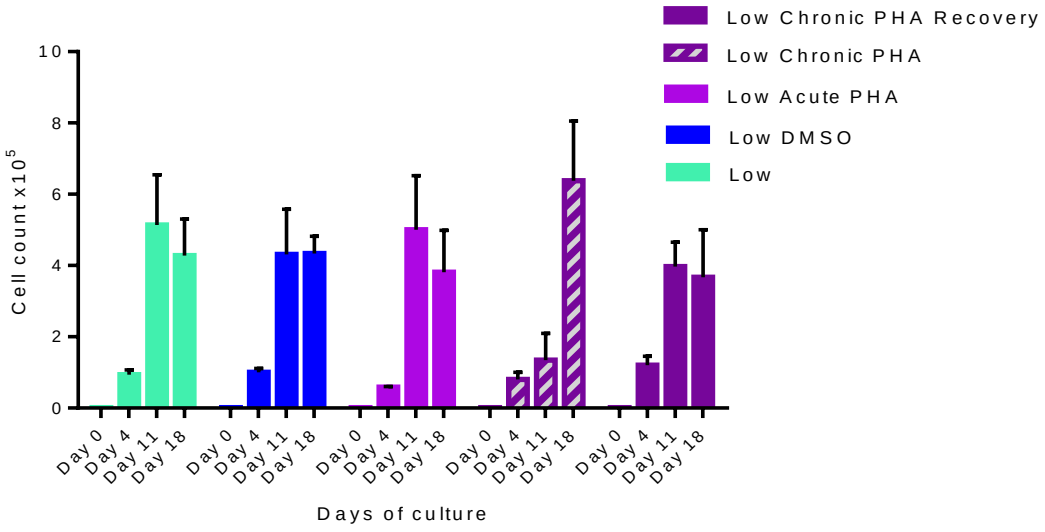
10
8
6
4
2
0
Cell count x10^5
Day 0
Day 4
Day 11
Day 18
Days of culture
Low Chronic PHA Recovery
Low Chronic PHA
Low Acute PHA
Low DMSO
Low

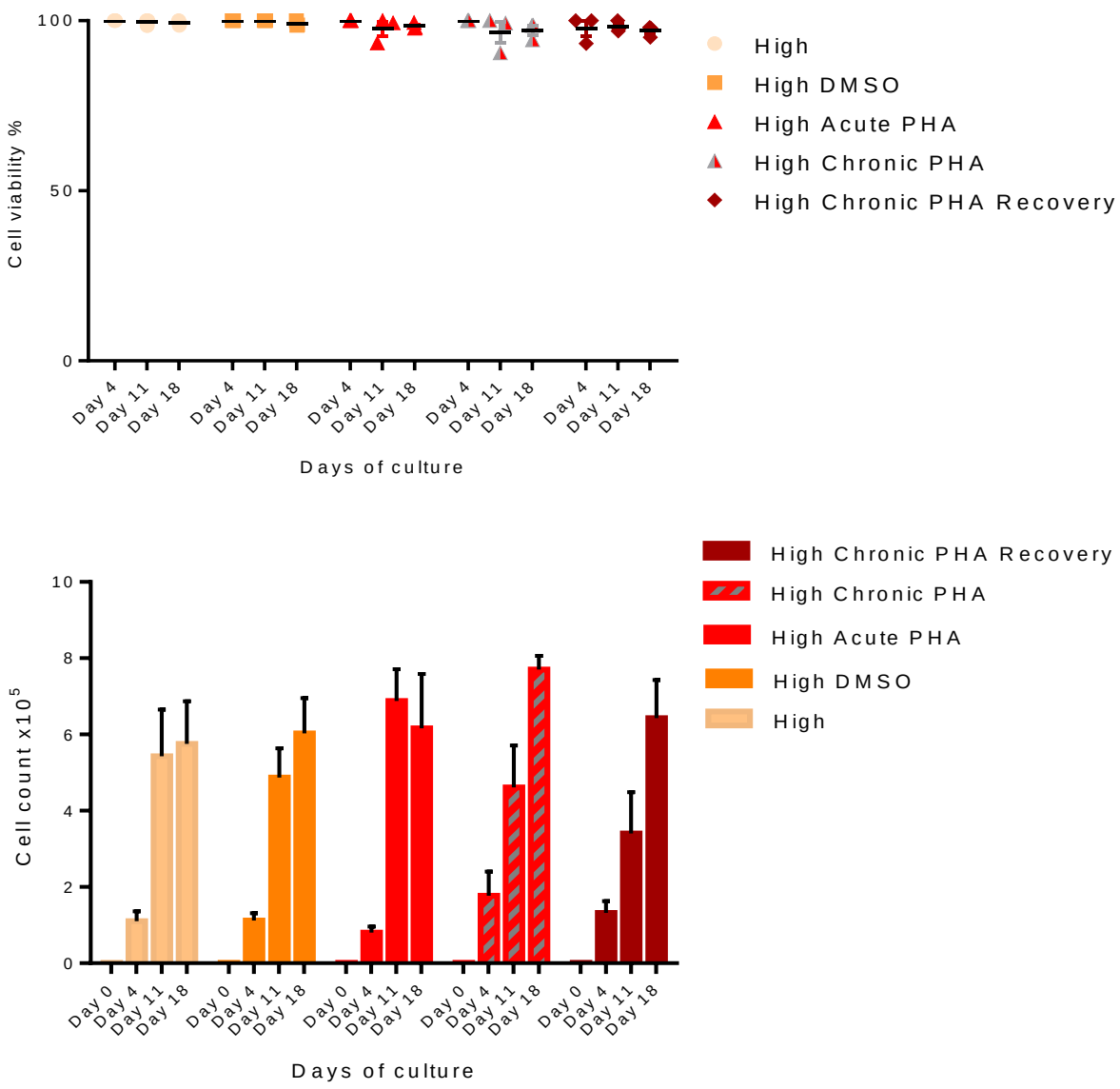

Figure 4.2-e Analysis of contact inhibition using cell count and viability following long term culture of ASC52telo cells treated with PHA-767491. ASC52telo cells were seeded at 2000 cells per well in 96 well plate in various conditions as per the PHA model, and incubated for the indicated number of days. At those points the cells were counted using haemocytometer and cell viability was measured using trypan blue. Graphs and error bars represent SEM of combined data from independent experiments as indicated in brackets, Low, Low DMSO, Low acute PHA-767491:P+14, P+16, P+17 (n=3), Low chronic PHA-867491, Low chronic PHA-767491 recovery: P+19, +20 (n=2). High, High DMSO, High acute PHA-767491, High chronic PHA-867491, High chronic PHA-767491 recovery:P+67, 69, P+70 (n=3). Morphology was observed and phase contrast images were taken using a Nikon Eclipse T5100 inverted microscope and DN100 camera with x4 and x10 objectives. Cell clumping was observed with high cell density during culture. White arrow – Normal cell elongation, Red arrow- cell debris, Black arrow – cell clumps. Cell viability across treatments was maintained <95%,

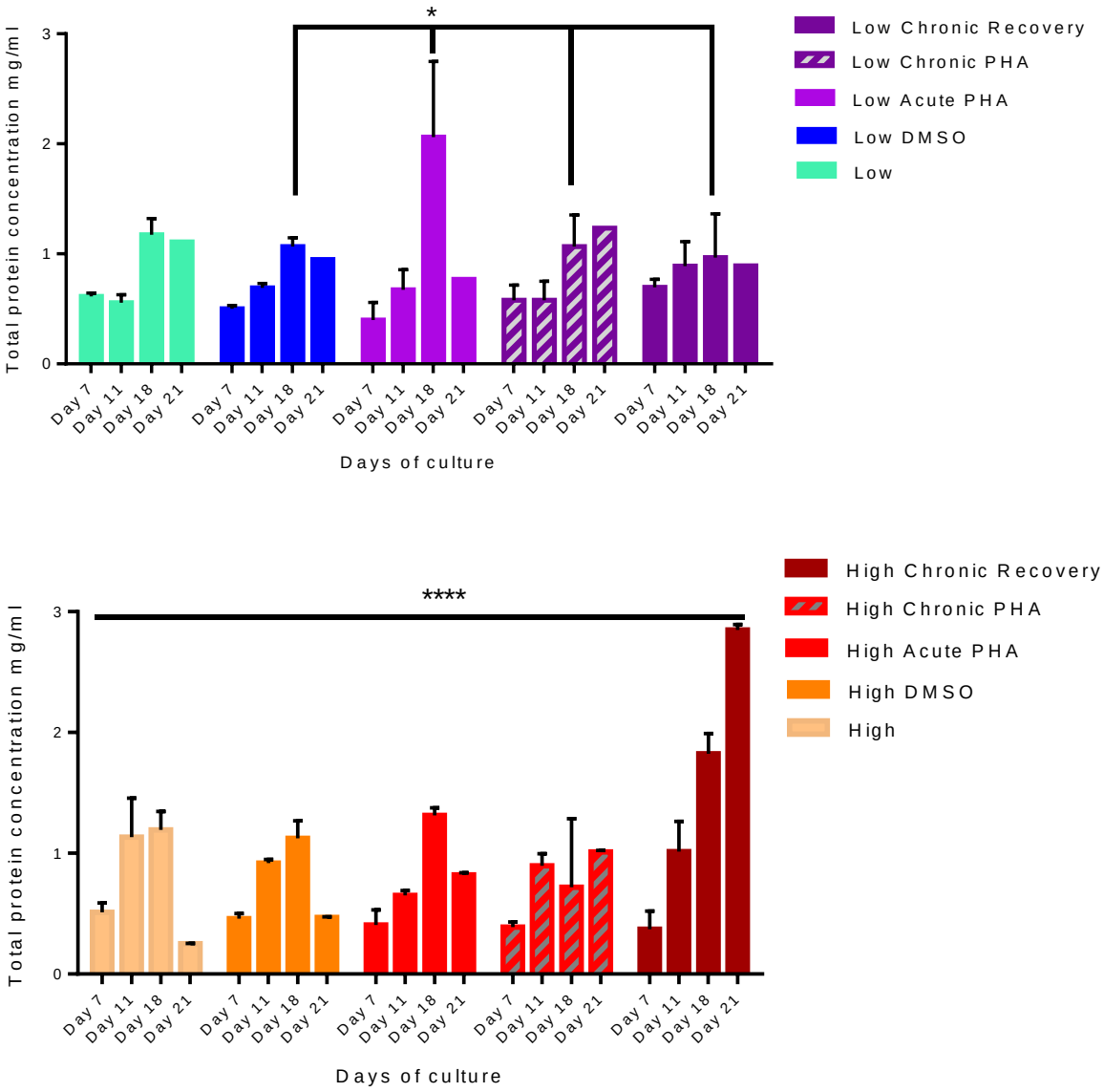

Figure 4.2-f Contact inhibition in ASC52telo cells treated long term with PHA-767491 analysed based on protein concentration. ASC52telo cells were seeded at 5000 cells per cm^2 on a 96 well plate in triplicates, under the various PHA conditions, as per the PHA model. Cells were incubated for the indicated number of days with media changes every 3 days. At the indicated days cell lysates were collected and protein concentrations were measured with Bradford assay. Day 7 and 11- Low: P+28,29,32 Low Chronic PHA/Recovery: P+31,32,35. High: P+81,82,85, High Chronic PHA/Recovery: P+72, 73,81 (n=3), Day 18 Low: P+28, 32, Low Chronic PHA/Recovery: P+31, 35. High: P+81, 85, High Chronic PHA/Recovery: P+72, 80, (n=2), Day 21- Low: P+29, Low Chronic PHA/Recovery: P+32. High: P+82, High Chronic PHA/Recovery: P+73 (n =1). Error bars represent SEM, statistical values were calculated by the Tukey post hoc test following two-way ANOVA analysis, * P≤0.05, Graphs represent combined data from independent experiments as indicated in brackets. Overall significant increase in continual growth in High passage chronic PHA-767491 treated cells under recovery.

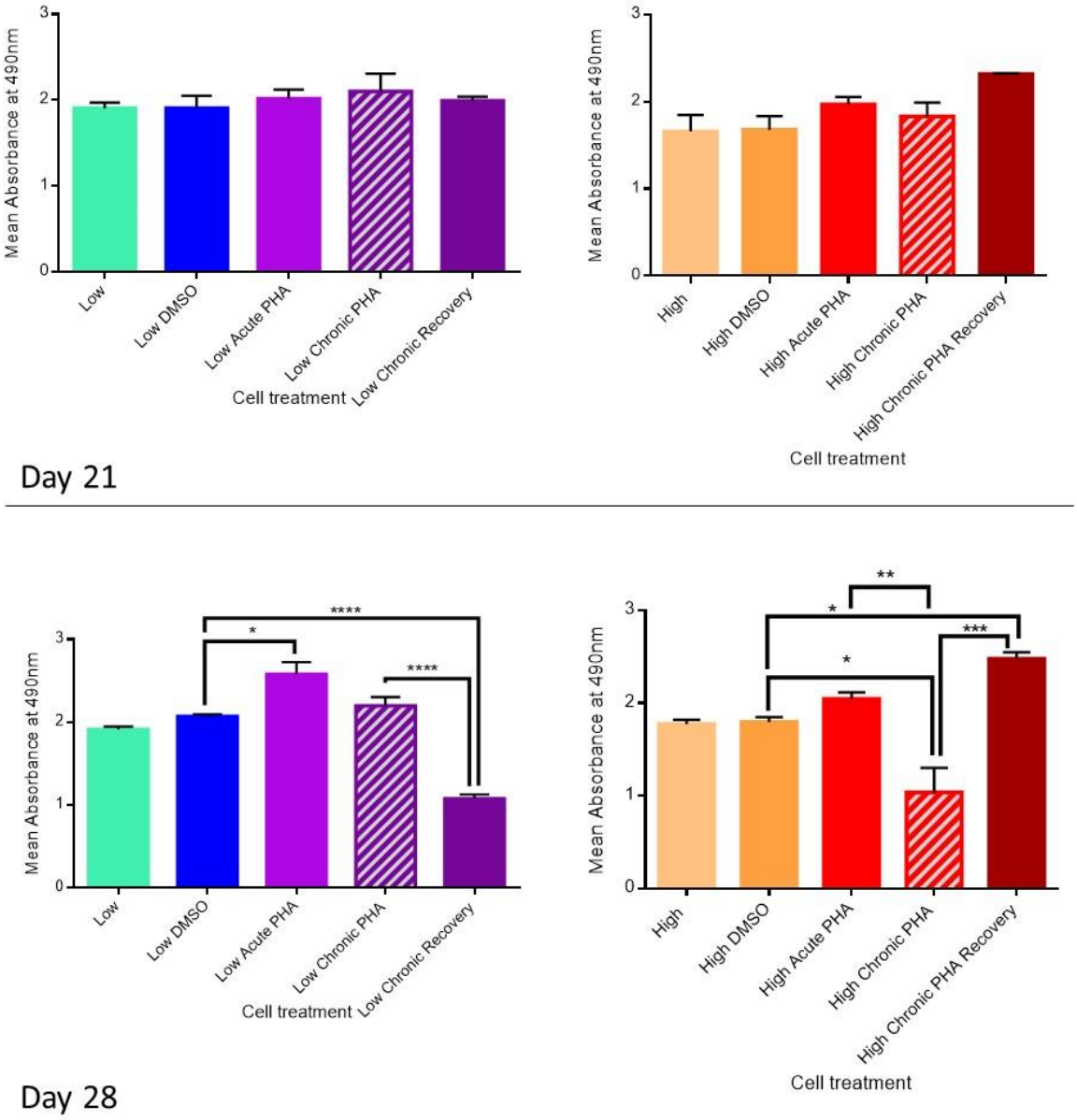

Figure 4.2-g Cell viability of ASC52telo cells following long term culture with PHA-767491 treatment, measured by MTS assay. ASC52telo cells were seeded at 5000 cells per cm^2 on a 96 well plate in triplicates, under conditions set out by the PHA model. Cells were incubated for the indicated number of days and the media was changed every 3 days. At the indicated days MTS assay was performed. Error represents SEM of triplicates; statistical values were calculated by the Tukey post hoc test following one-way ANOVA analysis, * P≤0.05, ** P≤0.01, ***P≤0.001, ****P≤0.0001. Graphs represent combined data from independent experiments as indicated in brackets. . Day 21- Low/Low DMSO/Low Acute PHA: P+29, 31, Low Chronic PHA/Recovery: P+32,34. High/ High DMSO/High Acute PHA: P+82, 84,(n=2). Day 28 - Low/Low DMSO/Low Acute PHA: P+34, Low Chronic PHA/Recovery: P+37. High/ High DMSO/High Acute PHA: P+87, High Chronic PHA/Recovery: P+82, (n=1). A higher increase in cell numbers was indicated by the MTS assay in high passage PHA-767491 treated cells under recovery, compared with controls, which increased further following longer culture time.

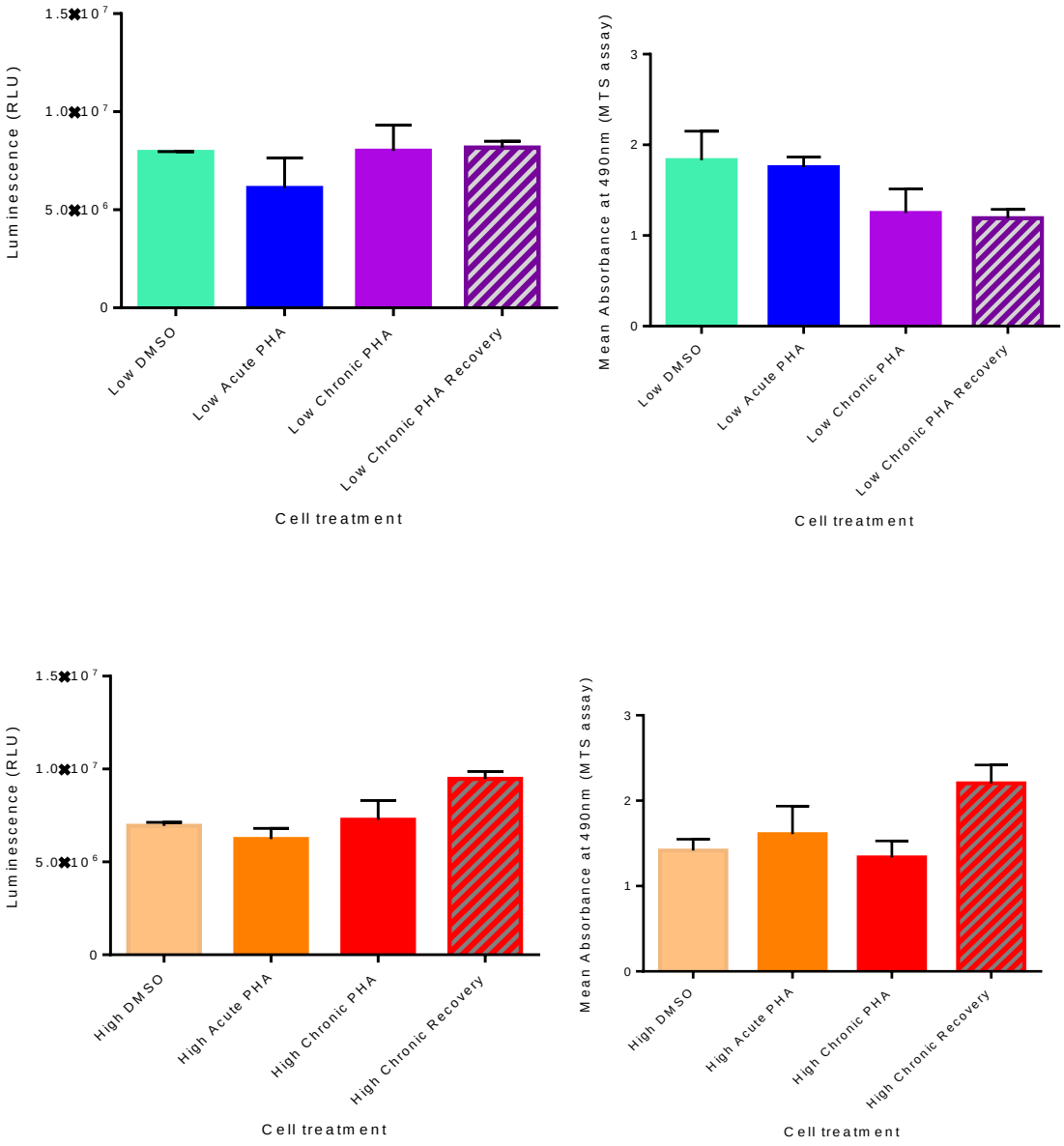

Figure 4.2-h Continual cell viability following long term culture and PHA-767491 in ASC52telo, measured using real-time-Glo MT assay followed by MTS assay. ASC52telo cells were seeded at 5000 cells per cm^2 on a 96 well plate in triplicates, under conditions defined by the PHA model. Cells were incubated for 21 days with media changes every 3 days. On day 21 the real-time-Glo MT assay was performed with luminescence reading. The media was changed and the cells maintained under the same conditions of PHA model; media was further changed every 3 days. At day 28 an MTS assay was performed. Error represents SEM of triplicates, statistical values were calculated by the Tukey post hoc test following one-way ANOVA analysis. Low DMSO/Acute PHA: P+32,33, Low Chronic PHA/Recovery: P+35, 36. High DMSO/Acute PHA: P+85,86, High Chronic PHA/Recovery: P+80,81, Graphs represent combined data from two independent experiments (n=2). A higher increase of cell numbers was indicated by the analysis over long term culture in high passage chronic PHA-767491 cells under recovery compared to untreated cells, although not significant, suggests continual growth.

4.3 Verification of STR genotypes

Following long term culture of ASC52telo cells in our study, it was important to verify the genotype of ASC52telo cell line, and rule out contamination. We originally obtained the ASC52telo cells from ATCC® hTERT immortalized adipose derived Mesenchymal stem cells (ATCC® SCRC 4000™), and cultured over long term, and under acute and chronic PHA-767491 treatment. The genotype of the cells was

analysed with DNA fingerprinting of polymorphism by profiling short tandem repeats by PCR amplification followed by capillary gel electrophoresis. For genotyping we used the Promega GenePrint 10 kit, which types the cell lines using 10 loci. In our analysis CSCF1PO was not seen which is likely due to not running the PCR products on the capillary electrophoresis equipment long enough. We are confident that the cell lines were not contaminated as matched genotype without overlapping signal was demonstrated (Figure 4.3-a).

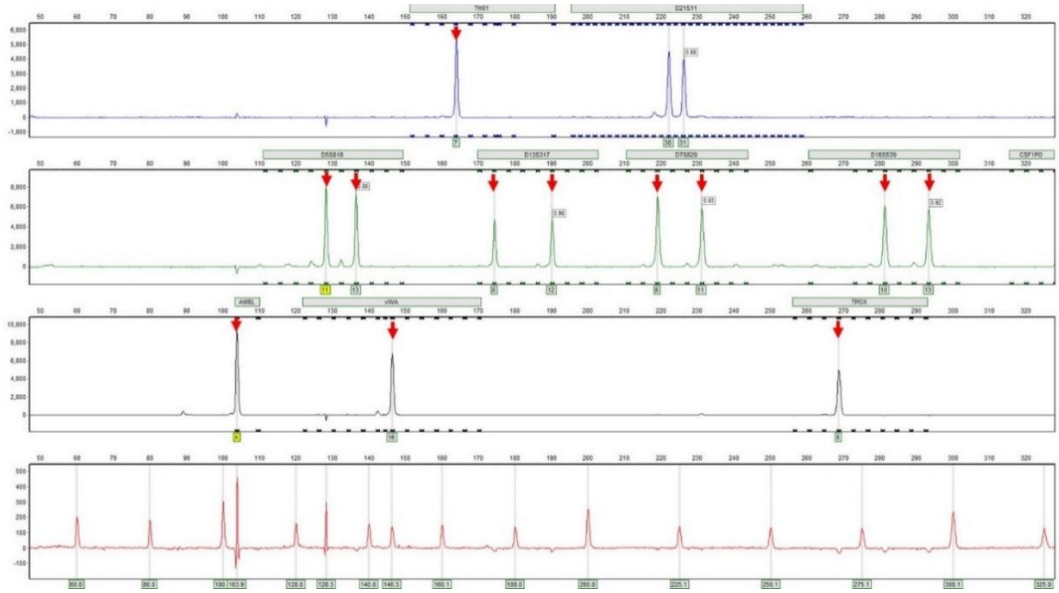

ASC52telo p+6

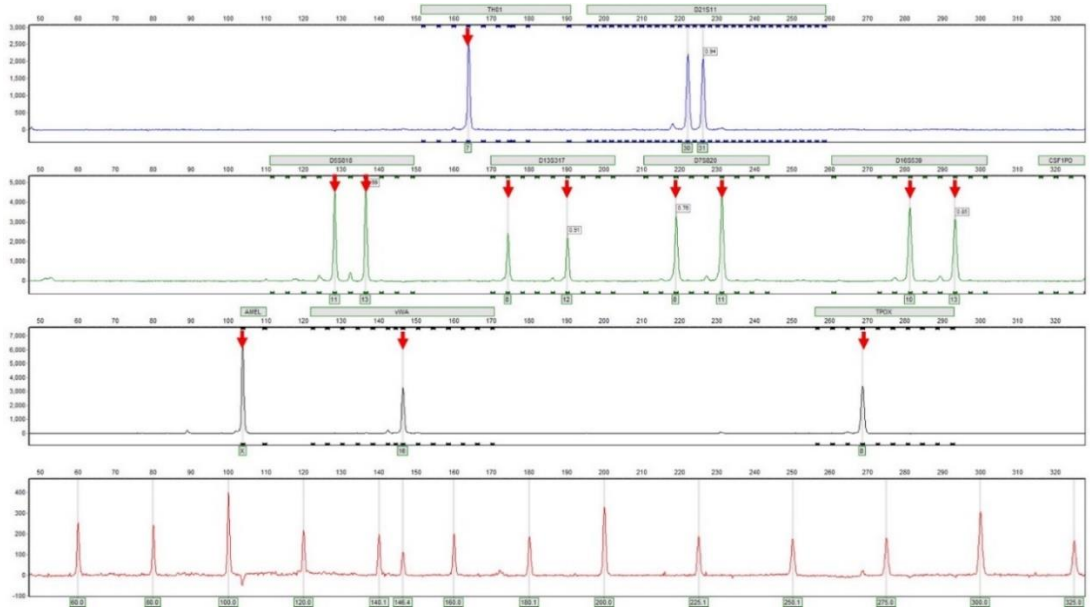

ASC52telo P+96

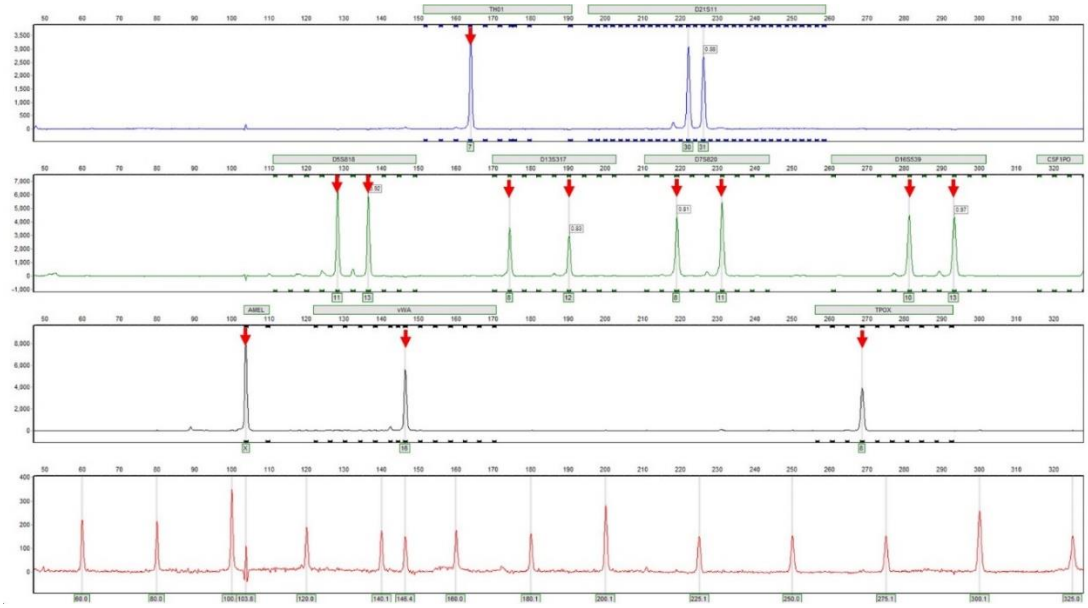

ASC52telo P+96 Chronic PHA

Figure 4.3-a STR profile of ASC52telo cell line with and without chronic PHA-767491 treatment. Amplicons were generated by PCR and separated by capillary gel electrophoresis on an Applied Biosystems ABI Prism 310 Genetic Analyser, and analysed using GeneMarker HID. Expected DNA profile (red arrows at peaks): Amelogenin: X, D13S317: 8, 12, D16S539: 10, 13, D5S818: 11, 13, D7S820: 8, 11, THO1: 7, TPOX: 8, vWA: 16, which match the genotype of our ASC52telo cell lines, high and low passage, and chronic PHA-767491 treated cells.

4.4 Summary

Overall, our data suggests that chronic interference with DNA replication initiation induced with PHA-767491 treatment leads to chromosomal instabilities. Inefficient DNA repair or avoiding apoptosis may result in the acquiring of sustained DNA damage and cell transformation. The genotype of long term culture of ASC52telo cells was maintained.

5 Chapter 3 RECQL4 dynamics and interacting partners

Results

We established that prolonged, mild interference with DNA replication initiation by inhibiting DDK can result in genomic instabilities and can contribute to the transformation of mesenchymal stem cells. DDK acts upstream of RECQL4 in the process of replication initiation (Labib, 2010; Im et al., 2015), which suggests that the changes we observed parallel to long-term inhibition of DDK could recapitulate changes shown by RTS patients who carry mutations that disable RECQL4 functions. RECQL4 mutations lead to a significant predisposition to OS development in RTS type II patients. The second aim of our work was to establish a system that models the effect of impaired / complete lack of RECQL4 in proliferating and differentiating mesenchymal stem cells.

We set out to identify if RTS cells lines show cellular changes similar to our previous findings using the PHA-767491 model, which may sensitize the cells to OS.

The results of RECQL4 mutations could also originate from disrupting protein-protein interactions and protein complexes, and as such could be secondary consequences of disrupted RECQL4 function. A number of RECQL4 interacting proteins have been described in the literature (Croteau et al., 2012b), and we aim to verify some of these to serve as controls in our search for novel interactions following posttranslational modifications. To enable further investigations relating to the knockdown and overexpression of RECQL4, and to further identify interacting RECQL4 proteins, Emerald-GFP tagged RECQL4 cell lines were established.

5.1 Establishing of expression characteristics of RECQL4

In our experiments, we interfere with RECQL4 expression in various ways, therefore it was important to establish the natural expression dynamics as well as expression characteristics following siRNA mediated knockdown.

To establish the influence of proliferation and RECQL4 expression, RECQL4 expression was monitored in U2OS-FLIPINTREX and HeLa LacZeo cells over 9 days without passaging. RECQL4 expression appears to vary over the 9 days; expression increases as cells proliferate, and generally decreases when cells appear to reach confluency, HeLa cells showed more variable expression levels

(Figure 5.1-a and Figure 5.1-b). Unfortunately, we were not able to show RECQL4 expression with immunofluorescence, the antibody turned out to be unsuitable for immunofluorescent staining (Figure 5.1-c).

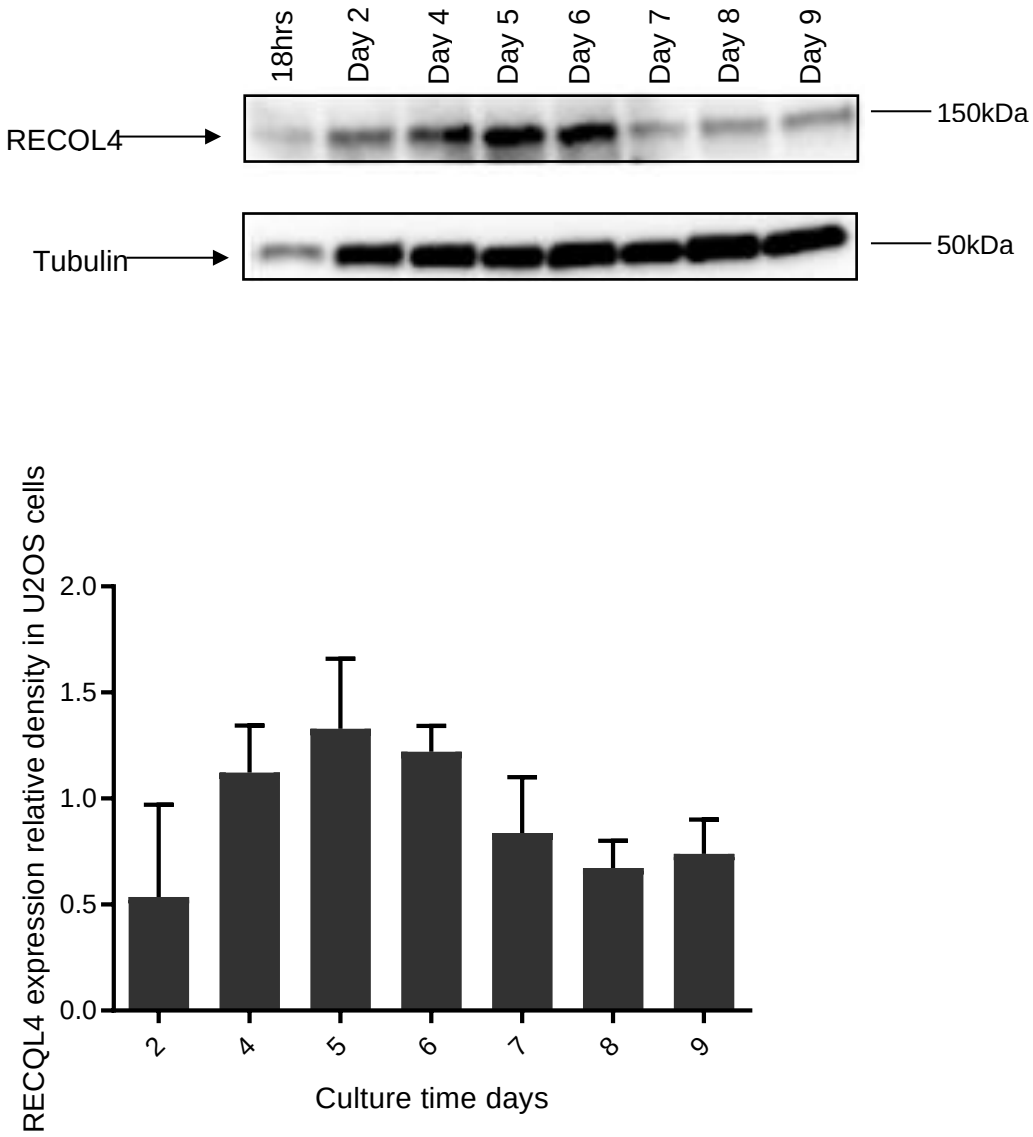

Figure 5.1-a RECQL4 expression in relation to cell confluence in U2OS-FLIPINTREX cells. 12,000 U2OS FLIPINTREX cells were seeded per well in a 96 well plate and incubated for 9 days. Each day cell lysate was collected. Western blot was performed and probed with Tubulin and RECQL4 antibodies. Tubulin verified uniformity of loading. Graph represents data combined from two independent experiments (n=2), error bars represent SEM, one representative western blot is shown. RECQL4 expression was shown to increase with cell proliferation and decrease as cells became confluent,

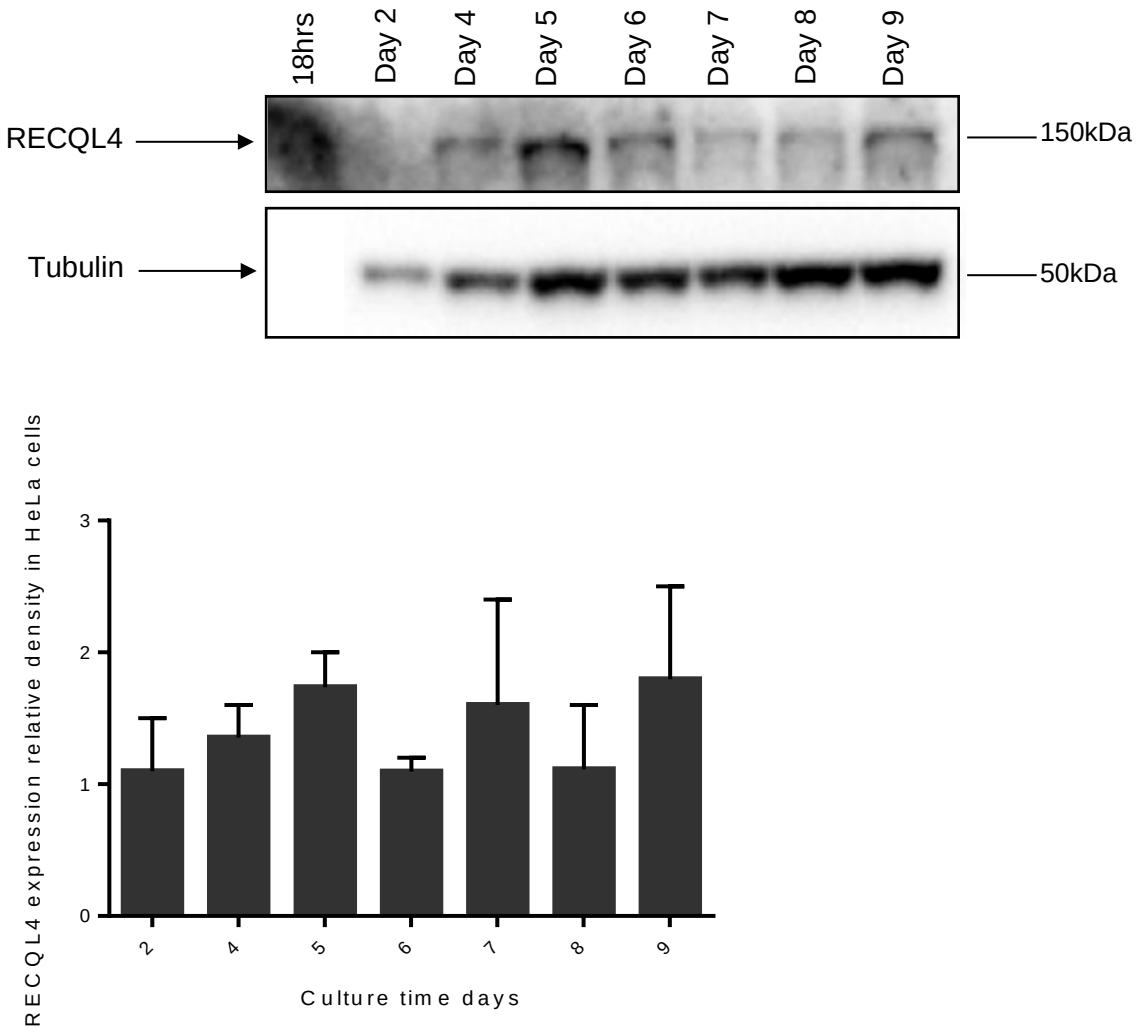

Figure 5.1-b RECQL4 expression in relation to cell confluence in HeLa cells over 9 days. 12,000 HeLa LacZeo cells were seeded per well in a 96 well plate and incubated for 9 days. Each day cell lysate was collected. Western blot was performed and probed with Tubulin and RECQL4 antibodies. Tubulin verified loading efficiency. Graph represents data combined from two independent experiments (n=2), error bars represent SEM, one representative western blot is shown. RECQL4 expression was variable but appeared to increase with cell proliferation and decrease as cells become confluent.

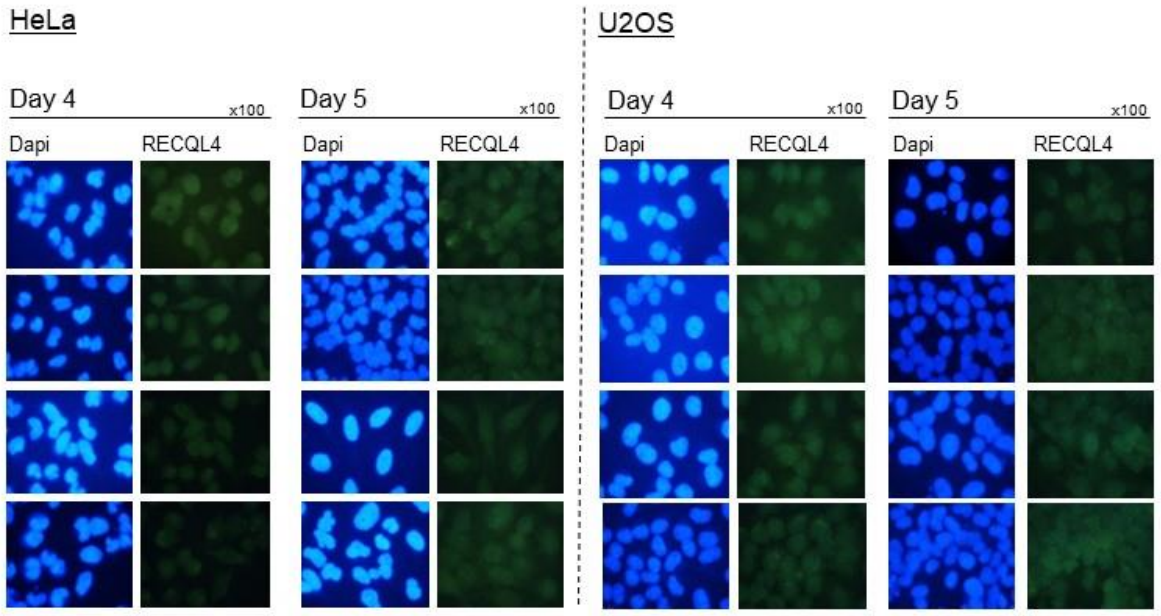

Figure 5.1-c Analysis of RECQL4 antibody in HeLa and U2OS cells. 72000 HeLa LacZeo and U2OS FLIPINTREX cells were seeded per well, in a 24 well plate on sterile glass coverslips and incubated for 4 and 5 days, with medium change on day 3. The cells were fixed with 4% paraformaldehyde and probed for RECQL4 expression. HeLa day 4 1:100 antibody dilution, HeLa day 5 1:75 antibody dilution, U2OS day 5 1:50 antibody dilution, U2OS day 4 1:30 antibody dilution. The cells were analysed by immunofluorescence. Green signal is due to auto-fluorescence detected in high gain setting; no RECQL4 expression was detected (Nikon gain 400); x100 objective.

RECQL4 expression and cellular proliferation was further invesitigated over 10 days. Cell count and viabilty was recorded daily. Cell viability was maintained over the culture time with a steady increase as cell proliferation occurred, and reduction with high cell density (Figure 5.1-d). U2OS cells overall, maintained cell viability and increased in cell count over the 10 day period (Figure 5.1-d). HeLa cells appeared to pick up following a reduction in cell viability and count before a decrease is observed again (Figure 5.1-d). The increase in cell count in HeLa and U2OS cells appears around day 4 or 5, similar to the RECQL4 expression levels previously shown (Figure 5.1-a and Figure 5.1-b). The expression of the Ki67 antigen in cells correlated with cell proliferation: lack of expression represents resting cells with reduced expression following extended culturing in U2OS and HeLa cells (Figure 5.1-e and Figure 5.1-f) as cells stopped cycling. The percentage of Ki67 'dim' cells defined at a threshold set at the lowest 10% of expression level at day 1 post seeding, was analysed and verified decrease in Ki67 expression as cells became confluent over extended culturing in HeLa and U2OS cells, which appeared to correlate with reduced RECQL4 expression in U2OS cells, however, this appeared more variable in HeLa cells (Figure 5.1-e and Figure 5.1-f).

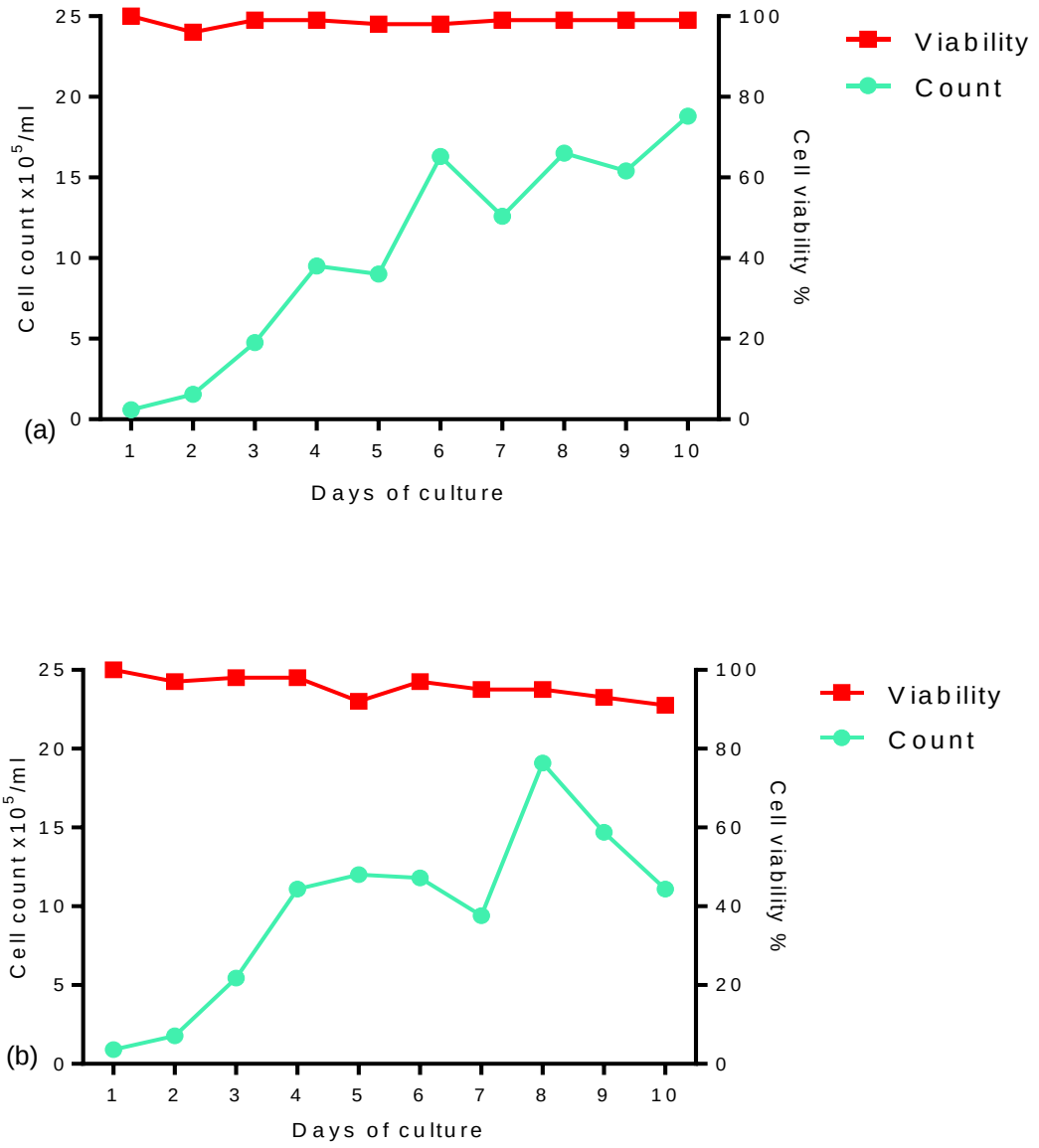

Figure 5.1-d U2OS and HeLa cell proliferation rate and viability over 10 days. 72000 HeLa LacZeo and U2OS FLIPINTREX cells were seeded per well in a 24 well plate and incubated for 10 days, with medium changes every 3 days. Cell count, using BioRad counter, and viability was recorded daily using trypan blue in (a) U2OS, (b) HeLa cells. Cell proliferation was demonstrated with an increase in cell count while maintaining cell viability. Graph represents one preliminary experiment (n=1). Over long-term culture, proliferation rate seems to decrease in HeLa cells,

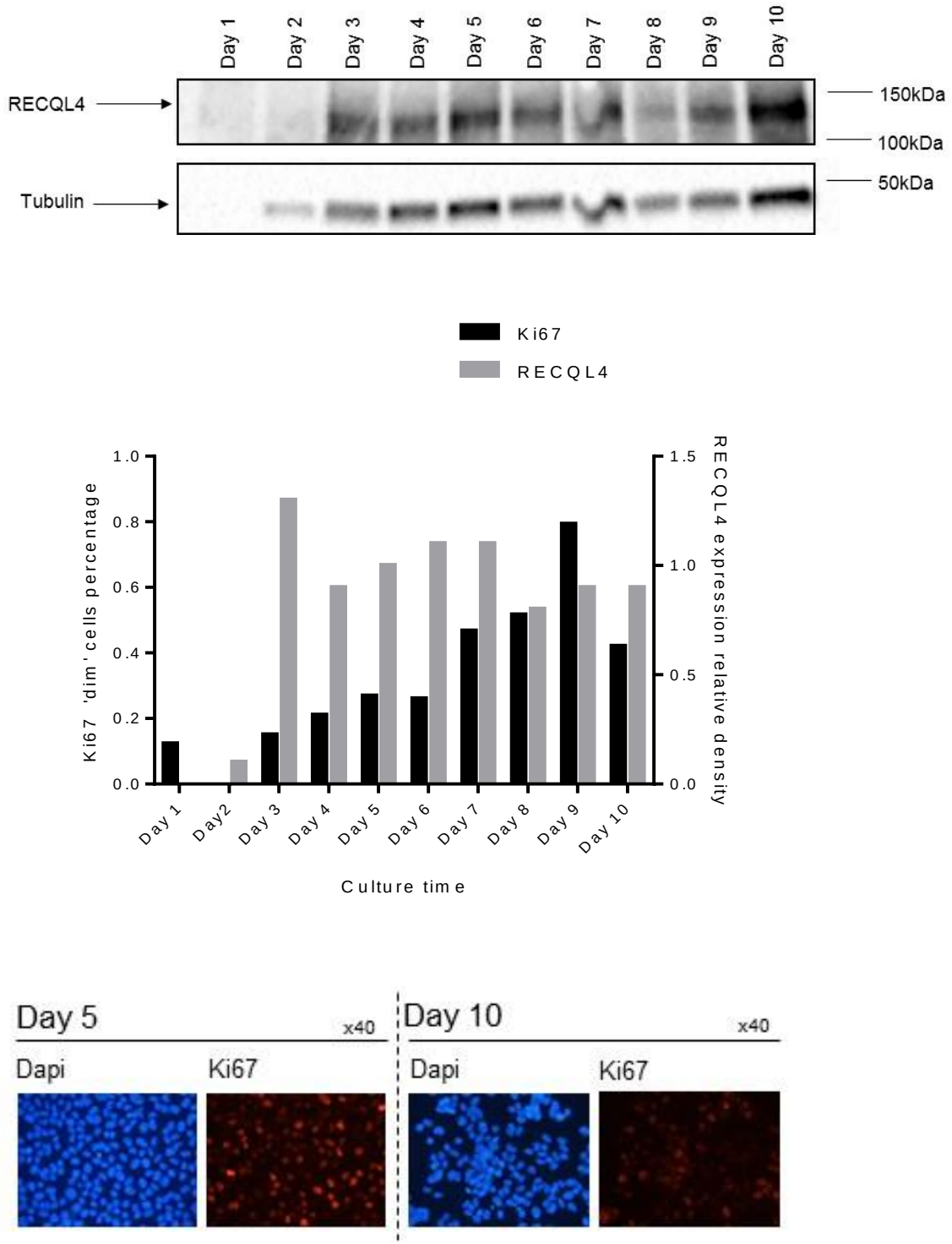

Figure 5.1-e The percentage of Ki67 'dim' cells in relation to RECQL4 expression in U2OS cells. 72000 U2OS FLIPINTREX cells were seeded per well in a 24 well plate in duplicates and incubated for 10 days with medium changes every 3 days. Each day cell lysate was collected from the appropriate well. SDS page and Western blot were performed and the membrane was probed for Tubulin and RECQL4. RECQL4 expression represented as relative density compared to Tubulin. Cells on a parallel well were also fixed with 4% paraformaldehyde and probed for Ki67 expression. The cells were analysed by immunofluorescence. One representative graph and western blot is shown. Red cells show Ki67 expressing cells. Ki67 expression decreased over 10 days of cell culturing. Representative images are shown from day 5 and 10. Ki67 signal was detected using Nikon E800 microscope with DN100 imaging camera, using DAPI and TRITC filters and imaging software, 40x objective. Ki67 expression quantified using CellProfiler. 'Dim' cells show low Ki67 signal and are non-proliferating.

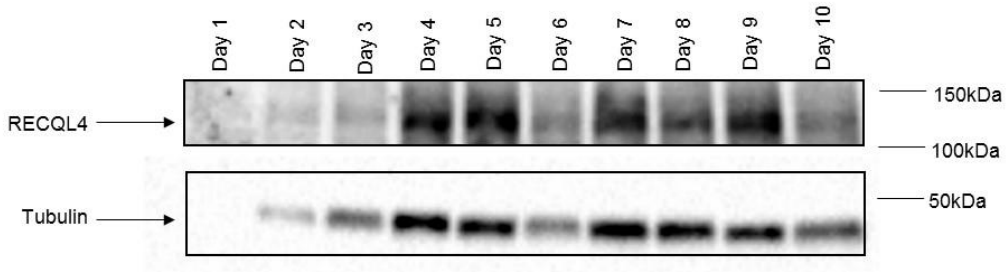

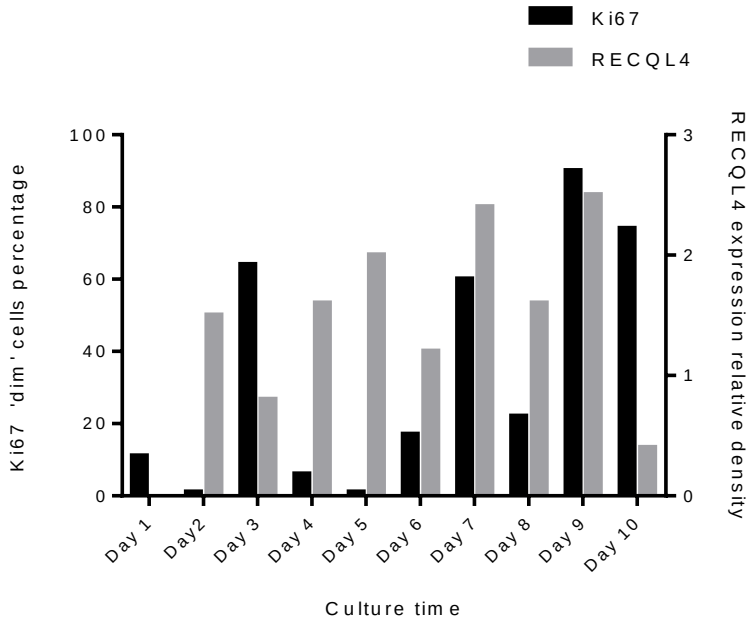

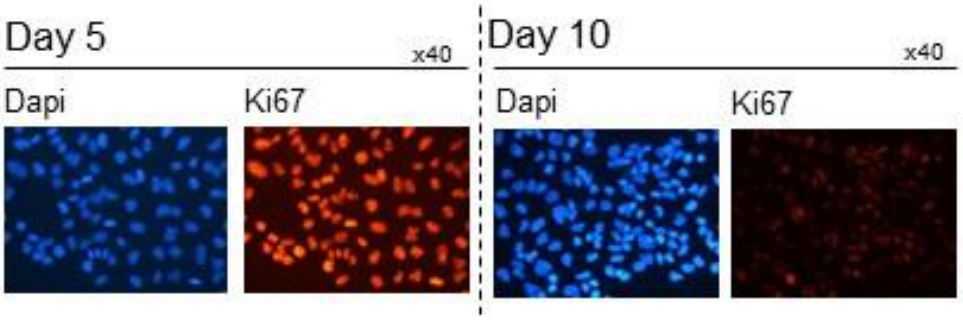

Figure 5.1-f Percentage of Ki67 'dim' cells in relation to RECQL4 expression in HeLa cells. 72000 HeLa cells were seeded per well in a 24 well plate in duplicates and incubated for 10 days with medium changes every 3 days. Each day cell lysate was collected from the appropriate well. SDS page and western blot were performed and the membrane was probed for Tubulin and RECQL4. RECQL4 expression represented as relative density. Cells from parallel wells were also fixed with 4% paraformaldehyde and probed for Ki67 expression. The cells were analysed by immunofluorescence. One representative graph and western blot is shown. Red cells show Ki67 expressing cells. Ki67 expression decreased over 10 days of cell culturing. Representative images from days 5 and 10 are shown. Ki67 signal was detected using Nikon E800 microscope with DN100 imaging camera, using DAPI and TRITC filters and imaging software, 40x objective. Ki67 expression was quantified using CellProfiler. 'Dim' cells show low Ki67 signal and are non-proliferating.

To identify if RECQL4 mutations affect proliferation and Ki67 expression levels, the proliferative capacity of primary RTS cells was tested. AG18375 RTS primary cells did not demonstrate reduced Ki67 levels, whereas AG03587 cells showed lower levels, suggesting reduced proliferative state. These experiments, however, need to be repeated and extended to other primary RTS cell lines; these lines are now available in the laboratory (Figure 5.1-g).

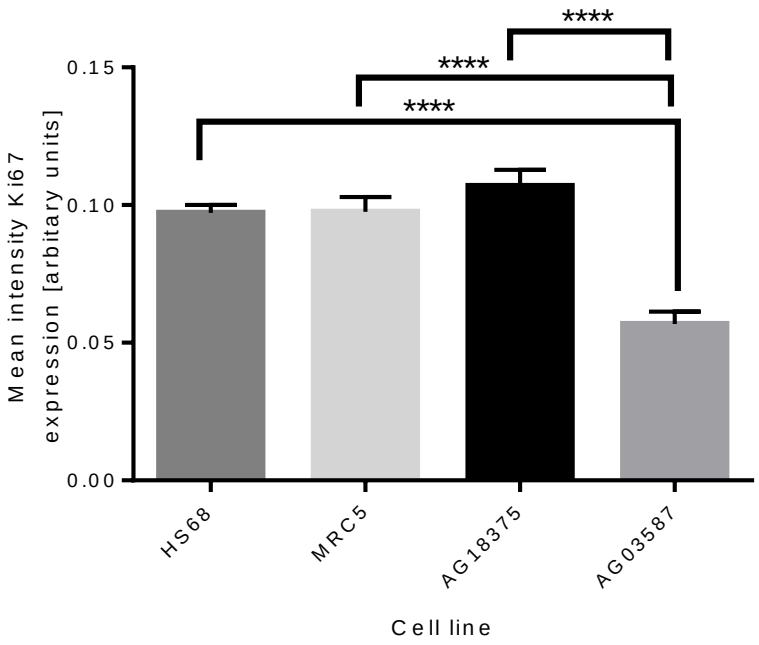

Figure 5.1-g Proliferation rate in a selection of primary RTS cell lines. AG18375 P+4, 5, AG03587 P+13, 14, HS68tert P+30, 31, and MRC5 P+33,34, were seeded onto glass coverslips in a 24 well plate and allowed to reach around 80% confluency. The cells were fixed in 4% paraformaldehyde, and stained for Ki67 and DAPI. Images were collected using a Leica SP8 confocal microscope, and analysed and quantified using CellProfiler. Error bar represents SEM, statistical significance was calculated by the Tukey post hoc test following one-way ANOVA analysis. ****P≤0.0001, graphs represent combined data from two independent experiments (n=2). Reduced Ki67 expression was seen in AG03587 cells.

5.2 Establishing overexpression and depletion of RECQL4

As discussed previously, it appears that RECQL4 overexpression and under-expression may contribute to tumourigenesis, suggesting that RECQL4 expression may be a double-edged sword (Buffart et al., 2005; Choi et al., 2007; Saglam et al., 2007; Maire et al., 2009; Sadikovic et al., 2010; Su et al., 2010; Fang et al., 2013; Ghosal and Chen, 2013). As we understand, RTS patients with identified RECQL4 mutations demonstrate a clear predisposition to OS (Tong, 1995; Lindor et al., 1996; Miozzo et al., 1998; Kitao et al., 1999; Lindor et al., 2000; Wang et al., 2001; Balraj et al., 2002; Wang et al., 2002b; Siitonen et al., 2003; Wang et al., 2003).

In order to study the influence of knockdown and overexpression of RECQL4 on the physiology of standard laboratory cell lines and mesenchymal cells, and to identify interacting partners of RECQL4 with GFP-pulldown, we established cell lines that express Emerald-GFP tagged RECQL4 in a Doxycycline inducible manner, verified the effect of commercially available siRNA molecules, and generated lentiviral vectors that express these siRNA molecules as short-hairpin RNAs (shRNAs).

5.2.1 Generation of Emerald–GFP tagged RECQL4 expression construct

Hitherto, there has been no reliable data available on the effect of overexpression of RECQL4 in cell culture. To avoid the potential effect of continuous overexpression we opted for a tetracycline inducible expression system. RECQL4 fused with Emerald-GFP also allowed for the immunopurification of interacting partners of RECQL4, as well as identifying its post-translational modifications.

5.2.1.1 Establishing a suitable plasmid delivery system

A suitable delivery system was identified and optimised for our cell lines. Lipofectamine 2000 and Fugene 6 transfection reagents were used at varying transfection reagent:DNA ratios in HeLa cells. pEYFP -C1 was used for verifying the efficiency of delivery. This vector contains a C-terminal enhanced yellow variant of green fluorescent protein. Its fluorescence can be easily analysed with fluorescence microscopy (Wilson et al., 2002; Karpova et al., 2003; Fahrner et al., 2014; Tanida et al., 2015; Uritu et al., 2015). Based on these experiments Lipofectamine 2000 was selected for further work in a ratio of 3:1 (Lipofectamine: DNA) (Figure 5.2-a).

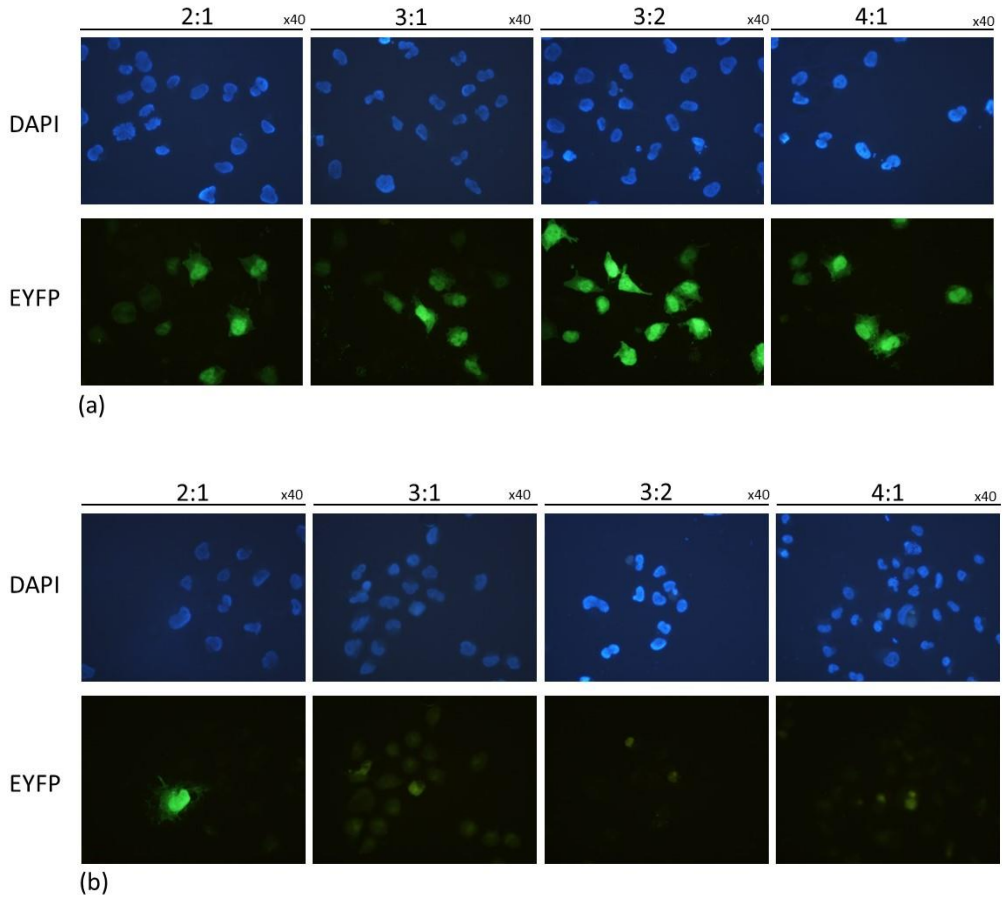

Figure 5.2-a Determining the optimal transfection ratio in HeLa cells. HeLa LacZeo cells were seeded at $1x10^5$ onto glass coverslips in 24 well plate and incubated overnight. The cells were transfected with variety of ratios of delivery and plasmid (a; lipofectamine, b; Fugene) and pEYFP-C1 plasmid (EYFP). 6 hours after transfection with Lipofectamine, media was removed and replaced with fresh media alone; additional media was added to Fugene transfected wells. 72 hours post seeding, cells were fixed with 4% paraformaldehyde and stained with DAPI. Cells were photographed using Nikon E800 microscope with DN100 imaging camera, using DAPI and FITC filters and imaging software, with x40 objective. Successful intracellular localisation in the nucleus and cytoplasm of pEYFP-C1 expression is shown in green. pEYFP-C1 was used as transfection control in further experiments.

An Emerald-GFP tagged expression construct was generated with the Gateway® site-specific recombination cloning system (Peakman et al., 1992; Boyd, 1993; Liu et al., 1998), (ThermoFisher Scientific), by recombining pENTR-RECQL4(F0) with the expression vector pDESTfrtto-Emerald-N0. This reaction resulted in an expression construct with the Emerald tag on the carboxy terminus of RECQL4. The entry clone and the destination vector have been available in our plasmid collection. Recombinant constructs were verified with restriction fragment mapping (Figure 5.2-b). Expression of RECQL4-Emerald from the verified constructs was confirmed with fluorescent microscopy following transient transfection of the miniprep DNA into U2OS-FLIPINTREX and HeLa-LacZeo cells (Figure 5.2-c). Maxiprep plasmid DNA was prepared from the verified clone 3 and was co-transfected into U2OS-FLIPINTREX cells with pOG44 to generate clones with stable chromosomal integration.

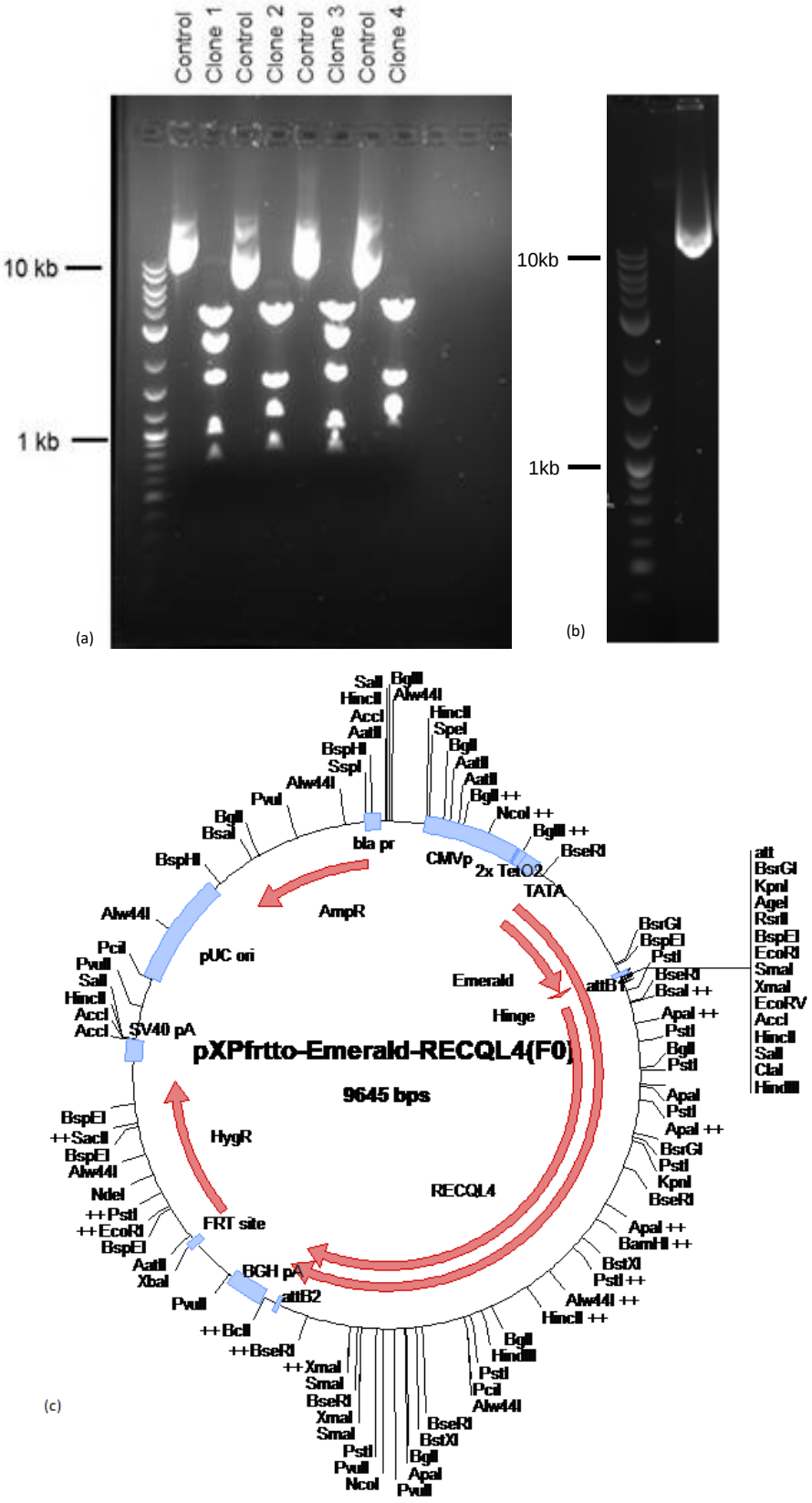

Figure 5.2-b Verification of recombinant constructs. *NcoI* digestion was performed on DNA from minipreps of clones #1-4 (a). (b) Maxiprep DNA of clone 3. Control lanes contain undigested plasmid from the same clone. (c) plasmid map.

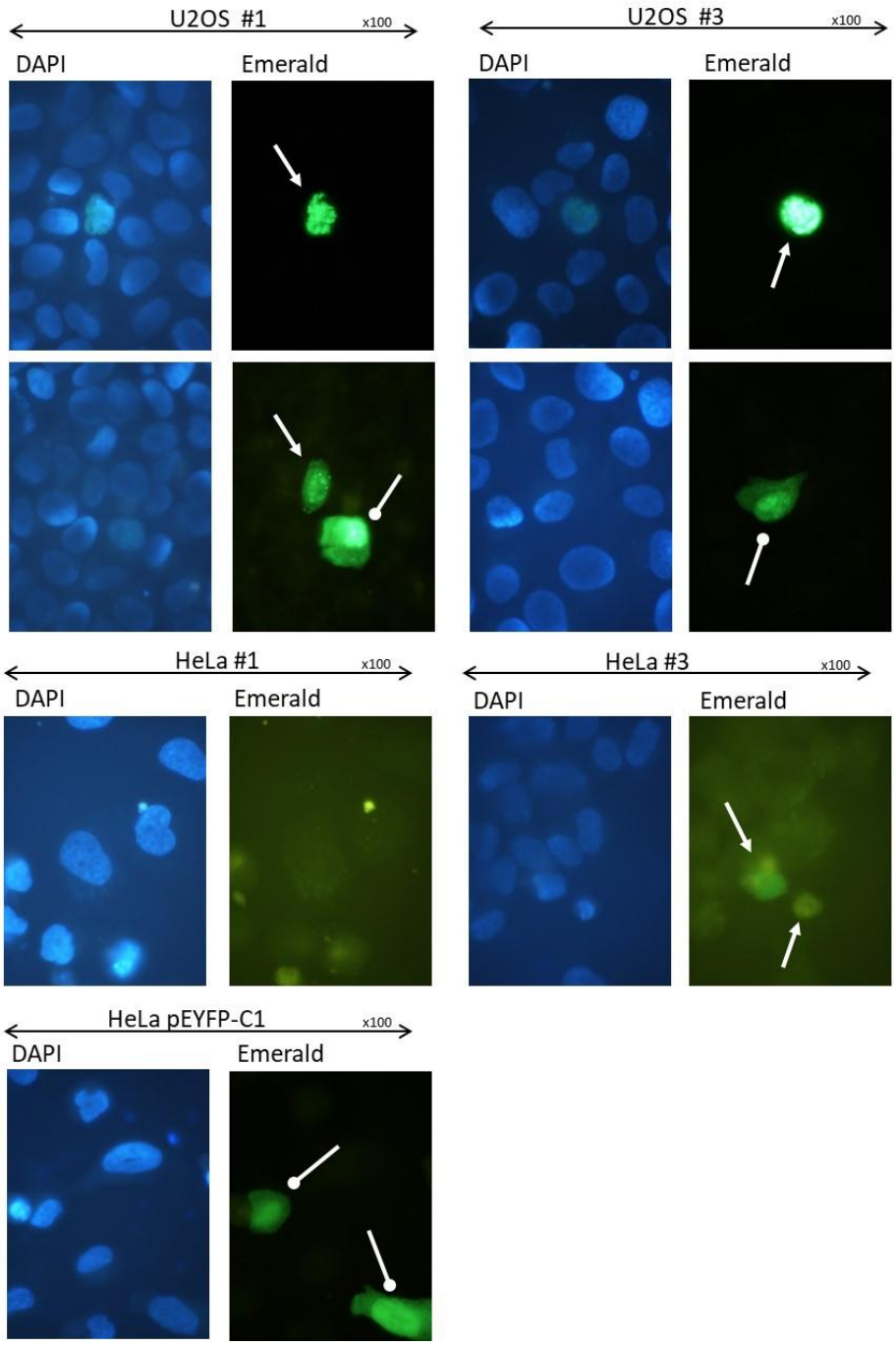

Figure 5.2-c Transiently transfected RECQL4-Emerald localisation in HeLa-LacZeo and U2OS-FLIPINTREX cells. HeLa and U2OS cells were seeded at 10^5 cells per well and incubated overnight on 24 well plate. Cells were transiently transfected with mini-prep DNA of clones #1 and #3 with Lipofectamine (1:3), fixed 48 hours post transfection and stained with Hoechst-33258. Signal was detected using Nikon E800 microscope with DN100 imaging camera, using FITC and DAPI filters and imaging software, x100 objective, FITC filter set for GFP and DAPI filter set for detecting Hoechst-33258-stained nuclei. Successful intracellular localisation of RECQL4-Emerald expression is shown in green; white arrow-nucleus, white oval arrow – cytoplasm and nucleus. pEYFP-C1 was used as transfection control.

The transfected cell population was selected for accurate integration and maintained under selection. The Hygromycin B resistance marker carried on the expression plasmid is only expressed if it is integrated into the target FLP recombination site as desired. The recipient cells are also resistant for Blasticidin-S; the construct that expresses the tetracycline receptor needed for inducibility

carries a Blasticydin S resistance marker. Optimal concentrations of Hygromycin B and Blasticidin-S required for successful selection were determined in cell survival experiments. The optimal concentrations for selection in HeLa cells were 4µg/ml Blasticidin-S and 225µg/ml Hygromycin B, and 4µg/ml Blasticidin-S and 150µg/ml Hygromycin B in U2OS cells. HeLa LacZeo#2 and U2OS FLIPINTREX#15 showed stable, inducible expression upon addition of doxycycline (Figure 5.2-d). These clones were further analysed, and induced RECQL4 expression was verified (Figure 5.2-e, Figure 5.2-f Figure 5.2-g). These clones were used for further work in GFP Nanotrap pulldown experiments.

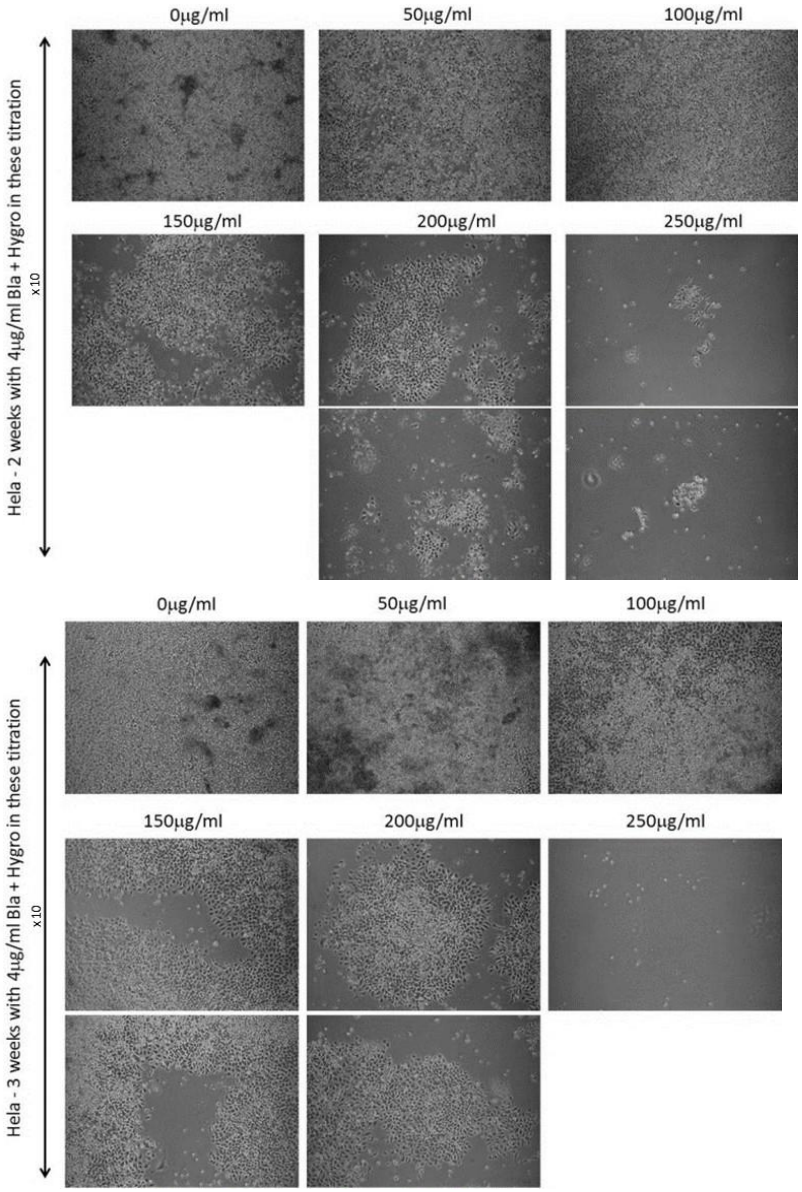

Figure 5.2-d Dual selection Hygromycin B titration with Blasticidin-S®. HeLa cells were seeded into petri dishes containing 10ml DMEM medium with 10% FBS, 4µg/ml Blasticidin-S® and variable Hygromycin B concentrations from 0 µg/ml to 250 µg/ml and incubated for 2 weeks and 3 weeks. The cells were observed microscopically using Nikon Eclipse TE2000 inverted stage microscope, x10 objective. 250µg/ml Hygromycin showed cell toxicity while 200µg/ml showed slight inhibition of cell selection. 4µg/ml Blasticidin-S® with 225µg/ml Hygromycin B was deemed suitable for further work.

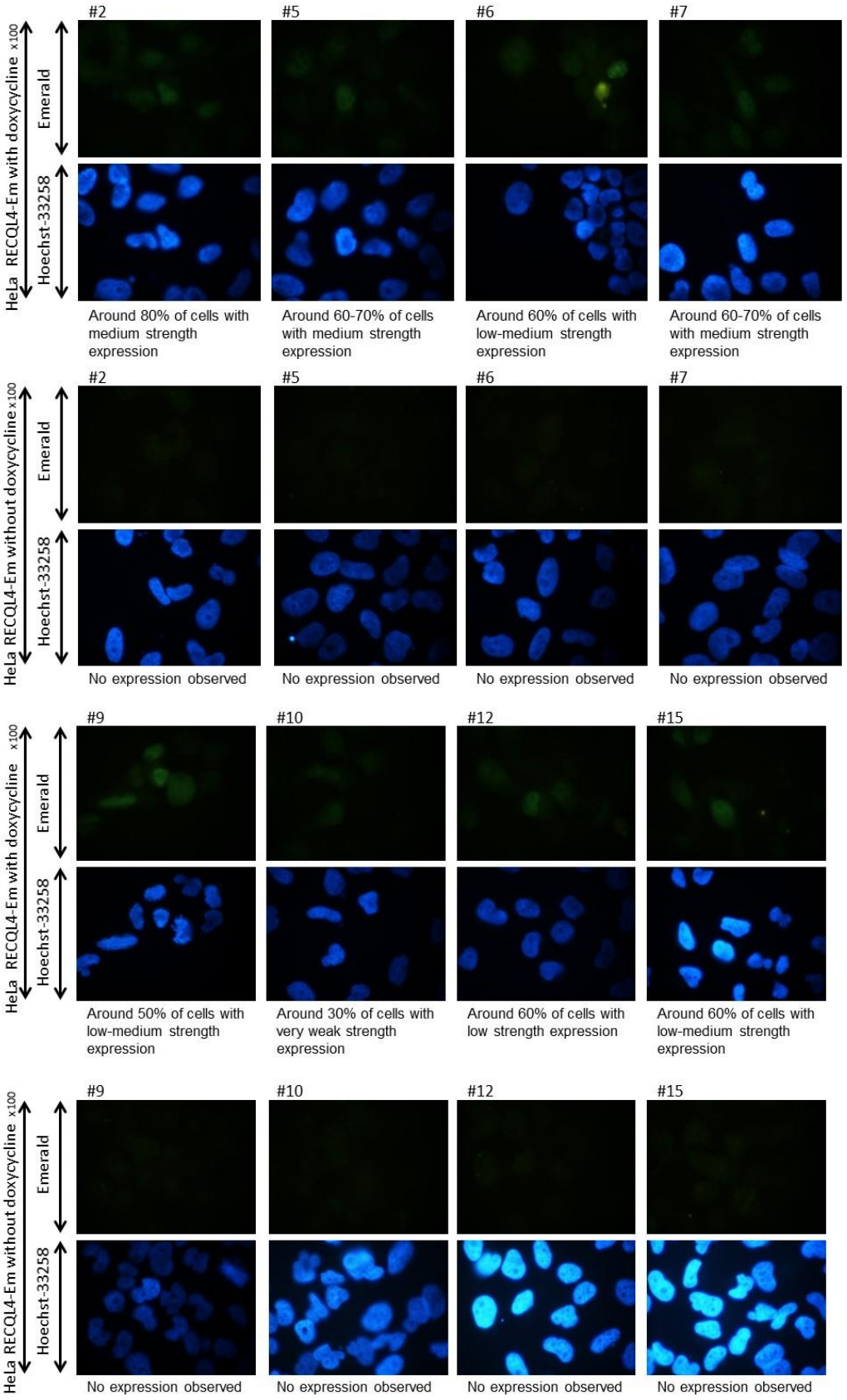
#2
#5
#6
#7
HeLa RECQL4-Em with doxycycline x100
Emerald
Hoechst-33258
Around 80% of cells with medium strength expression
Around 60-70% of cells with medium strength expression
Around 60% of cells with low-medium strength expression
Around 60-70% of cells with medium strength expression
#2
#5
#6
#7
HeLa RECQL4-Em without doxycycline x100
Emerald
Hoechst-33258
No expression observed
No expression observed
No expression observed
No expression observed
#9
#10
#12
#15
HeLa RECQL4-Em with doxycycline x100
Emerald
Hoechst-33258
Around 50% of cells with low-medium strength expression
Around 30% of cells with very weak strength expression
Around 60% of cells with low strength expression
Around 60% of cells with low-medium strength expression
#9
#10
#12
#15
HeLa RECQL4-Em without doxycycline x100
Emerald
Hoechst-33258
No expression observed
No expression observed
No expression observed
No expression observed

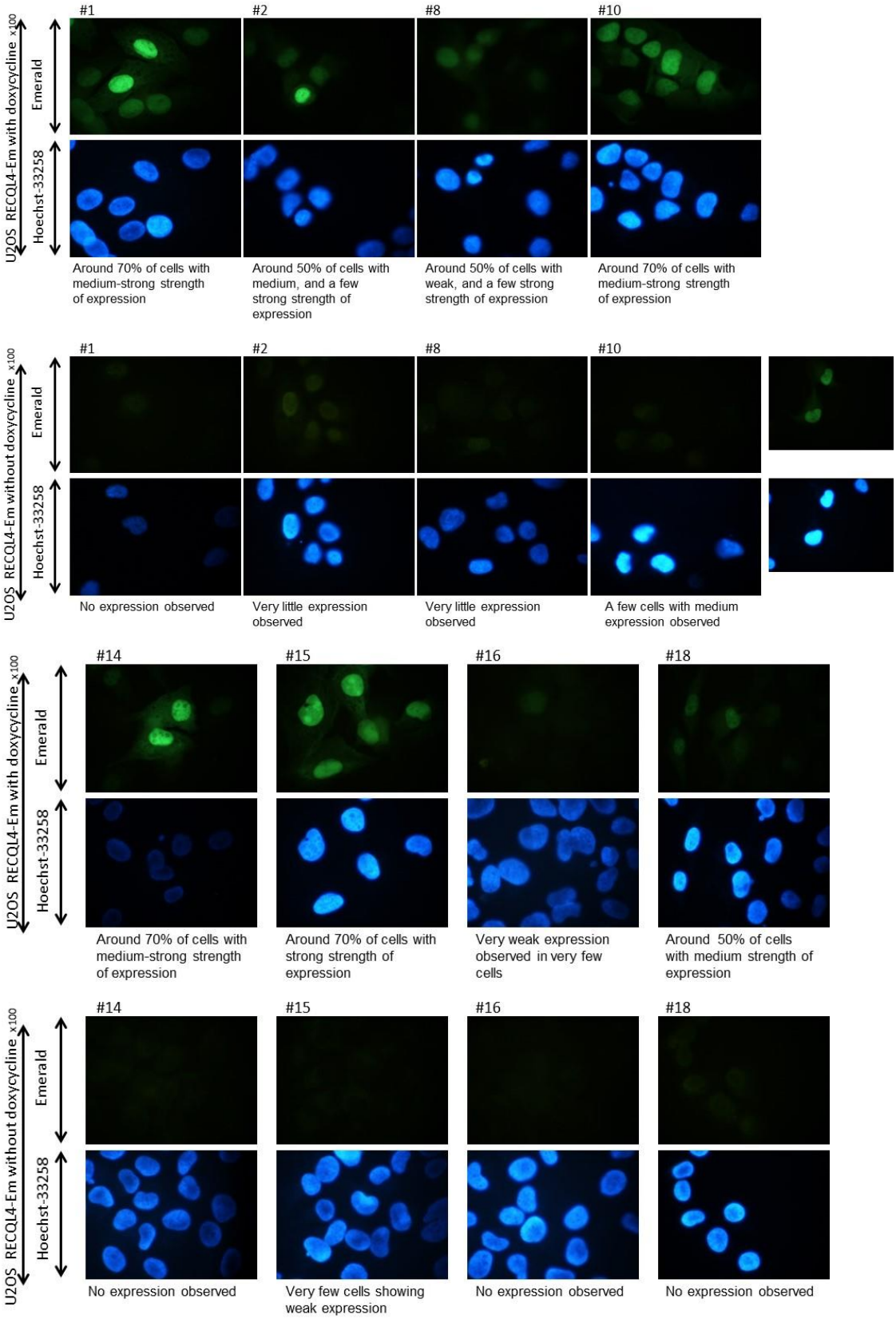

Figure 5.2-e Inducible expression of Emerald-GFP tagged RECQL4. RECQL4-Emerald HeLa and U2OS clones under selection were harvested using trypsin and seeded in a 24 well plate layout with or without 2µg/ml doxycycline. 48 hours following induction cells were fixed and nuclei were stained with Hoechst-33258. Images were collected on a Nikon Eclipse E800 microscope with DN100 imaging camera and imaging software, at x100 magnification, using FITC and DAPI filters. Induced expression seen with doxycycline treatment. Blue – cell nuclei, Green – Emerald tagged expression. HeLa LacZeo # 2 and U2OS FLIPINTREX # 15 clones were selected for further analysis.

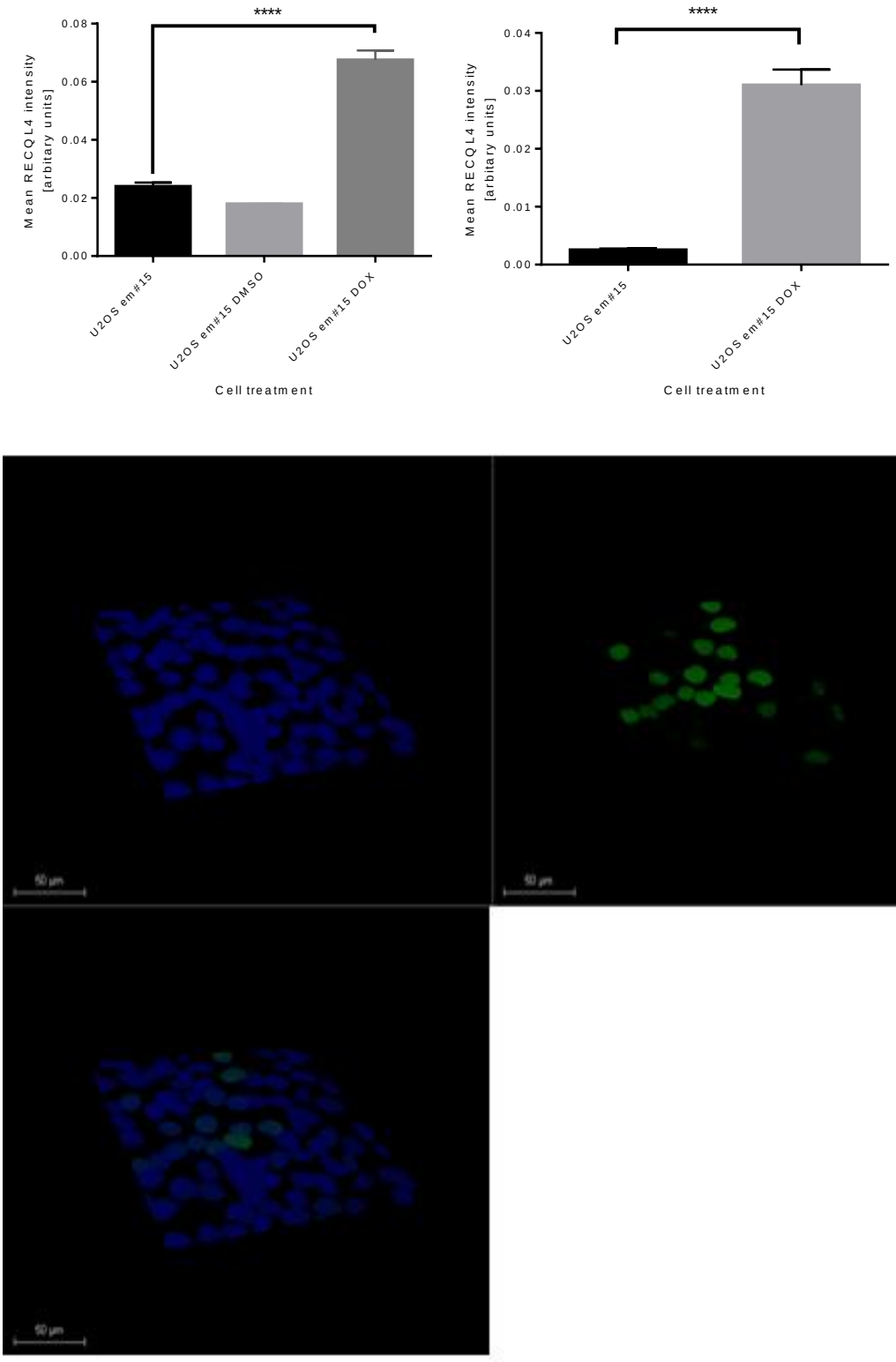

Figure 5.2-f Expression intensity in U2OS cells expressing RECQL4 Emerald. U2OS FLIPINTREX RECQL4-Emerald clone # 15 cells were seeded at 12,000 cells per well on glass coverslips with or without induction using doxycycline (DOX) at 2ug/ml, and allowed to reach around 70% confluency (3 days). The cells were fixed in 4% paraformaldehyde Emerald-GFP signal was detected using Leica SP8, confocal laser scanning microscope, and images analysed and quantified using CellProfiler. U2OS em #15: U2OS FLIPINTREX RECQL4-Emerald clone # 15. Graphs represent data combined from three independent experiments (n=3), ****P≤0.0001 unpaired t test. Significantly induced RECQL4 expression demonstrated in U2OS FLIPINTREX RECQL4-Emerald # 15 clone.

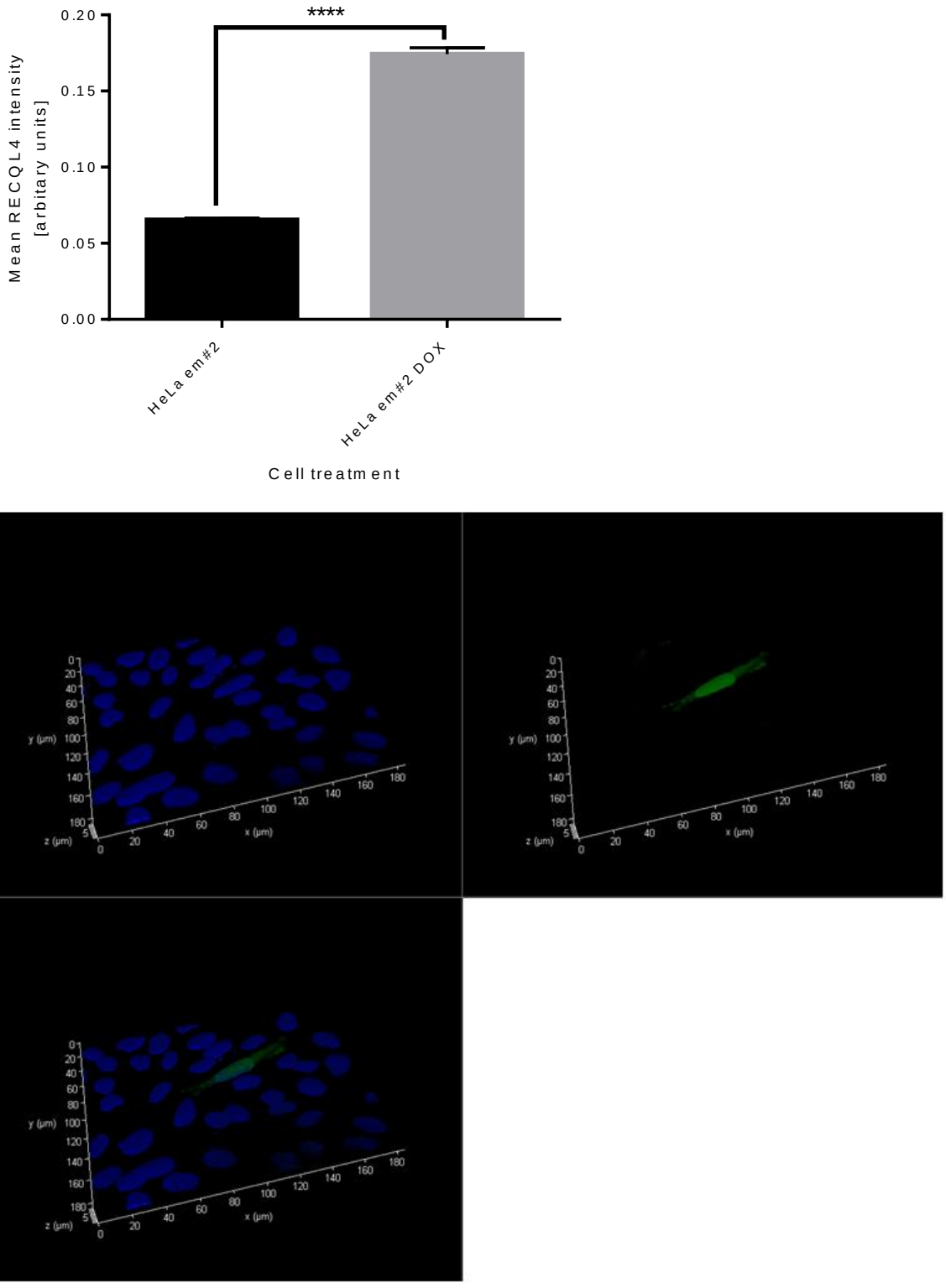

Figure 5.2-g Expression intensity in HeLa cells expressing RECQL4-Emerald. HeLa LacZeo RECQL4-Emerald clone #2, cells were seeded at 12,000 cells per well on glass coverslips with or without induction using doxycycline (DOX) at 2ug/ml, and allowed to reach around 70% confluency (3 days). The cells were fixed in 4% paraformaldehyde. Emerald signal was detected using Leica SP8 confocal laser scanning microscope. Images were analysed and quantified using CellProfiler. Hela em#2: HeLa LacZeo RECQL4-Emerald clone #2. Graphs represent data combined from three independent experiments (n=3) ****P≤0.0001 unpaired t test. Significantly induced RECQL4 expression demonstrated in HeLa LacZeo RECQL4-Emerald #2.

5.2.2 Establishing conditions for siRNA-mediated depletion of RECQL4

In order to identify suitable conditions and dynamics of RECQL4 depletion RECQL4 knockdown was performed in HeLa and U2OS cells transfected with RECQL4 siRNA molecules. Efficient RECQL4 siRNA knockdown was demonstrated over 7 and 9 days using siRNA molecules that target the coding region of the mRNA (#1, #2, #3 and #4 see table 2.2-b; (Figure 5.2-m), and the 3' untranslated region (#9 and #10 see table 2.2-b; Figure 5.2-i) however, intrinsic changes in RECQL4 expression due to the proliferative state of the cells also has to be considered as previously discussed.

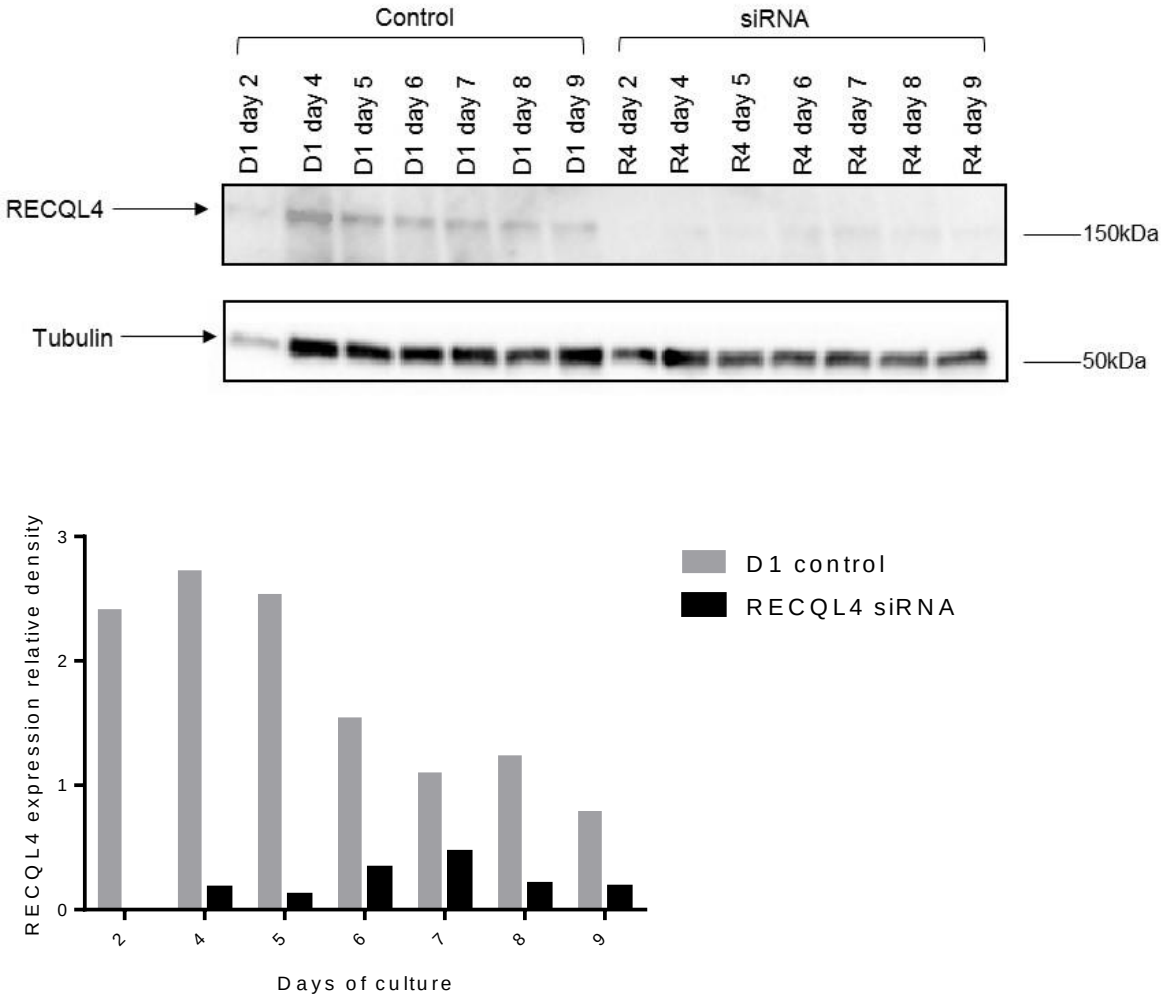

Figure 5.2-h Dynamics of siRNA mediated knockdown in HeLa LacZeo cells. Reverse transfection was performed using 2µM RECQL4 siRNA pool (containing siRNAs #1, #2, #3, #4) and Dharmafect only as a control. 12,000 HeLa cells were seeded and incubated overnight. 18 hours post transfection the medium was topped up. 42 hours post transfection and each day afterwards, cell lysate was collected and analysed with SDS page and western blotting. One representative graph and western blot is shown (n=1). RECQL4 expression was shown to increase indicating cell proliferation, and decrease as cells became confluent. RECQL4 pool siRNA transfection showed little expression indicating successful knockdown. The loading was verified with tubulin.

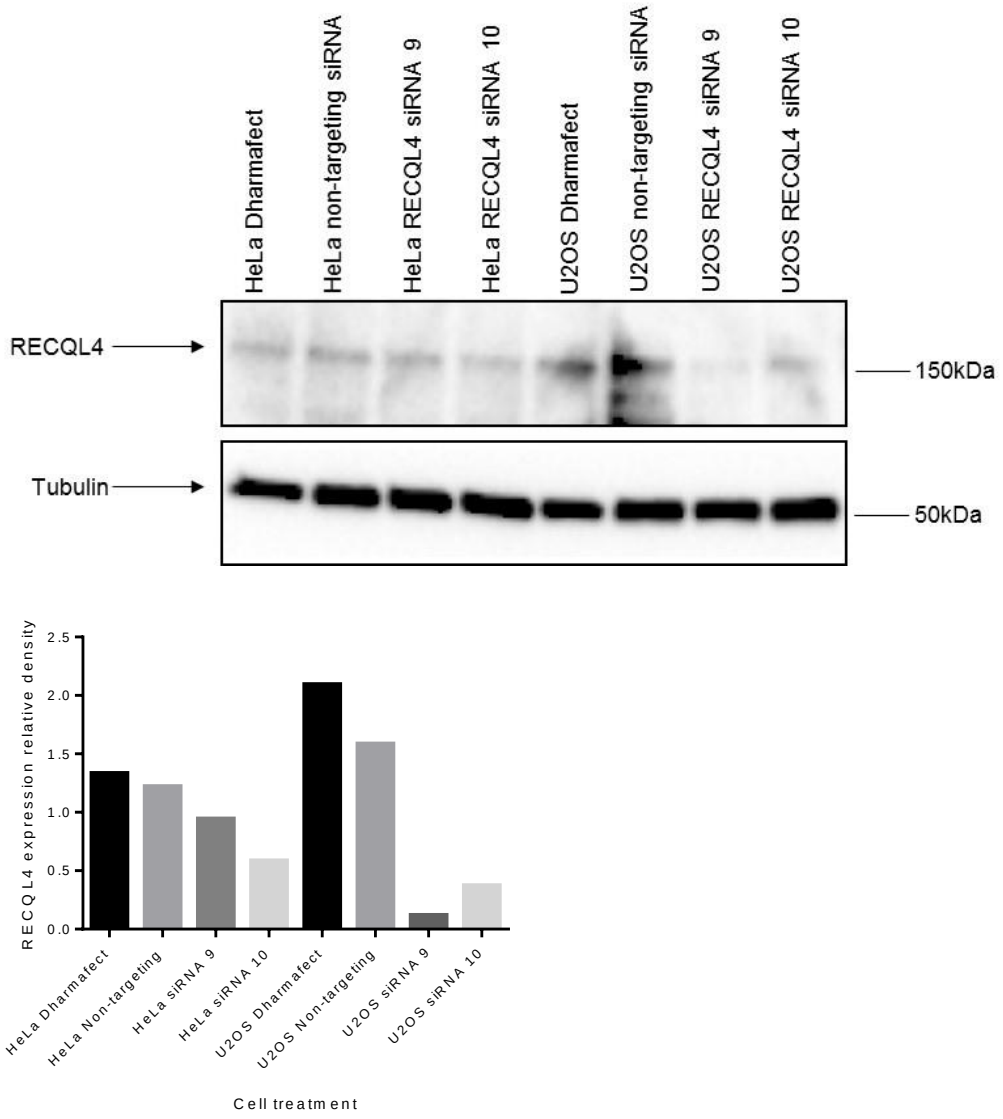

Figure 5.2-i RECQL4 knockdown efficiency using RECQL4 siRNA 9 and 10 in HeLa and U2OS cells, western blot. 12,000 U2OS FLIPINTREX and HeLa LacZeo cells were seeded per well in a 96 well plate and reverse transfected with the indicated siRNAs. The medium was topped up after 18 hrs and the cells were lysed 3 days post transfection. Western blot was performed and probed with Tubulin and RECQL4 antibodies. Loading was normalised and verified with Tubulin. One representative graph and western blot is shown (n=1). In HeLa cells RECQL4 expression appeared to not change and expression was low. In U2OS cell line RECQL4 knockdown was shown to be efficient in both RECQL4 siRNA 9 and 10 with little expression seen and high expression in the non-targeting control siRNA and Dharmafect only cells.

5.2.3 Generation of shRNA constructs

A number of primary cell lines are extremely difficult to transfect with traditional methods, and this limitation extends to introduction of siRNA molecules into these cell types. Although successful transfection methods have been described in mesenchymal stem cells (Jaiswal et al., 2000; Yoshikawa et al., 2004) we sought for a more efficient approach that generates stable knockdown. In order to mediate knockdown in ASC52telo cells a fourth-generation lentiviral transduction system was employed, and an shRNA expression construct was generated.

Two oligonucleotides harbouring the siRNA sequences that target the 3' untranslated region of RECQL4, and identical in the core sequence to siRNAs 9 and 10 described above, were custom synthesised, annealed and cloned into the pLKO.1 lentiviral vector. The ligated plasmids were transformed into NEB-Stable competent *E.coli* host cells. Miniprep DNA was purified from emerging colonies and mapped with *XhoI* and *HinfI* digestions. RECQL4sh 10A3 and RECQL4 9A1 showed fragment bands at the expected sizes following restriction digest (Figure 5.2-j and Figure 5.2-k). Confirmed clones were further verified by sequencing, and selected for maxiprep, lentiviral packaging and downstream applications.

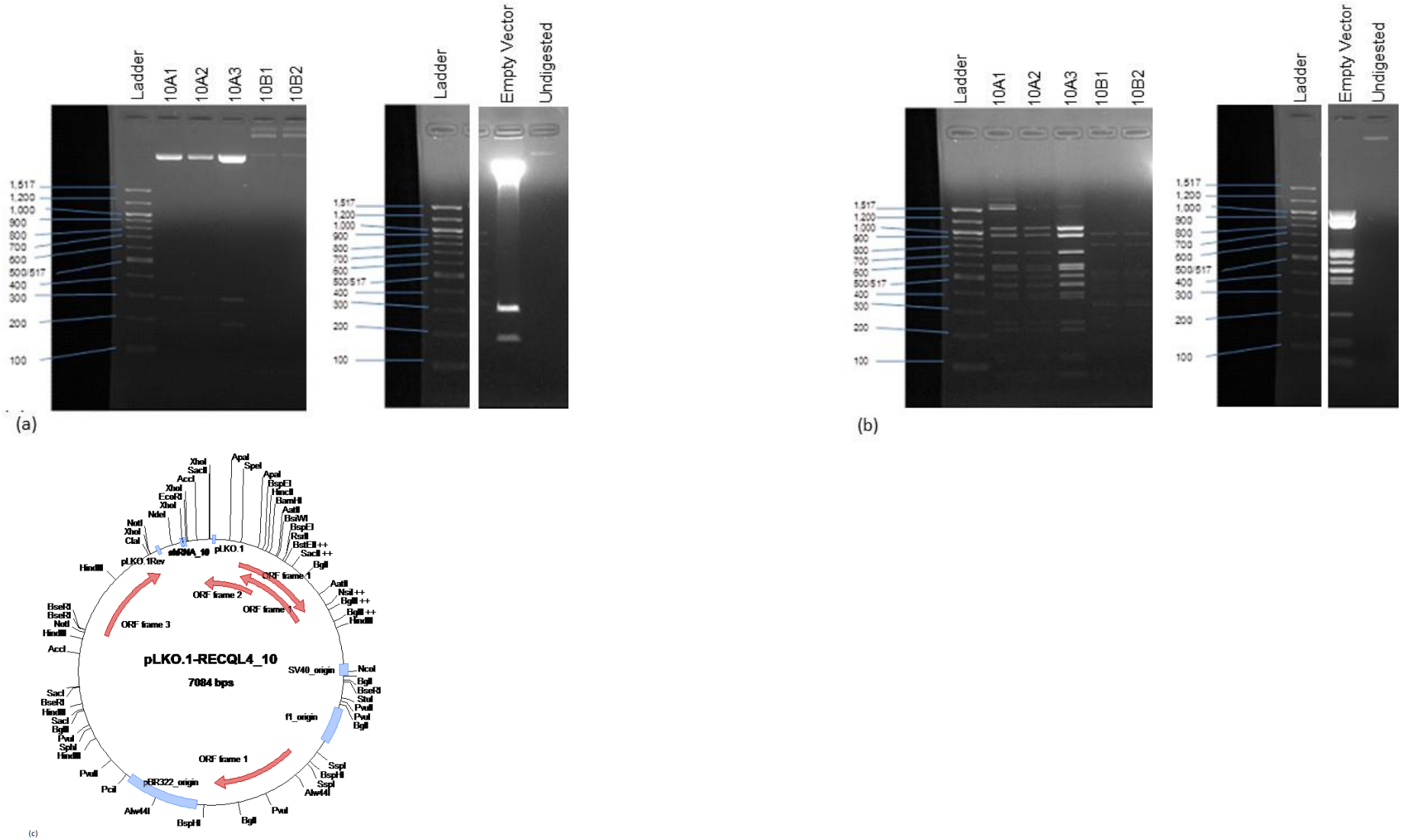

Figure 5.2-j Verification of recombinant shRNA constructs. Restriction digest was performed on the miniprep plasmid DNA. ladder- 100 bp ladder (NEB). (a) *XhoI* digested fragments; empty vector: 6556, 304, 190; shRNA clone: 6556, 295, 190, 43. (b) *HinfI* digested fragments; empty vector: 1074, 948, 947, 597, 571, 517, 456, 454, 396, 380, 224, 133, 118, 75, 73, 65, 22; shRNA clone: 1074, 947, 724, 597, 571, 517, 456, 454, 396, 380, 253,133, 118, 75, 73, 65, 22, 5. (c) Plasmid map.

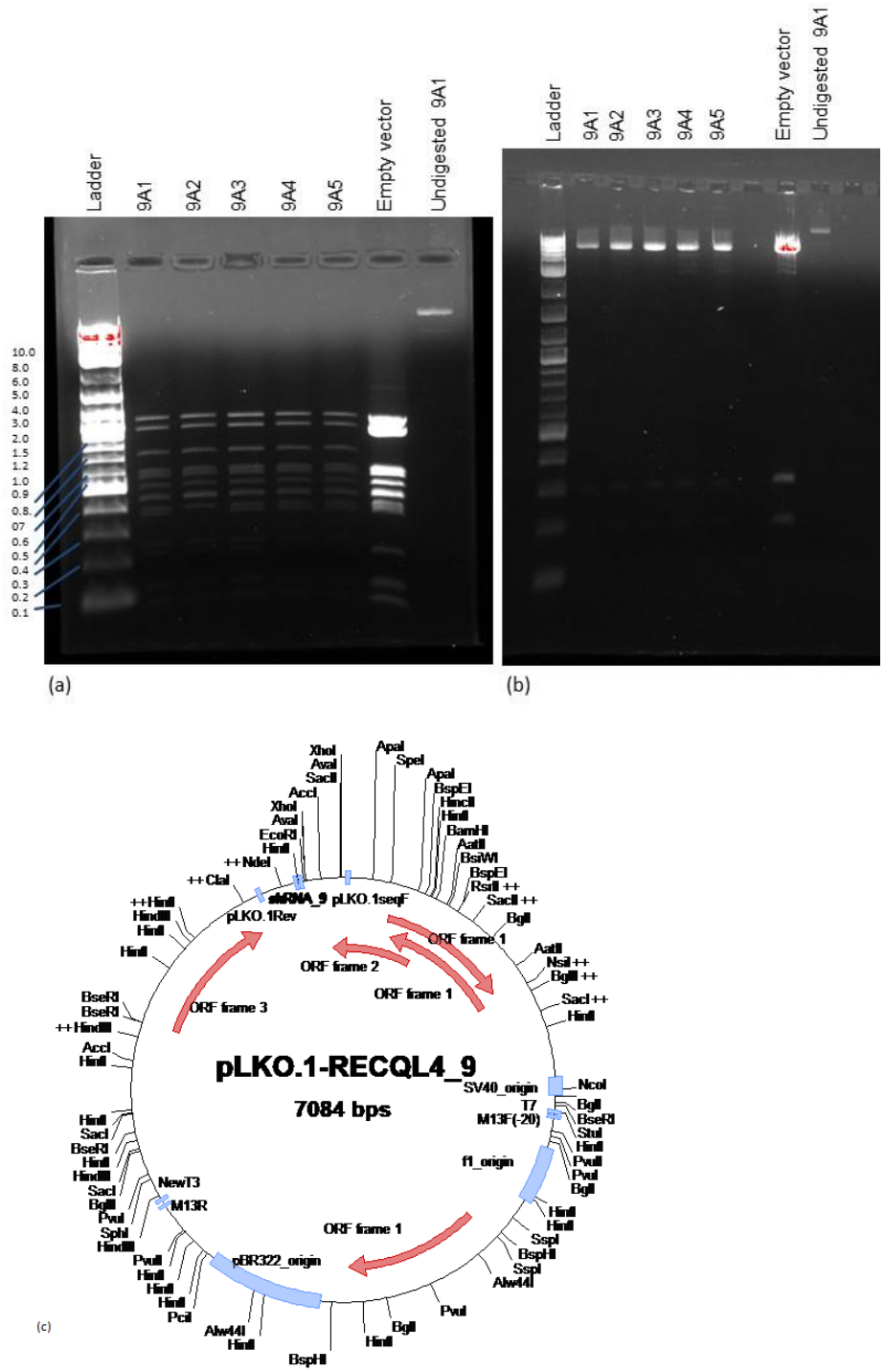

Figure 5.2-k Recombinant construct RECQL4 9A verification. Restriction digest was performed on the Mini-prep plasmid DNA. ladder- 100 bp. (a) HinfI digested fragments, (b) *XhoI* digested fragments. XhoI sizes: empty vector: 6556, 304, 190; shRNA clone: 6556, 295, 190, 43. *HinfI* sizes: empty vector: 1074, 948, 947, 597, 571, 517, 456, 454, 396, 380, 224, 133, 118, 75, 73, 65, 22; shRNA clone: 1074, 947, 724, 597, 571, 517, 456, 454, 396, 380, 253,133, 118, 75, 73, 65, 22, 5. 2 log ladder. (c) Plasmid map.

5.2.4 RTS cell lines and PHA Sensitivity

RECQL4 holds an important role in DNA replication initiation. To determine if RECQL4 mutation sensitizes cells to interference of DNA replication, RTS cell line AG05013 and RECQL4 knockdown U2OS and HeLa cells were treated with PHA-767491. We established previously that media changes were required in PHA-767491 treated cells (see section 3.1). AG05013tert, HS68tert, and MRC5 cells were re-tested with medium changes (Figure 5.2-l), which confirmed that the RECQL4 mutated cell line (AG05013tert) is indeed more sensitive to inhibition of replication initiation inhibitors than wild-type cells. We suggest that RTS cells are more sensitive to this drug, because of their inherent problem with replication initiation due to the lack of RECQL4. Whether this finding represents a general feature of RTS cells or specific to AG05013 needs to be verified using other RTS cell lines.

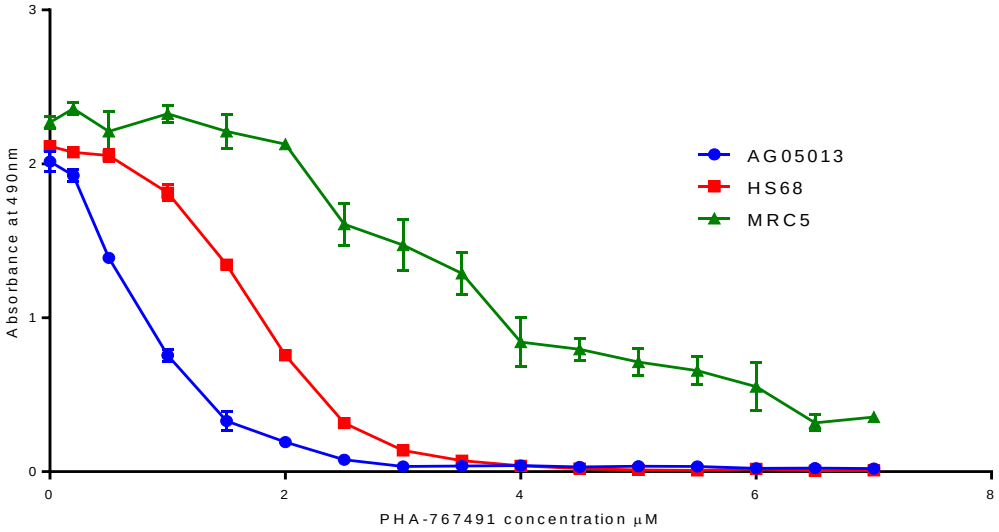

Figure 5.2-l Sensitivity of AG05013tert, HS68tert, and MRC5 cells to PHA-767491. Cells were seeded at 2000 cells per well in 96 well plate, and were treated with the indicated concentration of the drug alongside controls. Medium was changed and treatment reapplied to the cells every 3 days. Cell viability was established post 7 days incubation using the MTS assay read at 490nm. Error bars represents SEM of triplicates, graph represents one of three independent experiments (n=1). The RECQL4 mutated cell line AG05013tert shows a higher sensitivity to replication inhibition than the control cell lines.

RECQL4 mutated cells (AG05013) appeared to demonstrate sensitivity to PHA-767491. To verify a link between RECQL4 expression and sensitivity, RECQL4 was depleted using siRNA, as previously verified (Figure 5.2-m), and cells were treated with PHA-767491. U2OS cells showed steadily reduced cell viability with increasing concentrations of PHA-767491 after 0.4 µM with Non-targeting siRNA treatment and in RECQL4 depleted cells (Figure 5.2-n). Viability measurement was variable in HeLa cells but fell sharply above 2.5 µM (Figure 5.2-o). Knockdown of RECQL4 in

these U2OS and HeLa cells was verified with western blotting; however, increased sensitivity to PHA following RECQL4 siRNA knockdown was not seen (Figure 5.2-n and Figure 5.2-o). This data suggests, contradicting to data obtained from primary fibroblasts, that siRNA mediated knockdown of RECQL4 in HeLa and U2OS cells does not sensitise these cells to inhibition of replication initiation.

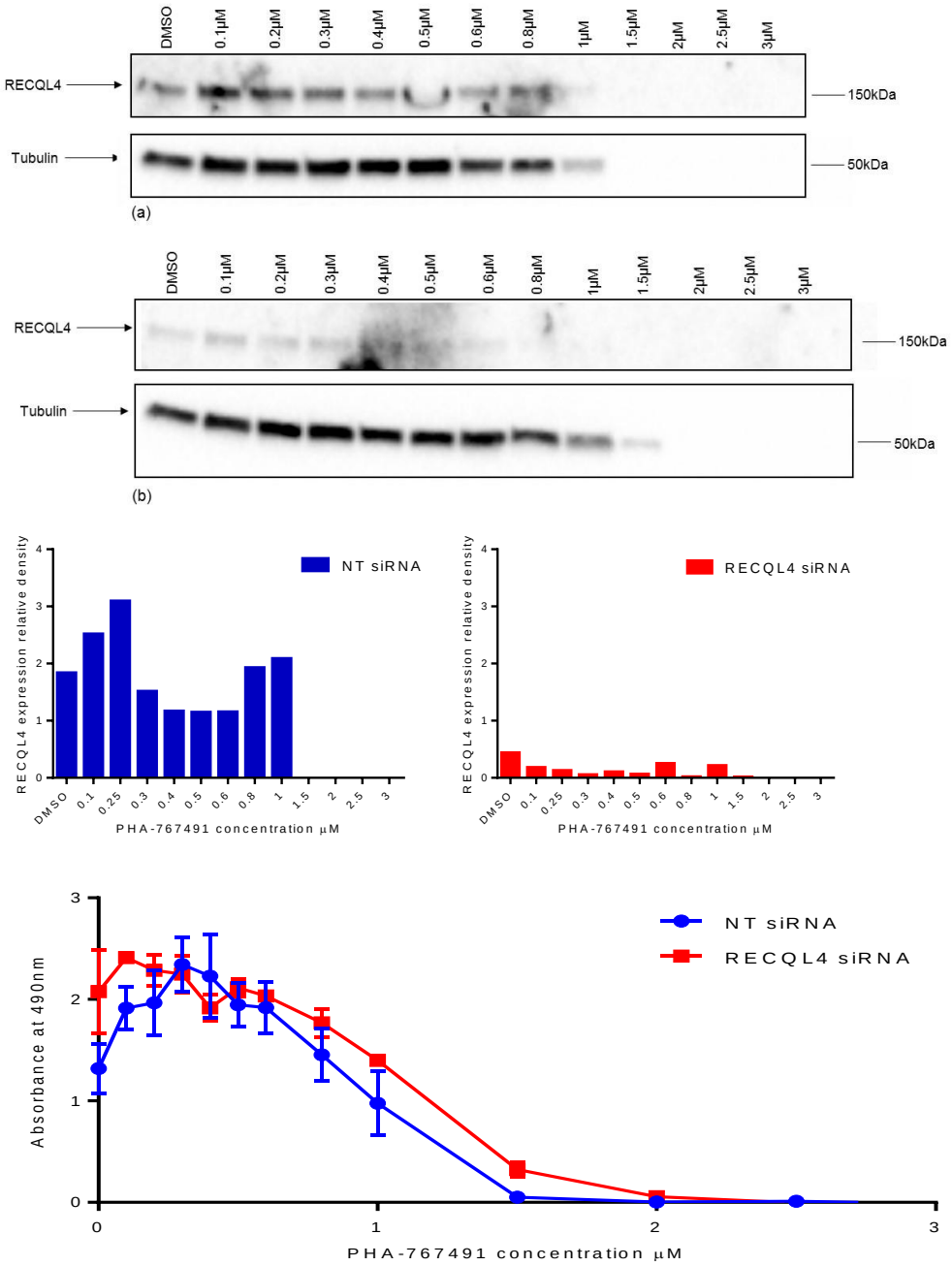

Figure 5.2-n Sensitivity of cells to PHA-767491 following siRNA mediated knockdown of RECQL4 in U2OS. 4000 U2OS cells were seeded per well in a 96 well plate and reverse transfected with RECQL4 siRNA pool (9 + 10) and the control Non-targeting siRNAs. 18 hours post transfection medium was changed with the addition of PHA-767491 at variable concentrations. Medium was replaced every 3 days with fresh medium containing the appropriate concentrations of PHA-767491. MTS absorbance was read at 490nm 7 days following initial PHA-767491 treatment. Data represent means ± SEM of triplicates, western blot and graphs is a representative of one of two independent experiments. Cells were lysed 7 days following initial PHA-767491 treatment, the lysates were run on SDS PAGE and western blot performed. Membrane was probed for Tubulin and RECQL4. Loss of both RECQL4 and tubulin signal represents the loss of cells. a:NT (non-targeting) siRNA b:RECQL4 siRNA. RECQL4 knockdown did not demonstrate sensitivity to PHA-767491.

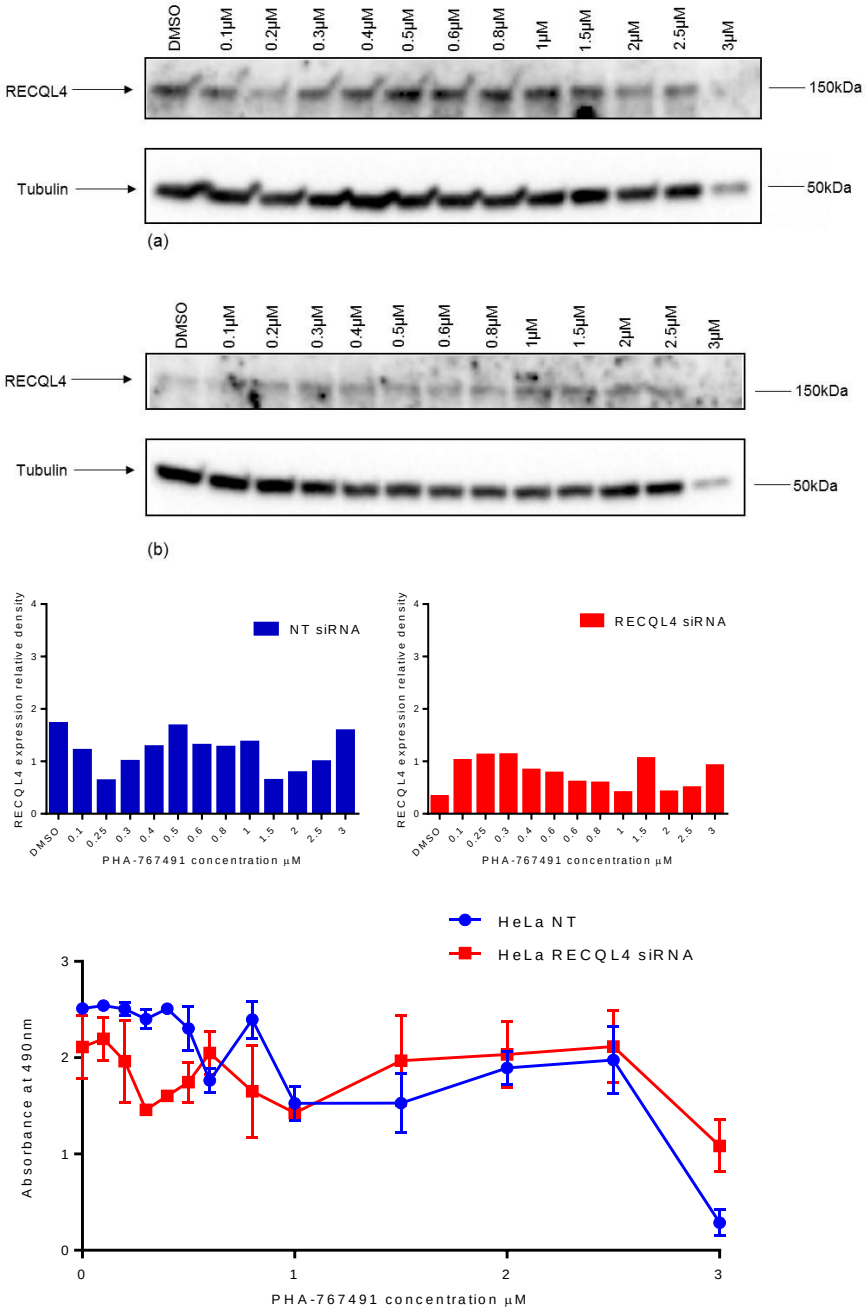

Figure 5.2-o– Sensitivity of cells to PHA-767491 following siRNA mediated knockdown of RECQL4 in HeLa cells. 4000 HeLa cells were seeded per well in a 96 well plate and reverse transfected with RECQL4 siRNA pool (9 + 10) and the control Non-targeting siRNAs. 18 hours post transfection medium was changed with the addition of PHA-767491 at variable concentrations. Medium was replaced every 3 days with fresh medium containing the appropriate concentrations of PHA-767491. MTS absorbance was read at 490nm 7 days following initial PHA-767491 treatment. Data represent means ± SEM of triplicates, western blot and graphs is a representative of one of two independent experiments. Cells were lysed 7 days following initial PHA-767491 treatment, the lysates were run on SDS PAGE and western blot performed. Membrane was probed for Tubulin and RECQL4. Loss of both RECQL4 and tubulin signal represents the loss of cells. a:NT (non-targeting) siRNA b:RECQL4 siRNA. RECQL4 knockdown did not demonstrate sensitivity to PHA-767491.

5.2.5 RECQL4 DNA damage

We found evidence of DNA damage in ASC52telo cells treated in the PHA-model. RTS cell lines (AG05013tert, AG18375, and AG03587) were investigated for the same markers. There was a significant increase seen in AG05013tert γH2AX and TRF2 expression intensity, with no significant changes seen in co-localisation of TRF2 and γH2AX foci (Figure 5.2-p)

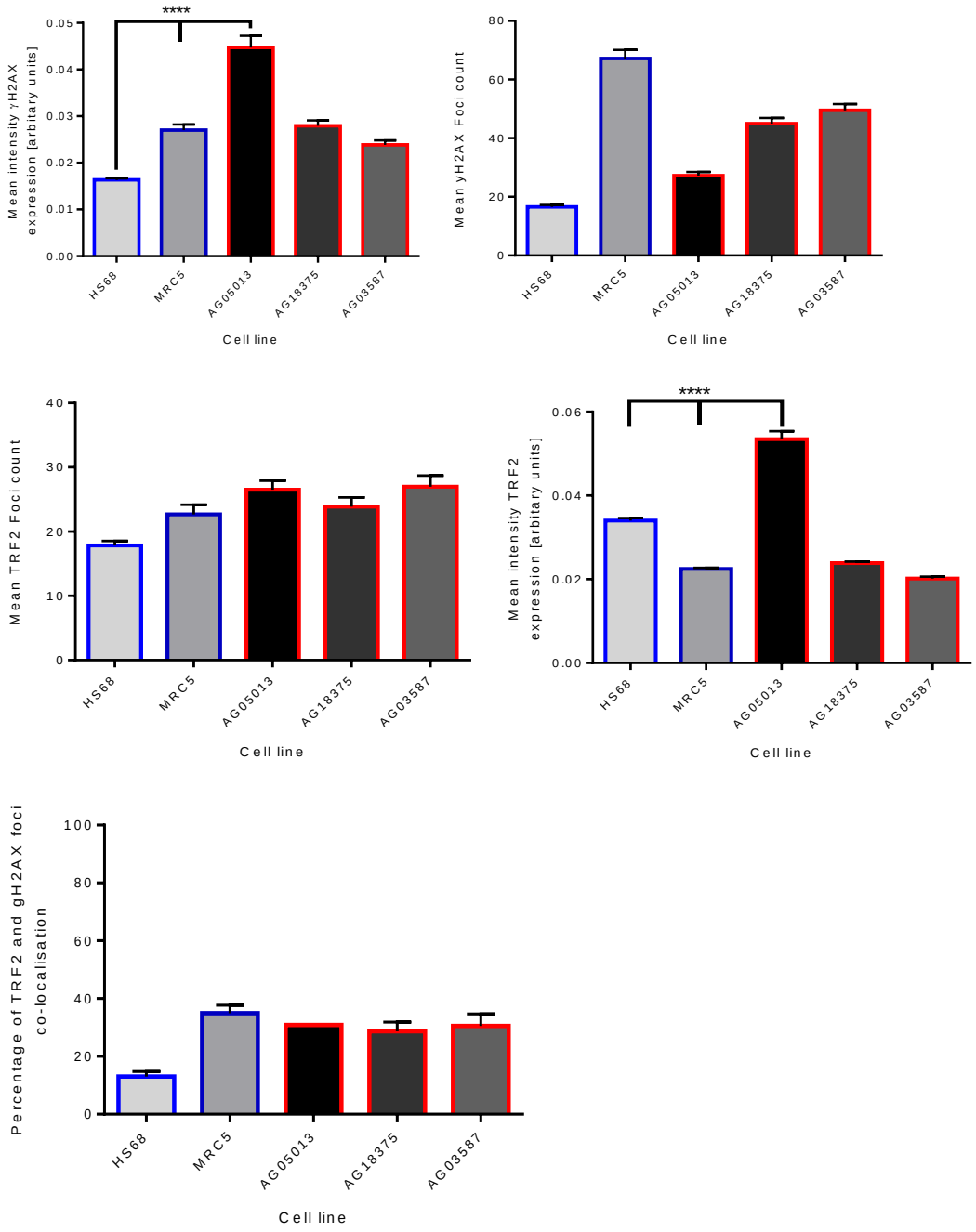

Figure 5.2-p Expression of DNA damage and telomeric markers in RTS cell lines. AG05013tert P+15,16,17, AG18375 P+4, 5, 6, AG03587 P+13, 14, 15, HS68tert P+35, 44,45, and MRC5 P+36, 45, 46, were seeded onto glass coverslips in 24 well plate and allowed to reach around 80% confluency. The cells were fixed in 4% paraformaldehyde, and stained for γH2AX and TRF2. Images were collected with a Leica SP8 confocal microscope and quantified using CellProfiler. Error bars represent SEM. Statistical values were calculated by the Tukey post hoc test following one-way ANOVA analysis, **P≤0.01,****P≤0.0001. Graph represents data combined from three independent experiments (n=3). An increase of γH2AX and TRF2 expression was shown in AG05013tert cells.

5.3 Isolation and identification of RECQL4 interacting partners.

The established HeLa#2 and U2OS#15 clones were expanded, and 9 10cm petri dishes were used per treatment as follows. RECQL4-Emerald expression was induced with 2 µg/ml doxycycline. To enrich the isolated RECQL4 population for post-translational modifications (Im et al., 2015), the cells were treated with 2µM Suberoylanilide hydroxamic acid (SAHA), 4mM hydroxyurea (HU) or DMSO as control. SAHA is an inhibitor of histone deacetylases (HDACs). SAHA was included in the experiment to permit identification of posttranslational acetylation modifications of RECQL4 and protein-protein interactions that depend on it. Hydroxyurea (HU) treatment was employed to facilitate isolation of S-phase specific binding partners and post-translational modifications of RECQL4. HU blocks DNA synthesis by inhibiting ribonucleotide reductase, which limits the accumulation of deoxyribonucleotides required for incorporation at replication forks, holding the cells at S phase (Butler et al., 2000; Koç et al., 2004; Karnani and Dutta, 2011). The isolation of GFP-Emerald tagged RECQL4 was performed using Chromotek GFP-trap®_A, then SDS PAGE and western blot was performed to determine efficiency of RECQL4-Emerald expression and pull-down. RECQL4-Emerald expression was demonstrated in the input samples of the GFP-Trap, which then decreases expectedly with the non-bound samples (wash), with higher expression seen on the bound beads, demonstrating efficient immunoprecipitation (Figure 5.3-a).

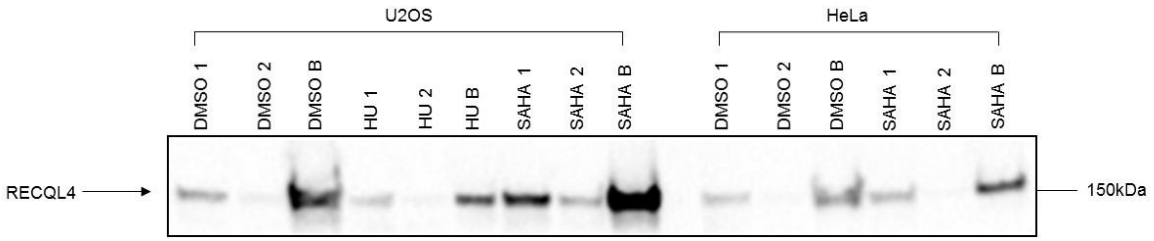

Figure 5.3-a GFP-trap pull-down of Emerald-GFP tagged RECQL4. RECQL4 expression was induced in the selected U2OS #15 cells with doxycycline in 10cm dishes. Post 3 days the cells were either treated with 2µm Suberoylanilide hydroxamic acid (SAHA), 4mM hydroxyurea (HU), or as a control with DMSO for 18 hours. GFP tagged RECQL4 was immunoprecipitated using GFP-Trap_A, then SDS-page and western blot were performed. The membrane was probed with RECQL4 (1:1000 in BSA blocking). 1 –Input, 2 – Non-bound, B – Bound; 2% input and unbound loaded. Bound lanes show strong signal of RECQL4-Emerald.

The SDS gel was cut to segments, and sent for identification of protein content by mass spectrometry (Table 5.3-a). Co-precipitated binding partners from a subsequent pull-down experiment were separated on SDS PAGE. A few previously identified positive 'hits' were also verified with western blot. Presence of PP2A

(protein phosphatase 2A) was demonstrated in the lysate and wash, but very little to no signal was seen in the pull-down fraction in U2OS cells (Figure 5.3-b). Little to strong expression was shown in HeLa cells (Figure 5.3-c). MCM10 is a known interacting protein of RECQL4. Its expression was demonstrated in the pull-down following SAHA treatment in both cell lines, although somewhat weaker in U2OS (Figure 5.3-b and Figure 5.3-c).

Cell treatment	RECQ4 pull down 'positive hits'
Blank- SAHA	Serine/threonine-protein phosphatase 2A
Control	Homeobox protein engrailed-2
Control	Homeobox protein engrailed-1
Hu	ATP-dependent DNA helicase Q4 (RECQL4)
SAHA	ATP-dependent DNA helicase Q4 (RECQL4)

Table 5.3-a A list of identified proteins from the RECQL4 pull down earmarked for follow-up analysis. RECQL4 expression was induced in the selected U2OS #15 cells with doxycycline in 10cm dishes. Post 3 days the cells were either treated with 2µm Suberoylanilide hydroxamic acid (SAHA), 4mM hydroxyurea (HU), or as a control treated with DMSO (control), untreated (blank) for 18 hours. GFP tagged RECQL4 was immunoprecipitated using GFP-Trap_A, then SDS-page and the gel was cut into pieces and sent for mass spectrometry.

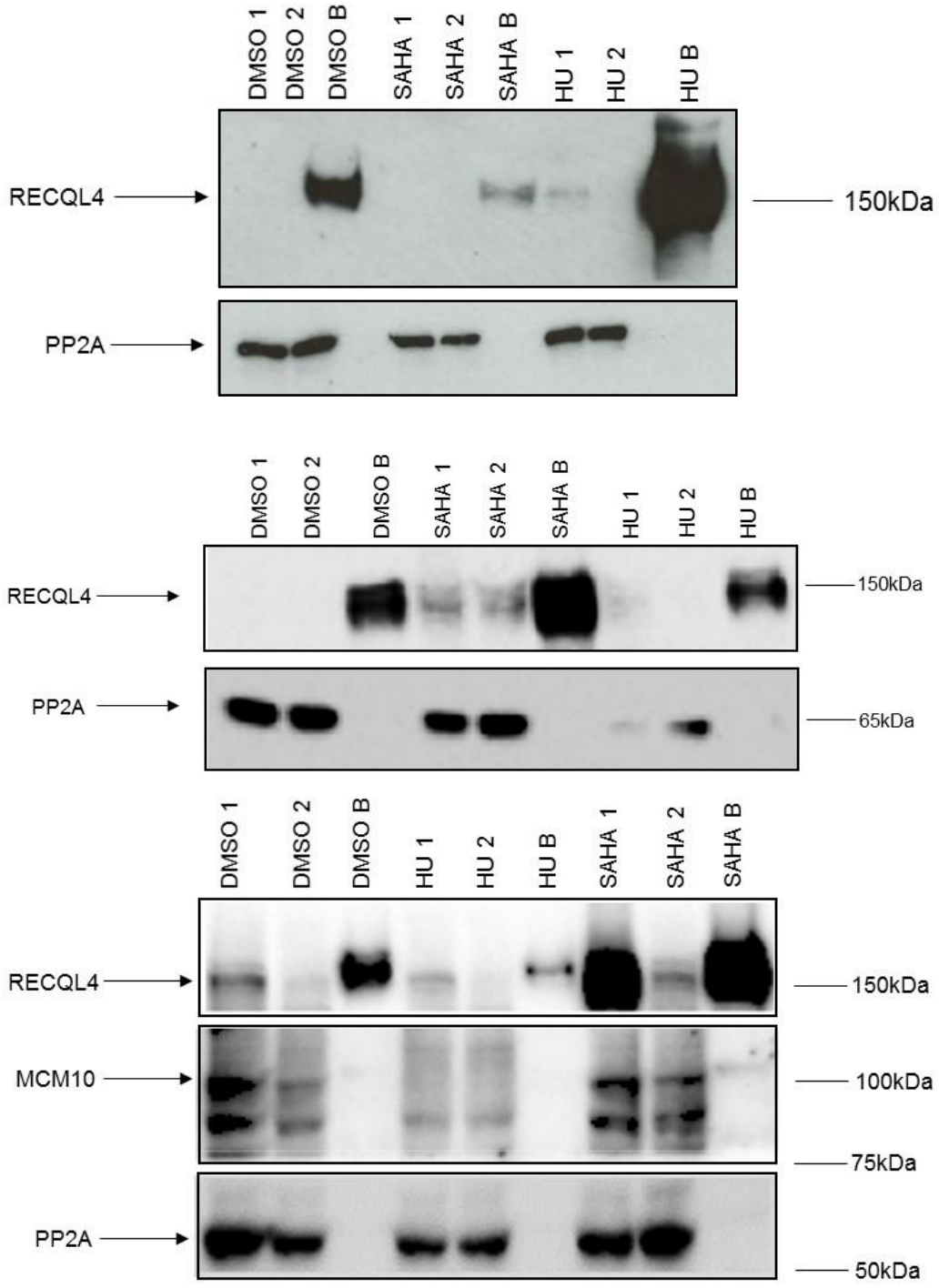

Figure 5.3-b Pull-down of RECQL4 interacting partners in U2OS clone #15 cells. RECQL4 expression was induced in the selected U2OS #15 cells with doxycycline in 10cm dishes. Post 3 days the cells were either treated with 2μm Suberoylanilide hydroxamic acid (SAHA), 4mM hydroxyurea (HU), or as a control treated with DMSO for 18 hours. GFP tagged RECQL4 was immunoprecipitated using GFP-Trap_A, then SDS-page and western blot were performed. The membrane was probed with PP2A (1:1000 in BSA blocking), RECQL4 (1:1000 in BSA blocking), and MCM10 (1:800), 1 – Input, 2 – Non-bound, B – Bound; 2% input and unbound were loaded. PP2A expression is not seen in the RECQL4-bound fraction, but weak signal of MCM10 is shown.

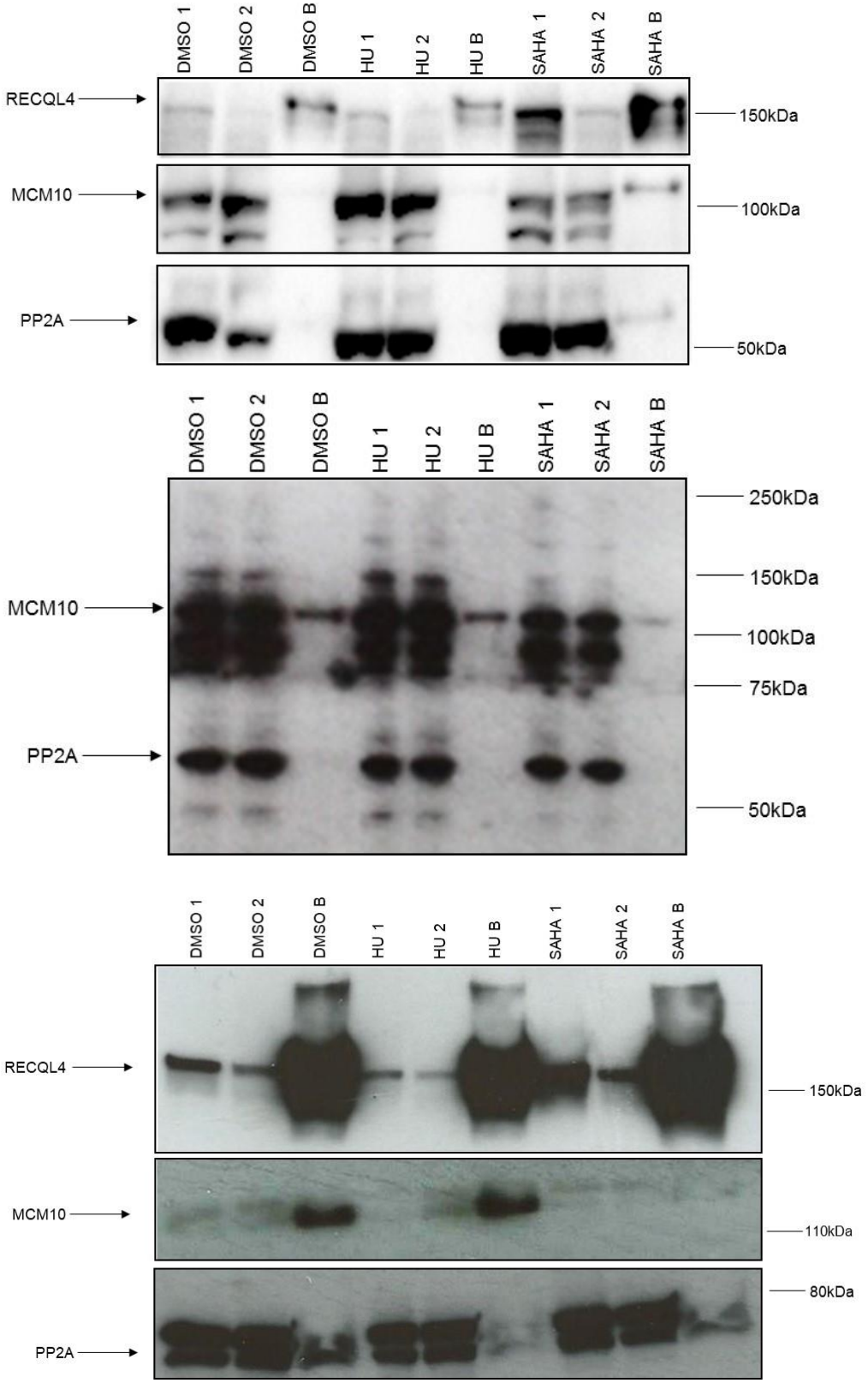

Figure 5.3-c Pull-down of RECQL4 interacting partners from HeLa clone #2 cells. RECQL4 expression was induced in the selected HeLa #2 cells with doxycycline in 10cm dishes. Post 3 days the cells were either treated with 2µm Suberoylanilide hydroxamic acid (SAHA), 4mM hydroxyurea (HU), or as a control treated with DMSO for 18 hours. Immunoprecipitation using GFP-Trap_A, SDS-page and western blot were performed. The membrane was probed with PP2A (1:1000 in BSA blocking), RECQL4 (1:1000 in BSA blocking), and MCM10 (1:800), 1 –Input, 2 – Non-bound, B – Bound; 2% input and unbound loaded. PP2A and MCM10 expression shown in RECQL4 bound fraction.

A novel RECQL4 interacting protein: Highly divergent homeobox (HDX) had been previously identified in other experiments (data not shown here). To explore this, further, a HDX antibody, which was not available before, was first verified following reverse siRNA transfection. Reduced expression was demonstrated following siRNA knockdown (Figure 5.3-d). RECQL4-GFP pulldown was performed, and the isolated proteins were analysed on western blot probed for HDX. HDX was found to be present in the GFP-bound fraction suggesting interaction with RECQL4 (Figure 5.3-e and Figure 5.3-f). The novel homeobox protein engrailed-2 (EN-2) was seen by mass spectrometry (Table 5.3-a), and was also found to be present in the RECQL4 bound fraction (Figure 5.3-e).

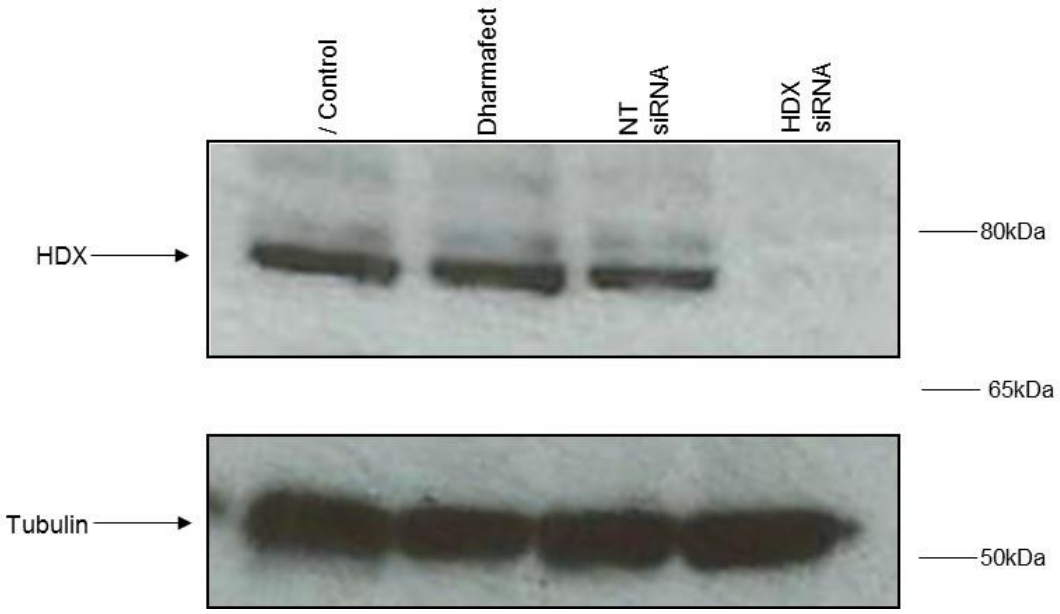

Figure 5.3-d Verification of HDX siRNA and antibody. Reverse transfection was performed using 2µM siRNA (pooled molecules 1, 2, 3 and 4) with Non-targeting and Dharmafect only as controls. 12,000 U2OS FLIPINTREX cells were then seeded per well in a 96 well plate. 18 hrs post transfection the medium was topped up and the cells were incubated until day 3. Cell lysate was collected and an SDS PAGE and western blot was performed. The membrane was probed with HDX antibody (abcam ab94475) at 1µg/ml in BSA blocking solution. / Control - no treatment, Dharmafect – Dharmafect 1, delivery vehicle only, NT siRNA - non-targeting siRNA, HDX siRNA – HDX pool siRNA. Reduced HDX expression was demonstrated following knockdown.

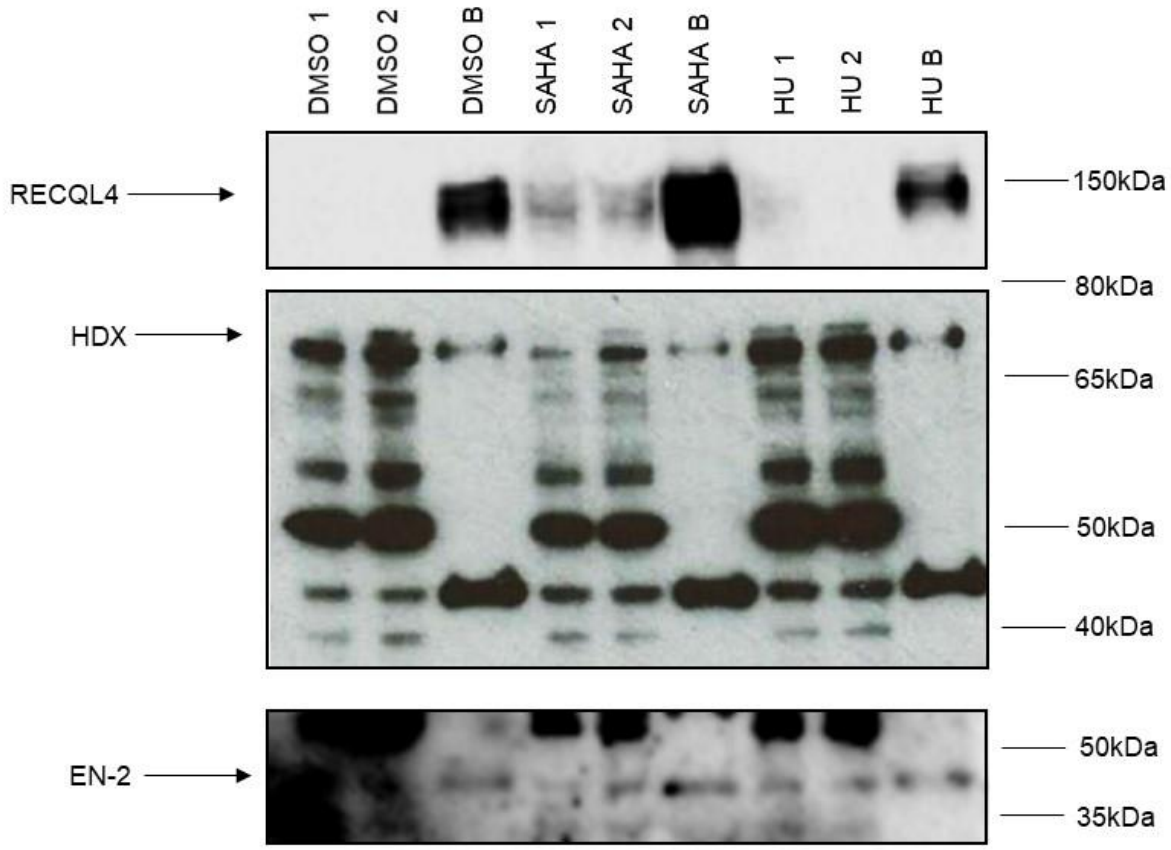

Figure 5.3-e Pull-down of RECQL4 interacting partners in U2OS clone #15 cells. RECQL4 expression was induced in the selected U2OS #15 cells with doxycycline in 10cm dishes. Post 3 days the cells were either treated with 2µm Suberoylanilide hydroxamic acid (SAHA), 4mM hydroxyurea (HU), or as a control treated with DMSO for 18 hours. GFP tagged RECQL4 was immunoprecipitated using GFP-Trap_A, then SDS-page and western blot were performed. The membrane was probed with Abcam anti-HDX antibody (ab94475) at 1µg/ml in BSA blocking solution, RECQL4 (1:1000 in BSA blocking) and Engrailed 2 (1:10000). 1 –Input, 2 – Non-bound, B – Bound; 2% input and unbound were loaded. RECQL4: 150kDa, HDX: 77kDa, EN-2: 42 kDa. HDX and EN-2 signal is shown in the RECQL4 bound fraction.

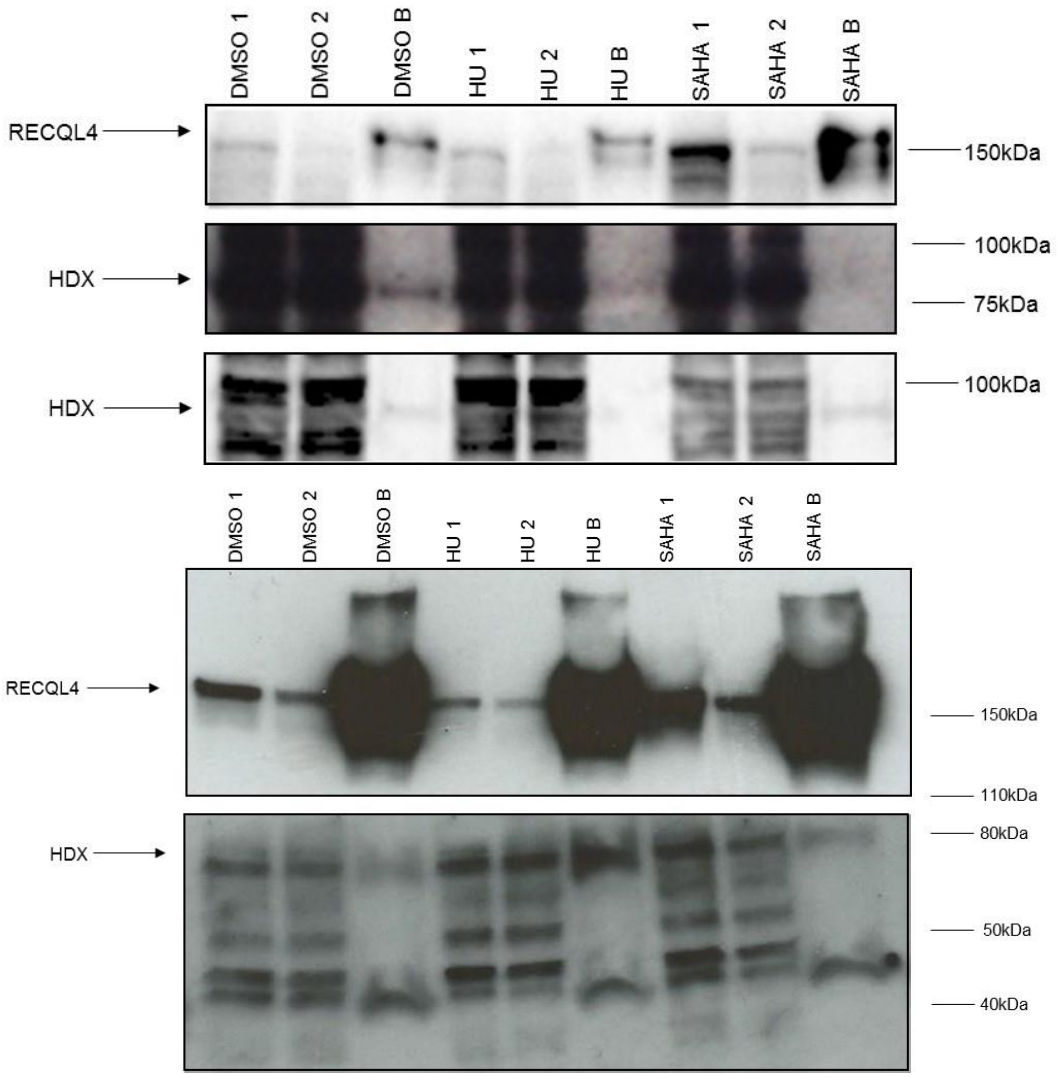

Figure 5.3-f Pull-down of RECQL4 interacting partners in HeLa clone #2 cells. RECQL4 expression was induced in the selected HeLa #2 cells with doxycycline in 10cm dishes. Post 3 days the cells were either treated with 2µm Suberoylanilide hydroxamic acid (SAHA), 4mM hydroxyurea (HU), or as a control treated with DMSO for 18 hours. Immunoprecipitation using GFP-Trap_A, SDS-page and western blot were performed. 2% input and unbound were loaded, 1 –Input, 2 – Non-bound, B – Bound. Membrane was probed for RECQL4 (Cell Signalling 1:1000) 150kDa, HDX -77kDa (Aviva Systems Biology ARP39832_P050), (top blots), and Abcam anti-HDX antibody (ab94475)(bottom blot) at 1µg/ml in BSA. HDX and EN-2 signal is shown in the RECQL4 bound fraction.

5.4 Summary

In summary, RECQL4 expression appeared variable in cell lines and RTS cells. The AG05013 RTS cell line appeared to demonstrate evidence of DNA damage with an increase in γH2AX and TRF2 intensity not seen in the other RTS cell lines (AG03587, AG18375). Further investigations are required to understand the reasons for this finding, perhaps sustained DNA damage from existing specific RECQL4 mutation. Further comparison of other RTS cell lines could better our understanding of the apparent alterations of DNA damage response seen in these cells, such as cell morphology, aneuploidy, proliferative rate, and preferred DNA damage response pathway.

The shRNA constructs generated during this work are used for follow-on work in the laboratory. Lentiviral vectors have been generated and used for transduction of ASC52telo cells. Phenotypic changes induced by stable knockdown are currently being characterised as part of an MSc by Research project.

We found a number of novel RECQL4 protein interactions that to date have not been reported. These preliminary findings are currently under follow-up investigation in the laboratory and could lead to new roles and pathways that involve RECQL4.

6 Discussion

6.1 Interfering with DNA replication initiation (chapter 1, section 3.1)

We set out to establish a model based on replication initiation stress and reduced proliferative rate, which mimics the potential effects of RECQL4 mutations identifying any subsequent cellular changes, such as damage to the cells (Sangrithi et al., 2005; Lu et al., 2014a; Lu et al., 2016).

PHA-767491 is a pyrrolopyrridinone molecule, the first well-characterized inhibitor of DBF4 dependent kinase (DDK) (Montagnoli et al., 2008; Vanotti et al., 2008). It is a dual Cdc7/Cdk9 inhibitor, and consequentially inhibits firing of replication origins without affecting replication fork progression (Montagnoli et al., 2008), due to specific inhibition of both Cdc7 kinase and the phosphorylation of MCM2 at the Cdc7-dependent Ser40 site (Montagnoli et al., 2008). PHA treatment was found to abolish MCM2 phosphorylation in HCC1954 cells further corresponding to cell growth and viability effects (Sasi et al., 2014). In normal cells Cdc7 inhibition arrests cell proliferation (Montagnoli et al., 2004; Tudzarova et al., 2010). The inhibition or depletion of Cdc7 leads to the triggering of the replication origin activation checkpoint, which generates a reversible G1 arrest, failure to progress to S phase, while the cells remain viable. Active Cdc7 levels are restored following withdrawal of treatment (Tudzarova et al., 2010).

An early study was the first to show that DDK depletion leads to the severe disruption of DNA replication in HeLa cells (Jiang et al., 1999). Further studies have demonstrated the depletion of DDK by siRNA in HeLa cells led to p53-independent apoptosis, in comparison to a normal human dermal fibroblast cell line, in which it led to reversible cell cycle arrest. This effect was further confirmed in other cell lines (Montagnoli et al., 2004; Im and Lee, 2008; Tudzarova et al., 2010; Ito et al., 2012). PHA-767491 has also been demonstrated to reduce proliferation in a number of other cell lines (Sasi et al., 2014).

Our aim was to establish a model of mild replication initiation inhibition in mesenchymal stem cells (ASC52telo) in culture using PHA. ASC52telo cells have been employed in many studies (Wolbank et al., 2009; Hasebe-Takada et al., 2016; Nardone et al., 2017; Pitrone et al., 2017). Our results indicated the degradation of PHA during cell culture, and media changes with fresh addition of PHA at day 3

maintained inhibition. There is little information on the stability of PHA in the literature, as studies appeared to use short term treatment of around 24 to 72 hours (Montagnoli et al., 2008; Natoni et al., 2013; Fitzgerald et al., 2014; Sasi et al., 2014; Erbayraktar et al., 2016). There are many conditions which can lead to degradation of a substance, including time, and environmental factors (Blessy et al., 2014).

A model of PHA-767491 was established in low and high passage ASC52telo cells with acute and chronic PHA treatment, and withdrawal of treatment in either case ('recovery'). This enabled us to further understand the effects of reduced replication over time and the potential cellular stress this generates, similar to the effect of RECQL4 mutations, and if and how the cells may recover following the cessation of treatment with PHA-767491. Interestingly, PHA-767491 treated cells appeared to lead to cell morphology changes, as the cells appeared larger, which is an indication of cellular morphological modifications that have been further explored in this study. Cells that are actively proliferating produce a range of proteins which can be utilised as markers using assays such as immunofluorescence. Ki67 is a nuclear antigen expressed in cycling cells, and is not expressed in quiescent cells (Sobecki et al, 2017). The role of Ki67 was not initially fully understood (Tsurusawa and Fujimoto, 1995), however, a more recent study has found Ki67 may be involved in the organisation of heterochromatin in proliferating cells (Sobecki et al., 2016). Early studies found levels of expression to appear in G1 phase, with a further increase during S phase and G2 phase, with the maximum level seen during mitosis at the surface of chromosomes (Gerdes et al., 1984; Sasaki et al., 1987; Manoir et al., 1991; Tsurusawa et al., 1992; Scholzen and Gerdes, 2000; Ladstein et al., 2010). Absent expression is seen in resting cells in G0 phase of the cell cycle (Scholzen and Gerdes, 2000). An early study, however, did find some tumour cells in G1 phase negative for Ki67 progressed into S phase of the cell cycle, following a long G1 phase duration (Tsurusawa and Fujimoto, 1995). We expected a decrease of Ki67 expression in PHA-767491 treated cells, as we have demonstrated reduced proliferation as reduced cell count. Somewhat surprisingly, we observed some high levels of Ki67 expression in these cells. This contradiction might be related to persisting Ki67 expression in G1; as described previously, PHA-767491 could hold the cells in G1 phase of the cell cycle. The reduced expression shown following long term PHA-767491 treatment could demonstrate increased sensitivity and/or more cells exiting the cell cycle into G0, as the cells were previously shown to demonstrate reduced proliferation via cell count. A study by Montagnoli et al, (2008),

demonstrated an increase of Ki67 following PHA-767491 using immunohistochemistry in HCT116 xenografts, which also remained unexplained (Montagnoli et al., 2008).

Topoisomerases are enzymes that hold important roles in uncoiling supercoiled DNA, and removing knots and catenates that form during DNA metabolism by causing transient breaks in the DNA double-helix (Wang, 1985; Wang, 2002). Topoisomerase 1 (TOP1) generates single-stranded breaks in double-stranded DNA, swivels the broken end around the non-scissile strand, then re-joins the break during transcription and replication (Bouwman and Crosetto, 2018). Camptothecin (CPT) inhibits topoisomerase I catalytic activity through the prevention of re-ligation, and stabilizes the TOP1-DNA cleavage complex (Hsiang et al., 1985; Huang et al., 2004; Darzynkiewicz et al., 2012; Zhao et al., 2012; Berniak et al., 2013), leading to a G2 delay and cytotoxicity (Janss et al., 1998). Camptothecin has been reported in many studies as an attractive anticancer drug (Hafian et al., 2004; Zhou et al., 2010; Gaur et al., 2014). At this stage of the study, we utilised CPT to demonstrate reduced cell proliferation, verified with reduced Ki67 expression, which has also been demonstrated in the literature (Zhou et al, 2010; Gaur et al, 2014).

There are many methods for the analysis of cell proliferation, each with their own advantages and limitations (Jones et al., 2001; Ng et al., 2005; Hutmacher et al., 2009; Mimeault and Batra, 2010; Quent et al., 2010). The simplest method using a haemocytometer was utilised in our study, and with the combination of trypan blue cell viability was measured alongside. Although simple and not expensive the main limitation can be human error and the same operator would introduce a constant level of this potential error (Pierre, 2002). We also utilised the indirect colorimetric MTS (3-(4,5-dimethylthiazol-2-yl)-5-(3-carboxymethoxyphenyl)-2-(4-sulfonyl)-2H-tetrazolium) assay. The MTS assay is based on the bioreduction of tetrazolium salts changing the colour from a pale yellow to dark blue dye by the formation of formazan catalysed by mitochondrial dehydrogenases, and measured by absorbance (Mosmann, 1983; Berridge et al., 2005). Limitations include a variable metabolic behaviour found in cells and under variable culture conditions such as pH changes, and as an end-point assay further analysis of cell survival cannot be achieved. High cell density has also been found to be inappropriate for measuring cell proliferation (Plumb et al., 1989; Hsu et al., 2003; Ng et al., 2005; Lopez-Barcons, 2010; Rattan et al., 2011). Additional chemical treatments may also interfere (Wang et al., 2010). In our study PHA and DMSO treated wells without cells were utilised as controls,

and demonstrated no modification of signal. The assay measures enzyme activity of mitochondrial dehydrogenases, that is metabolic activity, rather than measuring the number of cells and viability (Mosmann, 1983; Quent et al., 2010). Nevertheless, this enzyme activity is proportional to the number of live cells as damaged or dead cells display no dehydrogenase activity (Mosmann, 1983; Jevprasesphant et al., 2003). The MTS assay has been utilised for analysing cell growth following PHA-767491 treatment in a recent study, and found inhibition of cell growth, as seen in our study (Liu et al., 2018). A cell count alongside the MTS is necessary to verify the cell number is suitably represented within our study.

6.1.1 PHA-767491 effect on osteocyte differentiation (chapter 1, section 3.1.1)

6.1.1.1 Differentiation of ASC52telo MSCs

The MSCs utilised in our study were isolated from adipose tissue obtained commercially, and can differentiate *in vitro* into mesodermal lineages; osteocytes, chondrocytes, and adipocytes (Hampel et al., 2005; Strem et al., 2005; Zhang et al., 2011), and non-mesenchymal lineages: skeletal myocytes (Strem et al., 2005), hepatocytes (Wang et al., 2014a), cardiomyocytes (Strem et al., 2005; Choi et al., 2010), pancreatic (Timper et al., 2006), and neuronal cells (Safford et al., 2002; Kang et al., 2003; Strem et al., 2005). It is not clear whether all these terminally differentiated cell types represent true *in vivo* routes of differentiation. We concentrated on differentiating the cells into adipocytes, osteoblasts, and chondrocytes, which was verified in low and high passage ASC52telo cells. Re-expression of hTERT in mesenchymal stem cells is also extensively studied (Wolbank et al., 2009), and in particular found that the ASC52telo cell line maintains mesenchymal surface markers, and osteocyte and adipocyte differentiation potential. However, adipocyte differentiation capabilities may become enhanced (Jun et al., 2004; Kang et al., 2004a; Wolbank et al., 2009). Other reports also found that hTERT immortalisation of ASCs leads to increased differentiation potential (Jun et al., 2004; Kang et al., 2004a), however, this may not be applicable to all transduced cell lines, as differentiation potential appears to be variable even across subclones derived from single adult stem cells (Guilak et al., 2006).

As the fibroblast like MSCs differentiate into chondrocytes, their morphology changes into a large round shape. The cells become surrounded by ECM that contains a highly organised network of collagens, proteoglycans and

glycosaminoglycans (Hardingham et al., 2006; Chang et al., 2008; Ding et al., 2010). The cells produce cartilage-related extracellular matrix molecules, including proteoglycans, collagen II and IV, PRELP and aggrecan (Caplan, 1991; Pittenger et al., 1999; Zuk et al., 2001; Erickson et al., 2002; Zuk et al., 2002; Dragoo et al., 2003; Siitonen et al., 2003; Wickham et al., 2003). Alcian blue stains highly sulphated proteoglycans in nodules, a characteristic of cartilaginous matrix, a sign of chondrocyte differentiation (Zuk et al., 2002; Ogawa et al., 2004).

The differentiation of adipocytes leads to changes of cell shape from the fibroblast like MSC, into spherical shape cells, expressing ECM proteins such as fibronectin, laminin, and collagen. Fibronectin initially forms a network, which is replaced by collagen network (Elbrecht et al., 1996; Kubo et al., 2000; Rosen and Macdougald, 2006; Vallee et al., 2009). Differentiation then leads to the accumulation of intracellular lipid-rich vacuoles, identifying the final stage of adipocyte differentiation. These vacuoles stain positive using Oil Red O (Vater et al., 2011). Oil Red O ($C_{26}H_{24}N_4O$) is a fat-soluble diazol dye which detects neutral lipids and cholesteryl esters (Ramirez-Zacarias et al., 1992). Oil Red O is a hydrophobic dye; minimally soluble in solvent which further decreases in water, associating with the lipids in tissue (Mehlem et al., 2013), or in our study with lipid droplets. The lipid droplet production appears proportional to the extent of differentiation (Kuri-Harcuch and Green, 1978). In our study, the outcome was determined using this method and qualitatively. To further this, data can be collected quantitatively by extracting the dye using isopropanol (Choi et al., 2008) or via measuring the activity of glycerol-3-phosphate dehydrogenase (GPDH) (Pairault and Green, 1979; Tsuji et al., 2008).

Following osteoblast differentiation, cell morphology modifies from fibroblast like cells into cuboidal shape, also demonstrated in our study. The cells produce extracellular matrix (ECM) which is composed of mainly collagen type I, and late differentiation aggregates and nodules form. Increased levels of alkaline phosphatase, and the accumulation of calcium is also seen during differentiation (Pittenger et al., 1999; Chamberlain et al., 2007). We analysed these calcium levels qualitatively using Alizarin Red S staining, often used within the literature (Stanford et al, 1995; Yang et al, 2004; Håkelien et al., 2014;Aveic et al, 2019). Alizarin Red S forms a chelate complex with calcium cations (Stanford et al., 1995). Strong staining was observed demonstrating osteoblast differentiation within our study. We often observed, although not always significant, stronger staining of the calcium deposits in differentiated ASC52telo cells with PHA-767491 treatment, which could

be investigated further by quantification to determine its significance. The stain can be further analysed following extraction for semi-quantification (Stanford et al., 1995), for example using acid extraction, which can be used to assay the kinetics of osteogenesis (Junqueira et al., 1998; Long, 2001; Gregory et al., 2004), and RNA-Seq analysis to determine the extent of differentiation (Håkelien et al., 2014).

Disrupting the balance of MSC differentiation into adipocytes and osteoblasts has been reported in many human diseases, with some physiological changes favouring adipocyte differentiation of bone marrow MSCs leading to loss of bone, and increased risk of bone fracture (Rodríguez et al., 2000; Sekiya et al., 2004; Muruganandan and Sinal, 2014). In aging an increase in bone marrow adipogenesis with decrease in bone marrow formation has been reported (Meunier et al., 1971; Burkhardt et al., 1987; Kajkenova et al., 1997; Nuttall and Gimble, 2000; Verma et al., 2002). The link between increasing age and the loss of bone mass and strength has been long established, with some points mentioned previously (Parfitt, 1984; Zebaze et al., 2010; Almeida, 2012). Reduced RECQL4 activity could be linked to reduced proliferation and impairment of osteoblasts, either directly, or providing a sensitised environment (Ng et al, 2015). RTS patients demonstrate clinical signs of premature aging, which may be related to changes in aging of MSCs. Accumulation of pre-osteoblastic cells with a decrease of mature osteoblasts have been reported in rats with increasing age (Roholl et al., 1994).

Genetic approaches have proposed that the committed osteoblast lineage is the cell of origin in OS (Berman et al., 2008; Walkley et al., 2008), which would explain previous studies as p53 deletion in pre-osteoblasts and osteoblast progenitors showed higher levels of OS compared to multi-lineage potential cells (Ng et al., 2012). Osteoblast progenitors have been found to be more committed than other mesenchymal stem cells, which correlates to lower levels of other sarcoma types observed (Lin et al., 2009). A large early study found 81% of osteosarcomas were undifferentiated or poorly differentiated (Dahlin, 1957), which was also reported in later studies (Thomas et al., 2004; Tataria et al., 2006; Haydon et al., 2007). We propose that mesenchymal stem cells or differentiating osteoblast may be the cells of origin of OS, which is also raised as a possibility by other laboratories (Conget and Minguell, 1999; Pittenger et al., 1999; Thomas et al., 2004; Tataria et al., 2006; Haydon et al., 2007; Deng et al., 2008). Many studies are in support of sarcomas being a differentiation disease, in support of our hypothesis, and suggest that

mutations that hinder differentiation are the cause, initiating different sarcomas depending on cell lineage and stage of differentiation. It is thought to be the reason for the many different subtypes seen in osteosarcoma as well (Tang et al., 2008). Studies in support of this model have demonstrated an overlap of gene expression signatures of differentiated stages of MSCs from normal tissues and sarcomas (Nielsen et al., 2002; Boeuf et al., 2008; Bovée et al., 2010; Mohseny and Hogendoorn, 2011). Other studies propose another model: the sarcoma originates from primitive MSCs following the acquired mutations that direct sarcoma genesis (Rubio et al., 2005; Tolar et al., 2007; Li et al., 2009), as the overlap of signatures is thought to be generated due to similar stroma of different tissues (Wunder et al., 2007; Li et al., 2009). Sarcomas may generate from mutated MSCs which are vulnerable to further mutations (Yang et al, 2014).

6.1.1.2 The role of RUNX2 in regulating MSC differentiation

RUNX2 is essential in the regulation of osteoblast differentiation through the expression of bone-specific genes, such as collagen type 1α-1, Osterix and Bone sialoprotein (BSP) Nakashima et al., 2002; Rutkovskiy et al, 2016). The activity of RUNX2 is regulated via many post-translational modifications such as phosphorylation, methylation, acetylation, and ubiquitination (Bae and Lee, 2006; Rajgopal et al., 2007; Zagami et al., 2009). The level of RUNX2 expression is cell cycle phase dependent, and variable depending on cell type and during osteogenesis in MSCs. Maximum expression has been shown in preosteoblasts, and again in early mature osteoblasts. A decline in expression occurs during osteoblast commitment, reducing further in mature osteoblasts and osteocytes (Ducy et al., 1997; Maruyama et al., 2007; Tang et al., 2008; Komori, 2010; Jönsson et al., 2012)**,** which we also demonstrated in our study. In osteoblasts the maximum peak is seen in early G1 phase of the cell cycle, which reduces in S and M phase (Galindo et al., 2005). A decrease of expression is also seen at the G1/S transition of the cell cycle and during mitosis (Nimmo and Woollard, 2008). RUNX2 represses the transcription of $p21^{CDKN1A/WAF1/CIP1}$, a cyclin-dependent kinase inhibitor that holds a role in cell cycle arrest at G1 (Westendorf et al., 2002; Galindo et al., 2005; Galindo et al., 2007). In our study, RUNX2 was increased in lower passage ASC52telo cells under PHA treatment upon osteoblast differentiation, however, this requires repeating to verify. As previously discussed, in normal cells PHA-767491 treatment would lead to the cells being held at G1 phase of the cell cycle (Rodriguez-Acebes et al., 2010; Tudzarova et al., 2010; Ahuja et al., 2016), which may explain the

increase in RUNX2 expression levels we observed. Further analysis is required such as cell cycle sorting to determine this.

Under genotoxic stress, RUNX2 interacts with the p53 tumour suppressor (Ozaki et al., 2013). Overexpression of RUNX2 leads to a downregulation of genes downstream of p53, while downregulation of RUNX2 leads to an elevation of these following DNA damage (Ozaki et al., 2013). RUNX2 may have an important role in DNA damage response (DDR) (Wysokinski et al., 2015). During differentiation some DDR-related factors may associate with RUNX2. The deficiency of p53 has been shown to enhance the ability of proliferation and differentiation of osteoblasts (An et al., 2010). An increased level of p53 upregulates RUNX2 in osteoblasts and inhibits osteoblast differentiation (Galindo et al., 2005; Lengner et al., 2006). High levels of RUNX2 have also been found in osteosarcoma with loss of p53 (Pereira et al., 2009; San Martin et al., 2009). High expression level of RUNX2 is associated with bone metastasis (Vladimirova et al., 2008; Zagami et al., 2009; Pratap et al., 2011), suggesting an involvement in forming a microenvironment that encourages tumour invasion.

RUNX2 and RECQL4 expression has been found to be increased in some OS patients (Martin et al, 2014). The lack of functional RUNX2 in osteoblasts leads to a loss of growth restraint (Pratap et al., 2003). Osteogenic differentiation leads to growth restraint and terminal cell cycle exit due to RUNX2- dependent induction of $p27^{KIP1}$ (Drissi et al., 1999), and growth arrest following the inhibition of S-phase cyclin complexes in mature osteoblasts (Thomas et al., 2001; Thomas et al., 2004).

6.1.1.3 The role of RECQL4 in bone morphogenesis

Ng et al, (2015), using conditional alleles that specifically inactivated *Recql4 in vivo* in osteoblastic progenitor stages of differentiation, described shorter bone formation and reduced bone volume. RECQL4 knockdown in the osteoblastic cell lineage and in primary osteoblasts did demonstrate cell cycle arrest, apoptosis, impaired differentiation and failed proliferation (Ng et al., 2015). The cells displayed a ‘flattened’ morphology, proliferation declined with a reduced Sca-1 expression, a marker of proliferation (Ng et al., 2015). Although other studies have observed senescence in human fibroblasts following RECQL4 knockdown (Lu et al., 2014a), this was not observed (Ng et al., 2015), however, some aspects of regulation of proliferation may be different between these cell types (Lu et al., 2014b). There are

important differences to consider between this mouse model system and human patients. RECQL4 mutant proteins are expressed throughout the human body during all the stages of skeletal development, while the OSX-CRE mediated conditional allele will not deplete Recql4 from all bone forming cells (Ng et al., 2015). However, the study does suggest an important intrinsic function for Recql4 in skeletal growth (Ng et al., 2015). Mice, that harbour Recql4 depleted cells committed to osteoblast differentiation, fail to produce mineralisation, as shown with alizarin red staining, while profiling revealed that all markers of osteoblastic maturation, except Runx2 were reduced in these cells (Ng et al., 2015). Interestingly the same depletion in more mature cell populations did not demonstrate this skeletal phenotype, suggesting that Recql4 may have a major role in pre-osteoblasts in mice (Ng et al., 2015). High expression of *Recql4* was reported in MC3T3.E1 mouse osteoblastic cells, and this level decreases as the cells differentiate in culture. Recql4 overexpression leads to increased proliferation, while siRNA-mediated depletion impeded growth (Yang et al., 2006). However, the decline of *RECQL4* mRNA was not demonstrated in human cells following *in vitro* differentiation of Fob1.19 human immortalised foetal osteoblast cells (Burks et al., 2007). The authors suggest this variable outcome could be due difference in species, and method of induction of differentiation (Burks et al., 2007).

Recql4 may play a role in the regulation of osteoprogenitor proliferation as its localization is observed in active osteoblasts surrounding the growth plates rather than differentiated osteocytes in adult mice (Yang et al., 2006). High expression in actively forming bone, in osteoblasts lining the trabecular surface, and in bone lining cells, also suggests an important role for RECQL4 in bone growth (Delagoutte and Von Hippel, 2003; Siitonen, 2008). This is not too surprising as we know differentiation leads to reduced proliferative state of the cells, and a correlation between RECQL4 expression and proliferation activity has been demonstrated (Yang et al., 2006). Recql4 expression in mice is also abundant in proliferating intestinal enterocytes and in immature cells and in chondrocytes of developing bones and cartilage of the growth plate (Delagoutte and Von Hippel, 2003). Yang and co-workers (2006) suggest that reduced RECQL4 expression may be required for full differentiation (Yang et al., 2006). RTS patients may harbour mutations that generate C-terminally truncated RECQL4 proteins, which preserve function in replication, but helicase activity is either diminished or limited (Ng et al., 2015). This suggests that tumour predisposition may be a feature of cells that retain the Sld2-

homology regions of RECQL4, which leads to proliferation with genomic instability (Kitao et al., 1999a; Abe et al., 2011; Kohzaki et al., 2012). In line with our thoughts, these genomic instabilities would lead to OS formation. Further to this, the previously mentioned study by Ng et al, (2015) suggests that tumourigenesis may require mutant *Recql4* activity (Ng et al., 2015). Double knockout mice that harbour deleted *p53* and *Recql4* in the osteoblastic lineage (**Osx**-Cre **p53$^{fl/fl}$Recql4$^{fl/fl}$**) do not always develop OS. The study suggests that mutant alleles of *Recql4*, and not null alleles, may lead to susceptibility to OS formation (Ng et al., 2015). However, previous mouse models were unable to demonstrate that *Recql4* mutations lead to OS in mice, due to transcription of the N-terminal region, and hypomorphic *Recql4* alleles (Hoki et al., 2003; Mann et al., 2005).

6.2 Relationship between disturbance of DNA replication initiation and cellular transformation (chapter 1, section 3.1.2)

Disruption of the process of differentiation can lead to severe diseases, such as cancer (Gray et al., 2004; Jögi et al., 2012). We identified cellular changes indicative of cell damage in ASC52telo cells under PHA-767491 treatment. Further to this, acquiring DNA damage may dysregulate differentiation. Chronic PHA-767491 treated cells demonstrated osteoblastic like characteristics, with increased RUNX2 expression and mineralised calcium deposits observed during culturing in normal media. The same was not seen in acute PHA-767491 treated cells. Interestingly, we would expect RUNX2 levels to be reduced with the evidence of calcium mineralisation, as it occurs at a later stage of differentiation (Stein et al., 2004; Rutkovskiy et al., 2016) Dysregulation of osteogenesis transcription factors could be establishing the features seen, and acquired over the long term PHA-767491 treatment. It is important to consider factors that regulate RUNX2, which also play a role in the regulation of osteoblast differentiation, as previously discussed (Long, 2011; Rutkovskiy et al., 2016). The induced overexpression of RUNX2 in adipose derived mesenchymal stem cells has been reported to enhance osteogenic activity and inhibit adipogenesis, with a significant increase in mineral deposition compared to control cells (Zhang et al., 2006). RUNX2 is known to target other genes in osteogenesis, including osteocalcin (Li et al., 2012). Our results would be strengthened by the analysis of osteocyte specific gene expression, such as osteocalcin. Wang et al. (2006) describes a method to measure the formation of calcified nodules with fluorescent dyes in living cells continuously without the

deleterious effects of Alizarin Red S. This would be useful to determine the initial stages and proposed continual dysregulation observed in our study. Adipose-derived stem cells may undergo spontaneous differentiation *in vitro* following aging or seeding at low density with concurrent RUNX2 expression, calcium mineralization, bone morphogenetic protein-2 and alkaline phosphatase activity (Liu et al., 2016). In our study, the same was not seen in the control cultures. Although the cells under continuous PHA-767491 treatment showed reduced proliferation rate, the same cell density was seeded for both treated and control cells. Early studies were thought to demonstrate spontaneous differentiation, however, many of these were later retracted due to the inability to reproduce the results, and cross-contamination (Rubio et al., 2005).

6.2.1 Membrane potential maintained in PHA-767491 treated ASC52telo cells (chapter 1, section 3.1.3)

Mitochondrial DNA (mtDNA) is important for mitochondrial function and biogenesis during development and differentiation (Larsson et al., 1998). mtDNA maintenance, expression and regulation is complex, including mtDNA replication, mtDNA transcription, RNA modifications, RNA stability, translation, and localisation of translated proteins (Hällberg and Larsson, 2014). It is not too surprising that genetic defects of mitochondrial function can lead to human diseases (Archer, 2013; Magalhães et al., 2014; Singer, 2014). RECQL4 has also been shown to have a regulatory role in mitochondrial DNA copy number (mtDNA) maintenance. mtDNA copy number was found to increase in HEK293 cells following the elevation of RECQL4 expression, while knockdown in U2OS cells lead to a decrease in mtDNA copy number. RECQL4 deficient human fibroblasts and RECQL4 suppressed cancer cells express elevated mitochondrial superoxide production with a decrease in repair function following oxidative DNA damage (Chi et al., 2012). Interestingly, mtDNA copy number was found to be significantly reduced in RTS cell line AG05013. Reduced levels were also demonstrated in cells without mitochondrial localization signal and showing localisation to the nucleus. Mitochondrial mass was also decreased and mitochondrial morphology was aberrant suggesting alterations in mitochondrial bioenergetics occur without RECQL4 localisation. Increased invasive capabilities in these cells were further evidenced, which may be a contributing factor of the predisposition of tumourigenesis found in RTS patients (Kumari et al., 2016). Interestingly, mitochondrial and metabolic changes are also regarded as hallmarks of differentiation of stem cells. During differentiation,

mitochondrial modifications occur (Folmes et al., 2011; Varum et al., 2011; Wanet et al., 2015). Osteoblasts have a high energy requirement, as they synthesize large amounts of extracellular matrix proteins (Esen and Long, 2014). Mitochondrial activity has been found to be regulated during osteoblast differentiation, and at later stages of differentiation an increase in glycolysis is observed and may have a key role in mature osteoblasts. This may enable the cells to become more adaptable to changes in O_2 levels and energy changes (Komarova et al., 2000).

The mitochondrial membrane potential, sometimes referred to as the protonmotive force, is a crucial parameter controlling respiratory rate, ATP synthesis, Ca2+ uptake and storage, ROS generation and detoxification, and may influence the regulation of mtDNA expression (Nicholls, 2004; Gustafsson et al., 2016). Usage of rhodamine 123 (R123), tetramethylrhodamine methyl ester (TMRM), and tetramethylrhodamine ethyl ester (TMRE) provides a simple method for analysis of membrane potential. These dyes bind to the inner and outer aspects of inner mitochondrial membrane due to their lipophilic cation properties, and accumulate by the mitochondria depending on membrane potential, which can then be measured as absorbance due to the exhibition of a red shift in excitation and emission (Vander Heiden et al., 1997; Scaduto and Grotyohann, 1999; Jayaraman, 2005; Masgras et al., 2012). Viable cells exhibit high fluorescence, with low levels in apoptotic cells, and under pathological condition such as mitochondrial membrane potential impairment (Cottet-Rousselle et al., 2011;Burbulla and Krüger, 2012).

In our study, the mitochondrial membrane appeared viable and no significant changes were seen in permeability in the TMRE assay. However, higher readings were demonstrated in higher passage cells under both normal conditions and PHA-767491 treated cells, the reasons for which is unclear. Culturing cells for long period *in vitro* can generate alterations in gene expression, and differentiation potential, as a result of culture induced stress (Somaiah et al., 2015). In aging, a decrease in energy production and increased oxidative stress are considered as major contribution to age related pathologies. Defects in mitochondrial activity are also often seen (Di Lisa and Bernardi, 2005; Conley et al., 2007; Pi et al., 2007; Bratic and Larsson, 2013). Although differences in membrane potential reading between young and aged cells have been reported, some uncertainty remains due to methodological limitations (Nicholls, 2004).

The effect of PHA-767491 treatment on mitochondria is not intensively studied in the literature. A study by Nantoni et al, (2011) showed that PHA-767491 induced Bax activation and a time-dependent increase in cells with low mitochondrial membrane potential in chronic lymphocytic leukemia (CLL) cells. They found the inhibition of Cdk9 lead to death of quiescent CLL cells through the intrinsic apoptotic pathway, suggesting a link with the transcriptional inhibition of Mcl-1 as a decrease of Mcl-1 protein was seen. Cdc7 inhibition caused a block of proliferation in CLL cells (Natoni et al., 2011). Our study did not appear to show significant changes to mitochondrial membrane potential in response to chronic or acute PHA-767491 treatment.

To further verify our findings, methods such as flow cytometry and confocal microscopy can be used (Cottet-Rousselle et al., 2011). They offer the visualisation and analysis of morphological changes of mitochondria (Cottet-Rousselle et al., 2011). We could also verify our findings with the use of oxygen electrodes to measure and analyse respiratory parameters.

6.3 PHA-767491 generates DNA damage in ASC52telo cells (chapter 2, section 4)

6.3.1 Morphological markers of genome instability

The cellular architecture not only provides structural basis to cellular shape, but involves many functions necessary for the survival and maintenance of the cell (Takai et al., 2005). In most cells under normal conditions the shape of nuclei is usually round or oval (Webster et al., 2009). Alterations can be seen during normal development and differentiation (Hampoelz and Lecuit, 2011), and during cell aging and genetic diseases (Khatau et al., 2009; Zwerger et al., 2011).

Cellular morphological changes are utilised as markers of chromosomal instabilities; aberrant mitotic structures are typically associated with unfinished replication in somatic cells, indicative of replicative stress (Mankouri et al., 2013). These include abnormalities found within the literature, such as micronuclei, nuclear budding, chromatin bridges, and enlarged nuclei (Yoon et al., 2002; Zhen et al., 2002; Hida et al., 2004; Hong et al., 2009; El Ghamrasni et al., 2011; Mcgranahan et al., 2012; Chen et al., 2014a; Tyagi et al., 2015; Yadav and Bhatia, 2017). Cellular aging has been reported to be an influential factor of baseline of these markers, and demonstrated in our study (Khatau et al., 2009; Zwerger et al., 2011). The initial

PHA treatment was sufficient to generate DNA damage which either maintained or increased with chronic treatment.

Measurement of the frequency of micronuclei is often used to quantify genotoxic stress, and the diagnosis of malignant diseases (Offer et al., 2005; El-Zein et al., 2006; Verma and Dey, 2014; Tyagi et al., 2015). Micronuclei were first identified in erythrocytes (Dawson and Bury, 1961). They are formed when fragments or entire chromosomes separate from the mitotic chromosome 'bundle'. A separate nuclear envelope, complete with nuclear lamina and Nuclear-pore complexes (NPCs), is formed around them after cytokinesis. Micronuclei are induced by genotoxic stress or loss of factors needed for chromosomal segregation, forming an independent nucleus like structure (Walker et al., 1996; Goshima et al., 2003; Salina et al., 2003; Offer et al., 2005; El-Zein et al., 2006). Micronuclei themselves may hold a role as an origin of chromosomal instability, following the reincorporation of defective micronuclear chromatin into daughter nuclei. The defects in micronuclei can affect DNA repair and replication, leading to the generation of genomic instability (Terradas et al., 2016). Scoring of micronuclei was performed within the criteria set by Fenech (2000), who considered them to be morphologically identical to but smaller than the cell nucleus, at no more than one third of its diameter. The boundary of micronuclei needs to also be easily distinguishable from the nuclear boundary as overlapping edges are referred to as blebs (Fenech, 2000). To further our investigation, we could probe ASC52telo cells for centromeric DNA to identify if the observed bridges and micronuclei contain α-satellite DNA, to further identify if defects in centric/pericentric heterochromatin are present (Pageau and Lawrence, 2006). We saw an increased expression of Ki67 in the micronuclei, which has also been observed by other laboratories, suggesting a faulty mitotic checkpoint leading to mitotic catastrophe, seen in carcinoma development with p53 overexpression (Caruso et al., 2011).

Nuclear buds are another form of nuclear abnormalities, often forming following genotoxic stress and γ-irradiation. They are also called 'Blebs' and 'Nuclear protrusions' (Zaharopoulos et al., 1998; Haaf et al., 1999; Serrano-García and Montero-Montoya, 2001; Fenech, 2009). The initiation of bud formation usually occurs during S phase of the cell cycle. They demonstrate the same morphology as micronuclei, however, they remain linked to the nucleus via a narrow or wide nucleoplasmic stalk (Fenech, 2006). Amplification of DNA becomes selectively localised to specific sites at the periphery of the nucleus, forming budding as the

surplus DNA is excluded via the nucleus, which can form micronuclei. The amplified DNA may also be eliminated through recombination between homologous regions within the sequence, this then forms minicircles of acentric and a telomeric DNA. These localise to regions within the nucleus or following segregation localise to the nucleus at distinct regions (Shimizu et al., 1998; Shimizu et al., 2000). This suggests that the nucleus has an ability to sense excess DNA, and induce a potential DNA repair mechanism to eliminate these (Fenech, 2006; Black and Giunta, 2018).

A further example of nuclear architecture defect is the formation of the doughnut-shaped nuclei (Reichert et al., 2010; Verstraeten et al., 2011; Dreesen et al., 2013). They have been found to form during chromatin decondensation during late mitosis, suggesting the involvement of centrosome separation and organization defects (Verstraeten et al., 2011). However, Jagannathan et al (2012), did not find a relation with centrosomes and suggested an indirect cause following cell cycle perturbation (Jagannathan et al., 2012). The observation of the doughnut-shaped nuclei has been linked to an increase of proteasomal degradation of pericentrin (Verstraeten et al., 2011). During cell division, the sister chromatids are often connected via DNA bridges, most apparently during anaphase. A subset of these has been found in human cells to link to chromosomal fragile sites (Chan et al., 2009; Lukas et al., 2011). These fragile sites can be susceptible to chromosome breakages, translocations, deletions, and associated often with genetic disorders and cancer (Durkin and Glover, 2007; Gandhi et al., 2010). The mis-repair of double stranded DNA breaks could generate dicentric chromosomes and forming bridges (Fenech, 2006; Black and Giunta, 2018), which may be the mechanism behind the chromosome bridges observed in our study.

PHA-767491 treated lung cells from p53R172H-KI mice demonstrated inhibition of origin firing and reduced micronuclei formation (Singh et al., 2017). However, these cells hold a *Tp53* mutation, supporting the relationship between p53 expression levels and the induction of micronuclei and level of p53 association with chromosomal damage reported in other studies (Driessens et al., 2003; Salazar et al., 2009). The study by Huggett et al (2016) did not report cell morphology changes using phase contrast light microscopy, and nuclei analysis using DAPI, in human (foetal) IMR90 lung fibroblast cells treated with acute PHA-767491, or CDC7 siRNA knockdown. Arrested growth was observed as smaller population of cells, consistent with G1 cell cycle arrest (Huggett et al., 2016), which was also demonstrated in other studies (Montagnoli et al., 2004; Rodriguez-Acebes et al.,

2010; Tudzarova et al., 2010). However, treatment in cancer cells showed detachment and cells floated into the media (Huggett et al., 2016). Altered morphology has been reported following PHA-767491 on pluripotent mesenchymal progenitor C3H10T1/cells. CDC7 reportedly holds an important role in α-actin filament reorganization and SMC morphology. Acute PHA-767491 treatment (10 hours) led to an inhibition of α-SMA expression, reduced actin filament-formed stress fibres in cells induced with TGF-β (Shi et al., 2012).

6.3.2 Protein markers of DNA damage

The micronuclei appeared to be stained positive for γH2AX, indicating they may have been generated following double stranded DNA breaks (Rogakou et al., 1998). Activation of H2AX can also occur as a result of typical DDR activation seen in senescent cells. In fibroblasts these foci were termed Persistent DNA Damage Foci (PDDF) (Rodier et al., 2009). Senescence analysis is required to determine PDDF as influential factor within our study.

We observed induction of γH2AX foci in response to acute and chronic PHA-767491 treatment. H2AX phosphorylation occurs in the chromatin structure surrounding the DSB site, and near the DSBs the chromatin rapidly de-condenses to allow efficient repair (Rogakou et al., 1998; Celeste et al., 2003a; Helt et al., 2005; Kruhlak et al., 2006; Heo et al., 2008; Li et al., 2010a). γH2AX foci start to form at the DSB site around 10-30 mins following damage, and remain there until the damage is repaired, reaching a plateau within 30 minutes (Nakamura et al., 2006).

The intrinsic low levels of γH2AX observed in the control cells represent H2AX phosphorylation that primarily occurs normally during DNA replication, initially reported as a result of stalled and collapsed replication forks (Yoshida et al., 2003). Induction can also occur in mitotic cells where they form nuclear foci that are not due to DNA damage, and importantly do not induce a DNA damage response via downstream proteins (Mcmanus and Hendzel, 2005; An et al., 2010). This suggests the cell cycle may play a role in γH2AX induction, and also a decrease seen may not accurately reflect reduced DNA damage (Ichijima et al., 2005; Tu et al., 2013). To verify our findings, cell cycle analysis would be performed using flow cytometry, to verify levels of H2AX found in proportion to intrinsic histone content, and cell cycle specific expression, particularly important in cells treated with PHA-767491 (Macphail et al., 2003; Kataoka et al., 2006).

γH2AX levels have been reported to increase with PHA-767491 treatment of Capan-1 pancreas adenocarcinoma, and PANC-1 pancreatic ductal epithelial carcinoma cells, but not in IMR90 lung fibroblasts cells. The cells were treated for 96 hours, in contrast to our prolonged treatment. Cancer cells maybe more sensitive**;** increased Cdc7 and Dbf4 has been demonstrated in many human malignancies (Bonte et al., 2008; Huggett et al., 2016); however, not all cancer cells demonstrate a similar effect (Montagnoli et al., 2004). Importantly, as we suspect within our PHA-767491 model, the expression levels of Cdc7-Dbf4 may hold a role in aiding survival of some cancer cells by enhancing replication stress tolerance following the induction of ssDNA and dsDNA breaks (Bonte et al., 2008; Cheng et al., 2017). Taken together, this suggests that some human malignancies may require a certain level of CDC7 expression to aid tumorigenesis.

A common way to measure γH2AX foci is performed by immunofluorescence, other methods include western blotting, or flow cytometry (Nakamura et al., 2006). The use of CellProfiler software to quantify foci excludes qualitative factors such as variation of the foci due to cell cycle phase, giving a further advantage of counting individual foci as opposed to overall intensity. We indeed observed discrepancies between data obtained with foci counts and intensity measurements. Nevertheless, analysis with flow cytometry alongside would verify our findings, and would be used to further our study.

TRF2 and other members of the shelterin protein complex prevent the recognition of telomeres as a DNA break that would lead to repair, repressing the repair at chromosomes ends. This is very important for maintaining genome organization into separate chromosomes. If repression does not occur this leads to chromosomal fusions and genomic instability (Reddel, 2014). Reduced levels of TRF2 observed in our work could represent TRF2 degradation following DNA damage, as reported in the literature (Saha et al., 2013). Changes of nuclear morphology indicative of chromosomal instability were shown to increase with both acute and chronic PHA treatment. A study by Saha, (2013) reported a link with TRF2 intensity with the degree of nuclear morphology changes (Saha et al., 2013). To further our study, nuclear contour ratios could be calculated to determine if a correlation between these markers occurs in our system.

DNA damage foci that occur at uncapped telomeres and identified by DNA damage response factors (53BP1, γH2AX, Rad17, ATM, and MRE11) that co-localise with

telomeres and shelterin proteins are referred to as Telomere dysfunction-Induced Foci (TIFs) (Karlseder et al., 1999; De Lange, 2002; Takai et al., 2003; Zhang et al., 2017a). In our study we determined TIFS by analysing the colocalization of γH2AX and TRF2 to identify damage at the telomeres. γH2AX foci have been demonstrated in many studies showing robust correlation with replicative telomere shortening reflecting age-dependent telomere dysfunction-induced foci (Takai et al., 2003; Sedelnikova et al., 2004; Sharma et al., 2012). Significant co-localisation was shown in low passage cells**,** however, the same was not seen in high passage cells. High passage control cells appeared to generate similar TRF2 levels in comparison to low passage control cells. In all cell passages and treatments, the evidence that not all γH2AX foci colocalised with TRF2 foci suggests that the DNA damage generated is not concentrated to the telomeres. There could also be reduced response, degradation of TRF2 over time, or reduced maintained telomerase (Chu et al., 2016). The damaged telomeres may fuse with broken DNA ends as the cell progresses through the cell cycle, generating a dicentric chromosomes (Vukovic et al., 2007). The consequent breakage of the anaphase bridge leads to new chromosome free ends, which fuse again with exposed DNA, initiates breakage-fusion-bridge cycles (Zheng et al., 1999) and could lead to the morphological signs of genome instability we also observed in or model. TIFs can be more easily detected by analysing the co-localisation of 53BP1 foci with TRF1 (Takai et al., 2003), Nevertheless, our model uses hTERT immortalised cells and telomerase expression may be an influential factor.

The DNA damage evidence in PHA-767491 cells led to analysing a DNA damage response by looking at expression levels of effector proteins CHK1, phosphorylated CHK1 and 53BP1. CHK1 holds many roles, including checkpoint control, a direct role in cell survival, and the regulation of DNA repair (Sanchez et al., 1997;Sørensen et al., 2005; Dai and Grant, 2010; van Jaarsveld et al., 2019), and has been shown to be important for cell proliferation (Takai et al., 2000; Shimada et al., 2008). Disruption can lead to cell death or cellular defects, or human disease following monoallelic loss of CHK1 (Zhang et al., 2005; Tang et al., 2006; Boles et al., 2010). Decrease in CHK1 levels under normal conditions or cellular stress is mainly due to proteasome-dependent degradation (Merry et al., 2010), which can be further influenced by nutrient restriction, histone deacetylase inhibition, and other interacting proteins (Xu et al., 2004; Zhang et al., 2005; Brazelle et al., 2010; Li et al., 2010b). Reduced levels can also be due to stresses that lead to the activation

of p53-dependent G1/S arrest, which inhibits E2F-dependent transcription of CHK1, found to be important in the rise of levels during G1 / S transition (Gottifredi et al., 2001). Genotoxic stress can lead to a delay of progression through S or G2 phases of the cell cycle, and is caused by the phosphorylation of CDC25A and CDC25C phosphatases by CHK1, which inhibits their activity, consequently inhibiting the dephosphorylation of cyclin-dependent kinases CDK1 and CDK2 (Bartek et al., 2004; Sørensen et al., 2005; Goto et al., 2019), thus delaying mitotic entry and allowing DNA repair mechanisms to follow (Sanchez et al., 1997; Brown and Baltimore, 2003). If CHK1 is inhibited, it can enable the cell to continue the cell cycle with sustained DNA damage, potentially leading to cell death (Sørensen et al., 2005).

The activation of CHK1 stabilizes the CDC7-DBF4 kinase complex, assisting in replication (Yamada et al., 2013), and is important for intra-S and G2/M cell cycle checkpoints (Sanchez et al., 1997; Zhao et al., 2002; Brown and Baltimore, 2003; Petermann et al., 2006; Heffernan et al., 2007; Segurado and Diffley, 2008). Certain number of the ASC52telo cells would be reversibly arrested at G1 phase within the cell cycle due to the PHA-767491 (Rodriguez-Acebes et al., 2010), therefore, we could expect this may influence CHK1 activity, also due to the inhibition of Cdc7 be it mild. Interestingly, Montagnoli and co-workers observed that PHA-767491 does not lead to a sustained DNA damage response (Montagnoli et al., 2008b). They did not detect CHK1 phosphorylation at Ser345, and only low levels of CHK2 phosphorylation at Thr68, following PHA-767491 treatment in HeLa cells. Although an increase in γH2AX expression was seen, they suggested this may be a secondary effect.. In our study, slight increase of phosphorylated CHK1 at endogenous levels was only seen in low passage chronic PHA-767491 treated cells, which requires further verification.

53BP1 has been shown to initiate the phosphorylation of H2AX and other proteins, to proceed a DNA repair response (Ward et al., 2005; Lee et al., 2010; Noon et al., 2010), and promotes DNA end linking during chromosome remodelling (Manis et al., 2004; Ward et al., 2004). 53BP1 has a role in the early event of tumour progression, influencing proliferation, apoptosis and cell cycle (Nuciforo et al., 2007; Bi et al., 2015). An increase of 53BP1 expression in cells under acute PHA-767491 could demonstrate an initial response; however, expression appears to be reduced. Nevertheless, in some chronic treated cells a significant increase was seen, suggesting that the long-term DNA replication interference could still generate

53BP1 response. Apoptosis or senescence often follows as a response to irreparable DNA damage (Elmore, 2007). The acute treated cells could be more sensitive to the initial treatment and induce cells into apoptosis as an alternative to repair. Quantifying apoptotic and senescent could determine if this is an influential factor within our study. Although not significant, reduced expression was seen in high passage chronic PHA-767491 cells under recovery, which could indicate during long term treatment these cells lost the capability to initiate a 53BP1 mediated response, indicating a reduced DNA damage response. The lack of expression may relate to the increase in genomic instabilities seen in these cells. If 53BP1 can activate CHK1 (Bartek and Lukas, 2003), we may have expected to see a correlation between them, which may be the case in high passage cells.

Deregulation of cell proliferation has been found to lead to DNA damage response activation mainly via the ATM and ATR pathways (Hahn et al., 1999) (Bartkova et al., 2005; Gorgoulis et al., 2005; Bartkova et al., 2010). Interestingly, this activation in normal cells would lead to a barrier against uncontrolled cell growth, a hallmark of cancer cells. In tumour cells this activation however leads to removal of this barrier through one or more losses of DNA damage response capabilities, increasing genomic instability, and the higher dependency on the remaining DNA damage response (Halazonetis et al., 2008; O'connor, 2015). A cancer cell acquires a number of central genetic lesions that enable alterations to the normal multicellular development and expansion of cells, allowing intratumoral diversification and the development of cancer subclones. These cells harbour variations of genomic modifications, which differ from the surrounding tumour cell population. Patients who present this heterogeneity show poor prognosis and increase in relapse following cancer treatment, which is a feature of OS (Landau et al., 2013; Landau et al., 2015; Andor et al., 2016; Mcgranahan et al., 2016). A driver of this process is chromosomal instability (Bakhoum and Landau, 2017).

6.3.3 Interference with DNA replication initiation leads to cellular transformation (chapter 2 section 4.2)

The degree of chromosomal instabilities is not the only influential factor for tumourigenesis. To assess whether the chromosomal instability we observed following chronic PHA treatment correlated with the acquisition of tumourigenic characteristics, we further analysed the cells for anchorage-independent growth and loss of contact inhibition, hallmarks of tumour cell development. Modification of adhesion is classed within the first change of cellular adaptation and is also involved

in the metastasis stage (Jinka et al., 2012). In normal cells the detachment from the extracellular matrix, or cell adhesion to an inappropriate location induces a type of apoptosis, often termed as anoikis, triggered by the loss of interaction between the cell and the extra-cellular matrix (ECM) that mediates cell death (Frisch and Ruoslahti, 1997; Frisch and Screaton, 2001; Lee et al., 2016). Anoikis was first described in epithelial and endothelial cells and protects cells when adherent on permissive ECM proteins (Frisch and Francis, 1994). Anoikis is a Greek word meaning loss of “home” or “homelessness”, and holds an important role in the prevention of detached cells adhering to new locations and potentially initiate dysplastic growth. The failure of this regulation can lead to adherent cells detaching from supportive matrix due to loss of survival signals from cell-ECM interactions, are able to survive under suspension conditions or capable of proliferation with alternative ECM proteins at ectopic sites. Tumour cells, including osteosarcoma, are able is to resist anoikis, and to grow and survive without anchorage to ECM (Liu et al., 2008; Taddei et al., 2012; Zhu et al., 2013; Gao et al., 2018). Osteoblasts secrete ECM that is a major component for mature bone, and important mechanical receptors that signal bone matrix formation and the promotion of mineralization following mechanical strain (Wozniak et al., 2000; Simmons et al., 2003). Secreted ECM-related proteins include osteonectin, osteopontin (OPN), osteocalcin (OCN), bone morphogenetic protein 2 (BMP-2), and type I collagen, and promote vascular endothelial growth factor (VEGF) synthesis (Bhatt et al., 2007).

Adult tissue derived MSCs retain adherence to plastic dishes in laboratory culture (Da Silva Meirelles et al., 2006). Adipose derived MSCs also hold this characteristic (Grossmann, 2002). Cell clump (spheroids) formation was observed in our PHA model indicating potential anchorage-independent cell growth. Although a few small spheroids were seen in some of the control conditions on ultra-low attachment plates, these appeared rare and indicated a growth rate significantly lower than the chronic treated high passage cells.

MSC spheroids have been shown to maintain differentiation, and allow a novel 3D culture model in comparison to adherent monolayer systems (Baraniak and Mcdevitt, 2011). Long term culturing of ASCs as 3D spheroid culture leads to efficient and enhanced proliferation, with unaltered adhesion capacity demonstrated with re-attachment. Alterations of cell-to-ECM interacting protein expression have also been found in MSC spheroids compared to scraped or trypsinised MSCs,

suggesting that spheroid growth leads to cellular changes advantageous to proliferation and growth (Lee et al., 2016).

The soft agar method has been the gold-standard, sensitive assay for many years for exploring anchorage-independent growth (Macpherson and Montagnier, 1964; Conery and Harlow, 2010; Hasebe-Takada et al., 2016); however, the soft agar assay is unsuitable to demonstrate tumourigenic conversion from hTERT transduction (Jiang et al., 1999; Wolbank et al., 2009; Zhang et al., 2017c). Instead, we grew the cells in plates treated to reduce attachment surface (Fukazawa et al., 1995). The ultra-low attachment plates used in our study have a neutrally charged, hydrophilic surface with covalently bonded hydrogel layer that minimises attachment (Corning 3474), (Basu-Roy et al.; Douma et al., 2004; Boschelli et al., 2008; Dottori et al., 2010; Neri et al., 2013). Several studies have used similar techniques and observations as to our study, to determine malignant transformation (Ward et al., 2013; Giannakouros et al., 2015).

To further our analysis staining using crystal violet dye can be used, binding to proteins and DNA, and indicating cell viability, colony formation (Zhang et al., 2017c), and anoikis *in vivo* (Pedanou et al., 2016). It is a method used often in the literature, however, similar to using the MTS assay, as the cell clumps appear large the permeability of the stain would be a concern. Another methodology for cell clump quantification would be the flow cytometry-based pulse-width assay, which is reported to show high level of accuracy, and sensitivity (Hickerson et al., 2014; Cui et al., 2016), Quantifying the clumps alone could be used, however, in our study, the treated cell clumps appeared larger, therefore the cells appeared to favour grouping together rather than producing smaller and many clumps. It would be interesting to analyse our PHA-767491 treated cells for anoikis *in vivo*, to determine if reduced regulation may be leading to the potential anchorage-independent growth observed (Kang et al., 2007; Rago et al., 2008).

Another cellular transformation hallmark includes the loss of contact inhibition. Our findings initially showed that acute PHA-767491 treatment reduced cell proliferative rate, however, we wanted to investigate if the cellular modifications that we observed, including anchorage-independent growth, led to a loss of contact inhibition in these cells. ASC52telo cells have been reported to display normal contact inhibition properties (Wolbank et al., 2009). In confluent adherent cell lines, contact inhibition is defined as a major decrease in cell mobility and mitotic rate in

relation to increasing cell density, and a stationary state insensitive to nutrient renewal following confluency, in spite of the availability of growth factors and nutrients (Levine et al., 1965; Huttenlocher et al., 1998; Halbleib and Nelson, 2006; Takai et al., 2008; Zeng and Hong, 2008; Heckman, 2009). In particular, fibroblast cells display density-dependent inhibition and the extent of quiescence is proportional to serum growth factor concentrations within the growth medium in culture (Cooper and Hausman, 2000).

The formation of cell clumping observed in our study in PHA-767491 treated cells could lead to under-represented cell quantity, as individual cells could not be quantified within the cell clumps. Grzesiak and co-workers (2011) observed similar cell clump formation following culture of equine adipose derived primary cells (Grzesiak et al., 2011). Undifferentiated adipose derived stem cells form spheres, thought to be neurospheres, spontaneously when cultured at high density (Kang et al., 2004b; Ivascu and Kubbies, 2007; Meyer and Walter, 2016; Schmidt et al., 2016; Zhang et al., 2017b). Chronic PHA treatment did cause more variable cell viability over the culture time measured by trypan blue; however, it remained above 95%, demonstrating good rate of cell survival in culture (Ribeiro et al., 2006).

We used protein concentration measurements to gain a better insight of cell growth. However, protein concentrations may alter due to conditions of the cell, and changes may occur when cells are under stress (Gasch et al., 2000; Brauer et al., 2008; Keren et al., 2013; Barenholz et al., 2015), or are in different cell cycle phase (Cookson et al., 2009). Changes in protein concentrations also relate to the proliferative state of the cell, an increase in bio-synthesis machinery genes leads to faster growth. Barenholz et al, (2015) suggested a model where cell growth leads to production of proteins at the same rate as protein degradation. These suggestions could explain the variable protein concentrations we observed. Nevertheless, results obtained with cell count and protein concentration measurements show some correlation. An increase was shown in general in acute PHA-767491 treated cells, although this did decrease following further culturing. High passage chronic treated cells following recovery demonstrated overall significant increase in proliferation over the 21 days of culture. Repeats are required to verify this finding, as not always seen, but suggests continual growth in these cells. We do need to consider that the cells may catch up following release of treatment. Further culturing and other analysis are required.

The RealTime-Glo MT cell viability assay (Promega) is a nonlytic assay. It measures the reducing potential of viable cells in an ATP-independent manner, is well tolerated by cells and luminescence signal can be retaken up to 72 hrs of incubation, which provides kinetic data allowing the possibility to monitor cellular changes over time. The assay utilises a pro-substrate, and an engineered luciferase added to the media. The MT cell viability pro-substrate is cell-permeant and diffuses into the cells in culture. This is reduced by metabolically active cells forming a NanoLuc® substrate that diffuses out of the cells, and rapidly used by A NanoLuc® Enzyme that is also added to the media, producing a luminescent signal (Hall et al., 2012). The assay result correlates with the quantity of metabolically active viable cells, and is affected by the number of cells per well, and their overall metabolic activity. High number of cells, however, results in loss of linearity (Riss et al., 2015). Our study showed the initial reading (day 21) appeared sufficient as demonstrated high cell density across the cultures, treated and controls, although no significant differences at time of reading. However, a high reduction of signal was observed after 72 hours in all cells, which was unexpected and could suggest loss of cell viability. When viewed microscopically the cells, however, appeared viable suggesting this was not the case. To verify cell viability, I performed an MTS assay following further culture time on the same cells, which demonstrated cell viability, and further that high passage cells released from chronic PHA treatment showed increased cell numbers. The same was not shown in low passage cells, suggesting potential cellular changes may occur following chronic treatment. There are a number of possible reasons for the reduced luminescence readings obtained with the RealTime-Glo MT kit, which occurred following experimental repeats. As a luminescent assay, exposure to sources of light could have led to the reduction of output. High light intensity may also lead to an increase in the decay rate of the reaction (Deluca et al., 1979). Further repeats and potential experimental design modifications would enable the use of the RealTime-Glo MT kit in further investigations in our study, but in this instance, it did not meet expectations. Nevertheless, the finding that chronic PHA-767491 recovery cells continue to proliferate was generally confirmed with each technique. Extending the time in culture would be important, and to distinguish between the loss of contact inhibition and slow growth further studies are required. β-galactosidase activity assay would highlight the cells under senescence, and contact inhibition as both are associated with lysosomal activation (Knecht et al., 1984; Severino et al., 2000; Leontieva et al., 2014). It would be important to determine if PHA-767491 treatment generates

senescent cells alone. Modifying the methodology by seeding the cells initially at high density has been used within the literature (Leontieva et al., 2014), and would enable further verification of our results.

A study by Røsland et al (2009), was the first to report spontaneous malignant transformations that occurred in 45.8% of long term cultured bone-marrow derived human mesenchymal stem cells (hMSC), followed by a number of other reports. However, contamination was admitted generating artefactual results and suggested to be the 'cause' of transformation (Rubio et al., 2005; Røsland et al., 2009; Torsvik et al., 2010). A more recent study, however, observed tumorigenic transformation during long-term culture, and was confirmed not to be due to contamination with other human cell lines (Pan et al., 2013). Due to risk of contamination during long term culturing it is therefore crucial that rigorous aseptic working procedures are followed to reduce artefactual results indicating transformation, observed in early reports. This also highlights the need to characterise the cell type, discussed in the next chapter.

In summary, our model of replicative stress in ASC52telo cells verified our thoughts as DNA damage was shown. In particular, prolonged replicative stress may lead to a reduced or impaired response leading to sustained DNA damage and cell transformation, as depicted in Schematic 6.3-1.

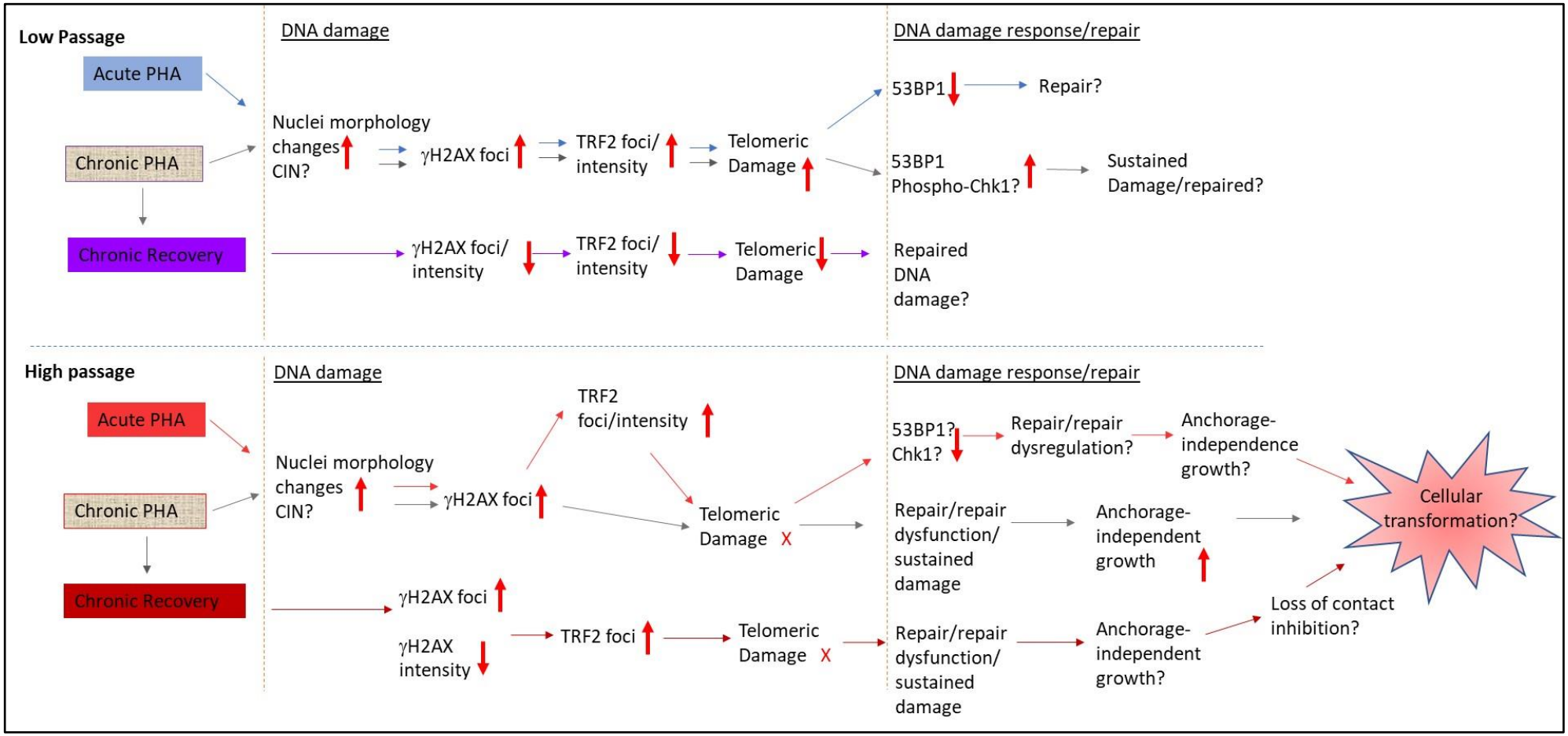

Schematic 6.3-1 cell damage response in ASC52telo cells treated with PHA-767491. ASC52telo cells under PHA model demonstrate increased DNA damage following replicative stress induced by PHA-767491. Chronic treatment appears necessary for sustaining DNA damage and developing features seen in cellular transformation.

6.4 ASC52telo genotype verified (chapter 2, section 4.3).

Throughout my investigations, to ensure cellular changes in high passage cells were considered, we used matched high passage number cells as a control to the long term treated cells, to demonstrate the cellular changes were due to conditions of treatment rather than passage.

Short tandem repeats (STRs) contain 3-7 base pair long sequence units repeated in tandem, dispersed across the genome. The number of repeat units at the same locus varies between individuals, and the haplotype of several loci combined together can identify individuals (Jeffreys et al., 1985b; Litt and Luty, 1989; Weber and May, 1989; Edwards et al., 1991; Rassmann et al., 1991; Moretti and Budowle, 1998), and as in our case cells and cell lines, at an astonishingly high power of probability. When amplified with PCR they can be differentiated using fluorescent primers that flank the repeat sequences at hypervariable regions (Jeffreys et al., 1985a; Jeffreys et al., 1985b; Saiki et al., 1985; Edwards et al., 1991; Warne et al., 1991; Edwards et al., 1992). It is crucial to determine origin, phenotype, and contamination in cell lines. The method utilised (GenePrint® 10 System) enabled co-amplification and detection of 10 human loci, following the amplification of STR regions of human genomic DNA with ILS, and run by capillary electrophoresis to determine the size of the amplified samples. The random match probability of the system is 1 in $2.92*10^9$ (Promega). Our ASC52telo cells at different stages of passage and treatment have been verified, and the possibility of contamination with other (tumour) cell lines was ruled out. Cell line authentication has been set as an important standard of the literature (Masters et al., 2001; Dunham and Guthmiller, 2009; Stacey et al., 2014; Yu et al., 2015). Standards have been issued regarding the authentication of the use of human cell lines by the American Tissue Culture Collection Standards Development Organization Workshop. To further our analysis the European Medicines Agency reported the analysis of senescence *in vitro* following several passages could be utilised to indicate the absence of immortalized/tumourigenic cells, aiding the quality control of MSCs, and highlighting cross contamination (Emea, 2009).

6.5 RECQL4 expression and proliferation (chapter 3, section 5)

The role of RECQL4 in DNA replication, repair and telomere maintenance is well documented, therefore, we would assume that loss leads to an effect on cellular growth and lifespan (Ghosh et al., 2012; Davis et al., 2013; Ferrarelli et al., 2013). RECQL4 expression has been found to correlate with cell proliferation activity (Bachrati and Hickson, 2003; Yang et al., 2006; Lu et al., 2014a). The study by Yang et al, (2006) demonstrated decrease of proliferation in MC3T3.E1 cells following the knockdown of *Recql4* using siRNA silencing. On the other hand, overexpression was shown to lead to cell growth in mouse osteoblastic cells (Yang et al., 2006). A more recent study found that the disruption of *Recql4* reduced proliferation in mouse osteoblasts (Ng et al., 2015), and in *Drosophila* (Xu et al., 2009a). Tissue and cell specific expression patterns have also been shown for RECQL4 mRNA with northern blotting analysis. High expression correlates to higher number of intensively proliferating cells. It is not surprising, therefore, that tissues and organs with the highest expression are strongly affected contributing to the pathological features seen in RECQL4 related syndromes (Larizza et al., 2010; Wang and Plon, 2016). The expression profile of RECQL4 has been found to be consistent with the skeletal defects most often seen in patients with RTS (Larizza et al., 2010; Wang and Plon, 2016). Interestingly, RTS patients usually have a normal lifespan in the absence of cancer despite presentations of premature aging (Hofer et al., 2005; Jin et al., 2008; Larizza et al., 2010).

In our study, RECQL4 expression levels appeared variable during cell culture between U2OS and HeLa cell lines. The study was small and repeats are needed, however, we employed different indicators of proliferation and viability to verify our findings. Nevertheless, a steady increase and decrease in RECQL4 expression in U2OS cells was found correlating to cell count levels.

In cancer cell lines, we would not expect to find contact inhibition. HeLa cells demonstrate rapid growth and a lack of contact inhibition (Stephenson, 1982). Other authors report that HeLa cells in culture maintain contact inhibition (Schwab, 2008), however, it might reflect clonal variability of this cell line that is used in laboratories all over the world. We observed reduced but apparently continual growth rate following confluency under our conditions. Other studies have reported long term culture leading to continual growth as cells pile up and detach in batches (Delinasios et al., 2015).

There are a few similarities in the expression pattern of RECQL4 involving ubiquity, showing higher levels in proliferating cells, and cell cycle phase specific distribution. Peak of expression is seen at S-phase of the cell cycle (Bachrati and Hickson, 2003; Dietschy et al., 2009; Croteau et al., 2012b). Certainly, there appears a correlation between RECQL4 expression with Ki67 expression and the proliferative state of the cells, however, repeats and further analysis are required to confirm.

We did experience difficulties culturing the AG03587 cell line; it appears to proliferate very slowly and goes into senescence more readily than the other RTS cells lines. Cell viability measurements alongside are also required to ensure this is not a contributing factor to the results obtained. The AG18375 cell line harbours a confirmed RECQL4 mutation at chromosomal location 8q24.3 (g.2626G>A and g.2886delT), and the patient presented with OS at 21 years of age (Gupta et al., 2013). *RECQL4* mutations are thought to lead to partially active protein in some RTS cases (Ouyang et al., 2008). In our study, the effect on proliferation in culture could be due to cell specific features, or specific *RECQL4* mutation.

6.6 Generation of Emerald-GFP tagged RECQL4 expression constructs (chapter 3, section 5.2)

RECQL4-emerald tagged HeLa and U2OS cells were established successfully, and following signal analysis, the induced expression appeared to be localised mainly in the nucleus, but also to cytoplasm in HeLa and U2OS cells. Of the RecQ helicase family, RECQL4 is the only one known to be found both in the nucleus and cytoplasm (Yin et al., 2004; Petkovic et al., 2005; Burks et al., 2007). There are contradicting results within the literature relating to RECQL4 localisation, which could be due to the antibodies and methods used, and could explain the diverse results (Yin et al., 2004; Petkovic et al., 2005: Schurman et al., 2009; Chi et al., 2012; Monaghan and Whitmarsh, 2015). RECQL4 has two signals regulating its presence in the nucleus. A nuclear localisation signal (NLS) is located at the N-terminus (amino acids 363-492) (Yin *et al*, 2004, (Burks et al., 2007), while the C-terminus harbours a functional nuclear export signal (NES), which may be important for cytoplasmic localisation and for mitochondrial maintenance. Diminished cytoplasmic localization was observed following the deletion of this NES (Chi et al., 2012). Localisation of RECQL4 may also be influenced by cell cycle phases (Petkovic et al., 2005). The phosphorylation of the NLS has been found to be important for many cell cycle related proteins for nuclear localisation (De et al., 2012;

Bauer et al., 2015), while acetylation has been reported to influence recognition of localisation signal. RECQL4 is acetylated by p300, a histone acetyltransferase, leading to localisation to the cytoplasm (Dietschy et al., 2009).

Interestingly, a recent study further suggests RECQL4 main activity may be located within the mitochondria, and re-location to the nucleus allowing nuclear genome maintenance. Mitochondrial localisation of RECQL4 has been found in a few other studies as well (Chi et al., 2012; Croteau et al., 2012a; De et al., 2012; Gupta et al., 2013; Wang et al., 2014b)**,** which could explain some of the phenotypic features seen in RTS patients (De et al., 2012). RECQL4 intracellular distribution and dynamic re-localization to sites of DNA damage has suggested to be a possible contribution to phenotypes and associated heterogeneity, which has been found in RECQL4-associated diseases (Croteau et al., 2012b).

Tagging of proteins with the small and versatile GFP provides a scalable method to study localisation and protein-protein interactions (Leonetti et al., 2016). Using the same direct method utilised in our study, GFP-tagged RECQL4 was also reported to be predominantly localised to the nucleus in U2OS cells, however, a small percentage was observed localised to the cytoplasm. Additionally, mitochondrial localisation was also seen (Woo et al., 2006; Chi et al., 2012). The GFP tag may influence the localisation of the protein. It has been reported that GFP translocates to the nucleus itself (Seibel et al., 2007), although it may be mediated by its capability diffusing through the nuclear pores passively. Overexpression of tagged proteins can lead to effects on structure, function, and localisation of the protein (Agbulut et al., 2006; Das et al., 2009), which also depends on whether the tag is on the amino or the carboxy terminus (Simpson et al., 2000; Giraldez et al., 2005). The promoter used on the plasmid vectors for transient transfection, such as CMV, can increase the protein amount present within the cell (Deer and Allison, 2004; Qin et al., 2010), which has been found to also influence sub-cellular localisation and function. Cells expressing low levels of fluorescent tagged protein under inducing conditions are ideal for further work, (Watanabe and Mitchison, 2002; Taylor et al., 2011), and in our study we chose low expressing clones.

6.6.1 siRNA

The study by Abe et al, (2011) suggests that a complete loss of *RECQL4* in humans would be lethal (Abe et al., 2011). Knockdown of RECQL4 has been shown to correlate with reduced proliferation in primary fibroblast (Lu et al., 2014).

Senescence was detected without an increase of apoptosis (Lu et al., 2014), consistent with studies in the literature of senescent cells being resistant to apoptosis (Hampel et al., 2005), however, an increase in cell death was demonstrated suggesting another pathway may be involved. Development of senescence could be a result of oxidative stress (Lu et al., 2014). Senescent cells have been shown to be irreversibly arrested in G1/G0 cell cycle phase (Sherwood et al., 1988), and RECQL4 knockdown was shown to lead to accumulation of cells in G0/G1 (Lu et al., 2014). Senescence induced by replication defects usually leads to cell cycle arrest during G1 or G2 of the cell cycle (Mao et al., 2012). Considering this, RECQL4 knockdown appears to lead to stress induced cell cycle arrest (Lu et al., 2014). In both mouse and human cells RECQL4 dysfunction generated an increase in DNA damage, and increases senescence (Lu et al., 2014).

RECQL4 siRNA 9 and 10, targets the 3' untranslated region of the RECQL4 mRNA. This mode of targeting found to be more effective than targeting the open reading frame (ORF) (Forman et al., 2008; Gayral et al., 2014). The targeting of these sequences occurs following perfect and imperfect complementarity. The direct cleavage and degradation of the mRNAs follows perfect complementarity, while imperfect complementarity leads to blockage of transcription and inhibition of protein synthesis from the target mRNA (Zhang et al., 2015), both leading to reduced protein content. Factors affecting these processes include flanking sequence, location within the 3'-UTR, and the accessibility of target mRNA (Grimson et al., 2007). A key issue described in the literature is off-target gene silencing which may also involve other influential factors (Jackson and Linsley, 2004; Birmingham et al., 2006; Jackson et al., 2006). In our work we used siRNA molecules that had been designed by the supplier, Qiagen using a novel algorithm that minimizes the risk of off-target effect (Li and Zamore, 2019).

Primary RTS fibroblasts (AG05013tert) demonstrated sensitivity to PHA-767491, not seen in HeLa and U2OS models. Repeats are needed to verify our initial findings, but this may not seem unexpected when taking into account that siRNA mediated knockdown did not reach 100%, and the effects are often reversed over time as previously described, compared to AG05013 cell line that carries an inactivating mutation of RECQL4. We also need to consider that these two cell lines originate from malignant cancers. Depleting RECQL4 in fibroblast cell lines such as hTERT immortalised HS68 might provide answers to this contradiction

6.6.2 shRNA

A long-term aim of our work is to interfere with RECQL4 expression in mesenchymal stem cells under standard culturing conditions or during osteogenic differentiation to establish why people with biallelic RECQL4 mutations develop osteosarcomas. To achieve this, we established a rescueable siRNA mediated knockdown system in standard laboratory cell lines, and vectors for lentivirus mediated transduction for shRNA knockdown. Unlike synthetic siRNA, which are effector molecules introduced directly into the cells, short-hairpin RNAs (shRNAs) are introduced indirectly. The constitutive expression of shRNA molecules can be achieved by RNA polymerase II or III -driven expression cassettes (Scherer and Rossi, 2003). shRNA integration via viral vectors into mammalian cell lines have been demonstrated to induce stable transduction, and long-term gene knockdown (Taxman et al., 2010). The recombinant constructs generated in our study were verified using standard protocols employed by a number of other laboratories successfully (Inouye et al., 1981; Roberts, 1987; Woollard et al., 1994; Yu et al., 2003; Seo et al., 2015; Yu et al., 2016). In the literature successful use of RECQL4 knockdown using shRNA have also been reported (Croteau et al., 2012a; Ghosh et al., 2012).

6.7 RECQL4 expression and DNA damage markers (chapter 3, section 5.24)

RECQL4 has an important role in replication initiation, and chromosomal instabilities could occur if altered RECQL4 expression leads to an extension in the time of exposure of single stranded DNA, whereas high expression could cause unmatched annealing, and depletion could lead to impaired reannealing (Macris et al., 2006). Maire and co-workers (2009) found a correlation between RECQL4 expression levels and a higher frequency of structural chromosomal changes (S-CIN) associated with OS, however they did not observe a relationship with N-CIN (numerical chromosomal instabilities) (Maire et al., 2009). RTS patients have been found to demonstrate both N- and S-CIN (Der Kaloustian et al., 1990; Ying et al., 1990; Orstavik et al., 1994; Lindor et al., 1996; Miozzo et al., 1998). Chromosomal instabilty *in vivo* may lead to neoplastic transformation of cancer stem/progenitor cells which are sensitive to RECQL4 mutations. Mesenchymal cells may be especially sensitive, which are thought to give rise to tumours in RTS patients (Larizza et al, 2010). Cells isolated from a mouse model of RTS type II showed aneuploidy due to defects in sister-chromatid cohesion, which suggested a role for the RECQL4 helicase in sister-chromatid cohesion and mitotic chromosome

segregation, a potential source of chromosomal instability and cancer predisposition (Mann et al., 2005).

RTS fibroblast cell lines showed slightly reduced growth rate, and appeared to be moderately sensitive to gamma-irradiation and generated higher levels of γH2AX and 53BP1 foci, in comparison to control fibroblasts (GM00323 and GM00969), suggestive of defective repair of DSBs (Singh et al., 2010). RECQL4 also found to colocalize with γH2AX, suggesting RECQL4 binds to DSB (Singh et al., 2010). γH2AX foci count has also been found to be increased, suggesting that deficiency of RECQL4 activated a DNA damage response using ATM (Lu et al, 2014); however, was not found to be significantly increased in our study. Our findings could be extended by probing for other markers of DNA damage, for example 53BP1.

The RECQL4 helicase resolves telomeric D-loop structures with the help of shelterin proteins TRF1, TRF2, and POT1, which stimulate its helicase activity. RECQL4 may also work synergistically with WRN by unwinding telomeric D-loops, and may assist WRN and BLM following oxidative stress. RECQL4 depletion induces crisis sites at telomeres via the activation of 53BP1 DNA damage response protein, although the cause could be due to replicative stress (Ghosh et al., 2012). The promotion of telomeric maintence may involve RECQL4 and the repair of the thymine glycol lesions that block DNA metabolism (Ferrarelli et al., 2013). A high level of fragile telomeres were observed in the AG05013 and AG18371 RTS cell lines (Ghosh et al., 2012). It is possible that binding of DNA repair factors or other proteins involved in telomere replication are inhibited in RECQL4 mutated cells (Ghosh et al., 2012). However, the fact that we were not able to show increase of telomeric damage in RTS cell lines, that is co-localisation of γH2AX and TRF2, does not support the above findings of the literature. The lack of co-localisation seen in our work could be due to short telomeres being scored as non-telomeric; chromatid ends in pre-senescent human cells that have extremely short telomeres may lack TRF2 foci (Nakamura et al., 2008). This is especially relevant to the data obtained where co-localisation was not observed and reduced or low TRF2 foci were also seen. Although, unlikely relevant as short telomeres should not be present in the AG05013tert cells, and low passages were utilised for all RTS cell lines.

6.8 Isolation and identification of RECQL4 interacting partners (chapter 3, section 5).

With the generated inducible RECQL4-Emerald tagged HeLa and U2OS clones, analysis of protein interactions was performed using the GFP-pulldown. RECQL4 has been found to interact with many proteins involving different pathways (Table 6.8-a), a few of which are discussed in detail below. GFP pulldown is a widely used technique (Trinkle-Mulcahy et al., 2008; Emmott and Goodfellow, 2014), however, there are limitations to be considered such as the influence the GFP tag fusion may have on the protein, discussed previously (see section 5.2.4.1).

Table 6.8-a Interacting protein with RECQL4. Adapted from (Croteau et al., 2012b)

Location	Protein	Recql4 region of interaction	Interaction activity	Reference
Nuclear	MCM10	1-200aa	Helicase inhibition, replication complex.	(Xu et al., 2009b)
	RAD51	unknown	DSBs repair	(Reinhardt and Schumacher, 2012)
	XPA	unknown	Nucleotide excision repair	(Yin et al., 2004), (Fan and Luo, 2008)
	POL β	unknown	DNA Polβ primer extension stimulation and activity	(Fan and Luo, 2008)
	APE1	unknown	Stimulation of APE1 endonuclease	(Fan and Luo, 2008)
	RPA	unknown	Stimulation of RECQL4 helicase	(Rossi et al., 2010)
	BLM	1-471aa	Stimulation of BLM	(Singh et al., 2012)
	p300	1-408aa	Cellular location of RECQL4 regulation	(Xu and Liu, 2009)
	Nucleophosmin (NPM)	Unknown	unknown	(Wang et al., 2014b)
Mitochondria	TOM20	13-18aa	Import into mitochondria	(Croteau et al., 2012a)
	p32		Promotes nuclear localization of RECQL4	(Wang et al., 2014b)
	TFAM	Unknown	unknown	(Singh et al., 2010)
	p53	270-400aa	Silencing of RECQL4 and p53 nuclear location signals	(Croteau et al., 2012a)
Nuclear / telomere	TRF1	Unknown	Stimulation of RECQL4 helicase and telomere maintenance	(Werner et al., 2006)
	TRF2	Unknown	Stimulation of RECQL4 helicase and telomere maintenance	(Werner et al., 2006)
	WRN	unknown	Stimulation of WRN on telomeric D-loop	(Werner et al., 2006)
Unknown	Cut5	unknown	DNA replication	(Burks et al., 2007)
	PARP1	833-1208aa	Base excision repair	(Petkovic et al., 2005), (Schurman et al., 2009).
	URB1/2	Unknown	Unknown	(Yin et al., 2004), (Woo et al., 2006)
Cytosolic	Protein Phosphatase 2A (PP2A)	unknown	unknown	(Wang et al., 2014b)

As an inhibitor of histone deacetylase, SAHA was used in our study to identify RECQL4 interacting proteins which rely on posttranslational acetylation modifications, for regulating protein activity and transmitting signals throughout the cell (Cohen, 2000). The study by Dietschy et al, (2009), was the first to demonstrate post-translational modifications of RECQL4, and following the acetylation of RECQL4 by p300, a significant proportion of RECQL4 protein was shifted from the nucleus to cytoplasm *in vivo.* We employed extended HU treatment to induce fork collapse and new origin firing (Park et al., 2006; Ghosh et al., 2012; Kohzaki et al., 2012; Sidorova et al., 2013) and to see if it influences interactions and modifications of RECQL4.

We found PP2A/A α and β isoforms in the pulldown from U2OS cells, however, we could not verify the interaction with western blot analysis. A low amount of PP2A was detected in the pulldown from SAHA treated HeLa cells. We were also able to detect MCM10 in the bound fraction of the pulldown, however, its abundance was mainly reflected by levels of RECQL4, and was not always seen. Wang et al (2014) suggested RECQL4 was transported to the mitochondria, and although MCM10 can also be found there, it mainly remained at the outer mitochondrial membrane. RECQL4 may dissociate from MCM10 via other protein interactions.

6.8.1 Novel RECQL4 interacting proteins (chapter 3, section 5.3)

Excitingly, novel RECQL4 protein interactions were detected; Engrailed-1 (EN-1), Engrailed-2 (EN-2), and Highly Divergent Homeobox (HDX). HU treatment appeared to induce an increase in HDX levels in the complex. HDX is a hitherto uncharacterised protein, also known as *CXorf43*. It belongs to the POU-class homeobox genes, which contains 16 related genes in the human genome. HDX, unlike the other members, does not encode a POU-specific domain, for which it has been placed into a new class within this family. HDX encodes a highly divergent atypical homeodomain (Holland et al., 2007). It has been found to be significantly enriched during embryonic development (Dennis et al., 2003), while its expression is reduced in breast and other cancer cells (Yamamoto et al., 2011). Missense mutations in HDX could be involved in the pathogenesis of acute promyelocytic leukemia (APL) (Greif et al., 2011). Homeobox transcription factors have a role in the regulation of cell identity, and are involved in normal and malignant haematopoesis; the dysregulation of the ‘Hox code’ may play an important role in myeloid malignancy development (Eklund, 2007). Following the knockdown of

osterix, HDX was found to be upregulated in mouse chondrogenic ATDC5 cells (Park and Kim, 2013). Another study suggested HDX may be relevant in mental retardation (Honda et al., 2010). Other homeobox gene mutations have also been linked to mental retardation, epilepsy, or other movement disorders (Wigle and Eisenstat, 2008).

Two further Homeobox proteins, EN-1 and EN-2 were detected by mass spectrometry. EN-2 was further analysed by western blot, and was confirmed to be present in RECQL4 bound fractions, however, this finding requires verification. SAHA treatment may cause an increase in the level of EN-2 in the complex. Homeobox genes are a superfamily of regulatory genes and encode homeodomain-containing transcription factors. The homeobox itself is a 183-bp DNA sequence that encodes a 61 amino acid homeodomain within the HOX proteins. The homeodomain recognises and binds sequence-specific DNA motifs (Mcginnis and Krumlauf, 1992). In humans 39 HOX genes have been identified, and shown to have roles in apoptosis, differentiation, receptor signalling, motility, and angiogenesis (Shah and Sukumar, 2010).

Engrailed is a member of the homeobox gene family, characterised first in *Drosophila* (Wedeen and Weisblat, 1991). The human genome contains two copies of Engrailed, EN-2 and EN-1, which hold important roles in early embryonic development and in normal human neuronal development (Sillitoe et al., 2008; Morgan et al., 2011; Mcgrath et al., 2013). The overexpression of EN-2 has been found in cancers, and it is suggested as a potential oncogene in breast cancer. Following the suppression of EN-2 in a human breast cancer cell line, a significant decrease in proliferation was found (Martin et al., 2005). Similarly, a decrease in prostate cancer cell proliferation was observed following siRNA mediated knockdown of EN-2, which in turn decreased PAX-2 expression (Martin et al., 2005; Bose et al., 2008). Hypermethylation of EN-1 has also been seen in colorectal cancer, prostate cancer, and astrocytoma (Mayor et al., 2009; Wu et al., 2010; Devaney et al., 2011). A number of homeodomain containing proteins of the HOX family were found to play roles in replication (De Stanchina et al., 2000; Comelli et al., 2009; Salsi et al., 2009; Falaschi et al., 2010; Marchetti et al., 2010; Miotto and Graba, 2010). Interestingly, a study found the N-terminus of RECQL4 to adopt a fold similar to homeodomains, and the domain is involved in the interaction with TopBP1 (Ohlenschläger et al., 2012).

7 Conclusion

RECQL4 holds an important role in DNA replication, further demonstrated by its known interactions with DNA replication factors crucial for the initiation of DNA replication (Im et al., 2009; Xu et al., 2009; Thangavel et al., 2010). To enable a model of mild replication interference, to an extent expected in RTS patients, PHA-767491 was used in our study to reduce the activity of CDC7/DBF4, a kinase with a key role upstream of RECQL4 in replication initiation. Reduced proliferative rate was demonstrated in PHA-767491 treated ASC52telo cells (under acute as well as chronic treatment), in agreement with literature results (Montagnoli et al., 2008; Vanotti et al., 2008; Natoni et al., 2013; Fitzgerald et al., 2014; Sasi et al., 2014; Erbayraktar et al., 2016).

RTS patients present predominantly osteoblastic OS (Sim et al., 1992; Werner et al., 2006; Hicks et al., 2007; Zils et al., 2015). Our findings using ASC52telo cells under PHA-767491 model did appear to influence osteoblastic markers; calcium and RUNX2, following osteocyte differentiation. Using qualitative methods, we found that calcium levels appeared to increase following PHA treatment post osteocyte differentiation, despite reduced cell numbers due to the mild proliferation inhibition. High calcium levels can lead to cellular disruption, and may influence cancer cell progression (Mundy, 2002; Santini et al., 2012; Daft et al., 2015). High calcium levels have also been reported in osteosarcoma patients (Kharb et al., 2012). Quantification methods are required to determine if the qualitative data within our study is a true representation of calcium levels. The expression of RUNX2 is suggestive of MSCs commitment towards differentiation into osteoblasts (Ducy et al., 1997; Komori et al., 1997; Tang et al., 2008; Komori, 2010). Interestingly, our findings suggest an elevation of RUNX2 expression following acute PHA-767491 treatment in ASC52telo osteocyte differentiated cells. An elevation of RUNX2 levels have been observed in OS cells (Nathan et al., 2009; Martin et al., 2014). The overexpression of RUNX2 has been reported as potentially leading to disrupted osteoblast differentiation. Impaired osteoblast differentiation can lead to genomic instability, and OS (Andela et al., 2005; Lu et al., 2008; Tang et al., 2008; Pereira et al., 2009; San Martin et al., 2009; Won et al., 2009; Kurek et al., 2010; Martin et al., 2010; Martin et al., 2014). We investigated further if these cells underwent cellular transformation. Our findings showed that PHA-767491 treated ASC5telo cells

demonstrate these osteoblastic differentiation markers under normal (non-differentiating) media, showing significant increase of RUNX2 levels and observation of high calcium levels. The data obtained suggest the dysregulation of osteoblast differentiation drivers under acute and chronic PHA-767491 treatment, however, further verification is required to support this conclusion.

The dysregulation of mitochondrial function can lead to diseases (Archer, 2013; Magalhães et al., 2014; Singer, 2014). Therefore, we considered mitochondrial maintenance in our PHA model. Our findings showed no significant changes of mitochondrial activity, measured by membrane potential, in acute and chronic PHA-767491 treated cells, demonstrating lack of mitochondrial alterations in these cells. However, RECQL4 may hold a role in mitochondrial maintenance (Croteau et al., 2012), which is likely to be independent of its role in replication initiation.

We found that ASC52telo cells under acute and chronic PHA-767491 treatment demonstrated the presence of DNA damage, with an increased occurrence of changes in nuclear morphology, suggestive of genomic instability. Phosphorylation of H2AX (γH2AX) occurs as a localised response to DSB (Rogakou et al., 1998). γH2AX forms foci rapidly (Rothkamm and Horn, 2009), and remains until the DNA damage is repaired (Nakamura et al., 2006). As expected from literature data, we found that ASC52telo cells responded to Camptothecin treatment with the generation of γH2AX foci. ASC52telo cells with acute and chronic PHA-767491 treatment demonstrated significantly high levels also, with levels returning to background in low passage cells released from treatment. Importantly, the same degree of return to normal levels was not seen in high passage cells released from PHA-767491 treatment under the same recovery conditions. Effect of inhibition of replication initiation on telomere maintenance only appeared to be present in low passage ASC52telo cells under acute and chronic PHA-767491 treatment. Not all of the DNA damage appears telomeric. We found signs of activated DNA damage response with Phospho-CHK1 following chronic PHA treatment in low passage ASC52telo cells, suggesting the involvement of the ATR pathway (Bartek et al., 2004; Dai and Grant, 2010). Interestingly, in correlation to this, the significant activation of 53BP1 was shown in low passage chronic PHA treated cells. However in acute treated cells the level of 53BP1 appeared reduced, compared to control cells, suggesting a lack or impairment of 53BP1 response in these cells. Taken together, our findings suggest, cells under chronic replicative stress lead to signs of

sustained DNA damage, which may generate cells susceptible or sensitive to transformation during sustained PHA-767491 treatment or post recovery. To gain further insights into this process, transformation characteristics were investigated.

ASC52telo cells under the PHA model were cultured over a prolonged time reaching a high cell density. Our findings suggest continual cell growth in ASC52telo high passage cells released from chronic PHA-767491 treatment, which indicates impaired or loss of contact inhibition, a hallmark of cancer cells (Abercrombie, 1979; Hanahan and Weinberg, 2000). Although we would expect these cells to recover from PHA-767491, which would lead to an increase of proliferation, the level of continual growth was not observed in low passage cells and controls. Further to this, high passage chronic PHA-767491 treated cells demonstrated signs of anchorage-independent growth, with spheroid cultures forming following the detachment from the extracellular matrix, which is another sign of transformation. The cells may have acquired resistance to anoikis or programmed cell death (Kang et al., 2007).

In conclusion, we developed a model of replicative stress in ASC52telo cells that induced cellular changes indicative of DNA damage following chronic PHA-767491 treatment. These changes were sustained following recovery and may lead to the development of transformation characteristics, as depicted in Figure 7-1 (blue arrows), alongside our hypothesis. RECQL4 mutations could generate chromosomal instabilities causing disruption to osteocyte differentiation. The dysregulation is likely to have pathological consequences, and may be relevant to characteristics of RTS disease and the predisposition to OS.

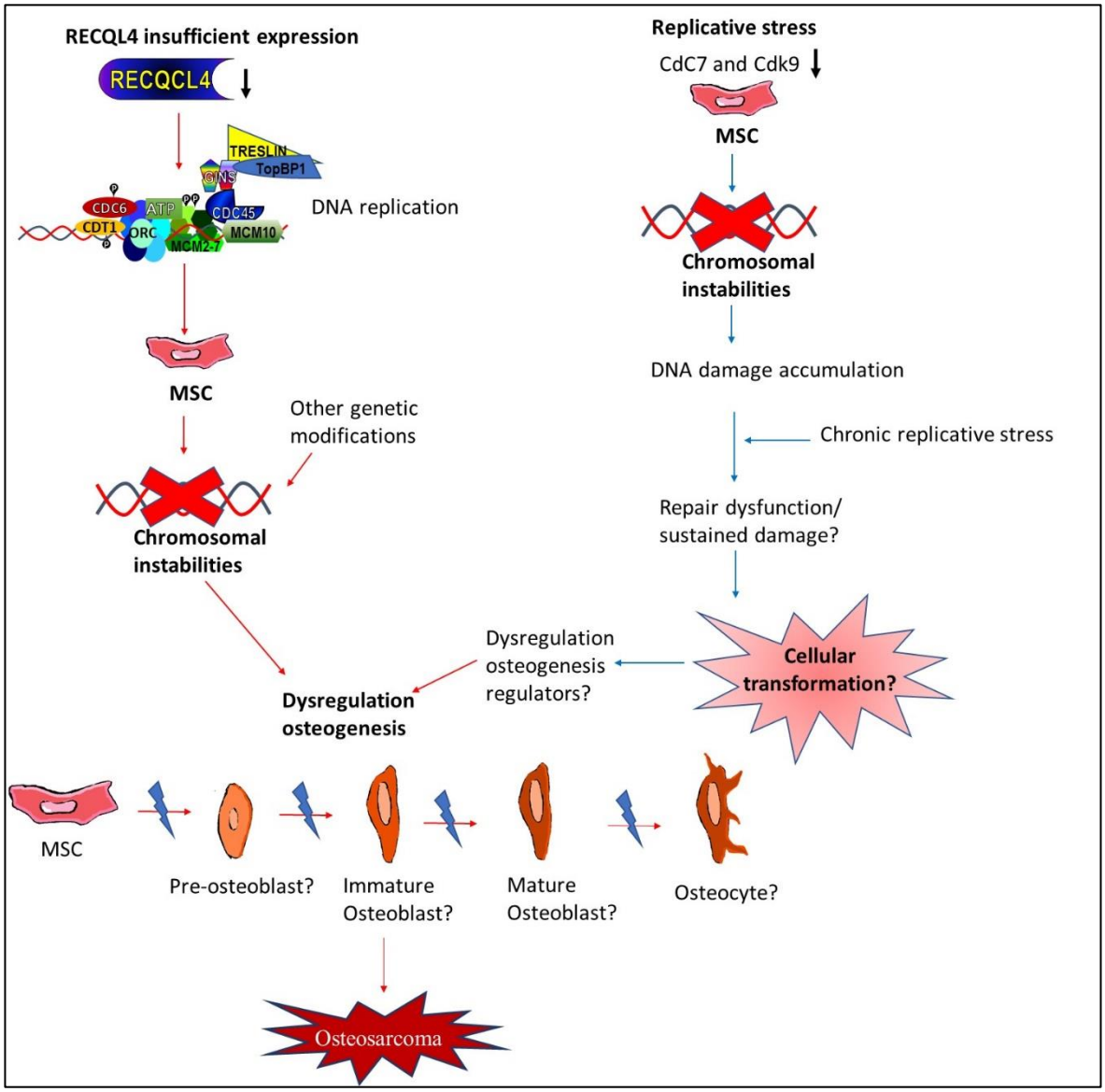

Figure 7-1 DNA damage resulting in dysregulation of osteoblast differentiation and OS development. Sustained DNA damage occurs following chronic mild inhibition of DNA replication initiation (PHA-767491 model) which may lead to dysregulation in osteogenesis regulator factors (our findings, blue arrows), which could lead to differentiation dysregulation and osteosarcoma. We suggest RECQL4 mutations lead to chromosomal instabilities causing the dysregulation of osteocyte differentiation and osteosarcoma development (red arrows).

The AG05013tert fibroblast cell line, a TERT immortalized RTS cell line with documented RECQL4 mutations (Kitao et al., 1999b), demonstrated sensitivity to acute PHA-767491 treatment, however, the same was not observed following the siRNA knockdown of RECQL4 in U2OS an HeLa cells. The lack of sensitivity to PHA-767491 in these cells could be explained by incomplete depletion of RECQL4 levels, or the reduction of siRNA efficiency over time (Jacobsen et al., 2004). Further investigations using other RTS cell lines would verify our findings. With the use of PHA-767491 treatment in ASC52telo we established an *in vitro* cell culture model under acute and chronic replicative stress, and recovery.

Our findings demonstrate induced chromosomal instabilities due to mild inhibition of DNA replication. Some of these markers were further investigated in a group of RTS cell lines: AG05013tert, AG18375, and AG03587 cells, to link to RECQL4 mutations. Patients with RTS have been found to demonstrate genomic instabilty (Der Kaloustian et al., 1990; Ying et al., 1990; Orstavik et al., 1994; Lindor et al., 1996; Miozzo et al., 1998). Although there appears to be variation of reports in the literature, an association has been suggested between RECQL4, S-CIN and OS (Maire et al, 2009), with truncating RECQL4 mutations associated with a higher risk (Wang et al., 2003). We found significant increase of γH2AX intensity in the AG05013tert RTS cell line, suggesting greater extent of DSB damage in these cells. An increase of telomeric DNA damage was observed in AG05013tert cells, but was not evidenced in AG18375 and AG03587 RTS fibroblasts, suggesting a potential role of RECQL4 in TERT mediated telomere maintenance, which warrants further investigations given the presence of DNA damage markers in this cell line. Overall, it is difficult to suggest a reason for the evidence of DNA damage in the RTS AG05013 cells, which is not found in the other RTS cell lines (AG18375 and AG03587), as some mutation characteristics known are shared. Similarly, proliferative rate was also found variable between specific RTS cell lines. We found variability of DNA damage response between RTS cell lines as well, which has also been reported in the literature (Smith and Paterson, 1982; Shinya et al., 1993; Kerr et al., 1996; Lindor et al., 2000), reflecting heterogeneity of these cells (Schurman et al., 2009). Further studies are required to perhaps identify if specific mutations are generating or providing a sensitised environment for DNA damage and tumorigenesis, conceivably through interacting proteins and pathways.

We investigated RECQL4 interacting proteins and identified known binding partners of RECQL4; MCM10, and low levels of Protein phosphate 2 A (PP2A), previously reported in the literature (Xu et al., 2009; Wang et al., 2014). The co-localisation of PP2A and RECQL4 was reported to be restricted to the cytosolic RECQL4 complex (Wang et al., 2014). This could explain the lack/low efficiency of pulldown of PP2A seen in our study, as RECQL4 expression was primarily observed in the nucleus of our cells. We found novel interactions with highly divergent homeobox (HDX) and homeobox protein EN-2. Although there is little information on HDX in the literature, HDX may have a role in human disease, and tumourigenesis (Honda et al., 2010; Greif et al., 2011; Yamamoto et al., 2011). EN-2 has been reported to play a role in proliferation and human disease, including cancer (Bose et al., 2008; Rissling et al.,

2009). Pulldown levels appeared variable following SAHA and HU treatment, which may be influenced by other parameters. These novel findings could lead to furthering our understanding of RECQL4 and potential novel pathways and roles.

6.9 Overall findings and future directions

Our study (Schematic 6.3-1), demonstrated the accumulation of chromosomal changes that may be required to drive tumourigenesis, and are acquired over several cell cycles in long term culture with cellular stress generated by chronic PHA-767491 treatment. Further to this, our findings suggest that chronic PHA-767491 treatment leads to the development of transformation characteristics, which become permanent, as after withdrawal of treatment the transformed phenotype is not reversed. Further investigations involving other markers of osteocyte differentiation would verify our findings and perhaps the dysregulation of differentiation regulation.

To verify our hypothesis, the ASC52telo cell line would be transduced using the generated RECQL4 shRNA lentiviral vector, enabling a model of ASC52telo cell line with stable and long term RECQL4 knockdown to be established, differentiated into osteoblasts, while analysing for DNA damage, during and post differentiation. We know from a recent study that adipose derived mesenchymal stem cells (ASCs) may play a role in OS development (Wang et al., 2017). It would be interesting to establish if impaired ASCs following RECQL4 knockdown may provide the microenvironment forming a niche that supports OS development (Hanahan and Coussens, 2012; Turley et al., 2016). This will enhance our understanding to establish a direct link between impaired replication initiation due to RECQL4 mutations, consequential chromosomal abnormalities and the development of malignancies, in particular osteosarcoma.

The novel protein interactions found with RECQL4 are exciting and verification of these could lead to new pathways or RECQL4 roles. Literature data suggest that RECQL4 is a double-edged sword, and perhaps RECQL4 depletion alone may not be the only driving force of osteosarcoma development. Depleting RECQL4 with lentivirus delivered shRNA in mesenchymal stem cells could verify our hypothesis of its involvement in osteoblast differentiation, and if dysregulation and/or impairment can lead to osteosarcoma.

8 References

Abe, T., Yoshimura, A., Hosono, Y., Tada, S., Seki, M. & Enomoto, T. 2011. The N-terminal region of RECQL4 lacking the helicase domain is both essential and sufficient for the viability of vertebrate cells: role of the N-terminal region of RECQL4 in cells. Biochimica et Biophysica Acta (BBA)-Molecular Cell Research, 1813, 473-479.

Abercrombie, M. 1979. Contact inhibition and malignancy. Nature, 281, 259-262.

Abraham, R. T. 2004. PI 3-kinase related kinases:'big'players in stress-induced signaling pathways. DNA repair, 3, 883-887.

Ahmed, H., Salama, A., Salem, S. E. & Bahnassy, A. A. 2012. A case of synchronous double primary breast carcinoma and osteosarcoma: Mismatch repair genes mutations as a possible cause for multiple early onset malignant tumors. The American journal of case reports, 13, 218.

Ahuja, A. K., Jodkowska, K., Teloni, F., Bizard, A. H., Zellweger, R., Herrador, R., Ortega, S., Hickson, I. D., Altmeyer, M. & Mendez, J. 2016. A short G1 phase imposes constitutive replication stress and fork remodelling in mouse embryonic stem cells. Nature communications, 7, 10660.

Akbari, M., Peña-Diaz, J., Andersen, S., Liabakk, N.-B., Otterlei, M. & Krokan, H. E. 2009. Extracts of proliferating and non-proliferating human cells display different base excision pathways and repair fidelity. DNA repair, 8, 834-843.

Akech, J., Wixted, J. J., Bedard, K., Van Der Deen, M., Hussain, S., Guise, T. A., Van Wijnen, A. J., Stein, J. L., Languino, L. R. & Altieri, D. C. 2010. Runx2 association with progression of prostate cancer in patients: mechanisms mediating bone osteolysis and osteoblastic metastatic lesions. Oncogene, 29, 811-821.

Alfranca, A., Martinez-Cruzado, L., Tornin, J., Abarrategi, A., Amaral, T., De Alava, E., Menendez, P., Garcia-Castro, J. & Rodriguez, R. 2015. Bone microenvironment signals in osteosarcoma development. Cellular and molecular life sciences, 72, 3097-3113.

Allen, M. R., Hock, J. M. & Burr, D. B. 2004. Periosteum: biology, regulation, and response to osteoporosis therapies. Bone, 35, 1003-1012.

Alman, B. A. 2015. The role of hedgehog signalling in skeletal health and disease. Nature reviews Rheumatology, 11, 552-560.

Almeida, K. H. & Sobol, R. W. 2007. A unified view of base excision repair: lesion-dependent protein complexes regulated by post-translational modification. DNA repair, 6, 695-711.

Almeida, M. 2012. Aging mechanisms in bone. BoneKEy reports, 1, 102.

Al-Romaih, K., Bayani, J., Vorobyova, J., Karaskova, J., Park, P., Zielenska, M. & Squire, J. 2003. Chromosomal instability in osteosarcoma and its association with centrosome abnormalities. Cancer genetics and cytogenetics, 144, 91-99.

Al-Tassan, N., Chmiel, N. H., Maynard, J., Fleming, N., Livingston, A. L., Williams, G. T., Hodges, A. K., Davies, D. R., David, S. S. & Sampson, J. R. 2002. Inherited variants of MYH associated with somatic G: C→ T: A mutations in colorectal tumors. Nature genetics, 30, 227-232.

An, J., Huang, Y.-C., Xu, Q.-Z., Zhou, L.-J., Shang, Z.-F., Huang, B., Wang, Y., Liu, X.-D., Wu, D.-C. & Zhou, P.-K. 2010. DNA-PKcs plays a dominant role in the regulation of H2AX phosphorylation in response to DNA damage and cell cycle progression. BMC molecular biology, 11, 18.

Anantha, R. W., Vassin, V. M. & Borowiec, J. A. 2007. Sequential and synergistic modification of human RPA stimulates chromosomal DNA repair. Journal of Biological Chemistry, 282, 35910-35923.

Anantha, R. W., Sokolova, E. & Borowiec, J. A. 2008. RPA phosphorylation facilitates mitotic exit in response to mitotic DNA damage. Proceedings of the National Academy of Sciences, 105, 12903-12908.

Andela, V., Siddiqui, F., Groman, A. & Rosier, R. 2005. An immunohistochemical analysis to evaluate an inverse correlation between Runx2/Cbfa1 and NFκB in human osteosarcoma. Journal of clinical pathology, 58, 328-330.

Andor, N., Graham, T. A., Jansen, M., Xia, L. C., Aktipis, C. A., Petritsch, C., Ji, H. P. & Maley, C. C. 2016. Pan-cancer analysis of the extent and consequences of intratumor heterogeneity. Nature medicine, 22, 105-113.
Anisimov, V. N. 2009. Carcinogenesis and aging 20 years after: escaping horizon. Mechanisms of ageing and development, 130, 105-121.
Anwer, A. G., Gosnell, M. E., Perinchery, S. M., Inglis, D. W. & Goldys, E. M. 2012. Visible 532 nm laser irradiation of human adipose tissue-derived stem cells: Effect on proliferation rates, mitochondria membrane potential and autofluorescence. Lasers in Surgery and Medicine, 44, 769-778.
Araujo, Ana r., Gelens, L., Sheriff, Rahuman s. M. & Santos, Silvia d. M. 2016. Positive Feedback Keeps Duration of Mitosis Temporally Insulated from Upstream Cell-Cycle Events. Molecular Cell, 64, 362-375.
Archer, S. L. 2013. Mitochondrial dynamics—mitochondrial fission and fusion in human diseases. New England Journal of Medicine, 369, 2236-2251.
Aria, V. and Yeeles, J.T. 2019. Mechanism of bidirectional leading-strand synthesis establishment at eukaryotic DNA replication origins. Molecular cell, 73,2, 199-211.
Artandi, S. E. & Depinho, R. A. 2009. Telomeres and telomerase in cancer. Carcinogenesis, 31, 9-18.
Atashi, F., Modarressi, A. & Pepper, M. S. 2015. The role of reactive oxygen species in mesenchymal stem cell adipogenic and osteogenic differentiation: a review. Stem cells and development, 24, 1150-1163.
Avnet, S., Longhi, A., Salerno, M., Halleen, J. M., Perut, F., Granchi, D., Ferrari, S., Bertoni, F., Giunti, A. & Baldini, N. 2008. Increased osteoclast activity is associated with aggressiveness of osteosarcoma. International journal of oncology, 33, 1231-1238.
Aveic, S., Davtalab, R., Vogt, M., Weber, M., Buttler, P., Tonini, G.P. & Fischer, H. 2019. Calcium phosphate scaffolds with defined interconnecting channel structure provide a mimetic 3D niche for bone marrow metastasized tumor cell growth. Acta biomaterialia, 88, 527-539.
Bachrati, C. Z. & Hickson, I. D. 2003. RecQ helicases: suppressors of tumorigenesis and premature aging. Biochemical Journal, 374, 577-606.
Bachrati, C. Z. & Hickson, I. D. 2008. RecQ helicases: guardian angels of the DNA replication fork. Chromosoma, 117, 219-233.
Bae, S.-C. & Lee, Y. H. 2006. Phosphorylation, acetylation and ubiquitination: the molecular basis of RUNX regulation. Gene, 366, 58-66.
Bakhoum, S. F. & Landau, D. A. 2017. Chromosomal Instability as a Driver of Tumor Heterogeneity and Evolution. Cold Spring Harbor Perspectives in Medicine, 7, a029611.
Bakkenist, C. J. & Kastan, M. B. 2003. DNA damage activates ATM through intermolecular autophosphorylation and dimer dissociation. Nature, 421, 499.
Bakkenist, C. J. & Kastan, M. B. 2004. Initiating cellular stress responses. Cell, 118, 9-17.
Ballabeni, A., Zamponi, R., Moore, J. K., Helin, K. & Kirschner, M. W. 2013. Geminin deploys multiple mechanisms to regulate Cdt1 before cell division thus ensuring the proper execution of DNA replication. Proceedings of the National Academy of Sciences, 110, E2848-E2853.
Ballock, R. T. & O'keefe, R. J. 2003. The biology of the growth plate. JBJS, 85, 715-726.
Baraniak, P. R. & Mcdevitt, T. C. 2011. Scaffold-free culture of mesenchymal stem cell spheroids in suspension preserves multilineage potential.
Barenholz, U., Keren, L. & Milo, R. 2016. A Minimalistic Resource Allocation Model to Explain Ubiquitous Increase in Protein Expression with Growth Rate. PLOS ONE 11, e0153344.
Baritaud, M., Cabon, L., Delavallée, L., Galan-Malo, P., Gilles, M., Brunelle-Navas, M. & Susin, S. 2012. AIF-mediated caspase-independent necroptosis requires ATM and DNA-PK-induced histone H2AX Ser139 phosphorylation. Cell death & disease, 3, e390.
Bartek, J. & Lukas, J. 2003. Chk1 and Chk2 kinases in checkpoint control and cancer. Cancer cell, 3, 421-429.
Bartek, J., Lukas, C. & Lukas, J. 2004. Checking on DNA damage in S phase. Nature reviews Molecular cell biology, 5, 792-804.

Bartkova, J., Hamerlik, P., Stockhausen, M., Ehrmann, J., Hlobilkova, A., Laursen, H., Kalita, O., Kolar, Z., Poulsen, H. S. & Broholm, H. 2010. Replication stress and oxidative damage contribute to aberrant constitutive activation of DNA damage signalling in human gliomas. Oncogene, 29, 5095-5102.

Bartkova, J., Hořejší, Z., Koed, K., Krämer, A., Tort, F., Zieger, K., Guldberg, P., Sehested, M., Nesland, J. M. & Lukas, C. 2005. DNA damage response as a candidate anti-cancer barrier in early human tumorigenesis. Nature, 434, 864-870.

Basu-Roy, U., Basilico, C. & Mansukhani, A. Sphere Formation (Osteosphere/Sarcopshere) Assay.

Bathurst, N., Sanerkin, N. & Watt, L. 1986. Osteoclast-rich osteosarcoma. The British journal of radiology, 59, 667-673.

Bauer, M., Goldstein, M., Christmann, M., Becker, H., Heylmann, D. & Kaina, B. 2011. Human monocytes are severely impaired in base and DNA double-strand break repair that renders them vulnerable to oxidative stress. Proceedings of the National Academy of Sciences, 108, 21105-21110.

Bauer, N. C., Doetsch, P. W. & Corbett, A. H. 2015. Mechanisms regulating protein localization. Traffic, 16, 1039-1061.

Bayani, J., Zielenska, M., Pandita, A., Al-Romaih, K., Karaskova, J., Harrison, K., Bridge, J. A., Sorensen, P., Thorner, P. & Squire, J. A. 2003. Spectral karyotyping identifies recurrent complex rearrangements of chromosomes 8, 17, and 20 in osteosarcomas. Genes, Chromosomes and Cancer, 36, 7-16.

Bayani, J., Selvarajah, S., Maire, G., Vukovic, B., Al-Romaih, K., Zielenska, M. & Squire, J. A. Genomic mechanisms and measurement of structural and numerical instability in cancer cells. Seminars in cancer biology, 2007. Elsevier, 5-18.

Bechter, O. E., Zou, Y., Shay, J. W. & Wright, W. E. 2003. Homologous recombination in human telomerase-positive and ALT cells occurs with the same frequency. EMBO reports, 4, 1138-1143.

Beghini, A., Castorina, P., Roversi, G., Modiano, P. & Larizza, L. 2003. RNA processing defects of the helicase gene RECQL4 in a compound heterozygous Rothmund–Thomson patient. American Journal of Medical Genetics Part A, 120, 395-399.

Bellido, T., Ali, A. A., Plotkin, L. I., Fu, Q., Gubrij, I., Roberson, P. K., Weinstein, R. S., O'brien, C. A., Manolagas, S. C. & Jilka, R. L. 2003. Proteasomal Degradation of Runx2 Shortens Parathyroid Hormone-induced Anti-apoptotic Signaling in Osteoblasts, a putative explanation for why intermittent administration is needed for bone anabolism. Journal of Biological Chemistry, 278, 50259-50272.

Bellido, T., Plotkin, L. I. & Bruzzaniti, A. 2014. Bone cells. Basic and Applied Bone Biology: Elsevier, 27-45.

Berkers, C. R., Maddocks, O. D. K., Cheung, E. C., Mor, I. & Vousden, K. H. 2013. Metabolic regulation by p53 family members. Cell metabolism, 18, 617-633.

Berman, S. D., Calo, E., Landman, A. S., Danielian, P. S., Miller, E. S., West, J. C., Fonhoue, B. D., Caron, A., Bronson, R. & Bouxsein, M. L. 2008. Metastatic osteosarcoma induced by inactivation of Rb and p53 in the osteoblast lineage. Proceedings of the National Academy of Sciences, 105, 11851-11856.

Berniak, K., Rybak, P., Bernas, T., Zarębski, M., Biela, E., Zhao, H., Darzynkiewicz, Z. & Dobrucki, J. W. 2013. Relationship Between DNA Damage Response, Initiated by Camptothecin or Oxidative Stress, and DNA Replication, Analyzed by Quantitative 3D Image Analysis. Cytometry. Part A : the journal of the International Society for Analytical Cytology, 83, 913-924.

Berridge, M. V., Herst, P. M. & Tan, A. S. 2005. Tetrazolium dyes as tools in cell biology: new insights into their cellular reduction. Biotechnology annual review, 11, 127-152.

Bertoli, C., Skotheim, J. M. & De Bruin, R. a. M. 2013. Control of cell cycle transcription during G1 and S phases. Nature reviews. Molecular cell biology, 14, 518.

Bhatt, K. A., Chang, E. I., Warren, S. M., Lin, S.-E., Bastidas, N., Ghali, S., Thibboneir, A., Capla, J. M., Mccarthy, J. G. & Gurtner, G. C. 2007. Uniaxial mechanical strain: an in vitro correlate to distraction osteogenesis. Journal of Surgical Research, 143, 329-336.

Bi, J., Huang, A., Liu, T., Zhang, T. & Ma, H. 2015. Expression of DNA damage checkpoint 53BP1 is correlated with prognosis, cell proliferation and apoptosis in colorectal cancer. International journal of clinical and experimental pathology, 8, 6070.
Bieback, K., Kern, S., Klüter, H. & Eichler, H. 2004. Critical parameters for the isolation of mesenchymal stem cells from umbilical cord blood. Stem cells, 22, 625-634.
Bielack, S. S., Kempf-Bielack, B., Delling, G., Exner, G. U., Flege, S., Helmke, K., Kotz, R., Salzer-Kuntschik, M., Werner, M. & Winkelmann, W. 2002. Prognostic factors in high-grade osteosarcoma of the extremities or trunk: an analysis of 1,702 patients treated on neoadjuvant cooperative osteosarcoma study group protocols. Journal of Clinical Oncology, 20, 776-790.
Bilkay, U., Tokat, C., Helvaci, E., Ozek, C., Zekioglu, O., Onat, T. & Songur, E. 2008. Osteogenic capacities of tibial and cranial periosteum: a biochemical and histologic study. Journal of Craniofacial Surgery, 19, 453-458.
Birmingham, A., Anderson, E. M., Reynolds, A., Ilsley-Tyree, D., Leake, D., Fedorov, Y., Baskerville, S., Maksimova, E., Robinson, K. & Karpilow, J. 2006. 3′ UTR seed matches, but not overall identity, are associated with RNAi off-targets. Nature methods, 3, 199-204.
Bishop, M. W., Janeway, K. A. & Gorlick, R. 2016. Future directions in the treatment of osteosarcoma. Current opinion in pediatrics, 28, 26-33.
Black, E.M. and Giunta, S. 2018. Repetitive Fragile Sites: Centromere Satellite DNA as a Source of Genome Instability in Human Diseases. Genes, 9,12, 615.
Blackburn, E. H. 2001. Switching and signaling at the telomere. Cell, 106, 661-673.
Blagosklonny, M. V. & Pardee, A. B. 2002. The restriction point of the cell cycle. Cell cycle, 1, 102-109.
Blessy, M., Patel, R. D., Prajapati, P. N. & Agrawal, Y. K. 2014. Development of forced degradation and stability indicating studies of drugs—A review. Journal of Pharmaceutical Analysis, 4, 159-165.
Boeuf, S., Kunz, P., Hennig, T., Lehner, B., Hogendoorn, P., Bovee, J. & Richter, W. 2008. A chondrogenic gene expression signature in mesenchymal stem cells is a classifier of conventional central chondrosarcoma. The Journal of pathology, 216, 158-166.
Bohr, V. A. 2002. Repair of oxidative DNA damage in nuclear and mitochondrial DNA, and some changes with aging in mammalian cells 1, 2. Free Radical Biology and Medicine, 32, 804-812.
Bolden, J. E., Peart, M. J. & Johnstone, R. W. 2006. Anticancer activities of histone deacetylase inhibitors. Nature reviews Drug discovery, 5, 769-784.
Boles, N. C., Peddibhotla, S., Chen, A. J., Goodell, M. A. & Rosen, J. M. 2010. Chk1 haploinsufficiency results in anemia and defective erythropoiesis. PloS one, 5, e8581.
Bonner, W. M., Redon, C. E., Dickey, J. S., Nakamura, A. J., Sedelnikova, O. A., Solier, S. & Pommier, Y. 2008. γH2AX and cancer. Nature reviews. Cancer, 8, 957.
Bonte, D., Lindvall, C., Liu, H., Dykema, K., Furge, K. & Weinreich, M. 2008a. Cdc7-Dbf4 Kinase Overexpression in Multiple Cancers and Tumor Cell Lines Is Correlated with p53 Inactivation. Neoplasia (New York, N.Y.), 10, 920-931.
Boonrungsiman, S., Gentleman, E., Carzaniga, R., Evans, N. D., Mccomb, D. W., Porter, A. E. & Stevens, M. M. 2012. The role of intracellular calcium phosphate in osteoblast-mediated bone apatite formation. Proceedings of the National Academy of Sciences, 109, 14170-14175.
Boschelli, F., Arndt, K. T. & Golas, J. M. 2008. 4-anilino-3-quinolinecarbonitriles for the treatment of chronic myelogenous leukemia (CML). Google Patents.
Bose, S. K., Bullard, R. S. & Donald, C. D. 2008. Oncogenic role of engrailed-2 (en-2) in prostate cancer cell growth and survival. Translational oncogenomics, 3, 37.
Botter, S. M., Neri, D. & Fuchs, B. 2014. Recent advances in osteosarcoma. Current opinion in pharmacology, 16, 15-23.
Bourin, P., Bunnell, B. A., Casteilla, L., Dominici, M., Katz, A. J., March, K. L., Redl, H., Rubin, J. P., Yoshimura, K. & Gimble, J. M. 2013. Stromal cells from the adipose tissue-derived stromal vascular fraction and culture expanded adipose tissue-derived stromal/stem cells: a joint statement of the International Federation for

Adipose Therapeutics and Science (IFATS) and the International Society for Cellular Therapy (ISCT). Cytotherapy, 15, 641-648.
Bouwman, B.A. & Crosetto, N. 2018. Endogenous DNA Double-Strand Breaks during DNA Transactions: Emerging Insights and Methods for Genome-Wide Profiling. Genes, 9, 632.
Bovée, J. V., Hogendoorn, P. C., Wunder, J. S. & Alman, B. A. 2010. Cartilage tumours and bone development: molecular pathology and possible therapeutic targets. Nature Reviews Cancer, 10, 481-488.
Bower, J. J., Karaca, G. F., Zhou, Y., Simpson, D. A., Cordeiro-Stone, M. & Kaufmann, W. K. 2010. Topoisomerase IIα maintains genomic stability through decatenation G2 checkpoint signaling. Oncogene, 29, 4787.
Boyd, A. C. 1993. Turbo cloning: a fast, efficient method for cloning PCR products and other blunt-ended DNA fragments into plasmids. Nucleic acids research, 21, 817-821.
Bratic, A. & Larsson, N.-G. 2013. The role of mitochondria in aging. The Journal of clinical investigation, 123, 951-957.
Brauer, M. J., Huttenhower, C., Airoldi, E. M., Rosenstein, R., Matese, J. C., Gresham, D., Boer, V. M., Troyanskaya, O. G. & Botstein, D. 2008. Coordination of growth rate, cell cycle, stress response, and metabolic activity in yeast. Molecular biology of the cell, 19, 352-367.
Brazelle, W., Kreahling, J. M., Gemmer, J., Ma, Y., Cress, W. D., Haura, E. & Altiok, S. 2010. Histone deacetylase inhibitors downregulate checkpoint kinase 1 expression to induce cell death in non-small cell lung cancer cells. PloS one, 5, e14335.
Bredella, M. A., Torriani, M., Ghomi, R. H., Thomas, B. J., Brick, D. J., Gerweck, A. V., Rosen, C. J., Klibanski, A. & Miller, K. K. 2011. Vertebral bone marrow fat is positively associated with visceral fat and inversely associated with IGF-1 in obese women. Obesity, 19, 49-53.
Broadhead, M. L., Clark, J., Myers, D. E., Dass, C. R. & Choong, P. F. 2011a. The molecular pathogenesis of osteosarcoma: a review. Sarcoma, 2011.
Brown, E. J. & Baltimore, D. 2003. Essential and dispensable roles of ATR in cell cycle arrest and genome maintenance. Genes & development, 17, 615-628.
Brubaker, K. D., Vessella, R. L., Brown, L. G. & Corey, E. 2003. Prostate cancer expression of runt-domain transcription factor Runx2, a key regulator of osteoblast differentiation and function. The Prostate, 56, 13-22.
Bryan, T. M., Englezou, A., Dalla-Pozza, L., Dunham, M. A. & Reddel, R. R. 1997. Evidence for an alternative mechanism for maintaining telomere length in human tumors and tumor-derived cell lines. Nature medicine, 3, 1271-1274.
Buffart, T. E., Coffa, J., Hermsen, M., Carvalho, B., Van Der Sijp, J. R. M., Ylstra, B., Pals, G., Schouten, J. P. & Meijer, G. A. 2005. DNA copy number changes at 8q11–24 in metastasized colorectal cancer. Analytical Cellular Pathology, 27, 57-65.
Burbulla, L. F. & Krüger, R. 2012. The Use of Primary Human Fibroblasts for Monitoring Mitochondrial Phenotypes in the Field of Parkinson's Disease. Journal of Visualized Experiments : JoVE, 4228.
Burgess, D. J. 2013. Specialist responses at telomeres. Nature Reviews Genetics, 14.
Burkhardt, R., Kettner, G., Böhm, W., Schmidmeier, M., Schlag, R., Frisch, B., Mallmann, B., Eisenmenger, W. & Gilg, T. H. 1987. Changes in trabecular bone, hematopoiesis and bone marrow vessels in aplastic anemia, primary osteoporosis, and old age: a comparative histomorphometric study. Bone, 8, 157-164.
Burks, L. M., Yin, J. & Plon, S. E. 2007. Nuclear import and retention domains in the amino terminus of RECQL4. Gene, 391, 26-38.
Burrell, R. A., Mcclelland, S. E., Endesfelder, D., Groth, P., Weller, M.-C., Shaikh, N., Domingo, E., Kanu, N., Dewhurst, S. M. & Gronroos, E. 2013. Replication stress links structural and numerical cancer chromosomal instability. Nature, 494, 492.
Burrow, K. L., Hoyland, J. A. & Richardson, S. M. 2017. Human Adipose-Derived Stem Cells Exhibit Enhanced Proliferative Capacity and Retain Multipotency Longer than Donor-Matched Bone Marrow Mesenchymal Stem Cells during Expansion In Vitro. Stem cells international, 2017.
Butler, L. M., Agus, D. B., Scher, H. I., Higgins, B., Rose, A., Cordon-Cardo, C., Thaler, H. T., Rifkind, R. A., Marks, P. A. & Richon, V. M. 2000. Suberoylanilide hydroxamic

acid, an inhibitor of histone deacetylase, suppresses the growth of prostate cancer cells in vitro and in vivo. Cancer research, 60, 5165-5170.
Cabral, R. E. C., Queille, S., Bodemer, C., De Prost, Y., Neto, J. B. C., Sarasin, A. & Daya-Grosjean, L. 2008. Identification of new RECQL4 mutations in Caucasian Rothmund–Thomson patients and analysis of sensitivity to a wide range of genotoxic agents. Mutation Research/Fundamental and Molecular Mechanisms of Mutagenesis, 643, 41-47.
Cai, J., Li, W., Su, H., Qin, D., Yang, J., Zhu, F., Xu, J., He, W., Guo, X. & Labuda, K. 2010. Generation of human induced pluripotent stem cells from umbilical cord matrix and amniotic membrane mesenchymal cells. Journal of Biological Chemistry, 285, 11227-11234.
Calo, E., Quintero-Estades, J. A., Danielian, P. S., Nedelcu, S., Berman, S. D. & Lees, J. A. 2010. Rb regulates fate choice and lineage commitment in vivo. Nature, 466, 1110.
Cao, F., Lu, L., Abrams, S. A., Hawthorne, K. M., Tam, A., Jin, W., Dawson, B., Shypailo, R., Liu, H. & Lee, B. 2017. Generalized Metabolic Bone Disease and Fracture Risk in Rothmund-Thomson Syndrome. Human Molecular Genetics.
Cao, J. J. 2011. Effects of obesity on bone metabolism. Journal of orthopaedic surgery and research, 6, 30.
Caplan, A. I. 1991. Mesenchymal stem cells. Journal of orthopaedic research, 9, 641-650.
Capp, C., Wu, J. & Hsieh, T.-S. 2009. Drosophila RecQ4 has a 3′-5′ DNA helicase activity that is essential for viability. Journal of Biological Chemistry, 284, 30845-30852.
Capp, C., Wu, J. & Hsieh, T.-S. 2010. RecQ4: the second replicative helicase? Critical reviews in biochemistry and molecular biology, 45, 233-242.
Carlson, A. M., Lindor, N. M. & Litzow, M. R. 2011. Therapy-related myelodysplasia in a patient with Rothmund–Thomson syndrome. European journal of haematology, 86, 536-540.
Carter, S. L., Eklund, A. C., Kohane, I. S., Harris, L. N. & Szallasi, Z. 2006. A signature of chromosomal instability inferred from gene expression profiles predicts clinical outcome in multiple human cancers. Nature genetics, 38, 1043-1048.
Caruso, R. A., Fedele, F., Crisafulli, C., Paparo, D., Parisi, A., Lucianò, R. & Cavallari, V. 2011. Abnormal nuclear structures (micronuclei, nuclear blebs, strings, and pockets) in a case of anaplastic giant cell carcinoma of the thyroid: an immunohistochemical and ultrastructural study. Ultrastructural pathology, 35, 14-18.
Celeste, A., Fernandez-Capetillo, O., Kruhlak, M. J., Pilch, D. R., Staudt, D. W., Lee, A., Bonner, R. F., Bonner, W. M. & Nussenzweig, A. 2003a. Histone H2AX phosphorylation is dispensable for the initial recognition of DNA breaks. Nature cell biology, 5, 675-679.
Celeste, A., Difilippantonio, S., Difilippantonio, M. J., Fernandez-Capetillo, O., Pilch, D. R., Sedelnikova, O. A., Eckhaus, M., Ried, T., Bonner, W. M. & Nussenzweig, A. 2003b. H2AX haploinsufficiency modifies genomic stability and tumor susceptibility. Cell, 114, 371-383.
Cenni, V., Maraldi, N. M., Ruggeri, A., Secchiero, P., Del Coco, R., De Pol, A., Cocco, L. & Marmiroli, S. 2004. Sensitization of multidrug resistant human ostesarcoma cells to Apo2 Ligand/TRAIL-induced apoptosis by inhibition of the Akt/PKB kinase. International journal of oncology, 25, 1599-1608.
Cesare, A. J. & Reddel, R. R. 2010. Alternative lengthening of telomeres: models, mechanisms and implications. Nature reviews. Genetics, 11, 319.
Chai, W., Ford, L. P., Lenertz, L., Wright, W. E. & Shay, J. W. 2002. Human Ku70/80 associates physically with telomerase through interaction with hTERT. Journal of Biological Chemistry, 277, 47242-47247.
Chamberlain, G., Fox, J., Ashton, B. & Middleton, J. 2007. Concise review: mesenchymal stem cells: their phenotype, differentiation capacity, immunological features, and potential for homing. Stem cells, 25, 2739-2749.
Chan, Q. K. Y., Lam, H.-M., Ng, C.-F., Lee, A. Y. Y., Chan, E. S. Y., Ng, H.-K., Ho, S.-M. & Lau, K.-M. 2010. Activation of GPR30 inhibits the growth of prostate cancer cells through sustained activation of Erk1/2, c-jun/c-fos-dependent upregulation of p21, and induction of G2 cell-cycle arrest. Cell Death & Differentiation, 17, 1511-1523.

Chan, L. H., Wang, W., Yeung, W., Deng, Y., Yuan, P. & Mak, K. K. 2014. Hedgehog signaling induces osteosarcoma development through Yap1 and H19 overexpression. Oncogene, 33, 4857.
Chandrasekar, C. R., Grimer, R. J., Carter, S. R., Tillman, R. M., Abudu, A., Jeys, L. M., Cheung, W. G. H. & Sharma, R. 2012. Pathological fracture of the proximal femur in osteosarcoma: need for early radical surgery? ISRN oncology, 2012.
Chang, H. H. Y., Pannunzio, N. R., Adachi, N. & Lieber, M. R. 2017. Non-homologous DNA end joining and alternative pathways to double-strand break repair. Nature Reviews Molecular Cell Biology.
Chen, C. T., Shih, Y. R. V., Kuo, T. K., Lee, O. K. & Wei, Y. H. 2008. Coordinated changes of mitochondrial biogenesis and antioxidant enzymes during osteogenic differentiation of human mesenchymal stem cells. Stem Cells, 26, 960-968.
Chen, L.-Y., Redon, S. & Lingner, J. 2012. The human CST complex is a terminator of telomerase activity. Nature, 488, 540-544.
Chen, P.-F., Singhal, S., Bushyhead, D., Broder-Fingert, S. & Wolfe, J. 2014a. Colchicine-induced degeneration of the micronucleus during conjugation in Tetrahymena. Biology open, 3, 353-361.
Chen, X., Bahrami, A., Pappo, A., Easton, J., Dalton, J., Hedlund, E., Ellison, D., Shurtleff, S., Wu, G. & Wei, L. 2014a. Recurrent somatic structural variations contribute to tumorigenesis in pediatric osteosarcoma. Cell reports, 7, 104-112.
Chen, Y., Wang, L., Cheng, X., Ge, X. & Wang, P. 2014b. An ultrasensitive system for measuring the USPs and OTULIN activity using Nanoluc as a reporter. Biochemical and biophysical research communications, 455, 178-183.
Chen, X., Pappo, A. & Dyer, M. A. 2015. Pediatric solid tumor genomics and developmental pliancy. Oncogene, 34, 5207-5215.
Chen, Q., Shou, P., Zheng, C., Jiang, M., Cao, G., Yang, Q., Cao, J., Xie, N., Velletri, T. & Zhang, X. 2016. Fate decision of mesenchymal stem cells: adipocytes or osteoblasts? Cell death and differentiation, 23, 1128.
Cheng, J., Fan, Y. H., Xu, X., Zhang, H., Dou, J., Tang, Y., Zhong, X., Rojas, Y., Yu, Y. & Zhao, Y. 2014. A small-molecule inhibitor of UBE2N induces neuroblastoma cell death via activation of p53 and JNK pathways. Cell death & disease, 5, e1079.
Cheng, A. N., Fan, C.-C., Lo, Y.-K., Kuo, C.-L., Wang, H.-C., Lien, I. H., Lin, S.-Y., Chen, C.-H., Jiang, S. S. & Chang, I. S. 2017. Cdc7-Dbf4-mediated phosphorylation of HSP90-S164 stabilizes HSP90-HCLK2-MRN complex to enhance ATR/ATM signaling that overcomes replication stress in cancer. Scientific reports, 7, 17024.
Chi, Z., Nie, L., Peng, Z., Yang, Q., Yang, K., Tao, J., Mi, Y., Fang, X., Balajee, A. S. & Zhao, Y. 2012. RecQL4 cytoplasmic localization: implications in mitochondrial DNA oxidative damage repair. The international journal of biochemistry & cell biology, 44, 1942-1951.
Chi, Z., Nie, L., Peng, Z., Yang, Q., Yang, K., Tao, J., Mi, Y., Fang, X., Balajee, A. S. & Zhao, Y. 2012. RecQL4 cytoplasmic localization: implications in mitochondrial DNA oxidative damage repair. The international journal of biochemistry & cell biology, 44, 1942-1951.
Chirgwin, J. M. & Guise, T. A. 2000. Molecular mechanisms of tumor-bone interactions in osteolytic metastases. Critical Reviews™ in Eukaryotic Gene Expression, 10.
Choi, Y. W., Bae, S. M., Kim, Y. W., Lee, H. N., Kim, Y. W., Park, T. C., Ro, D. Y., Shin, J. C., Shin, S. J. & Seo, J. S. 2007. Gene expression profiles in squamous cell cervical carcinoma using array-based comparative genomic hybridization analysis. International Journal of Gynecological Cancer, 17, 687-696.
Choi, K.-M., Seo, Y.-K., Yoon, H.-H., Song, K.-Y., Kwon, S.-Y., Lee, H.-S. & Park, J.-K. 2008. Effect of ascorbic acid on bone marrow-derived mesenchymal stem cell proliferation and differentiation. Journal of bioscience and bioengineering, 105, 586-594.
Choi, Y. S., Dusting, G. J., Stubbs, S., Arunothayaraj, S., Han, X. L., Collas, P., Morrison, W. A. & Dilley, R. J. 2010. Differentiation of human adipose-derived stem cells into beating cardiomyocytes. Journal of cellular and molecular medicine, 14, 878-889.
Choi, B. H., Xie, S. & Dai, W. 2017. PTEN is a negative regulator of mitotic checkpoint complex during the cell cycle. Experimental Hematology & Oncology, 6, 19.

Chou, A. J., Merola, P. R., Wexler, L. H., Gorlick, R. G., Vyas, Y. M., Healey, J. H., Laquaglia, M. P., Huvos, A. G. & Meyers, P. A. 2005. Treatment of osteosarcoma at first recurrence after contemporary therapy. Cancer, 104, 2214-2221.
Choudhery, M. S., Badowski, M., Muise, A. & Harris, D. T. 2013. Comparison of human mesenchymal stem cells derived from adipose and cord tissue. Cytotherapy, 15, 330-343.
Chu, T.W., MacNeil, D.E. & Autexier, C. 2016. Multiple mechanisms contribute to the cell growth defects imparted by human telomerase insertion in fingers domain mutations associated with premature aging diseases. Journal of Biological Chemistry, 291, 8374-8386.
Chung, F.-L., Chen, H.-J. C. & Nath, R. G. 1996. Lipid peroxidation as a potential endogenous source for the formation of exocyclic DNA adducts. Carcinogenesis, 17, 2105-2111.
Cisyk, A. L., Singh, H. & Mcmanus, K. J. 2014. Establishing a biological profile for interval colorectal cancers. Digestive diseases and sciences, 59, 2390-2402.
Cleaver, J. E. 1977. Nucleosome structure controls rates of excision repair in DNA of human cells. Nature, 270, 451-453.
Cleton-Jansen, A.-M., Anninga, J. K., Briaire-De Bruijn, I. H., Romeo, S., Oosting, J., Egeler, R. M., Gelderblom, H., Taminiau, A. H. & Hogendoorn, P. C. 2009. Profiling of high-grade central osteosarcoma and its putative progenitor cells identifies tumourigenic pathways. British journal of cancer, 101, 1909-1918.
Clevers, H., Loh, K. M. & Nusse, R. 2014. An integral program for tissue renewal and regeneration: Wnt signaling and stem cell control. Science, 346, 1248012.
Cohen, P. 2000. The regulation of protein function by multisite phosphorylation–a 25 year update. Trends in biochemical sciences, 25, 596-601.
Cohen, D.M. and Chen, C.S. 2008. Mechanical control of stem cell differentiation.
Cohen, A., Dempster, D. W., Stein, E. M., Nickolas, T. L., Zhou, H., Mcmahon, D. J., Müller, R., Kohler, T., Zwahlen, A. & Lappe, J. M. 2012. Increased marrow adiposity in premenopausal women with idiopathic osteoporosis. The Journal of Clinical Endocrinology & Metabolism, 97, 2782-2791.
Cohnheim, J. 1867. Ueber entzündung und eiterung. Archiv für pathologische Anatomie und Physiologie und für klinische Medicin, 40, 1-79.
Colter, D. C., Sekiya, I. & Prockop, D. J. 2001. Identification of a subpopulation of rapidly self-renewing and multipotential adult stem cells in colonies of human marrow stromal cells. Proceedings of the National Academy of Sciences, 98, 7841-7845.
Comelli, L., Marchetti, L., Arosio, D., Riva, S., Abdurashidova, G., Beltram, F. & Falaschi, A. 2009. The homeotic protein HOXC13 is a member of human DNA replication complexes. Cell Cycle, 8, 454-459.
Conery, A. R. & Harlow, E. 2010. High-throughput screens in diploid cells identify factors that contribute to the acquisition of chromosomal instability. Proceedings of the National Academy of Sciences, 107, 15455-15460.
Cong, Y.-S., Wright, W. E. & Shay, J. W. 2002. Human Telomerase and Its Regulation. Microbiology and Molecular Biology Reviews, 66, 407-425.
Conget, P. A. & Minguell, J. J. 1999. Phenotypical and functional properties of human bone marrow mesenchymal progenitor cells. Journal of cellular physiology, 181, 67-73.
Conley, K. E., Marcinek, D. J. & Villarin, J. 2007. Mitochondrial dysfunction and age. Current Opinion in Clinical Nutrition & Metabolic Care, 10, 688-692.
Cookson, N. A., Cookson, S. W., Tsimring, L. S. & Hasty, J. 2009. Cell cycle-dependent variations in protein concentration. Nucleic acids research, gkp1069.
Coon, E.A. and Benarroch, E.E. 2018. DNA damage response: Selected review and neurologic implications. Neurology, 90,8, 367-376.
Cooper, G. M. & Hausman, R. E. 2000. The cell, Sinauer Associates Sunderland.
Costantini, S., Woodbine, L., Andreoli, L., Jeggo, P. A. & Vindigni, A. 2007. Interaction of the Ku heterodimer with the DNA ligase IV/Xrcc4 complex and its regulation by DNA-PK. DNA repair, 6, 712-722.
Cottet-Rousselle, C., Ronot, X., Leverve, X. & Mayol, J. F. 2011. Cytometric assessment of mitochondria using fluorescent probes. Cytometry Part A, 79, 405-425.

Coudreuse, D. & Nurse, P. 2010. Driving the cell cycle with a minimal CDK control network. Nature, 468, 1074.
Coxon, F. P. & Taylor, A. 2008. Vesicular trafficking in osteoclasts. 19, 424-433.
Crevel, G., Vo, N., Crevel, I., Hamid, S., Hoa, L., Miyata, S. & Cotterill, S. 2012. Drosophila RecQ4 is directly involved in both DNA replication and the response to UV damage in S2 cells. PloS one, 7, e49505.
Crisan, M., Yap, S., Casteilla, L., Chen, C.-W., Corselli, M., Park, T. S., Andriolo, G., Sun, B., Zheng, B. & Zhang, L. 2008. A perivascular origin for mesenchymal stem cells in multiple human organs. Cell stem cell, 3, 301-313.
Cromie, G. A., Connelly, J. C. & Leach, D. R. F. 2001. Recombination at double-strand breaks and DNA ends: conserved mechanisms from phage to humans. Molecular cell, 8, 1163-1174.
Croteau, D. L., Popuri, V., Opresko, P. L. & Bohr, V. A. 2014. Human RecQ helicases in DNA repair, recombination, and replication. Annual review of biochemistry, 83, 519-552.
Croteau, D. L., Rossi, M. L., Canugovi, C., Tian, J., Sykora, P., Ramamoorthy, M., Wang, Z., Singh, D. K., Akbari, M. & Kasiviswanathan, R. 2012a. RECQL4 localizes to mitochondria and preserves mitochondrial DNA integrity. Aging cell, 11, 456-466.
Croteau, D. L., Singh, D. K., Ferrarelli, L. H., Lu, H. & Bohr, V. A. 2012b. RECQL4 in genomic instability and aging. Trends in Genetics, 28, 624-631.
Cui, L.-L., Kinnunen, T., Boltze, J., Nystedt, J. & Jolkkonen, J. 2016. Clumping and viability of bone marrow derived mesenchymal stromal cells under different preparation procedures: a flow cytometry-based in vitro study. Stem cells international, 2016.
Cui, Y., Zhu, J.-J., Ma, C.-B., Cui, K., Wang, F., Ni, S.-H. & Zhang, Z.-Y. 2016. Interleukin 10 gene− 1082A/G polymorphism is associated with osteosarcoma risk and poor outcomes in the Chinese population. Tumor Biology, 37, 4517-4522.
Currall, V. A. & Dixon, J. H. 2006. Synchronous multifocal osteosarcoma: case report and literature review. Sarcoma, 2006.
Curtis, E. M., Moon, R. J., Dennison, E. M., Harvey, N. C. & Cooper, C. 2016. Recent advances in the pathogenesis and treatment of osteoporosis. Clinical Medicine, 16, 360-364.
Da Silva Meirelles, L., Chagastelles, P. C. & Nardi, N. B. 2006. Mesenchymal stem cells reside in virtually all post-natal organs and tissues. Journal of cell science, 119, 2204-2213.
Daft, P. G., Yang, Y., Napierala, D. & Zayzafoon, M. 2015. The growth and aggressive behavior of human osteosarcoma is regulated by a CaMKII-controlled autocrine VEGF signaling mechanism. PLoS One, 10, e0121568.
Dahlin, D. C. 1957. Bone tumors: general aspects and an analysis of 2,276 cases, Thomas.
Dai, Y. & Grant, S. 2010. New insights into checkpoint kinase 1 in the DNA damage response signaling network. Clinical Cancer Research, 16, 376-383.
Dai, J.-Q., Huang, Y.-G. & He, A.-N. 2015. Dihydromethysticin kavalactone induces apoptosis in osteosarcoma cells through modulation of PI3K/Akt pathway, disruption of mitochondrial membrane potential and inducing cell cycle arrest. International journal of clinical and experimental pathology, 8, 4356.
Damron, T. A., Ward, W. G. & Stewart, A. 2007. Osteosarcoma, chondrosarcoma, and Ewing's sarcoma: National Cancer Data Base Report. Clinical orthopaedics and related research, 459, 40-47.
Daniel, J. A. & Nussenzweig, A. 2013. The AID-induced DNA damage response in chromatin. Molecular cell, 50, 309-321.
Darzynkiewicz, Z., Zhao, H., Halicka, H. D., Rybak, P., Dobrucki, J. & Wlodkowic, D. 2012. DNA Damage Signaling Assessed in Individual Cells in Relation to the Cell Cycle Phase and Induction of Apoptosis. Critical reviews in clinical laboratory sciences, 49, 199-217.
Das, S. C., Panda, D., Nayak, D. & Pattnaik, A. K. 2009. Biarsenical labeling of vesicular stomatitis virus encoding tetracysteine-tagged m protein allows dynamic imaging of m protein and virus uncoating in infected cells. Journal of virology, 83, 2611-2622.
Davis, A. J. & Chen, D. J. 2013. DNA double strand break repair via non-homologous end-joining. Translational cancer research, 2, 130.

Davis, T., Tivey, H. S. E., Brook, A. J. C., Grimstead, J. W., Rokicki, M. J. & Kipling, D. 2013. Activation of p38 MAP kinase and stress signalling in fibroblasts from the progeroid Rothmund–Thomson syndrome. Age, 35, 1767-1783.

Daw, N. C., Billups, C. A., Rodriguez-Galindo, C., Mccarville, M. B., Rao, B. N., Cain, A. M., Jenkins, J. J., Neel, M. D. & Meyer, W. H. 2006. Metastatic osteosarcoma. Cancer, 106, 403-412.

Dawson, D. & Bury, H. 1961. The significance of Howell-Jolly bodies and giant metamyelocytes in marrow smears. Journal of clinical pathology, 14, 374-380.

De Lange, T. 2002. Protection of mammalian telomeres. Oncogene, 21, 532.

De Stanchina, E., Gabellini, D., Norio, P., Giacca, M., Peverali, F. A., Riva, S., Falaschi, A. & Biamonti, G. 2000. Selection of homeotic proteins for binding to a human DNA replication origin. Journal of molecular biology, 299, 667-680.

De, S., Kumari, J., Mudgal, R., Modi, P., Gupta, S., Futami, K., Goto, H., Lindor, N. M., Furuichi, Y. & Mohanty, D. 2012. RECQL4 is essential for the transport of p53 to mitochondria in normal human cells in the absence of exogenous stress. J Cell Sci, 125, 2509-2522.

Deer, J. R. & Allison, D. S. 2004. High-Level Expression of Proteins in Mammalian Cells Using Transcription Regulatory Sequences from the Chinese Hamster EF-1α Gene. Biotechnology progress, 20, 880-889.

Delagoutte, E. & Von Hippel, P. H. 2003. Helicase mechanisms and the coupling of helicases within macromolecular machines Part ii: Integration of helicases into cellular processes. Quarterly reviews of biophysics, 36, 1-69.

Delinasios, J. G., Angeli, F., Koumakis, G., Kumar, S., Kang, W.-H., Sica, G., Iacopino, F., Lama, G., Lamprecht, S. & Sigal-Batikoff, I. 2015. Proliferating fibroblasts and HeLa cells co-cultured in vitro reciprocally influence growth patterns, protein expression, chromatin features and cell survival. Anticancer research, 35, 1881-1916.

Deluca, M., Wannlund, J. & Mcelroy, W. D. 1979. Factors affecting the kinetics of light emission from crude and purified firefly luciferase. Analytical biochemistry, 95, 194-198.

Denchi, E. L. & De Lange, T. 2007. Protection of telomeres through independent control of ATM and ATR by TRF2 and POT1. Nature, 448, 1068-1071.

Deng, Z.-L., Sharff, K. A., Tang, N. I., Song, W.-X., Luo, J., Luo, X., Chen, J., Bennett, E., Reid, R. & Manning, D. 2008. Regulation of osteogenic differentiation during skeletal development. Front Biosci, 13, 2001-2021.

Dennis, G., Sherman, B. T., Hosack, D. A., Yang, J., Gao, W., Lane, H. C. & Lempicki, R. A. 2003. DAVID: database for annotation, visualization, and integrated discovery. Genome biology, 4, 1.

Depamphilis, M. L., Blow, J. J., Ghosh, S., Saha, T., Noguchi, K. & Vassilev, A. 2006. Regulating the licensing of DNA replication origins in metazoa. Current opinion in cell biology, 18, 231-239.

Der Kaloustian, V. M., Mcgill, J. J., Vekemans, M. & Kopelman, H. R. 1990. Clonal lines of aneuploid cells in Rothmund-Thomson syndrome. American journal of medical genetics, 37, 336-339.

Devaney, J., Stirzaker, C., Qu, W., Song, J. Z., Statham, A. L., Patterson, K. I., Horvath, L. G., Tabor, B., Coolen, M. W. & Hulf, T. 2011. Epigenetic deregulation across chromosome 2q14. 2 differentiates normal from prostate cancer and provides a regional panel of novel DNA methylation cancer biomarkers. Cancer Epidemiology Biomarkers & Prevention, 20, 148-159.

Di Lisa, F. & Bernardi, P. 2005. Mitochondrial function and myocardial aging. A critical analysis of the role of permeability transition. Cardiovascular Research, 66, 222-232.

Díaz-Montero, C. M., Wygant, J. N. & Mcintyre, B. W. 2006. PI3-K/Akt-mediated anoikis resistance of human osteosarcoma cells requires Src activation. European Journal of Cancer, 42, 1491-1500.

Dick, D. C., Morley, W. N. & Watson, J. T. 1982. Rothmund-Thomson syndrome and osteogenic sarcoma. Clinical and experimental dermatology, 7, 119-123.

Dicker, A., Le Blanc, K., Åström, G., Van Harmelen, V., Götherström, C., Blomqvist, L., Arner, P. & Rydén, M. 2005. Functional studies of mesenchymal stem cells derived from adult human adipose tissue. Experimental cell research, 308, 283-290.

Dietschy, T., Shevelev, I. & Stagljar, I. 2007. The molecular role of the Rothmund-Thomson-, RAPADILINO-and Baller-Gerold-gene product, RECQL4: recent progress. Cellular and molecular life sciences, 64, 796-802.

Dietschy, T., Shevelev, I., Pena-Diaz, J., Hühn, D., Kuenzle, S., Mak, R., Miah, M. F., Hess, D., Fey, M. & Hottiger, M. O. 2009. p300-mediated acetylation of the Rothmund-Thomson-syndrome gene product RECQL4 regulates its subcellular localization. Journal of cell science, 122, 1258-1267.

Diller, L., Kassel, J., Nelson, C. E., Gryka, M. A., Litwak, G., Gebhardt, M., Bressac, B., Ozturk, M., Baker, S. J. & Vogelstein, B. 1990. p53 functions as a cell cycle control protein in osteosarcomas. Molecular and cellular biology, 10, 5772-5781.

Ding, L., Sun, X., You, Y., Liu, N. & Fu, Z. 2010. Expression of focal adhesion kinase and phosphorylated focal adhesion kinase in human gliomas is associated with unfavorable overall survival. Translational Research, 156, 45-52.

Doksani, Y., Wu, J. Y., De Lange, T. & Zhuang, X. 2013. Super-resolution fluorescence imaging of telomeres reveals TRF2-dependent T-loop formation. Cell, 155, 345-356.

Doll, R. & Peto, R. 1981. The causes of cancer: quantitative estimates of avoidable risks of cancer in the United States today. Journal of the National Cancer Institute, 66, 1192-1308.

Dominici, M., Le Blanc, K., Mueller, I., Slaper-Cortenbach, I., Marini, F. C., Krause, D. S., Deans, R. J., Keating, A., Prockop, D. J. & Horwitz, E. M. 2006. Minimal criteria for defining multipotent mesenchymal stromal cells. The International Society for Cellular Therapy position statement. Cytotherapy, 8, 315-317.

Dorfman, H. D. & Czerniak, B. 1998. Bone tumors. St. Louis: Mosby,1997.

Dottori, M., Pebay, A. & Pera, M. F. 2010. Neural differentiation of human embryonic stem cells. Protocols for Neural Cell Culture: Fourth Edition, 75-86.

Douma, S., Van Laar, T., Zevenhoven, J., Meuwissen, R., Van Garderen, E. & Peeper, D. S. 2004. Suppression of anoikis and induction of metastasis by the neurotrophic receptor TrkB. Nature, 430, 1034-1039.

Dragoo, J. L., Samimi, B., Zhu, M., Hame, S. L., Thomas, B. J., Lieberman, J. R., Hedrick, M. H. & Benhaim, P. 2003. Tissue-engineered cartilage and bone using stem cells from human infrapatellar fat pads. Bone & Joint Journal, 85, 740-747.

Dreesen, O., Ong, P. F., Chojnowski, A. & Colman, A. 2013. The contrasting roles of lamin B1 in cellular aging and human disease. Nucleus, 4, 283-290.

Driessens, G., Harsan, L., Robaye, B., Waroquier, D., Browaeys, P., Giannakopoulos, X., Velu, T. & Bruyns, C. 2003. Micronuclei to detect in vivo chemotherapy damage in a p53 mutated solid tumour. British journal of cancer, 89, 727.

Drissi, H., Hushka, D., Aslam, F., Nguyen, Q., Buffone, E., Koff, A., Van Wijnen, A. J., Lian, J. B., Stein, J. L. & Stein, G. S. 1999. The cell cycle regulator p27kip1 contributes to growth and differentiation of osteoblasts. Cancer research, 59, 3705-3711.

Drouin, C. A., Mongrain, E., Sasseville, D., Bouchard, H.-L. & Drouin, M. 1993. Rothmund-Thomson syndrome with osteosarcoma. Journal of the American Academy of Dermatology, 28, 301-305.

Ducy, P., Zhang, R., Geoffroy, V., Ridall, A. L. & Karsenty, G. 1997. Osf2/Cbfa1: a transcriptional activator of osteoblast differentiation. cell, 89, 747-754.

Ducy, P., Starbuck, M., Priemel, M., Shen, J., Pinero, G., Geoffroy, V., Amling, M. & Karsenty, G. 1999. A Cbfa1-dependent genetic pathway controls bone formation beyond embryonic development. Genes & development, 13, 1025-1036.

Ducy, P., Schinke, T. & Karsenty, G. 2000. The osteoblast: a sophisticated fibroblast under central surveillance. Science, 289, 1501-1504.

Dudley, D. D., Chaudhuri, J., Bassing, C. H. & Alt, F. W. 2005. Mechanism and control of V (D) J recombination versus class switch recombination: similarities and differences. Advances in immunology, 86, 43-112.

Dudley-Javoroski, S. & Shields, R. K. 2008. Dose estimation and surveillance of mechanical loading interventions for bone loss after spinal cord injury. Physical therapy, 88, 387-396.

Duesberg, P., Li, R., Fabarius, A. & Hehlmann, R. 2006. Aneuploidy and cancer: from correlation to causation. Infection and inflammation: impacts on oncogenesis. Karger Publishers.
Dunham, J. H. & Guthmiller, P. 2009. Doing good science: Authenticating cell line identity. Promega Notes, 101, 15-18.
Duong, L. T., Lakkakorpi, P. T., Nakamura, I., Machwate, M., Nagy, R. M. & Rodan, G. A. 1998. PYK2 in osteoclasts is an adhesion kinase, localized in the sealing zone, activated by ligation of alpha (v) beta3 integrin, and phosphorylated by src kinase. Journal of Clinical Investigation, 102, 881.
Durkin, S. G. & Glover, T. W. 2007. Chromosome fragile sites. Annu. Rev. Genet., 41, 169-192.
Dwek, J. R. 2010. The periosteum: what is it, where is it, and what mimics it in its absence? Skeletal radiology, 39, 319-323.
Dworaczek, H. & Xiao, W. 2007. Xeroderma pigmentosum: a glimpse into nucleotide excision repair, genetic instability, and cancer. Critical Reviews™ in Oncogenesis, 13.
Edwards, A., Civitello, A., Hammond, H. A. & Caskey, C. T. 1991. DNA typing and genetic mapping with trimeric and tetrameric tandem repeats. American journal of human genetics, 49, 746.
Edwards, A., Hammond, H. A., Jin, L., Caskey, C. T. & Chakraborty, R. 1992. Genetic variation at five trimeric and tetrameric tandem repeat loci in four human population groups. Genomics, 12, 241-253.
Eklund, E. A. 2007. The role of HOX genes in malignant myeloid disease. Current opinion in hematology, 14, 85-89.
El Ghamrasni, S., Pamidi, A., Halaby, M. J., Bohgaki, M., Cardoso, R., Li, L., Venkatesan, S., Sethu, S., Hirao, A. & Mak, T. W. 2011. Inactivation of chk2 and mus81 leads to impaired lymphocytes development, reduced genomic instability, and suppression of cancer. PLoS genetics, 7, e1001385.
Elbrecht, A., Chen, Y., Cullinan, C. A., Hayes, N., Leibowitz, M. D., Moller, D. E. & Berger, J. 1996. Molecular cloning, expression and characterization of human peroxisome proliferator activated receptors γ1 and γ2. Biochemical and biophysical research communications, 224, 431-437.
El-Deiry, W. S., Kern, S. E. & Pietenpol, J. 1992. p53 binding sites in transposons. Nat. Genet, 1, 45-49.
El-Khoury, J. M., Haddad, S. N. & Atallah, N. G. 1997. Osteosarcomatosis with Rothmund-Thomson syndrome. The British journal of radiology, 70, 215-218.
Elmore, S. 2007. Apoptosis: a review of programmed cell death. Toxicologic pathology, 35, 495-516.
El-Zein, R. A., Schabath, M. B., Etzel, C. J., Lopez, M. S., Franklin, J. D. & Spitz, M. R. 2006. Cytokinesis-blocked micronucleus assay as a novel biomarker for lung cancer risk. Cancer Research, 66, 6449-6456.
Emea 2009. assessment report for ChondroCelect Europena Medciines Agency 724428/2009
Emmott, E. & Goodfellow, I. 2014. Identification of Protein Interaction Partners in Mammalian Cells Using SILAC-immunoprecipitation Quantitative Proteomics. Journal of Visualized Experiments : JoVE, 51656.
Engler, A. J., Sen, S., Sweeney, H. L. & Discher, D. E. 2006. Matrix elasticity directs stem cell lineage specification. Cell, 126, 677-689.
Erbayraktar, Z., Alural, B., Erbayraktar, R. S. & Erkan, E. P. 2016. Cell division cycle 7-kinase inhibitor PHA-767491 hydrochloride suppresses glioblastoma growth and invasiveness. Cancer Cell International, 16, 88.
Erices, A., Conget, P. & Minguell, J. J. 2000. Mesenchymal progenitor cells in human umbilical cord blood. British journal of haematology, 109, 235-242.
Erickson, G. R., Gimble, J. M., Franklin, D. M., Rice, H. E., Awad, H. & Guilak, F. 2002. Chondrogenic potential of adipose tissue-derived stromal cells in vitro and in vivo. Biochemical and biophysical research communications, 290, 763-769.
Esen, E. & Long, F. 2014. Aerobic glycolysis in osteoblasts. Current osteoporosis reports, 12, 433-438.

Espejel, S., Franco, S., Sgura, A., Gae, D., Bailey, S. M., Taccioli, G. E. & Blasco, M. A. 2002. Functional interaction between DNA-PKcs and telomerase in telomere length maintenance. The EMBO journal, 21, 6275-6287.

Esterbauer, H., Eckl, P. & Ortner, A. 1990. Possible mutagens derived from lipids and lipid precursors. Mutation Research/Reviews in Genetic Toxicology, 238, 223-233.

Everts, V., De Vries, T. J. & Helfrich, M. H. 2009. Osteoclast heterogeneity:: Lessons from osteopetrosis and inflammatory conditions. Biochimica et Biophysica Acta (BBA) - Molecular Basis of Disease, 1792, 757-765.

Fahrner, M., Muik, M., Schindl, R., Butorac, C., Stathopulos, P., Zheng, L., Jardin, I., Ikura, M. & Romanin, C. 2014. A coiled-coil clamp controls both conformation and clustering of stromal interaction molecule 1 (STIM1). Journal of Biological Chemistry, 289, 33231-33244.

Falaschi, A., Abdurashidova, G. & Biamonti, G. 2010. DNA replication, development and cancer: a homeotic connection? Critical reviews in biochemistry and molecular biology, 45, 14-22.

Fan, W. & Luo, J. 2008. RecQ4 facilitates UV light-induced DNA damage repair through interaction with nucleotide excision repair factor xeroderma pigmentosum group A (XPA). Journal of Biological Chemistry, 283, 29037-29044.

Fang, H., Nie, L., Chi, Z., Liu, J., Guo, D., Lu, X., Hei, T. K., Balajee, A. S. & Zhao, Y. 2013. RecQL4 Helicase Amplification Is Involved in Human Breast Tumorigenesis. PLoS ONE, 8, e69600.

Fenech, M. 2000. The in vitro micronucleus technique. Mutation Research/Fundamental and Molecular Mechanisms of Mutagenesis, 455, 81-95.

Fenech, M. 2006. Cytokinesis-block micronucleus assay evolves into a “cytome” assay of chromosomal instability, mitotic dysfunction and cell death. Mutation Research/Fundamental and Molecular Mechanisms of Mutagenesis, 600, 58-66.

Fenech, M. 2009. A lifetime passion for micronucleus cytome assays—reflections from Down Under. Mutation Research/Reviews in Mutation Research, 681, 111-117.

Feng, J., Funk, W. D., Wang, S.-S., Weinrich, S. L., Avilion, A. A., Chiu, C.-P., Adams, R. R., Chang, E., Allsopp, R. C. & Yu, J. 1995. The RNA component of human telomerase. Science, 269, 1236-1241.

Ferrarelli, L. K., Popuri, V., Ghosh, A. K., Tadokoro, T., Canugovi, C., Hsu, J. K., Croteau, D. L. & Bohr, V. A. 2013. The RECQL4 protein, deficient in Rothmund–Thomson syndrome is active on telomeric D-loops containing DNA metabolism blocking lesions. DNA repair, 12, 518-528.

Fisher, D., Krasinska, L., Coudreuse, D. & Novák, B. 2012. Phosphorylation network dynamics in the control of cell cycle transitions. J Cell Sci, 125, 4703-4711.

Fitzgerald, J., Murillo, L. S., O'brien, G., O'connell, E., O'connor, A., Wu, K., Wang, G.-N., Rainey, M. D., Natoni, A. & Healy, S. 2014. A high through-put screen for small molecules modulating MCM2 phosphorylation identifies Ryuvidine as an inducer of the DNA damage response. PloS one, 9, e98891.

Flach, J., Bakker, S. T., Mohrin, M., Conroy, P. C., Pietras, E. M., Reynaud, D., Alvarez, S., Diolaiti, M. E., Ugarte, F. & Forsberg, E. C. 2014. Replication stress is a potent driver of functional decline in ageing haematopoietic stem cells. Nature, 512, 198.

Fletcher, C. D. M. 2014. The evolving classification of soft tissue tumours–an update based on the new 2013 WHO classification. Histopathology, 64, 2-11.

Foley, E. A. & Kapoor, T. M. 2013. Microtubule attachment and spindle assembly checkpoint signaling at the kinetochore. Nature reviews. Molecular cell biology, 14, 25.

Folmes, C. D. L., Nelson, T. J., Martinez-Fernandez, A., Arrell, D. K., Lindor, J. Z., Dzeja, P. P., Ikeda, Y., Perez-Terzic, C. & Terzic, A. 2011. Somatic oxidative bioenergetics transitions into pluripotency-dependent glycolysis to facilitate nuclear reprogramming. Cell metabolism, 14, 264-271.

Fontaine, C., Cousin, W., Plaisant, M., Dani, C. & Peraldi, P. 2008. Hedgehog signaling alters adipocyte maturation of human mesenchymal stem cells. Stem Cells, 26, 1037-1046.

Forman, J. J., Legesse-Miller, A. & Coller, H. A. 2008. A search for conserved sequences in coding regions reveals that the let-7 microRNA targets Dicer within its coding sequence. Proceedings of the National Academy of Sciences, 105, 14879-14884.
Forsburg, S. L. 2004. Eukaryotic MCM proteins: beyond replication initiation. Microbiology and Molecular Biology Reviews, 68, 109-131.
Fortini, P., Parlanti, E., Sidorkina, O. M., Laval, J. & Dogliotti, E. 1999. The type of DNA glycosylase determines the base excision repair pathway in mammalian cells. Journal of Biological Chemistry, 274, 15230-15236.
Fortini, P. & Dogliotti, E. 2007. Base damage and single-strand break repair: mechanisms and functional significance of short-and long-patch repair subpathways. DNA repair, 6, 398-409.
Franz-Odendaal, T. A., Hall, B. K. & Witten, P. E. 2006. Buried alive: how osteoblasts become osteocytes. Developmental Dynamics, 235, 176-190.
Fraser, J. K., Wulur, I., Alfonso, Z. & Hedrick, M. H. 2006. Fat tissue: an underappreciated source of stem cells for biotechnology. Trends in biotechnology, 24, 150-154.
Freire-Maia, N. 1971. Ectodermal dysplasias. Human heredity, 21, 309-312.
Friedberg, E. C., Walker, G. C., Siede, W. & Wood, R. D. 2005. DNA repair and mutagenesis, American Society for Microbiology Press.
Friedel, A. M., Pike, B. L. & Gasser, S. M. 2009. ATR/Mec1: coordinating fork stability and repair. Current opinion in cell biology, 21, 237-244.
Friedenstein, A. J., Chailakhjan, R. K. & Lalykina, K. S. 1970. The development of fibroblast colonies in monolayer cultures of guinea-pig bone marrow and spleen cells. Cell Proliferation, 3, 393-403.
Frisch, S. M. & Francis, H. 1994. Disruption of epithelial cell-matrix interactions induces apoptosis. The Journal of cell biology, 124, 619-626.
Frisch, S. M. & Ruoslahti, E. 1997. Integrins and anoikis. Current opinion in cell biology, 9, 701-706.
Frisch, S. M. & Screaton, R. A. 2001. Anoikis mechanisms. Current opinion in cell biology, 13, 555-562.
Frost, H. M. & Straatsma, C. R. 1964. Bone remodelling dynamics. LWW.
Fukazawa, H., Mizuno, S. & Uehara, Y. 1995. A microplate assay for quantitation of anchorage-independent growth of transformed cells. Analytical biochemistry, 228, 83-90.
Gagos, S. & Irminger-Finger, I. 2005. Chromosome instability in neoplasia: chaotic roots to continuous growth. The International Journal of Biochemistry & Cell Biology, 37, 1014-1033.
Galindo, M., Pratap, J., Young, D. W., Hovhannisyan, H., Im, H.-J., Choi, J.-Y., Lian, J. B., Stein, J. L., Stein, G. S. & Van Wijnen, A. J. 2005. The bone-specific expression of Runx2 oscillates during the cell cycle to support a G1-related antiproliferative function in osteoblasts. Journal of Biological Chemistry, 280, 20274-20285.
Galindo, M., Kahler, R. A., Teplyuk, N. M., Stein, J. L., Lian, J. B., Stein, G. S., Westendorf, J. J. & Van Wijnen, A. J. 2007. Cell cycle related modulations in Runx2 protein levels are independent of lymphocyte enhancer-binding factor 1 (Lef1) in proliferating osteoblasts. Journal of molecular histology, 38, 501-506.
Gandhi, M., Dillon, L. W., Pramanik, S., Nikiforov, Y. E. & Wang, Y.-H. 2010. DNA breaks at fragile sites generate oncogenic RET/PTC rearrangements in human thyroid cells. Oncogene, 29, 2272-2280.
Gao, H., Prasad, G. L. & Zacharias, W. 2014. Combusted but not smokeless tobacco products cause DNA damage in oral cavity cells. Environmental toxicology and pharmacology, 37, 1079-1089.
Gao, Z., Zhao, G. S., Lv, Y., Peng, D., Tang, X., Song, H. & Guo, Q N. 2019. Anoikis-resistant human osteosarcoma cells display significant angiogenesis by activating the Src kinase-mediated MAPK pathway. Oncology reports, 41,1, 235-245.
Garimella, R., Tadikonda, P., Tawfik, O., Gunewardena, S., Rowe, P. & Van Veldhuizen, P. 2017. Vitamin D Impacts the Expression of Runx2 Target Genes and Modulates Inflammation, Oxidative Stress and Membrane Vesicle Biogenesis Gene Networks in 143B Osteosarcoma Cells. International journal of molecular sciences, 18, 642.

Gasch, A. P., Spellman, P. T., Kao, C. M., Carmel-Harel, O., Eisen, M. B., Storz, G., Botstein, D. & Brown, P. O. 2000. Genomic expression programs in the response of yeast cells to environmental changes. Molecular biology of the cell, 11, 4241-4257.
Gaur, S., Wang, Y., Kretzner, L., Chen, L., Yen, T., Wu, X., Yuan, Y.-C., Davis, M. & Yen, Y. 2014. Pharmacodynamic and pharmacogenomic study of the nanoparticle conjugate of camptothecin CRLX101 for the treatment of cancer. Nanomedicine: Nanotechnology, Biology and Medicine, 10, 1477-1486.
Gayral, M., Jo, S., Hanoun, N., Vignolle-Vidoni, A., Lulka, H., Delpu, Y., Meulle, A., Dufresne, M., Humeau, M. & Du Rieu, M. C. 2014. MicroRNAs as emerging biomarkers and therapeutic targets for pancreatic cancer. World J Gastroenterol, 20, 11199-11209.
Geiersbach, K. B. & Samowitz, W. S. 2011. Microsatellite instability and colorectal cancer. Archives of pathology & laboratory medicine, 135, 1269-1277.
Geigl, J. B., Obenauf, A. C., Schwarzbraun, T. & Speicher, M. R. 2008. Defining 'chromosomal instability'. Trends in Genetics, 24, 64-69.
Gelfand, C. A., Plum, G. E., Grollman, A. P., Johnson, F. & Breslauer, K. J. 1998. Thermodynamic consequences of an abasic lesion in duplex DNA are strongly dependent on base sequence. Biochemistry, 37, 7321-7327.
Georgess, D., Machuca-Gayet, I., Blangy, A. & Jurdic, P. 2014. Podosome organization drives osteoclast-mediated bone resorption. Cell adhesion & migration, 8, 192-204.
Gerdes, J., Lemke, H., Baisch, H., Wacker, H.-H., Schwab, U. & Stein, H. 1984. Cell cycle analysis of a cell proliferation-associated human nuclear antigen defined by the monoclonal antibody Ki-67. The Journal of Immunology, 133, 1710-1715.
Ghosal, G. & Chen, J. 2013. DNA damage tolerance: a double-edged sword guarding the genome. Translational cancer research, 2, 107.
Ghosh, A. K., Rossi, M. L., Singh, D. K., Dunn, C., Ramamoorthy, M., Croteau, D. L., Liu, Y. & Bohr, V. A. 2012. RECQL4, the protein mutated in Rothmund-Thomson syndrome, functions in telomere maintenance. Journal of Biological Chemistry, 287, 196-209.
Giannakouros, P., Matte, I., Rancourt, C. & Piché, A. 2015. Transformation of NIH3T3 mouse fibroblast cells by MUC16 mucin (CA125) is driven by its cytoplasmic tail. International journal of oncology, 46, 91-98.
Gilbert, S. F. 2000. Osteogenesis: the development of bones. Developmental biology, 6.
Gillet, L. C. J. & Schärer, O. D. 2006. Molecular mechanisms of mammalian global genome nucleotide excision repair. Chemical reviews, 106, 253-276.
Giraldez, T., Hughes, T. E. & Sigworth, F. J. 2005. Generation of functional fluorescent BK channels by random insertion of GFP variants. The Journal of general physiology, 126, 429-438.
Girish, G., Finlay, K., Fessell, D., Pai, D., Dong, Q. & Jamadar, D. 2012. Imaging review of skeletal tumors of the pelvis malignant tumors and tumor mimics. The Scientific World Journal, 2012.
Godwin, J. W., Pinto, A. R. & Rosenthal, N. A. 2013. Macrophages are required for adult salamander limb regeneration. Proceedings of the National Academy of Sciences, 110, 9415-9420.
Gönczy, P. 2008. Mechanisms of asymmetric cell division: flies and worms pave the way. Nature reviews. Molecular cell biology, 9, 355.
Gonzalez-Suarez, E., Jacob, A. P., Jones, J., Miller, R., Roudier-Meyer, M. P., Erwert, R., Pinkas, J., Branstetter, D. & Dougall, W. C. 2010. RANK ligand mediates progestin-induced mammary epithelial proliferation and carcinogenesis. Nature, 468, 103-107.
Gonzalo, S., García-Cao, M., Fraga, M. F., Schotta, G., Peters, A. H. F. M., Cotter, S. E., Eguía, R., Dean, D. C., Esteller, M. & Jenuwein, T. 2005. Role of the RB1 family in stabilizing histone methylation at constitutive heterochromatin. Nature cell biology, 7, 420-428.
Goodarzi, A. A., Jeggo, P. & Lobrich, M. 2010. The influence of heterochromatin on DNA double strand break repair: Getting the strong, silent type to relax. DNA repair, 9, 1273-1282.

Goodarzi, A. A. & Jeggo, P. A. 2012. The heterochromatic barrier to DNA double strand break repair: how to get the entry visa. International journal of molecular sciences, 13, 11844-11860.
Goodwin, H. S., Bicknese, A. R., Chien, S. N., Bogucki, B. D., Oliver, D. A., Quinn, C. O. & Wall, D. A. 2001. Multilineage differentiation activity by cells isolated from umbilical cord blood: expression of bone, fat, and neural markers. Biology of Blood and Marrow Transplantation, 7, 581-588.
Gorgoulis, V. G., Vassiliou, L.-V. F., Karakaidos, P., Zacharatos, P., Kotsinas, A., Liloglou, T., Venere, M., Ditullio, R. A., Kastrinakis, N. G. & Levy, B. 2005. Activation of the DNA damage checkpoint and genomic instability in human precancerous lesions. Nature, 434, 907-913.
Gorgoulis, V.G., Pefani, D.E., Pateras, I.S. and Trougakos, I.P. 2018. Integrating the DNA damage and protein stress responses during cancer development and treatment. The Journal of pathology, 246,1,12-40.
Gorlick, R. 2002. Osteosarcoma: clinical practice and the expanding role of biology. Journal of Musculoskeletal and Neuronal Interactions, 2, 549-551.
Goshima, G., Kiyomitsu, T., Yoda, K. & Yanagida, M. 2003. Human centromere chromatin protein hMis12, essential for equal segregation, is independent of CENP-A loading pathway. The Journal of cell biology, 160, 25-39.
Goto, H., Natsume, T., Kanemaki, M.T., Kaito, A., Wang, S., Gabazza, E.C., Inagaki, M. & Mizoguchi, A. 2019. Chk1-mediated Cdc25A degradation as a critical mechanism for normal cell cycle progression. Journal of Cell Science, 132,2, 223123.
Gottifredi, V., Karni-Schmidt, O., Shieh, S.-Y. & Prives, C. 2001. p53 down-regulates CHK1 through p21 and the retinoblastoma protein. Molecular and cellular biology, 21, 1066-1076.
Granger, M. P., Wright, W. E. & Shay, J. W. 2002. Telomerase in cancer and aging. Critical reviews in oncology/hematology, 41, 29-40.
Grant, S. G., Wenger, S. L., Latimer, J. J., Thull, D. & Burke, L. 2000. Analysis of genomic instability using multiple assays in a patient with Rothmund–Thomson syndrome. Clinical genetics, 58, 209-215.
Gray, L. S., Perez-Reyes, E., Gamorra, J. C., Haverstick, D. M., Shattock, M., Mclatchie, L., Harper, J., Brooks, G., Heady, T. & Macdonald, T. L. 2004. The role of voltage gated T-type Ca 2+ channel isoforms in mediating “capacitative” Ca 2+ entry in cancer cells. Cell Calcium, 36, 489-497.
Greaves, M. & Maley, C. C. 2012. Clonal evolution in cancer. Nature, 481, 306-313.
Gregory, C. A., Gunn, W. G., Peister, A. & Prockop, D. J. 2004. An Alizarin red-based assay of mineralization by adherent cells in culture: comparison with cetylpyridinium chloride extraction. Analytical biochemistry, 329, 77-84.
Greider, C. W. 1999. Telomeres do D-loop–T-loop. Cell, 97, 419-422.
Greif, P., Yaghmaie, M., Konstandin, N., Ksienzyk, B., Alimoghaddam, K., Ghavamzadeh, A., Hauser, A., Graf, A., Krebs, S. & Blum, H. 2011. Somatic mutations in acute promyelocytic leukemia (APL) identified by exome sequencing. Leukemia, 25, 1519-1522.
Griffith, J. D., Comeau, L., Rosenfield, S., Stansel, R. M., Bianchi, A., Moss, H. & De Lange, T. 1999. Mammalian telomeres end in a large duplex loop. Cell, 97, 503-514.
Grimson, A., Farh, K. K.-H., Johnston, W. K., Garrett-Engele, P., Lim, L. P. & Bartel, D. P. 2007. MicroRNA targeting specificity in mammals: determinants beyond seed pairing. Molecular cell, 27, 91-105.
Grossmann, J. 2002. Molecular mechanisms of “detachment-induced apoptosis—Anoikis”. Apoptosis, 7, 247-260.
Grundy, G. J., Rulten, S. L., Zeng, Z., Arribas-Bosacoma, R., Iles, N., Manley, K., Oliver, A. & Caldecott, K. W. 2013. APLF promotes the assembly and activity of non-homologous end joining protein complexes. The EMBO journal, 32, 112-125.
Grzesiak, J., Marycz, K., Czogala, J., Wrzeszcz, K. & Nicpon, J. 2011. Comparison of behavior, morphology and morphometry of equine and canine adipose derived mesenchymal stem cells in culture. International Journal of Morphology, 29, 1012-1017.

Guck, J., Schinkinger, S., Lincoln, B., Wottawah, F., Ebert, S., Romeyke, M., Lenz, D., Erickson, H. M., Ananthakrishnan, R., Mitchell, D., Käs, J., Ulvick, S. & Bilby, C. 2005. Optical Deformability as an Inherent Cell Marker for Testing Malignant Transformation and Metastatic Competence. Biophysical Journal, 88, 3689-3698.

Guilak, F., Lott, K. E., Awad, H. A., Cao, Q., Hicok, K. C., Fermor, B. & Gimble, J. M. 2006. Clonal analysis of the differentiation potential of human adipose-derived adult stem cells. Journal of cellular physiology, 206, 229-237.

Guo, Z., Kumagai, A., Wang, S. X. & Dunphy, W. G. 2000. Requirement for Atr in phosphorylation of Chk1 and cell cycle regulation in response to DNA replication blocks and UV-damaged DNA in Xenopus egg extracts. Genes & development, 14, 2745-2756.

Guo, Y., Liu, J., Li, Y.-H., Song, T.-B., Wu, J., Zheng, C.-X. & Xue, C.-F. 2005. Effect of vector-expressed shRNAs on hTERT expression. World Journal of Gastroenterology: WJG, 11, 2912.

Gupta, A., Cao, W. & Chellaiah, M. A. 2012. Integrin αvβ3 and CD44 pathways in metastatic prostate cancer cells support osteoclastogenesis via a Runx2/Smad 5/receptor activator of NF-κB ligand signaling axis. Molecular cancer, 11, 66.

Gupta, S., De, S., Srivastava, V., Hussain, M., Kumari, J., Muniyappa, K. & Sengupta, S. 2013. RECQL4 and p53 potentiate the activity of polymerase γ and maintain the integrity of the human mitochondrial genome. Carcinogenesis, bgt315.

Gustafsson, C. M., Falkenberg, M. & Larsson, N.-G. 2016. Maintenance and expression of mammalian mitochondrial DNA. Annual review of biochemistry, 85, 133-160.

Haaf, T., Raderschall, E., Reddy, G., Ward, D. C., Radding, C. M. & Golub, E. I. 1999. Sequestration of mammalian Rad51-recombination protein into micronuclei. The Journal of cell biology, 144, 11-20.

Hafian, H., Venteo, L., Sukhanova, A., Nabiev, I., Lefevre, B. T. & Pluot, M. 2004. Immunohistochemical study of DNA topoisomerase I, DNA topoisomerase IIα, p53, and Ki-67 in oral preneoplastic lesions and oral squamous cell carcinomas. Human pathology, 35, 745-751.

Hahn, W. C., Counter, C. M., Lundberg, A. S., Beijersbergen, R. L., Brooks, M. W. & Weinberg, R. A. 1999. Creation of human tumour cells with defined genetic elements. Nature, 400, 464-468.

Hahn, W. C. 2003. Role of telomeres and telomerase in the pathogenesis of human cancer. Journal of Clinical Oncology, 21, 2034-2043.

Håkelien, A. M., Bryne, J. C., Harstad, K. G., Lorenz, S., Paulsen, J., Sun, J., Mikkelsen, T. S., Myklebost, O. & Meza-Zepeda, L. A. 2014. The regulatory landscape of osteogenic differentiation. Stem Cells, 32, 2780-2793.

Halazonetis, T. D., Gorgoulis, V. G. & Bartek, J. 2008. An oncogene-induced DNA damage model for cancer development. science, 319, 1352-1355.

Halbleib, J. M. & Nelson, W. J. 2006. Cadherins in development: cell adhesion, sorting, and tissue morphogenesis. Genes & development, 20, 3199-3214.

Hall, M. P., Unch, J., Binkowski, B. F., Valley, M. P., Butler, B. L., Wood, M. G., Otto, P., Zimmerman, K., Vidugiris, G. & Machleidt, T. 2012. Engineered luciferase reporter from a deep sea shrimp utilizing a novel imidazopyrazinone substrate. ACS chemical biology, 7, 1848.

Hällberg, B. M. & Larsson, N.-G. 2014. Making proteins in the powerhouse. Cell metabolism, 20, 226-240.

Hameed, O., Wei, S. & Siegal, G. P. 2011. Bone/Osteoid Producing Lesions. Frozen Section Library: Bone. Springer.

Hampel, B., Wagner, M., Teis, D., Zwerschke, W., Huber, L. A. & Jansen-Dürr, P. 2005. Apoptosis resistance of senescent human fibroblasts is correlated with the absence of nuclear IGFBP-3. Aging cell, 4, 325-330.

Hampel, B., Wagner, M., Teis, D., Zwerschke, W., Huber, L. A. & Jansen-Dürr, P. 2005. Apoptosis resistance of senescent human fibroblasts is correlated with the absence of nuclear IGFBP-3. Aging cell, 4, 325-330.

Hampoelz, B. & Lecuit, T. 2011. Nuclear mechanics in differentiation and development. Current opinion in cell biology, 23, 668-675.

Hanahan, D. & Weinberg, R. A. 2000. The hallmarks of cancer. cell, 100, 57-70.

Hanahan, D. & Coussens, L. M. 2012. Accessories to the crime: functions of cells recruited to the tumor microenvironment. Cancer cell, 21, 309-322.
Hanasoge, S. & Ljungman, M. 2007. H2AX phosphorylation after UV irradiation is triggered by DNA repair intermediates and is mediated by the ATR kinase. Carcinogenesis, 28, 2298-2304.
Hanawalt, P. C. & Spivak, G. 2008. Transcription-coupled DNA repair: two decades of progress and surprises. Nature reviews. Molecular cell biology, 9, 958.
Hanssen-Bauer, A., Solvang-Garten, K., Sundheim, O., Peña-Diaz, J., Andersen, S., Slupphaug, G., Krokan, H. E., Wilson, D. M., Akbari, M. & Otterlei, M. 2011. XRCC1 coordinates disparate responses and multiprotein repair complexes depending on the nature and context of the DNA damage. Environmental and molecular mutagenesis, 52, 623-635.
Harada, S.-I. & Rodan, G. A. 2003. Control of osteoblast function and regulation of bone mass. Nature, 423, 349-355.
Hardingham, T. E., Oldershaw, R. A. & Tew, S. R. 2006. Cartilage, SOX9 and Notch signals in chondrogenesis. Journal of anatomy, 209, 469-480.
Harley, C. B., Vaziri, H., Counter, C. M. & Allsopp, R. C. 1992. The telomere hypothesis of cellular aging. Experimental gerontology, 27, 375-382.
Harrison, D.J., Geller, D.S., Gill, J.D., Lewis, V.O. and Gorlick, R. 2018. Current and future therapeutic approaches for osteosarcoma. Expert review of anticancer therapy, 18,1, 39-50.
Hartwell, L. H. & Kastan, M. B. 1994. Cell cycle control and cancer. Science-AAAS-Weekly Paper Edition, 266, 1821-1828.
Hasebe-Takada, N., Kono, K., Yasuda, S., Sawada, R., Matsuyama, A. & Sato, Y. 2016. Application of cell growth analysis to the quality assessment of human cell-processed therapeutic products as a testing method for immortalized cellular impurities. Regenerative Therapy, 5, 49-54.
Hausman, G. J., Hausman, D. B. & Martin, R. J. 1992. Biochemical and cytochemical studies of preadipocyte differentiation in serum-free culture of porcine stromal-vascular cells: interaction of dexamethasone and growth hormone. Cells Tissues Organs, 143, 322-329.
Haydon, R. C., Luu, H. H. & He, T.-C. 2007. Osteosarcoma and osteoblastic differentiation: a new perspective on oncogenesis. Clinical orthopaedics and related research, 454, 237-246.
Hayflick, L. & Moorhead, P. S. 1961. The serial cultivation of human diploid cell strains. Experimental cell research, 25, 585-621.
Hayflick, L. 1965. The limited in vitro lifetime of human diploid cell strains. Experimental cell research, 37, 614-636.
Haynes, L., Kaste, S. C., Ness, K. K., Wu, J., Ortega-Laureano, L., Bishop, M., Neel, M., Rao, B. & Fernandez-Pineda, I. 2017. Pathologic fracture in childhood and adolescent osteosarcoma: A single-institution experience. Pediatric blood & cancer, 64.
He, Y. & Smith, R. 2009. Nuclear functions of heterogeneous nuclear ribonucleoproteins A/B. Cellular and molecular life sciences, 66, 1239-1256.
Heaphy, C. M., De Wilde, R. F., Jiao, Y., Klein, A. P., Edil, B. H., Shi, C., Bettegowda, C., Rodriguez, F. J., Eberhart, C. G., Hebbar, S., Offerhaus, G. J., Mclendon, R., Rasheed, B. A., He, Y., Yan, H., Bigner, D. D., Oba-Shinjo, S. M., Marie, S. K. N., Riggins, G. J., Kinzler, K. W., Vogelstein, B., Hruban, R. H., Maitra, A., Papadopoulos, N. & Meeker, A. K. 2011a. Altered Telomeres in Tumors with ATRX and DAXX Mutations. Science, 333, 425-425.
Heaphy, C. M., Subhawong, A. P., Hong, S.-M., Goggins, M. G., Montgomery, E. A., Gabrielson, E., Netto, G. J., Epstein, J. I., Lotan, T. L. & Westra, W. H. 2011b. Prevalence of the alternative lengthening of telomeres telomere maintenance mechanism in human cancer subtypes. The American journal of pathology, 179, 1608-1615.
Hecht, S. S., Mcintee, E. J. & Wang, M. 2001. New DNA adducts of crotonaldehyde and acetaldehyde. Toxicology, 166, 31-36.

Heckman, C. A. 2009. Contact inhibition revisited. Journal of cellular physiology, 220, 574-575.
Hees, C. L. M., Duinen, C. L. M., Bruijin, J. A. & Vermeer, B. J. 1996. Malignant eccrine poroma in a patient with Rothmiund-Thomson syndrome. British Journal of Dermatology, 134, 813-815.
Heffernan, T. P., Ünsal-Kaçmaz, K., Heinloth, A. N., Simpson, D. A., Paules, R. S., Sancar, A., Cordeiro-Stone, M. & Kaufmann, W. K. 2007. Cdc7-Dbf4 and the human S checkpoint response to UVC. Journal of Biological Chemistry, 282, 9458-9468.
Heinsohn, S., Evermann, U., Zur Stadt, U., Bielack, S. & Kabisch, H. 2007. Determination of the prognostic value of loss of heterozygosity at the retinoblastoma gene in osteosarcoma. International journal of oncology, 30, 1205-1214.
Helman, L. J. & Meltzer, P. 2003. Mechanisms of sarcoma development. Nature reviews. Cancer, 3, 685.
Helt, C. E., Cliby, W. A., Keng, P. C., Bambara, R. A. & O'reilly, M. A. 2005. Ataxia telangiectasia mutated (ATM) and ATM and Rad3-related protein exhibit selective target specificities in response to different forms of DNA damage. Journal of Biological Chemistry, 280, 1186-1192.
Henson, J. D., Neumann, A. A., Yeager, T. R. & Reddel, R. R. 2002. Alternative lengthening of telomeres in mammalian cells. oncogene, 21, 598.
Heo, K., Kim, H., Choi, S. H., Choi, J., Kim, K., Gu, J., Lieber, M. R., Yang, A. S. & An, W. 2008. FACT-mediated exchange of histone variant H2AX regulated by phosphorylation of H2AX and ADP-ribosylation of Spt16. Molecular cell, 30, 86-97.
Hernandez, C., Beaupre, G. & Carter, D. 2003. A theoretical analysis of the relative influences of peak BMD, age-related bone loss and menopause on the development of osteoporosis. Osteoporosis international, 14, 843-847.
Hickerson, D. H. M., White, H. S., Nguyen, A., Nieman, E., Meadows, N., Gentry, T., Foster, S. J., Balber, A. E., Fiordalisi, M. & Hinson, J. M. 2014. Development of a flow cytometry–based pulse-width assay for detection of aggregates in cellular therapeutics to be infused by catheter. Cytotherapy, 16, 1545-1557.
Hicks, M. J., Roth, J. R., Kozinetz, C. A. & Wang, L. L. 2007. Clinicopathologic features of osteosarcoma in patients with Rothmund-Thomson syndrome. Journal of clinical oncology, 25, 370-375.
Hida, K., Hida, Y., Amin, D. N., Flint, A. F., Panigrahy, D., Morton, C. C. & Klagsbrun, M. 2004. Tumor-associated endothelial cells with cytogenetic abnormalities. Cancer research, 64, 8249-8255.
Hoege, C. & Hyman, A. A. 2013. Principles of PAR polarity in Caenorhabditis elegans embryos. Nature reviews. Molecular cell biology, 14, 315.
Hofer, A. C., Tran, R. T., Aziz, O. Z., Wright, W., Novelli, G., Shay, J. & Lewis, M. 2005. Shared phenotypes among segmental progeroid syndromes suggest underlying pathways of aging. The Journals of Gerontology Series A: Biological Sciences and Medical Sciences, 60, 10-20.
Hoki, Y., Araki, R., Fujimori, A., Ohhata, T., Koseki, H., Fukumura, R., Nakamura, M., Takahashi, H., Noda, Y. & Kito, S. 2003. Growth retardation and skin abnormalities of the Recql4-deficient mouse. Human molecular genetics, 12, 2293-2299.
Holland, P. W., Booth, H. a. F. & Bruford, E. A. 2007. Classification and nomenclature of all human homeobox genes. BMC biology, 5, 1.
Holliday, R. & Ho, T. 1998. Gene silencing and endogenous DNA methylation in mammalian cells. Mutation Research/Fundamental and Molecular Mechanisms of Mutagenesis, 400, 361-368.
Honda, S., Hayashi, S., Imoto, I., Toyama, J., Okazawa, H., Nakagawa, E., Goto, Y.-I. & Inazawa, J. 2010. Copy-number variations on the X chromosome in Japanese patients with mental retardation detected by array-based comparative genomic hybridization analysis. Journal of human genetics, 55, 590-599.
Hong, K. U., Kim, E., Bae, C.-D. & Park, J. 2009. TMAP/CKAP2 is essential for proper chromosome segregation. Cell Cycle, 8, 314-324.
Hong, A.M., Millington, S., Ahern, V., McCowage, G., Boyle, R., Tattersall, M., Haydu, L. and Stalley, P.D. 2013. Limb preservation surgery with extracorporeal irradiation in

the management of malignant bone tumor: the oncological outcomes of 101 patients. Annals of Oncology, 24, 10, 2676-2680.
Horwitz, E. M., Prockop, D. J., Fitzpatrick, L. A., Koo, W. W. K., Gordon, P. L., Neel, M., Sussman, M., Orchard, P., Marx, J. C. & Pyeritz, R. E. 1999. Transplantability and therapeutic effects of bone marrow-derived mesenchymal cells in children with osteogenesis imperfecta. Nature medicine, 5.
Hoshino, A., Costa-Silva, B., Shen, T.-L., Rodrigues, G., Hashimoto, A., Mark, M. T., Molina, H., Kohsaka, S., Di Giannatale, A. & Ceder, S. 2015. Tumour exosome integrins determine organotropic metastasis. Nature, 527, 329.
Howell, S. M. & Bray, D. W. 2008. Amelanotic melanoma in a patient with Rothmund-Thomson syndrome. Archives of dermatology, 144, 416-417.
Hsiang, Y.-H., Hertzberg, R., Hecht, S. & Liu, L. F. 1985. Camptothecin induces protein-linked DNA breaks via mammalian DNA topoisomerase I. Journal of Biological Chemistry, 260, 14873-14878.
Hsu, S., Bollag, W. B., Lewis, J., Huang, Q., Singh, B., Sharawy, M., Yamamoto, T. & Schuster, G. 2003. Green tea polyphenols induce differentiation and proliferation in epidermal keratinocytes. Journal of Pharmacology and Experimental Therapeutics, 306, 29-34.
Hu, J., Selby, C.P., Adar, S., Adebali, O. and Sancar, A. 2017. Molecular mechanisms and genomic maps of DNA excision repair in Escherichia coli and humans. Journal of Biological Chemistry, 292,38, 15588-15597.
Huang, J. I., Kazmi, N., Durbhakula, M. M., Hering, T. M., Yoo, J. U. & Johnstone, B. 2005. Chondrogenic potential of progenitor cells derived from human bone marrow and adipose tissue: A patient-matched comparison. Journal of Orthopaedic Research, 23, 1383-1389.
Huang, G.-J., Gronthos, S. & Shi, S. 2009a. Mesenchymal stem cells derived from dental tissues vs. those from other sources: their biology and role in regenerative medicine. Journal of dental research, 88, 792-806.
Huang, S., Ernberg, I. & Kauffman, S. 2009b. Cancer attractors: a systems view of tumors from a gene network dynamics and developmental perspective. Seminars in cell & developmental biology. Elsevier, 869-876.
Huang, S. 2013. Genetic and non-genetic instability in tumor progression: link between the fitness landscape and the epigenetic landscape of cancer cells. Cancer and Metastasis Reviews, 32, 423-448.
Huggett, M. T., Tudzarova, S., Proctor, I., Loddo, M., Keane, M. G., Stoeber, K., Williams, G. H. & Pereira, S. P. 2016. Cdc7 is a potent anti-cancer target in pancreatic cancer due to abrogation of the DNA origin activation checkpoint. Oncotarget, 7, 18495-18507.
Hughes, D. P. M., Thomas, D. G., Giordano, T. J., Mcdonagh, K. T. & Baker, L. H. 2006. Essential erbB family phosphorylation in osteosarcoma as a target for CI-1033 inhibition. Pediatric blood & cancer, 46, 614-623.
Hutmacher, D. W., Horch, R. E., Loessner, D., Rizzi, S., Sieh, S., Reichert, J. C., Clements, J. A., Beier, J. P., Arkudas, A. & Bleiziffer, O. 2009. Translating tissue engineering technology platforms into cancer research. Journal of cellular and molecular medicine, 13, 1417-1427.
Huttenlocher, A., Lakonishok, M., Kinder, M., Wu, S., Truong, T., Knudsen, K. A. & Horwitz, A. F. 1998. Integrin and cadherin synergy regulates contact inhibition of migration and motile activity. The Journal of cell biology, 141, 515-526.
Huvos, A. 1993. Osteosarcoma in adolescents and young adults: new developments and controversies. Commentary on pathology. Cancer treatment and research, 62, 375.
Ichijima, Y., Sakasai, R., Okita, N., Asahina, K., Mizutani, S. & Teraoka, H. 2005. Phosphorylation of histone H2AX at M phase in human cells without DNA damage response. Biochemical and biophysical research communications, 336, 807-812.
Ichikawa, K., Noda, T. & Furuichi, Y. 2002. [Preparation of the gene targeted knockout mice for human premature aging diseases, Werner syndrome, and Rothmund-Thomson syndrome caused by the mutation of DNA helicases]. Nihon yakurigaku zasshi. Folia pharmacologica Japonica, 119, 219-226.

Im, J.-S. & Lee, J.-K. 2008. ATR-dependent activation of p38 MAP kinase is responsible for apoptotic cell death in cells depleted of Cdc7. Journal of Biological Chemistry, 283, 25171-25177.
Im, J.-S., Ki, S.-H., Farina, A., Jung, D.-S., Hurwitz, J. & Lee, J.-K. 2009. Assembly of the Cdc45-Mcm2–7-GINS complex in human cells requires the Ctf4/And-1, RecQL4, and Mcm10 proteins. Proceedings of the National Academy of Sciences, 106, 15628-15632.
Im, J. S., Park, S. Y., Cho, W. H., Bae, S. H., Hurwitz, J. & Lee, J. K. 2015. RecQL4 is required for the association of Mcm10 and Ctf4 with replication origins in human cells. Cell Cycle, 14, 1001-9.
Inoue, R., Matsuki, N. A., Jing, G., Kanematsu, T., Abe, K. & Hirata, M. 2005. The inhibitory effect of alendronate, a nitrogen-containing bisphosphonate on the PI3K–Akt–NFκB pathway in osteosarcoma cells. British journal of pharmacology, 146, 633-641.
Inouye, H., Michaelis, S., Wright, A. & Beckwith, J. 1981. Cloning and restriction mapping of the alkaline phosphatase structural gene (phoA) of Escherichia coli and generation of deletion mutants in vitro. Journal of bacteriology, 146, 668-675.
Ionov, Y., Peinado, M. A., Malkhosyan, S., Shibata, D. & Perucho, M. 1993. Ubiquitous somatic mutations in simple repeated sequences reveal a new mechanism for colonic carcinogenesis. Nature, 363, 558-561.
Ishikawa, F., Matunis, M. J., Dreyfuss, G. & Cech, T. R. 1993. Nuclear proteins that bind the pre-mRNA 3'splice site sequence r (UUAG/G) and the human telomeric DNA sequence d (TTAGGG) n. Molecular and cellular biology, 13, 4301-4310.
Ito, S., Ishii, A., Kakusho, N., Taniyama, C., Yamazaki, S., Fukatsu, R., Sakaue-Sawano, A., Miyawaki, A. & Masai, H. 2012. Mechanism of cancer cell death induced by depletion of an essential replication regulator. PloS one, 7, e36372.
Ito, Y., Bae, S.-C. & Chuang, L. S. H. 2015. The RUNX family: developmental regulators in cancer. Nature Reviews. Cancer, 15, 81.
Ito, Y., Fitzsimmons, J. S., Sanyal, A., Mello, M. A., Mukherjee, N. & O'driscoll, S. W. 2001. Localization of chondrocyte precursors in periosteum. Osteoarthritis and Cartilage, 9, 215-223.
Ivascu, A. & Kubbies, M. 2007. Diversity of cell-mediated adhesions in breast cancer spheroids. International journal of oncology, 31, 1403-1414.
Jackson, A. L. & Loeb, L. A. 2001. The contribution of endogenous sources of DNA damage to the multiple mutations in cancer. Mutation Research/Fundamental and Molecular Mechanisms of Mutagenesis, 477, 7-21.
Jackson, A. L. & Linsley, P. S. 2004. Noise amidst the silence: off-target effects of siRNAs? TRENDS in Genetics, 20, 521-524.
Jackson, A. L., Burchard, J., Schelter, J., Chau, B. N., Cleary, M., Lim, L. & Linsley, P. S. 2006. Widespread siRNA “off-target” transcript silencing mediated by seed region sequence complementarity. Rna, 12, 1179-1187.
Jacobsen, L. B., Calvin, S. A., Colvin, K. E. & Wright, M. 2004. FuGENE 6 transfection reagent: the gentle power. Methods, 33, 104-112.
Jagannathan, M., Sakwe, A. M., Nguyen, T. & Frappier, L. 2012. The MCM-associated protein MCM-BP is important for human nuclear morphology. Journal of Cell Science, 125, 133-143.
Jaiswal, R. K., Jaiswal, N., Bruder, S. P., Mbalaviele, G., Marshak, D. R. & Pittenger, M. F. 2000. Adult human mesenchymal stem cell differentiation to the osteogenic or adipogenic lineage is regulated by mitogen-activated protein kinase. Journal of Biological Chemistry, 275, 9645-9652.
Jakob, B., Splinter, J., Conrad, S., Voss, K.-O., Zink, D., Durante, M., Löbrich, M. & Taucher-Scholz, G. 2011. DNA double-strand breaks in heterochromatin elicit fast repair protein recruitment, histone H2AX phosphorylation and relocation to euchromatin. Nucleic acids research, 39, 6489-6499.
Janss, A. J., Levow, C., Bernhard, E. J., Muschel, R. J., Mckenna, W. G., Sutton, L. & Phillips, P. C. 1998. Caffeine and staurosporine enhance the cytotoxicity of cisplatin and camptothecin in human brain tumor cell lines. Experimental cell research, 243, 29-38.

Javed, A., Barnes, G. L., Pratap, J., Antkowiak, T., Gerstenfeld, L. C., Van Wijnen, A. J., Stein, J. L., Lian, J. B. & Stein, G. S. 2005. Impaired intranuclear trafficking of Runx2 (AML3/CBFA1) transcription factors in breast cancer cells inhibits osteolysis in vivo. Proceedings of the National Academy of Sciences of the United States of America, 102, 1454-1459.

Jayaraman, S. 2005. Flow cytometric determination of mitochondrial membrane potential changes during apoptosis of T lymphocytic and pancreatic beta cell lines: Comparison of tetramethylrhodamineethylester (TMRE), chloromethyl-X-rosamine (H2-CMX-Ros) and MitoTracker Red 580 (MTR580). Journal of Immunological Methods, 306, 68-79.

Jee, W. S. S. 1988. The skeletal tissues. Cell and tissue biology: a textbook of histology, 213-217.

Jeffreys, A., Wilson, V. & Thein, S. L. 1985a. Individual-specific 'fingerprints' of human DNA. Nature, 316, 4.

Jeffreys, A. J., Wilson, V. & Thein, S. L. 1985b. Hypervariable'minisatellite' regions in human DNA. Nature, 314, 67-73.

Jeggo, P. A. & Löbrich, M. 2015. How cancer cells hijack DNA double-strand break repair pathways to gain genomic instability. Biochemical Journal, 471, 1-11.

Jevprasesphant, R., Penny, J., Jalal, R., Attwood, D., Mckeown, N. B. & D'emanuele, A. 2003. The influence of surface modification on the cytotoxicity of PAMAM dendrimers. International Journal of Pharmaceutics, 252, 263-266.

Jiang, X.-R., Jimenez, G., Chang, E., Frolkis, M., Kusler, B., Sage, M., Beeche, M., Bodnar, A. G., Wahl, G. M. & Tlsty, T. D. 1999. Telomerase expression in human somatic cells does not induce changes associated with a transformed phenotype. Nature genetics, 21, 111-114.

Jin, W., Liu, H., Zhang, Y., Otta, S. K., Plon, S. E. & Wang, L. L. 2008. Sensitivity of RECQL4-deficient fibroblasts from Rothmund–Thomson syndrome patients to genotoxic agents. Human genetics, 123, 643-653.

Jinka, R., Kapoor, R., Sistla, P. G., Raj, T. A. & Pande, G. 2012. Alterations in cell-extracellular matrix interactions during progression of cancers. International journal of cell biology, 2012.

Jögi, A., Vaapil, M., Johansson, M. & Påhlman, S. 2012. Cancer cell differentiation heterogeneity and aggressive behavior in solid tumors. Upsala Journal of Medical Sciences, 117, 217-224.

Jones, L. J., Gray, M., Yue, S. T., Haugland, R. P. & Singer, V. L. 2001. Sensitive determination of cell number using the CyQUANT® cell proliferation assay. Journal of immunological methods, 254, 85-98.

Jones, D. H., Nakashima, T., Sanchez, O. H., Kozieradzki, I., Komarova, S. V., Sarosi, I., Morony, S., Rubin, E., Sarao, R. & Hojilla, C. V. 2006. Regulation of cancer cell migration and bone metastasis by RANKL. Nature, 440, 692-696.

Jones, D. S., Podolsky, S. H. & Greene, J. A. 2012. The burden of disease and the changing task of medicine. New England Journal of Medicine, 366, 2333-2338.

Jönsson, S., Hjorth-Hansen, H., Olsson, B., Wadenvik, H., Sundan, A. & Standal, T. 2012. Imatinib inhibits proliferation of human mesenchymal stem cells and promotes early but not late osteoblast differentiation in vitro. Journal of bone and mineral metabolism, 30, 119-123.

Jun, E. S., Lee, T. H., Cho, H. H., Suh, S. Y. & Jung, J. S. 2004. Expression of telomerase extends longevity and enhances differentiation in human adipose tissue-derived stromal cells. Cellular Physiology and Biochemistry, 14, 261-268.

Jung, S., Panchalingam, K. M., Wuerth, R. D., Rosenberg, L. & Behie, L. A. 2012. Large-scale production of human mesenchymal stem cells for clinical applications. Biotechnology and applied biochemistry, 59, 106-120.

Junqueira, L., Carneiro, J. & Kelley, R. O. 1998. Basic histology. 9th. Stamford, Conn.: Appleton & Lange. x.

Justesen, J., Stenderup, K., Ebbesen, E. N., Mosekilde, L., Steiniche, T. & Kassem, M. 2001. Adipocyte tissue volume in bone marrow is increased with aging and in patients with osteoporosis. Biogerontology, 2, 165-171.

Kajkenova, O., Lecka-Czernik, B., Gubrij, I., Hauser, S. P., Takahashi, K., Parfitt, A. M., Jilka, R. L., Manolagas, S. C. & Lipschitz, D. A. 1997. Increased adipogenesis and myelopoiesis in the bone marrow of SAMP6, a murine model of defective osteoblastogenesis and low turnover osteopenia. Journal of Bone and Mineral Research, 12, 1772-1779.

Kalkwarf, H. J., Laor, T. & Bean, J. A. 2011. Fracture risk in children with a forearm injury is associated with volumetric bone density and cortical area (by peripheral QCT) and areal bone density (by DXA). Osteoporosis international, 22, 607-616.

Kamma, H., Fujimoto, M., Fujiwara, M., Matsui, M., Horiguchi, H., Hamasaki, M. & Satoh, H. 2001. Interaction of hnRNP A2/B1 isoforms with telomeric ssDNA and the in vitro function. Biochemical and biophysical research communications, 280, 625-630.

Kang, S. K., Lee, D. H., Bae, Y. C., Kim, H. K., Baik, S. Y. & Jung, J. S. 2003. Improvement of neurological deficits by intracerebral transplantation of human adipose tissue-derived stromal cells after cerebral ischemia in rats. Experimental neurology, 183, 355-366.

Kang, S. K., Putnam, L., Dufour, J., Ylostalo, J., Jung, J. S. & Bunnell, B. A. 2004a. Expression of Telomerase Extends the Lifespan and Enhances Osteogenic Differentiation of Adipose Tissue–Derived Stromal Cells. Stem cells, 22, 1356-1372.

Kang, S. K., Putnam, L. A., Ylostalo, J., Popescu, I. R., Dufour, J., Belousov, A. & Bunnell, B. A. 2004b. Neurogenesis of Rhesus adipose stromal cells. Journal of cell science, 117, 4289-4299.

Kang, H.-G., Jenabi, J. M., Zhang, J., Keshelava, N., Shimada, H., May, W. A., Ng, T., Reynolds, C. P., Triche, T. J. & Sorensen, P. H. B. 2007. E-cadherin cell-cell adhesion in ewing tumor cells mediates suppression of anoikis through activation of the ErbB4 tyrosine kinase. Cancer research, 67, 3094-3105.

Kang, S., Kang, M.S., Ryu, E. & Myung, K. 2018. Eukaryotic DNA replication: Orchestrated action of multi-subunit protein complexes. Mutation Research/Fundamental and Molecular Mechanisms of Mutagenesis, 809, 58-69.

Kapinas, K., Grandy, R., Ghule, P., Medina, R., Becker, K., Pardee, A., Zaidi, S. K., Lian, J., Stein, J. & Van Wijnen, A. 2013. The abbreviated pluripotent cell cycle. Journal of cellular physiology, 228, 9-20.

Karimian, E., Chagin, A. S. & Sävendahl, L. 2011. Genetic regulation of the growth plate. Frontiers in endocrinology, 2.

Karimian, E., Chagin, A. S., Gjerde, J., Heino, T., Lien, E. A., Ohlsson, C. & Sävendahl, L. 2008. Tamoxifen impairs both longitudinal and cortical bone growth in young male rats. Journal of Bone and Mineral Research, 23, 1267-1277.

Karlseder, J., Broccoli, D., Dai, Y., Hardy, S. & De Lange, T. 1999. p53-and ATM-dependent apoptosis induced by telomeres lacking TRF2. Science, 283, 1321-1325.

Karnani, N. & Dutta, A. 2011. The effect of the intra-S-phase checkpoint on origins of replication in human cells. Genes & development, 25, 621-633.

Karpova, T. S., Baumann, C. T., He, L., Wu, X., Grammer, A., Lipsky, P., Hager, G. L. & Mcnally, J. G. 2003. Fluorescence resonance energy transfer from cyan to yellow fluorescent protein detected by acceptor photobleaching using confocal microscopy and a single laser. Journal of microscopy, 209, 56-70.

Kataoka, Y., Bindokas, V. P., Duggan, R. C., Murley, J. S. & Grdina, D. J. 2006. Flow cytometric analysis of phosphorylated histone H2AX following exposure to ionizing radiation in human microvascular endothelial cells. Journal of radiation research, 47, 245-257.

Kavanagh, J. N., Redmond, K. M., Schettino, G. & Prise, K. M. 2013. DNA double strand break repair: a radiation perspective. Antioxidants & redox signaling, 18, 2458-2472.

Kawai, M., De Paula, F. J. A. & Rosen, C. J. 2012. New insights into osteoporosis: the bone–fat connection. Journal of internal medicine, 272, 317-329.

Kawanishi, S., Hiraku, Y., Pinlaor, S. & Ma, N. 2006. Oxidative and nitrative DNA damage in animals and patients with inflammatory diseases in relation to inflammation-related carcinogenesis. Biological chemistry, 387, 365-372.

Kaya, M., Wada, T., Akatsuka, T., Kawaguchi, S., Nagoya, S., Shindoh, M., Higashino, F., Mezawa, F., Okada, F. & Ishii, S. 2000. Vascular endothelial growth factor

expression in untreated osteosarcoma is predictive of pulmonary metastasis and poor prognosis. Clinical Cancer Research, 6, 572-577.
Kellermayer, R., Siitonen, H. A., Hadzsiev, K., Kestilä, M. & Kosztolányi, G. 2005. A patient with Rothmund-Thomson syndrome and all features of RAPADILINO. Archives of dermatology, 141, 617-620.
Kennedy, B. K., Berger, S. L., Brunet, A., Campisi, J., Cuervo, A. M., Epel, E. S., Franceschi, C., Lithgow, G. J., Morimoto, R. I. & Pessin, J. E. 2014. Geroscience: linking aging to chronic disease. Cell, 159, 709-713.
Keren, L., Zackay, O., Lotan-Pompan, M., Barenholz, U., Dekel, E., Sasson, V., Aidelberg, G., Bren, A., Zeevi, D. & Weinberger, A. 2013. Promoters maintain their relative activity levels under different growth conditions. Molecular systems biology, 9, 701.
Kern, S., Eichler, H., Stoeve, J., Klüter, H. & Bieback, K. 2006. Comparative analysis of mesenchymal stem cells from bone marrow, umbilical cord blood, or adipose tissue. Stem cells, 24, 1294-1301.
Kerr, B., Ashcroft, G., Scott, D., Horan, M., Ferguson, M. & Donnai, D. 1996. Rothmund-Thomson syndrome: two case reports show heterogeneous cutaneous abnormalities, an association with genetically programmed ageing changes, and increased chromosomal radiosensitivity. Journal of medical genetics, 33, 928-934.
Khanna, K. K. & Jackson, S. P. 2001. DNA double-strand breaks: signaling, repair and the cancer connection. Nature genetics, 27, 247-254.
Khatau, S. B., Hale, C. M., Stewart-Hutchinson, P. J., Patel, M. S., Stewart, C. L., Searson, P. C., Hodzic, D. & Wirtz, D. 2009. A perinuclear actin cap regulates nuclear shape. Proceedings of the National Academy of Sciences, 106, 19017-19022.
Kim, Y.-J. & M Wilson Iii, D. 2012. Overview of base excision repair biochemistry. Current molecular pharmacology, 5, 3-13.
Kim, J., Nakasaki, M., Todorova, D., Lake, B., Yuan, C. Y., Jamora, C. & Xu, Y. 2014. p53 induces skin aging by depleting Blimp1+ sebaceous gland cells. Cell death & disease, 5, e1141.
Kinner, A., Wu, W., Staudt, C. & Iliakis, G. 2008. γ-H2AX in recognition and signaling of DNA double-strand breaks in the context of chromatin. Nucleic acids research, 36, 5678-5694.
Kinzler, K. W. and Vogelstein, B. 1996. Lessons from hereditary colorectal cancer. Cell, 87,2,159-170.
Kiss, F. & Anstey, A. V. 2013. A review of UVB-mediated photosensitivity disorders. Photochemical & Photobiological Sciences, 12, 37-46.
Kitao, S., Lindor, N. M., Shiratori, M., Furuichi, Y. & Shimamoto, A. 1999a. Rothmund–Thomson syndrome responsible gene, RECQL4: genomic structure and products. Genomics, 61, 268-276.
Kitao, S., Shimamoto, A., Goto, M., Miller, R. W., Smithson, W. A., Lindor, N. M. & Furuichi, Y. 1999b. Mutations in RECQL4 cause a subset of cases of Rothmund-Thomson syndrome. Nature genetics, 22, 82-84.
Knecht, E., Hernández-Yago, J. & Grisolía, S. 1984. Regulation of lysosomal autophagy in transformed and non-transformed mouse fibroblasts under several growth conditions. Experimental cell research, 154, 224-232.
Knoblich, J. A. 2010. Asymmetric cell division: recent developments and their implications for tumour biology. Nature reviews. Molecular cell biology, 11, 849.
Knoell, K. A., Sidhu-Malik, N. K. & Malik, R. K. 1999. Aplastic anemia in a patient with Rothmund-Thomson syndrome. Journal of pediatric hematology/oncology, 21, 444-446.
Kobayashi, J. 2004. Molecular mechanism of the recruitment of NBS1/hMRE11/hRAD50 complex to DNA double-strand breaks: NBS1 binds to γ-H2AX through FHA/BRCT domain. Journal of radiation research, 45, 473-478.
Koç, A., Wheeler, L. J., Mathews, C. K. & Merrill, G. F. 2004. Hydroxyurea arrests DNA replication by a mechanism that preserves basal dNTP pools. Journal of Biological Chemistry, 279, 223-230.
Kögler, G., Sensken, S., Airey, J. A., Trapp, T., Müschen, M., Feldhahn, N., Liedtke, S., Sorg, R. V., Fischer, J. & Rosenbaum, C. 2004. A new human somatic stem cell

from placental cord blood with intrinsic pluripotent differentiation potential. Journal of Experimental Medicine, 200, 123-135.
Kohzaki, M., Chiourea, M., Versini, G., Adachi, N., Takeda, S., Gagos, S. & Halazonetis, T. D. 2012. The helicase domain and C-terminus of human RecQL4 facilitate replication elongation on DNA templates damaged by ionizing radiation. Carcinogenesis, 33, 1203-10.
Komarova, S. V., Ataullakhanov, F. I. & Globus, R. K. 2000. Bioenergetics and mitochondrial transmembrane potential during differentiation of cultured osteoblasts. American Journal of Physiology-Cell Physiology, 279, C1220-C1229.
Komori, T., Yagi, H., Nomura, S., Yamaguchi, A., Sasaki, K., Deguchi, K., Shimizu, Y., Bronson, R. T., Gao, Y. H. & Inada, M. 1997. Targeted disruption of Cbfa1 results in a complete lack of bone formation owing to maturational arrest of osteoblasts. cell, 89, 755-764.
Komori, T. 2007. Regulation of bone development and maintenance by Runx2. Frontiers in bioscience: a journal and virtual library, 13, 898-903.
Komori, T. 2010. Regulation of bone development and extracellular matrix protein genes by RUNX2. Cell and tissue research, 339, 189-195.
Kovac, M., Blattmann, C., Ribi, S., Smida, J., Mueller, N. S., Engert, F., Castro-Giner, F., Weischenfeldt, J., Kovacova, M. & Krieg, A. 2015. Exome sequencing of osteosarcoma reveals mutation signatures reminiscent of BRCA deficiency. Nature communications, 6, 8940.
Krejci, L., Altmannova, V., Spirek, M. & Zhao, X. 2012. Homologous recombination and its regulation. Nucleic acids research, 40, 5795-5818.
Krokan, H. E. & Bjørås, M. 2013. Base Excision Repair. Cold Spring Harbor Perspectives in Biology, 5.
Kruhlak, M. J., Celeste, A., Dellaire, G., Fernandez-Capetillo, O., Müller, W. G., Mcnally, J. G., Bazett-Jones, D. P. & Nussenzweig, A. 2006. Changes in chromatin structure and mobility in living cells at sites of DNA double-strand breaks. The Journal of cell biology, 172, 823-834.
Kubo, Y., Kaidzu, S., Nakajima, I., Takenouchi, K. & Nakamura, F. 2000. Organization of extracellular matrix components during differentiation of adipocytes in long-term culture. In Vitro Cellular & Developmental Biology-Animal, 36, 38-44.
Kumagai, A., Shevchenko, A., Shevchenko, A. & Dunphy, W. G. 2010. Treslin collaborates with TopBP1 in triggering the initiation of DNA replication. Cell, 140, 349-359.
Kumar, A. & Singh, U. 2017. KEYWORDS Primary Bone Malignancies, Secondary Bone Malignancies, Epidemiology. MALIGNANT BONE TUMOURS-A RETROSPECTIVE ANALYSIS IN RELATION TO AGE, SEX AND SITE.
Kumari, J., Hussain, M., De, S., Chandra, S., Modi, P., Tikoo, S., Singh, A., Sagar, C., Sepuri, N. B. V. & Sengupta, S. 2016. Mitochondrial functions of RECQL4 are required for the prevention of aerobic glycolysis-dependent cell invasion. J Cell Sci, 129, 1312-1318.
Kundu, Z. S. 2014. Classification, imaging, biopsy and staging of osteosarcoma. Indian Journal of Orthopaedics, 48, 238-246.
Kurek, K. C., Del Mare, S., Salah, Z., Abdeen, S., Sadiq, H., Lee, S.-H., Gaudio, E., Zanesi, N., Jones, K. B. & Deyoung, B. 2010. Frequent attenuation of the WWOX tumor suppressor in osteosarcoma is associated with increased tumorigenicity and aberrant RUNX2 expression. Cancer research, 70, 5577-5586.
Kuri-Harcuch, W. & Green, H. 1978. Adipose conversion of 3T3 cells depends on a serum factor. Proceedings of the National Academy of Sciences, 75, 6107-6109.
Kurucu, N., Şahin, G., Sarı, N., Ceylaner, S. and İlhan, İ.E. 2019. Association of vitamin D receptor gene polymorphisms with osteosarcoma risk and prognosis. Journal of bone oncology, 14, 100208.
Kwon, Y. T., Xia, Z., An, J. Y., Tasaki, T., Davydov, I. V., Seo, J. W., Sheng, J., Xie, Y. & Varshavsky, A. 2003. Female lethality and apoptosis of spermatocytes in mice lacking the UBR2 ubiquitin ligase of the N-end rule pathway. Molecular and cellular biology, 23, 8255-8271.
Labib, K., Tercero, J. A. & Diffley, J. F. X. 2000. Uninterrupted MCM2-7 function required for DNA replication fork progression. Science, 288, 1643-1647.

Labib, K. 2010. How do Cdc7 and cyclin-dependent kinases trigger the initiation of chromosome replication in eukaryotic cells? Genes & development, 24, 1208-1219.
Ladstein, R. G., Bachmann, I. M., Straume, O. & Akslen, L. A. 2010. Ki-67 expression is superior to mitotic count and novel proliferation markers PHH3, MCM4 and mitosin as a prognostic factor in thick cutaneous melanoma. BMC cancer, 10, 1.
Landau, D. A., Carter, S. L., Stojanov, P., Mckenna, A., Stevenson, K., Lawrence, M. S., Sougnez, C., Stewart, C., Sivachenko, A. & Wang, L. 2013. Evolution and impact of subclonal mutations in chronic lymphocytic leukemia. Cell, 152, 714-726.
Landau, D. A., Tausch, E., Taylor-Weiner, A. N., Stewart, C., Reiter, J. G., Bahlo, J., Kluth, S., Bozic, I., Lawrence, M. & Böttcher, S. 2015. Mutations driving CLL and their evolution in progression and relapse. Nature, 526, 525-530.
Lane, D. P. & Crawford, L. V. 1979. T antigen is bound to a host protein in SY40-transformed cells. Nature, 278, 261-263.
Lao, V. V., Welcsh, P., Luo, Y., Carter, K. T., Dzieciatkowski, S., Dintzis, S., Meza, J., Sarvetnick, N. E., Monnat, R. J. & Loeb, L. A. 2013. Altered RECQ helicase expression in sporadic primary colorectal cancers. Translational oncology, 6, 458IN7-469IN10.
Larizza, L., Magnani, I. & Roversi, G. 2006. Rothmund–Thomson syndrome and RECQL4 defect: splitting and lumping. Cancer letters, 232, 107-120.
Larizza, L., Roversi, G. & Volpi, L. 2010. Rothmund-thomson syndrome. Orphanet journal of rare diseases, 5, 1.
Larsen, N. B. & Hickson, I. D. 2013. RecQ helicases: conserved guardians of genomic integrity. DNA Helicases and DNA Motor Proteins. Springer.
Larsson, N.-G., Wang, J., Wilhelmsson, H., Oldfors, A., Rustin, P., Lewandoski, M., Barsh, G. S. & Clayton, D. A. 1998. Mitochondrial transcription factor A is necessary for mtDNA maintenance and embryogenesis in mice. Nature genetics, 18, 231-236.
Latypov, V. F., Tubbs, J. L., Watson, A. J., Marriott, A. S., Mcgown, G., Thorncroft, M., Wilkinson, O. J., Senthong, P., Butt, A. & Arvai, A. S. 2012. Atl1 regulates choice between global genome and transcription-coupled repair of O 6-alkylguanines. Molecular cell, 47, 50-60.
Lau, E. & Jiang, W. 2006. Is there a pre-RC checkpoint that cancer cells lack? Cell Cycle, 5, 1602-1606.
Lau, E., Tsuji, T., Guo, L., Lu, S.-H. & Jiang, W. 2007. The role of pre-replicative complex (pre-RC) components in oncogenesis. The FASEB Journal, 21, 3786-3794.
Lee, K.-S., Kim, H.-J., Li, Q.-L., Chi, X.-Z., Ueta, C., Komori, T., Wozney, J. M., Kim, E.-G., Choi, J.-Y. & Ryoo, H.-M. 2000. Runx2 is a common target of transforming growth factor β1 and bone morphogenetic protein 2, and cooperation between Runx2 and Smad5 induces osteoblast-specific gene expression in the pluripotent mesenchymal precursor cell line C2C12. Molecular and cellular biology, 20, 8783-8792.
Lee, O. K., Kuo, T. K., Chen, W.-M., Lee, K.-D., Hsieh, S.-L. & Chen, T.-H. 2004. Isolation of multipotent mesenchymal stem cells from umbilical cord blood. Blood, 103, 1669-1675.
Lee, J. H., Goodarzi, A. A., Jeggo, P. A. & Paull, T. T. 2010. 53BP1 promotes ATM activity through direct interactions with the MRN complex. The EMBO journal, 29, 574-585.
Lee, A. J., Endesfelder, D., Rowan, A. J., Walther, A., Birkbak, N. J., Futreal, P. A., Downward, J., Szallasi, Z., Tomlinson, I. P. & Howell, M. 2011a. Chromosomal instability confers intrinsic multidrug resistance. Cancer research, 71, 1858-1870.
Lee, J. A., Jung, J. S., Kim, D. H., Lim, J. S., Kim, M. S., Kong, C. B., Song, W. S., Cho, W. H., Jeon, D. G. & Lee, S. Y. 2011b. RANKL expression is related to treatment outcome of patients with localized, high-grade osteosarcoma. Pediatric blood & cancer, 56, 738-743.
Lee, H.-S., Lee, N. C. O., Kouprina, N., Kim, J.-H., Kagansky, A., Bates, S., Trepel, J. B., Pommier, Y., Sackett, D. & Larionov, V. 2016. Effects of anticancer drugs on chromosome instability and new clinical implications for tumor-suppressing therapies. Cancer research, 76, 902-911.
Lee, J.-M., Song, W.-W., Lee, J.-Y., Hwang, D.-S., Kim, Y.-D., Shin, S.-H., Chung, I.-K. & Kim, U.-K. 2012. Clinical study of benign and malignant fibrous-osseous lesions of

the jaws. Journal of the Korean Association of Oral and Maxillofacial Surgeons, 38, 29-37.
Lee, J. H., Han, Y.-S. & Lee, S. H. 2016. Long-Duration Three-Dimensional Spheroid Culture Promotes Angiogenic Activities of Adipose-Derived Mesenchymal Stem Cells. Biomolecules & Therapeutics, 24, 260-267.
Lemos, D. R., Eisner, C., Hopkins, C. I. & Rossi, F. M. V. 2015. Skeletal muscle-resident MSCs and bone formation. Bone, 80, 19-23.
Lengauer, C., Kinzler, K. W. & Vogelstein, B. 1997. Genetic instability in colorectal cancers. Nature, 386, 623-627.
Lengauer, C., Kinzler, K. W. & Vogelstein, B. 1998. Genetic instabilities in human cancers. Nature, 396, 643.
Lengner, C. J., Steinman, H. A., Gagnon, J., Smith, T. W., Henderson, J. E., Kream, B. E., Stein, G. S., Lian, J. B. & Jones, S. N. 2006. Osteoblast differentiation and skeletal development are regulated by Mdm2–p53 signaling. The Journal of cell biology, 172, 909-921.
Leonard, A. C. & Méchali, M. 2013. DNA replication origins. Cold Spring Harbor perspectives in biology, 5, a010116.
Leonetti, M. D., Sekine, S., Kamiyama, D., Weissman, J. S. & Huang, B. 2016. A scalable strategy for high-throughput GFP tagging of endogenous human proteins. Proceedings of the National Academy of Sciences, 113, E3501-E3508.
Leong, D. T., Lim, J., Goh, X., Pratap, J., Pereira, B. P., Kwok, H. S., Nathan, S. S., Dobson, J. R., Lian, J. B. & Ito, Y. 2010. Cancer-related ectopic expression of the bone-related transcription factor RUNX2 in non-osseous metastatic tumor cells is linked to cell proliferation and motility. Breast Cancer Research, 12, 1.
Leontieva, O. V., Demidenko, Z. N. & Blagosklonny, M. V. 2014. Contact inhibition and high cell density deactivate the mammalian target of rapamycin pathway, thus suppressing the senescence program. Proceedings of the National Academy of Sciences of the United States of America, 111, 8832-8837.
Levine, E. M., Becker, Y., Boone, C. W. & Eagle, H. 1965. Contact inhibition, macromolecular synthesis, and polyribosomes in cultured human diploid fibroblasts. Proceedings of the National Academy of Sciences, 53, 350-356.
Levine, A. J., Momand, J. & Finlay, C. A. 1991. The p53 tumour supressor gene. Nature, 351, 453.
Li, D., Firozi, P. F., Zhang, W., Shen, J., Digiovanni, J., Lau, S., Evans, D., Friess, H., Hassan, M. & Abbruzzese, J. L. 2002. DNA adducts, genetic polymorphisms, and K-ras mutation in human pancreatic cancer. Mutation Research/Genetic Toxicology and Environmental Mutagenesis, 513, 37-48.
Li, N., Yang, R., Zhang, W., Dorfman, H., Rao, P. & Gorlick, R. 2009. Genetically transforming human mesenchymal stem cells to sarcomas. Cancer, 115, 4795-4806.
Li, A., Yu, Y., Lee, S.-C., Ishibashi, T., Lees-Miller, S. P. & Ausió, J. 2010a. Phosphorylation of histone H2A. X by DNA-dependent protein kinase is not affected by core histone acetylation, but it alters nucleosome stability and histone H1 binding. Journal of biological chemistry, 285, 17778-17788.
Li, D.-Q., Ohshiro, K., Khan, M. N. & Kumar, R. 2010b. Requirement of MTA1 in ATR-mediated DNA damage checkpoint function. Journal of Biological Chemistry, 285, 19802-19812.
Li, Y., Ge, C., Long, J. P., Begun, D. L., Rodriguez, J. A., Goldstein, S. A. & Franceschi, R. T. 2012. Biomechanical stimulation of osteoblast gene expression requires phosphorylation of the RUNX2 transcription factor. Journal of Bone and Mineral Research, 27, 1263-1274.
Li, R., Zhang, W., Cui, J., Shui, W., Yin, L., Wang, Y., Zhang, H., Wang, N., Wu, N. & Nan, G. 2014. Targeting BMP9-promoted human osteosarcoma growth by inactivation of notch signaling. Current cancer drug targets, 14, 274-285.
Li, L., Ng, D. S. W., Mah, W. C., Almeida, F. F., Rahmat, S. A., Rao, V. K., Leow, S. C., Laudisi, F., Peh, M. T. & Goh, A. M. 2015. A unique role for p53 in the regulation of M2 macrophage polarization. Cell death and differentiation, 22, 1081.

Li, C. and Zamore, P D. 2019. RNA interference and small RNA analysis. Cold Spring Harbor Protocols, 4.
Lieber, M. R. 2010. The mechanism of double-strand DNA break repair by the nonhomologous DNA end joining pathway. Annual review of biochemistry, 79, 181.
Lieber, M. R. 2016. Mechanisms of human lymphoid chromosomal translocations. Nat Rev Cancer, 16, 387-398.
Lim, M., Zhong, C., Yang, S., Bell, A. M., Cohen, M. B. & Roy-Burman, P. 2010. Runx2 regulates survivin expression in prostate cancer cells. Laboratory investigation; a journal of technical methods and pathology, 90, 222.
Lin, G. L. & Hankenson, K. D. 2011. Integration of BMP, Wnt, and notch signaling pathways in osteoblast differentiation. Journal of cellular biochemistry, 112, 3491-3501.
Lin, P. P., Pandey, M. K., Jin, F., Raymond, A. K., Akiyama, H. & Lozano, G. 2009. Targeted mutation of p53 and Rb in mesenchymal cells of the limb bud produces sarcomas in mice. Carcinogenesis, 30, 1789-1795.
Lindahl, T. 1993. Instability and decay of the primary structure of DNA. nature, 362, 709-715.
Lindahl, T. 2001. Keynote: past, present, and future aspects of base excision repair. Progress in nucleic acid research and molecular biology, 68, xvii-xxx.
Lindor, N. M., Devries, E. M. G., Michels, V. V., Schad, C. R., Jalal, S. M., Donovan, K. M., Smithson, W. A., Kvols, L. K., Thibodeau, S. N. & Dewald, G. W. 1996. Rothmund-Thomson syndrome in siblings: evidence for acquired in vivo mosaicism. Clinical genetics, 49, 124-129.
Lindor, N. M., Furuichi, Y., Kitao, S., Shimamoto, A., Arndt, C. & Jalal, S. 2000. Rothmund-Thomson syndrome due to RECQ4 helicase mutations: Report and clinical and molecular comparisons with Bloom syndrome and Werner syndrome. American journal of medical genetics, 90, 223-228.
Litt, M. & Luty, J. A. 1989. A hypervariable microsatellite revealed by in vitro amplification of a dinucleotide repeat within the cardiac muscle actin gene. American journal of human genetics, 44, 397.
Liu, G., Meng, X., Jin, Y., Bai, J., Zhao, Y., Cui, X., Chen, F. & Fu, S. 2008. Inhibitory role of focal adhesion kinase on anoikis in the lung cancer cell A549. Cell biology international, 32, 663-670.
Liu, H.-Y., Tuckett, A. Z., Fennell, M., Garippa, R. & Zakrzewski, J. L. 2018. Repurposing of the CDK inhibitor PHA-767491 as a NRF2 inhibitor drug candidate for cancer therapy via redox modulation. Investigational new drugs, 1-11.
Liu, Q., Li, M. Z., Leibham, D., Cortez, D. & Elledge, S. J. 1998. The univector plasmid-fusion system, a method for rapid construction of recombinant DNA without restriction enzymes. Current biology, 8, 1300-S1.
Liu, W., Toyosawa, S., Furuichi, T., Kanatani, N., Yoshida, C., Liu, Y., Himeno, M., Narai, S., Yamaguchi, A. & Komori, T. 2001. Overexpression of Cbfa1 in osteoblasts inhibits osteoblast maturation and causes osteopenia with multiple fractures. J Cell Biol, 155, 157-166.
Liu, Y., Zhang, Z., Zhang, C., Deng, W., Lv, Q., Chen, X., Huang, T. & Pan, L. 2016. Adipose-derived stem cells undergo spontaneous osteogenic differentiation in vitro when passaged serially or seeded at low density. Biotechnic & histochemistry: official publication of the Biological Stain Commission, 91, 369.
Liu, Z., Liu, Q., Xu, B., Wu, J., Guo, C., Zhu, F., Yang, Q., Gao, G., Gong, Y. & Shao, C. 2009. Berberine induces p53-dependent cell cycle arrest and apoptosis of human osteosarcoma cells by inflicting DNA damage. Mutation Research/Fundamental and Molecular Mechanisms of Mutagenesis, 662, 75-83.
Loew, L. M., Tuft, R. A., Carrington, W. & Fay, F. S. 1993. Imaging in five dimensions: time-dependent membrane potentials in individual mitochondria. Biophysical journal, 65, 2396-2407.
Long, F. 2011. Building strong bones: molecular regulation of the osteoblast lineage. Nature reviews Molecular cell biology, 13, nrm3254.
Long, M. W. 2001. Osteogenesis and bone-marrow-derived cells. Blood Cells, Molecules, and Diseases, 27, 677-690.

Longhi, A., Errani, C., Gonzales-Arabio, D., Ferrari, C. & Mercuri, M. 2008. Osteosarcoma in patients older than 65 years. Journal of Clinical Oncology, 26, 5368-5373.
Lopez-Barcons, L. A. 2010. Serially heterotransplanted human prostate tumours as an experimental model. Journal of cellular and molecular medicine, 14, 1385-1395.
Lovejoy, C. A., Li, W., Reisenweber, S., Thongthip, S., Bruno, J., De Lange, T., De, S., Petrini, J. H. J., Sung, P. A. & Jasin, M. 2012. Loss of ATRX, genome instability, and an altered DNA damage response are hallmarks of the alternative lengthening of telomeres pathway. PLoS genetics, 8, e1002772.
Lu, X.-Y., Lu, Y., Zhao, Y.-J., Jaeweon, K., Kang, J., Xiao-Nan, L., Ge, G., Meyer, R., Perlaky, L. & Hicks, J. 2008. Cell cycle regulator gene CDC5L, a potential target for 6p12-p21 amplicon in osteosarcoma. Molecular Cancer Research, 6, 937-946.
Lu, H., Fang, E. F., Sykora, P., Kulikowicz, T., Zhang, Y., Becker, K. G., Croteau, D. L. & Bohr, V. A. 2014a. Senescence induced by RECQL4 dysfunction contributes to Rothmund–Thomson syndrome features in mice. Cell death & disease, 5, e1226.
Lu, L., Jin, W., Liu, H. & Wang, L. L. 2014b. RECQ DNA helicases and osteosarcoma. Current Advances in Osteosarcoma. Springer.
Lu, L., Harutyunyan, K., Jin, W., Wu, J., Yang, T., Chen, Y., Joeng, K. S., Bae, Y., Tao, J. & Dawson, B. C. 2015. RECQL4 regulates p53 function in vivo during skeletogenesis. Journal of Bone and Mineral Research, 30, 1077-1089.
Lu, L., Jin, W. & Wang, L. L. 2017. Aging in Rothmund-Thomson syndrome and related RECQL4 genetic disorders. Ageing research reviews, 33, 30-35.
Lukas, C., Savic, V., Bekker-Jensen, S., Doil, C., Neumann, B., Pedersen, R. S., Grøfte, M., Chan, K. L., Hickson, I. D. & Bartek, J. 2011. 53BP1 nuclear bodies form around DNA lesions generated by mitotic transmission of chromosomes under replication stress. Nature cell biology, 13, 243-253.
Luukkonen, J., Hilli, M., Nakamura, M., Ritamo, I., Valmu, L., Kauppinen, K., Tuukkanen, J. and Lehenkari, P. 2019. Osteoclasts secrete osteopontin into resorption lacunae during bone resorption. Histochemistry and cell biology, 1-13.
Macphail, S. H., Banáth, J. P., Yu, Y., Chu, E. & Olive, P. L. 2003. Cell cycle-dependent expression of phosphorylated histone H2AX: reduced expression in unirradiated but not X-irradiated G1-phase cells. Radiation research, 159, 759-767.
Macpherson, I. & Montagnier, L. 1964. Agar suspension culture for the selective assay of cells transformed by polyoma virus. Virology, 23, 291-294.
Macris, M. A., Krejci, L., Bussen, W., Shimamoto, A. & Sung, P. 2006. Biochemical characterization of the RECQ4 protein, mutated in Rothmund-Thomson syndrome. DNA repair, 5, 172-180.
Magalhães, J., Venditti, P., Adhihetty, P. J., Ramsey, J. J. & Ascensão, A. 2014. Mitochondria in Health and Disease. Oxidative medicine and cellular longevity, 2014.
Maire, G., Yoshimoto, M., Chilton-Macneill, S., Thorner, P. S., Zielenska, M. & Squire, J. A. 2009. Recurrent RECQL4 imbalance and increased gene expression levels are associated with structural chromosomal instability in sporadic osteosarcoma. Neoplasia, 11, 260-IN6.
Malumbres, M. & Barbacid, M. 2009. Cell cycle, CDKs and cancer: a changing paradigm. Nature Reviews Cancer, 9, 153-166.
Manis, J. P., Morales, J. C., Xia, Z., Kutok, J. L., Alt, F. W. & Carpenter, P. B. 2004. 53BP1 links DNA damage-response pathways to immunoglobulin heavy chain class-switch recombination. Nature immunology, 5, 481-487.
Mankouri, H. W., Huttner, D. & Hickson, I. D. 2013. How unfinished business from S-phase affects mitosis and beyond. The EMBO journal, 32, 2661-2671.
Mann, M. B., Hodges, C. A., Barnes, E., Vogel, H., Hassold, T. J. & Luo, G. 2005. Defective sister-chromatid cohesion, aneuploidy and cancer predisposition in a mouse model of type II Rothmund–Thomson syndrome. Human molecular genetics, 14, 813-825.
Manoir, S. D., Guillaud, P., Camus, E., Seigneurin, D. & Brugal, G. 1991. Ki-67 labeling in postmitotic cells defines different Ki-67 pathways within the 2c compartment. Cytometry, 12, 455-463.
Mao, Z., Ke, Z., Gorbunova, V. & Seluanov, A. 2012. Replicatively senescent cells are arrested in G1 and G2 phases. Aging (Albany NY), 4, 431-435.

Marchetti, L., Comelli, L., D'innocenzo, B., Puzzi, L., Luin, S., Arosio, D., Calvello, M., Mendoza-Maldonado, R., Peverali, F. & Trovato, F. 2010. Homeotic proteins participate in the function of human-DNA replication origins. Nucleic acids research, 38, 8105-8119.

Marcomini, I. & Gasser, S. M. 2015. Nuclear organization in DNA end processing: Telomeres vs double-strand breaks. DNA repair, 32, 134-140.

Mareschi, K., Biasin, E., Piacibello, W., Aglietta, M., Madon, E. & Fagioli, F. 2001. Isolation of human mesenchymal stem cells: bone marrow versus umbilical cord blood. haematologica, 86, 1099-1100.

Mari, P.-O., Florea, B. I., Persengiev, S. P., Verkaik, N. S., Brüggenwirth, H. T., Modesti, M., Giglia-Mari, G., Bezstarosti, K., Demmers, J. a. A. & Luider, T. M. 2006. Dynamic assembly of end-joining complexes requires interaction between Ku70/80 and XRCC4. Proceedings of the National Academy of Sciences, 103, 18597-18602.

Marina, N., Gebhardt, M., Teot, L. & Gorlick, R. 2004. Biology and Therapeutic Advances for Pediatric Osteosarcoma. The Oncologist, 9, 422-441.

Mariotti, L. G., Pirovano, G., Savage, K. I., Ghita, M., Ottolenghi, A., Prise, K. M. & Schettino, G. 2013. Use of the γ-H2AX assay to investigate DNA repair dynamics following multiple radiation exposures. PloS one, 8, e79541.

Marteijn, J. A., Bekker-Jensen, S., Mailand, N., Lans, H., Schwertman, P., Gourdin, A. M., Dantuma, N. P., Lukas, J. & Vermeulen, W. 2009. Nucleotide excision repair–induced H2A ubiquitination is dependent on MDC1 and RNF8 and reveals a universal DNA damage response. The Journal of cell biology, 186, 835-847.

Marteijn, J. A., Lans, H., Vermeulen, W. & Hoeijmakers, J. H. J. 2014. Understanding nucleotide excision repair and its roles in cancer and ageing. Nature reviews. Molecular cell biology, 15, 465.

Martin, N. L., Saba-El-Leil, M. K., Sadekova, S., Meloche, S. & Sauvageau, G. 2005. EN2 is a candidate oncogene in human breast cancer. Oncogene, 24, 6890-6901.

Martin, J. W., Zielenska, M., Stein, G. S., Van Wijnen, A. J. & Squire, J. A. 2010. The role of RUNX2 in osteosarcoma oncogenesis. Sarcoma, 2011.

Martin, J. W., Squire, J. A. & Zielenska, M. 2012. The genetics of osteosarcoma. Sarcoma, 2012.

Martin, J. W., Chilton-Macneill, S., Koti, M., Van Wijnen, A. J., Squire, J. A. & Zielenska, M. 2014. Digital expression profiling identifies RUNX2, CDC5L, MDM2, RECQL4, and CDK4 as potential predictive biomarkers for neo-adjuvant chemotherapy response in paediatric osteosarcoma. PloS one, 9, e95843.

Martínez-Diez, M., Santamaría, G., Ortega, Á. D. & Cuezva, J. M. 2006. Biogenesis and dynamics of mitochondria during the cell cycle: significance of 3′ UTRs. PloS one, 1, e107.

Maruyama, Z., Yoshida, C. A., Furuichi, T., Amizuka, N., Ito, M., Fukuyama, R., Miyazaki, T., Kitaura, H., Nakamura, K. & Fujita, T. 2007. Runx2 determines bone maturity and turnover rate in postnatal bone development and is involved in bone loss in estrogen deficiency. Developmental dynamics, 236, 1876-1890.

Marzona, L. & Pavolini, B. 2009. Play and players in bone fracture healing match. Clinical cases in mineral and bone metabolism, 6, 159-162.

Maser, R. S. & Depinho, R. A. 2002. Connecting chromosomes, crisis, and cancer. Science, 297, 565-569.

Masgras, I., Carrera, S., De Verdier, P. J., Brennan, P., Majid, A., Makhtar, W., Tulchinsky, E., Jones, G. D., Roninson, I. B. & Macip, S. 2012. Reactive oxygen species and mitochondrial sensitivity to oxidative stress determine induction of cancer cell death by p21. Journal of Biological Chemistry, 287, 9845-9854.

Masters, J. R., Thomson, J. A., Daly-Burns, B., Reid, Y. A., Dirks, W. G., Packer, P., Toji, L. H., Ohno, T., Tanabe, H. & Arlett, C. F. 2001. Short tandem repeat profiling provides an international reference standard for human cell lines. Proceedings of the National Academy of Sciences, 98, 8012-8017.

Matsumoto, M., Yaginuma, K., Igarashi, A., Imura, M., Hasegawa, M., Iwabuchi, K., Date, T., Mori, T., Ishizaki, K. & Yamashita, K. 2007. Perturbed gap-filling synthesis in nucleotide excision repair causes histone H2AX phosphorylation in human quiescent cells. Journal of cell science, 120, 1104-1112.

Matsuno, K., Kumano, M., Kubota, Y., Hashimoto, Y. & Takisawa, H. 2006. The N-terminal noncatalytic region of Xenopus RecQ4 is required for chromatin binding of DNA polymerase α in the initiation of DNA replication. Molecular and cellular biology, 26, 4843-4852.

Matsuoka, S., Rotman, G., Ogawa, A., Shiloh, Y., Tamai, K. & Elledge, S. J. 2000. Ataxia telangiectasia-mutated phosphorylates Chk2 in vivo and in vitro. Proceedings of the National Academy of Sciences, 97, 10389-10394.

Matsutani, N., Yokozaki, H., Tahara, E., Tahara, H., Kuniyasu, H., Haruma, K., Chayama, K., Yasui, W. & Tahara, E. 2001. Expression of telomeric repeat binding factor 1 and 2 and TRF1-interacting nuclear protein 2 in human gastric carcinomas. International Journal of Oncology, 19, 507-512.

Mayor, R., Casadome, L., Azuara, D., Moreno, V., Clark, S., Capella, G. & Peinado, M. 2009. Long-range epigenetic silencing at 2q14. 2 affects most human colorectal cancers and may have application as a non-invasive biomarker of disease. British journal of cancer, 100, 1534-1539.

Mccardle, A. 2013. Skeletal muscle loss: sarcopenia and inactivity. Presented at the European Calcified Tissue Society Conference ECTS, Bone Abstracts, 1.

Mcelhinny, S. a. N., Snowden, C. M., Mccarville, J. & Ramsden, D. A. 2000. Ku recruits the XRCC4-ligase IV complex to DNA ends. Molecular and cellular biology, 20, 2996-3003.

Mcgee-Lawrence, M. E., Carpio, L. R., Schulze, R. J., Pierce, J. L., Mcniven, M. A., Farr, J. N., Khosla, S., Oursler, M. J. & Westendorf, J. J. 2016. Hdac3 deficiency increases marrow adiposity and induces lipid storage and glucocorticoid metabolism in osteochondroprogenitor cells. Journal of Bone and Mineral Research, 31, 116-128.

Mcginnis, W. & Krumlauf, R. 1992. Homeobox genes and axial patterning. Cell, 68, 283-302.

Mcgranahan, N., Burrell, R. A., Endesfelder, D., Novelli, M. R. & Swanton, C. 2012. Cancer chromosomal instability: therapeutic and diagnostic challenges. EMBO reports, 13, 528-538.

Mcgranahan, N., Furness, A. J. S., Rosenthal, R., Ramskov, S., Lyngaa, R., Saini, S. K., Jamal-Hanjani, M., Wilson, G. A., Birkbak, N. J. & Hiley, C. T. 2016. Clonal neoantigens elicit T cell immunoreactivity and sensitivity to immune checkpoint blockade. Science, 351, 1463-1469.

Mcgrath, S. E., Michael, A., Pandha, H. & Morgan, R. 2013. Engrailed homeobox transcription factors as potential markers and targets in cancer. FEBS letters, 587, 549-554.

Mcmanus, K. J. & Hendzel, M. J. 2005. ATM-dependent DNA damage-independent mitotic phosphorylation of H2AX in normally growing mammalian cells. Molecular biology of the cell, 16, 5013-5025.

Medagli, B., Di Crescenzio, P., De March, M. & Onesti, S. 2016. Structure and Activity of the Cdc45-Mcm2–7-GINS (CMG) Complex, the Replication Helicase. The Initiation of DNA Replication in Eukaryotes. Springer.

Mehlem, A., Hagberg, C. E., Muhl, L., Eriksson, U. & Falkevall, A. 2013. Imaging of neutral lipids by oil red O for analyzing the metabolic status in health and disease. Nature protocols, 8, 1149-1154.

Mehollin-Ray, A. R., Kozinetz, C. A., Schlesinger, A. E., Guillerman, R. P. & Wang, L. L. 2008. Radiographic abnormalities in Rothmund-Thomson syndrome and genotype–phenotype correlation with RECQL4 mutation status. American Journal of Roentgenology, 191, W62-W66.

Melrose, J., Hayes, A. J., Whitelock, J. M. & Little, C. B. 2008. Perlecan, the “jack of all trades” proteoglycan of cartilaginous weight-bearing connective tissues. Bioessays, 30, 457-469.

Merry, C., Fu, K., Wang, J., Yeh, I. J. & Zhang, Y. 2010. Targeting the checkpoint kinase Chk1 in cancer therapy. Cell Cycle, 9, 279-283.

Meunier, P., Aaron, J., Edouard, C. & Vlgnon, G. 1971. Osteoporosis and the replacement of cell populations of the marrow by adipose tissue: a quantitative study of 84 iliac bone biopsies. Clinical orthopaedics and related research, 80, 147-154.

Meyer, F. R. L. & Walter, I. 2016. Establishment and Characterization of New Canine and Feline Osteosarcoma Primary Cell Lines. Veterinary Sciences, 3, 9.
Mimeault, M. & Batra, S. K. 2010. Recent advances on skin-resident stem/progenitor cell functions in skin regeneration, aging and cancers and novel anti-aging and cancer therapies. Journal of cellular and molecular medicine, 14, 116-134.
Miotto, B. & Graba, Y. 2010. Control of DNA replication: a new facet of Hox proteins? Bioessays, 32, 800-807.
Miozzo, M., Castorina, P., Riva, P., Dalpra, L., Fuhrman Conti, A. M., Volpi, L., Hoe, T. S., Khoo, A., Wiegant, J. & Rosenberg, C. 1998. Chromosomal instability in fibroblasts and mesenchymal tumors from 2 sibs with Rothmund-Thomson syndrome. International journal of cancer, 77, 504-510.
Miozzo, M., Castorina, P., Riva, P., Dalpra, L., Fuhrman Conti, A. M., Volpi, L., Hoe, T. S., Khoo, A., Wiegant, J. & Rosenberg, C. 1998. Chromosomal instability in fibroblasts and mesenchymal tumors from 2 sibs with Rothmund-Thomson syndrome. International journal of cancer, 77, 504-510.
Mirabello, L., Troisi, R. J. & Savage, S. A. 2009. Osteosarcoma incidence and survival rates from 1973 to 2004. Cancer, 115, 1531-1543.
Mirabello, L., Yeager, M., Mai, P. L., Gastier-Foster, J. M., Gorlick, R., Khanna, C., Patiño-Garcia, A., Sierrasesúmaga, L., Lecanda, F. & Andrulis, I. L. 2015. Germline TP53 variants and susceptibility to osteosarcoma. JNCI: Journal of the National Cancer Institute, 107.
Moerman, E. J., Teng, K., Lipschitz, D. A. & Lecka-Czernik, B. 2004. Aging activates adipogenic and suppresses osteogenic programs in mesenchymal marrow stroma/stem cells: the role of PPAR-γ2 transcription factor and TGF-β/BMP signaling pathways. Aging cell, 3, 379-389.
Mohseny, A. B., Szuhai, K., Romeo, S., Buddingh, E. P., Briaire-De Bruijn, I., De Jong, D., Van Pel, M., Cleton-Jansen, A. M. & Hogendoorn, P. C. W. 2009. Osteosarcoma originates from mesenchymal stem cells in consequence of aneuploidization and genomic loss of Cdkn2. The Journal of pathology, 219, 294-305.
Mohseny, A. B. & Hogendoorn, P. C. 2011. Concise review: mesenchymal tumors: when stem cells go mad. Stem cells, 29, 397-403.
Moiseeva, T.N. and Bakkenist, C.J. 2018. Regulation of the initiation of DNA replication in human cells. DNA repair, 99-106.
Monaghan, R. M. & Whitmarsh, A. J. 2015. Mitochondrial proteins moonlighting in the nucleus. Trends in biochemical sciences, 40, 728-735.
Montagnoli, A., Valsasina, B., Croci, V., Menichincheri, M., Rainoldi, S., Marchesi, V., Tibolla, M., Tenca, P., Brotherton, D. & Albanese, C. 2008. A Cdc7 kinase inhibitor restricts initiation of DNA replication and has antitumor activity. Nature chemical biology, 4, 357-365.
Morales-Sánchez, M. A., Peralta-Pedrero, M. L., Jurado-Santa Cruz, F., Pomerantz, H. & Barajas-Nava, L. A. 2016. Interventions for preventing keratinocyte cancer in high-risk groups not receiving immunosuppressive therapy. The Cochrane Library.
Moretti, T. & Budowle, B. The CODIS STR Project: evaluation of fluorescent multiplex STR systems. Proceedings of the 50th Annual Meeting of the American Academy of Forensic Sciences, 1998. American Academy of Forensic Sciences, 9-14.
Morgan, D. O. 1997. Cyclin-dependent kinases: engines, clocks, and microprocessors. Annual review of cell and developmental biology, 13, 261-291.
Morgan, R., Boxall, A., Bhatt, A., Bailey, M., Hindley, R., Langley, S., Whitaker, H. C., Neal, D. E., Ismail, M. & Whitaker, H. 2011. Engrailed-2 (EN2): a tumor specific urinary biomarker for the early diagnosis of prostate cancer. Clinical Cancer Research, 17, 1090-1098.
Mori, K., Berreur, M., Blanchard, F., Chevalier, C., Guisle-Marsollier, I., Masson, M., Rédini, F. & Heymann, D. 2007. Receptor activator of nuclear factor-κB ligand (RANKL) directly modulates the gene expression profile of RANK-positive Saos-2 human osteosarcoma cells. Oncology reports, 18, 1365-1371.
Mori, S., Chang, J. T., Andrechek, E. R., Matsumura, N., Baba, T., Yao, G., Kim, J. W., Gatza, M., Murphy, S. & Nevins, J. R. 2009. Anchorage-independent cell growth signature identifies tumors with metastatic potential. Oncogene, 28, 2796-2805.

Mosmann, T. 1983. Rapid colorimetric assay for cellular growth and survival: application to proliferation and cytotoxicity assays. Journal of immunological methods, 65, 55-63.
Motyl, K. J., Raetz, M., Tekalur, S. A., Schwartz, R. C. & Mccabe, L. R. 2011. CCAAT/enhancer binding protein β-deficiency enhances type 1 diabetic bone phenotype by increasing marrow adiposity and bone resorption. American Journal of Physiology-Regulatory, Integrative and Comparative Physiology, 300, R1250-R1260.
Mueller, S. M. & Glowacki, J. 2001. Age-related decline in the osteogenic potential of human bone marrow cells cultured in three-dimensional collagen sponges. Journal of cellular biochemistry, 82, 583-590.
Mulhern, D. M. & Van Gerven, D. P. 1997. Patterns of femoral bone remodeling dynamics in a medieval Nubian population. American Journal of Physical Anthropology, 104, 133-146.
Mundlos, S. & Olsen, B. R. 2002. Defects in skeletal morphogenesis. in: Steinmann, B.
Mundy, G. R. 2002. Metastasis: Metastasis to bone: causes, consequences and therapeutic opportunities. Nature Reviews Cancer, 2, 584-593.
Muñoz, P., Blanco, R. & Blasco, M. A. 2006. Role of the TRF2 telomeric protein in cancer and aging. Cell Cycle, 5, 718-721.
Muramatsu, S., Hirai, K., Tak, Y.-S., Kamimura, Y. & Araki, H. 2010. CDK-dependent complex formation between replication proteins Dpb11, Sld2, Pol ε, and GINS in budding yeast. Genes & development, 24, 602-612.
Murray, A. 1993. The cell cycle: an introduction.
Muruganandan, S. & Sinal, C. J. 2014. The impact of bone marrow adipocytes on osteoblast and osteoclast differentiation. IUBMB life, 66, 147-155.
Mutsaers, A. J., Ng, A. J. M., Baker, E. K., Russell, M. R., Chalk, A. M., Wall, M., Liddicoat, B. J. J., Ho, P. W. M., Slavin, J. L. & Goradia, A. 2013. Modeling distinct osteosarcoma subtypes in vivo using Cre: lox and lineage-restricted transgenic shRNA. Bone, 55, 166-178.
Nagaraju, G. & Scully, R. 2007. Minding the gap: the underground functions of BRCA1 and BRCA2 at stalled replication forks. DNA repair, 6, 1018-1031.
Nahhas, A.F., Oberlin, D.M., Braunberger, T.L. and Lim, H.W. 2018. Recent Developments in the Diagnosis and Management of Photosensitive Disorders. American journal of clinical dermatology,1-25.
Nakamura, T. M., Morin, G. B., Chapman, K. B., Weinrich, S. L., Andrews, W. H., Lingner, J., Harley, C. B. & Cech, T. R. 1997. Telomerase catalytic subunit homologs from fission yeast and human. Science, 277, 955-959.
Nakamura, A., Sedelnikova, O. A., Redon, C., Pilch, D. R., Sinogeeva, N. I., Shroff, R., Lichten, M. & Bonner, W. M. 2006. Techniques for γ-H2AX Detection. Methods in Enzymology. Academic Press.
Nakamura, A. J., Chiang, Y. J., Hathcock, K. S., Horikawa, I., Sedelnikova, O. A., Hodes, R. J. & Bonner, W. M. 2008. Both telomeric and non-telomeric DNA damage are determinants of mammalian cellular senescence. Epigenetics & chromatin, 1, 6.
Nakanishi, K., Kawai, T., Kumaki, F., Hiroi, S., Mukai, M., Ikeda, E., Koering, C. E. & Gilson, E. 2003. Expression of mRNAs for telomeric repeat binding factor (TRF)-1 and TRF2 in atypical adenomatous hyperplasia and adenocarcinoma of the lung. Clinical Cancer Research, 9, 1105-1111.
Nakashima, K., Zhou, X., Kunkel, G., Zhang, Z., Deng, J. M., Behringer, R. R. & De Crombrugghe, B. 2002. The novel zinc finger-containing transcription factor osterix is required for osteoblast differentiation and bone formation. Cell, 108, 17-29.
Narayan, S., Fleming, C., Trainer, A. & Craig, J. 2001. Rothmund–Thomson syndrome with myelodysplasia. Pediatric dermatology, 18, 210-212.
Narciso, L., Fortini, P., Pajalunga, D., Franchitto, A., Liu, P., Degan, P., Frechet, M., Demple, B., Crescenzi, M. & Dogliotti, E. 2007. Terminally differentiated muscle cells are defective in base excision DNA repair and hypersensitive to oxygen injury. Proceedings of the National Academy of Sciences, 104, 17010-17015.
Nardone, G., Oliver-De La Cruz, J., Vrbsky, J., Martini, C., Pribyl, J., Skládal, P., Pešl, M., Caluori, G., Pagliari, S. & Martino, F. 2017. YAP regulates cell mechanics by controlling focal adhesion assembly. Nature Communications, 8.

Nathan, S. S., Pereira, B. P., Zhou, Y. F., Gupta, A., Dombrowski, C., Soong, R., Pho, R. W., Stein, G. S., Salto-Tellez, M., Cool, S. M. & Van Wijnen, A. J. 2009. Elevated expression of Runx2 as a key parameter in the etiology of osteosarcoma. Mol Biol Rep, 36, 153-8.

Natoni, A., Murillo, L. S., Kliszczak, A. E., Catherwood, M. A., Montagnoli, A., Samali, A., O'dwyer, M. & Santocanale, C. 2011. Mechanisms of action of a dual Cdc7/Cdk9 kinase inhibitor against quiescent and proliferating CLL cells. Molecular cancer therapeutics, 10, 1624-1634.

Natoni, A., Coyne, M. R. E., Jacobsen, A., Rainey, M. D., O'brien, G., Healy, S., Montagnoli, A., Moll, J., O'dwyer, M. & Santocanale, C. 2013. Characterization of a Dual CDC7/CDK9 Inhibitor in Multiple Myeloma Cellular Models. Cancers, 5, 901-918.

Nelson, C. M. & Bissell, M. J. Modeling dynamic reciprocity: engineering three-dimensional culture models of breast architecture, function, and neoplastic transformation. 2005 2005. Elsevier, 342-352.

Neri, D., Kaspar, M. & Trachsel, E. 2013. Anti-EDB antibody-targeted IL-10 cytokine for therapy of rheumatoid arthritis. Google Patents.

Ng, K. W., Leong, D. T. W. & Hutmacher, D. W. 2005. The challenge to measure cell proliferation in two and three dimensions. Tissue Engineering, 11, 182-191.

Ng, A. J. M., Mutsaers, A. J., Baker, E. K. & Walkley, C. R. 2012. Genetically engineered mouse models and human osteosarcoma. Clinical sarcoma research, 2, 19.

Ng, A. J. M., Walia, M. K., Smeets, M. F., Mutsaers, A. J., Sims, N. A., Purton, L. E., Walsh, N. C., Martin, T. J. & Walkley, C. R. 2015. The DNA helicase recql4 is required for normal osteoblast expansion and osteosarcoma formation. PLoS

Nicholls, D. G. 2004. Mitochondrial membrane potential and aging. Aging cell, 3, 35-40.

Nicholls, D.G., 2018. Fluorescence Measurement of Mitochondrial Membrane Potential Changes in Cultured Cells. In Mitochondrial Bioenergetics,Humana Press, New York, NY. 121-135

Nielsen, T. O., West, R. B., Linn, S. C., Alter, O., Knowling, M. A., O'connell, J. X., Zhu, S., Fero, M., Sherlock, G. & Pollack, J. R. 2002. Molecular characterisation of soft tissue tumours: a gene expression study. The Lancet, 359, 1301-1307.

Nijjar, T., Bassett, E., Garbe, J., Takenaka, Y., Stampfer, M. R., Gilley, D. & Yaswen, P. 2005. Accumulation and altered localization of telomere-associated protein TRF2 in immortally transformed and tumor-derived human breast cells. Oncogene, 24, 3369-3376.

Nimmo, R. & Woollard, A. 2008. Worming out the biology of Runx. Developmental biology, 313, 492-500.

Nishida, S., Endo, N., Yamagiwa, H., Tanizawa, T. & Takahashi, H. E. 1999. Number of osteoprogenitor cells in human bone marrow markedly decreases after skeletal maturation. Journal of bone and mineral metabolism, 17, 171-177.

Nishitani, H. & Lygerou, Z. 2002. Control of DNA replication licensing in a cell cycle. Genes to Cells, 7, 523-534.

Noatynska, A., Tavernier, N., Gotta, M. & Pintard, L. 2013. Coordinating cell polarity and cell cycle progression: what can we learn from flies and worms? Open biology, 3, 130083.

Noon, A. T., Shibata, A., Rief, N., Löbrich, M., Stewart, G. S., Jeggo, P. A. & Goodarzi, A. A. 2010. 53BP1-dependent robust localized KAP-1 phosphorylation is essential for heterochromatic DNA double-strand break repair. Nature cell biology, 12, 177-184.

Novarina, D., Amara, F., Lazzaro, F., Plevani, P. & Muzi-Falconi, M. 2011. Mind the gap: keeping UV lesions in check. DNA repair, 10, 751-759.

Nuciforo, P. G., Luise, C., Capra, M., Pelosi, G. & Di Fagagna, F. D. A. 2007. Complex engagement of DNA damage response pathways in human cancer and in lung tumor progression. Carcinogenesis, 28, 2082-2088.

Nuttall, M. E. & Gimble, J. M. 2000. Is there a therapeutic opportunity to either prevent or treat osteopenic disorders by inhibiting marrow adipogenesis? Bone, 27, 177-184.

O'connor, M. J. 2015. Targeting the DNA damage response in cancer. Molecular cell, 60, 547-560.

Oda, E., Ohki, R., Murasawa, H., Nemoto, J., Shibue, T., Yamashita, T., Tokino, T., Taniguchi, T. & Tanaka, N. 2000. Noxa, a BH3-only member of the Bcl-2 family and candidate mediator of p53-induced apoptosis. Science, 288, 1053-1058.
Offer, T., Ho, E., Traber, M. G., Bruno, R. S., Kuypers, F. A. & Ames, B. N. 2005. A simple assay for frequency of chromosome breaks and loss (micronuclei) by flow cytometry of human reticulocytes. The FASEB journal, 19, 485-487.
Ogawa, R., Mizuno, H., Watanabe, A., Migita, M., Shimada, T. & Hyakusoku, H. 2004. Osteogenic and chondrogenic differentiation by adipose-derived stem cells harvested from GFP transgenic mice. Biochemical and biophysical research communications, 313, 871-877.
Oh, H., Wang, S. C., Prahash, A., Sano, M., Moravec, C. S., Taffet, G. E., Michael, L. H., Youker, K. A., Entman, M. L. & Schneider, M. D. 2003. Telomere attrition and Chk2 activation in human heart failure. Proceedings of the National Academy of Sciences, 100, 5378-5383.
Oh, B.-K., Kim, Y.-J., Park, C. & Park, Y. N. 2005. Up-regulation of telomere-binding proteins, TRF1, TRF2, and TIN2 is related to telomere shortening during human multistep hepatocarcinogenesis. The American journal of pathology, 166, 73-80.
Ohlenschläger, O., Kuhnert, A., Schneider, A., Haumann, S., Bellstedt, P., Keller, H., Saluz, H.-P., Hortschansky, P., Hänel, F. & Grosse, F. 2012. The N-terminus of the human RecQL4 helicase is a homeodomain-like DNA interaction motif. Nucleic acids research, 40, 8309-8324.
Okamoto, K., Bartocci, C., Ouzounov, I., Diedrich, J. K., Yates Iii, J. R. & Denchi, E. L. 2013. A two-step mechanism for TRF2-mediated chromosome-end protection. Nature, 494, 502-505.
O'keefe, R. J., Puzas, J. E., Loveys, L., Hicks, D. G. & Rosier, R. N. 1994. Analysis of type II and type X collagen synthesis in cultured growth plate chondrocytes by in situ hybridization: rapid induction of type X collagen in culture. Journal of Bone and Mineral Research, 9, 1713-1722.
Olivier, M., Hollstein, M. & Hainaut, P. 2010. TP53 mutations in human cancers: origins, consequences, and clinical use. Cold Spring Harbor perspectives in biology, 2, a001008.
Orstavik, K. H., Mcfadden, N., Hagelsteen, J., Ormerod, E. & Van Der Hagen, C. 1994. Instability of lymphocyte chromosomes in a girl with Rothmund-Thomson syndrome. Journal of medical genetics, 31, 570-572.
Ottaviani, G. & Jaffe, N. 2009. The etiology of osteosarcoma. Pediatric and Adolescent Osteosarcoma. Springer.
Ouyang, K. J., Woo, L. L. & Ellis, N. A. 2008. Homologous recombination and maintenance of genome integrity: cancer and aging through the prism of human RecQ helicases. Mechanisms of ageing and development, 129, 425-440.
Overholtzer, M., Rao, P. H., Favis, R., Lu, X.-Y., Elowitz, M. B., Barany, F., Ladanyi, M., Gorlick, R. & Levine, A. J. 2003. The presence of p53 mutations in human osteosarcomas correlates with high levels of genomic instability. Proceedings of the National Academy of Sciences, 100, 11547-11552.
Overmeer, R. M., Moser, J., Volker, M., Kool, H., Tomkinson, A. E., Van Zeeland, A. A., Mullenders, L. H. F. & Fousteri, M. 2011. Replication protein A safeguards genome integrity by controlling NER incision events. The Journal of cell biology, 192, 401-415.
Ozaki, T., Nakagawara, A. & Nagase, H. 2013. RUNX family participates in the regulation of p53-dependent DNA damage response. International journal of genomics, 2013.
Pageau, G. J. & Lawrence, J. B. 2006. BRCA1 foci in normal S-phase nuclei are linked to interphase centromeres and replication of pericentric heterochromatin. J Cell Biol, 175, 693-701.
Pagliuca, F. W., Collins, M. O., Lichawska, A., Zegerman, P., Choudhary, J. S. & Pines, J. 2011. Quantitative proteomics reveals the basis for the biochemical specificity of the cell-cycle machinery. Molecular cell, 43, 406-417.
Pairault, J. & Green, H. 1979. A study of the adipose conversion of suspended 3T3 cells by using glycerophosphate dehydrogenase as differentiation marker. Proceedings of the National Academy of Sciences, 76, 5138-5142.

Palm, W. & De Lange, T. 2008. How shelterin protects mammalian telomeres. Annual review of genetics, 42, 301-334.
Pan, Q., Fouraschen, S. M., De Ruiter, P. E., Dinjens, W. N., Kwekkeboom, J., Tilanus, H. W. & Van Der Laan, L. J. 2013. Detection of spontaneous tumorigenic transformation during culture expansion of human mesenchymal stromal cells. Experimental Biology and Medicine, 1535370213506802.
Pâques, F. & Haber, J. E. 1999. Multiple pathways of recombination induced by double-strand breaks in Saccharomyces cerevisiae. Microbiology and molecular biology reviews, 63, 349-404.
Pardee, A. B. 1974. A restriction point for control of normal animal cell proliferation. Proceedings of the National Academy of Sciences, 71, 1286-1290.
Pardo, B., Gomez-Gonzalez, B. & Aguilera, A. 2009. DNA repair in mammalian cells. Cellular and Molecular Life Sciences, 66, 1039-1056.
Parfitt, A. M. 1980. Morphologic basis of bone-mineral measurements-transient and steady-state effects of treatment in osteoporosis. Karger allschwilerstrasse 10, ch-4009 basel, switzerland.
Parfitt, A. M. 1984. Age-related structural changes in trabecular and cortical bone: cellular mechanisms and biomechanical consequences. Calcified Tissue International, 36, S123-S128.
Parfitt, A. M. 1990. Bone-forming cells in clinical conditions. Bone, 1, 351-429.
Parfitt, A. M. 1994. The two faces of growth: benefits and risks to bone integrity. Osteoporosis International, 4, 382-398.
Parfitt, A. M., Travers, R., Rauch, F. & Glorieux, F. H. 2000. Structural and cellular changes during bone growth in healthy children. Bone, 27, 487-494.
Park, S.-J., Lee, Y.-J., Beck, B. D. & Lee, S.-H. 2006. A positive involvement of RecQL4 in UV-induced S-phase arrest. DNA and cell biology, 25, 696-703.
Park, S.-Y. & Kim, J.-E. 2013. Differential gene expression by Osterix knockdown in mouse chondrogenic ATDC5 cells. Gene, 518, 368-375.
Park, H. W., Kim, Y. C., Yu, B., Moroishi, T., Mo, J.-S., Plouffe, S. W., Meng, Z., Lin, K. C., Yu, F.-X. & Alexander, C. M. 2015. Alternative Wnt signaling activates YAP/TAZ. Cell, 162, 780-794.
Parkin, D. M., Stiller, C. A., Draper, G. J. & Bieber, C. A. 1988. The international incidence of childhood cancer. International Journal of Cancer, 42, 511-520.
Parsa, N. 2012. Environmental Factors Inducing Human Cancers. Iranian Journal of Public Health, 41, 1-9.
Patel, D. M., Shah, J. & Srivastava, A. S. 2013. Therapeutic potential of mesenchymal stem cells in regenerative medicine. Stem cells international, 2013.
Peakman, T. C., Harris, R. A. & Gewert, D. R. 1992. Highly efficient generation of recombinant baculoviruses by enzymatically mediated site-specific in vitro recombination. Nucleic acids research, 20, 495-500.
Pedanou, V. E., Gobeil, S., Tabaries, S., Simone, T. M., Zhu, L. J., Siegel, P. M. & Green, M. R. 2016. The histone H3K9 demethylase KDM3A promotes anoikis by transcriptionally activating pro-apoptotic genes BNIP3 and BNIP3L. Elife, 5.
Pereira, B. P., Zhou, Y., Gupta, A., Leong, D. T., Aung, K. Z., Ling, L., Pho, R. W., Galindo, M., Salto-Tellez, M. & Stein, G. S. 2009. Runx2, p53, and pRB status as diagnostic parameters for deregulation of osteoblast growth and differentiation in a new pre-chemotherapeutic osteosarcoma cell line (OS1). Journal of cellular physiology, 221, 778-788.
Perry, S. W., Norman, J. P., Barbieri, J., Brown, E. B. & Gelbard, H. A. 2011. Mitochondrial membrane potential probes and the proton gradient: a practical usage guide. BioTechniques, 50, 98-115.
Petermann, E., Maya-Mendoza, A., Zachos, G., Gillespie, D. a. F., Jackson, D. A. & Caldecott, K. W. 2006. Chk1 requirement for high global rates of replication fork progression during normal vertebrate S phase. Molecular and cellular biology, 26, 3319-3326.
Petermann, E. & Helleday, T. 2010. Pathways of mammalian replication fork restart. Nature reviews Molecular cell biology, 11, 683-687.

Petkovic, M., Dietschy, T., Freire, R., Jiao, R. & Stagljar, I. 2005. The human Rothmund-Thomson syndrome gene product, RECQL4, localizes to distinct nuclear foci that coincide with proteins involved in the maintenance of genome stability. Journal of cell science, 118, 4261-4269.

Pfeifer, G. P., Denissenko, M. F., Olivier, M., Tretyakova, N., Hecht, S. S. & Hainaut, P. 2002. Tobacco smoke carcinogens, DNA damage and p53 mutations in smoking-associated cancers. Oncogene, 21, 7435.

Pi, Y., Goldenthal, M. J. & Marín-García, J. 2007. Mitochondrial channelopathies in aging. Journal of Molecular Medicine, 85, 937-951.

Pianigiani, E., De Aloe, G., Andreassi, A., Rubegni, P. & Fimiani, M. 2001. Rothmund-Thomson Syndrome (Thomson-Type) and Myelodysplasia. Pediatric dermatology, 18, 422-425.

Pierre, R. V. 2002. Peripheral blood film review: the demise of the eyecount leukocyte differential. Clinics in laboratory medicine, 22, 279-297.

Pino, A. M., Rosen, C. J. & Rodríguez, J. P. 2012. In osteoporosis, differentiation of mesenchymal stem cells (MSCs) improves bone marrow adipogenesis. Biological research, 45, 279-287.

Pitrone, M., Pizzolanti, G., Tomasello, L., Coppola, A., Morini, L., Pantuso, G., Ficarella, R., Guarnotta, V., Perrini, S. & Giorgino, F. 2017. NANOG Plays a Hierarchical Role in the Transcription Network Regulating the Pluripotency and Plasticity of Adipose Tissue-Derived Stem Cells. International Journal of Molecular Sciences, 18, 1107.

Pittenger, M. F., Mackay, A. M., Beck, S. C., Jaiswal, R. K., Douglas, R., Mosca, J. D., Moorman, M. A., Simonetti, D. W., Craig, S. & Marshak, D. R. 1999. Multilineage potential of adult human mesenchymal stem cells. science, 284, 143-147.

Plumb, J. A., Milroy, R. & Kaye, S. B. 1989. Effects of the pH dependence of 3-(4, 5-dimethylthiazol-2-yl)-2, 5-diphenyltetrazolium bromide-formazan absorption on chemosensitivity determined by a novel tetrazolium-based assay. Cancer research, 49, 4435-4440.

Podhorecka, M., Skladanowski, A. & Bozko, P. 2010. H2AX phosphorylation: its role in DNA damage response and cancer therapy. Journal of nucleic acids, 2010.

Polig, E. & Jee, W. S. S. 1990. A model of osteon closure in cortical bone. Calcified tissue international, 47, 261-269.

Porter, W., Hardman, C., Abdalla, S. & Powles, A. 1999. Haematological disease in siblings with Rothmundą Thomson syndrome. Clin Exp Dermatol, 24, 452ą454.

Pratap, J., Galindo, M., Zaidi, S. K., Vradii, D., Bhat, B. M., Robinson, J. A., Choi, J.-Y., Komori, T., Stein, J. L. & Lian, J. B. 2003. Cell growth regulatory role of Runx2 during proliferative expansion of preosteoblasts. Cancer research, 63, 5357-5362.

Pratap, J., Lian, J. B. & Stein, G. S. 2011. Metastatic bone disease: role of transcription factors and future targets. Bone, 48, 30-36.

Pujol, L. A., Erickson, R. P., Heidenreich, R. A. & Cunniff, C. 2000. Variable presentation of Rothmund-Thomson syndrome. American journal of medical genetics, 95, 204-207.

Qiagen. 2018. Telomere Extension by Telomerase [Online]. https://www.qiagen.com/eg/shop/genes-and-pathways/pathway-details/?pwid=430. [Accessed 2018].

Qin, J. Y., Zhang, L., Clift, K. L., Hulur, I., Xiang, A. P., Ren, B.-Z. & Lahn, B. T. 2010. Systematic comparison of constitutive promoters and the doxycycline-inducible promoter. PloS one, 5, e10611.

Qiu, S., Rao, D. S., Palnitkar, S. & Parfitt, A. M. 2002. Relationships between osteocyte density and bone formation rate in human cancellous bone. Bone, 31, 709-711.

Quent, V., Loessner, D., Friis, T., Reichert, J. C. & Hutmacher, D. W. 2010. Discrepancies between metabolic activity and DNA content as tool to assess cell proliferation in cancer research. Journal of cellular and molecular medicine, 14, 1003-1013.

Quist, T., Jin, H., Zhu, J.-F., Smith-Fry, K., Capecchi, M. R. & Jones, K. B. 2015. The impact of osteoblastic differentiation on osteosarcomagenesis in the mouse. Oncogene, 34, 4278.

Rago, A. P., Napolitano, A. P., Dean, D. M., Chai, P. R. & Morgan, J. R. 2008. Miniaturization of an Anoikis assay using non-adhesive micromolded hydrogels. Cytotechnology, 56, 81-90.

Rajagopalan, H., Nowak, M. A., Vogelstein, B. & Lengauer, C. 2003. Opinion: The significance of unstable chromosomes in colorectal cancer. Nature reviews. Cancer, 3, 695.
Rajgopal, A., Young, D. W., Mujeeb, K. A., Stein, J. L., Lian, J. B., Van Wijnen, A. J. & Stein, G. S. 2007. Mitotic control of RUNX2 phosphorylation by both CDK1/cyclin B kinase and PP1/PP2A phosphatase in osteoblastic cells. Journal of cellular biochemistry, 100, 1509-1517.
Ramirez-Zacarias, J. L., Castro-Munozledo, F. & Kuri-Harcuch, W. 1992. Quantitation of adipose conversion and triglycerides by staining intracytoplasmic lipids with Oil red O. Histochemistry, 97, 493-497.
Rassmann, K., Schlötterer, C. & Tautz, D. 1991. Isolation of simple-sequence loci for use in polymerase chain reaction-based DNA fingerprinting. Electrophoresis, 12, 113-118.
Ratnakumar, K. & Bernstein, E. 2013. ATRX: the case of a peculiar chromatin remodeler. Epigenetics, 8, 3-9.
Rattan, R., Giri, S., Hartmann, L. C. & Shridhar, V. 2011. Metformin attenuates ovarian cancer cell growth in an AMP-kinase dispensable manner. Journal of cellular and molecular medicine, 15, 166-178.
Rauch, F., Travers, R. & Glorieux, F. H. 2007. Intracortical remodeling during human bone development—a histomorphometric study. Bone, 40, 274-280.
Rauch, T., Wang, Z., Zhang, X., Zhong, X., Wu, X., Lau, S. K., Kernstine, K. H., Riggs, A. D. & Pfeifer, G. P. 2007. Homeobox gene methylation in lung cancer studied by genome-wide analysis with a microarray-based methylated CpG island recovery assay. Proceedings of the National Academy of Sciences, 104, 5527-5532.
Rauch, F. 2012. The dynamics of bone structure development during pubertal growth. J Musculoskelet Neuronal Interact, 12, 1-6.
Reddel, R. R. 2014. Telomere Maintenance Mechanisms in Cancer: Clinical Implications. Current Pharmaceutical Design, 20, 6361-6374.
Reichert, N., Wurster, S., Ulrich, T., Schmitt, K., Hauser, S., Probst, L., Götz, R., Ceteci, F., Moll, R. & Rapp, U. 2010. Lin9, a subunit of the mammalian DREAM complex, is essential for embryonic development, for survival of adult mice, and for tumor suppression. Molecular and cellular biology, 30, 2896-2908.
Reinhardt, H. C. & Schumacher, B. 2012. The p53 network: cellular and systemic DNA damage responses in aging and cancer. Trends in Genetics, 28, 128-136.
Resnick, D. 1995. Tumors and tumor-like lesions of bone: radiographic principles. Diagnosis of bone and joint disorder. 3rd ed. Philadelphia, PA: WB Saunders, 3613-27.
Ribeiro, D. A., Lima, P. L. a. D., Marques, M. E. A. & Salvadori, D. M. F. 2006. Lack of DNA damage induced by fluoride on mouse lymphoma and human fibroblast cells by single cell gel (comet) assay. Brazilian dental journal, 17, 91-94.
Riggi, N., Cironi, L., Provero, P., Suvà, M.-L., Kaloulis, K., Garcia-Echeverria, C., Hoffmann, F., Trumpp, A. & Stamenkovic, I. 2005. Development of Ewing's sarcoma from primary bone marrow–derived mesenchymal progenitor cells. Cancer research, 65, 11459-11468.
Riss, T. L., Moravec, R. A., Niles, A. L., Benink, H. A., Worzella, T. J. & Minor, L. 2015. Cell viability assays.
Rissling, I., Strauch, K., Höft, C., Oertel, W. H. & Möller, J. C. 2009. Haplotype analysis of the engrailed-2 gene in young-onset Parkinson's disease. Neurodegenerative Diseases, 6, 102-105.
Rizzari, C., Bacchiocchi, D., Rovelli, A., Biondi, A., Cantu, -. R. A., Uderzo, C. & Masera, G. 1996. Myelodysplastic syndrome in a child with Rothmund-Thomson syndrome: a case report. Journal of pediatric hematology/oncology, 18, 96-97.
Roberts, R. J. 1987. Restriction enzymes and their isoschizomers. Nucleic acids research, 15, r189-r217.
Robertson, A. B., Klungland, A., Rognes, T. & Leiros, I. 2009. DNA repair in mammalian cells. Cellular and molecular life sciences, 66, 981-993.
Robles, A. I. & Harris, C. C. 2010. Clinical outcomes and correlates of TP53 mutations and cancer. Cold Spring Harbor perspectives in biology, 2, a001016.

Rodier, F., Coppé, J.-P., Patil, C. K., Hoeijmakers, W. A., Muñoz, D. P., Raza, S. R., Freund, A., Campeau, E., Davalos, A. R. & Campisi, J. 2009. Persistent DNA damage signalling triggers senescence-associated inflammatory cytokine secretion. Nature cell biology, 11, 973-979.

Rodríguez, J. P., Montecinos, L., Ríos, S., Reyes, P. & Martínez, J. 2000. Mesenchymal stem cells from osteoporotic patients produce a type I collagen-deficient extracellular matrix favoring adipogenic differentiation. Journal of cellular biochemistry, 79, 557-565.

Rodriguez, R., Tornin, J., Suarez, C., Astudillo, A., Rubio, R., Yauk, C., Williams, A., Rosu-Myles, M., Funes, J. M. & Boshoff, C. 2013. Expression of FUS-CHOP fusion protein in immortalized/transformed human mesenchymal stem cells drives mixoid liposarcoma formation. Stem cells, 31, 2061-2072.

Rodriguez-Acebes, S., Proctor, I., Loddo, M., Wollenschlaeger, A., Rashid, M., Falzon, M., Prevost, A. T., Sainsbury, R., Stoeber, K. & Williams, G. H. 2010. Targeting DNA replication before it starts: Cdc7 as a therapeutic target in p53-mutant breast cancers. The American journal of pathology, 177, 2034-2045.

Rogakou, E. P., Pilch, D. R., Orr, A. H., Ivanova, V. S. & Bonner, W. M. 1998. DNA double-stranded breaks induce histone H2AX phosphorylation on serine 139. Journal of biological chemistry, 273, 5858-5868.

Rogakou, E. P., Boon, C., Redon, C. & Bonner, W. M. 1999. Megabase chromatin domains involved in DNA double-strand breaks in vivo. The Journal of cell biology, 146, 905-916.

Roholl, P. J. M., Blauw, E., Zurcher, C., Dormans, J. & Theuns, H. M. 1994. Evidence for a diminished maturation of preosteoblasts into osteoblasts during aging in rats: an ultrastructural analysis. Journal of Bone and Mineral Research, 9, 355-366.

Roos, W. P., Batista, L. F. Z., Naumann, S. C., Wick, W., Weller, M., Menck, C. F. M. & Kaina, B. 2007. Apoptosis in malignant glioma cells triggered by the temozolomide-induced DNA lesion O6-methylguanine. Oncogene, 26, 186-197.

Roos, W. P. & Kaina, B. 2013. DNA damage-induced cell death: from specific DNA lesions to the DNA damage response and apoptosis. Cancer letters, 332, 237-248.

Roschke, A. V., Glebov, O. K., Lababidi, S., Gehlhaus, K. S., Weinstein, J. N. & Kirsch, I. R. 2008. Chromosomal instability is associated with higher expression of genes implicated in epithelial-mesenchymal transition, cancer invasiveness, and metastasis and with lower expression of genes involved in cell cycle checkpoints, DNA repair, and chromatin maintenance. Neoplasia, 10, 1222-IN26.

Rosen, E. D. & Macdougald, O. A. 2006. Adipocyte differentiation from the inside out. Nature reviews Molecular cell biology, 7, 885-896.

Rosenberg, A. E. 2010. Robbins and Cotran-Pathologic Basis of Disease. Bones, joints and soft tissue tumors. Elsevier.

Røsland, G. V., Svendsen, A., Torsvik, A., Sobala, E., Mccormack, E., Immervoll, H., Mysliwietz, J., Tonn, J.-C., Goldbrunner, R. & Lønning, P. E. 2009. Long-term cultures of bone marrow–derived human mesenchymal stem cells frequently undergo spontaneous malignant transformation. Cancer research, 69, 5331-5339.

Rossi, M. L., Ghosh, A. K., Kulikowicz, T., Croteau, D. L. & Bohr, V. A. 2010. Conserved helicase domain of human RecQ4 is required for strand annealing-independent DNA unwinding. DNA repair, 9, 796-804.

Rothkamm, K. & Horn, S. 2009. gamma-H2AX as protein biomarker for radiation exposure. Ann Ist Super Sanita, 45, 265-71.

Rothmund, A. 1868. Über Cataracten in Verbindung mit einer eigenthümlichen Hautdegeneration. Archiv für Ophthalmologie, 14, 159-182.

Rubio, D., Garcia-Castro, J., Martín, M. C., De La Fuente, R., Cigudosa, J. C., Lloyd, A. C. & Bernad, A. 2005. Spontaneous human adult stem cell transformation. Cancer research, 65, 3035-3039.

Rucci, N. & Teti, A. 2010. 1. Abstract 2. The metastasis process 3. Bone as preferential site of metastasis 4. Osteomimicry 4.1. Osteomimicry in osteolytic bone metastases 4.2. Osteomimicry in osteoblastic bone metastases. Frontiers in bioscience, 2, 907-915.

Rustamov, V., Keller, F., Klicks, J., Hafner, M. and Rudolf, R. 2019. Bone sialoprotein shows enhanced expression in early, high-proliferation stages of three-dimensional

spheroid cell cultures of breast cancer cell line MDA-MB-231. Frontiers in oncology, 9.
Rutkovskiy, A., Stensløkken, K.-O. & Vaage, I. J. 2016. Osteoblast differentiation at a glance. Medical science monitor basic research, 22, 95.
Sadikovic, B., Thorner, P., Chilton-Macneill, S., Martin, J. W., Cervigne, N. K., Squire, J. & Zielenska, M. 2010. Expression analysis of genes associated with human osteosarcoma tumors shows correlation of RUNX2 overexpression with poor response to chemotherapy. Bmc Cancer, 10, 1.
Safford, K. M., Hicok, K. C., Safford, S. D., Halvorsen, Y.-D. C., Wilkison, W. O., Gimble, J. M. & Rice, H. E. 2002. Neurogenic differentiation of murine and human adipose-derived stromal cells. Biochemical and biophysical research communications, 294, 371-379.
Saglam, O., Shah, V. & Worsham, M. J. 2007. Molecular differentiation of early and late stage laryngeal squamous cell carcinoma: an exploratory analysis. Diagnostic Molecular Pathology, 16, 218-221.
Saha, B., Zitnik, G., Johnson, S., Nguyen, Q., Risques, R. A., Martin, G. M. & Oshima, J. 2013. DNA damage accumulation and TRF2 degradation in atypical Werner syndrome fibroblasts with LMNA mutations. Frontiers in Genetics, 4, 129.
Saiki, R. K., Scharf, S., Faloona, F., Mullis, K. B., Horn, G. T., Erlich, H. A. & Arnheim, N. 1985. Enzymatic amplification of b-globin genomic sequences and restriction site analysis for diagnosis of sickle cell anemia. Science, 230, 1350-1354.
Salazar, A. M., Sordo, M. & Ostrosky-Wegman, P. 2009. Relationship between micronuclei formation and p53 induction. Mutation Research/Genetic Toxicology and Environmental Mutagenesis, 672, 124-128.
Salina, D., Enarson, P., Rattner, J. B. & Burke, B. 2003. Nup358 integrates nuclear envelope breakdown with kinetochore assembly. The Journal of cell biology, 162, 991-1001.
Salsi, V., Ferrari, S., Ferraresi, R., Cossarizza, A., Grande, A. & Zappavigna, V. 2009. HOXD13 binds DNA replication origins to promote origin licensing and is inhibited by geminin. Molecular and cellular biology, 29, 5775-5788.
San Filippo, J., Sung, P. & Klein, H. 2008. Mechanism of eukaryotic homologous recombination. Annu. Rev. Biochem., 77, 229-257.
San Martin, I. A., Varela, N., Gaete, M., Villegas, K., Osorio, M., Tapia, J. C., Antonelli, M., Mancilla, E. E., Pereira, B. P. & Nathan, S. S. 2009. Impaired cell cycle regulation of the osteoblast-related heterodimeric transcription factor Runx2-Cbfβ in osteosarcoma cells. Journal of cellular physiology, 221, 560-571.
Sancar, A., Lindsey-Boltz, L. A., Ünsal-Kaçmaz, K. & Linn, S. 2004. Molecular mechanisms of mammalian DNA repair and the DNA damage checkpoints. Annual review of biochemistry, 73, 39-85.
Sanchez, Y., Wong, C., Thoma, R. S., Richman, R., Wu, Z., Piwnica-Worms, H. & Elledge, S. J. 1997. Conservation of the Chk1 checkpoint pathway in mammals: linkage of DNA damage to Cdk regulation through Cdc25. Science, 277, 1497-1501.
Sanchez, Y., Bachant, J., Wang, H., Hu, F., Liu, D., Tetzlaff, M. & Elledge, S. J. 1999. Control of the DNA damage checkpoint by chk1 and rad53 protein kinases through distinct mechanisms. Science, 286, 1166-1171.
Sangrithi, M. N., Bernal, J. A., Madine, M., Philpott, A., Lee, J., Dunphy, W. G. & Venkitaraman, A. R. 2005. Initiation of DNA replication requires the RECQL4 protein mutated in Rothmund-Thomson syndrome. Cell, 121, 887-898.
Santarpia, L., Iwamoto, T., Di Leo, A., Hayashi, N., Bottai, G., Stampfer, M., André, F., Turner, N. C., Symmans, W. F. & Hortobágyi, G. N. 2013. DNA repair gene patterns as prognostic and predictive factors in molecular breast cancer subtypes. The oncologist, 18, 1063-1073.
Santini, D., Pantano, F., Vincenzi, B., Tonini, G. & Bertoldo, F. 2012. The role of bone microenvironment, vitamin D and calcium. Prevention of Bone Metastases. Springer.
Sasaki, K., Murakami, T., Kawasaki, M. & Takahashi, M. 1987. The cell cycle associated change of the Ki-67 reactive nuclear antigen expression. Journal of cellular physiology, 133, 579-584.

Sasi, N. K., Tiwari, K., Soon, F.-F., Bonte, D., Wang, T., Melcher, K., Xu, H. E. & Weinreich, M. 2014. The Potent Cdc7-Dbf4 (DDK) Kinase Inhibitor XL413 Has Limited Activity in Many Cancer Cell Lines and Discovery of Potential New DDK Inhibitor Scaffolds. PLoS ONE, 9, e113300.

Savage, S. A. & Mirabello, L. 2011. Using epidemiology and genomics to understand osteosarcoma etiology. Sarcoma, 2011.

Sbodio, J. I. & Chi, N.-W. 2002. Identification of a Tankyrase-binding Motif Shared by IRAP, TAB182, and Human TRF1 but Not Mouse TRF1 NuMA CONTAINS THIS RXXPDG MOTIF AND IS A NOVEL TANKYRASE PARTNER. Journal of Biological Chemistry, 277, 31887-31892.

Scaduto, R. C. & Grotyohann, L. W. 1999. Measurement of Mitochondrial Membrane Potential Using Fluorescent Rhodamine Derivatives. Biophysical Journal, 76, 469-477.

Schärer, O. D. 2003. Chemistry and biology of DNA repair. Angewandte Chemie International Edition, 42, 2946-2974.

Schärer, O. D. 2013. Nucleotide excision repair in eukaryotes. Cold Spring Harbor perspectives in biology, 5, a012609.

Scheel, C., Schaefer, K.-L., Jauch, A., Keller, M., Wai, D., Brinkschmidt, C., Van Valen, F., Boecker, W., Dockhorn-Dworniczak, B. & Poremba, C. 2001. Alternative lengthening of telomeres is associated with chromosomal instability in osteosarcomas. Oncogene, 20, 3835.

Scherer, L. J. & Rossi, J. J. 2003. Approaches for the sequence-specific knockdown of mRNA. Nature biotechnology, 21, 1457-1465.

Scherjon, S. A., Kleijburg-Van Der Keur, C., Noort, W. A., Claas, F. H. J., Willemze, R., Fibbe, W. E. & Kanhai, H. H. H. 2003. Amniotic fluid as a novel source of mesenchymal stem cells for therapeutic transplantation. Blood, 102, 1548-1549.

Schmidt, M., Scholz, C.-J., Polednik, C. & Roller, J. 2016. Spheroid-based 3-dimensional culture models: Gene expression and functionality in head and neck cancer. Oncology reports, 35, 2431-2440.

Scholzen, T. & Gerdes, J. 2000. The Ki-67 protein: from the known and the unknown. Journal of cellular physiology, 182, 311-322.

Schüring, A. N., Schulte, N., Kelsch, R., Röpke, A., Kiesel, L. & Götte, M. 2011. Characterization of endometrial mesenchymal stem-like cells obtained by endometrial biopsy during routine diagnostics. Fertility and sterility, 95, 423-426.

Schurman, S. H., Hedayati, M., Wang, Z., Singh, D. K., Speina, E., Zhang, Y., Becker, K., Macris, M., Sung, P. & Wilson Iii, D. M. 2009. Direct and indirect roles of RECQL4 in modulating base excision repair capacity. Human molecular genetics, 18, 3470-3483.

Schwab, M. 2008. Encyclopedia of cancer, Springer Science & Business Media.

Sedelnikova, O. A., Horikawa, I., Zimonjic, D. B., Popescu, N. C., Bonner, W. M. & Barrett, J. C. 2004. Senescing human cells and ageing mice accumulate DNA lesions with unrepairable double-strand breaks. Nature cell biology, 6, 168.

Segurado, M. & Diffley, J. F. X. 2008. Separate roles for the DNA damage checkpoint protein kinases in stabilizing DNA replication forks. Genes & Development, 22, 1816-1827.

Seibel, N. M., Eljouni, J., Nalaskowski, M. M. & Hampe, W. 2007. Nuclear localization of enhanced green fluorescent protein homomultimers. Analytical biochemistry, 368, 95-99.

Seifrtová, M., Havelek, R., Ćmielová, J., Jiroutova, A., Soukup, T., Brůčková, L., Mokrý, J., English, D. & Řezáčová, M. 2012. The response of human ectomesenchymal dental pulp stem cells to cisplatin treatment. International endodontic journal, 45, 401-412.

Sekiya, I., Larson, B. L., Vuoristo, J. T., Cui, J. G. & Prockop, D. J. 2004. Adipogenic differentiation of human adult stem cells from bone marrow stroma (MSCs). Journal of Bone and Mineral Research, 19, 256-264.

Selvarajah, S., Yoshimoto, M., Ludkovski, O., Park, P. C., Bayani, J., Thorner, P., Maire, G., Squire, J. A. & Zielenska, M. 2008. Genomic signatures of chromosomal instability and osteosarcoma progression detected by high resolution array CGH and interphase FISH. Cytogenetic and genome research, 122, 5-15.

Sengupta, S., Van Deursen, F., De Piccoli, G. & Labib, K. 2013. Dpb2 integrates the leading-strand DNA polymerase into the eukaryotic replisome. Current Biology, 23, 543-552.
Seo, B., Kim, C., Hills, M., Sung, S., Kim, H., Kim, E., Lim, D. S., Oh, H.-S., Choi, R. M. J. & Chun, J. 2015. Telomere maintenance through recruitment of internal genomic regions. Nature communications, 6.
Serrano-García, L. & Montero-Montoya, R. 2001. Micronuclei and chromatid buds are the result of related genotoxic events. Environmental and molecular mutagenesis, 38, 38-45.
Severino, J., Allen, R. G., Balin, S., Balin, A. & Cristofalo, V. J. 2000. Is β-galactosidase staining a marker of senescence in vitro and in vivo? Experimental cell research, 257, 162-171.
Sfeir, A., Kosiyatrakul, S. T., Hockemeyer, D., Macrae, S. L., Karlseder, J., Schildkraut, C. L. & De Lange, T. 2009. Mammalian telomeres resemble fragile sites and require TRF1 for efficient replication. cell, 138, 90-103.
Shah, N. & Sukumar, S. 2010. The Hox genes and their roles in oncogenesis. Nature Reviews Cancer, 10, 361-371.
Shamanna, R. A., Singh, D. K., Lu, H., Mirey, G., Keijzers, G., Salles, B., Croteau, D. L. & Bohr, V. A. 2014. RECQ helicase RECQL4 participates in non-homologous end joining and interacts with the Ku complex. Carcinogenesis, 35, 2415-2424.
Sharma, A., Singh, K. & Almasan, A. 2012. Histone H2AX phosphorylation: a marker for DNA damage. DNA repair protocols. Springer.
Shaw, P., Bovey, R., Tardy, S., Sahli, R., Sordat, B. & Costa, J. 1992. Induction of apoptosis by wild-type p53 in a human colon tumor-derived cell line. Proceedings of the National Academy of Sciences, 89, 4495-4499.
Shaw, C. S., Jones, D. A. & Wagenmakers, A. J. M. 2008. Network distribution of mitochondria and lipid droplets in human muscle fibres. Histochemistry and cell biology, 129, 65-72.
Shay, J.W. and Wright, W.E. 2004. Senescence and immortalization: role of telomeres and telomerase. Carcinogenesis, 26, 5, 867-874.
Shay, J. W. & Wright, W. E. 2006. Telomerase therapeutics for cancer: challenges and new directions. Nature reviews. Drug discovery, 5, 577.
Shay, J. W. & Wright, W. E. Role of telomeres and telomerase in cancer. 2011 2011. Elsevier, 349-353.
Shay, J.W. and Wright, W.E. 2019. Telomeres and telomerase: three decades of progress. Nature reviews. Genetics.
Sheng, J. Q., Chan, T. L., Chan, Y. W., Huang, J. S., Chen, J. G., Zhang, M. Z., Guo, X. L., Mu, H., Chan, A. S. & Li, S. R. 2006. Microsatellite instability and novel mismatch repair gene mutations in northern Chinese population with Hereditary non-polyposis colorectal cancer. Journal of Digestive Diseases, 7, 197-205.
Sherwood, S. W., Rush, D., Ellsworth, J. L. & Schimke, R. T. 1988. Defining cellular senescence in IMR-90 cells: a flow cytometric analysis. Proceedings of the National Academy of Sciences, 85, 9086-9090.
Shi, N., Xie, W.-B. & Chen, S.-Y. 2012. Cell division cycle 7 is a novel regulator of transforming growth factor-β-induced smooth muscle cell differentiation. Journal of Biological Chemistry, 287, 6860-6867.
Shieh, S.-Y., Ahn, J., Tamai, K., Taya, Y. & Prives, C. 2000. The human homologs of checkpoint kinases Chk1 and Cds1 (Chk2) phosphorylate p53 at multiple DNA damage-inducible sites. Genes & development, 14, 289-300.
Shimada, M., Niida, H., Zineldeen, D. H., Tagami, H., Tanaka, M., Saito, H. & Nakanishi, M. 2008. Chk1 is a histone H3 threonine 11 kinase that regulates DNA damage-induced transcriptional repression. Cell, 132, 221-232.
Shimizu, N., Itoh, N., Utiyama, H. & Wahl, G. M. 1998. Selective entrapment of extrachromosomally amplified DNA by nuclear budding and micronucleation during S phase. The Journal of cell biology, 140, 1307-1320.
Shimizu, N., Shimura, T. & Tanaka, T. 2000. Selective elimination of acentric double minutes from cancer cells through the extrusion of micronuclei. Mutation Research/Fundamental and Molecular Mechanisms of Mutagenesis, 448, 81-90.

Shimizu, T., Tanaka, T., Iso, T., Matsui, H., Ooyama, Y., Kawai-Kowase, K., Arai, M. & Kurabayashi, M. 2011. Notch signaling pathway enhances bone morphogenetic protein 2 (BMP2) responsiveness of Msx2 gene to induce osteogenic differentiation and mineralization of vascular smooth muscle cells. Journal of Biological Chemistry, 286, 19138-19148.

Shinya, A., Nishigori, C., Moriwaki, S.-I., Takebe, H., Kubota, M., Ogino, A. & Imamura, S. 1993. A case of Rothmund-Thomson syndrome with reduced DNA repair capacity. Archives of dermatology, 129, 332-336.

Siddiqui, J. A. & Partridge, N. C. 2016. Physiological bone remodeling: systemic regulation and growth factor involvement. Physiology, 31, 233-245.

Sidorova, J. M., Kehrli, K., Mao, F. & Monnat, R. 2013. Distinct functions of human RECQ helicases WRN and BLM in replication fork recovery and progression after hydroxyurea-induced stalling. DNA repair, 12, 128-139.

Sidorova, J.M. and Monnat Jr, R.J. 2015. Human RECQ helicases: roles in cancer, aging, and inherited disease. Advances in. Genomics Genetics, 5, 19-33.

Siitonen, A. 2008. Molecular genetics of RECQL4 syndromes. Kansanterveyslaitoksen julkaisuja. A: A

Siitonen, H. A., Kopra, O., Kääriäinen, H., Haravuori, H., Winter, R. M., Säämänen, A.-M., Peltonen, L. & Kestilä, M. 2003. Molecular defect of RAPADILINO syndrome expands the phenotype spectrum of RECQL diseases. Human molecular genetics, 12, 2837-2844.

Siitonen, H. A., Sotkasiira, J., Biervliet, M., Benmansour, A., Capri, Y., Cormier-Daire, V., Crandall, B., Hannula-Jouppi, K., Hennekam, R. & Herzog, D. 2009. The mutation spectrum in RECQL4 diseases. European journal of human genetics, 17, 151-158.

Sillitoe, R. V., Stephen, D., Lao, Z. & Joyner, A. L. 2008. Engrailed homeobox genes determine the organization of Purkinje cell sagittal stripe gene expression in the adult cerebellum. The Journal of Neuroscience, 28, 12150-12162.

Silva, J. M., Mizuno, H., Brady, A., Lucito, R. & Hannon, G. J. 2004. RNA interference microarrays: high-throughput loss-of-function genetics in mammalian cells. Proceedings of the National Academy of Sciences of the United States of America, 101, 6548-6552.

Sim, F. H., Devries, E. M. G., Miser, J. S. & Unni, K. K. 1992. Case report 760. Skeletal radiology, 21, 543-545.

Simmons, C. A., Matlis, S., Thornton, A. J., Chen, S., Wang, C.-Y. & Mooney, D. J. 2003. Cyclic strain enhances matrix mineralization by adult human mesenchymal stem cells via the extracellular signal-regulated kinase (ERK1/2) signaling pathway. Journal of biomechanics, 36, 1087-1096.

Simon, T., Kohlhase, J., Wilhelm, C., Kochanek, M., De Carolis, B. & Berthold, F. 2010. Multiple malignant diseases in a patient with Rothmund–Thomson syndrome with RECQL4 mutations: Case report and literature review. American Journal of Medical Genetics Part A, 152, 1575-1579.

Simpson, J. C., Wellenreuther, R., Poustka, A., Pepperkok, R. & Wiemann, S. 2000. Systematic subcellular localization of novel proteins identified by large-scale cDNA sequencing. EMBO reports, 1, 287-292.

Sims, N. A. & Martin, T. J. 2014. Coupling the activities of bone formation and resorption: a multitude of signals within the basic multicellular unit. BoneKEy Rep, 3.

Singer, M. 2014. The role of mitochondrial dysfunction in sepsis-induced multi-organ failure. Virulence, 5, 66-72.

Singh, D. K., Karmakar, P., Aamann, M., Schurman, S. H., May, A., Croteau, D. L., Burks, L., Plon, S. E. & Bohr, V. A. 2010. The involvement of human RECQL4 in DNA double strand break repair. Aging cell, 9, 358-371.

Singh, D. K., Popuri, V., Kulikowicz, T., Shevelev, I., Ghosh, A. K., Ramamoorthy, M., Rossi, M. L., Janscak, P., Croteau, D. L. & Bohr, V. A. 2012. The human RecQ helicases BLM and RECQL4 cooperate to preserve genome stability. Nucleic acids research, 40, 6632-6648.

Singh, S., Vaughan, C. A., Frum, R. A., Grossman, S. R., Deb, S. & Palit Deb, S. 2017. Mutant p53 establishes targetable tumor dependency by promoting unscheduled replication. The Journal of Clinical Investigation, 127, 1839-1855.

Smith, P. J. & Paterson, M. C. 1982. Enhanced radiosensitivity and defective DNA repair in cultured fibroblasts derived from Rothmund Thomson syndrome patients. Mutation Research/Fundamental and Molecular Mechanisms of Mutagenesis, 94, 213-228.
Sobecki, M., Mrouj, K., Camasses, A., Parisis, N., Nicolas, E., Llères, D., Gerbe, F., Prieto, S., Krasinska, L., David, A., Eguren, M., Birling, M.-C., Urbach, S., Hem, S., Déjardin, J., Malumbres, M., Jay, P., Dulic, V., Lafontaine, D. L. J., Feil, R. & Fisher, D. 2016. The cell proliferation antigen Ki-67 organises heterochromatin. eLife, 5, e13722.
Sobecki, M., Mrouj, K., Colinge, J., Gerbe, F., Jay, P., Krasinska, L., Dulic, V. & Fisher, D. 2017. Cell-cycle regulation accounts for variability in Ki-67 expression levels. Cancer research, 77, 2722-2734.
Solomon, H., Sharon, M. & Rotter, V. 2014. Modulation of alternative splicing contributes to cancer development: focusing on p53 isoforms, p53β and p53γ. Cell death and differentiation, 21, 1347.
Somaiah, C., Kumar, A., Mawrie, D., Sharma, A., Patil, S. D., Bhattacharyya, J., Swaminathan, R. & Jaganathan, B. G. 2015. Collagen promotes higher adhesion, survival and proliferation of mesenchymal stem cells. PloS one, 10, e0145068.
Song, B.-Q., Chi, Y., Li, X., Du, W.-J., Han, Z.-B., Tian, J.-J., Li, J.-J., Chen, F., Wu, H.-H. & Han, L.-X. 2015. Inhibition of notch signaling promotes the adipogenic differentiation of mesenchymal stem cells through autophagy activation and PTEN-PI3K/AKT/mTOR pathway. Cellular Physiology and Biochemistry, 36, 1991-2002.
Sonnenschein, C. & Soto, A. M. Theories of carcinogenesis: an emerging perspective. 2008 2008. Elsevier, 372-377.
Sørensen, C. S., Hansen, L. T., Dziegielewski, J., Syljuåsen, R. G., Lundin, C., Bartek, J. & Helleday, T. 2005. The cell-cycle checkpoint kinase Chk1 is required for mammalian homologous recombination repair. Nature cell biology, 7, 195-201.
Spinella-Jaegle, S., Rawadi, G., Kawai, S., Gallea, S., Faucheu, C., Mollat, P., Courtois, B., Bergaud, B., Ramez, V. & Blanchet, A. M. 2001. Sonic hedgehog increases the commitment of pluripotent mesenchymal cells into the osteoblastic lineage and abolishes adipocytic differentiation. Journal of cell science, 114, 2085-2094.
Spurney, C., Gorlick, R., Meyers, P. A., Healey, J. H. & Huvos, A. G. 1998. Multicentric osteosarcoma, Rothmund-Thomson syndrome, and secondary nasopharyngeal non-Hodgkin's lymphoma: a case report and review of the literature. Journal of pediatric hematology/oncology, 20, 494-497.
Squier, C. A., Ghoneim, S. & Kremenak, C. R. 1990. Ultrastructure of the periosteum from membrane bone. Journal of anatomy, 171, 233.
Stacey, G. N., Byrne, E. & Hawkins, J. R. 2014. DNA profiling and characterization of animal cell lines. Animal Cell Biotechnology: Methods and Protocols, 57-73.
Stanford, C. M., Jacobson, P. A., Eanes, E. D., Lembke, L. A. & Midura, R. J. 1995. Rapidly forming apatitic mineral in an osteoblastic cell line (UMR 10601 BSP). Journal of Biological Chemistry, 270, 9420-9428.
Stein, G. S., Lian, J. B., Van Wijnen, A. J., Stein, J. L., Montecino, M., Javed, A., Zaidi, S. K., Young, D. W., Choi, J.-Y. & Pockwinse, S. M. 2004. Runx2 control of organization, assembly and activity of the regulatory machinery for skeletal gene expression. Oncogene, 23, 4315.
Stenderup, K., Justesen, J., Clausen, C. & Kassem, M. 2003. Aging is associated with decreased maximal life span and accelerated senescence of bone marrow stromal cells. Bone, 33, 919-926.
Stephenson, E. M. 1982. Locomotory invasion of human cervical epithelium and avian fibroblasts by HeLa cells in vitro. Journal of cell science, 57, 293-314.
Stern, B. & Nurse, P. 1996. A quantitative model for the cdc2 control of S phase and mitosis in fission yeast. Trends in Genetics, 12, 345-350.
Stiller, C. 2007. Childhood Cancer in Britain: Incidence. Survival, Mortality.
Stinco, G., Governatori, G., Mattighello, P. & Patrone, P. 2008. Multiple cutaneous neoplasms in a patient with Rothmund–Thomson syndrome: case report and published work review. The Journal of dermatology, 35, 154-161.

Strem, B. M., Hicok, K. C., Zhu, M., Wulur, I., Alfonso, Z., Schreiber, R. E., Fraser, J. K. & Hedrick, M. H. 2005. Multipotential differentiation of adipose tissue-derived stem cells. Keio journal of medicine, 54, 132.

Su, Y., Meador, J. A., Calaf, G. M., De-Santis, L. P., Zhao, Y., Bohr, V. A. & Balajee, A. S. 2010. Human RecQL4 helicase plays critical roles in prostate carcinogenesis. Cancer research, 70, 9207-9217.

Sun, Z., Wang, S. & Zhao, R. C. 2014. The roles of mesenchymal stem cells in tumor inflammatory microenvironment. Journal of hematology & oncology, 7, 14.

Svilar, D., Goellner, E. M., Almeida, K. H. & Sobol, R. W. 2011. Base excision repair and lesion-dependent subpathways for repair of oxidative DNA damage. Antioxidants & redox signaling, 14, 2491-2507.

Symeonidou, I.-E., Taraviras, S. & Lygerou, Z. 2012. Control over DNA replication in time and space. FEBS letters, 586, 2803-2812.

Szekely, A. M., Bleichert, F., Nümann, A., Van Komen, S., Manasanch, E., Nasr, A. B., Canaan, A. & Weissman, S. M. 2005. Werner protein protects nonproliferating cells from oxidative DNA damage. Molecular and cellular biology, 25, 10492-10506.

Ta, H. T., Dass, C. R., Choong, P. F. M. & Dunstan, D. E. 2009. Osteosarcoma treatment: state of the art. Cancer and Metastasis Reviews, 28, 247-263.

Taddei, M. L., Giannoni, E., Fiaschi, T. & Chiarugi, P. 2012. Anoikis: an emerging hallmark in health and diseases. The Journal of pathology, 226, 380-393.

Taitz, J., Cohn, R. J., White, L., Russell, S. J. & Vowels, M. R. 2004. Osteochondroma after total body irradiation: An age-related complication. Pediatric blood & cancer, 42, 225-229.

Takai, H., Tominaga, K., Motoyama, N., Minamishima, Y. A., Nagahama, H., Tsukiyama, T., Ikeda, K., Nakayama, K., Nakanishi, M. & Nakayama, K.-I. 2000. Aberrant cell cycle checkpoint function and early embryonic death in Chk1−/− mice. Genes & development, 14, 1439-1447.

Takai, H., Smogorzewska, A. & De Lange, T. 2003. DNA damage foci at dysfunctional telomeres. Current Biology, 13, 1549-1556.

Takai E, C. K., Shaheen a, Hung Ct, Guo Xe 2005. Osteoblast elastic modulus measured by atomic force microscopy is substrate dependent. Ann Biomed Eng, 33, 963–71.

Takai, Y., Miyoshi, J., Ikeda, W. & Ogita, H. 2008. Nectins and nectin-like molecules: roles in contact inhibition of cell movement and proliferation. Nature Reviews Molecular Cell Biology, 9, 603-615.

Tanaka, S. & Araki, H. 2011. Multiple regulatory mechanisms to inhibit untimely initiation of DNA replication are important for stable genome maintenance. PLoS Genet, 7, e1002136.

Tanaka, S., Komeda, Y., Umemori, T., Kubota, Y., Takisawa, H. & Araki, H. 2013. Efficient initiation of DNA replication in eukaryotes requires Dpb11/TopBP1-GINS interaction. Molecular and cellular biology, 33, 2614-2622.

Tanck, E., Hannink, G., Ruimerman, R., Buma, P., Burger, E. H. & Huiskes, R. 2006. Cortical bone development under the growth plate is regulated by mechanical load transfer. Journal of anatomy, 208, 73-79.

Tang, J., Erikson, R. L. & Liu, X. 2006. Checkpoint kinase 1 (Chk1) is required for mitotic progression through negative regulation of polo-like kinase 1 (Plk1). Proceedings of the National Academy of Sciences, 103, 11964-11969.

Tang, N., Song, W.-X., Luo, J., Haydon, R. C. & He, T.-C. 2008. Osteosarcoma development and stem cell differentiation. Clinical orthopaedics and related research, 466, 2114-2130.

Tanida, T., Matsuda, K. I., Yamada, S., Hashimoto, T. & Kawata, M. 2015. Estrogen-related Receptor β Reduces the Subnuclear Mobility of Estrogen Receptor α and Suppresses Estrogen-dependent Cellular Function. Journal of Biological Chemistry, 290, 12332-12345.

Tataria, M., Quarto, N., Longaker, M. T. & Sylvester, K. G. 2006. Absence of the p53 tumor suppressor gene promotes osteogenesis in mesenchymal stem cells. Journal of pediatric surgery, 41, 624-632.

Taxman, D. J., Moore, C. B., Guthrie, E. H. & Huang, M. T.-H. 2010. Short hairpin RNA (shRNA): design, delivery, and assessment of gene knockdown. RNA Therapeutics: Function, Design, and Delivery, 139-156.
Taylor, W. B. 1957. Rothmund's Syndrome—Thomson's Syndrome: Congenital Poikiloderma With or Without Juvenile Cataracts A Review of the Literature, Report of a Case, and Discussion of the Relationship of the Two Syndromes. AMA archives of dermatology, 75, 236-244.
Taylor, S. S. & Mckeon, F. 1997. Kinetochore localization of murine Bub1 is required for normal mitotic timing and checkpoint response to spindle damage. Cell, 89, 727-735.
Taylor, M. J., Perrais, D. & Merrifield, C. J. 2011. A high precision survey of the molecular dynamics of mammalian clathrin-mediated endocytosis. PLoS biology, 9, e1000604.
Terradas, M., Martín, M. & Genescà, A. 2016. Impaired nuclear functions in micronuclei results in genome instability and chromothripsis. Archives of toxicology, 90, 2657.
Tesser-Gamba, F., Petrilli, A. S., De Seixas Alves, M. T., Garcia Filho, R. J., Juliano, Y. & Toledo, S. R. C. 2012. MAPK7 and MAP2K4 as prognostic markers in osteosarcoma. Human pathology, 43, 994-1002.
Thomas, D. M., Carty, S. A., Piscopo, D. M., Lee, J.-S., Wang, W.-F., Forrester, W. C. & Hinds, P. W. 2001. The retinoblastoma protein acts as a transcriptional coactivator required for osteogenic differentiation. Molecular cell, 8, 303-316.
Thomas, D. M., Johnson, S. A., Sims, N. A., Trivett, M. K., Slavin, J. L., Rubin, B. P., Waring, P., Mcarthur, G. A., Walkley, C. R. & Holloway, A. J. 2004. Terminal osteoblast differentiation, mediated by runx2 and p27KIP1, is disrupted in osteosarcoma. J Cell Biol, 167, 925-934.
Thomassen, M., Tan, Q. & Kruse, T. A. 2009. Gene expression meta-analysis identifies chromosomal regions and candidate genes involved in breast cancer metastasis. Breast cancer research and treatment, 113, 239-249.
Thompson, B. J. 2013. Cell polarity: models and mechanisms from yeast, worms and flies. Development, 140, 13-21.
Thomson, M. S. 1936. Poikiloderma congenitale: two cases for diagnosis. SAGE Publications.
Tichy, E. D., Liang, L., Deng, L., Tischfield, J., Schwemberger, S., Babcock, G. & Stambrook, P. J. 2011. Mismatch and base excision repair proficiency in murine embryonic stem cells. DNA repair, 10, 445-451.
Timper, K., Seboek, D., Eberhardt, M., Linscheid, P., Christ-Crain, M., Keller, U., Müller, B. & Zulewski, H. 2006. Human adipose tissue-derived mesenchymal stem cells differentiate into insulin, somatostatin, and glucagon expressing cells. Biochemical and biophysical research communications, 341, 1135-1140.
Tirode, F., Surdez, D., Ma, X., Parker, M., Le Deley, M. C., Bahrami, A., Zhang, Z., Lapouble, E., Grossetête-Lalami, S. & Rusch, M. 2014. Genomic landscape of Ewing sarcoma defines an aggressive subtype with co-association of STAG2 and TP53 mutations. Cancer discovery, 4, 1342-1353.
Tolar, J., Nauta, A. J., Osborn, M. J., Panoskaltsis Mortari, A., Mcelmurry, R. T., Bell, S., Xia, L., Zhou, N., Riddle, M. & Schroeder, T. M. 2007. Sarcoma derived from cultured mesenchymal stem cells. Stem cells, 25, 371-379.
Torsvik, A., Røsland, G. V., Svendsen, A., Molven, A., Immervoll, H., Mccormack, E., Lønning, P. E., Primon, M., Sobala, E. & Tonn, J.-C. 2010. Spontaneous malignant transformation of human mesenchymal stem cells reflects cross-contamination: putting the research field on track–letter. Cancer Research, 70, 6393-6396.
Trinkle-Mulcahy, L., Boulon, S., Lam, Y. W., Urcia, R., Boisvert, F.-M., Vandermoere, F., Morrice, N. A., Swift, S., Rothbauer, U., Leonhardt, H. & Lamond, A. 2008. Identifying specific protein interaction partners using quantitative mass spectrometry and bead proteomes. The Journal of Cell Biology, 183, 223-239.
Tsai, Y.-L., Tseng, S.-F., Chang, S.-H., Lin, C.-C. & Teng, S.-C. 2002. Involvement of replicative polymerases, Tel1p, Mec1p, Cdc13p, and the Ku complex in telomere-telomere recombination. Molecular and cellular biology, 22, 5679-5687.

Tsai, M. S., Lee, J. L., Chang, Y. J. & Hwang, S. M. 2004. Isolation of human multipotent mesenchymal stem cells from second-trimester amniotic fluid using a novel two-stage culture protocol. Human reproduction, 19, 1450-1456.
Tsuji, W., Inamoto, T., Yamashiro, H., Ueno, T., Kato, H., Kimura, Y., Tabata, Y. & Toi, M. 2008. Adipogenesis induced by human adipose tissue–derived stem cells. Tissue Engineering Part A, 15, 83-93.
Tsurusawa, M., Ito, M., Zha, Z., Kawai, S., Takasaki, Y. & Fujimoto, T. 1992. Cell-cycle-associated expressions of proliferating cell nuclear antigen and Ki-67 reactive antigen of bone marrow blast cells in childhood acute leukemia. Leukemia, 6, 669-674.
Tu, W.-Z., Li, B., Huang, B., Wang, Y., Liu, X.-D., Guan, H., Zhang, S.-M., Tang, Y., Rang, W.-Q. & Zhou, P.-K. 2013. γH2AX foci formation in the absence of DNA damage: Mitotic H2AX phosphorylation is mediated by the DNA-PKcs/CHK2 pathway. FEBS Letters, 587, 3437-3443.
Tubbs, J. L., Latypov, V., Kanugula, S., Butt, A., Melikishvili, M., Kraehenbuehl, R., Fleck, O., Marriott, A., Watson, A. J. & Verbeek, B. 2009. Alkylated DNA damage flipping bridges base and nucleotide excision repair. Nature, 459, 808.
Tudzarova, S., Trotter, M. W., Wollenschlaeger, A., Mulvey, C., Godovac-Zimmermann, J., Williams, G. H. & Stoeber, K. 2010. Molecular architecture of the DNA replication origin activation checkpoint. The EMBO journal, 29, 3381-3394.
Turley, E. A., Wood, D. K. & Mccarthy, J. B. 2016. Carcinoma cell hyaluronan as a “portable” cancerized prometastatic microenvironment. Cancer research, 76, 2507-2512.
Turnpenny, P. D. & Ellard, S. 2016. Emery's Elements of Medical Genetics E-Book, Elsevier Health Sciences.
Tyagi, R., Dey, P., Uppal, R. & Rajwanshi, A. 2015. Analysis of morphological markers of chromosomal instability in ascitic fluid. Diagnostic cytopathology, 43, 855-858.
Uccelli, A., Moretta, L. & Pistoia, V. 2008. Mesenchymal stem cells in health and disease. Nature reviews. Immunology, 8, 726.
Uematsu, N., Weterings, E., Yano, K.-I., Morotomi-Yano, K., Jakob, B., Taucher-Scholz, G., Mari, P.-O., Van Gent, D. C., Chen, B. P. C. & Chen, D. J. 2007. Autophosphorylation of DNA-PKCS regulates its dynamics at DNA double-strand breaks. The Journal of cell biology, 177, 219-229.
Uhlmann, F., Bouchoux, C. & López-Avilés, S. 2011. A quantitative model for cyclin-dependent kinase control of the cell cycle: revisited. Phil. Trans. R. Soc. B, 366, 3572-3583.
Ullah, I., Subbarao, R. B. & Rho, G. J. 2015. Human mesenchymal stem cells-current trends and future prospective. Bioscience reports, 35, e00191.
Unni, K. K. 1996. Dahlin's bone tumors: general aspects and data on 11,087 cases, Lippincott Williams & Wilkins.
Uritu, C. M., Varganici, C. D., Ursu, L., Coroaba, A., Nicolescu, A., Dascalu, A. I., Peptanariu, D., Stan, D., Constantinescu, C. A. & Simion, V. 2015. Hybrid fullerene conjugates as vectors for DNA cell-delivery. Journal of Materials Chemistry B, 3, 2433-2446.
Utani, K.-I., Kohno, Y., Okamoto, A. & Shimizu, N. 2010. Emergence of micronuclei and their effects on the fate of cells under replication stress. PLoS One, 5, e10089.
Valko, M., Rhodes, C. J., Moncol, J., Izakovic, M. M. & Mazur, M. 2006. Free radicals, metals and antioxidants in oxidative stress-induced cancer. Chemico-biological interactions, 160, 1-40.
Vallee, M., Côté, J. F. & Fradette, J. 2009. Adipose-tissue engineering: taking advantage of the properties of human adipose-derived stem/stromal cells. Pathologie Biologie, 57, 309-317.
Van Der Deen, M., Akech, J., Lapointe, D., Gupta, S., Young, D. W., Montecino, M. A., Galindo, M., Lian, J. B., Stein, J. L. & Stein, G. S. 2012. Genomic promoter occupancy of runt-related transcription factor RUNX2 in Osteosarcoma cells identifies genes involved in cell adhesion and motility. Journal of Biological Chemistry, 287, 4503-4517.

Van Jaarsveld, M.T., Deng, D., Wiemer, E.A. & Zi, Z. 2019. Tissue-Specific Chk1 Activation Determines Apoptosis by Regulating the Balance of p53 and p21. iScience, 12, 27-40.

Van Maldergem, L., Siitonen, H. A., Jalkh, N., Chouery, E., De Roy, M., Delague, V., Muenke, M., Jabs, E. W., Cai, J. & Wang, L. L. 2006. Revisiting the craniosynostosis-radial ray hypoplasia association: Baller-Gerold syndrome caused by mutations in the RECQL4 gene. Journal of medical genetics, 43, 148-152.

Vander Heiden, M. G., Chandel, N. S., Williamson, E. K., Schumacker, P. T. & Thompson, C. B. 1997. Bcl-xL Regulates the Membrane Potential and Volume Homeostasis of Mitochondria. Cell, 91, 627-637.

Vanotti, E., Amici, R., Bargiotti, A., Berthelsen, J., Bosotti, R., Ciavolella, A., Cirla, A., Cristiani, C., D'alessio, R. & Forte, B. 2008. Cdc7 kinase inhibitors: pyrrolopyridinones as potential antitumor agents. 1. Synthesis and structure–activity relationships. Journal of medicinal chemistry, 51, 487-501.

Varughese, M., Leavey, P., Smith, P., Sneath, R., Breatnach, F. & O'meara, A. 1992. Osteogenic sarcoma and Rothmund Thomson syndrome. Journal of cancer research and clinical oncology, 118, 389-390.

Varum, S., Rodrigues, A. S., Moura, M. B., Momcilovic, O., Easley Iv, C. A., Ramalho-Santos, J., Van Houten, B. & Schatten, G. 2011. Energy metabolism in human pluripotent stem cells and their differentiated counterparts. PloS one, 6, e20914.

Vasseur, F., Delaporte, E., Zabot, M., Sturque, M., Barrut, D., Savary, J., Thomas, L. & Thomas, P. 1999. Excision repair defect in Rothmund Thomson syndrome. ACTA DERMATOVENEREOLOGICA-STOCKHOLM-, 79, 150-152.

Vater, C., Kasten, P. & Stiehler, M. 2011. Culture media for the differentiation of mesenchymal stromal cells. Acta biomaterialia, 7, 463-477.

Velletri, T., Xie, N., Wang, Y., Huang, Y., Yang, Q., Chen, X., Chen, Q., Shou, P., Gan, Y. & Cao, G. 2016. P53 functional abnormality in mesenchymal stem cells promotes osteosarcoma development. Cell death & disease, 7, e2015.

Vennos, E. M., Collins, M. & James, W. D. 1992. Rothmund-Thomson syndrome: review of the world literature. Journal of the American Academy of Dermatology, 27, 750-762.

Verma, S., Rajaratnam, J. H., Denton, J., Hoyland, J. A. & Byers, R. J. 2002. Adipocytic proportion of bone marrow is inversely related to bone formation in osteoporosis. Journal of clinical pathology, 55, 693-698.

Verma, S. & Dey, P. 2014. Correlation of morphological markers of chromosomal instability in fine needle aspiration cytology with grade of breast cancer. Cytopathology, 25, 259-263.

Verstraeten, V. L. R. M., Peckham, L. A., Olive, M., Capell, B. C., Collins, F. S., Nabel, E. G., Young, S. G., Fong, L. G. & Lammerding, J. 2011. Protein farnesylation inhibitors cause donut-shaped cell nuclei attributable to a centrosome separation defect. Proceedings of the National Academy of Sciences, 108, 4997-5002.

Vi, L., Baht, G. S., Whetstone, H., Ng, A., Wei, Q., Poon, R., Mylvaganam, S., Grynpas, M. & Alman, B. A. 2015. Macrophages promote osteoblastic differentiation in vivo: implications in fracture repair and bone homeostasis. Journal of Bone and Mineral Research, 30, 1090-1102.

Visinoni, A. F., Lisboa-Costa, T., Pagnan, N. a. B. & Chautard-Freire-Maia, E. A. 2009. Ectodermal dysplasias: clinical and molecular review. American Journal of Medical Genetics Part A, 149, 1980-2002.

Vladimirova, V., Waha, A., Lückerath, K., Pesheva, P. & Probstmeier, R. 2008. Runx2 is expressed in human glioma cells and mediates the expression of galectin-3. Journal of neuroscience research, 86, 2450-2461.

Vukovic, B., Beheshti, B., Park, P., Lim, G., Bayani, J., Zielenska, M. & Squire, J. A. 2007. Correlating breakage-fusion-bridge events with the overall chromosomal instability and in vitro karyotype evolution in prostate cancer. Cytogenetic and genome research, 116, 1-11.

Wagner, W., Wein, F., Seckinger, A., Frankhauser, M., Wirkner, U., Krause, U., Blake, J., Schwager, C., Eckstein, V. & Ansorge, W. 2005. Comparative characteristics of mesenchymal stem cells from human bone marrow, adipose tissue, and umbilical cord blood. Experimental hematology, 33, 1402-1416.

Wagner, E. R., Luther, G., Zhu, G., Luo, Q., Shi, Q., Kim, S. H., Gao, J.-L., Huang, E., Gao, Y. & Yang, K. 2011. Defective osteogenic differentiation in the development of osteosarcoma. Sarcoma, 2011.
Walker, J. A., Boreham, D. R., Unrau, P. & Duncan, A. M. V. 1996. Chromosome content and ultrastructure of radiation-induced micronuclei. Mutagenesis, 11, 419-424.
Walkley, C. R., Qudsi, R., Sankaran, V. G., Perry, J. A., Gostissa, M., Roth, S. I., Rodda, S. J., Snay, E., Dunning, P. & Fahey, F. H. 2008. Conditional mouse osteosarcoma, dependent on p53 loss and potentiated by loss of Rb, mimics the human disease. Genes & development, 22, 1662-1676.
Wallace, S. S., Murphy, D. L. & Sweasy, J. B. 2012. Base excision repair and cancer. Cancer letters, 327, 73-89.
Walther, A., Houlston, R. & Tomlinson, I. 2008. Association between chromosomal instability and prognosis in colorectal cancer: a meta-analysis. Gut.
Wanet, A., Arnould, T., Najimi, M. & Renard, P. 2015. Connecting mitochondria, metabolism, and stem cell fate. Stem cells and development, 24, 1957-1971.
Wang, J. C. 1985. DNA topoisomerases. Annual review of biochemistry, 54, 665-697.
Wang, S., Wang, Q., Crute, B., Melnikova, I., Keller, S. & Speck, N. 1993. Cloning and characterization of subunits of the T-cell receptor and murine leukemia virus enhancer core-binding factor. Molecular and cellular biology, 13, 3324-3339.
Wang, L. L., Levy, M. L., Lewis, R. A., Chintagumpala, M. M., Lev, D., Rogers, M. & Plon, S. E. 2001. Clinical manifestations in a cohort of 41 Rothmund-Thomson syndrome patients. American journal of medical genetics, 102, 11-17.
Wang, J. C. 2002. Cellular roles of DNA topoisomerases: a molecular perspective. Nature reviews Molecular cell biology, 3, 430-440.
Wang, B., Matsuoka, S., Carpenter, P. B. & Elledge, S. J. 2002a. 53BP1, a mediator of the DNA damage checkpoint. Science, 298, 1435-1438.
Wang, L. L., Worley, K., Gannavarapu, A., Chintagumpala, M. M., Levy, M. L. & Plon, S. E. 2002b. Intron-size constraint as a mutational mechanism in Rothmund-Thomson syndrome. The American Journal of Human Genetics, 71, 165-167.
Wang, L. L., Gannavarapu, A., Kozinetz, C. A., Levy, M. L., Lewis, R. A., Chintagumpala, M. M., Ruiz-Maldanado, R., Contreras-Ruiz, J., Cunniff, C. & Erickson, R. P. 2003. Association between osteosarcoma and deleterious mutations in the RECQL4 gene in Rothmund–Thomson syndrome. Journal of the National Cancer Institute, 95, 669-674.
Wang, R. C., Smogorzewska, A. & De Lange, T. 2004. Homologous recombination generates T-loop-sized deletions at human telomeres. Cell, 119, 355-368.
Wang, Y. U. E., Liu, V. W., Ngan, H. & Nagley, P. 2005. Frequent Occurrence of Mitochondrial Microsatellite Instability in the D-Loop Region of Human Cancers. Annals of the New York Academy of Sciences, 1042, 123-129.
Wang, P., Henning, S. M. & Heber, D. 2010. Limitations of MTT and MTS-Based Assays for Measurement of Antiproliferative Activity of Green Tea Polyphenols. PLoS ONE, 5, e10202.
Wang, E., Zou, J., Zaman, N., Beitel, L. K., Trifiro, M. & Paliouras, M. 2013a. Cancer systems biology in the genome sequencing era: Part 1, dissecting and modeling of tumor clones and their networks. Seminars in Cancer Biology, Elsevier, 279-285.
Wang, E., Zou, J., Zaman, N., Beitel, L. K., Trifiro, M. & Paliouras, M. 2013b. Cancer systems biology in the genome sequencing era: Part 2, evolutionary dynamics of tumor clonal networks and drug resistance. Seminars in Cancer Biology, Elsevier, 286-292.
Wang, Y., Wang, F., Zhao, H., Zhang, X., Chen, H. & Zhang, K. 2014a. Human adipose-derived mesenchymal stem cells are resistant to HBV infection during differentiation into hepatocytes in vitro. International journal of molecular sciences, 15, 6096-6110.
Wang, J.-T., Xu, X., Alontaga, A. Y., Chen, Y. & Liu, Y. 2014b. Impaired p32 regulation caused by the lymphoma-prone RECQ4 mutation drives mitochondrial dysfunction. Cell reports, 7, 848-858.
Wang, Y., Chu, Y., Yue, B., Ma, X., Zhang, G., Xiang, H., Liu, Y., Wang, T., Wu, X. & Chen, B. 2017a. Adipose-derived mesenchymal stem cells promote osteosarcoma

proliferation and metastasis by activating the STAT3 pathway. Oncotarget, 8, 23803.
Wang, Y., Wang, W., Wang, N., Tall, A. R. & Tabas, I. 2017b. Mitochondrial Oxidative Stress Promotes Atherosclerosis and Neutrophil Extracellular Traps in Aged Mice. Arteriosclerosis, Thrombosis, and Vascular Biology, ATVBAHA-117.
Ward, I. M. & Chen, J. 2001. Histone H2AX is phosphorylated in an ATR-dependent manner in response to replicational stress. Journal of Biological Chemistry, 276, 47759-47762.
Ward, I. M., Reina-San-Martin, B., Olaru, A., Minn, K., Tamada, K., Lau, J. S., Cascalho, M., Chen, L., Nussenzweig, A. & Livak, F. 2004. 53BP1 is required for class switch recombination. The Journal of cell biology, 165, 459-464.
Ward, I. M., Difilippantonio, S., Minn, K., Mueller, M. D., Molina, J. R., Yu, X., Frisk, C. S., Ried, T., Nussenzweig, A. & Chen, J. 2005. 53BP1 cooperates with p53 and functions as a haploinsufficient tumor suppressor in mice. Molecular and cellular biology, 25, 10079-10086.
Ward, K. K., Tancioni, I., Lawson, C., Miller, N. L., Jean, C., Chen, X. L., Uryu, S., Kim, J., Tarin, D. & Stupack, D. G. 2013. Inhibition of focal adhesion kinase (FAK) activity prevents anchorage-independent ovarian carcinoma cell growth and tumor progression. Clinical & experimental metastasis, 30, 579-594.
Warne, D., Watkins, C., Bodfish, P., Nyberg, K. & Spurr, N. K. 1991. Tetranucleotide repeat polymorphism at the human betaactin related pseudogene 2 (ACTBP2) detected using the polymerase chain reaction. Nucleic Acids Research, 19, 6980-6980.
Watanabe, N. & Mitchison, T. J. 2002. Single-molecule speckle analysis of actin filament turnover in lamellipodia. Science, 295, 1083-1086.
Weber, J. L. & May, P. E. 1989. Abundant class of human DNA polymorphisms which can be typed using the polymerase chain reaction. American journal of human genetics, 44, 388.
Webster, M., Witkin, K. L. & Cohen-Fix, O. 2009. Sizing up the nucleus: nuclear shape, size and nuclear-envelope assembly. Journal of cell science, 122, 1477-1486.
Wedeen, C. J. & Weisblat, D. A. 1991. Segmental expression of an engrailed-class gene during early development and neurogenesis in an annelid. Development, 113, 805-814.
Wei, L., Griego, A. M., Chu, M. & Ozbun, M. A. 2014. Tobacco exposure results in increased E6 and E7 oncogene expression, DNA damage and mutation rates in cells maintaining episomal human papillomavirus 16 genomes. Carcinogenesis, 35, 2373-2381.
Weinberg, R. A. The biology of cancer. 2007. New York: Garland Science, 1.
Weisenberger, D. J., Siegmund, K. D., Campan, M., Young, J., Long, T. I., Faasse, M. A., Kang, G. H., Widschwendter, M., Weener, D. & Buchanan, D. 2006. CpG island methylator phenotype underlies sporadic microsatellite instability and is tightly associated with BRAF mutation in colorectal cancer. Nature genetics, 38, 787.
Weissenbach, J., Gyapay, G., Dib, C., Vignal, A., Morissette, J., Millasseau, P., Vaysseix, G. & Lathrop, M. 1992. A second-generation linkage map of the human genome. Nature, 359, 794-801.
Weng, L.-P., Brown, J. L. & Eng, C. 2001. PTEN coordinates G1 arrest by down-regulating cyclin D1 via its protein phosphatase activity and up-regulating p27 via its lipid phosphatase activity in a breast cancer model. Human molecular genetics, 10, 599-604.
Werner, S. R., Prahalad, A. K., Yang, J. & Hock, J. M. 2006. RECQL4-deficient cells are hypersensitive to oxidative stress/damage: Insights for osteosarcoma prevalence and heterogeneity in Rothmund-Thomson syndrome. Biochemical and Biophysical Research Communications, 345, 403-409.
West, S. C. 2003. Molecular views of recombination proteins and their control. Nature reviews. Molecular cell biology, 4, 435.
Westendorf, J. J., Zaidi, S. K., Cascino, J. E., Kahler, R., Van Wijnen, A. J., Lian, J. B., Yoshida, M., Stein, G. S. & Li, X. 2002. Runx2 (Cbfa1, AML-3) interacts with histone deacetylase 6 and represses the p21CIP1/WAF1 promoter. Molecular and cellular biology, 22, 7982-7992.

Wexler, S. A., Donaldson, C., Denning-Kendall, P., Rice, C., Bradley, B. & Hows, J. M. 2003. Adult bone marrow is a rich source of human mesenchymal 'stem'cells but umbilical cord and mobilized adult blood are not. British journal of haematology, 121, 368-374.

Wickham, M. Q., Erickson, G. R., Gimble, J. M., Vail, T. P. & Guilak, F. 2003. Multipotent stromal cells derived from the infrapatellar fat pad of the knee. Clinical orthopaedics and related research, 412, 196-212.

Wigle, J. & Eisenstat, D. 2008. Homeobox genes in vertebrate forebrain development and disease. Clinical genetics, 73, 212-226.

Wilkens, L., Flemming, P., Gebel, M., Bleck, J., Terkamp, C., Wingen, L., Kreipe, H. & Schlegelberger, B. 2004. Induction of aneuploidy by increasing chromosomal instability during dedifferentiation of hepatocellular carcinoma. Proceedings of the National Academy of Sciences of the United States of America, 101, 1309-1314.

Wilson, M. C., Meredith, D. & Halestrap, A. P. 2002. Fluorescence resonance energy transfer studies on the interaction between the lactate transporter MCT1 and CD147 provide information on the topology and stoichiometry of the complex in situ. Journal of Biological Chemistry, 277, 3666-3672.

Wogan, G. N., Hecht, S. S., Felton, J. S., Conney, A. H. & Loeb, L. A. 2004. Environmental and chemical carcinogenesis. 14, 473-486.

Wolbank, S., Stadler, G., Peterbauer, A., Gillich, A., Karbiener, M., Streubel, B., Wieser, M., Katinger, H., Van Griensven, M. & Redl, H. 2009. Telomerase immortalized human amnion-and adipose-derived mesenchymal stem cells: maintenance of differentiation and immunomodulatory characteristics. Tissue Engineering Part A, 15, 1843-1854.

Won, K. Y., Park, H.-R. & Park, Y.-K. 2009. Prognostic implication of immunohistochemical Runx2 expression in osteosarcoma. Tumori, 95, 311.

Wong, L. H., Mcghie, J. D., Sim, M., Anderson, M. A., Ahn, S., Hannan, R. D., George, A. J., Morgan, K. A., Mann, J. R. & Choo, K. H. A. 2010. ATRX interacts with H3. 3 in maintaining telomere structural integrity in pluripotent embryonic stem cells. Genome research, 20, 351-360.

Woo, L. L., Futami, K., Shimamoto, A., Furuichi, Y. & Frank, K. M. 2006. The Rothmund-Thomson gene product RECQL4 localizes to the nucleolus in response to oxidative stress. Experimental cell research, 312, 3443-3457.

Woollard, J., Schmitz, C. B., Freeman, A. E. & Tuggle, C. K. 1994. Rapid communication: HinfI polymorphism at the bovine Pit-1 locus. Journal of animal science, 72, 3267.

World Health, O. 2013. classification of tumours: Pathology and genetics of tumors of soft tissue and bone.

Wozniak, M., Fausto, A., Carron, C. P., Meyer, D. M. & Hruska, K. A. 2000. Mechanically Strained Cells of the Osteoblast Lineage Organize Their Extracellular Matrix Through Unique Sites of αVβ3-Integrin Expression. Journal of bone and mineral research, 15, 1731-1745.

Wright, W. E. & Shay, J. W. 1992. The two-stage mechanism controlling cellular senescence and immortalization. Experimental gerontology, 27, 383-389.

Wu, X., Rauch, T. A., Zhong, X., Bennett, W. P., Latif, F., Krex, D. & Pfeifer, G. P. 2010. CpG island hypermethylation in human astrocytomas. Cancer research, 70, 2718-2727.

Wunder, J. S., Nielsen, T. O., Maki, R. G., O'sullivan, B. & Alman, B. A. 2007. Opportunities for improving the therapeutic ratio for patients with sarcoma. The lancet oncology, 8, 513-524.

Wysokinski, D., Pawlowska, E. & Blasiak, J. 2015. RUNX2: A master bone growth regulator that may be involved in the DNA damage response. DNA and cell biology, 34, 305-315.

Xavier, J. M., Morgado, A. L., Solá, S. & Rodrigues, C. M. P. 2014. Mitochondrial translocation of p53 modulates neuronal fate by preventing differentiation-induced mitochondrial stress. Antioxidants & redox signaling, 21, 1009-1024.

Xi, Y. & Chen, Y. 2017. PTEN Plays Dual Roles As a Tumor Suppressor in Osteosarcoma Cells. Journal of cellular biochemistry.

Xu, X., Lee, J. & Stern, D. F. 2004. Microcephalin is a DNA damage response protein involved in regulation of CHK1 and BRCA1. Journal of Biological Chemistry, 279, 34091-34094.
Xu, X. & Liu, Y. 2009. Dual DNA unwinding activities of the Rothmund–Thomson syndrome protein, RECQ4. The EMBO journal, 28, 568-577.
Xu, Y., Lei, Z., Huang, H., Dui, W., Liang, X., Ma, J. & Jiao, R. 2009a. dRecQ4 is required for DNA synthesis and essential for cell proliferation in Drosophila. PloS one, 4, e6107.
Xu, X., Rochette, P. J., Feyissa, E. A., Su, T. V. & Liu, Y. 2009b. MCM10 mediates RECQ4 association with MCM2-7 helicase complex during DNA replication. The EMBO journal, 28, 3005-3014.
Xu, L., Li, S. & Stohr, B. A. 2013. The role of telomere biology in cancer. Annual Review of Pathology: Mechanisms of Disease, 8, 49-78.
Yadav, S. & Bhatia, A. 2017. Morphology based scoring of Chromosomal instability and its correlation with cell viability. Pathology-Research and Practice.
Yager, J. D. & Leihr, J. G. 1996. Molecular mechanisms of estrogen carcinogenesis. Annual review of pharmacology and toxicology, 36, 203-232.
Yamada, M., Watanabe, K., Mistrik, M., Vesela, E., Protivankova, I., Mailand, N., Lee, M., Masai, H., Lukas, J. & Bartek, J. 2013. ATR–Chk1–APC/CCdh1-dependent stabilization of Cdc7–ASK (Dbf4) kinase is required for DNA lesion bypass under replication stress. Genes & development, 27, 2459-2472.
Yamaguchi, R., Matsumoto, S., Ae, K., Tanizawa, T., Gokita, T., Hayakawa, K., Funauchi, Y., Kito, M., Ishii, H. & Motoi, N. 2015. Case Report: Asymptomatic Osteosarcoma. Case Reports in Clinical Medicine, 4, 369.
Yamamoto, M., Cid, E., Bru, S. & Yamamoto, F. 2011. Rare and frequent promoter methylation, respectively, of TSHZ2 and 3 genes that are both downregulated in expression in breast and prostate cancers. PLoS One, 6, e17149.
Yang, J., Murthy, S., Winata, T., Werner, S., Abe, M., Prahalad, A. K. & Hock, J. M. 2006. Recql4 haploinsufficiency in mice leads to defects in osteoblast progenitors: Implications for low bone mass phenotype. Biochemical and biophysical research communications, 344, 346-352.
Yang, D.-C., Tsay, H.-J., Lin, S.-Y., Chiou, S.-H., Li, M.-J., Chang, T.-J. & Hung, S.-C. 2008. cAMP/PKA regulates osteogenesis, adipogenesis and ratio of RANKL/OPG mRNA expression in mesenchymal stem cells by suppressing leptin. PLoS One, 3, e1540.
Yano, K. I., Morotomi-Yano, K., Wang, S. Y., Uematsu, N., Lee, K. J., Asaithamby, A., Weterings, E. & Chen, D. J. 2008. Ku recruits XLF to DNA double-strand breaks. EMBO reports, 9, 91-96.
Ye, J. Z.-S., Donigian, J. R., Van Overbeek, M., Loayza, D., Luo, Y., Krutchinsky, A. N., Chait, B. T. & De Lange, T. 2004. TIN2 binds TRF1 and TRF2 simultaneously and stabilizes the TRF2 complex on telomeres. Journal of Biological Chemistry, 279, 47264-47271.
Yellowley, C. E., Li, Z., Zhou, Z., Jacobs, C. R. & Donahue, H. J. 2000. Functional gap junctions between osteocytic and osteoblastic cells. Journal of bone and mineral research, 15, 209-217.
Yin, J., Kwon, Y. T., Varshavsky, A. & Wang, W. 2004. RECQL4, mutated in the Rothmund–Thomson and RAPADILINO syndromes, interacts with ubiquitin ligases UBR1 and UBR2 of the N-end rule pathway. Human molecular genetics, 13, 2421-2430.
Ying, K. L., Oizumi, J. & Curry, C. J. 1990. Rothmund-Thomson syndrome associated with trisomy 8 mosaicism. Journal of medical genetics, 27, 258-260.
Yonish-Rouach, E. & Resnitzky, D. 1991. Wild-type p53 induces apoptosis of myeloid leukaemic cells that is inhibited by interleukin-6. Nature, 352, 345.
Yoon, D.-S., Wersto, R. P., Zhou, W., Chrest, F. J., Garrett, E. S., Kwon, T. K. & Gabrielson, E. 2002. Variable levels of chromosomal instability and mitotic spindle checkpoint defects in breast cancer. The American journal of pathology, 161, 391-397.
Yoshida, C. A., Furuichi, T., Fujita, T., Fukuyama, R., Kanatani, N., Kobayashi, S., Satake, M., Takada, K. & Komori, T. 2002. Core-binding factor β interacts with Runx2 and is required for skeletal development. Nature genetics, 32, 633-638.

Yoshikawa, T., Uchimura, E., Kishi, M., Funeriu, D. P., Miyake, M. & Miyake, J. 2004. Transfection microarray of human mesenchymal stem cells and on-chip siRNA gene knockdown. Journal of controlled release, 96, 227-232.
Yu, J.-Y., Taylor, J., Deruiter, S. L., Vojtek, A. B. & Turner, D. L. 2003. Simultaneous inhibition of GSK3α and GSK3β using hairpin siRNA expression vectors. Molecular Therapy, 7, 228-236.
Yu, M., Selvaraj, S. K., Liang-Chu, M. M. Y., Aghajani, S., Busse, M., Yuan, J., Lee, G., Peale, F., Klijn, C., Bourgon, R., Kaminker, J. S. & Neve, R. M. 2015. A resource for cell line authentication, annotation and quality control. Nature, 520, 307-311.
Yu, J.-G., Lim, J.-A., Song, Y.-R., Heu, S., Kim, G. H., Koh, Y. J. & Oh, C.-S. 2016. Isolation and Characterization of Bacteriophages Against Pseudomonas syringae pv. actinidiae Causing Bacterial Canker Disease in Kiwifruit. Journal of microbiology and biotechnology, 26, 385-393.
Zagami, C. J., Zusso, M. & Stifani, S. 2009. Runx transcription factors: Lineage-specific regulators of neuronal precursor cell proliferation and post-mitotic neuron subtype development. Journal of cellular biochemistry, 107, 1063-1072.
Zaharopoulos, P., Wong, J. & Wen, J. W. 1998. Nuclear protrusions in cells from Cytologic Specimens. Acta cytologica, 42, 317-329.
Zambetti, G. P. 2014. Expanding the reach of the p53 tumor suppressor network. Cell death and differentiation, 21, 505.
Zamore, P. D., Tuschl, T., Sharp, P. A. & Bartel, D. P. 2000. RNAi: double-stranded RNA directs the ATP-dependent cleavage of mRNA at 21 to 23 nucleotide intervals. Cell, 101, 25-33.
Zebaze, R. M., Ghasem-Zadeh, A., Bohte, A., Iuliano-Burns, S., Mirams, M., Price, R. I., Mackie, E. J. & Seeman, E. 2010. Intracortical remodelling and porosity in the distal radius and post-mortem femurs of women: a cross-sectional study. The Lancet, 375, 1729-1736.
Zebaze, R., Ghasem-Zadeh, A., Mbala, A. & Seeman, E. 2013. A new method of segmentation of compact-appearing, transitional and trabecular compartments and quantification of cortical porosity from high resolution peripheral quantitative computed tomographic images. Bone, 54, 8-20.
Zeman, M. K. & Cimprich, K. A. 2014. Causes and consequences of replication stress. Nature cell biology, 16, 2.
Zeng, Q. & Hong, W. 2008. The emerging role of the hippo pathway in cell contact inhibition, organ size control, and cancer development in mammals. Cancer cell, 13, 188-192.
Zhang, Y.-W., Otterness, D. M., Chiang, G. G., Xie, W., Liu, Y.-C., Mercurio, F. & Abraham, R. T. 2005. Genotoxic stress targets human Chk1 for degradation by the ubiquitin-proteasome pathway. Molecular cell, 19, 607-618.
Zhang, X., Yang, M., Lin, L., Chen, P., Ma, K. T., Zhou, C. Y. & Ao, Y. F. 2006. Runx2 overexpression enhances osteoblastic differentiation and mineralization in adipose-derived stem cells in vitro and in vivo. Calcified tissue international, 79, 169-178.
Zhang, X., Hirai, M., Cantero, S., Ciubotariu, R., Dobrila, L., Hirsh, A., Igura, K., Satoh, H., Yokomi, I. & Nishimura, T. 2011. Isolation and characterization of mesenchymal stem cells from human umbilical cord blood: reevaluation of critical factors for successful isolation and high ability to proliferate and differentiate to chondrocytes as compared to mesenchymal stem cells from bone marrow and adipose tissue. Journal of cellular biochemistry, 112, 1206-1218.
Zhang, J., Yan, Y.-G., Wang, C., Zhang, S.-J., Yu, X.-H. & Wang, W.-J. 2015. MicroRNAs in osteosarcoma. Clinica Chimica Acta, 444, 9-17.
Zhang, B., Zhang, Y., Zou, X., Chan, A. W. H., Zhang, R., Lee, T. K. W., Liu, H., Lau, E. Y. T., Ho, N. P. Y. & Lai, P. 2017a. The CCCTC-binding factor (CTCF)–forkhead box protein M1 axis regulates tumour growth and metastasis in hepatocellular carcinoma. The Journal of pathology, 243, 418-430.
Zhang, K., Song, L., Wang, J., Yan, S., Li, G., Cui, L. & Yin, J. 2017b. Strategy for constructing vascularized adipose units in poly (l-glutamic acid) hydrogel porous scaffold through inducing in-situ formation of ASCs spheroids. Acta biomaterialia, 51, 246-257.

Zhang, Y., Huang, L., Zhao, Y. & Hu, T. 2017c. Musk xylene induces malignant transformation of human liver cell line L02 via repressing the TGF-β signaling pathway. Chemosphere, 168, 1506-1514.
Zhao, B., Li, L., Lei, Q. & Guan, K.-L. 2010. The Hippo–YAP pathway in organ size control and tumorigenesis: an updated version. Genes & development, 24, 862-874.
Zhao, H., Rybak, P., Dobrucki, J., Traganos, F. & Darzynkiewicz, Z. 2012. Relationship of DNA Damage Signaling to DNA Replication Following Treatment with DNA Topoisomerase Inhibitors Camptothecin/Topotecan, Mitoxantrone, or Etoposide. Cytometry. Part A: the journal of the International Society for Analytical Cytology, 81, 45-51.
Zhao, H., Watkins, J. L. & Piwnica-Worms, H. 2002. Disruption of the checkpoint kinase 1/cell division cycle 25A pathway abrogates ionizing radiation-induced S and G2 checkpoints. Proceedings of the National Academy of Sciences, 99, 14795-14800.
Zhen, Y.-Y., Libotte, T., Munck, M., Noegel, A. A. & Korenbaum, E. 2002. NUANCE, a giant protein connecting the nucleus and actin cytoskeleton. Journal of cell science, 115, 3207-3222.
Zheng, Y.-Z., Roseman, R. R. & Carlson, W. R. 1999. Time course study of the chromosome-type breakage-fusion-bridge cycle in maize. Genetics, 153, 1435-1444.
Zhou, B.-B. S. & Bartek, J. 2004. Targeting the checkpoint kinases: chemosensitization versus chemoprotection. Nature Reviews Cancer, 4, 216-225.
Zhou, L., Du, L., Chen, X., Li, X., Li, Z., Wen, Y., Li, Z., He, X., Wei, Y. & Zhao, X. 2010. The antitumor and antimetastatic effects of N-trimethyl chitosan-encapsulated camptothecin on ovarian cancer with minimal side effects. Oncology reports, 24, 941-948.
Zhu, L., McManus, M. M. & Hughes, D P. 2013. Understanding the biology of bone sarcoma from early initiating events through late events in metastasis and disease progression. Frontiers in Oncology, 3.
Zils, K., Klingebiel, T., Behnisch, W., Mueller, H. L., Schlegel, P.-G., Fruehwald, M., Suttorp, M., Simon, T., Werner, M. & Bielack, S. 2015. Osteosarcoma in Patients with Rothmund–Thomson Syndrome. Pediatric hematology and oncology, 32, 32-40.
Ziv, Y., Bielopolski, D., Galanty, Y., Lukas, C., Taya, Y., Schultz, D. C., Lukas, J., Bekker-Jensen, S., Bartek, J. & Shiloh, Y. 2006. Chromatin relaxation in response to DNA double-strand breaks is modulated by a novel ATM-and KAP-1 dependent pathway. Nature cell biology, 8, 870.
Zoetis, T., Tassinari, M. S., Bagi, C., Walthall, K. & Hurtt, M. E. 2003. Species comparison of postnatal bone growth and development. Birth Defects Research Part B Developmental and Reproductive Toxicology, 68, 86-110.
Zou, L. & Elledge, S. J. 2003. Sensing DNA damage through ATRIP recognition of RPA-ssDNA complexes. Science, 300, 1542-1548.
Zou, Y., Liu, Y., Wu, X. & Shell, S. M. 2006. Functions of human replication protein A (RPA): from DNA replication to DNA damage and stress responses. Journal of cellular physiology, 208, 267-273.
Zuk, P. A., Zhu, M., Mizuno, H., Huang, J., Futrell, J. W., Katz, A. J., Benhaim, P., Lorenz, H. P. & Hedrick, M. H. 2001. Multilineage cells from human adipose tissue: implications for cell-based therapies. Tissue engineering, 7, 211-228.
Zuk, P. A., Zhu, M., Ashjian, P., De Ugarte, D. A., Huang, J. I., Mizuno, H., Alfonso, Z. C., Fraser, J. K., Benhaim, P. & Hedrick, M. H. 2002. Human adipose tissue is a source of multipotent stem cells. Molecular biology of the cell, 13, 4279-4295.
Zwerger, M., Ho, C. Y. & Lammerding, J. 2011. Nuclear mechanics in disease. Annual review of biomedical engineering, 13, 397.